CONGRESS

MINAR 9

JULY
2023

المؤتمر الدولي

التاسع
للعلوم الصرفة
والتطبيقية والتكنولوجية

Rimar Academy
أكاديمية ريمار

Minar Journal
مجلة مينار

IX

International Congress of

Pure and Applied Technological Sciences

Issued By
RIMAR ACADEMY

July 6th-8th 2023

PROCEEDINGS BOOK

كتاب الوقائع

CONGRESS

MINAR 9

ISBN 978-625999348-5



Publisher	Rimar Academy
Editor-in-Chief	Prof. Dr. Ghuson H. MOHAMMED
Design Coordinator	Ali HIJAZI
ISBN	978-625-99934-8-5
DOI	10.47832/MinarCongress9
Printing Date	August 2023
Conference Dates	06 - 07 - 08, July / 2023
Number of Pages	402
URL	www.rimaracademy.com
Printing Certificate Number	47843

CO-SPONSORED BY

الجهات الراعية



الرؤساء الفخريون
Honorary Committee



الأستاذ الدكتور وعد محمود رؤوف
Prof. Dr. Waad Mahmood RAOOF

رئيس جامعة تكريت
Rector of Tikrit University

العراق - Iraq



الأستاذ الدكتور محمد حقي ألما
Prof. Dr. Mehmet Hakkı ALMA

رئيس جامعة اغدير
Rector of Iğdır University

تركيا-Türkiye



الأستاذ الدكتور قصي كمال الدين الاحمدي
Prof. Dr. Kossay K. Al-AHMADY

رئيس جامعة الموصل
Rector of the University of Mosul

العراق - Iraq



الأستاذ الدكتور مازن حسن جاسم الحسني
Prof. Dr. Mazin Hasan Jasim ALHASANY

رئيس جامعة واسط
Rector of the University of Wasit

العراق - Iraq



الأستاذ الدكتور زكريا ظلام
Prof. Dr..Zakaria ZALLAM

جامعة غازي عنتاب
Gaziantep University

تركيا-Türkiye



الأستاذ الدكتور علياء عباس علي العطار
Prof. Dr. Alyaa A. Ali Al-ATTAR

رئيس الجامعة التقنية الشمالية
Rector of Northern Technical University

العراق - Iraq



الأستاذ الدكتور غصون حميد محمد
Prof. Dr. Ghuson H. MOHAMMED

جامعة بغداد
University of Baghdad

العراق - Iraq

رئيس المؤتمر
Chair of Congress



الأستاذ الدكتور خميس عواد زيدان
Prof. Dr. Khamis A. ZIDAN

نائب رئيس الجامعة العراقية للشؤون العلمية
Vice Rector of Al-Iraqia University for Scientific Affairs

العراق - Iraq

رئيس الهيئة الإستشارية
Chairman of Consultative Committee



الأستاذ الدكتور منير سالم طه
Prof. Dr. Muneer salim TAHA

نائب رئيس جامعة الموصلة للشؤون العلمية
Vice-president for Scientific Affairs of the University of Mosul
العراق - Iraq

رئيس الهيئة التحضيرية
Chairman of Organizing Committee



الأستاذ الدكتور عماد حسن رضا
Prof. Dr. Emad Hasaan Ridha

جامعة البصرة للنفط والغاز / مساعد رئيس الجامعة للشؤون العلمية
Vice - Chancellor for Scientific Affairs Basrah University for Oil and Gas

العراق - Iraq

رئيس الهيئة العلمية
Chairman of scientific committe



أ. د. عبد الكريم دهش علي
Prof. Dr. Abdulkareem Dash ALI

عميد كلية التربية للعلوم الصرفة – جامعة تكريت
Dean of the College of Education Pure Science-Tikrit University

العراق - Iraq

الأمين العام للمؤتمر
General Secretary

الهيئة الإستشارية
Consultative Committee



Prof. Dr. Mohammed Kadhim JAWAD
University of Baghdad
Iraq



Prof. Dr. Kamal Hamid YASSER
University of Thi-Qar
Iraq



Prof. Dr. Khazaal Yaseen MUSTFA
University of Al-Hamdaniya
Iraq



Prof. Dr. Jafar Ramadhan MOHAMMED
Ninevah University
Iraq



Prof. Dr. Nawras Abdelah ALWAN
University Of Basrah
Iraq



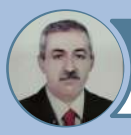
Prof. Dr. Hiyam Adil Ibrahim Ismail ALTAII
University of Mosul
Iraq



Prof. Dr. Derar ELEYAN
Palestine Technical University
Palestine



Prof. Dr. Sattar Jaber KHALLAWY
Wasit University
Iraq



Prof. Dr. Basim N. ABOOD
Wasit University
Iraq



Assist. Prof. Dr. sameera ahmed EBRAHIEM
University of Baghdad
Iraq



Dr. Osman TÜRK
Harran University
Türkiye



Dr. Nabil Mohie Abdel–Hamid ALY
Kafrelsheikh University
Egypt

الهيئة التحضيرية
Organizing Committee



Prof. Dr. Nihad Abdul-Lateef ALI
Al-Qasim Green University
Iraq



Prof. Dr. Abdelmonnem S. KAHLEL
University of Mosul
Iraq



Prof. Dr. kifah Saed DOOSH
University of Baghdad
Iraq



Prof. Dr. Sawsan Muhammed Abdulla AL-SORCHEE
Baghdad University
Iraq



Assist. Prof. Dr. Jalil Talab ABDULLA
Wasit University
Iraq



Assist. Prof. Iman radha JASIM
University of Mosul
Iraq



Assist. Prof. Dr. Methaq Abd Muslim GUDA
University of Kufa
Iraq



Assist. Prof. Alyaa M. Abdul Majeed HALEEM
University of Mosul
Iraq



Assist. Prof. Farah Tareq MOHAMMED
University of Mosul
Iraq



Lect. Ammar Al-ZUBADE
University of Baghdad
Iraq



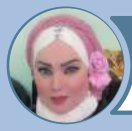
Lect. Dr. Ali Muhsen ALİ
University of Kerbala
Iraq



Dr. Amel D. HUSSEIN
Wasit University
Iraq



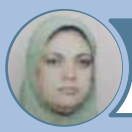
Dr. Haleemah Jaber MOHAMMED
Ministry of Science and Technology-Iraq



Dr. Liqaa Zeki Hummady ALTAMIMI
University of Baghdad
Iraq



Dr. Ali M. HUSSEIN
University of Mosul
Iraq



Dr. Huda Y.AL-ATTAR
University of Mosul
Iraq



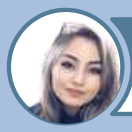
Dr. Hayder AbdulMunem AbdulAmeer TURK
Ministry of Education
Iraq



Dr. may TAHA
University of Mosul
Iraq



Assist. Prof. Dr. Zaid Salim SULIMAN
University of Baghdad
Iraq



Dr. Dinara MAZHITOVNA
Rimar Academy
Qazakistan

الهيئة العلمية



Prof. Dr. Ebtahag .Z.SULYMAN
University of Mosul
Iraq



Prof. Dr. Kamal Hussein Ahmad Al-SAMARRAI
Samarra University
Iraq



Prof. Dr. Samira NEGRICHI
Larbi Tebessi University
Algeria



Prof. Dr. Sawsan Yousef KARA
Ministry of Education
Palestine



Prof. Dr. Amera Mahmood ALRAWI
University of Mosul
Iraq



Prof. Dr. Nazih Wayes ZAİD
University of Baghdad
Iraq



Prof. Chèrif Fatima ZOHRA
Professor off Général Surgery and Oncology
Algeria



Prof. Dr. Oruba Kuttof Hussein AL-BERMANİ
Babylon University
Iraq



Assist. prof. intisar ghanim TAHA
University of Mosul
Iraq



Assist. Prof. Dr. Rana Tariq YAHYA
University of Mosul
Iraq



Assist. Prof. Dr. Nihad Taha Mohammed JADDOA
University of Baghdad
Iraq



Assist. Prof. Dr. Fatima Rammadan ABDUL
Mustansiriyah University
Iraq



Assist. Prof. Dr.Ekhlas Hmeyem SHALLAL
University of Baghdad
Iraq



Assist. Prof. Dr.Israa abdul razzaq ALDOBAİSSİ
Mustansiriyah University
Iraq



Asst. Prof. Dr. Anmar Ahmed AL-TAIE
University Of Mosul
Iraq



Assist. Prof. Dr. Sura Safi Obayes KHAFAJI
Al-Qasim Green University
Iraq



Assist. prof. Farah Tariq SAEED
University of Mosul
Iraq



Lect. Dr. Adil Hatem NAWAR
University of Anbar
Iraq



Lect. Dr. Ikhlas Ali Hammoodi AL-HADEETHI
Wasit University
Iraq



Lect. Dr. Sabah Noori HAMMOODİ
AShur University Collage
Iraq



Lect. Dr. Hanan Ali Hammoodi AL-HADEETHI
Uruk University
Iraq



Dr. Anaam Kadhim HADI
Ministry of Science and Technology
Iraq



Dr. Husam R. ABED
Ministry of Education
Iraq



Dr. Bader AL-AİFAN
Kuwait University
Kuwait



Dr. Batool Abd Al Ameer Baqer ALSAFAR
Al Mustansiriyah University
Iraq



Dr. Zhazıra ZHAUYNSHIYEVA
ABAI University
Kazakistan



Dr. Najah sobhi nayyef AL OMAR
University of Mosul
Iraq



Dr. Fatiha HACHANI
KASDI Merbah University-Ouargla
Algeria



Dr. Asia A. M.SAADULLAH
University of Duhok
Iraq



Dr. Ahmed Chaloob SADDAM
University of Baghdad
Iraq



Dr. Zahraa Hasan RAHEEM
University of Baghdad
Iraq



Dr. Ali Abdulwahab RİDHA
University of Technology and Applied Sciences, Rustaq
Oman

الهيئة العلمية



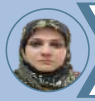
Dr. Amel ABBAS
Medecine faculty-University of Kasdi Merbah Ouargla
Algeria



Dr. Mayson Thafir HADI
University of Baghdad
Iraq



Dr. SANDUGASH TLEUBAY
ABAI University
Kazakistan



Dr. Rana Ramzi ABED
University of Mosul
Iraq



Dr. Mira Ausama Al-KATIB
University of Mosul
Iraq



Dr.Naina DERAOUI
University of Kasdi Merbah Ouargla
Algeria



Dr. Mustafa M.Khalifa JABIRY
Management & Science University
Malaysia



Khalid EL BEKKAYE
University Mohammed I Oujda
Morocco



Dr. Roukia HAMMODI
University of Kasdi Merbah Ouargla
Algeria



Dr. Tawfiq Mohammed Mustafa Al-ANTARY
University of Jordan
Jordan



Dr.Abdelbaset Abdelsameaa Ahmed ALKHARPOTLY
Aswan University
Egypt



Dr. Mohammed nuh Al KHAFAF
Northern Technical University
Iraq



Dr. Muslim Muhsin ALI
University of Missouri
USA



Dr. FOUZIA Youcef
University of Kasdi Merbah Ouargla
Algeria



Dr. Ghassan H. Abdul-MAJEED
University of Baghdad
Iraq



Dr. Symbat YESSIMKULOVA
ABAI University
Kazakistan



Dr. Mutasim Ali Mohamed ELAGAB
Gezera University
Sudan



Dr. ZHAXYLYK ORALKANOVA
ABAI University
Kazakistan



Dr. Hanane ARBIA
Kasdi Merbah University
Algeria



Dr. Shatha Hizem SHAKER
Tikrit University
Iraq



Dr. Hussein Hadi NAHI
Al-qasim Green University
Iraq



Dr. Ibrahem Rahem Jassim Al-AADILY
University of Sheffield
UK



Dr. Zainab H. MAHMOOD
University of Baghdad
Iraq



Dr. Ahmed Yossif EL-AGHA
Second Assalam School
Qatar



Dr. Shaymaa Z.AL RUMAIDH
University of Thi-Qar
Iraq



Dr. Jenan Atiyah GHAFIL
University of Baghdad
Iraq



Dr. Amjed mohammed SHAREEF
Al-Karkh University of Science
Iraq



Dr. Mohamed RMAIDA
Libyan Iron and Steel Company(LISCO)
Libya



Dr. Ielaf O. Abdul Majeed DAHL
University of Mosul
Iraq



Dr. Morooj A. ABOOD
Ministry of Science and Technology
Iraq



Dr. Likaa Hamied MAHDI
Mustansyriah university
Iraq



Dr. Sheren Fadhal ABBAS
University of Basrah
Iraq



Dr. Rana Adnan MOHAMMED
University of Baghdad
Iraq



Dr. Refag Suleiman Hamed MOHAMMED
University of Gezira
Sudan



Dr. Souad Ahmed ABUMARYAM
Sirte University
Libya



Dr. Abdelaziz KEROUM
EPH MOHAMMADIA. MASCARA
Algeria

Rimar Academy

PREFACE

The 9th International Conference on Applied Sciences and Technology Research "MINAR CONGRESS", was organized by Istanbul Gedik University in collaboration with Remar Academy. The primary objective of this event was to compile and disseminate valuable scientific knowledge and make a meaningful contribution to the future.

Remarkably, a substantial number of researchers, both from local and international backgrounds, demonstrated their interest in this conference. The scientific committee meticulously reviewed the submissions and ultimately accepted a select group of individuals, totaling 84 applicants, 62 of them were accepted by the scientific committee.

This conference was truly a global endeavor, as it drew participation from 23 attendees who joined in person, alongside 39 who engaged in the event remotely. These participants collectively enriched the conference with their expertise and insights.

The core of this conference was the presentation of 33 complete research papers, while the remaining articles and research findings are set to be featured in forthcoming issues of the MINAR Journal.

I would like to extend my sincere appreciation to all the contributors and scholars who played an essential role in making this conference a resounding success. Your dedication and valuable contributions are deeply respected and acknowledged.

Editor-in-Chief
Prof. Dr. Ghuson H. MOHAMMED

Table of Contents

Evaluating The Interface Shear Strength with Different Degree of Compaction of Clay Subgrade Soil Using Biaxial Geogrid BX1100 — 1

Qais Sahib Banyhussan, Ahmed Al-Bdairi, Manar Mahmood Alghrairi & Ali Basher Muhesen

Some Biological Aspects of Sea Bream (Acanthopagrus Latus) In Shatt Al-Arab River, Iraq — 14

Layla A. Aufy & Shaymaa A.J. Al-Jumaiee

Effect of Rheumatoid Arthritis on Alkaline Phosphatase Activity and Some Biochemical Variables — 26

Huda Y. Al-Attar & Eman Sameer Al-Soffi

Detection of Proteus Mirabilis Carrying blaCTX-M, blaSHV, and blaTEM Genes Related to Urinary Tract Infections — 38

Miaad K. Alkhudhairy, Mahasin Sifir Madkhur & Layla Saleh Abdul-Hassan

Solving Some Nonlinear Partial Differential Equations by GERFM — 49

Zaniab Mohamed Ridha Al-Fatlawy

Evaluation The Efficacy of Ocimum Basilicum Extract & Antifungal Agents Against Some Pathogenic Filamentous Fungi — 65

Ihsan Ali Alzamily, Hassan Ali Tamur & Murtadha M Hussein

Codebook Design Method for Astronomical Images Compression — 77

Maha A. Hameed

Rimar Academy

Table of Contents

Fabrication and Characterization of Polyvinyl Alcohol Nanofibers with Silver in Different Ratios for No2 Gas Sensing
Dalia Y. Salahaddin & Nadim K. Hassan
83

Study of Artin Cokernel of the Group (D_n×C_11), Where n is an Even Number
Bassim Kareem Mihsin
95

Inhibitory Effect and Antioxidant Activity of the Internal Membrane Decomposition of Egg Shells
Sheren Fadhel Abbas
113

Effect of Gibberellin Spraying On Yield of Bean and Its Components
Raam Shaker Mahmoud & Ammar Al-Zubade
121

Synthesis and Characterization of Ultraviolet Photodetector Based On Zns/PEDOT: PSS Organic/Inorganic P–N Heterojunction
Ikhlas H. Shallal, Morooj A.Aboode & Nisreen S.Turki
128

Evaluation of Some Heavy Metals and Microbial Contamination in Some Imported Food Sauce
Miyada Kh Hassan
140

The Effect of Moringa Oleifera Powder On the Ability of Fusarium Spp Isolates to Produce Toxic Metabolites On Wild Eggplant, Atropa Belladonna
Ali F. Merjan, Hala Jumaah Asree & Hanan Ali Kareem
150

Rimar Academy

Table of Contents

The Possible Protective Effect of Rutin to Reduce the Effect of Formaldehyde on Lung Tissue and Oxidative Stress in Rats
Arjwan A Alsudani & Hadeel Jabar Neama Almuoswi
157

Material Removal Rate Prediction in Abrasive Water Jet (AWJ) Process Using Artificial Neural Network
Mostafa Adel Abdullah, Safaa Kadhim Ghazi & Atheer R. Mohammed
173

Image Captioning System Using Merge Conventional and Recurrent Neural Networks
Rasha Talib Gdeeb
189

Cyanobacteria and Microalgae Microcystin-LR of the Reverse Osmosis House Filter Drinking Water in Babel Province, Iraq
Sabaa Hilal Hadi, Rana H. Raheema, M.A. Al-Khafaji & Abdulazeez A. Hassooni
209

Quintic Spline Exponential Methods for Numerical Solutions of Two-Point Boundary Value Problems in Mid Knots
Ahmed R Khlefh
219

Speed Control for the DC Motor Based on Feedforward PID Controller
Ghaidaa Hadi Salih Elias
230

Security Challenges and Threats in Wireless Sensor Networks: A Review
Maytham S. Jabor , Aqeel Salman Azez, Azhar Hasan Nsaif, Azhar Sabah Abdulaziz & Worud Mahdi Saleh
245

Rimar Academy

Table of Contents

Study The Effects of Different Doses of Tylosin Tartrate On Hematological Parameter and Some Reproductive Hormones On Male White Mice 265

Awatif I. Muhammed & Ban Sahib Abdul-Nabi AL- Nasiry

Using Walnut Peel as a Natural Dye with Natural Wool Fibers 273

Hiba Swadi, Nagham Swadi, Meena M.Abdul-Hussain & Ola Subhi

Evaluation the Pharmacodynamics Interaction of Cyclosporine and Azacitidine On the Treatment of Induced Aplastic Anemia in Rat 284

Ghanem T. Abdulrazzaq & Huda F. Hasan

Optimization of Wire EDM Parameters for Machining HSS (8X200) by using Grey Relational Analysis (GRA) 293

Athraa M. S. Ahmed, Abd Ulrahman I. Jihad, Heba Saad Qasim & Saad K. Shather

Effect of Toxoplasmosis On Zinc and Thyroid Hormones Levels with Pregnant Women 307

Aya R. Abduwahab Alheany & Ammer Abd. Mohammed

Antimicrobial Effect of Gaultheria Procumbens On Multidrug Resistant Bacteria Causing Wound Infections 313

Layla Fouad Ali & Nagham Shakir AlAttar

أثر التكيّف على الشوارع الحضرية 329

Adaptation Impact of Urban Alleyways

Inas Hasan Shukur & Ahmad N. Al-Shammaa

Rimar Academy

Table of Contents

دراسة المحتوى الميكروبي لأنواع مختلفة من الخبز والحلويات والمعجنات المباعة في الأسواق المحلية 345

Study The Microbial Content About Different Types of Bread, Pastries and Sweets Sold in Local Market

Sahar Sabeeh George

النشاط المضاد للأكسدة لبروتينات الشرش المعزولة من حليب الجمل المتحللة انزيميا واستعمالها في إطالة العمر الخزني للزيوت 359

Antioxidant Activity of Whey Proteins Isolated from Enzymatically Hydrolyzed Camel's Milk and Their Using in Extending the Shelf Life of Oils

Orass T. AL-Ibresam, Rawdah M. AL-Ali & Sawsan A. AL-Hilifi

The Effect of Serum Glypican-4 (GLY-4) in Patients with Cardiovascular Disease in Iraq 374

Bayader Abdul Hussein Mahmeed, Hend Ahmed Abass, Wasan T. Al-Rubayee & Rayah Sulaiman Baban

The Effect of Alcoholic Extract of Infected Ceratonia Fruits Infected with Some Fungi On Some Histological Characteristics of White Male Swiss Ratus Rattus Ratus 380

Zainab Jawad Naki AL-Busaid, Zainab Abd Al -Ameer Mohammed,
Zainab Shnewer Mahdi Al- Turfi & Wijdan Kamal Noor Shalan Al_Qraawy

Identification and Diagnosis of Some Types of Pathogenic Bacteria That Cause Dental Caries in Diabetic Patients 389

Sumyah H. Torki, Salih S. Yagoub, Haneen M. Hammed, Tabarak S. Jassim,
Mastafa H. AL-Musawi & Hanan A. AL-Naymi

Determination of Vitamin D Levels in Patients with Autism by High Performance Liquid Chromatography HPLC 395

Hadeel Sameer Abd Alwahab

Rimar Academy

Evaluating The Interface Shear Strength with Different Degree of Compaction of Clay Subgrade Soil Using Biaxial Geogrid BX1100

Qais Sahib Banyhussan [1], Ahmed Al-Bdairi [2], Manar Mahmood Alghrairi [3], Ali Basher Muhesen [4]

© 2023 The Author(s). This open access article is distributed under a Creative CommonsAttribution (CC-BY) 4.0 license.

Abstract: Using geogrid in road pavements can enhance pavement performance by enhancing bearing capacity, lateral confinement, and overall stiffness, in addition to lowering lateral and vertical pavement deformations. A Number of large-scale direct shear experiments were applied in this paper to assess the influence of compaction degree on the mechanical interaction among a clay subgrade soil and a subbase layer in both cases of using and not using reinforcement at the interface. Clay subgrade soil, Subbase granular materials as Type B, and Biaxial Geogrid BX1100 were employed as reinforcing materials in this investigation. In the current investigation, direct shear test was employed by fabricating a large-scale direct shear apparatus consisting of a square upper box with dimensions of (200 mm × 200 mm × 100 mm), and a rectangular lower box with dimensions of (200 mm × 250 mm × 100 mm). On specimens with and without reinforcement, 40 interface tests were performed for five degrees of compaction (100, 98, 93, 90, and 84%), which corresponded to (60, 55, 50, 45, and 40 blows/layer) for the shear box, with the regular loads applied for each combination being (25 – 50 - 75 – 100) kPa. The results demonstrate that the interface shear stress curves grew and trailed a similar pattern for the four normal stress (25 – 50 - 75 – 100) kPa. At their optimal moisture levels, the effect of dry density on the interface properties of these combinations (geogrid-soil) was also examined. The interface shear failure envelopes grew with increasing molding dry densities (i.e. degree of compaction), reaching a maximum value at 97% degree of compaction.

Key Words: Shear strength; large scale direct shear test; geogrid; degree of compaction.

Author details

[1– 2 – 4] Highway and Transportation Department, Engineering College, Mustansiriyah University, Baghdad, Iraq

[3] Civil Engineering Department, Engineering College, Istanbul Gedik University, Isanbul, Turkey

Citation information

Cite this article as:

Banyhussan, Q.A., Al-Bdairi, A., Alghrairi, M.M., Muhesen, A.B., (July 2023), *Evaluating The Interface Shear Strength with Different Degree of Compaction of Clay Subgrade Soil Using Biaxial Geogrid BX1100*, Proceedings of the Minar Congress, Turkey, (9) pp 1-13, DOI: http://dx.doi.org/10.47832/MinarCong9-1

http://dx.doi.org/10.47832/MinarCong9-1

1 qaisalmusawi@uomustansiriyah.edu.iq

2 ahmed_shaker_eng87@uomustansiriyah.edu.iq

3 manarma0822@gmail.com

4 alibasher@yahoo.com

Introduction

In pavement engineering, geogrid reinforcements are primarily utilized for two purposes: base reinforcement (embedded inside the subbase layers or base) and subgrade stabilization (embedded between the granular base course and the subgrade). By enhancing the pavement carrying capacity, lateral confinement as well as overall stiffness in addition to lowering lateral pavement and the vertical deformations, the addition of geogrid to road pavements can enhance pavement performance (Shukla, 2002; Zornberg, 2011). Additionally, the use of geogrid can minimize fracture propagation and stop reflected cracking. Antireflective cracking systems may also include numerous layers of geosynthetic materials in the interlayer zone. From a financial standpoint, also it can (i) reduce the base course amount that is needed, (ii) lower the cost of maintaining the roads, and (iii) extend the lifespan of the road pavement. Additionally, the geonet layer strengthens the soil, which reduces settlement results compared to unreinforced soil (Nareeman and Fattah, 2012).

In order to be constructed, pavements need a solid and strong base, which is not always feasible. When building roads, certain sites have subgrade that is of extremely low quality, thus this needs to be fixed before paving. Rutting and persistent deformation of the pavement arise from failing to restore the subbase to a robust and stable state (Giroud and Ha, 2004).

The shape, geometry, tensile stiffness, and strength of the reinforcement as well as the soil's physical and mechanical characteristics (distribution of particle size, particle size and shape, moisture content, and density) all affect the soil-reinforcement interface properties. The soil-reinforcement interaction mechanism (direct shear mode or pullout mode) is one of these variables (Banyhussan et al., 2023).

While direct shear equipment is frequently used to assess the interface shear characteristics of reinforcement and fill materials, triaxial and direct shear tests are customarily utilized to determine the shear strength parameters. When geotextile was utilized at the interface, several researchers used direct shear equipment to acquire interface parameters using a device that preserved a rigid block as the substratum. Others have evaluated interface qualities using a system in which the shear box (both parts) were filled with soil and at the horizontal shear plane a geogrid was installed to imitate field circumstances Arulrajah et al. (2015), Choudhary and Krishna (2014), and Kandolkar and Mandal (2013).

Aim of the Study

Geogrids have been extensively employed to build solid subgrade foundations and to give builders a working surface over brittle and fragile soils. By minimizing excessive deformation and cracking, using geogrid reinforcement in a pavement system assures a good pavement structure with long lasting.

The mechanical interaction among a clay subgrade soil and a subbase layer with using a geogrid and without at the interface was examined in this work using a numbers of large-scale direct shear experiments.

Materials Used

Subbase Material

The study used subbase granular materials (SGM) Type B. This type of SGM has been obtained from Sabeaa Al- bour area north of Baghdad city in Iraq. Table (1) illustrates the gradation of subbase granular materials. The chemical as well as physical properties of SGM are presented in Table (2) complied with (SCRB /R6, 2003).

Table 1. Gradation of the subbase granular materials

% Passing by the weight		
Size of the Sieve mm	**Passing (%)**	**Limits of SCRB/R6, 2003**
75	100	-
50	100	100
25	88.5	75-95
9.5	74.5	40-75
4.75	51.2	30-60
2.36	41.4	21-47
0.3	27	14-28
0.075	14.30	5-15

Table 2. The physical properties and results of chemical analysis

Characteristics	**Results**	**Limits of SCRB/R6,2003**
Max. dry density (gm/cm^3)	2.240	Not limited
Optimum moisture content %	7.0	Not limited
Organic matter ,%	0.84	Max. 2
T.S.S ,%	7.58	Max. 10
(SO_3) content , %	2.60	Max. 5
Gypsum content , %	5.59	Max. 10.75

Clay Soil

The clay soil is taken from Al-Muthanaa Airport location in Baghdad city. Table (3) shows the soil properties for clay soil.

Table 3. Properties of clay soil

Characteristics	Results	Specification requirement
Max. dry density (gm/cm^3)	1.88	AASHTO T99 – 95
Optimum moisture content (%)	10.1	AASHTO T99 – 95
Liquid limit (%)	34.5	AASHTO T89 – 96
Plastic limit (%)	21.8	AASHTO T90 – 96

Geogrid

The Biaxial Geogrid BX1100, produced by Tensar International Company, depicted in Figure (1). The mechanical and physical characteristics of the BX1100 geogrid are displayed in Table (4).



Figure 1. Biaxial geogrid reinforcement used in the study.

Table 4. Biaxial geogrid Physical and mechanical properties (Tensar International Co)

The physical properties	Data		
Color	Black		
Polymer	PP		
Rib shape	Rectangular		
Polymer type	Biaxial geogrid		
Index properties	**Units**	**MD Values**	**XMD Values**
Aperture Dimensions	mm	25	33
Rib Thickness	mm	0.76	0.76
Tensile Strength @ 2% Strain	kN/m	4.1	6.6
Tensile Strength @ 5% Strain	kN/m	8.5	13.4
Ultimate Tensile Strength	kN/m	12.4	19.0

4- Direct Shear Test

The manufactured direct shear tool with large-scale by (Banyhussan 2023) consisted of In the current investigation, a square upper box with dimensions (200 mm × 200 mm × 100 mm), and a rectangular lower box with dimensions (20 mm× 250 mm× 100 mm) are employed. In order to keep the shearing area consistent throughout the experiments, the bottom box's size was kept greater than the top box's.

4.1 Interface Test Program

For the current study, the impact of compaction on the shear interface strength was studied. The equivalent numbers of blows that achieved maximum dry density in the shear box at optimum moisture content was found by try and error to be (60 blows/layer) with 3 layers used in the box.

40 interface examinations were done on specimens as a total in both case of using and not using reinforcement for five degree of compaction (100, 98, 93, 90 and 84%), that equivalent to (60, 55, 50, 45, and 40 blows/layer) for the shear box, where the loads applied for each combination normally were taken to be equal to (25 – 50 - 75 – 100) kPa (Xu, et al. (2020).). ASTM D3080 [ASTM D3080/ D3080M (2011)] and ASTM D5321 [ASTM D5321/ D5321M (2014)] For interface testing without and with reinforcement, normal test techniques were used. The ASTM D5321 [ASTM D5321/ D5321M (2014)] interface test procedure requires the box size must be at least five times larger than the reinforcement's opening size. This ratio was equal to 8.0 in this investigation for the geogrid utilized.

Procedure

A produced large-size direct shear apparatus with box dimensions box with dimensions of (200 mm × 250 mm × 100 mm) was utilized in this work to investigate the interface parameters with and without geogrid. Two linear variable differential transducers (LVDTs) with a range of 50 mm made up the test equipment, which also included two horizontal load cells with a capacity of 50 kN. The sample's horizontal and vertical deformations during the shearing process were measured using LVDTs. Through the use of a Data Acquisition System (DAQ), the measurements were automated. The reinforcement was positioned at the lower-to-upper interface during interface testing.

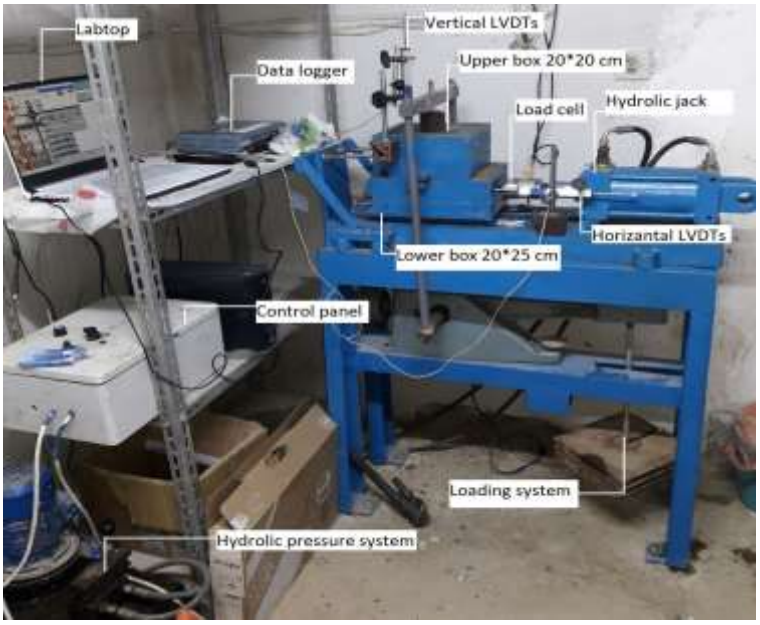


Figure 2. Large-scale direct shear apparatus (Banyhussan et. al.,2023)

Failure Criterion

The specimen must be sheared to a horizontal displacement that is at least 10% of the box size, or 20 mm for a 200 mm wide shear box, in accordance with ASTM D3080 [ASTM D3080/ D3080M (2011)]. Failure criteria were used by Youwai et al. (2004) based on the peak shear stress or the shear stress that corresponded to the test's end (equivalent to about 15% of the box's size, or about 30 mm). The test can be conducted until the horizontal displacement surpasses 75 mm or another amount specified by the user, or it can be stopped sooner if the shear stress is reached, in accordance with ASTM D5321 [ASTM D5321/ D5321M (2014)].

Results and Discussion

Interface Shear Strength

Figure 3 shows the photograph of geogrid used that fixed to the shear box at the shearing plane. A total of tests are 40; with five degree of compaction of subgrade soil (100, 98, 93, 90 and 84 %), reinforced and without reinforced subgrade interface, interface shear strength were evaluated under four normal stress (25 – 50 - 75 – 100) kPa.

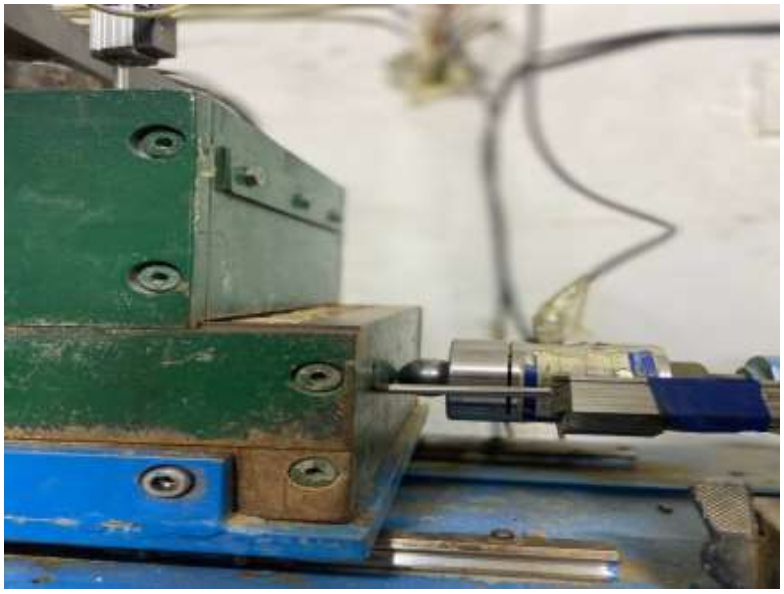


Figure3. Geogrid reinforcement fixed to the shear box

For degree of compaction (100%) with optimum moisture content, Figure 4 and 5 illustrate the a typical displacement with shear stress with different normal stresses (25 – 50 - 75 – 100) kPa respectively, of subbase-clay in both case of using and not using reinforcement. It is appear that, increasing normal strength leads to increase shear stresses for all cases. Figure 6 and 7 show the Mohr–Coulomb shear strength envelopes at end for the four cases under consideration for degree of compaction (100%) with optimum moisture content. The angle of friction and adhesion are shown in Table 5 and Table 6 for without and geogrid reinforcement, respectively.

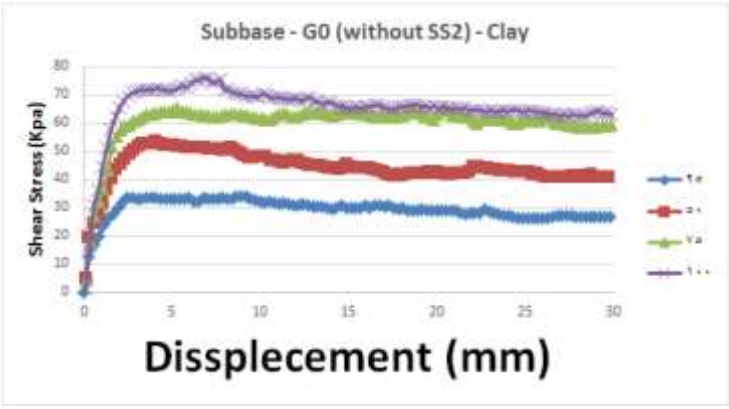


Figure4. shear stress with horizontal displacement for without reinforcement for 100% degree of compaction with optimum moisture content

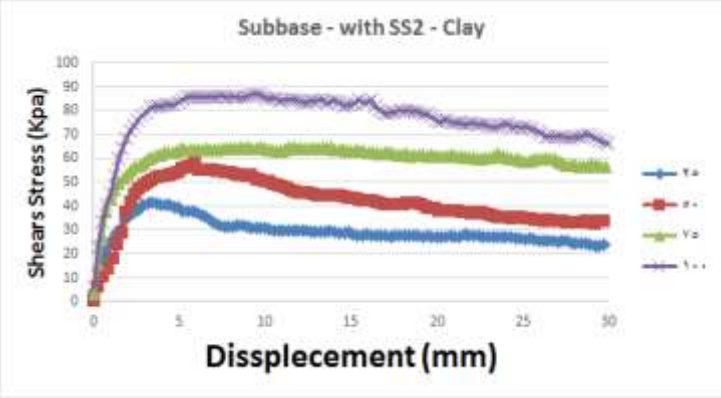


Figure5. shear stress with horizontal displacement for with geogrid for 100% degree of compaction with optimum moisture content

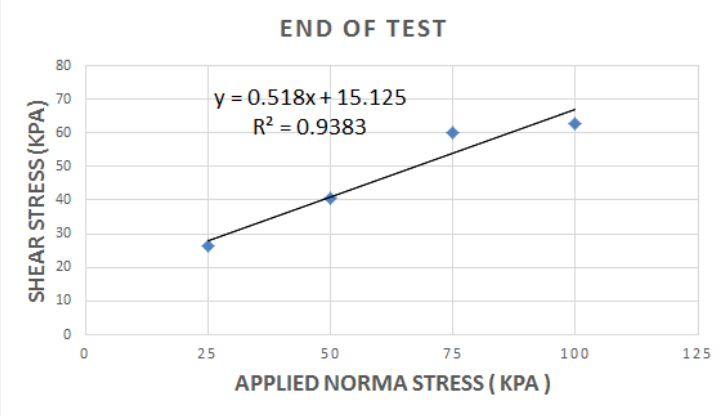


Figure 6. Mohr–Coulomb interface shear strength envelopes at end without reinforcement for 100% degree of compaction with optimum moisture content

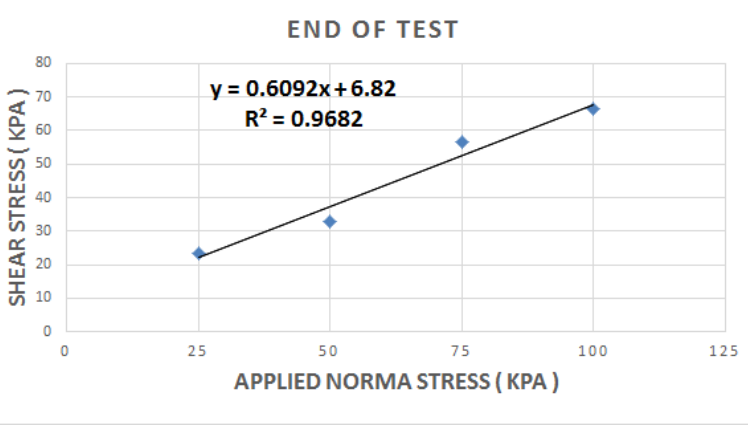


Figure 7. Mohr–Coulomb interface shear strength envelopes at end with geogrid for 100% degree of compaction with optimum moisture content

Table 5. Shear properties of different interfaces without geogrid

	Interface shear strength (kPa) (end of test)				**Adhesion intercept c (kPa) (end of test)**	**Interface friction angle δ(degree) end of test)**
	Normal strength (Kpa)					
No. Of blows (Degree of compaction)	**25**	**50**	**75**	**100**		
60 (100%)	26.25	40.75	60	63	15.125	26.104
55 (98%)	20.25	30	51	62.75	3.875	29.538
50 (93%)	30	40	60	62.25	18.875	23.267
45 (90%)	25	42.25	55.5	66.25	13	28.810
40 (84%)	32.5	38.5	51	62.25	14.875	31.798

Table 6. Shear properties of different interfaces with geogrid

	Interface shear strength (kPa) (end of test)				Adhesion intercept c (kPa) (end of test)	Interface friction angle δ(degree) end of test)
	Normal strength (Kpa)					
No. Of blows (Degree of compaction)	**25**	**50**	**75**	**100**		
60 (100%)	23.57	33	56.5	66.5	6.82	29.786
55 (98%)	34.75	42	47.25	66.25	22.625	22.782
50 (93%)	27	42.25	67.25	84.75	5.75	37.596
45 (90%)	23.5	42	56.25	70	9.5	31.798
40 (84%)	25	44.25	62.50	73.45	8.62	30.25

Interaction Coefficient of Reinforcement

The ratio of the shear strength at of reinforced soil (τ reinforced) at interface to the shear strength of the soil without reinforcement (τ unreinforced) at same normal stress is defined as interaction coefficient (η). The interaction coefficient of the reinforcement is calculated using Equation 1 (Goud and Umashankar, 2018).

$$\eta = \frac{\tau_{reinforced}}{\tau_{unreinforced}} \quad \ldots\ldots\ldots\ldots\ldots\ldots \quad (1)$$

When the value of interaction coefficient is larger than one, it is mean a better using of reinforcement in pavement systems. Table 7 presents the shear interaction coefficients of different degree of compaction at normal stress equal to (25 – 50 - 75 – 100) kPa. At their optimal moisture levels, the effect of dry density on the interface properties of these geogrid-soil combinations was also examined. As expected, interface shear failure envelopes generally enlarged with the increase in molding dry densities (i.e degree of compaction), and it reach maximum value at degree of compaction 97% as shown in Figure 6. It may attributed to that, the reduction in interface shear resistance caused by the increase in density (MDD) led to increase pore water pressure, As a result, it is suggested that soil interface shear characteristics at 95% maximum dry density be employed in soil–geogrid reinforcement design (Abu-Farsakh, et.al (2007)).

Table 7. Shear Interaction coefficients for degree of compaction

	Shear Interaction coefficients (end of test)				Average shear Interaction coefficients	Max. Dry Density (g/cm3)
	Normal strength (Kpa)					
No. Of blows (Degree of compaction)	**25**	**50**	**75**	**100**		
60 (100%)	0.771	0.894	0.959	0.998	0.906	1.880
55 (98%)	1.836	1.354	1.167	1.067	1.356	1.842
50 (93%)	0.862	1.095	1.242	1.337	1.134	1.748
45 (90%)	0.934	1	1.032	1.051	1.004	1.692
40 (84%)	0.877	0.929	0.950	0.824	0.90	1.579

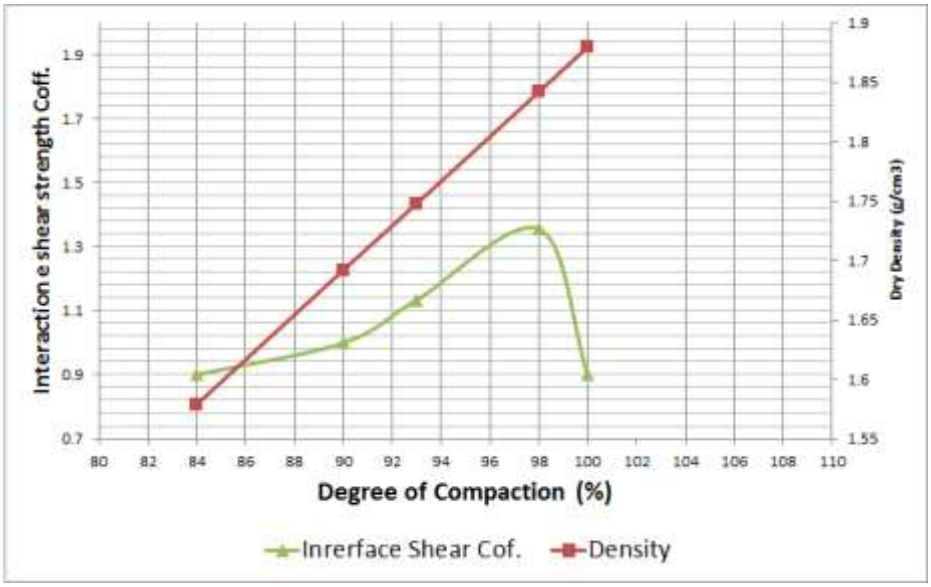


Figure 6. Effect of degree of compaction on the shear Interaction coefficient

Conclusions

Based on extensive testing of selected subbase over clay subgrade soil as well as a numbers of large-scale direct in both cases of using and not using reinforcement. A total of 40 tests with five degree of compaction of subgrade soil (100, 98, 93, 90 and 84 %) were evaluated under four normal stress (25 - 50 - 75 - 100) kPa. the following conclusions are found:

1. For the four normal stresses (25 - 50 - 75 -100) kPa, the interface shear stress curves rose and followed a similar trend.
2. Interface shear failure envelopes normally rise with increasing molding dry densities (i.e., degree of compaction), reaching their maximum value at 97% degree of compaction.

References

1. Abu-Farsakh M, Coronel J, Tao M (2007) Effect of soil moisture content and dry density on cohesive soil-geosynthetic interactions using large direct shear tests. J Mater Civ Eng 19(7):540–549. https://doi.org/10.1061/(ASCE)0899-1561(2007)19:7(540)
2. Arulrajah A, Rahman MA, Piratheepan J, Bo MW, Imteaz MA (2014) Evaluation of interface shear strength properties of geogrid-reinforced construction and demolition materials using a modified large-scale direct shear testing apparatus. J Mater Civil Eng, ASCE, Vol. 26, No. 5. https://doi.org/10.1061/(ASCE)MT.1943-5533.0000897.
3. Arulrajah A, Horpibulsuk S, Maghoolpilehrood F, Samingthong W, Du Y-J, Shen S-L (2015) Evaluation of interface shear strength properties of geogrid reinforced foamed recycled glass using a large-scale direct shear testing apparatus. Adv Mater SciEng.https://doi.org/10.1155/2015/235424.
4. ASTM (2018) Standard Specifications Manual, American Society for Testing and Materials.
5. Banyhussan, Q. S., Mosa, A. M., Hussein, A. N., & Sigar, E. J. (2023). Evaluating the Shear Strength of Subbase-subgrade Interface Using Large Scale Direct Shear Test. International Journal of Innovation in Engineering, 3(1), 35-47.
6. Bergado DT, Youwai S, Teerawattanasuk C, Visudmedanukul P (2003) The interaction mechanism and behaviour of hexagonal wire mesh reinforced embankment with silty sand backfill on soft clay. Comput Geotech 30(6):517–534. https://doi.org/10.1016/S0266-352X(03)00054-5.
7. Choudhary AK, Krishna AM (2014) Influence of different types of soils on soil- geosynthetics interaction behavior. IJIRSET 3(SPI 4):60–68.
8. Dafalla MA (2013) Effects of clay and moisture content on direct shear tests for clay-sand mixtures. Adv Mater Sci Eng. https://doi.org/10.1155/2013/562726.
9. Giroud, J.P. and Han, J. 2004. Design method for geogridreinforced unpaved roads–I. Journal of Geotechnical and Geoenvironmental Engineering, Volume 130, Issue 8, pp. 775-786.
10. Goud, G. N., & Umashankar, B. (2018). Interface shear strength properties of gravel bases and subgrades with various reinforcements. *International Journal of Geosynthetics and Ground Engineering*, *4*, 1-14.
11. Kamalzare M, Ziaie-Moayed R (2011) Influence of geosynthetic reinforcement on shear strength characteristics of two-layer subgrade. Acta Geotech Slov 8:39–49 Jewell, R. A. (1996). Soil reinforcement with geotextiles. London: Thomas Telford.
12. Kandolkar SS, Mandal JN (2013) Direct shear tests on stone dust. In: Proceedings of Indian Geotechnical Conference, Roorkee, pp 1–6.
13. Liu, C. N., Zornberg, J. G., Chen, T. C., Ho, Y. H., & Lin, B. H. (2009). Behavior of geogrid-sand interface in direct shear mode. Journal of Geotechnical and Geoenvironmental Engineering, 135(12), 1863–1871.

14. Lopes, M. L. (2002). Soil-geosynthetic interaction. In S. K. Shukla (Ed.), Geosynthetics and their applications (pp. 57–61). London: Thomas Telford.
15. Nareeman, BJ, Fattah, MY, (2012), Effect of Soil Reinforcement on Shear Strength and Settlement of Cohesive-Frictional Soil, International Journal of GEOMATE, Vol. 3, No. 1 (Sl. No. 5), pp. 308-313 Geotec., Const. Mat. & Env., ISSN:2186-2982(P), 2186-2990(O), Japan.
16. Nicks JE, Gebrenegus T, Adams M (2015) Strength characterization of open-graded aggregates for structural backfills (No.FHWA-HRT-15-034).
17. Sakleshpur, V. A., Prezzi, M., Salgado, R., Siddiki, N. Z., & Choi, Y. S. (2019). Large-scale direct shear testing of geogrid-reinforced aggregate base over weak subgrade. International Journal of Pavement Engineering, 20(6), 649-658.
18. Sayeed MMA, Ramaiah BJ, Rawal A (2013) Interface shear characteristics of jute/polypropylene hybrid nonwoven geotextiles and sand using large size direct shear test. Geotext Geomembr 42:63–68. https://doi.org/10.1016/j.geotexmem.2013.12.001.
19. SCRB /R6, 2003, Standards and Specifications for Roads and Bridges (2003) (Iraqi Standard Code), Ministry of Housing and Reonstruction.
20. Umashankar B, Hariprasad C, Sasanka Mouli S (2015) Interface Properties of Metal-Grid and Geogrid Reinforcements with Sand. In: International foundations congress and equipment expo 2015, San Antonio, pp 1–9.
21. Voottipruex P, Bergado DT, Ounjaichon P (2000) Pullout and direct shear resistance of hexagonal wire mesh reinforcement in weathered Bangkok clay. Geotech Eng 31(1):43–62
22. Xu, Y., Williams, D. J., & Serati, M. (2020). Investigation of shear strength of interface between roadbase and geosynthetics using large-scale single-stage and multi-stage direct shear test. Road Materials and Pavement Design, 21(6), 1588-1611.

Some Biological Aspects of Sea Bream (Acanthopagrus Latus) In Shatt Al-Arab River, Iraq

Layla A. Aufy [1], Shaymaa A.J. Al-Jumaiee [2]

© 2023 The Author(s). This open access article is distributed under a Creative CommonsAttribution (CC-BY) 4.0 license.

Abstract: Acanthopagrus latus caught from Shatt Al-Arab river, then its growth pattern, age, length-weight relationship, condition factor, as well as reproduction were investigated. Samples were monthly collected from September 2020 to August 2021 by gill nets. Total length and wet weight were recorded, and fish were sexed by extracted gonads out of the body cavity and examined and weighted, and using scales to determine the age of the species. The total lengths of species ranging from 10.7 to 23.7 cm. The length-weight relationships of males and females together were estimated as W=0.016 L3.007 and exhibited isometric growth (b=3.007). Mean relative condition factor (Kn) was 1.09 and 1.34 for males and females respectively. The maximum age was four years according to the reading of scales. The growth equation (von Bertalanffy) represented as: [Lt = 50.4(1-e-0.25(t+0.277)] using back calculated length. The growth performance index (Φ) was 2.56. The ratio of sex was 1:1.13 male to female. The peak of Gonadosomatic index (GSI) for both sexes was in March. The spawning period from March to May. The results generally showed that this species was slow growing relatively and had along live, which should be taken into account for sustainable management and exploitation to prevent excessive utilization in the studying area.

Key Words: Acanthopagrus latus, growth, reproduction, age, shatt al-arab river.

Author details

[1 – 2] Department of marine vertebrates, Marine Science Centre, University of Basrah, Basrah, Iraq

Citation information

Cite this article as:

Aufy, L.A., Al-Jumaiee, S.A.J., (July 2023), *Some Biological Aspects of Sea Bream (Acanthopagrus Latus) in Shatt Al-Arab River, Iraq*, Proceedings of the Minar Congress, Turkey, (9) pp 14-25, DOI: http://dx.doi.org/10.47832/MinarCong9-2

http://dx.doi.org/10.47832/MinarCong9-2

[1] layla.awfi@uobasrah.edu.iq

[2] shaymaa.jaber@uobasrah.edu.iq

Introduction

Sea breams, species of the Sparidae family, found in both temperate coastal water and tropical waters (Randall et al., 1997). The sea breams (Sparidae), which consist of roughly 36 genera and 130 species, are found within shallow temperate as well as tropical seas of the Atlantic, Indian, and Pacific oceans (Eschmeyer & Fong 2011). A broadly widespread fish with significant economic and ecological importance in the Indo-West Pacific is the yellowfin seabream (Acanthopagrus latus) (Xia et al., 2008).

This fish, a protandrous hermaphrodite like many other sparidae, typically spans a large biogeographic spectrum but is particularly common in shallow warm coastal waters, frequently reaching estuaries and mouths of river (Li and Ou, 2000; Xia et al., 2008). Fish growth patterns in both applied and fundamental management, are useful for estimating fish weight from its length measures (Hossain et al., 2009), calculating the biomass and productivity of the population of fishes (Hossain et al., 2016), and providing data about the stock's health (Hossen et al., 2020). Among the previous studies on this species in the Shatt al-Arab and Khor al-Zubayr is the study of Al-Hassan (1990) studied the genetic and phenotypic changes among the species in the Shatt Al-Arab. Al-Dubakel & Abdullah (2006) noted that there was a positive correlation between otolith's weight with both the weight and the total body length of three studied species, including A.latus in Khor Al-Zubayr, and Abdulsamad (2010) studied the age and growth of this species in the Shatt al-Arab river . The aim of the current study is to ascertain some biological parameter such as the age, growth pattern, condition factor, length-weight relationship, and reproduction of A.latus within the Shatt Al-Arab River from September 2020 to August 2021.

Materials and Methods

Gill nets with length of 200 to500 m and mesh size of 25x25 mm were used to collect 273 individual every month from September 2020 to August 2021 from Shatt Al-Arab river (Abu Al-Khasib location) south of the Abu Al-Khasib area (30° 46' 37" N, 47° 77' 11" E) (Figure 1).

Crushed ice was used to reserve samples and transport them to the laboratory, where they underwent immediate analysis. The length and weight of each fish were measured to the nearest 0.1 cm and 0.01 gm, respectively. Five to ten scales between the lateral line and the base of the dorsal fin from each fish were collected and placed in labeled envelopes. In between two glass slides, scales were placed after being washed with warm water. Using a micro-projector (20X magnification) to estimate age, determine the radius of the scale and the expanse between each annulus.

The length-weight relationship's regression equation is estimated using exponential regression :W= a Lb, where; W = total weight (gm), L = total length (cm), a = regression's intercept, and b = regression coefficient (slope) (Froese 2006). The Student's t-test was used to determine whether allometric coefficient "b" deviated regarding the predicted of isometric

growth value (b = 3). The formula Kn = W-/W (Le Cren, 1951) has been used to obtain the relative condition factor (Kn) in terms of sex as well as months; where W- = observed weight, and W= estimated weight.

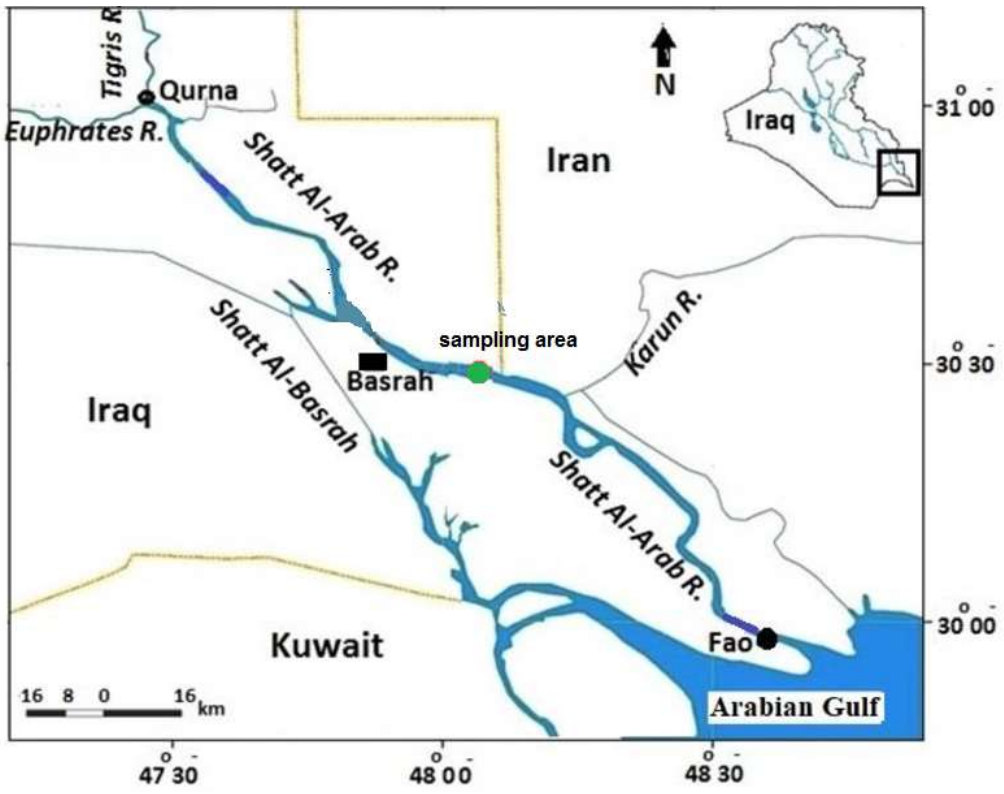


Figure 1. Map showing the Location of studying area.

The scale was read using a Projectina microscope [Form: 4014 BK-2] at 10x magnification. The radius of every annulus in addition to the scale's edge was measured from the enlarged image. The formula □L=a + bS□ (Bagenal and Tesch, 1978) as (a) represents intercept [correction factor] while (b) represents regression line, was used to determine the relationship between the length of fish at the time of capture (L) and scale radius (S). Following equation is employed to calculate total length at age: □Ln= a + Sn /S (L-a)□; as (Ln) represents length of fish at the age (n) and (a) is the correction factor, while annulus' radius was represented by (Sn); also (S) = radius of the scale, and (L) represented the length of fish at a moment it was captured.

The equation of von Bertalanffy was used to examine hypothetical growth in length: Lt = L∞ (1 – e -K (t - t0)), where (Lt) = the length of fish at age (t) ; (L∞) = the asymptotic length of fish , (K) = the coefficient growth, and (t0) represents hypothetical age at which the fish had zero length (Ricker, 1975).

The following formula was using to estimate the index of growth performance (Φ) = log10 K + 2 log10L∞ (Pauly and Munro, 1984).

The gonads were then taken out of the body cavity, weighed, and inspected macroscopically to determine their sex. Only fish with clearly distinguishable male and female gonads had their monthly male to female specimen ratios calculated. The chi-square (X2) method was used to determine the sex ratio (Sokal and Rohlf, 1995). Using monthly changes of the gonado-somatic index (GSI) to determine the spawning period of the species. GSI= Gonad weight / Body weight) * 100 (King,2013).

Results

Length-weight relationship

The relationship between total length and body weight regarding A.latus is calculated on the entire sample, with total lengths ranging from 10.7 to 23.7 cm and weights ranging from 24.21 to 214.9gm, as there was no statistically significant differences between sexes in regressions (t= 0.335, P>0.05). Figure(2) demonstrates how body weight increased exponentially with overall length: W=0.016 L3.007 (r2= 0.955). The t-test revealed that the relationship's regression coefficient (b) was very close to 3, demonstrating isometric growth.

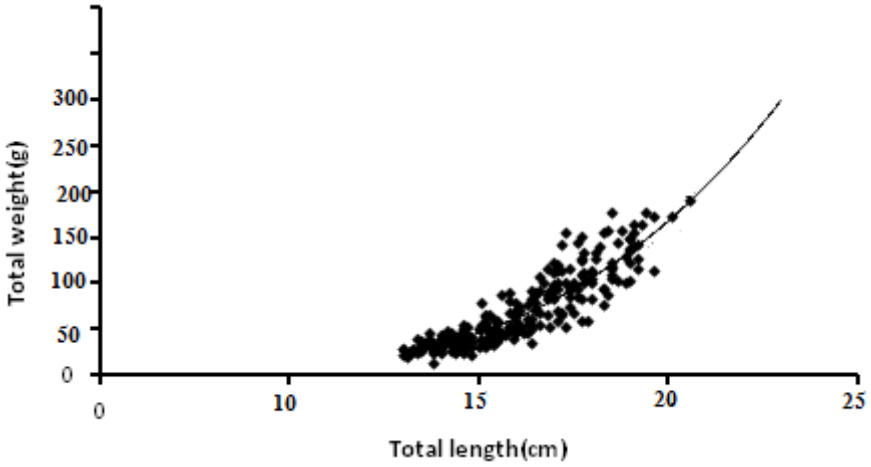


Figure 2. The length-weight relationships of A.Latus

Relative condition factor

Similar tendencies were seen in both sexes in the monthly change of the relative condition factor (Kn) between A. latus (Figure 3). Kn for males ranged from 0.91 in August to 1.09 in April, whereas it was 0.89 in August to 1.34 in April for females.

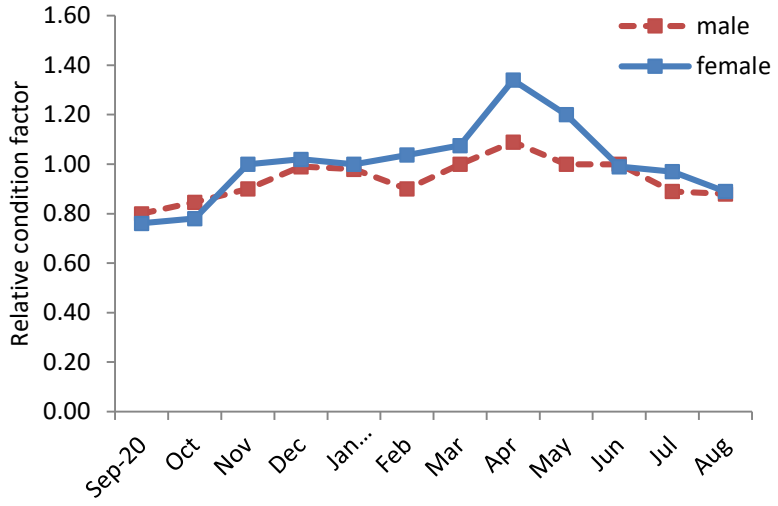


Figure 3. Relative condition factor (Kn) of A.latus

Age and Growth

Scales provided an estimated age range of 1 to 4 years, with the majority of samples being one year old. The equation for the relationship between the fish's total length (L) and the scale radius (S) was L = 1.941 + 0.87S. Increased coefficient correlation (r2 =0.902) showed the relationship's linear agreement. Based on a back lengths calculation from various age fish, the average length of A.latus for every annulus is displayed in (Table I).

The first year of life showed occurrence of rapid development in length, which was subsequent to an interval of slower growth rate among left life years. The annual increment percentage was fluctuated from 50.6% in the first life's year to 10.9% in the fourth life's year (Table I). Age/length data for A. latus were adjusted using the von Bertalanffy growth model, which is represented like the following: {Lt = 50.4 (1 - e-0.25 (t + 0.277))}. The growth performance index of A. latus is estimated to be 2.56.

Table 1. A.latus's average observing and back-calculated total lengths.

Age	Number of fish	Length at age (cm)			
		1	2	3	4
1	32	12.7			
2	45	13.1	16.3		
3	11	14.7	16	19.3	
4	5	14.8	17.9	19.5	22.3
Mean length (cm)		12.8	16.9	22.1	25.3
Annual increment (cm)		13.2	4.5	3.2	2.7
% Growth increment		15.6	7.2	5.3	2.9

Reproduction

GSI for both males and females of A.latus reached its peak in March, with the principal spawning season lasting until June. The Gonado-somatic index start reaches its maximum value in March, when it reached 8.9 for males and 9.3 for females, indicating that the maturity of gonads starting from October, and their weight increases until it reaches its maximum during the March, then it decreases. The values of the GSI decreased with the period of spawning from April until June, the lowest value of GSI recorded in August was 0.32 and 0.45 for males and females respectively (Figure 4).

The gonads of A. latus did not have any macroscopically identifiable ovaries during the summer (July to September) or include rather large volumes of both immature ovarian. Due to the process of sex change, there were a greater number of fish ovotestes in August that had great amounts of both immature testis and ovary. The number of females significantly raised their contributions during the winter. The general sex ratio (M : F) was 1:1.13 and did not deviate substantially from 1:1.

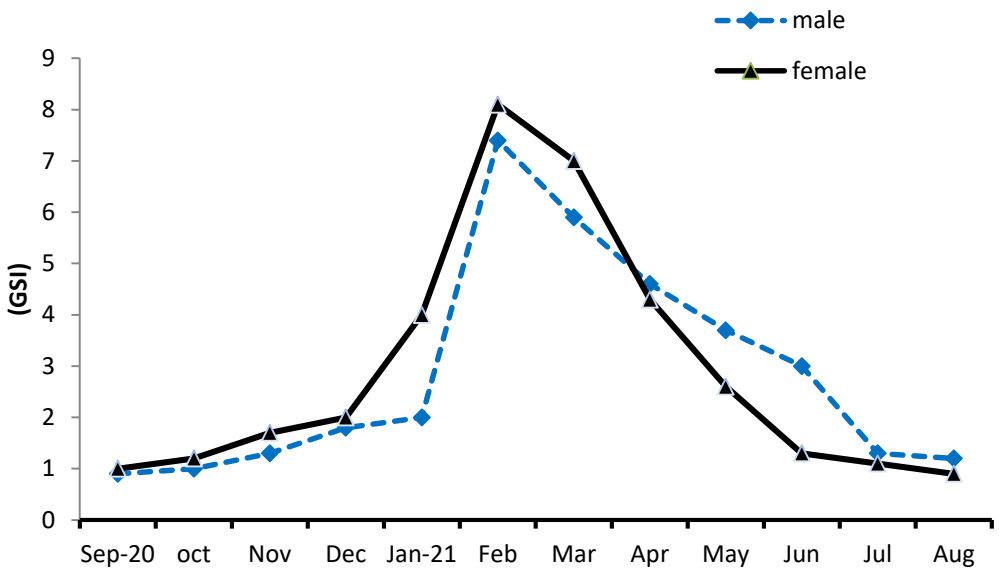


Figure 4. GSI for males and females of A.latus

Discussion

Studying the biology of sea bream A. latus is crucial for figuring out the nature of fish populations and if these communities are made up of one or many groups (Ghasemi and Shadi, 2018). Interestingly, the majority of local studies dealt with the presence and growth of A. latus in Iraqi waters, whether marine, Shatt al-Arab, Shatt al-Basra as well as the southern marshes due to their great ability to be present in various sizes and stages of different maturity in more than one different Iraqi environment, local studies focused on the presence and growth of A. latus in Iraqi waters (Mohamed,et al., 2010). The lengths of A. latus individuals in the current study ranging from 10.7 to 23.7 cm and were compared with various

authors in other geographic localities such as 11.6 -29.7 cm in the River of Shatt al-Arab, (Abdulsamad ,2010) and 10.2 – 38.0 in Al-Razzaza Lake (Mansour, 2004) These differences could be due to environmental conditions, nutrition, density of population, fishing stress, and may be use of various fishing gear (Mohamed and Abood, 2020).

That study examined the relationships of length and weight of species obtained from the Shatt Al-Arab river. Determining length-weight relationship has an important role in fisheries evaluations and can reveal a lot of information about the demographic composition of the stock, (Dauod et al., 2010; Taheri Mirghaed et al., 2020). The results of the present study showed that body weight rose exponentially with overall length. The relationship's regression coefficient (b) was 3.007, showed isometric growth for A. latus and the matching significant correlation value also indicated a significantly linear length-weight relationship. In agreement with these results, in Al-Razzaza Lake, (Mansour, 2004) (b) was 2.98 and (Abdulsamad, 2010) (b) was 3.045 in Shatt al-Arab River, revealed isometric growth and there was a strong length-weight relationship. In contrast with this study, Vahabnezhad,et al.,2017 indicate allometric growth (b) was 2.57 for the same species in the Persian Gulf. The reason for these differences can be attributed to seasonal fluctuations, changes in environmental indicators such as temperature and salinity, physiological condition of the fish at the time of sample collection, gender, nutritional conditions and reproductive stages of the fish (Sourinejad et al., 2014, Cuadrado,2019).

The relative condition factor showed similar pattern among males and females. The range of relative condition factor regarding males range from 0.91 in August –1.09 in April, while for females varied range was 0.89 –1.34 within August - April. In Awan et al., (2017) study, in Narreri lagoon in Pakistan, the condition factor of A. latus was found to be 0.46 indicating poor condition. On the other hand, Nikkhah Khajeataei and Kamrani, (2014) found that condition factor was 2.132 in the Persian Gulf waters. In addition, condition factor has declined from January toward March and then raised from April toward the end of autumn.

In the study of Abdulsamad (2010), it was noticed that there is an inflexion in the relative condition factor (Kn) at the length range of 20.1-22.0 and 22.1-24.0 cm in males and females, respectively, and such an inflexion is an appropriate indicator of the length at which sexual maturity begins. Also, the high value of (Kn) indicates that the rate of weight gain is greater than the rate of increase in length (Al- Hassan, 1990), and one of the reasons for this may be due to the effect of the weight of the gonads on body weight, especially if this coincides with the maturation of the gonads during the prespawning stage (Abdulsamad, 2010).

In general, many factors affecting the changes in the condition index such as conditions and environmental factors and its fluctuations, the physiological conditions of the fish during sample collection, age and sex, fullness of stomach, the reproduction stage of fishes and the nutritional conditions of the fish (King, 2013).

The basis of longitudinal structure is very important for determining fisheries management solutions in the field of stock assessment (DeMartini et al., 2000). For this

reason, the age or length of maturity of the population is a factor that is very important in the evaluation of the population status during fishing. The present study revealed a range of ages from 1 to 4 years. It was shown that the quick growth incidence among length of A. latus was discovered during the first year of life, and then there was a time when the growth rate was slowed throughout the rest of life. In agreement with the present results, Abdulsamad (2010) found the same age results in Shatt al-Arab River. On the other hand Mansour,2004 and Dauod et al.,2010 reported fish individuals up to 8 years old in Al-Razzaza Lake for the studying species. The growth parameter in compare with other study that recorded $L\infty$=37cm in Shatt al-Arab River (Abdulsamad, 2010), $L\infty$ =50.4 cm in Bushehr province south of Persian Gulf (Vahabnezhad,et al.,2017), $L\infty$=55cm at the Abu Dhabi waters (Grandcourt et al., 2004), and $L\infty$=57.8cm in the Gulf of Aden, southern Persian Gulf (Edwards et al., 1985). The growth performance index (Φ) of A.latus in our study (2.56) was in similar with Vahabnezhad,et al.,(2017) study that recorded (Φ)= 2.76 in Bushehr province south of Persian Gulf. Like other Sparidea species, A. latus, appears to be a relatively long-lived fish. The variation in environmental factors, such as water temperature, diversity, the availability of food, and overexploitation of natural resources, may be responsible for the differences in growth characteristics among populations of the same species in different geographic locations (Wootton,2011).

The total sex ratio (males: females) of A. latus population was determined to be 1:1.13 in the current study, which is in agreement with . The male-to-female sex ratio in Al-Razzaza lake was 1:1.18 (Mansour,2004), in the Bushehr province south of Persian Gulf it was 1:1.03 (Vahabnezhad,et al.,2017) and in the Narreri Lagoon Badin, Pakistan it was 1:1.44 (Panhwar,2017). Variation of sex ratio of fish population affected by several factor such as life stage, the spawning season and ground, migration and fishing area. (Nikolsky,1963, Bartulovic, et al.,2004).

The peak in the (GSI) for both males and females A.latus was shown in March, with the main spawning period enduring to June. These results were in agreement with Mansour(2004)who indicated the spawning period of these species took place from March to May in Al-Razzaza lake. Vahabnezhad et al. (2017) stated that the highest Gonado-somatic index was shown in February, and it's annual cycle also showed that A.latus spawning season (in Persian Gulf) lasted from February toward May. That also was in line with Hoseini and Savari (2004) in Persian Gulf . Conversely, Abou-Seedo et al., (2003) reviewed evidence suggesting that despite mature fish occurred within December, and the numbers were very little to be taken into account. This was done by the examination of Gonado-somatic index of this species. In Kuwaiti waters, the majority of the individuals start to spawn in January, (Abou-Seedo et al., 2003), on the other hand, noted the end of spawning within April rather than March. However, depending on their locales, A.latus' spawning season within the northern hemisphere differed significantly. Hence, it was found that A.latus possessed an extended spawning season in the Shatt Al-Arab River, according to information about how the stages of maturation change with season and the existence of mature fish.

Conclusion:

Based on current findings, it is concluded that for A.latus, there was a significantly linear length-weight relationship. The incidence of quick growth regarding length of A. latus was present in life's first year. The peak of (GSI) in both males and females of A.latus was revealed in March.

Recommendations:

1. Control fishing and prevent catching of immature and adult during the spawning period to aoid harmful to fish stock.
2. Study the possibility of cultivation this species.
3. Studying on other biological feature on this species such as feeding and ecological feature.

References

1. Abdulsamad S.(2010). Some Observations about Age and Growth of Shanag Acanthopagrus latusm (Houttuyn) in Shatt Al-Arab River. JOURNAL OF THI-QAR SCIENCE, 2(2).
2. Abou-Seedo, F. S.,Dadzie, S.,and Al-Kanaan, K. A.(2003). Sexuality, sex change and maturation patterns in the yellowfin seabream, Acanthopagrus latus (Teleostei: Sparidae)(Houttuyn, 1782). Journal of Applied Ichthyology, 19(2), 65-73.
3. Al-Dubakel ,A.Y; Abdullah ,J.N.(2006). Relationship of body size with somebody structures of three young marine fish species collected from Khor Al-Zubair, Iraq. Anales de Biología 28: 95-99.
4. Al-Hassan, L.A.J. (1990). Genetic and morphological variation in Acanthopagrus latus (Sparidae) in Iraq. Asian Fish. Sci. 2:269-273.
5. Awan, K. P., Qamar, N., Farooq, N., and Panhwar, S. K. (2017). Sex ratio, length weight relationships and condition of eight fish species collected from Narreri Lagoon, Badin, Sindh. Pakistan. J. Aquac. Mar. Biol, 5(4), 1-4.
6. Bagenal TB, Tesch FW. (1978) Age and Growth. In: Bagenal TB, editor. Methods for assessment of fish production in freshwater. Blackwell, Oxford, England.
7. Bartulovic V, Glamuzina B, Conides A, Dulcic J, Lucic D, Njire J, Kozul V.(2004). Age, growth, mortality and sex ratio of sand smelt, Atherina boyeri, Risso, 1810 (Pisces: Atherinidae) in the estuary of the Mala Neretva River (Middle-Eastern Adriatic, Croatia). J. Appl. Ichthyol.20:427-430.
8. Cuadrado JT, Lim DS, Alcontin RMS,Calang JL, Jumawan JC. (2019). Species Composition and length-weight relationship of twelve fish species in the two lakes ofEsperanza, Agusan del Sur, Philippines. Fish Taxa.4(1):1-8.
9. Dauod, H. A. M., Al-Aamery, R. A., Ali, A. I., Chabuk, F. M., & Abbas, K. M. (2010). Observations on the Age and Growth of Shank (Acanthopagrus latus (Houttuyn, 1782)) from Al-Razzazah Lake. Ibn AL-Haitham Journal For Pure and Applied Science, 23(1), 50-61.
10. DeMartini, E. E., Uchiyama, J. H., and Williams, H. A. (2000). Sexual maturity, sex ratio, and sizecomposition of swordfish, Xiphias gladius, caught by the Hawaii-based pelagic longlinefishery. Fishery Bulletin, 98(3), 489-489.
11. Edwards, R.R.C., Bakhader, A. and Shaher, S., (1985). Growth, mortality, age composition and fishery yields of fish from the Gulf of Aden. J.Fish Biol., 27, 13-21.
12. Eschmeyer, W.N. and Fong, J.D. (2011). Pisces. In: Zhang, Z.-Q. (Ed.). Animal biodiversity: An outline of higher level classification and survey of taxonomic richness. Zootaxa 3148: 26-38.
13. Froese, R. (2006). Cube law, condition factor and weight length relationship: history meta-analysis and recommendations. J. Appl. Ichthyol., 22: 241-253.

14. Ghasemi, A., and Shadi, A. (2018). Population Structure of Acanthopagrus latus from the Northern Persian Gulf and Gulf of Oman Based on Microsatellite Markers. Turkish Journal of Fisheries and Aquatic Sciences, 18(8), 983-990.
15. Grandcourt, E.M., Al Abdessalaam, T.Z., Francis, F.and Al Shamsi, A.T.,(2004). Biology and stock assessment of the Sparids, Acanthopagrus bifasciatus and Argyrops spinifer (Forsskål, 1775), in the Southern Arabian Gulf. Fisheries Research, 69, 7-20.
16. Hoseini, H. and Savari, A.,(2004). Some aspects of reproductive biology of A. latus in Boushehr water (Persian Gulf). Journal of Iranian Fisheries Science, 3(1), 45-52 .
17. Hossain, M.Y. Naser, S.M.A.; Bahkali, A.H.; Yahya, K.; Hossen, M.A.; Elgorban, A. M.; Islam, M.M. and Rahman, M.M.(2016). Life History Traits of the Flying Barb Esomus danricus (Hamilton, 1822) (Cyprinidae) in the Ganges River, Northwestern Bangladesh. Pak. J.Zool., 48(2): 399-408.
18. Hossain, M.Y.; Ohtomi, J.; Ahmed, Z.F.; Ibrahim, A.H.M. and Jasmine, S.(2009). Length-weight and morphometric relationships of the tank goby Glossogobius giuris (Hamilton, 1822) (Perciformes: Gobiidae) in the Ganges of the northwestern Bangladesh. Asian Fish. Sci., 22(3): 961-969.
19. Hossen, M.A.; Hossain, M.Y.; Khatun, D.; Pramanik, M.N.U.; Parvin, M.F.; Jasmin, J.; Sharmin, S.; Rahman, O.; Mawa, Z.; Rahman, M.A. and Hasan, M.R. (2020). Morphometric and meristic traits of three ambassid fish species (Chanda nama, Parambassis lala and Parambassis ranga). Indian J. Mar. Sci., 49 (03): 398-405
20. King, M. (2013). Fisheries biology, assessment and management. John Wiley & Sons.
21. Le Cren ED.(1951). The length-weight relationship and seasonal cycle in gonad weight and condition in the perch (Perca fluviatilis). J.Anim. Ecol. 20:201-219.
22. Li, J. Ou, Y.J. (2000). Studies on the reproduc-tive biology of the pond-cultured Sparus latus Houttuyn, in the coast of Shenzhen bay. Journal of Zhejiang Ocean University (Natural Science), 19: 139-143.
23. Mansour, R.H. (2004). Some biological characteristics of silver sheim (Shank) Acanthopagrus latus (Houttuyn, 1782) in Razzaza lake. M. Sc. Thesis, Technical College of Al-M ussayib. (In Arabic).
24. Mohamed ARM, Abood AN.(2020). Population dynamics of three mullets species (Mugilidae) from the Shatt Al- Arab River, Iraq. Journal of Agriculture and Veterinary Science.13(9):22-31.
25. Mohamed, A. R. M., Jasim, B. M., and Asmail, A. K. (2010). Comparative Morphometric And Merstic Study On Yellow Fin Seabream, Acanthopagrus Latus In Iraqi Waters. Basrah Journal of Agricultural Sciences, 23.
26. Nikkhah Khajeataei, Sand Kamrani, E. (2014). Growth pattern, condition factor and length at first maturity of Yellowfin Seabream Acanthopagrus latus in the Persian Gulf. Utilization and Cultivation of Aquatics, 3(2), 1-14.
27. Nikolsky,G.V.(1969). Theory of population denuding as the biological back ground for rational exploitation and management of the fishery resources. Oliver & Boyd :323pp.

28. Panhwar,S.K. Qamar,N. Farooq,N.and AwanK.P.(2017). Sex ratio, length weight relationships and condition of eight fish species collected from Narreri Lagoon, Badin, Sindh, Pakistan. Journal of Aquaculture & Marine Biology, 5 (4),12-14.
29. Pauly, D. and Munro, J.,(1984). Once more on the comparison of growth in fish and invertebrates, Fishbyte. 2,21.
30. Randall, J.E., Allen, G.R. and Steene, R.C.,(1997). Fishes of the Great Barrier Reef and Coral Sea. University of Hawaii Press, Honolulu, Hawaii, 507P.
31. Ricker,W.E.(1975). Computation and interpretation of biological statistics of fish populations.Bull.Fish.Res.Board Can.,(191) :382pp.
32. Sokal, R.R. and Rohlf, F.J.,(1995). Biometry The Principles and Practice of Statistics in Biological Research, third ed., W.H. Freeman and Co., New York, 887P.
33. Sourinejad, I., Ataei N. K., Kamrani, and Shojaei G. (2014). Growth pattern, condition index and length of the first sexual maturity of the yellowfin Acanthopagrus latus in the Persian Gulf. Journal of Aquaculture, 3(2), 1-14
34. Taheri Mirghaed, A., Ghodrati Shojaei, M., Weigt, M., Ebrahimzadeh, S. M., Jahangard, A., Abbasi, M., and Abdolahian, M. (2020). Length–weight and length–length relationships of six fish species from the Persian Gulf. Aquaculture Sciences, 8(1), 102-111.
35. Vahabnezhad A.1; Taghavimotlagh S.A.1; Ghodrati Shojaei M.. (2017). Growth pattern and reproductive biology of Acanthopagrus latus from the Persian Gulf. Journal of Survey in Fisheries Sciences. 4(1) 18-28.
36. Wootton RJ.(2011). Growth: environmental effects. In: Farrell AP, editor. Encyclopedia of fish physiology: from genome to environment. Elsevier Science Publishing Co. Inc, United States.
37. Xia, J.H., Huang, J.H., Gong, J.B., Jiang, S.G.(2008). Significant population genetic structure of yellowfin Seabream Acanthopagrus latus in China. Journal of Fish Biology, 73: 1979-1992.

Effect of Rheumatoid Arthritis on Alkaline Phosphatase Activity and Some Biochemical Variables

Huda Y. Al-Attar [1], Eman Sameer Al-Soffi [2]

© 2023 The Author(s). This open access article is distributed under a Creative CommonsAttribution (CC-BY) 4.0 license.

Abstract: The study included measuring the concentrations of each Alkaline phosphatase enzyme, Calcium, Vitamin D in (45) blood samples (30) of patients with rheumatoid arthritis (15 males, 15 females), ages (55-83) years from arrivals to some laboratories in the city of Mosul/ Iraq. The results indicated a significant increasing the activity of Alkaline phosphatase a significant decrease in the concentration of calcium and vitamin D in rheumatoid arthritis compared to control groups, and the results also showed a significant increase in the activity of Alkaline phosphatase in females compared to males. There were no significant differences in the concentration of calcium and vitamin D between males and females.

Key Words: Rheumatoid arthritis, Alkaline phosphatase, biochemical variables.

Author details

[1 – 2] Department of Biology, College of Science, University of Mosul, Mosul, Iraq

Citation information

Cite this article as:

Al-Attar, H.Y., Al-Soffi, E.S., (July 2023), *Effect of Rheumatoid Arthritis on Alkaline Phosphatase Activity and Some Biochemical Variables*, Proceedings of the Minar Congress, Turkey, (9) pp 26-37, DOI: http://dx.doi.org/10.47832/MinarCong9-3

http://dx.doi.org/10.47832/MinarCong9-3

[1] hudaYounis1991@uomosul.edu.iq

[2] imasbio91@uomosul.edu.iq

Introduction

Rheumatoid Arthritis it is one of the chronic inflammatory autoimmune diseases, and it is considered one of the most common diseases in the world. (Dey *et al.*,2021). It often affects people during the most productive times, and the ability to carry out normal occupational activities may decrease significantly over time (Sajad and Mohammad, 2020).

The World Health (WHO) Organization confirmed that half of patients with rheumatoid arthritis in developed countries are unable to work full-time within (10) years of the onset of the disease (Gianinini et al., 2020). It is a misconception about arthritic conditions that it only affect The elderly or that they are the result of aging, but it includes all ages, including children and adolescents, and about (1-3)% of women develop rheumatoid arthritis in their lives, and the disease often begins between the fourth and sixth decades of life (Mian et al., 2019).

There are about 1% of the world's population infected with rheumatoid arthritis, which is a chronic disease of unknown cause that mainly affects the synovial membarane, which is a thin membrane that surrounds the joint area, and produces synovial fluid used for joint movement, which leads to swelling, stiffness and pain in the joints. Rheumatoid arthritis is the most common type of autoimmune arthritis (Dey et al., 2021). It causes pain, stiffness, swelling, and limited movement and function in many joints, and may affect organs such as the eyes and lungs. Stiffness often appears worse in the morning, and may last from one to two hours or throughout the day. There are several factors that increase the risk of injury, including weight gain, joint injuries. and infections, genetic factors (Duan et al., 2018).

Research indicates that people with cardiovascular disease, high blood pressure, cholesterol, and malignancies are at risk of developing rheumatoid arthritis because they use drugs that target the immune system, cause inflammation, and damage joints and tissues (Cüzdan et al., 2020).

The main clinical symptoms appear in the form of chronic inflammation in the joints, which leads to gradual destruction of the joints, deformities and disability if it is not controlled, and it may be accompanied by systemic diseases such as vasculitis. and chronic inflammation, and elevated blood levels of C-reactive Protein (CRP), Rheumatoid Factor, peptide antibodies, and anti-cerulin protein (Lin et al., 2020).

There are several tests that are considered as indicators for the detection of cases of arthritis in rheumatoid arthritis, including alkaline phosphatase, calcium, vitamin D. Alkaline phosphatase belongs to the class of hydrolases, as it facilitates the transport of metabolites, especially waxy substances across cell membranes, and includes a group of enzymes attached to the outer part of the cell membrane, which catalyze the hydrolysis of extracellular organophosphate ester (Park *et al.*, 2020).

This enzyme is mainly found in the liver and bones, and in small amounts in the intestines, placenta, kidneys, white blood cells, ileum and mucous membrane (Gonzalez et al., 2020). Among the main sources of basal phosphatase are the liver and bones, as it is found at 80% and its levels found in the liver and bone, and its levels in the blood vary according to age and sex. It is high during childhood and puberty due to bone growth and development, and it decreases in the age groups (15-50) years. The enzymatic activity of alkaline phosphatase increases in a number of diseases such as bone diseases such as Paget's disease, rickets, bone cancer, liver diseases, hepatic bile obstruction, tumors, pregnancy, rheumatoid arthritis, and decreases in kidney diseases, vitamin C deficiency, hypothyroidism (Suzuki et al., 2019).

Calcium is found mainly in the bones and teeth, but in the blood it is in three forms, either in the form of a free ion Ca++ at (50%) of the total percentage, or bound with protein (albumin), which constitutes (45%), or bound with other organic compounds Citrate by (5%), and it is physiologically effective (AL-Bedri et al., 2019). Calcium is an essential element in the process of bone hardening, due to its contribution to its formation and composition. It is associated with the phosphorus ion, as phosphorus participates in maintaining the balance in the blood, any imbalance in one of which leads to an imbalance in the amount of the other ion.

Calcium intake is especially important for rheumatoid arthritis patients who are prone to osteoporosis. It works with vitamin D to treat many rheumatoid diseases, and directly enhances osteoblasts and bone cells (Kravchenko et al., 2022).

Among the vitamins that affect many biological functions, and are necessary in maintaining the mineral balance in the body, is vitamin D, as it is considered one of the fat-soluble vitamins. Diseases such as cancer, autoimmunity, diabetes and its complications (Harrison et al., 2018).

As patients with rheumatoid arthritis suffer from vitamin D deficiency, as well as its association with the severity of the disease, and an increased risk of developing rheumatoid arthritis. (Aleksadrova and Budko, 2016), vitamin D is essential for the absorption of calcium and phosphorus, as well as helps stimulate the enzyme alkaline phosphatase, thus increasing the release of phosphate from its intracellular compounds, and sharing it with calcium for bone formation (Liang et al., 2022). An increase in vitamin D leads to an increase in calcium in the blood, hypocalcaemia, and thus an increase in bone density and calcium deposition in the cells and channels of the kidneys, in addition to the occurrence of calcium deposition in the joints and arteries, and an increase in blood vessel contraction and blood pressure, and its deficiency leads to rickets and osteomalacia (Pallivalappi et al., 2022).

Material and Methods

Thirty (30) blood samples (15 males, 15 females) were collected from patients with rheumatoid arthritis, with different ages ranging from (55-83) years, and compared with (15)

blood samples from healthy people of the same age groups, and the following tests were conducted on serum the blood:

1. Measurement of the alkaline phosphatase enzyme with a measuring kit from BIOLABO, using a spectrophotometer.
2. Measurement of calcium concentration with a multimeter from BIOLABO, using a device Spectrophotometer.
3. Measurement of vitamin D concentration with a VEDA-LAB measuring kit using the VEDA-LAB device.

Statistical Analysis

The results were statistically analyzed using Mann-whitney U-test and in terms of probability P-Value ($\propto = 0.01$, $\propto = 0.05$), as well as a comparison between male and female patients with healthy subjects (Kikwood, 1988).

Results and Discussion

The results of Table (1) showed a significant increase in the concentration of the enzyme alkaline phosphatase (ALP) in rheumatoid arthritis for both sexes compared to the control groups. When any cell damage occurs, the enzyme leaks into the extracellular fluid, causing enzyme elevation (Krupaa et al., 2020).

Table1. Number and mean + S.D. Concentrations of biochemical variables in the serum of rheumatoid arthritis patients compared to control groups

Samples	Variables	N	Mean	Std. Deviation	95% Confidence Interval $Mean \pm (\frac{t\propto}{2})\ S_{\bar{y}}$	
Patient	Vitamin D	30	10.45	6.82145	Lower	7.9028
					Upper	12.9972
	S.Ca^{++}	30	1.97	.13966	Lower	1.9180
					Upper	2.0220
	ALP	30	131	31.50041	Lower	119.2367
					Upper	142.7624
control	Vitamin D	15	28.6333	8.93266	Lower	23.6866
					Upper	33.5801
	S.Ca^{++}	15	2.3533	.14573	Lower	2.2726
					Upper	2.4340
	ALP	15	58.5333	21.26992	Lower	46.7544
					Upper	70.3122

The results of Table (1) also showed a significant decrease in the concentrations of calcium and vitamin D in patients of both sexes compared to control groups, and the reason is that vitamin D deficiency leads to calcium deficiency, which causes a high risk of developing rheumatoid arthritis, and vitamin D works With calcium in bone formation and remodeling, normal blood levels must be maintained to protect against bone fracture, and vitamin D deficiency is related to rheumatic diseases and muscle inflammation (Bullock et al., 2017). Also, low calcium directly affects bone cells, which leads to a decrease in bone density and easy fracture, so we must take adequate amounts of vitamin D and calcium, especially patients at risk of developing autoimmune diseases such as rheumatoid arthritis and osteoporosis, because calcium is with vitamin D is used to treat rheumatic diseases (Kravchenko et al., 2022).

The results of Table (2) showed a significant increase in the activity of the enzyme alkaline phosphatase in females compared to males, and the reason may be attributed to vitamin D deficiency and osteoporosis, and early menstruation and irregular menstrual periods increase the risk of developing rheumatoid arthritis (AL-Bedri et al. al., 2019).

Table 2. Concentrations of biochemical variables in the serum of male and female patients compared to control groups

Samples	Sex	Variables	N	Mean	Std. Deviation	95% Confidence Interval $Mean \pm (\frac{t\alpha}{2})\ S_{\bar{y}}$	
Patient	Male	Vitamin D	15	9.9533	5.78309	Lower	6.7508
						Upper	13.1559
		S.Ca^{++}	15	1.9800	.14736	Lower	18984
						Upper	2.0616
		ALP	15	120.9333	30.96188	Lower	103.7872
						Upper	138.0795
	female	Vitamin D	15	10.9467	7.90035	Lower	6.5716
						Upper	15.3217
		S.Ca^{++}	15	1.9600	.13522	Lower	1.8851
						Upper	2.0349
		ALP	15	141.0667	29.65869	Lower	124.6422
						Upper	157.4911

Samples	Sex	Variables	N	Mean	Std. Deviation	Minimum	maximum
Control	Male	Vitamin D	8	32.3750	8.81488	19.20	48.90
		S.Ca^{++}	8	2.4000	.14142	2.10	2.50
		ALP	8	65.0000	19.69046	28.00	90.00
	female	Vitamin D	7	24.3571	7.45181	16.40	37.50
		S.Ca^{++}	7	2.3000	.14142	2.10	2.50

Testing the probability distribution of the variables studied is one of the basic conditions in any statistical analysis, as most estimation methods and testing hypotheses require a prerequisite that the studied variables have a probability distribution, and usually this

distribution is the normal distribution, and if this condition is not fulfilled, it requires the use of parametric and non-parametric tests (Which does not require a normal distribution of variables), by applying statistical hypotheses testing, and making comparisons, and the (Shapiro-Wilk) criterion is one of the statistical criteria used to test the normal distribution as in the following table:

Table 3.

Variables	Samples	Tests of Normality		
		Shapiro-Wilk		
		Statistic	Df	P-value
Vitamin D	Patient	.801	30	.000
	Control	.954	15	.593
S.Ca^{++}	Patient	.943	30	.109
	Control	.859	15	.023
ALP	Patient	.897	30	.007
	Control	.936	15	.337

From the observation of Table (3), we find that some variables follow a normal distribution in terms of the probability value (P-Value), which appeared greater than (0.05), as in the activity of the alkaline phosphatase enzyme (ALP-control), and the concentrations of (Ca++-patient), (V.D-control), while others were found to not follow the normal distribution, with a probability less than (0.05) as in the activity of (AIP.patient) enzyme, and the concentrations of (V.D- patient), (Ca++- control), and based on these results In Table (3), one of the non-parametric tests must be used in making comparisons, which is the (Mann-whitney U-test) for independent comparisons, as in the following table:

Table 4.

	Null Hypothesis	Test	Samples	Mean rank	Test value	P-value	Decision
1	The distribution of Vitamin D is the same across categories of case	Independent Samples mann-Whitney U Test	Patient	16.13	431	.000	Reject the null hypothesis
			Control	36.37			
2	The distribution of S.Ca^{++} is the same across categories of case		Patient	16	435	.000	Reject the null hypothesis
			Control	37			

The results of this test showed significant differences between patients and control groups in the activity of (AIP) enzyme, as indicated by the probability value (0.000), which is less than (0.05).), as well as significant differences appeared between patients and control groups in (V.D) and (Ca++) concentrations, in terms of the probability value (0.000), which is less than (0.05), with regard to (Ca++) concentration, the mean ranks of the control groups (37), which is higher than the mean The ranks of the patient samples are (16), while the mean (V.D) concentrations are (36.37), which is higher than the average ranks of the patient samples (16.13).

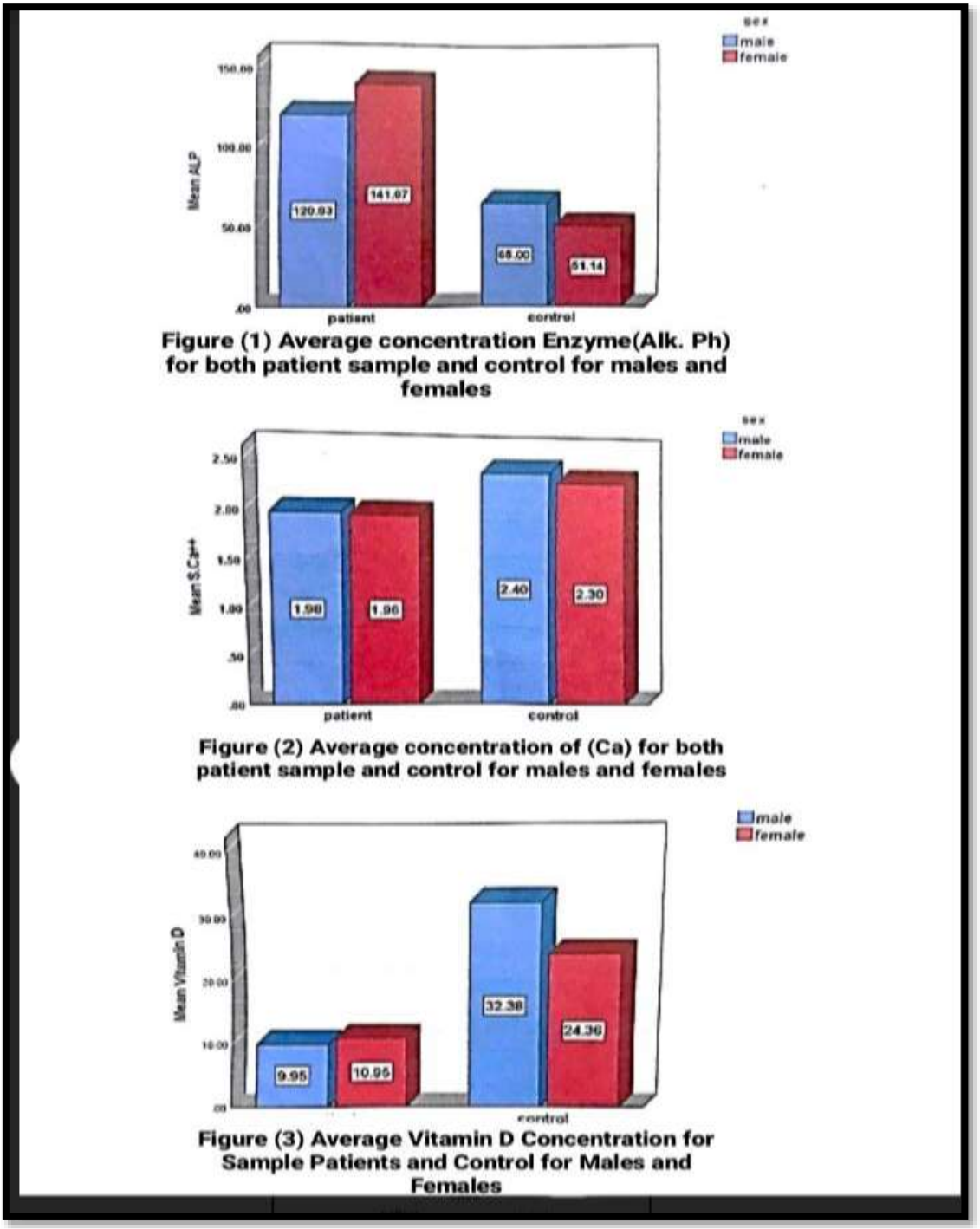
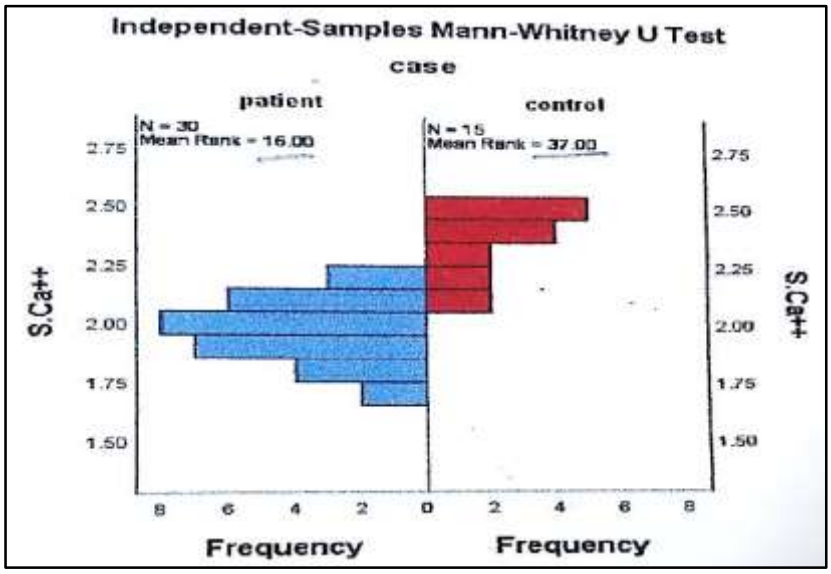
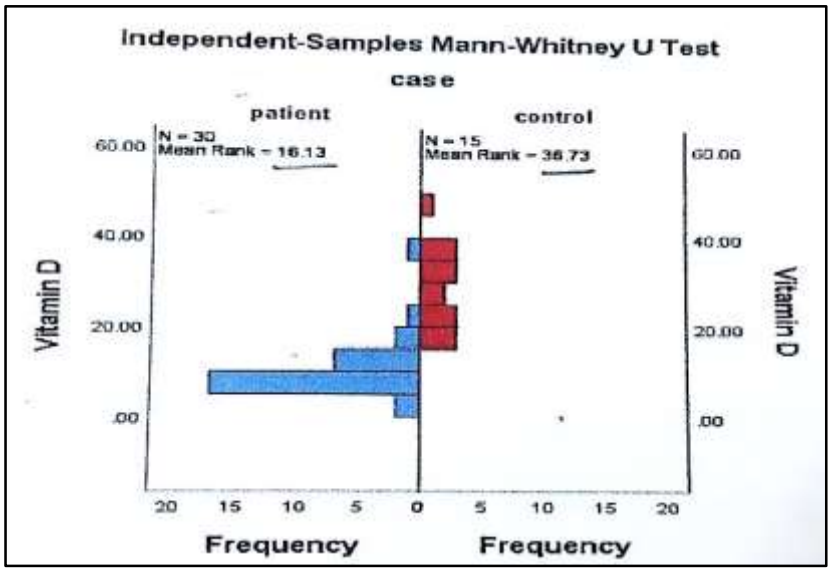


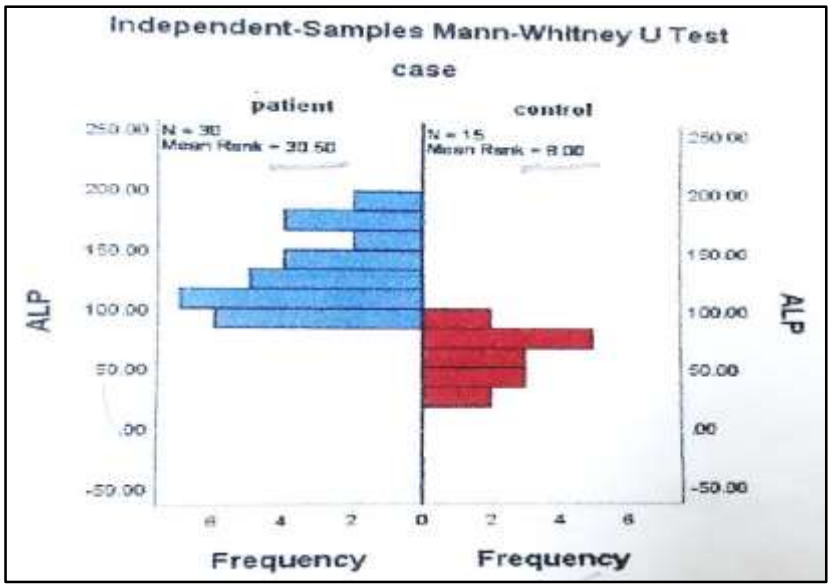
Figure (1) Average concentration Enzyme(Alk. Ph) for both patient sample and control for males and females

Figure (2) Average concentration of (Ca) for both patient sample and control for males and females

Figure (3) Average Vitamin D Concentration for Sample Patients and Control for Males and Females


Independent-Samples Mann-Whitney U Test
case
patient
control
N = 30
Mean Rank = 16.00
N = 15
Mean Rank = 37.00
S.Ca++
2.75
2.50
2.25
2.00
1.75
1.50
8 6 4 2 0 2 4 6 8
Frequency
Frequency


Independent-Samples Mann-Whitney U Test
case
patient
control
N = 30
Mean Rank = 16.13
N = 15
Mean Rank = 36.73
Vitamin D
60.00
40.00
20.00
.00
20 15 10 5 0 5 10 15 20
Frequency
Frequency


Independent-Samples Mann-Whitney U Test
case
patient
control
N = 30
Mean Rank = 30.50
N = 15
Mean Rank = 8.00
ALP
250.00
200.00
150.00
100.00
50.00
.00
-50.00
6 4 2 0 2 4 6
Frequency
Frequency

Before making a comparison between male and female patients, the normal distribution of male and female patients must be revealed, as in the following table:

Table 5.

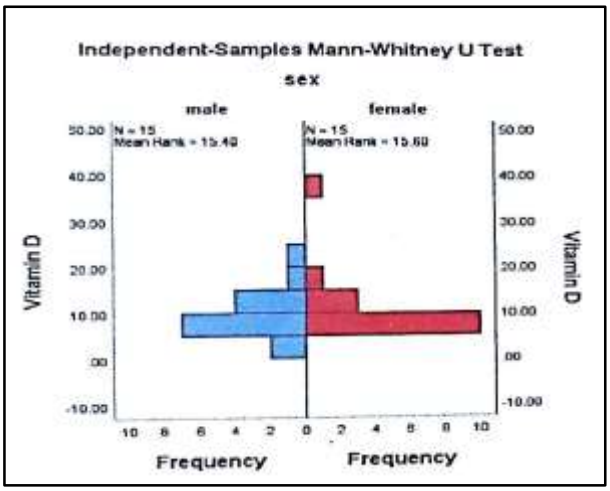
Variables	Sex	Tests of Normality		
		Shapiro-Wilk		
		Statistic	Df	Sig.
Vitamin D	Male	.947	15	.474
	Female	.639	15	.000
S.Ca^{++}	Male	.952	15	.560
	Female	.960	15	.692
ALP	Male	.814	15	.006
	Female	.929	15	.263

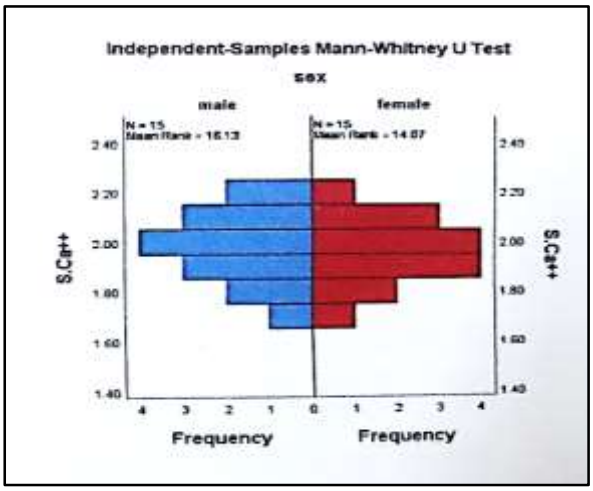
We note the results of Table (5) that the variables follow the normal distribution, in terms of the probability value (P-Value), as in (AIP-Female), (Ca++-Male, Female), and (V.D-Male), while the rest of the variables show that they do not. The normal distribution is traced in terms of the probability value less than (0.05) as in (AIP-Female), (V.D-Male), and based on the results that appeared in Table (5), it is necessary to use non-parametric tests, which is the (Mann-whitney U-test). For independent comparisons, as shown in the following table

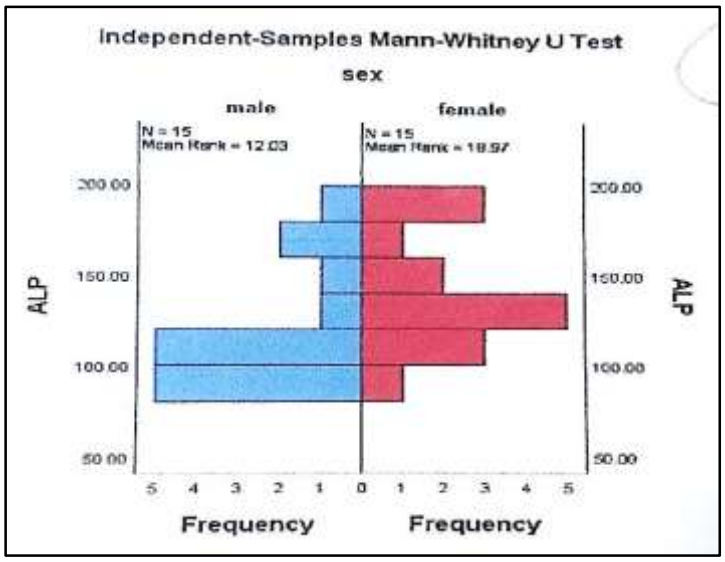
Table 6.

Variables	Sex	Tests of Normality		
		Shapiro-Wilk		
		Statistic	Df	Sig.
Vitamin D	Male	.947	15	.474
	Female	.639	15	.000
S.Ca^{++}	Male	.952	15	.560
	Female	.960	15	.692
ALP	Male	.814	15	.006
	Female	.929	15	.263

The results of Table (6) showed that there are significant differences between male and female patients in the activity of the enzyme (AIP) in terms of the probability value (0.029), which is less than (0.05).), while there were no significant differences between male and female patients in the concentration of (Ca++) in terms of the probability value (0.713), which is greater than (0.05), as we note that the average ranks for males (16.13), which is almost equal to the average ranks for females (14.87). Also, there are no significant differences between male and female patients in the concentration of (V.D) in terms of the probability value (0.967), which is greater than (0.05), as we note that the average ranks for males are (15.40), which is almost equal to the average ranks for females (15.60).


Independent-Samples Mann-Whitney U Test
sex
male
female
N = 15
Mean Rank = 15.40
N = 15
Mean Rank = 15.60
Vitamin D
Frequency
Frequency


Independent-Samples Mann-Whitney U Test
sex
male
female
N = 15
N = 15
S.Ca++
Frequency
Frequency


Independent-Samples Mann-Whitney U Test
sex
male
female
N = 15
Mean Rank = 12.03
N = 15
ALP
Frequency
Frequency

References

1. Al-bedri, k. z. Elias, A.A and Al-Derwibee, F.A. (2019). Serum Calcium and Serum Alkaline phosphatase levels and their Correlation with Disease Activity in Patients with Rheumatoid Arthritis. Medico - legal, Vol. 20, No.4.
2. Aleksadrova, V.. and Budko, N. P. (2016). Biochemistry of Vitamin Zapori Zhya state Medical university. P. 73.
3. Cüzdan, N; Benliday, I.C.; Basaran, S, and... Sarpel, T. (2020). Comparison of Vitamin D Profile between patients with inflammatory rheumatic diseases. Gulhane Med J. 62: 254-9.
4. Duan, W. and Li, H. (2018). Combination of NF-KB targeted siRNA and methrexate nano carrier towards the effective in a hybrid-treated in rheumatoid arthrit Duan and Li J. Nanobiotechnol. 16:58.
5. Gonzalez, M., Imam, 2., wong, R. L. 3. Zu, M., Trudeau, S., Gordan, S., Imam, M. and Gish, R. L. (2020). Normal alkaline phosphatase level dependent on vace/ethnicity: National GEF Health and Nutrition Examination Survey data Gastro. 7: enausoz. doi:10.11.1156/braigast–an0502.
6. Harrison, S. R., Li, O., Jeffery, L..E, Raza, K. and Hewison, M. (2018). Vitamin D Autammune Disease and Rheumatoid Arthritis Calcified Tissue International." 11.
7. Kikwood, B. R. (1988) Essential of medical Statistics, Balchwell Scientific publications Oxford ", 1st, pp. 43-56.
8. Kravchenko, D., Karakosta, P., Kuetting D Meyer,c, Brossart, P., Behning.C. and Schäfer, V.S. (2022). "The role of dual energy computed tomography the differentiation of acute gout a I acute Calcium Pyrophosphate Crystal arthritis". clinical Rheumatology. 41: 223- 233.
9. Krupaa, R. J., Hariharan, R., Babu, N. A. and Masthan, K. M.K. (2020). Alkaline phosphatase And Its Clinical Importance- A Review European J. of Molecular and Clinical Medicine ISSA- 2515-8260. Vol. 07, Issues 5.
10. Liang, L, Tong, T,Qin, L,Xie, J,Xu, Y, Lansen,Z, Liu, D.,Niu,X. and Tong, X. (2022). "Effects of Vitamin D with or without calcium on pathological ossification: Aretrospective clinical study Experimental and therapeutic Medicne", 23:285.
11. Lin , Y. J., Anzaghe, M. and Schülke, S... (2020). Update on the pathomechanism, Diagnosis, and Treatment options for Rheumatoid Arthritis. Cells, 9,880, doi:10.3390/Cells90.40.880 .
12. Mian, A., Ibrahim, and Scott, D.L. (2019 Asystematic review of guidelines for Managing rheumatoid arthritis BMC Rheumatology 3:42
13. Pallivalappil, S., Sasidaran, P. K. and Thulaseedarain. K. (2021) Serum Vitamin D levels In Rheumatoid Arthritis RCR, Vol. 11 Iss 3
14. No:1000281.

15. Park, H. M., Lee, J. H and Lee, Y.J. (2020). Positive Association of Serum Alkaline Phosphatase Level with Severe Knee Osteoarthritis: A Nationwide a Population-Based Study. Diagnostics, 10, 1016..
16. Raczkiewicz, A. and Tlustochowicz, W. (2016)Vitamin D in rheumatoid arthritis Post N Med XXIX (10): 753-755.
17. Suzuki, T., Nakamura, I and Kato, H. Calcium and vitamin D) Supplementation with 3-year denosumab treatment is beneficia to enhance bone mineral density in Postmenopausal Patients with osteoporosis. and Rheumatoid arthritis. Therapeutics and Clinical Risk Management: 15.
18. Giannini, D., Antonucci, M., Petrelli, Bilia, S., Alunno, A. and Puxeddu, I. (2020). "One Year in review 2020: Pathogenesis of rheumatoid arthritis", clinical and Experimental Rheumatology, 38: 387-397.
19. Simons, G., Caplan, J., Disanto te fano, R. L., Veldwijk, J., Englbrecht, M., Bywall, K. S., Kihlbom, U., Raza, K. and Falahee, M. (2022). "Systematic review of quantitative Preference studies of treatments for rheumatoid arthritis among Patients and at-risk populations", Arthritis Research and therapy, 24:55.
20. Bullock, J., Rizvi, S. A. A., Saleh, A. M., Ahmed, S. S, Do, D. P., Ansari, R. A. and Ahmed, J. (2018). "Rheumatoid Arthritis: A Brief Overview of the Treatment", Med Princ Parct. 27:501-507.
21. Dey, M., Busby, A., Elwell, Hog Cempp, L., Pratt, وه A., Young, A., Isaacs, J. and Nikiphorou, E. (2022). "Association between social deprivation and disease activity in rheumatoid arthritis: asystematic literature review", RMD open. doi:10.1136/rmdopen-2021-002058.
22. Chandrakar, B. L., Sharma, H. C. and Chandrakar, K. S. (2017). "Activity of Alkaline Phosphatase in Rheumatoid Arthritis for Diagnosis and Management. Int. J. Med Res Prof: 3(3): 28-84.
23. Mutsatsa, S., Mushore, M., Ncube, K. and Cursid, T. J. (2013). "Vitamin D the role of sunshine Vitamin", British J. of Mental Health Nursing. 2(4), 182-187.
24. Lee,Y.H.and B,S.C.(2016) "Vitamin D level in rheumatoid arthritis and its Corrleation with the disease activity: a meta – analysis clinical and Experimental Rheumatology : 34:827-833
25. Athanassiou, I. K, Athanassiou, P., Lyraki, A., Raftakis, I. and Antoniadis,C.(2012) . " Vitamin D and rheumatoid arthritis " Ther Adv Endocrinol Metab . 3(6) 181-187 .
26. Sajad, H. and Mohammad, G. (2020) . " Investigating the importance and causes of rheumatoid arthritis and its effective treatments : areviw study " perRevista Latinoamericana de Hipertension. Vol.15 – N.1

Detection of Proteus Mirabilis Carrying blaCTX-M, blaSHV, and blaTEM Genes Related to Urinary Tract Infections

Miaad K. Alkhudhairy [1], Mahasin Sifir Madkhur [2], Layla Saleh Abdul-Hassan [3]

© 2023 The Author(s). This open access article is distributed under a Creative CommonsAttribution (CC-BY) 4.0 license.

Abstract: Background: Proteus mirabilis is a bacterium that causes many serious systematic infections. The aim of the study: Determination of Proteus mirabilis carrying blaCTX-M, blaSHV, and blaTEM genes related to urinary tract infections.

Materials and Methods: 402 samples of urine were randomly collected from patients with symptomatic urinary tract infections at Al-Sadder Hospital in Al-Najaf Governorate, Iraq, from October 2022 to December 2023.

Results: 71 (17.7%) isolates of P. mirabilis were identified according to microscopic, culture, and biochemical characteristics, then were tested for their ability to produce extended-spectrum β-lactamases by the two phenotypic methods: double disc synergy test and modified Hodge test. 19 (26.8%) extended-spectrum β-lactamases-producers, which had previously been evaluated using the phenotypic method, were subjected to the investigation of β-lactamases encoding genes by using the polymerase chain reaction technique. This molecular technique detected 8 (42.1%) isolates carrying single β-lactamases encoding gene, 7 (36.8%) isolates had blaCTX-M gene, only one isolate (5.3%) carried blaSHV gene, and no single blaTEM gene was detected in any isolate. 3 (15.8%) isolates harbored multiple genes: blaCTX-M and blaTEM.

Conclusions: blaCTX-M gene was found to be more predominant among the extended-spectrum β-lactamases-producer under study than other genes.

Key Words: Proteus mirabilis, ESBLs, blaCTX-M, blaTEM, blaSHV.

Author details

[1–3] College of Health and Medical Techniques, Al-Furat Al-Awsat Technical University, Kufa, Iraq

[2] Al-Hamza General Hospital, Al-Diwaniyah Health Department, Iraq

Citation information

Cite this article as:

Alkhudhairy, M.K., Madkhur, M.S., Abdul-Hassan, L.S., (July 2023), *Detection of Proteus Mirabilis Carrying blaCTX-M, blaSHV, and blaTEM Genes Related to Urinary Tract Infections*, Proceedings of the Minar Congress, Turkey, (9) pp 38-48, DOI: http://dx.doi.org/10.47832/MinarCong9-4

http://dx.doi.org/10.47832/MinarCong9-4

[1] kuh.mead@atu.edu.iq. orcid.org/0000-0003-0890-3653

[2] ahmed.as1188@gmail.com orcid.org/0000-0002-9049-6040

[3] kuh.lyla12@atu.edu.iq

Introduction

Proteus mirabilis (P. mirabilis) is an opportunistic pathogen implicated in many diseases particularly infections associated with the urinary tract. It poses an unexpected global health threat by producing extended-spectrum β-lactamases (ESBLs), which reduces the efficiency of antibiotic therapy and increases mortality and morbidity in patients with suppressed immunity, catheterized patients, hospitalized patients, and those with renal functional complications [1, 2]. It also possesses virulence factors that help increase the expression of the disease and the complications of the disease, as well as prolong the recovery period and contribute directly to the difficulty of eliminating chronic and acute diseases. Proteus exhibits several virulence factors that contribute to increased pathogenicity, such as endotoxins, protease, hemolysin, urease, motility, and adhesions [1].

Flagella are significant virulence agents because they facilitate the swarming phenomena on solid media surfaces, allowing them to readily penetrate and infect the kidney. Thus P. mirabilis is a virulent pathogen responsible for both acute and chronic urinary tract infections (UTIs) [3, 4]. ESBLs are β-lactamase enzymes capable of effectively hydrolyzing penicillins, broad, narrow spectrum cephalosporins, and monobactams, but they cannot hydrolyze carbapenems or cefamycins and can be inhibited by β-lactamase inhibitors such as tazobactam and sulbactam. AmpC enzymes confer resistance to β-lactamase inhibitors, monobactams, cefamycins, cephalosporins, and penicillins. The deficiency of inhibition by β-lactamases inhibitors and cefamycins distinguishes AmpC-producing strains from ESBL-producing strains. β-lactamase enzymes are encoded by genes carried on different types of plasmids to protect bacteria from the effect of β-lactams, and these genes are often multiple and accountable for encoding many enzymes to resist many antibiotics such as trimethoprim, tetracyclines, sulfonamides, quinolones, chloramphenicol, and aminoglycosides, which limit therapeutic options and increase the consequences of infections.

On the other hand, carbapenems are one of the β-lactam generations that are effective in counteracting β-lactamases and are one of the preferred treatments for eradicating serious infections caused by virulent ESBL-producers. Since genes for resistance to β-lactams and multiple antibiotics are transmissible horizontally between different species and species via plasmids and transposons [2, 3, 4]. The main causes of antibiotic resistance in Gram-negative bacteria are the transfer of resistance genes through mobile genetic elements such as plasmids, transposons, and integrons, which may swiftly transfer between nations and pass through mutant clones. The other reason is those normal human floras acquire resistance genes, so those genes become a silent source of internal infection without realizing the role of this source in the dissemination of resistance genes [4]. It is worthwhile to test the ability of isolates under study to produce β-lactamases and highlight the types of genes encoding them to enable local and global health authorities to form a clear picture of the prevalent genotype and take the right measures to eradicate the virulent strains or at least reduce their virulence. Therefore, this study aimed to characterize the local genotype encoding the isolates in P. mirabilis isolates and to determine their characteristics

Materials and Methods

1. Isolation and Identification of Proteus mirabilis

Urine samples were randomly collected from 402 patients with symptomatic UTIs at Al-Sadder Hospital in Al-Najaf Governorate, Iraq, from October 2022 to December 2023. 71 (17.7%) isolates of P. mirabilis were identified according to microscopic, culture, and biochemical characteristics [5].

2. Phenotypic Detection of ESBLs Production

Modified Hodge Test (MHT)

The swab was used to inoculate the MHA medium with Escherichia coli ATCC 25922. A Ceftazidime disk (30µg) was situated in the medium's center and then 4 isolates of P. mirabilis were streaked radially starting from the disk's Ceftazidime outer edge to the inner plate edge. Then it was immediately incubated aerobically for 18 hours at degree 37◦C. The isolates that show a cloverleaf form in the middle of the culture medium are considered to be ESBLs-producers [6].

Double Discs Synergy Test (DDST)

According to the disc diffusion procedure, this test was carried out; a few fresh colonies from each P. mirabilis isolate were inoculated in nutrient broth (NB) overnight at 37oC. The turbidity of cultured NB was modified such that it conformed to the 0.5 McFarland standards. The streaking technique was used to inoculate bacterial suspension onto Mueller-Hinton agar (MHA), Amoxicillin/ Clavulanate (30µg) disk was situated in the exact plate's middle. Around four corners of Amoxicillin/ Clavulanic acid a disk of Ceftazidime (30µg), Ceftriaxone (10µg), Cefotaxime (30µg), and Aztreonam (30µg) were positioned such that there was a space of 1.5 cm from the center of one Amoxicillin/ Clavulanate disc to the centers of the other disks. Then it was immediately incubated aerobically for 18 hours at degree 37◦C. When the inhibition zones expanded beyond 5 mm in the direction of the Amoxicillin/ Clavulanate disk, the findings were regarded to be positive for ESBLs production [7].

3. Genotypic Detection of ESBLs Production

Three primer pairs were selected to amplify fragments of 593 bp (blaCTX-M), 445 bp (blaTEM), and 369 bp (blaSHV). The primer pairs were: blaCTX-M-F-5′ATGTGCAGYACCAGTAARGTKATGGC3′/ R- 5′TGGGTRAARTARGTSAC CAGAAYCAGCGG′; blaTEM-F 5′CGCCGCATACACTATTCTCAGAATGA3′/ R-5′ACGCTCACCGGCTCCAGATTTAT3′; blaSHV-F-5'CTTTATCGGCCCTCACT CAA3'/ R-5'AGGTGCTCATCATGGGAAAG3' [8].

Ethical Considerations

The study was approved by the Postgraduate Studies Committee of the College of Health and Medical Techniques, Al-Furat Al-Awsat Technical University, Kufa, Iraq. Patients' consent was taken before clinical samples were collected, and medical professionals at the burn center oversaw the collection of study samples.

Statistical Analysis

The statistical software SPSS v20.0, developed by IBM Corporation, Armonk, New York, USA, was used to analyze the data of the current study.

Results

Out of 402 urine samples collected from patients with UTIs, 71 (17.7%) isolates of P. mirabilis were identified according to microscopic, culture, and biochemical characteristics. All isolates under study were tested for their ability to produce ESBLs by DDST and MHT [Figure 1]. 19 (26.8%) ESBLs-producers, which had previously been evaluated using the phenotypic method, were subjected to the investigation of ESBLs-encoding genes by using the PCR technique. This molecular technique detected 8 (42.1%) isolates carried a single ESBLs-encoding gene, 7 (36.8%) isolates had blaCTX-M gene, only one isolate (5.3%) carried blaSHV gene, and no single blaTEM gene was detected in any isolate. 3 (15.8%) isolates harbored multiple genes: blaCTX-M and blaTEM [Table 1] and [Figure 2].

Table 1. Frequency of ESBLs-encoding genes among 14 ESBLs-producers

ESBLs-encoding genes type	No. of ESBLs encoding-genes N= 11/19 (57.9%) n (%)	Type of ESBLs-encoding genes association	N= 11/19 (57.9%) n (%)
bla$_{CTX-M}$	7 (36.8)	Single	
bla$_{TEM}$	0 (0.0)	-	8 (42.1)
bla$_{SHV}$	1 (5.3)	Single	
bla$_{CTX-M}$ + *bla*$_{TEM}$	3 (15.8)	Multiple	3 (15.8)

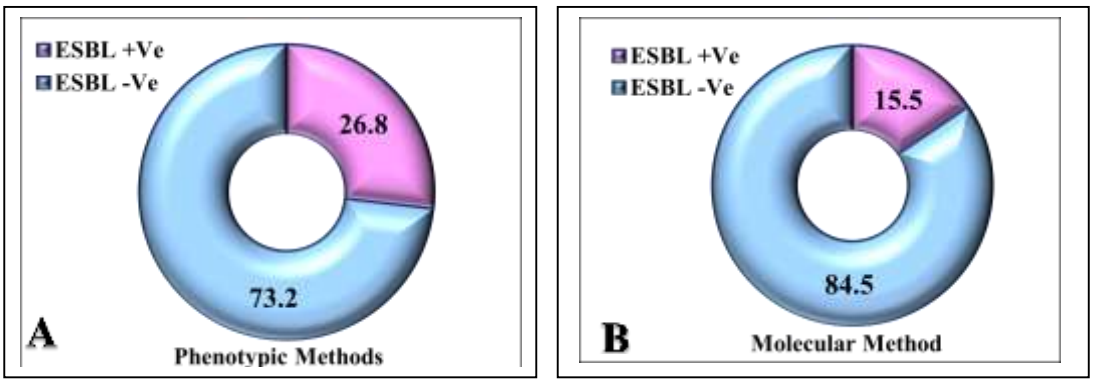


Figure 1. Phenotypic and molecular detection of ESBLs-producing *P. mirabilis* isolates.

(A): Phenotypic detection by DDST and MHT, (B): Molecular detection by PCR technique. The percentage of ESBLs-producers in phenotypic detection was higher than the percentage of ESBLs-producers in molecular detection.



Figure 2. Phenotypic techniques for detecting ESBLs-producing P. mirabilis isolates.

(A): An isolate of P. mirabilis 35 produced a keyhole appearance on MHA as a positive result for the ESBLs-production by using the DDST; (B): Isolates 15, 110, and 78 produced a cloverleaf appearance on MHA as a positive result for the ESBLs- production by using the MHT.

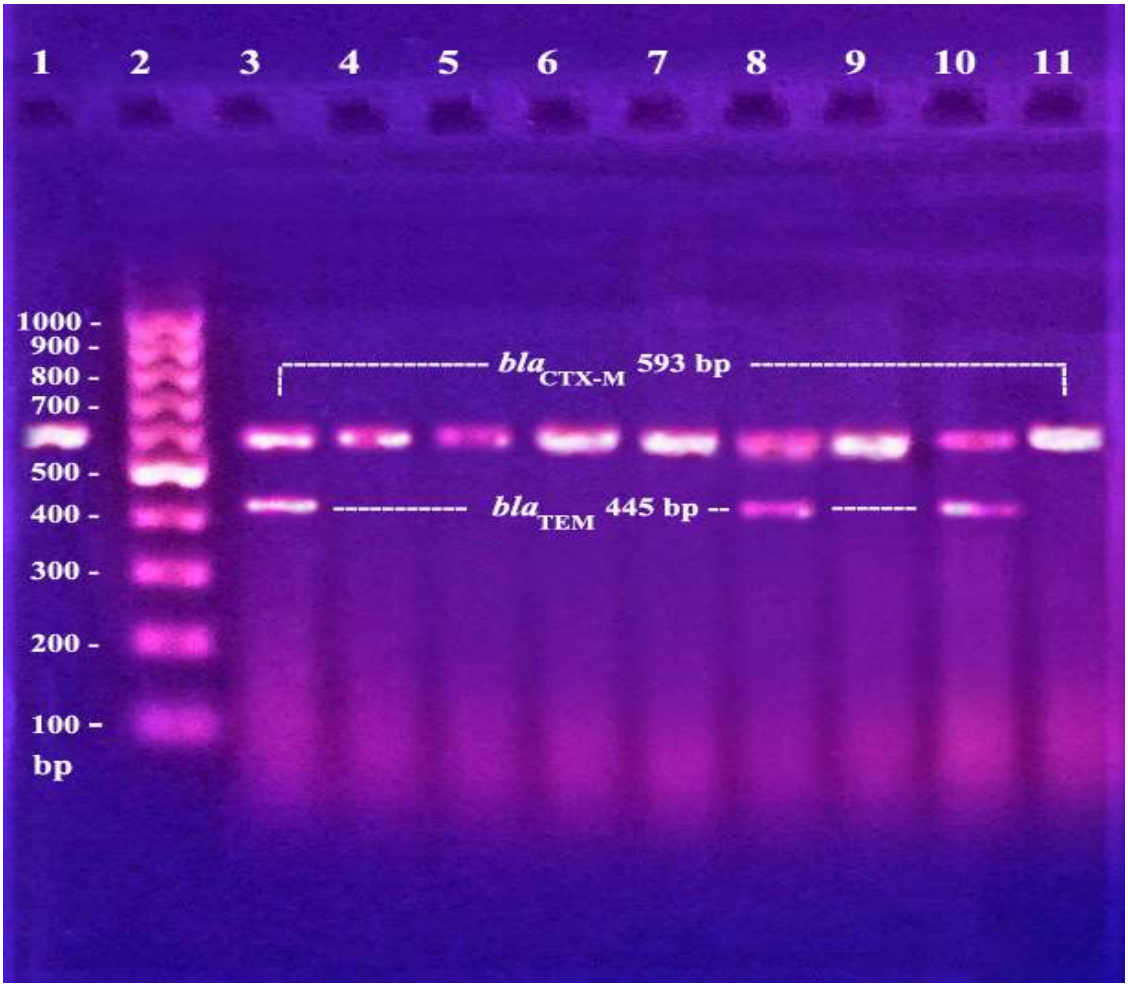


Figure 3. Detection of ESBLs-producers by PCR technique.

The amplicon size of the blaCTX-M gene is 593 bp and blaTEM gene 445 bp. Electrophoresis was used to separate the PCR products on an agarose gel weighing 0.750 g. For 1.5 hours, 70 Volts were used to conduct the electrophoresis. Lane 2: Marker; lane: 1, 3-11 positive blaCTX-M gene; lane: 3, 8, 10 positive blaTEM gene.

Discussion

Resistance to β-lactams has been frequently reported in P. mirabilis by producing different types of β-lactamase enzymes such as ESBLs, AmpC, and carbapenemases. Infections and diseases caused by P. mirabilis strains that can produce ESBLs represent a serious global threat because these producers exhibit coresistance to many classes of antibiotics including sulfa drugs, aminoglycosides, and quinolones. Formerly, blaTEM, blaSHV, and blaCTX-M genes were the main genotypes of ESBLs found in Enterobacteriaceae isolates [3, 4].

In this study, it was observed that the prevalence of ESBLs-producers identified by phenotypic methods was higher than that of the molecular method. The reason for these differences may be attributed to the fact that phenotypic methods are sensitive to ESBLs without specifying the type of encoded gene. The phenotypic methods are often easy, fast, low-cost, and do not require highly qualified technicians, while molecular technique, unlike phenotypic methods, is high cost, difficult, and requires technicians with high skills. However, PCR is a standard technique for detecting genes, but it is only sensitive to the selected primers, thus, it cannot identify the ESBLs-producers unless it is provided with the required primers. The other reason for the existence of a difference between phenotypic and molecular detection methods is perhaps because there are genes encoding the production of ESBLs are still not discovered despite their existence. This means that ESBLs negative isolates can express but rather that molecular technology requires feeding the device with advanced data to obtain satisfactory results and conform to the apparent detection [9, 10, 11].

According to the molecular results in the current study, the single blaCTX-M (36.8%) and linked blaCTX-M + blaTEM (15.8%) gene was the most dominant, and this may be due to the ease of gene transmission between Gram-negative bacteria, especially blaCTX-M. Several investigations indicated that other ESBLs, such as TEM and SHV variants, were replaced by CTX-M enzymes in Enterobacteriaceae [12, 13, 14]. These investigations explained the dominance of blaCTX-M genes encoding CTXM enzymes in this investigation. The reason for the translocation may be attributed to the accelerated spread of blaCTX-M genes across transposons and plasmids and because of the ease of crossing over and association of transposons and plasmids within successful clones. It is also widely believed that the cause of the increased CTX-M prevalence is the phenomenon of co-resistance in CTX-M-producing organisms, particularly aminoglycosides and fluoroquinolones which may simplify the occurrence of co-selection [13, 15].

Few nearby bacterial clones, plasmids, and genetic structures have all been linked to the extraordinary adaptive success of blaCTX-M genes in Enterobacteriaceae. Successful

connections of blaCTX-M genes and other resistance factors may have aided in the remarkable expansion of the CTX-M necessitating an uncontrollable pandemic scenario. Co-selection mechanisms will ensure the blaCTX-M genes' future survival within bacterial communities given that additional resistance genes, particularly newly developing ones like carbapenemases, are often found in CTX-M-producing species [13].

The genes of the isolates under study were diversified, and this may be due to genetic mutations and the ease of gene transmission between strains of Gram-negative bacteria. Bonnet et al [16] interpreted diversity in genes as diversity in mutations and confirmed the validity of this interpretation by identifying five types of mutations in the TEM gene, represented by: TEM-74, TEM-73, TEM-65, TEM -66, and TEM -57. Bonnet et al also predicted that this genetic diversity in β-lactamase enzymes related to the high occurrence of β-lactams resistance raises concern and fear that strains resistant to P. mirabilis could negatively participate in nosocomial infections and could take hold in hospitals infections. Indeed, P. mirabilis, which has genetic diversity in the production of ESBLs, has become one of the most important virulent pathogens in hospitals [4]. This diversity of β-lactamases, combined with the high prevalence of resistance to β-lactams, raises the possibility that antibiotic-resistant P. mirabilis will become entrenched in hospitals and become involved in nosocomial infections, in which case monitoring for susceptibility to β-lactams will be necessary. Production ESBLs have been linked to serious negative outcomes such as increased expenses, the discontinuation of chronic care, delays in appropriate treatment, an increase in length of stay, and an increase in overall infection-related mortality [17, 18].

Globally, until half of the past decade, it was reported that most of the ESBLs enzymes in P. mirabilis are of the type TEM-1, 2, and SHV-1, and it was believed that these types arose from single mutation or several point genetic mutations [3, 18]. Some literature reported that TEM was prevalent in P. mirabilis [19, 20]. TEM-72 was first presented in Italy in 2000 and TEM-92 was isolated in French in 2001. In another study was detected 106 isolates had TEM-20, 26, 47, 52, 87 [18, 21]. However, later reports continued to reveal the presence of CTX-M-type ESBLs enzyme in P. mirabilis along with SHV and TEM enzymes. The appearance of an increasing number of CTX-M in P. mirabilis has caused widespread worry. CTX-M-13 and 14 in P. mirabilis were discovered in Hong Kong [17, 18]. In 2017, Paulitsch-Fuchs et al [22] detected CTX-M-2 and VEB-6 enzymes in one isolate and three isolates of P. mirabilis, respectively. Schwaber et al [17] concluded in 2006 that CTX-M circulates at a rapid rate globally and was less prevalent than TEM in P. mirabilis based on the studies of others. However, recent studies showed that the CTX-M enzyme was more dominant and widespread among P. mirabilis than other ESBLs-enzymes. In Asian, USA, and European countries, the prevalence of CTX-M-producing bacteria has increased, reflecting a shift of ESBLs from the SHV or TEM lineage [23].

Conclusions

The prevalence of P. mirabilis isolates that produce ESBLs was worrisome, especially since it is a pathogenic bacterium that increases the complications of UTIs. The current study demonstrated the effectiveness of phenotypic methods in identifying ESBLs, which facilitates the identification of resistant isolates, prescribing treatment, and reducing complications. The blaCTX-M gene was distinguished by being more dominant than the rest of the genes, whether it was single or linked, while the gene expression of the blaSHV enzyme was so weak. Therefore, the current study recommends adopting phenotypic methods in local laboratories and rationing the prescription of β-lactams in the treatment of UTIs.

REFERENCES

1. Kamil, T. D. A., & Jarjes, S. F. (2021). Molecular Characterization of Proteus spp. from Patients Admitted to Hospitals in Erbil City. Polytechnic, 11(2), 95–99. https://doi.org/10.25156/ptj.v11n2y2021.pp95-99
2. Pal, N., Hooja, S., Sharma, R., & Maheshwari, R. K. (2016). Phenotypic detection and antibiogram of β-lactamase-producing proteus species in a tertiary care hospital, India. Annals of Medical and Health Sciences Research, 6(5), 267. https://doi.org/10.4103/amhsr.amhsr_413_15
3. Song, W., Kim, J., Bae, I. K., Jeong, S., Seo, Y. J., Shin, J. H., Jang, S. J., Uh, Y., Shin, J. H., Lee, M., & Lee, K. (2011). Chromosome-Encoded AmpC and CTX-M Extended-Spectrum β-Lactamases in Clinical Isolates of Proteus mirabilis from Korea. Antimicrobial Agents and Chemotherapy, 55(4), 1414–1419. https://doi.org/10.1128/aac.01835-09
4. Shaaban, M., Elshaer, S. L., & El-Rahman, O. a. A. (2022). Prevalence of extended-spectrum β-lactamases, AmpC, and carbapenemases in Proteus mirabilis clinical isolates. BMC Microbiology, 22(1). https://doi.org/10.1186/ s12866-022-02662-3
5. McFadden, J. F. (2000). Biochemical Tests for Identification of Medical Bacteria. 3rded. Lippincott Williams and Wilkins, USA.
6. Ghasemnejad A, Doudi M, Amirmozafari N. Evaluation of modified Hodge test as a non-molecular assay for accurate detection of KPC-producing Klebsiella pneumoniae. Pol J Microbiol. 2018;67(3):291-295. doi: 10.21307/pjm-2018-034.
7. Laudy AE, Róg P, Smolińska-Król K, Ćmiel M, Słoczyńska A, Patzer J, Dzierżanowska D, Wolinowska R, Starościak B, Tyski S. Prevalence of ESBL-producing Pseudomonas aeruginosa isolates in Warsaw, Poland, detected by various phenotypic and genotypic methods. PLoS One. 2017;12(6):e0180121. doi: 10.1371/journal.pone.0180121.
8. Fang, H., Ataker, F., Hedin, G., & Dornbusch, K. (2008). Molecular Epidemiology of Extended-Spectrum β-Lactamases among Escherichia coli Isolates Collected in a Swedish Hospital and Its Associated Health Care Facilities from 2001 to 2006. Journal of Clinical Microbiology, 46(2), 707–712. https://doi.org/10.1128/jcm.01943-07
9. Bajpai, T., Pandey, M., Varma, M., & Bhatambare, G. S. (2017). Prevalence of TEM, SHV, and CTX-M Beta-Lactamase genes in the urinary isolates of a tertiary care hospital. Avicenna Journal of Medicine, 07(01), 12–16. https://doi.org/10.4103/2231-0770.197508
10. Miao, Z., Li, S., Wang, L., Song, W., & Zhou, Y. (2017). Antimicrobial Resistance and Molecular Epidemiology of ESBL-Producing Escherichia coli Isolated from Outpatients in Town Hospitals of Shandong Province, China. Frontiers in Microbiology, 8. https://doi.org/10.3389/fmicb.2017.00063
11. Alkhudhairy, M. K., & Alshammari, M. M. M. (2019). Extended-spectrum β -lactamase-producing Escherichia coli isolated from pregnant women with asymptomatic UTI in Iraq. Eurasian Journal of Biosciences, 13(2), 1881–1889.

http://www.ejobios.org/download/extended-spectrum-lactamase-producing-escherichia-coli-isolated-from-pregnant-women-with-7348.pdf

12. Rodriguez-Villalobos, H., Bogaerts, P., Berhin, C., Bauraing, C., Deplano, A., Montesinos, I., De Mendonça, R., Jans, B., & Glupczynski, Y. (2010). Trends in production of extended-spectrum-lactamases among Enterobacteriaceae of clinical interest: results of a nationwide survey in Belgian hospitals. Journal of Antimicrobial Chemotherapy, 66(1), 37–47. https://doi.org/10.1093/jac/dkq388
13. Cantón, R., González-Alba, J. M., & Galán, J. C. (2012). CTX-M Enzymes: Origin and Diffusion. Frontiers in Microbiology, 3. https://doi.org/10.3389/ fmicb.2012.00110
14. Alkhudhairy, M. K., & Alshammari, M. M. M. (2020). Prevalence of metallo-β-lactamase–producing Pseudomonas aeruginosa isolated from diabetic foot infections in Iraq. New Microbes and New Infections, 35, 100661. https://doi. org/10.1016/j.nmni.2020.100661
15. Cantón, R., & Ruiz-Garbajosa, P. (2011). Co-resistance: an opportunity for the bacteria and resistance genes. Current Opinion in Pharmacology, 11(5), 477–485. https://doi.org/10.1016/j.coph.2011.07.007
16. Bonnet, R., De Champs, C., Sirot, D., Chanal, C., Labia, R., & Sirot, J. (1999). Diversity of TEM Mutants in Proteus mirabilis. Antimicrobial Agents and Chemotherapy, 43(11), 2671–2677. https://doi.org/10.1128/aac.43.11.2671
17. Schwaber, M. J., Navon-Venezia, S., Kaye, K. S., Ben-Ami, R., Schwartz, D. A., & Carmeli, Y. (2006). Clinical and Economic Impact of Bacteremia with Extended-Spectrum-β-Lactamase-Producing Enterobacteriaceae. Antimicrobial Agents and Chemotherapy, 50(4), 1257–1262. https://doi.org/10.1128/aac.50.4. 1257-1262.2006
18. Huang, Y., Xu, Y., Wang, Z., & Lin, X. (2014). Antimicrobial Resistance and Genotype Analysis of Extended-Spectrum-β-Lactamase-Producing Proteus Mirabilis. Open Journal of Clinical Diagnostics, 04(01), 57–62. https://doi.org/10.4236/ojcd.2014.41011
19. Luzzaro, F., Perilli, M., Amicosante, G., Lombardi, G., Belloni, R., Zollo, A., Bianchi, C., & Toniolo, A. (2001). Properties of multidrug-resistant, ESBL-producing Proteus mirabilis isolates and the possible role of β-lactam/β-lactamase inhibitor combinations. International Journal of Antimicrobial Agents, 17(2), 131–135. https://doi.org/10.1016/s0924-8579(00)00325-3
20. Perilli, M., Dell'Amico, E., Segatore, B., De Massis, M. R., Bianchi, C., Luzzaro, F., Rossolini, G. M., Toniolo, A., Nicoletti, G., & Amicosante, G. (2002). Molecular Characterization of Extended-Spectrum β-Lactamases Produced by Nosocomial Isolates of Enterobacteriaceae from an Italian Nationwide Survey. Journal of Clinical Microbiology, 40(2), 611–614. https://doi.org/10.1128/jcm.40.2.611-614.2002

21. Ho, P. M., Ho, A. W., Chow, K. H., Wong, R. C. W., Duan, R. S., Ho, W., Mak, G. C., Tsang, K. W., Yam, W., & Yuen, K. (2005). Occurrence and molecular analysis of extended-spectrum β-lactamase-producing Proteus mirabilis in Hong Kong, 1999–2002. Journal of Antimicrobial Chemotherapy, 55(6), 840–845. https://doi.org/10.1093/jac/dki135
22. Paulitsch-Fuchs, A. H., Melchior, N., Haitzmann, T., Fingerhut, T., Feierl, G., Baumert, R., Kittinger, C., & Zarfel, G. (2022). Analysis of Extended Spectrum Beta Lactamase (ESBL) Genes of Non-Invasive ESBL Enterobacterales in Southeast Austria in 2017. Antibiotics, 12(1), 1. https://doi.org/10.3390/antibiotic s12010001
23. Kanayama, A., Kobayashi, I., & Shibuya, K. (2015). Distribution and antimicrobial susceptibility profile of extended-spectrum β-lactamase-producing Proteus mirabilis strains recently isolated in Japan. International Journal of Antimicrobial Agents, 45(2), 113–118. https://doi.org/10.1016/j.ijantimicag.2014. 06.005

Solving Some Nonlinear Partial Differential Equations by GERFM

Zaniab Mohamed Ridha Al-Fatlawy [1]

© 2023 The Author(s). This open access article is distributed under a Creative CommonsAttribution (CC-BY) 4.0 license.

Abstract: We study using the method of generalized Hexponential rational function method (GERFM) to acquire some exact optical solitons for the dimensionless form of some equations such as (1 + 1) generalized Benjamin–Bona–Mahony (GBBM) equation. To this end, by transformation:

$$u(x,t) = \psi(\eta), \ \ \eta = kx - \theta t.$$

Where k and θ are constant values, the equations are converted into a nonlinear ODE. Second, the nonlinear ODE is solved according to a linear combination of the given basis functions. In this case, an algebraic equation is constructed. The solution of the nonlinear ODE yields the same solution of the original nonlinear PDE. In this paper, we will discuss about exact solutions of Generalized Benjamin-Bona-Mahony, Wu-Zhang equation and Fisher equation. we present generalized exponential rational function method that is abbreviated by GERFM. We use it to find an exact solution for some equations that we present in the sequel.

Key Words: Exact solutions; the generalized Benjamin–Bona–Mahony equation; generalized exponential rational function method.

Author details

[1] General Directorate of Education, Najaf Al-Ashraf Governorate, Iraq

Citation information

Cite this article as:

Al-Fatlawy, Z.M.R., (July 2023), *Solving Some Nonlinear Partial Differential Equations by GERFM*, Proceedings of the Minar Congress, Turkey, (9) pp 49-64, DOI: http://dx.doi.org/10.47832/MinarCong9-5

http://dx.doi.org/10.47832/MinarCong9-5

[1] hgthdyhd@gmail.com

Introduction

Numerous specialists and academics,have[studied and published significant research findings on fractional partial differential equations, and the techniques for solving thesepproblems are alwaysiimproving.lFirst integral method, alternate banding parallel difference method,, Laplacetransform method, extended trial equation method, expansion method, etc. are a few examples.[1]

Mathematician Maccari used the Fourier expansion and space-time reconstruction asymptotically precise reduction approach to deduce the space-time fractional j(2 + 1) dimensional Maccari equations from then Kadomtsev-Petviashvili equation in 1996.

The equations are frequently used in the fields of ocean and optical research to describe undisturbed waves in wave dynamicsk.KP hierarchy reduction was used to get both bright and dark N-soliton solutions. The exponential rational function approach was used in this paper to[2] Benjamin Bona Mahony, and the space–time fractionallcoupled Burgers' equations.

In this peaper, we describeh the exponential rational function method.

Preliminaries

1. Differential equationl

The mathematical formulation ,of most k problems in science involving rates of change n in terms of 2 or more independent variables, usually representing length, time or angle leads to a partial differential equation or to a set of such equations.

An equation in terms of dependent and independent variables along with derivatives is called a differential equation.

Examples:

$$y' + 2xy = 1$$

The differential equations are divided into two categories Ordinary Differential Equation (ODE) and Partial Differential Equation (PDE) that are defined as below:

2. Ordinary differential equation:

A differential equation is said ordinary if its dependent variable is in terms of just one independent variable.

Examples:

$$y' + 2xy = 1$$

$$\left(\frac{dy}{dx}\right)^3 + \frac{x^2 dy}{dx} = 1$$

3. Partial differential equation:

Variable is in terms of more than one independent variable.

Examples:

$$\frac{\partial u}{\partial x}+\frac{\partial u}{\partial t}-x=0$$

$$i\frac{\partial^2 u}{\partial x^2}-\frac{\partial u}{\partial t}=1, \qquad i=\sqrt{-1}$$

4. Degree and order of Differential equation:

The degree of a differential equation is the largest power of the equation and the order of differential is largest derivative of the equation.

Examples:

$$\frac{\partial u}{\partial x}+\frac{\partial u}{\partial t}-x=0, \quad degree\ 1\ and\ order\ 1$$

$$i\frac{\partial^2 u}{\partial x^2}-\frac{\partial u}{\partial t}=1, \qquad i=\sqrt{-1} \qquad degree\ 1\ and\ order\ 2$$

$$(y'')^3+y'^4=1, \quad degree\ 4\ and\ order\ 2$$

5. Homogeneous differential equation:

A (partial or ordinary) differential equation is said homogeneous if the term without dependent variable is zero.

Examples: The following differential equations are homogeneous:

$$\frac{\partial u}{\partial x}+\frac{\partial u}{\partial t}=0$$

$$\left(\frac{dy}{dx}\right)^3+\frac{x^2dy}{dx}=0$$

The following differential equations are NOT homogeneous:

$$\frac{\partial u}{\partial x}+\frac{\partial u}{\partial t}-x=0$$

$$\left(\frac{dy}{dx}\right)^3+\frac{x^2dy}{dx}=1$$

6. Linear and nonlinear differential equations

7. Linear differential equation:

A differential equation is said linear if in its terms the dependent variable or its derivatives is appeared at most one times, the dependent variable is of order 1.

Examples: Laplace's equation

$$\Delta w = \frac{\partial^2 w}{\partial x^2} + \frac{\partial^2 w}{\partial y^2} = 0.$$

Helmholtz's (or eigenvalue) equation

$$-\Delta w = \lambda w.$$

Linear transport equation

$$\frac{\partial w}{\partial t} + \sum_{i=1}^{n} b^i \frac{\partial w}{\partial x_i} = 0$$

Liouville's equation

$$\frac{\partial w}{\partial t} - \sum_{i=1}^{n} \frac{\partial (b^i w)}{\partial x_i} = 0.$$

Heat (or diffusion) equation

$$\frac{\partial w}{\partial t} - \Delta w = 0.$$

Schrödinger's equation

$$i\frac{\partial w}{\partial t} + \Delta w = 0., \quad i = \sqrt{-1}$$

Kolmogorov's equation

$$\frac{\partial w}{\partial t} - \sum_{i,j=1}^{n} a^{ij} \frac{\partial^2 w}{\partial x_i \partial x_j} + \sum_{i=1}^{n} b^i \frac{\partial w}{\partial x_i} = 0.$$

Fokker-Planck equation

$$\frac{\partial w}{\partial t} - \sum_{i,j=1}^{n} \frac{\partial^2 (a^{ij} w)}{\partial x_i \partial x_j} - \sum_{i=1}^{n} \frac{\partial (b^i w)}{\partial x_i} = 0.$$

Wave equation

$$\frac{\partial^2 w}{\partial t^2} - \Delta w = 0.$$

8. Nonlinear differential equation:

If a differential equation is not linear, it will be nonlinear.

Examples:

Nonliear Poisson's equation

$$-\Delta w = f(w).$$

Scalar conversation law

$$\frac{\partial w}{\partial t} + div\, F(w) = 0$$

Scalar reaction diffusion

$$\frac{\partial w}{\partial t} - \Delta w = f(w)$$

Korteweg-de Vries (KdV) equation

$$\frac{\partial w}{\partial t} + w\frac{\partial w}{\partial x} + \frac{\partial^3 w}{\partial x^3} = 0.$$

KdV equation

In 1895, Diederick Korteweg who is a Dutch physicist with his student Gustav de Vries (KdV) extracted a nonlinear partial differential equation as follows

$$\frac{\partial u}{\partial t} + \frac{\partial^3 u}{\partial x^3} + 6u\frac{\partial u}{\partial x} = 0. \qquad (*)$$

This equation that now is famous to KdV equation can describe Russe11's experiments. A nonlinear term that is the amplitude effect and Adispersive term that will be caused to the waves with different wave lengths can travel with different velocities.

In addition to a Korteweg and de Vries found a periodic that aroseasf a result of a balance between dispersion *j* and nonlinearity. A solution of (*) can be given by

$$u(x,t) = \frac{\xi}{2}\operatorname{sech}^2\left\{\frac{\sqrt{\xi}}{2}(x - \xi t - x_0)\right\},$$

whereξ shows the velocity of the wave. Figure 1.1 shows this wave with $\xi = 5, x_0 = 0$and $t = 0$.[6]

$$u(x,0)$$

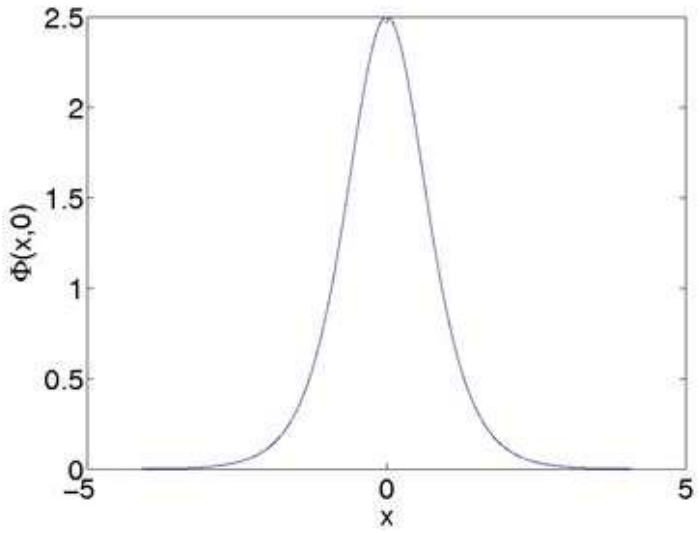


Figure 1. A solution of the equation (*) at $t = 0$

Exponential rational function method.

Exponential function method is a powerful tool for finding exact solutions of many nonlinear partial differential equations. It is a direct and efficient approach that is applicable for many nonlinear PDE's such as space–time fractional Fokas equation, the space–time fractional ZakharovKuznetsov Benjamin Bona Mahony, and the space–time fractional coupled Burgers' equations.

In this chapter, we describe the exponential rational function method. In order to describe the exponential rational function method, we consider the following nonlinear differential equation:

$$P(u, u_x, u_t, u_{xx}, u_{xt}, \dots) = 0, \qquad (1)$$

where$P$ is a (non)linear operator. For example, the following are some examples of nonlinear equations:

$$\frac{\partial u}{\partial t} + u\frac{\partial u}{\partial x} + \frac{\partial^3 u}{\partial x^3} = 0,$$

that is referred to as Korteweg-de Vries (KdV) equation.

In this chapter, we discuss the exact solution of the Benjamin–Bona–Mahony equation (in short BBM equation).

In 1972, the equation Korteweg–de Vries (KdV) has been improved by Benjamin, Bona, and Mahony to model long surface gravity waves including small amplitude propagating 1+1 dimensions. It is given by

$$\frac{\partial u}{\partial t}+\frac{\partial u}{\partial x}+u\frac{\partial u}{\partial x}-\frac{\partial^3 u}{\partial x^2\partial t}=0. \qquad (2)$$

The remarkable behavior of the solution for the equation (1) is similar to the following (KdV) equation ([1]):

$$\frac{\partial u}{\partial t}+\frac{\partial u}{\partial x}+u\frac{\partial u}{\partial x}+\frac{\partial^3 u}{\partial x^3}=0. \qquad (3)$$

Let us consider the equation (2) with the initial value

$$u(x,0)=\phi(x), \quad x\in\mathbb{R} \qquad (4)$$

Where ϕ is a positive and sufficiently smooth function and decays at infinity. In [1] it is shown that the equation (3) with initial condition (4) has at least soluiton wave propagating undiminished in amplitude as t increases. The BBM equation (3) includes many applications especially in hydromagnetic waves in cold plasma, acoustic-gravity waves in compressible fluids and the acoustic waves in anharmonic crystals [2,7]. One of the important differences of KdV equation and BBM equation is that the BBM equation has unique solution and stable while the KdV equation is unstable as wavenumber components increases. Another difference is that the BBM equation has just three number of motion integrals while the KdV has infinite number [4,9].

The linearized form of (1) is as follows:

$$\frac{\partial u}{\partial t}+\frac{\partial u}{\partial x}-\frac{\partial^3 u}{\partial x^2\partial t}=0. \qquad (5)$$

The general solution of this equation can be given by

$$u(x,t)=ae^{i(kx-wt)}. \qquad (6)$$

Substituting the solution (6) in (5), we have

$$-awie^{i(kx-wt)}+kaie^{i(kx-wt)}+ak^2wi^3e^{i(kx-wt)}=0.$$

Multiplying both side of this equation in i implies

$$aw-ka+ak^2w=0.$$

This means

$$w=\frac{k}{1+k^2},$$

where$w$ is the angular frequency and k is the wavenumber.

A generalization of BBM equation (1) can be given as follows

$$\frac{\partial u}{\partial t}+\frac{\partial u}{\partial x}+(au^n+bu^{2n})\frac{\partial u}{\partial x}-c\frac{\partial^3 u}{\partial x^2\partial t}=0, \qquad (7)$$

where the parameters a, b, c and n are constant values.

It is well known that the solution of equation (4) has exact solution in the particular case of $b = 0$and $n = 1$, that is in the following case:

$$\frac{\partial u}{\partial t}+\frac{\partial u}{\partial x}+au\frac{\partial u}{\partial x}-c\frac{\partial^3 u}{\partial x^2\partial t}=0. \qquad (8)$$

A generalization of BBM equation (2) also can be given as follows

$$\frac{\partial u}{\partial t}+a\frac{\partial u}{\partial x}+(bu^n+cu^{2n})\frac{\partial u}{\partial x}+d\frac{\partial^3 u}{\partial x^3}=0, \qquad (9)$$

Generalized exponential rational function method

In this section, we present generalized exponential rational function method that is abbreviated by GERFM. We use it to find an exact solution for some equations that we present in the sequel. The main step of this method is given as follows [3]:

Let the nonlinear form of a partial differential equation be given by

$$L\left\{\psi,\frac{\partial\psi}{\partial x},\frac{\partial\psi}{\partial t},\frac{\partial^2\psi}{\partial x^2},\cdots\right\}=0. \qquad (10)$$

Taking

$$\eta=\lambda\, x-\xi t, \qquad (11)$$

convert the equation (10) into the following nonlinear ordinary differential equation

$$L\{\psi,\psi',\psi'',\cdots\}=0, \qquad (12)$$

where

$$\psi=\psi(\eta),$$

and

$$\psi'=\frac{d\psi}{d\eta}, \qquad \psi''=\frac{d^2\psi}{d\eta^2}, \quad \cdots.$$

Let

$$\Theta(\eta)=\frac{a_1e^{b_1\eta}+a_2e^{b_2\eta}}{a_3e^{b_3\eta}+a_4e^{b_4\eta}}. \qquad (13)$$

Now, assume that the solution of (12) is in the following form:

$$\psi(\eta) = p_0 + \sum_{k=1}^{M} p_k\big(\Theta(\eta)\big)^k + \sum_{k=1}^{M} q_k\big(\Theta(\eta)\big)^{-k}. \qquad (14)$$

Note: The constant values in (14) are considered in such a way that the solution of (14) is a solution for (12). The value of M is determined by the principle of homogenous balancing.

Substituting (14) into (12) ,we get an equation in terms of $\Theta(\eta)$ and from there, we derive an equation in terms of

$$e^{b_i\eta}, \qquad i = 1,2,3,4.$$

Taking zero the coefficients of

$$e^{\lambda_i\eta}, \ \ i = 0,1,\cdots$$

one can obtain the constant values

$$p_i, q_j, i = 0,1,\cdots,M, \qquad j = 1,2,\cdots,M$$

and

$$a_i, b_i, \ \ i = 1,2,3,4.$$

Solving GBBM equation by GERFM

In this section, we will discuss about a new exact solution for a class of improved KdV equation called Generalized Benjamin-Bona-Mahony that we abbreviate it by GBBM and it is defined by

$$\frac{\partial u}{\partial t} + a\frac{\partial u}{\partial x} + (bu^v + cu^{2v})\frac{\partial u}{\partial x} - d\frac{\partial^3 u}{\partial x^2 \partial t} = 0, \qquad (15)$$

where$u$ is the unknown value in terms of x and t and also the values of a, b, c, d and v are constant. Most of the statements in this chapter is presented in [2,5].

The solution exists in the case of $c = 0$ and $v = 1$ (see [1,7]). That is,

$$\frac{\partial u}{\partial t} + a\frac{\partial u}{\partial x} + bu\frac{\partial u}{\partial x} - d\frac{\partial^3 u}{\partial x^2 \partial t} = 0. \qquad (16)$$

We will use GERFM to find an exact solution for GBBM equation (1). For this sake, consider the transformation

$$u(x,t) = \psi(\eta), \qquad (17)$$

where

$$\eta = \lambda x - \xi t, \qquad (18)$$

withλ and ξ as constant values. Now, by (15), (17) and (18) we have$0 = \frac{\partial u}{\partial t} + a\frac{\partial u}{\partial x} + (bu^v + cu^{2v})\frac{\partial u}{\partial x} - d\frac{\partial^3 u}{\partial x^2 \partial t} = \frac{\partial \psi}{\partial t} + a\frac{\partial \psi}{\partial x} + (b\psi^v + c\psi^{2v})\frac{\partial \psi}{\partial x} - d\frac{\partial^3 \psi}{\partial x^2 \partial t} = \frac{d\psi}{d\eta} \times \frac{\partial \eta}{\partial t} + a\left(\frac{d\psi}{d\eta} \times \frac{\partial \eta}{\partial x}\right) + (b\psi^v + c\psi^{2v})\left(\frac{d\psi}{d\eta} \times \frac{\partial \eta}{\partial x}\right) - d\frac{\partial^2}{\partial x^2}\left(\frac{d\psi}{d\eta} \times \frac{\partial \eta}{\partial t}\right) = -\xi\frac{d\psi}{d\eta} + a\lambda\frac{d\psi}{d\eta} + (b\psi^v + c\psi^{2v})\lambda\frac{d\psi}{d\eta} - d\frac{\partial^2}{\partial x^2}\left(-\xi\frac{d\psi}{d\eta}\right) = [-\xi + a\lambda + (b\psi^v + c\psi^{2v})\lambda]\frac{d\psi}{d\eta} + d \times \xi\frac{\partial^2}{\partial x^2}\left(\frac{d\psi}{d\eta}\right) = [-\xi + a\lambda + (b\psi^v + c\psi^{2v})\lambda]\frac{d\psi}{d\eta} + d \times \xi\frac{\partial}{\partial x}\left(\frac{d\left(\frac{d\psi}{d\eta}\right)}{d\eta} \times \frac{\partial \eta}{\partial x}\right) = [-\xi + a\lambda + (b\psi^v + c\psi^{2v})\lambda]\frac{d\psi}{d\eta} + d \times \xi \times \lambda\frac{\partial}{\partial x}\left(\frac{d^2\psi}{d\eta^2}\right) = [-\xi + a\lambda + (b\psi^v + c\psi^{2v})\lambda]\frac{d\psi}{d\eta} + d \times \xi \times \lambda \times \left(\frac{d\left(\frac{d^2\psi}{d\eta^2}\right)}{d\eta} \times \frac{\partial \eta}{\partial x}\right) = [-\xi + a\lambda + (b\psi^v + c\psi^{2v})\lambda]\frac{d\psi}{d\eta} + d \times \xi \times \lambda \times \lambda \times \frac{d^3\psi}{d\eta^3} = [-\xi + a\lambda + (b\psi^v + c\psi^{2v})\lambda]\frac{d\psi}{d\eta} + d \times \xi\lambda^2\frac{d^3\psi}{d\eta^3}$. So, we have

$$0 = (-\xi + a\lambda)\frac{d\psi}{d\eta} + (b\psi^v + c\psi^{2v})\lambda\frac{d\psi}{d\eta} + d \times \xi\lambda^2\frac{d^3\psi}{d\eta^3}. \qquad (19)$$

Integrating both side of (19) reduce the order of equation (19) as follows:

$$0 = (-\xi + a\lambda)\psi + \left(b\frac{\psi^{v+1}}{v+1} + c\frac{\psi^{2v+1}}{2v+1}\right)\lambda + d \times \xi\lambda^2\frac{d^2\psi}{d\eta^2}. \qquad (20)$$

Taking the transformation

$$\psi := \psi^n$$

from (20), we have

$$0 = (-\xi + a\lambda)\psi^n + \left(b\frac{(\psi^n)^{v+1}}{v+1} + c\frac{(\psi^n)^{2v+1}}{2v+1}\right)\lambda + d \times \xi\lambda^2\frac{d^2(\psi^n)}{d\eta^2}$$
$$= (-\xi + a\lambda)\psi^n + \left(b\frac{\psi^{nv+n}}{v+1} + c\frac{\psi^{2nv+n}}{2v+1}\right)\lambda + d \times \xi\lambda^2\frac{d^2(\psi^n)}{d\eta^2}. \qquad (21)$$

On the other hand,

$$\frac{d^2(\psi^n)}{d\eta^2} = \frac{d}{d\eta}\left(\frac{d\psi^n}{d\eta}\right) = \frac{d}{d\eta}\left(n\frac{d\psi}{d\eta} \times \psi^{n-1}\right) = n\frac{d}{d\eta}\left(\frac{d\psi}{d\eta} \times \psi^{n-1}\right) = n\left(\psi^{n-1}\frac{d^2\psi}{d\eta^2} + (n-1)\frac{d\psi}{d\eta}\psi^{n-2} \times \frac{d\psi}{d\eta}\right)$$
$$= n\psi^{n-1}\frac{d^2\psi}{d\eta^2} + n(n-1)\psi^{n-2}\left(\frac{d\psi}{d\eta}\right)^2. \qquad (22)$$

Substituting (22) into (21) implies that $0 = (-\xi + a\lambda)\psi^n + \left(b\frac{\psi^{nv+n}}{v+1} + c\frac{\psi^{2nv+n}}{2v+1}\right)\lambda + d \times \xi\lambda^2 \frac{d^2(\psi^n)}{d\eta^2} = (-\xi + a\lambda)\psi^n + \left(b\frac{\psi^{nv+n}}{v+1} + c\frac{\psi^{2nv+n}}{2v+1}\right)\lambda + d \times \xi\lambda^2 \left[n\psi^{n-1}\frac{d^2\psi}{d\eta^2} + n(n-1)\psi^{n-2}\left(\frac{d\psi}{d\eta}\right)^2\right] = \psi^n \left[(-\xi + a\lambda) + \left(b\frac{\psi^{nv}}{v+1} + c\frac{\psi^{2nv}}{2v+1}\right)\lambda + d \times \xi\lambda^2 \left[n\psi^{-1}\frac{d^2\psi}{d\eta^2} + n(n-1)\psi^{-2}\left(\frac{d\psi}{d\eta}\right)^2\right]\right]$. (23)

By cancelling ψ^n both side of (23), we have

$$0 = (-\xi + a\lambda) + \left(b\frac{\psi^{nv}}{v+1} + c\frac{\psi^{2nv}}{2v+1}\right)\lambda + d \times \xi\lambda^2 \left[n\psi^{-1}\frac{d^2\psi}{d\eta^2} + n(n-1)\psi^{-2}\left(\frac{d\psi}{d\eta}\right)^2\right]. \quad (24)$$

Multiplying both side of (24) in ψ^2 yields:

$$0 = (-\xi + a\lambda)\psi^2 + \left(b\frac{\psi^{nv+2}}{v+1} + c\frac{\psi^{2nv+2}}{2v+1}\right)\lambda + d \times \xi\lambda^2 \left[n\psi\frac{d^2\psi}{d\eta^2} + n(n-1)\left(\frac{d\psi}{d\eta}\right)^2\right]. \quad (25)$$

By reordering the terms of (25), we have

$$0 = d \times \xi\lambda^2 n\left[\psi\frac{d^2\psi}{d\eta^2} + \frac{(-\xi + a\lambda)}{d \times \xi\lambda^2 n}\psi^2 + \frac{b}{d \times \xi\lambda n(v+1)}\psi^{nv+2} + \frac{c}{(2v+1)d \times \xi\lambda n}\psi^{2nv+2} + (n-1)\left(\frac{d\psi}{d\eta}\right)^2\right]. \quad (26)$$

This is simplified by

$$0 = \psi\frac{d^2\psi}{d\eta^2} + \frac{(-\xi + a\lambda)}{d \times \xi\lambda^2 n}\psi^2 + \frac{b}{d \times \xi\lambda n(v+1)}\psi^{nv+2} + \frac{c}{(2v+1)d \times \xi\lambda n}\psi^{2nv+2} + (n-1)\left(\frac{d\psi}{d\eta}\right)^2. \quad (27)$$

Taking

$$n = \frac{1}{v},$$

from (27), we have

$$0 = \psi\frac{d^2\psi}{d\eta^2} + \frac{v(-\xi + a\lambda)}{d \times \xi\lambda^2}\psi^2 + \frac{bv}{d \times \xi\lambda(v+1)}\psi^{1+2} + \frac{cv}{(2v+1)d \times \xi\lambda}\psi^{2+2} + \left(\frac{1}{v} - 1\right)\left(\frac{d\psi}{d\eta}\right)^2,$$

that is simplified by

$$0 = \psi\frac{d^2\psi}{d\eta^2} + \alpha_1\psi^2 + \alpha_2\psi^{1+2} + \alpha_3\psi^{2+2} + \alpha_4\left(\frac{d\psi}{d\eta}\right)^2, \quad (28)$$

where

$$\alpha_1 = \frac{v(-\xi + a\lambda)}{d \times \xi\lambda^2},$$

$$\alpha_2 = \frac{bv}{d \times \xi\lambda(v+1)},$$

$$\alpha_3 = \frac{cv}{(2v+1)d \times \xi\lambda},$$

and

$$\alpha_4 = \frac{1-v}{v}.$$

So, we have

$$0 = \psi\frac{d^2\psi}{d\eta^2} + \alpha_1\psi^2 + \alpha_2\psi^3 + \alpha_3\psi^4 + \alpha_4\left(\frac{d\psi}{d\eta}\right)^2. \qquad (29)$$

Now, in order to find the solitary solution of GBBM (15), we use the balancing principle between the order of ψ^4 and $\left(\frac{d\psi}{d\eta}\right)^2$. In other words, by putting (14) into (29), the greatest order of ψ^4 is $4M$ and the smallest degree of $\left(\frac{d\psi}{d\eta}\right)^2$ is $-2M-2$. Now, by taking

$$4M - 2M - 2 = 0,$$

We will have

$$M = 1.$$

So, the solution (14) will be

$$\psi(\eta) = p_0 + p_1\Theta(\eta) + q_1\Theta(\eta)^{-1}. \qquad (30)$$

Now, by putting (30) into (29), we have

$$\begin{aligned} 0 = (p_0 + p_1\Theta(\eta) + q_1\Theta(\eta)^{-1})\left(p_1\frac{d^2\Theta}{d\eta^2} - q_1\frac{d^2\Theta}{d\eta^2}\Theta(\eta)^{-2} + 2q_1\frac{d\Theta}{d\eta}\Theta^{-3}\right) + \alpha_1(p_0 + p_1\Theta(\eta) + q_1\Theta(\eta)^{-1})^2 \\ + \alpha_2(p_0 + p_1\Theta(\eta) + q_1\Theta(\eta)^{-1})^3 + \alpha_3(p_0 + p_1\Theta(\eta) + q_1\Theta(\eta)^{-1})^4 \\ + \alpha_4\left(p_1\frac{d\Theta}{d\eta} - q_1\frac{d\Theta}{d\eta}\Theta^{-2}\right)^2. \qquad (31) \end{aligned}$$

Substituting $\Theta(\eta)$ into (31) we will arrive a nonlinear equation in terms of $e^{\lambda_i\eta}$, for some i.

Taking zero the coefficients of $e^{\lambda_i\eta}$ we will arrive a nonlinear system of the equations. Solving this system by software MAPLE generate some solutions. Next, the solution $u(x,t)$ is derived from

$$u(x,t) = \psi^n = \psi^{1/v}.$$

By using GERFM, one can solve the equation (32).

Example01 We consider Equation (32) in which $v = \delta = 1$. In this case, the equation (24), will be

$$0 = a_1\psi\frac{d^2\psi}{d\eta^2} + a_2\frac{d\psi}{d\eta} + a_3\psi\frac{d\psi}{d\eta} - a_4\left(\frac{d\psi}{d\eta}\right)^2$$

We have considered

$$\Theta = \frac{1}{1+e^{\eta}},$$

Also,

$$\alpha_1 = -\epsilon\lambda^2,$$

$$\alpha_2 = -\xi + a\lambda,$$

$$\alpha_3 = b,$$

and

$$\alpha_4 = 0.$$

The exact solution will be

$$w(x,t) = \frac{1 - e^x + x(e-1)}{1 + t(e-1)}.$$

Example02 Wu-Zhang equation

In this section, we use the GERFM to find an exact solution for Wu-Zhang equation **[8]** whose general form is as follows:

$$\frac{\partial^2 u}{\partial t^2} + 2\frac{\partial u}{\partial x}\frac{\partial^2 u}{\partial x \partial t} + \frac{\partial u}{\partial t}\frac{\partial^2 u}{\partial x^2} + \frac{3}{2}\left(\frac{\partial u}{\partial x}\right)^2\frac{\partial^2 u}{\partial x^2} - \frac{1}{3}\frac{\partial^3 u}{\partial x^3} = 0. \qquad (33)$$

For this sake, again we consider the transformation

$$u(x,t) = \psi(\eta), \qquad (34)$$

where

$$\eta = \lambda x - \xi t,$$

withλ and ξ as constant values. Now, by (32), (33) and (34) we have

$$0 = \frac{\partial}{\partial t}\left(\frac{d\psi}{d\eta}\frac{\partial\eta}{\partial t}\right) + 2\left(\frac{d\psi}{d\eta}\frac{\partial\eta}{\partial x}\right)\frac{\partial}{\partial x}\left(\frac{d\psi}{d\eta}\frac{\partial\eta}{\partial t}\right) + \left(\frac{d\psi}{d\eta}\frac{\partial\eta}{\partial t}\right)\frac{\partial}{\partial x}\left(\frac{d\psi}{d\eta}\frac{\partial\eta}{\partial x}\right) + \frac{3}{2}\left(\frac{d\psi}{d\eta}\frac{\partial\eta}{\partial x}\right)^2\frac{\partial}{\partial x}\left(\frac{d\psi}{d\eta}\frac{\partial\eta}{\partial x}\right) - \frac{1}{3}\frac{\partial^2}{\partial x^2}\left(\frac{d\psi}{d\eta}\frac{\partial\psi}{\partial x}\right)$$

$$= -\xi\left(\frac{d^2\psi}{d\eta^2}\frac{\partial\eta}{\partial t}\right) + 2\lambda\frac{d\psi}{d\eta}\times(-\xi)\left(\frac{d^2\psi}{d\eta^2}\frac{\partial\eta}{\partial x}\right) - \xi\frac{d\psi}{d\eta}\times\lambda\left(\frac{d^2\psi}{d\eta^2}\frac{\partial\eta}{\partial x}\right) + \frac{3}{2}\lambda^2\left(\frac{d\psi}{d\eta}\right)^2$$

$$\times\lambda\left(\frac{d^2\psi}{d\eta^2}\frac{\partial\eta}{\partial x}\right) - \frac{1}{3}\lambda\frac{\partial}{\partial x}\left(\frac{d^2\psi}{d\eta^2}\frac{\partial\eta}{\partial x}\right)$$

$$= \xi^2\frac{d^2\psi}{d\eta^2} - 2\lambda^2\xi\frac{d\psi}{d\eta}\frac{\partial^2\psi}{\partial\eta^2} - \lambda^2\xi\frac{d\psi}{d\eta}\frac{\partial^2\psi}{\partial\eta^2} + \frac{3}{2}\lambda^4\left(\frac{d\psi}{d\eta}\right)^2\frac{d^2\psi}{d\eta^2} - \frac{1}{3}\lambda^3\frac{d^3\psi}{d\eta^3}.$$

So, we have

$$0 = \xi^2\frac{d^2\psi}{d\eta^2} - 3\lambda^2\xi\frac{d\psi}{d\eta}\frac{d^2\psi}{d\eta^2} + \frac{3}{2}\lambda^4\left(\frac{d\psi}{d\eta}\right)^2\frac{d^2\psi}{d\eta^2} - \frac{1}{3}\lambda^3\frac{d^3\psi}{d\eta^3}. \qquad (35)$$

Now, we consider the solution (7) by

$$\psi(\eta) = p_0 + p_1\Theta(\eta) + q_1\Theta(\eta)^{-1}. \qquad (36)$$

Now, by putting (36) into (35), we will arrive a nonlinear equation in terms of $e^{\lambda_i\eta}$, for some i.

Taking zero the coefficients of $e^{\lambda_i\eta}$ we will arrive a nonlinear system of the equations. Solving this system by software MAPLE generate some solutions. Next, the solution $u(x,t)$ is derived from

$$u(x,t) = \psi(\eta).$$

By using GERFM,we find

$$p_0 = 0, p_1 = 1, q_1 = 0,$$

$$a_1 = 2k, \qquad b_1 = k, a_2 = 0, a_3 = 1, b_3 = 1, a_4 = 1, b_4 = k.$$

Also,

$$\xi = -\frac{1}{\sqrt{3}}ik^2, \quad \lambda = 1.$$

Example03 Fisher equation

In this section, we will use the GERFM to find an exact solution for a type of nonlinear Fisher equation [11] given as follows:

$$\frac{\partial u}{\partial t} = \frac{\partial^2 u}{\partial x^2} + 2u(1-u^2) + \mu(1-u^2). \qquad (37)$$

For this sake, again we consider the transformation

$$u(x,t) = \psi(\eta), \qquad (38)$$

where

$$\eta = \lambda x - \xi t, \qquad (39)$$

withλ and ξ as constant values. Now, by (37), (38) and (39) we have

$$0 = \frac{d\psi}{d\eta}\frac{\partial \eta}{\partial t} - \frac{\partial}{\partial x}\left(\frac{d\psi}{d\eta}\frac{\partial \eta}{\partial x}\right) - 2\psi(1-\psi^2) - \mu(1-\psi^2) = -\xi\frac{d\psi}{d\eta} - \lambda\left(\frac{d^2\psi}{d\eta^2}\frac{\partial \eta}{\partial x}\right) - 2\psi(1-\psi^2) - \mu(1-\psi^2)$$
$$= -\xi\frac{d\psi}{d\eta} - \lambda^2\frac{d^2\psi}{d\eta^2} - 2\psi(1-\psi^2) - \mu(1-\psi^2)$$

So, we have

$$0 = \lambda^2\frac{d^2\psi}{d\eta^2} + \xi\frac{d\psi}{d\eta} + (2\psi+\mu)(1-\psi^2). \qquad (40)$$

Now, we consider the solution (14) by

$$\psi(\eta) = p_0 + p_1\Theta(\eta) + q_1\Theta(\eta)^{-1}. \qquad (41)$$

Now, by putting (41) into (37), we will arrive a nonlinear equation in terms of $e^{\lambda_i \eta}$, for some i.

Taking zero the coefficients of $e^{\lambda_i \eta}$ we will arrive a nonlinear system of the equations. Solving this system by software MAPLE generate some solutions. Next, the solution $u(x,t)$ is derived from :

$$u(x,t) = \psi(\eta).$$

By using GERFM, we find

$$p_0 = 1, p_1 = 1, q_1 = 0,$$

$$a_1 = -4a, \quad b_1 = 0, a_2 = (\mu+2)b, b_2 = 1, \quad a_3 = 2a, b_3 = 0, a_4 = 2b, b_4 = 1.$$

Also,

$$\xi = -\frac{(5\mu^2 + 36\mu + 36)}{4}, \quad \lambda = \frac{\mu+6}{2}.$$

Figure 2. shows this solution in the interval $[-1,1] \times [-1,1]$. In this figure, we considered $a = 1, b = 2, \mu = 1$.

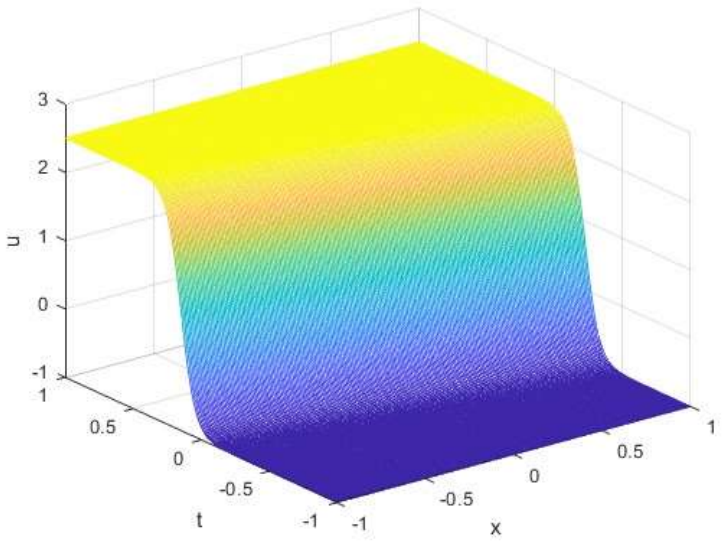


Figure 2. Exact solution for Fisher equation (1.2)

References

1. Albert J. (1989). On the Decay of Solutions of the Generalized Benjamin-Bona-Mahony Equation, Journal of mathematical analysis and applications, 141, 527-537.
2. Alsayyed, O., Jaradat, H. M., Jaradat, M. M. M., Mustafa, Z. &Shata, F. (2016). Multi-soliton solutions of the BBM equation arisen in shallow water, Journal of Nonlinear Sciences and its Applications, 9, 1807–1814.
3. Belobo, D.B.; Das, T. Solitary and Jacobi elliptic wave solutions of the generalized Benjamin–Bona–Mahony equation. Commun. Nonlinear Sci. Numer. Simulat. 2017, 48, 270–277.
4. Benjamin, T. B., Bona, J. L.&Mahony, J. J. (1972), Model Equations for Long Waves in Nonlinear Dispersive Systems, Philosophical Transactions of the Royal Society of London. Series A, Mathematical and Physical Sciences, 272 (1220): 47–78.
5. Ghanbari, B., Baleanu, D. & Al Qurashi, M. (2019). New Exact Solutions of the Generalized Benjamin–Bona–Mahony Equation. Symmetry. 11, 20. https://doi.org/10.3390/sym11010020
6. Gündoğdu H. &Gözükızıl O. F. (2017), Solving Benjamin-Bona-Mahony equation by using the sn-ns method and the tanh-coth method. MathematicaMoravica, 21(1), 95–103
7. Muatjetjeja, B. &Khalique, C. M. (2014). Benjamin–Bona–Mahony Equation with Variable Coefficients: Conservation Laws. Symmetry, 6, 1026–1036.
8. Mustafa, Kilic, Bulent, Karatas, Esra, Mohamed Al Qurashi, Maysaa', Baleanu, Dumitru and Tchier, Fairouz. "On soliton solutions of the Wu-Zhang system" Open Physics, vol. 14, no. 1, 2016, pp. 76-80. https://doi.org/10.1515/phys-2016-0004
9. Oliver, P. J. (1979), "Euler operators and conservation laws of the BBM equation", Mathematical Proceedings of the Cambridge Philosophical Society, 85: 143–160.
10. Earl D. Rainville ,Phillip E. Bedient (1981).Elementarydifferentionequation,sixthedation ,Macmillan Publishing Co., Inc.Printed in the United States of America,ISBN 0-02-397770-1.
11. 11.Taghizadeh N., Mirzazadeh M , Samiei A., Paghaleh S. &Vahidi J. (2012), Exact solutions of nonlinear evolution equations by using the modified simple equation method. Ain Shams Engineering Journal. 3(3), 321-32

[1] Zhang , Y., and Chen, Z. H.,2020,"A new exact solution of the space-fractional MKDV-ZK equation is obtained by the first integral method,"Practice and understanding of mathematics,50(13),pp. 243-250.

[2] Khalil, R., Alhorani, M., and Yousef, A., 2014," A new definition of fractional derivative," Journal of Computational and Applied Mathematics,264,pp. 65-70.

Evaluation The Efficacy of Ocimum Basilicum Extract & Antifungal Agents Against Some Pathogenic Filamentous Fungi

Ihsan Ali Alzamily [1], Hassan Ali Tamur [2], Murtadha M Hussein [3]

© 2023 The Author(s). This open access article is distributed under a Creative CommonsAttribution (CC-BY) 4.0 license.

Abstract: The widespread availability of chemical-based medications opened a way for researchers to look for alternatives, returning to the primary source of drugs. Plants have been utilized for their healing abilities since ancient times since they have been proved to cure diseases. some filamentous fungi used such as Aspergillus, Penicillium, Fusarium, Trichophyton and Cladosporium. The study included use of four types of antifungals agents, Ketoconazole, Fluconazole, Itraconazole and Nystatin, the study conducted that Fluconazole have the highest effect with inhibition zone of (37mm) against Aspergillus niger followed by Nystatin (24mm) against Trichophyton verrucosum, the antifungal Itraconazole came third with (23mm) against Trichophyton verrucosum and finally Ketoconazole with (21mm) against Aspergillus niger. Regarding to Ocimum basilicum extract, four concentrations 50%,25%,12.5% and 6.250 % respectively were used, the concentration of 25% had the highest effect with inhibition zone of (36mm) against Aspergillus flavus followed by concentration of 6.25 % with (35mm) against Penicillium expansum, concentration of 12.5 % with (33mm) against Penicillium expansum and finally concentration of 50 % with (22mm) against Aspergillus flavus. Synergistic test was done by mixing Ocimum basilicum extract with four types of antifungal agents, itraconazole with different concentrations gave good results with (Itra + 25% 39 mm) against Fusarium oxysporum followed by ketoconazole with (Keto+ 50% 30 mm) against Aspergillus Flavus, Nystatin with (Nyst + 50% 28 mm) against Aspergillus Flavus and finally Fluconazole with (Flu+12.5% 23 mm) against Trichophyton Verrucosum.

Key Words: Ocimum basilicum, Itraconazole, Synergistic, Trichophyton verrucosum.

Author details

[1– 2 – 3] Al-Qasim Green University, College of Biotechnology, Babylon, Iraq

Citation information

Cite this article as:

Alzamily, I.A., Tamur, H.A., Hussein, M.M., (July 2023), *Evaluation The Efficacy of Ocimum Basilicum Extract & Antifungal Agents Against Some Pathogenic Filamentous Fungi*, Proceedings of the Minar Congress, Turkey, (9) pp 65-76, DOI: http://dx.doi.org/10.47832/MinarCong9-6

http://dx.doi.org/10.47832/MinarCong9-6

1 ihsan@biotech.uoqasim.edu.iq orcid.org/0000-0003-1603-2966

2 hassanalsoltani805@gmail.com

3 murtada.bt85@gmail.com

Introduction

Fungi represent an eukaryotic organisms that are exist all over the world. It can be parasites or saprophytes, the former obtaining nutrients from a living host and the latter getting nutrients from decaying organic materials. Therefore, it is responsible for animal & plant diseases, having substantial medical & agricultural effects. Only a few fungi are primary pathogens. Fungal pathogens can cause diseases in both immunocompetent and immunocompromised individuals. Contrarily, most of filamentous fungi that cause disease in humans are opportunistic and demand the fulfillment of particular host requirements in order for infection to occur .Patients with impaired immune systems are most likely to become invasively infected by opportunistic microorganisms. (1). These fungi are categorized as a different kingdom from bacteria, protists, mammals, and plants.They are widespread in the inconspicuous & environment due to their small structures & mysterious lifestyles on the substrates they live on, with cell walls which consists of chitin, as opposed to walls of plant cell that consist of cellulose and walls of bacterial cell. It occurs naturally in various regions of the ecosystem & environment (2).A large number of known filamentous fungi belonging to the sub-Phylum "Pezizomycotina," that is part of Phylum "Ascomycota," which is also part of sub-kingdom Dikarya (3).Aspergillus, Fusarium,Penicillium, Cladosporium,Alternaria, Eurotium, Emericella, Curvularia, Paecilomyces, etc. are among the many genera of fungi that fall under the category of filamentous fungi.These genera have been more studied and found to occur more frequently than the other genera (4).

Currently, azoles,echinocandins and polyenes are three main types of antifungal drugs that clinicians utilize to treat fungal infections. Due to the limited availability of antifungal drugs, resistance has become a problem since some fungi can develop resistance to all three categories of antifungal drugs (5).Additionally, it is well recognized that amphotericin B, antifungal drug utilized for treatment of systemic infections, is linked to nephrotoxicity.Despite having a life-threatening fungal infection, its adverse effects and toxicity may be so severe that treatment must be discontinued (6). the emergence of resistance, the limits of currently existing antifungal medications and the increasing of fungal infections highlight the need of development of novel antifungal drugs, ideally with a different mode of action.After extraction and purification, many plants exhibit inhibitory efficiency against infections due to their phytochemicals and beneficial components because the prolonged and intensive utilization of industrial drugs, such as antibiotics, has different negative effects on human health, including allergies, poisoning, and other symptoms as well as different symptoms that result due to misuse of those antibiotics resulted the acquisition of pathogenic microbes resulting in formation of mutations against it (7).

Antimicrobial capabilities of medicinal plants are increasingly being documented worldwide.80% of the world's population, according to the World Health Organization, utilized plant extracts or their active ingredients as folk medicine in conventional treatments (8).Originally from Asia, sweet basil (Ocimum basilicum L.), also famous as "feslegen or reyhan" in Turkey, is grown frequently from seed as an ornamental or field crop in

Mediterranean nations. (9). O. basilicum leaves and flowering parts have traditionally been utilized as aromatic, antispasmodic, digestive, carminative, stomachic,galactogogue and tonic agents (10). They've also been utilized as a folk treatment to cure poor digestion,feverish illnesses, abdominal pains,nausea, gastro-enteritis, insomnia,migraine, gonorrhea, melancholy, chronic diarrhea exhaustion and dysentery.They have been used topically to treat skin infections, acne, snake bites ,insect stings and smell loss (11).Anyway, O. basilicum, as many other Ocimum species, has received little attention in terms of antibacterial activity.In recent years, {multiple drug resistance (MDR)} have developed in both human and plant pathogenic bacteria due to excessive consumption of commercial antimicrobial drugs frequently utilized to treat infectious diseases. Besides to this issue, antibiotics can also be linked with adverse effects in the host such as immunosuppression, allergic reactions and hypersensitivity.As a result, alternative antimicrobial medications for the treatment of infectious diseases from other sources, especially medicinal plants, are required. (10).

Research aim to assess the efficacy of O. basilicum extract against some filamentous fungi and compare its effect with antifungal agents. Also assessment the synergism role between these extracts and antifungal agents.

Materials and methods

Organisms source:

Isolation

Fungal strains were collected from Alqasim green university Laboratories.

Morphological identification

Morphological identification depending on the macro-features including appearance of the colony, such as its color and shape, and texture and micro-features under microscope such as fungal hyphae, sporangia and sporangiophore (12).

Preparation of plant extract

Leaves of plant was purchased from local markets of AlQasim city.plant materials were properly washed to eliminate soil and other contaminants and it was air dried before before milling the leaves in a miller for powder and storing the powder in glassy tins for the duration of the extraction.Using a Soxhlet extractor, the air-dried plant materials were extracted twice in room temperature with ethanol 95% (500 ml/100 g of plant material per run). The final ethanol extract of plant parts was filtered utilizing filter paper (Whatman), then evaporated at a 40°C in oven, and kept at -20 °C for additional analysis (13).

Preparation of serial dilutions of plant extract:

Two fold serial dilution of alcoholic plant extracts were prepared in sterilized test tubes with sterile DMSO beginning from undiluted 100% and 50%, 25%, 12.5% and 6.25%.

Antifungal Drug Susceptibility Testing

Preparation of fungal inoculum

A suspension containing fungal conidia was made by harvesting 10-day-old samples grown on a PDA. To release and capture conidia from the mycelium, 20 mL of 0.1% Tween 80 was added to the surface of the fungal cultures. By adding saline, the density of the fungal conidia inoculum was adjusted to 10^6 CFU/mL (McFarland 2) (14). This inoculum used for both antibiotics and plant extract assay.

Disc diffusion method:

Antifungal susceptibility testing was carried out in accordance with the National Committee for Clinical Laboratory Standards (M38-A) proposals.Strains are subcultured on PDA and incubated at 28 C for one week in order to promote sporulation.Conidia extracted in sterile saline after growth, then the conidial suspension was adjusted to 10×10^6. The discs used were Itraconazole, Fluconazole Ketoconazole and Nystatin. A sterile cotton swab dipped into the suspension of the standardized inoculums was used to streak the plates uniformly in three directions. After allowing the plates to dry, antifungal discs were added to the medium.every disc firmly placed on the agar surface, distributed equally. After that, plates were incubated at 28 °C. plates were checked 3-5 days after it had been incubated.Inhibition zones were all consistently circular, with a confluent lawn of growth. Zones diameters of complete inhibition were measured with an inhibition zone scale (15).

Disc Diffusion Method for plant extract:

O. basilicum (sweet basil) was utilized to test antifungal activity against fungal isolates. Six (6) mm sterile paper discs were soaked in the alcoholic extract for around (60 min) to allow the extracts absorption. The discs were carefully inoculated into the plates with the labeled test organisms. For 5 days, the plates were incubated. Zones of Inhibition were measured after 5 days of incubation (16).

Synergistic test

The same test done as the four types of antifungals were saturated with alcoholic extracts for around (60 min) to allow extracts absorption and then discs inoculated into the plates that incubated for 5 days and then the inhibition zone diameter was measured (17).

4- Results and discussion

4-1- Identification of isolates

Isolates provided from the source were revived, subcultured on Sabouraud's agar then incubated for 5 days at 28 °C. the resulting of subcultured was five genera as follwos in **table (1)**:

Table 1.

No	Fungal isolates	
1	Aspergillus	*Aspergillus niger*
		Aspergillus flavus
2	Penicillium	*Penicillium expansum*
3	Trichophyton	*Trichophyton verrucosum*
4	Fusarium	*Fusarium oxysporum*
5	Cladosporium spp.	

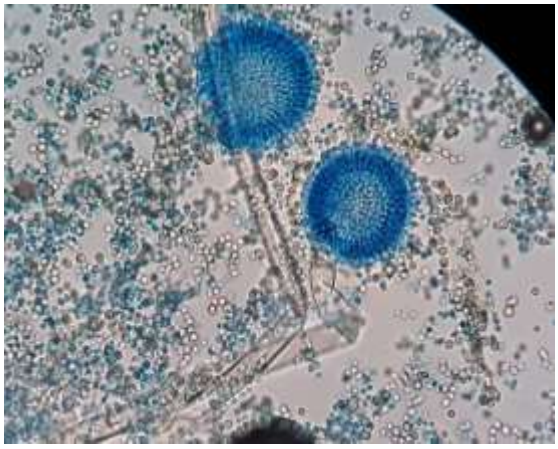


Figure 1. *Aspergillus niger (100x)*



Figure 2. Penicillium expansum (100x)

4-2- Effect of antibiotics against fungal isolates

The results as shown in Table No. 3, regarding to the effect of antifungal Fluconazole had the highest effect on the fungi under study, as highest inhibition zone was against the fungus, *Aspergillus niger* (37mm) , *Fusarium oxysporum* (35mm), *Aspergillus flavus* (33mm), *Penicillium expansum*(30mm), Cladosporium spp. (23mm), *Trichophyton verrucosum* (22mm) respectively. As for the antifungal Nystatin was the second in terms of effect on *Trichophyton verrucosum* (24mm), *Aspergillus niger* and *Fusarium oxysporum* (22mm), *Penicillium expansum* and Cladosporium spp. (20mm) and finally *Aspergillus flavus* (19mm).The third antifungal Itraconazole in terms of impact on *Trichophyton verrucosum* (23mm), *Aspergillus niger* and *Fusarium oxysporum* (21mm), *Penicillium expansum* (19mm), *Aspergillus flavus* and Cladosporium spp.(18mm).Finally,the antifungal Ketoconazole was less effect on fungal isolates , *Aspergillus niger* (21mm), *Trichophyton verrucosum* (15mm), *Fusarium oxysporum* (14mm), *Penicillium expansum* (11mm), Cladosporium spp. (10mm)and *Aspergillus flavus*

(5mm) respectively.According to certain findings, higher concentrations of Itraconazole & Ketoconazole were required to inhibit the filamentous fungal isolates (18).The triazole type of antifungal medications acts via interfering with sterol biosynthesis, which is a multistep process that involves conversion of lanosterol to ergosterol.Azoles, in particular, inhibiting lanosterol 14-demethylase (P45014dm), a cytochrome P450-dependent enzyme with a heme moiety in its active site. The iron atom in the P45014dm heme group is bound to azole compounds via an unrestricted nitrogen in the azole ring Through an unconstrained nitrogen in the azole ring, azole compounds bond to the iron atom within the P45014dm heme group. The azole-heme complex then prevents lanosterol demethylation, which is required for ergosterol synthesis. The loss of ergosterol, together with the accumulation of lanosterol and other methylated sterol precursors, impairs fungal membrane function and structure (1).



Figure 3. Effect of antifungal agents on *Trichophyton verrucosum*



Figure 4. Effect of antifungal agents on *Aspergiluus niger*

Table .2 Antibiotics against fungal isolates (Inhibition zone/ mm)

No	Fungal isolates	Keto	Flu	Itra	Nyst
1	*Aspergillus niger*	**21**	**37**	**21**	**22**
2	*Aspergillus flavus*	**5**	**33**	**18**	**19**
3	*Penicillium expansum*	**11**	**30**	**19**	**20**
4	*Trichophyton verrucosum*	**15**	**22**	**23**	**24**
5	*Fusarium oxysporum*	**14**	**35**	**21**	**22**
6	Cladosporium spp.	**10**	**23**	**18**	**20**

4-3- Effect of *Ocimum basilicum* extract on fungal isolates

Basil extracts effect on the fungal isolates done via four different concentrations: 50%, 25%, 12.5%, and 6.25% respectively. As we can see in the table (4), the results are uneven, as the concentration of 25% recorded the highest rates of inhibition for the fungi used in the study, *Aspergillus flavus* (36mm), *Trichophyton verrucosum* (26mm), *Penicillium expansum* and

Fusarium oxysporum (25mm), Cladosporium spp. (20mm) and finally *Aspergillus niger* (17mm).Also the concentration 6.25 % came second , *Penicillium expansum* (35mm), *Aspergillus flavus* (24mm), *Trichophyton verrucosum* and *Fusarium oxysporum* (20mm), *Aspergillus niger* and Cladosporium spp. (15mm).The third concentration 12.5 % , *Penicillium expansum* (33mm), *Aspergillus flavus* (25mm), *Fusarium oxysporum* (19mm), *Trichophyton verrucosum* (18mm), *Aspergillus niger* (15mm) and finally Cladosporium spp. (14mm).The last concentration was 50 % , Aspergillus flavus (22mm), Trichophyton verrucosum (20mm), Penicillium expansum (19mm), Cladosporium spp. (15mm), Fusarium oxysporum (10mm) and finally Aspergillus niger (12mm). Reuveni et al. (19) investigated the proportion of inhibition of basil components against *Fusarium oxysporum*. They observed that the eugenol had the highest percentage of inhibition (100%) against *Fusarium oxysporum*, while linalol and methyl chavicol had inhibition percentages of 26.4 and 30.3%.As well as inhibiting growth, the basil extract induced alterations in the micro & macro morphology of fungi. Reduced aerial mycelium growth was found at greater concentrations in all tested Fusarium species, with higher medium pigmentation in the case of F. verticillioides & F. proliferatum (20). O. basilicum has over 100 bioactive components, which include electrolytes,vitamins, phytonutrients and minerals (21). The chemicalcompositions of essential oils of O. basilicum contain cineole, methyl chavicol (estragole), eugenol, elemicin, methyl eugenol, rosmarinic acid, myristicin, apigenin,linalool, methyl cinnamate and ursolic acid (22).

Table 3. Ocimum basilicum extracts against fungal isolates (Inhibition zone /mm)

No	**Fungal isolates**	***Ocimum basilicum* extract**			
		50%	**25%**	**12.5%**	**6.25%**
1	*Aspergillus niger*	**12**	**17**	**15**	**15**
2	*Aspergillus flavus*	**22**	**36**	**25**	**24**
3	*Penicillium expansum*	**19**	**25**	**33**	**35**
4	*Trichophyton verrucosum*	**20**	**26**	**18**	**20**
5	*Fusarium oxysporum*	**10**	**25**	**19**	**20**
6	Cladosporium spp.	**15**	**20**	**14**	**15**



Figure 5. Effect of Ocimum basilicum extract on fungal isolates (*Trichophyton verrucosum*)



Figure 6. Effect of Ocimum basilicum extract on fungal isolates *(Aspergillus niger*)



Figure 7. Effect of Ocimum basilicum extracts on fungal isolates (*Aspergillus flavus*)

Effect of Synergistic between *Ocimum basilicum* extract and antifungal agents

The results showed in Table No. (5) the potent effect on the isolates as a result of mixing the antibiotic with basil extract, as mixing the antibiotic itraconazole with different concentrations gave good results, which are: *Fusarium oxysporum* (Itra + 25% 39 mm), *Aspergillus flavus* (Itra + 50% 37 mm), *Trichophyton verrucosum* (Itra + 12.5%32 mm) and finally *Penicillium expansum* (Itra + 6.25% 21mm). The second potent effect was by mixing the antifungal ketoconazole with different concentrations, *Aspergillus Flavus* (Keto+ 50% 30 mm) and *Trichophyton verrucosum* (Keto+ 12.5% 30 mm), *Penicillium expansum* (Keto+ 6.25% 20 mm) and finally *Fusarium oxysporum* (Keto+ 25% 9 mm). The antifungal Nystatin followed the Itraconazole and Ketoconazole by affecting the fungal isolates , *Aspergillus Flavus* (Nyst +

50% 28 mm), *Penicillium Expansum* (Nyst + 6.25% 26 mm), Trichophyton Verrucosum (Nyst + 12.5% 25 mm) and *Fusarium Oxysporum* (Nyst + 25% 12 mm) respectively. Finally, the antifungal Fluconazole was the last one in affecting fungal strains , *Trichophyton Verrucosum* (Flu+12.5% 23 mm), *Aspergillus Flavus* (Flu+50% 22 mm), Penicillium Expansum (Flu+6.25% 20 mm) and Fusarium Oxysporum (Flu+25% 11 mm) respectively.Basil essential oils' antibacterial properties are mostly related to their principal constituents. One compound's synergistic or antagonistic effects with minor percentage in the mixture as a whole must be taken into account (23).

Table 4. Synergism between Ocimum basilicum extract concentrations and antibiotics

No	**Fungal isolates**	**Synergistic test**			
1	*Aspergillus flavus*	**Keto+ 50%**	**Flu+ 50%**	**Itra + 50%**	**Nyst + 50%**
		30 mm	**22 mm**	**37 mm**	**28 mm**
2	*Fusarium oxysporum*	**Keto+ 25%**	**Flu+ 25%**	**Itra + 25%**	**Nyst + 25%**
		9 mm	**11 mm**	**39 mm**	**12 mm**
3	*Trichophyton verrucosum*	**Keto+ 12.5%**	**Flu+ 12.5%**	**Itra + 12.5%**	**Nyst + 12.5%**
		30 mm	**23 mm**	**32 mm**	**25 mm**
4	*Penicillium expansum*	**Keto+ 6.25%**	**Flu+ 6.25%**	**Itra + 6.25%**	**Nyst + 6.25%**
		20 mm	**20 mm**	**21mm**	**26 mm**



Figure 8. Synergistic between antifungals and plant extratct concentration (25%)



Figure 9. Synergistic between antifungals and plant extratct concentration (50%)



Figure 10. Synergistic between antifungals and plant extratct concentration (12.5%)



Figure 11. Synergistic between antifungals and plant extratct concentration (6.25%)

Conclusions

According to the findings, it is possible to draw the conclusion that sweet basil's alcoholic extract contain eight of the main phytochemicals, which include saponin,tannins, alkaloids, flavonoids, terpenoids, steroids, glycosides and resins, that are crucial for the antifungal & antibacterial activity found in these. Additionally, due to these phytochemicals, sweet basil extracts may be effective in therapeutic treatment due to their antibacterial & antifungal properties.Aromatic and medicinal plant components, such as leaves,shoots, seeds,roots, etc. are important sources of therapeutic substances in alternative and complementary medicine.Additionally, the abundance of bioactive chemicals, sometimes referred to as secondary metabolites, found in these plants, such as flavonoids, alkaloids, saponins,phenols, etc., has been linked to their antioxidant potential.

References

1. Powers-Fletcher MV, Kendall BA, Griffin AT, Hanson KE. 2016. Filamentous fungi. Microbiol Spectrum 4(3):DMIH2-0002-2015. doi:10.1128/microbiolspec.DMIH2-0002-2015.
2. Pitt, J.I., Samson, R.A. and Frisvad, J.C. (2000) List of Accepted Species and Their Synonyms in the Family Trichocomaceae. In: Samson, R.A. and Pitt, J.I., Eds., Integration of Modern Taxonomic Methods for Penicillium and Aspergillus Classification, Harwood, Amsterdam, 9-49.
3. Moretti, A.N. (2009) Taxonomy of Fusarium Genus, a Continuous Fight between Lumpers and Splitters. Proceedings of the National Academy of Sciences, 117, 7-13. https://doi.org/10.2298/zmspn0917007m.
4. Pitt, J.I. and Hocking, A.D. (1997) Primary Keys and Miscellaneous Fungi. Fungi and Food Spoilage, 2nd Edition, Blackie Academic and Professional, London, Weinheim, New York, Tokyo, Melbourne, Madras, 59-171. https://doi.org/10.1007/978-1-4615-6391-4_5.
5. Ostrowsky, B.; Greenko, J.; Adams, E.; Quinn, M.; O'Brien, B.; Chaturvedi, V.; Berkow, E.; Vallabhaneni, S.; Forsberg, K.; Chaturvedi, S.; et al. Candida auris isolates resistant to three classes of antifungal medications—New York, 2019. MMWR. Morb. Mortal. Wkly. Rep. 2020, 69, 6–9.
6. White, J.K.; Lund Nielsen, J.; Poulsen, J.S.; Madsen, A.M.; Lenart-Boró, A.; Chmiel, M.; Colbeck, I. Antifungal resistance in isolates of aspergillus from a pig farm. Atmosphere 2021, 12, 826.
7. Al- Janabi, J. K.; and Saberin, A. K.; (2014). The efficiency of green tea extracts and scholars in the growth of mentagrophytes mushrooms, The Journal of The University of Babylon Pure and Applied Sciences, 22 (2): 651-660.
8. Ahmad I, Beg AZ. Antimicrobial and phtytochemical studies on 45 Indian medicinal plants against multi-drug resistant human pathogens. J Ethnopharmacol 74: 113-123, 2001.
9. Reuveni R, Raviv M, Krasnovsky A et al. Compost inducesprotection against Fusarium oxysporum in sweet basil. Crop Protection 21: 583-587, 2002.
10. Adigüzel, A., Güllüce, M., Şengül, M., Öğütcü, H., Şahin, F., & Karaman, İ. (2005). Antimicrobial effects of Ocimum basilicum (Labiatae) extract. Turkish Journal of Biology, 29(3), 155-160.
11. Martin KW, Ernst E. Herbal medicines for treatment of fungal infections: a systematic review of controlled clinical trials. Mycoses 47: 87-92, 2004.
12. Webster, J. and Weber, R. (2007). Introduction to fungi. Cambridge university press.
13. Mahasneh, A.M. (2002). Screening of some indigenous Qatari medicinal plants for antimicrobial activity. Phytother Res., 16: 751-753.
14. Harčárová, M., Čonková, E., Proškovcová, M., Váczi, P., Marcinčáková, D., & Bujňák, L. (2021). Comparison of antifungal activity of selected essential oils against Fusarium

graminearum in vitro. Annals of Agricultural and Environmental Medicine, 28(3), 414-418.

15. Namidi, M. H., Ananthnaraja, T., & Satyasai, B. (2021). Antifungal Susceptibility Testing of Dermatophytes by ABDD and E-Test, a Comparative Study. Open Journal of Medical Microbiology, 11(3), 129-143.
16. Jacob, J. K. S., Carlos, R. C. A., & Divina, C. C. (2016). Phytochemical composition, antibacterial and antifungal activities of sweet basil (Ocimum basilicum). Advances in Environmental Biology, (7), 84-90.
17. Ahmad, A., Khan, A., Manzoor, N. & Khan, L. A. (2010). Evolution of ergosterol biosynthesis inhibitors as fungicidal against Candida. Microb Pathog 48, 35–41.
18. Shobana, C. S., Mythili, A., Homa, M., Galgóczy, L., Priya, R., Singh, Y. B., ... & Manikandan, P. (2015). In vitro susceptibility of filamentous fungi from mycotic keratitis to azole drugs. Journal de Mycologie Médicale, 25(1), 44-49.
19. Reuveni R, Fleisher A, Putievsky E (1984). Fungistatic activity of essential oils from Ocimum basilicum chemotypes. J. Phytopathol., 110: 20-22.
20. Kocić-Tanackov, S., Dimić, G., Lević, J., Tanackov, I., & Tuco, D. (2011). Antifungal activities of basil (Ocimum basilicum L.) extract on Fusarium species. African Journal of Biotechnology, 10(50), 10188-10195.
21. Da Costa, A. S., Arrigoni-Blank, M. D. F., Carvalho Filho, J. L. S. D., De Santana, A. D. D., Santos, D. D. A., Alves, P. B., et al. (2015). Chemical Diversity in Basil (Ocimum sp.) Germplasm. Scientific World J. 2015, 352638. doi:10.1155/2015/352638.
22. Senthoorraja, R., Subaharan, K., Manjunath, S., Pragadheesh, V. S., Bakthavatsalam, N., Mohan, M. G., et al. (2021). Electrophysiological, Behavioural and Biochemical Effect of Ocimum Basilicum Oil and its Constituents Methyl Chavicol and Linalool on Musca domestica L. Environ. Sci. Pollut. Res. Int. 28, 50565–50578. doi:10.1007/s11356-021-14282-x.
23. Daferera DJ, Ziogas BN, Polissiou MG (2003). The effectiveness of plant essential oils in the growth of Botrytis cinerea, Fusarium sp. And Clavibacter michiganensis subsp. michiganensis. Crop Prot., 22: 39- 44.

Codebook Design Method for Astronomical Images Compression

Maha A. Hameed [1]

© 2023 The Author(s). This open access article is distributed under a Creative CommonsAttribution (CC-BY) 4.0 license.

Abstract: The searching in binary codebook of a combination the Block Truncation Coding and Vector Quantization methods BTC and VQ desires a time consuming process because the full codebook search for every input vector toward discovery the best matched codevector or code word, so, in this paper, at first, a small binary codebook has been designed then by applying a new way which has been adopted by rotating each codevector such as the idea of codevector rotation in four direction then classified all these codevectors depending on direction of rotation to involve four codebooks (i.e. I, II, III and IV). In this case, the time of coding procedure is decreased with very small Distortion for each block additionally to that, an efficiency of coding process is improved with increasing in the compression ratio.

Key Words: Images compression, BTC and VQ method, bit map, codevector and rotating of block.

Author details

[1] Department of Astronomy and space, College of Science, University of Baghdad, Iraq

Citation information

Cite this article as:

Hameed, M.A., (July 2023), *Codebook Design Method for Astronomical Images Compression*, Proceedings of the Minar Congress, Turkey, (9) pp 77-82, DOI: http://dx.doi.org/10.47832/MinarCong9-7

http://dx.doi.org/10.47832/MinarCong9-7

[1] maha.hameed@sc.uobaghdad.edu.iq

Introduction

The idea of implementing the compression methods on images is to help the user towards reduce the space which is required to transmit the data of images or store the information of these images, this idea can be by applying many numerous methods on an original of digital image for compressing its data. At first the method of BTC was introduced via Delp and Mitchell. This method achieves 2 bits/pixel also the complexity of computational will be small [1], where BTC has an improvement of being very simple in an implement compared with VQ [2]. In BTC coding's system, firstly the image is divided into a number of uniform blocks, the two reconstruction values and the bit plane (binary image), for every block, are founded, but in the system of decoding, coded blocks are reconstructed using this bit plane and these reconstruction values. In this work, Vector Quantization is used in order to code the bit map of this image, where this method is a very popular method for compressing image, the main advantages for using this method are succeed high ratio of compression and easy process in decoding (Look- Up table), the problem in this method is that it requires a larger time in the process of matching [3]. In this paper, after designing a small binary codebook, an improvement method of coding is adaptive when the coder rotate the codevector blocks in four direction, after that classify all these codevectors depending on rotation's direction to involve four codebooks (i.e. multi- codebook design) instead of the small binary codebook, where the number of codebook (no. of codevectors) increased three times, thus the chance will be good to find the best matching codevector for each input vector, this leads to lessening in the bit rate then increasing in the ratio of compression all these enables to decrease the coding time with small deterioration in performance; in other word, the improved method is enable to increase the coding efficiency.

Block Truncation Compression method

BTC includes low storage requirements through simple and fast coding - decoding procedures [1, 4]. This technique can easily describe as follow, at first, an image is divided into uniform blocks, each block has size "*N*x*N*", the mean μ and the standard deviation σ (i.e. the two reconstruction levels) are computed for each block because these values change from block to another. the bit plane form is created too as follow, in every block. If a value of any pixel is equal to or larger than μ of this block's pixels the corresponding pixel in bit-map or binary image will take "1" value, else it will take "0" value. In decoding, for any block in bit-map, the pixel positions which has "1" value is changed by *a* value, but the remained pixels which has "0" value is changed by *b* value. These values (*a* and *b*) are given by;

$$a = \mu - \sigma\sqrt{q \div (n-q)} \qquad (1)$$

$$b = \mu + \sigma\sqrt{(n-q) \div q} \qquad (2)$$

Where, in each block, μ is used as threshold, *n* is number of pixels and *q* is number of pixels in any block which have values larger than or equal to threshold value.

Vector Quantization

Vector Quantization can be implement in these steeps, the first step is vector formatting, that is divided the input image into number of input vectors X_i. In the second steep, the Codebook C is designed where it has K codevectors Cv_1, Cv_2,.., Cv_k. Finally, Any input vector is quantized by determining the closest codevectors Cv_j (i.e. best matching) in this Codebook and the corresponding index of matched codevector is transmitted [2]. where the best matching is calculated using the minimum square distortion equation;

$$d_i = d_{\min(X_i, Cv_j)} \qquad (3)$$

In this process, compression is achieved when the coder transmit an index, where in this method the user requires fewer bits than transmitting vector itself.

The main advantage of this method is simplifying in decoding process, but the encoding process is, really, intensive in computationally process [5].

Block Rotation

In this paper, we solve and advance the problem of the time consuming in coding process when run the matching procedure in VQ method (i.e. the full searching in large codebook), by choosing small number of codevectors (small codebook) and rotating these in three dimensions, in other word, the result of this product is a multi- codebook design from small codebook.

The procedure method's description

The proposed method depends on the fact that, the quantization by using only a few number of the obtainable codevectors to code a large number of successive input image's vectors. Consequently, a codevector which has just been used in likely it has used again after rotating it to code the following entering vectors. In adopted method, the overall procedures can be describe in steps;

- Step 1: Design a binary codebook of small size (i.e. C), then divided an image into number of uniform blocks k.
- Step 2: Take an input vector from input image.
- Step 3: Compare each input vector with the codevectors using eq. 3, if they matched with each other then go to step 6. Else continue.
- Step 4: Compare this input vector with the rotational modes of the codevectors into (***II, III and IV***), it may be identify the best matching with one of these rotation codevectors.
- Step 5: Transmit an index of the nearest coded vector which identify the best matching and an index of rotational modes which identify the best matching too (i.e. **1 for *II*, 2 for *III* or 3 for *IV***) to the receiver. Go to step 7.

- Step 6: Transmit an index of this coded vector (which identify the best matching) and put its rotational mode ***I*** as index **0** then transmit these indices.
- Step 7: Increment the number of input image's blocks 'one' (i.e. no=no+1).
- Step 8: If no = k then end, otherwise go to step 2.

Experimental results

In this work, we have adopted a method for achieving the high ratio in compression of the gray image, where, firstly, designing a small binary codebook after that, rotating each codevector in the codebook in order to involve four codebooks instead of the small binary codebook, in this case, one can achieve increasing in compression ratio also decreasing in the bit rate and reducing in the time of searching with same quality for decoding image that achieved through implement full search method using large codebook (i.e. original method of VQ). In experimental results we have implemented several simulations when we applying our method on Astronomical image "Moon" in different codebook size and block size, After that finding the efficiencies of applying our scheme all these can be illustrate in table 1.

Table 1. The performance of the proposed method on "Moon" image.

Codebook size	Block size	Compression ratio	Bit rate	Distortion per block	PSNR
16	4x4	6.40	1.250	6.166	32.444
	8x8	23.60	.313	27.003	29.961
32	4x4	6.10	1.312	5.373	33.11
	8x8	22.38	0.338	25.907	30.02
64	4x4	5.82	1.375	4.767	33.68
	8x8	20.27	0.344	25.022	30.13



a **b** **c** **d**

a. Original image.
b. Decoding image, 4x4 block size and 64 codebook size.
c. Decoding image, 4x4 block size and 32 codebook size.
d. Decoding image, 8x8 block size and 32 codebook size.

Figure 1. Coding- decoding "Moon" image.

Illustration the proposed method which will be very efficient when we Rotate each codevector in the codebook. In this case the number of codevector will increase three times.

Conclusion

The quantization method which was adopted produced the best results and the best quality of decoded image when we compared these with the full search with very small distortion per block, see table.1, In other word, our proposed method can be used for improving the quality of decoding image even further where the number of codevector in the codebook increased three times, so the chance may be good to find the best matching codevector for every input vector. Our mentioned method can be useful for decreasing the bit rate then increasing in the compression ratio with reducing in the search time. Finally, from table. 1, one can see that the compression ratios depend on the codebook and block size, when the compression ratios increase the quality of decoded image decrease.

References

1. Pasi Franti, Olli Nevalainen and Timo Kaukoranta, " Compression of Digital Images by Block Truncation Coding: A Survey", The Computer Journal, Vol. 37, No. 4, pp. 308-332, 1994.
2. Rishav Chatterjee, " Image Compression and Resizing using Vector Quantization and Other Efficient Algorithms", International Journal of Engineering Science and Computing, Vol. 7, No. 6, pp. 13243-13246, 2017.
3. Maha A. Hameed, Saif B. Al-Khoja and Rafah R. Ismail, " Small Binary Codebook design depending on Rotating Blocks", Iraqi Journal of Science, Vol.62, No. 10, pp.3719-3723, 2021.
4. Yung- Gi Wu, "Block truncation image bit plane coding", Leader University Institute of Applied Information, Dept of computer Science & Information Engineering, Vol. 41, No. 10, pp.2476-2478, 2002.
5. Fast search method by block categorization and multi codebook designing based on block edge

Fabrication and Characterization of Polyvinyl Alcohol Nanofibers with Silver in Different Ratios for No2 Gas Sensing

Dalia Y. Salahaddin [1], Nadim K. Hassan [2]

© 2023 The Author(s). This open access article is distributed under a Creative CommonsAttribution (CC-BY) 4.0 license.

Abstract: In the current study, glass substrates were coated with Poly Vinyl Alcohol (PVA) nanofibers that were electrospun. The solution was electrospun at 20 KV while it was still warm using various concentrations of AgNO3 (1%, 2%, and 3% (wt.). The samples collected on the collectors were subjected to scanning electron microscopy (SEM) analysis and X-ray diffraction (XRD) analysis. The typical fiber diameter ranged from 100 nm to 250 nm. The PVA matrix successfully accommodates the Ag particles. PVA/ (1%,2%, and 3%) AgNO3 thin films have also been evaluated as gas sensors for (NO2) at various temperatures, including (120°C, 160°C, and 200°C). Doping is known to increase gas sensitivity. The results of sensing in these films are better than that of other similar materials and suggest that they can be used as high temperature sensors.

Key Words: Electrospinning PVA Nanofibers Ag Sensitivity.

Author details

[1– 2] Department of Physics, College of Pure Science, University of Tikrit, Tikrit, Iraq

Citation information

Cite this article as:

Salahaddin, D.Y., Hassan, N.K., (July 2023), *Fabrication and Characterization of Polyvinyl Alcohol Nanofibers with Silver in Different Ratios for No2 Gas Sensing*, Proceedings of the Minar Congress, Turkey, (9) pp 83-94, DOI: http://dx.doi.org/10.47832/MinarCong9-8

http://dx.doi.org/10.47832/MinarCong9-8

[1] University of Tikrit, Iraq

[2] University of Tikrit, Iraq

Introduction

Due to its routine usage and control, electrospinning is the method most frequently employed to create nanofibers [1]. Spinning creates fibers with sizes ranging from microns to less than 100 nanometers. These fibers have good surface areas, high porosities, and other qualities that make them appropriate for a wide range of applications in several industries. ideal [2]. Due to its superior chemical and thermal stability, water solubility, biocompatibility, and non-toxicity, polyvinyl alcohol (PVA) was chosen for the Ag spinning process. PVA is utilized extensively in a variety of applications because of its ability to produce fibers [3] [4].

Due to the design flexibility of electrospun nanofibers, customized functionalization may be accomplished either during the electrospinning process or by using post-treatment techniques. For instance, electrospun polymer nanofibers can be combined with metal nanoparticles like silver or gold to create functional composite nanofibers[5][6].

Because electrospun nanofibers have a surface area that is between one and two orders of magnitude bigger than continuous films, the thin membrane made of these fibers has a significant potential for use as a sensor [7]. To get high efficiency and effective performance from these nanofibrous composite materials, it is important to take into account the size and homogenous distribution of metal nanoparticles throughout the nanofiber matrix. Silver nanoparticles, for instance, have drawn a lot of interest because of their unusual optical, electrical, catalytic, and antibacterial properties [8][9]. Studies have focused on incorporating silver nanoparticles into electrospun nanofibers in order to produce functional nanofibrous composites by fusing those Ag nanoparticles with the special qualities of nanofibers.[10][6]. In this study, one of the electro spinning methods was used to manufacture a membrane of nanofibers by using an aqueous solution of pure PVA and PVA with different amount (1%, 2%, and 3%)(wt.) AgNO3 on a glass plate. The samples were characterized in detail using scanning electron microscopy (SEM) and X-ray diffraction (XRD), and their gas detection properties for NO2 emissions were analyzed.

Experimental

In this study, polyvinyl alcohol PVA with molecular weight Mw = 85,000 - 1.24,000 was used to prepare spinning solutions. Take an appropriate amount of commercially available PVA powder, place it in a 60°C water bath, heat it gently with a magnetic stirrer for 72 minutes, and dissolve it with distilled water. The solution was stirred until the polymer was completely dissolved and a homogeneous, clear, viscous solution was obtained. The doping solution was used to produce silver nitrate AgNO3 0.084g. Use 10 mL of distilled water as a solvent, stir with a magnetic stirrer for 5 min at room temperature, and add different amounts of He-AgNO3 solution (1%, 2%, 3% wt). Added to PVA matrix. The mixture was stirred for about 3-5 minutes to obtain a homogeneous solution.

Figure 1 shows a schematic diagram of the electrospinning process. The electrospinning system is a relatively basic system comprised of three major components: a DC high voltage

power supply, a syringe pump, and a conductive collector such as a magnet. As an example, consider aluminum. A valve, a DC high-voltage power source, and a syringe with a metal needle attached to the power supply's positive pole to positively charge the polymer solution comprise the system construction. a syringe with a metal needle connected to the positive pole of the power supply to positively charge the polymer solution, and a syringe pump to determine the composition of the polymer solution. The flow rate of the solution in the syringe is controlled by a metal needle. Adjust the distance between the needle and collector so that the fibers form on the glass plate. Table (1) shows the range and control parameters used in this study after conducting a series of tests to select the optimal control parameters that would achieve the desired non-fiber production.

Table 1. Optimum parameters are used in the preparation of pure PVA and PVA/Ag nanofibers at different ratios

parameters	DC high Voltage power supply	Needle size	Flow rat	Distance between the needle and the collector
Range	0-50kv	21-30 gauge	0.1-100 ml/h	1-20 cm
setat	20kv	21 gauge	0.1 ml/h	18 cm

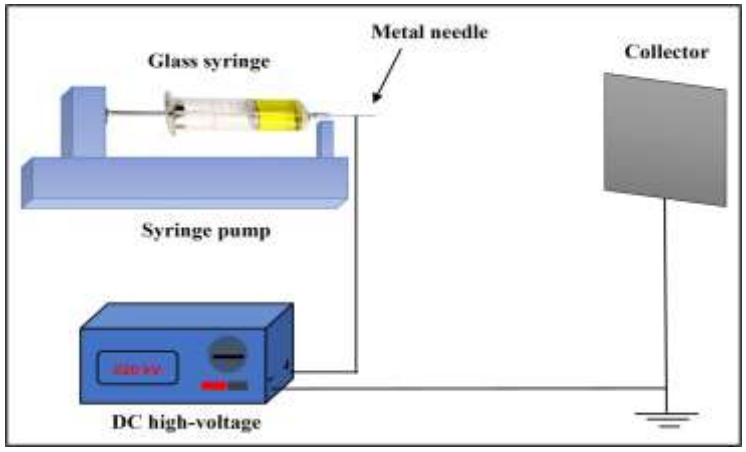


Figure 1. Schematic of the electrospinning process

Results and discussion

1. X-ray diffraction results

XRD was performed to confirm the phase structure of pure PVA and PVA/(2%, 3%) Ag thus prepared. Figure 2 shows the XRD patterns of PVA and PVA/(2%, 3%)Ag. From the XRD pattern of PVA, we can see that PVA has no trend peaks. Meanwhile, the presence of distinct peaks in the X-ray diffraction spectra indicated that the PVA/(2%, 3%) Ag nanofibers

possessed a face-centered (cubic) (fcc) single crystal structure [11]. Figure (2) shows a typical XRD pattern of Ag thin film. The peaks appearing at (38.269, 44.142, 60.026, 77.549, and 81.506) belong to the Ag crystal diagram (111), (200), (220), (311), and (222) [12][13]. Estimate the particle size (d) by davg = (0.9λ)/(β cos θ). where λ is the wavelength of the X-ray beam, β is the full width at half maximum intensity in radians, and θ is the angle. Span average, sweep average. The particle size (d) of PVA/(2%, 3%) Ag nanofibers was calculated to be (59.63 nm and 65.32 nm, respectively). This indicates a slight increase in particle size with increasing concentration of (Ag) nanoparticles.

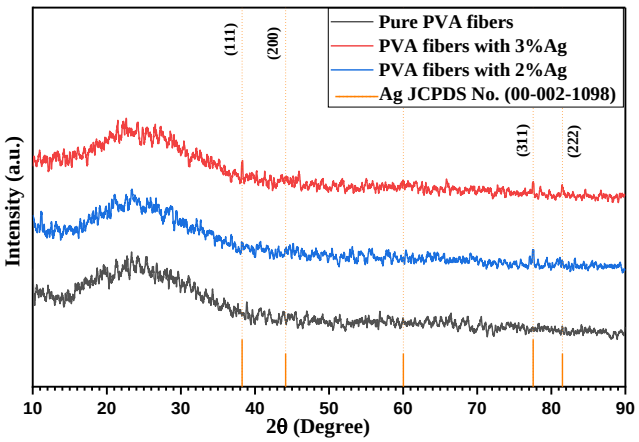


Figure 2. X-ray diffraction PVA and PVA/(1%, 2%)wt. Ag..

2. Field emission scanning electron microscopy (FESEM) result

The bare (PVA) and PVA/(1%, 2%, and 3%) Ag nanofibers underwent morphological examination using microscopy-FESEM. The existence of vacancies, the homogeneity of doped nanofibers, the presence of aggregates, the dispersion of particles in a continuous polymer matrix, and the potential orientation of nanoparticles are all things that may be learned by FESEM [14]. virgin (PVA) and doped (1.2 and 3) wt% FESEM pictures. The structure of silver nanofibers is depicted in Figures 3-(a), (b), (c), and (d). The end product was uniform, continuous, and bead-free fibers. The nanofibers had a diameter that varied from 150 to 400 nm, with an average diameter of 164.9 to 182.6 nm. Both pure PVA and PVA/(1,2,3)% wt. application were spun using the electrospinning technique. Ag solutions were used to create nanofibrous mats, which were subsequently examined for The addition of the proper Ag ratio changes Agitation and prolongs the flow of steroids [15], resulting in nanofibers with smaller diameters than the diameters of the incoming polymer nanofibers.[16] . A standard pure PVA fibers mat's morphology appears to be unaffected by the addition of one, two, or three percent weight of Ag to the PVA matrix. Within the fibers, the particles were densely packed. Analyzing this morphology, there is one main reason for the smoothness of the PVA (1, 2 and 3)% wt. Ag resulted fibers: high voltage during the electrospinning process can fragment particles (or decrease particle agglomerations), resulting in particle size reduction[17].

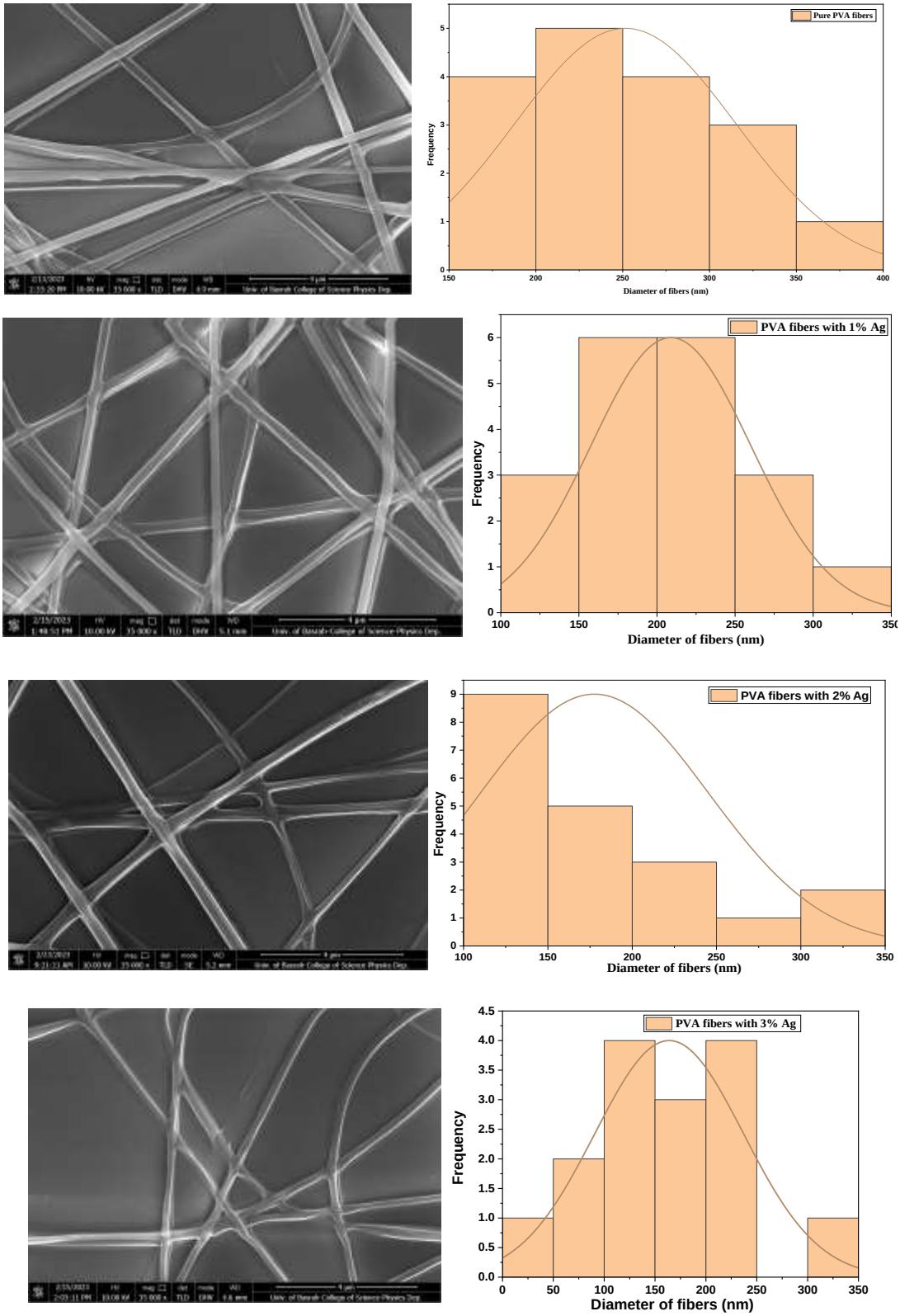
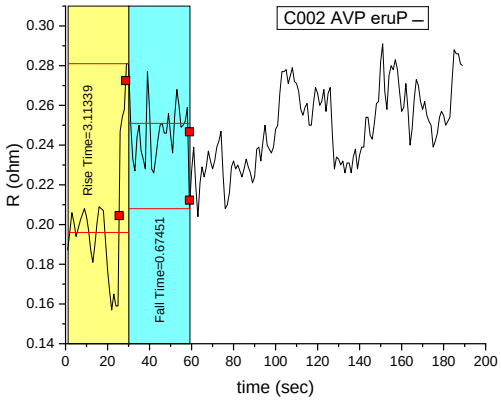
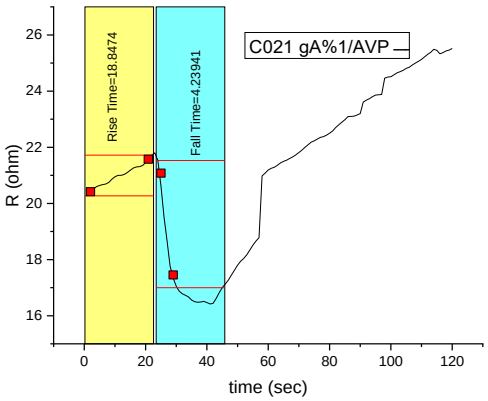
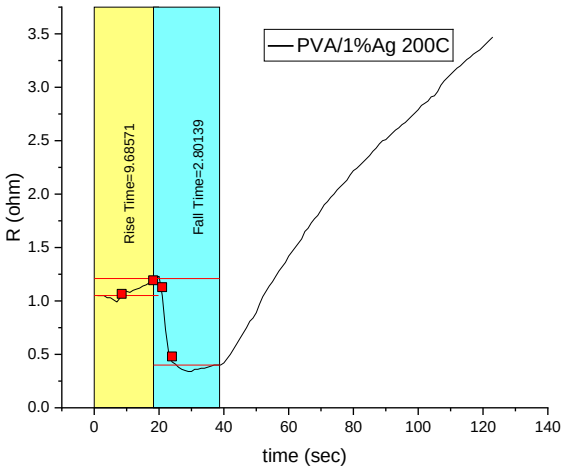
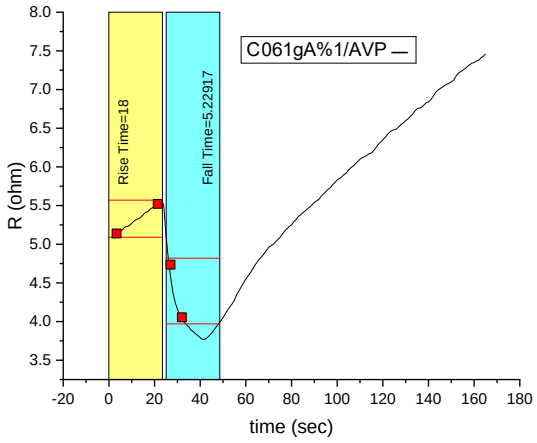


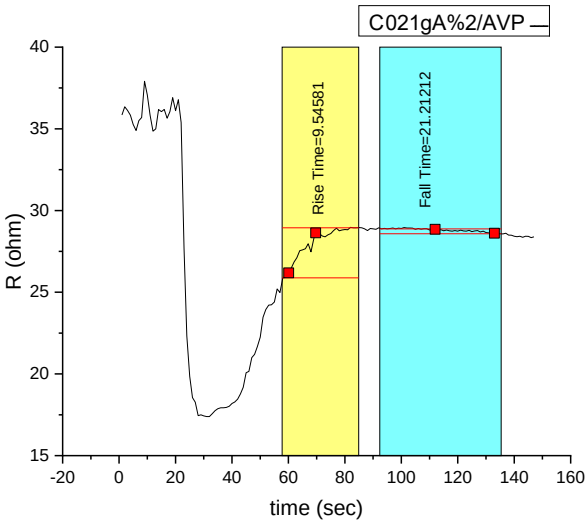
Figure 3. SEM images of(a) pure PVA, (b) PVA/1%Ag, (c) PVA/2%Ag, (d) PVA/3%Ag

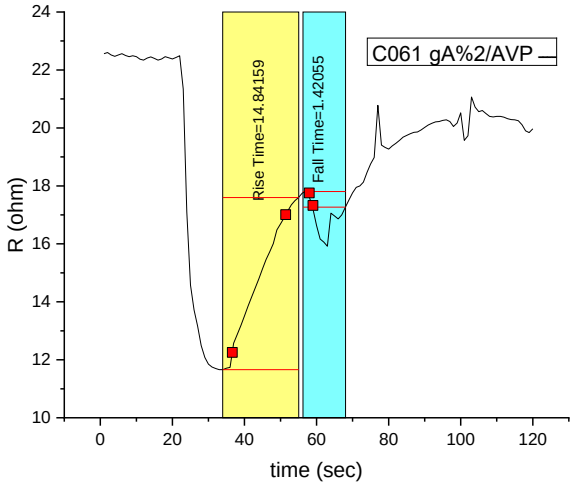

C002 AVP eruP
Rise Time=3.11339
Fall Time=0.67451
R (ohm)
time (sec)

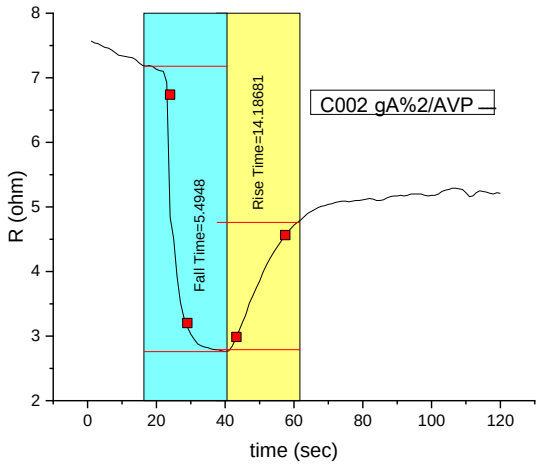

C021 gA%1/AVP
Rise Time=18.8474
Fall Time=4.23941
R (ohm)
time (sec)


PVA/1%Ag 200C
Rise Time=9.68571
Fall Time=2.80139
R (ohm)
time (sec)


C061gA%1/AVP
Rise Time=18
Fall Time=5.22917
R (ohm)
time (sec)


C021gA%2/AVP
Rise Time=9.54581
Fall Time=21.21212
R (ohm)
time (sec)


C061 gA%2/AVP
Rise Time=14.84159
Fall Time=1.42055
R (ohm)
time (sec)


C002 gA%2/AVP
Fall Time=5.4948
Rise Time=14.18681
R (ohm)
time (sec)

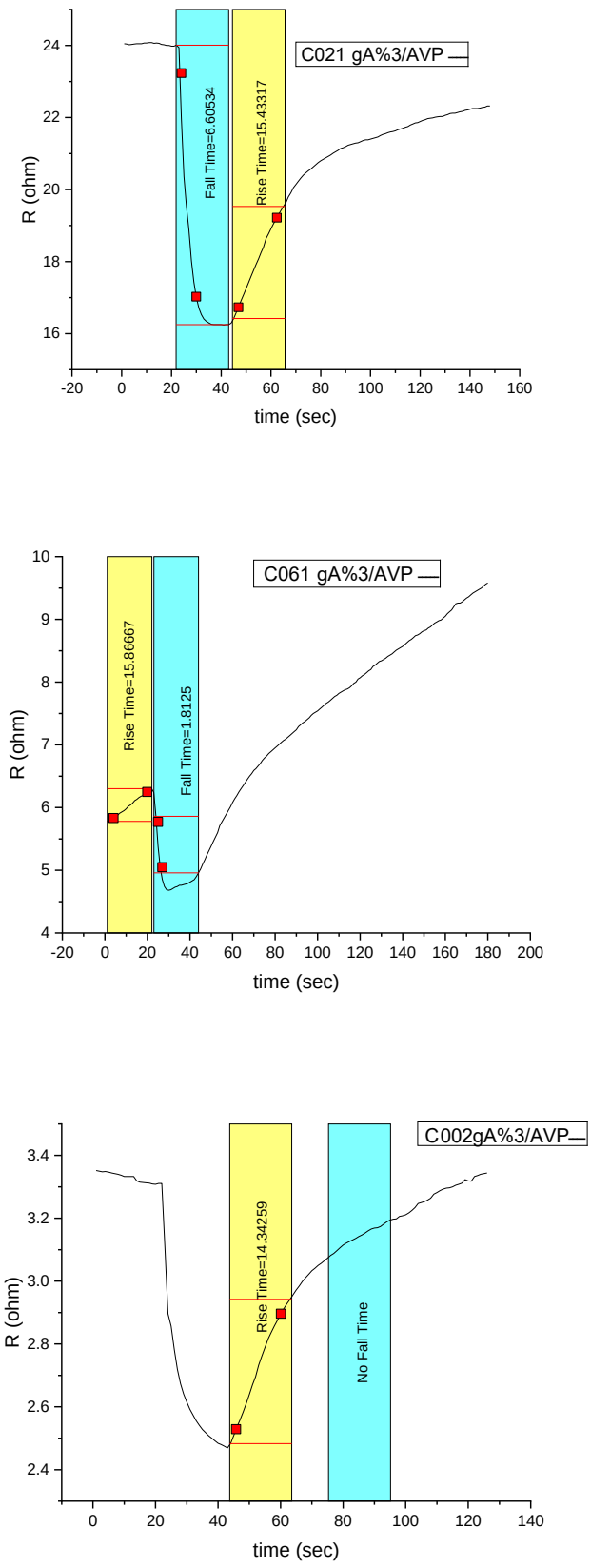


Figure 4. Shows the dynamic resistance of pure PVA sensor for NO2 and PVA with different concentrations from Ag at (120, 160, 200)°C (Pure PVA, PVA/3wt%Ag, PVA/2wt%Ag, PVA/1wt%Ag)

3. Sensing test results

This doped PVA film was manufactured as a film on a glass substrate, and the sensor performance was examined as a first step toward deploying it as a commercial sensor. Test gas NO2 was included in four sets of foils: pure PVA, PVA/1 wt% Ag, PVA/2 wt% Ag, and PVA/3 wt% Ag. At room temperature, neither the pure PVA nor the composite membranes responded to the tested gases. Significant reactions were seen for pure PVA and composite sheets with the lowest concentrations of silver (1 and 2 wt% Ag) compared to higher concentrations (3 wt% Ag) when the temperature rose to 200°C. At temperatures as high as 200 °C, pure PVA interacts with gases. The enhanced activation of the sensor material may be the cause of this[18]. As opposed to that,

Figure (4) shows the rapid increase in resistance of the nanofibrous film sensor when exposed to NO2 gas. In these systems, when the nanoparticles are embedded in the polymer PVA, thin-film conduction between the nanoparticles occurs mainly through a hopping mechanism. The presence of NO2 reduces the charge-carrying electrons in the nanoparticles, thereby reducing the total charge carriers and increasing the sheet resistance. The change in resistivity of the composite film was attributed to the presence of nanofillers, as no sensor response was observed for pure PVA at different temperatures (120, 160) °C. This enhanced gas sensing behavior can be demonstrated by the electron exchange between Ag nanoparticles and nanofiber molecules. Therefore, the change in resistance is greater than that of pure nanofibers (PVA), which is consistent with [19].

Sensitivity, response time, and recovery time:

Sensitivity, reaction time, and recovery time are the metrics that show how effective the sensor is. The response time of a gas sensor (τres) is defined as the time required for the sensor to reach 90% of the maximum reactions when the reducing/oxidizing gas is introduced to it, as it is a measure of the ability of the electronic circuit to respond to the signal, similarly, the recovery time (retrieval) (τrec) as the time for the sensor signal to decline to its initial value after removing the flow of reducing / oxidizing gas and reaching 10% [20]. Figure 5 depicts a typical NO2 sensitivity plot. (b) It is clear that when the working temperature is raised to 200 °C, the sensitivities of PVA/2%Ag and PVA/1%Ag sensors are 60% and 65%, respectively, and the reaction times are 16.2 s and 15.3 s, respectively. With rising operating temperature, it was discovered that the reaction time and recovery time both decreased. The recovery time was 55.8 and 56.7 seconds, respectively. The lower availability of surfaces with possible reaction sites on the film surface may be the cause of the diminished sensitivity at higher Ag concentrations[21].

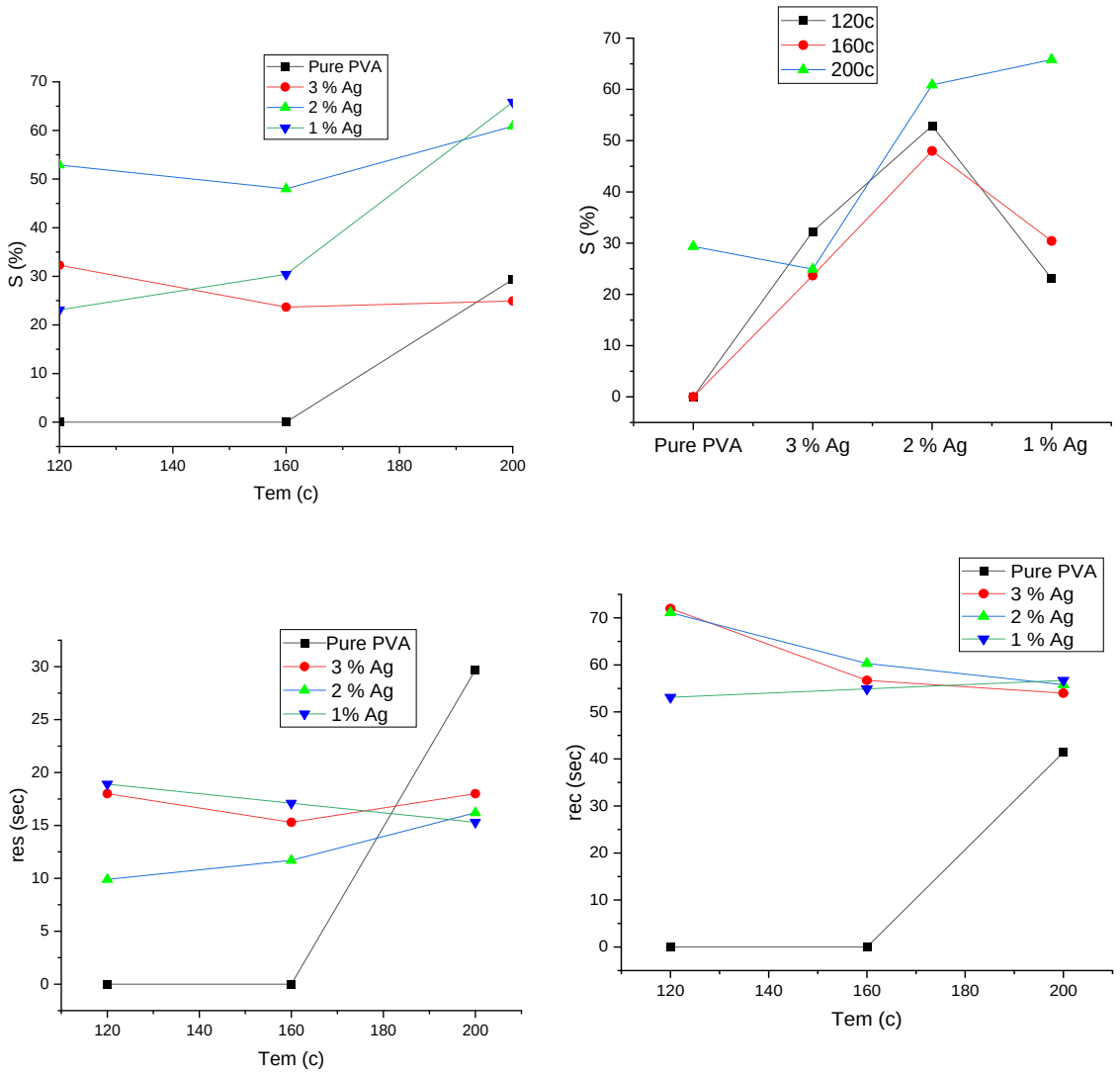


Figure 5. Shows the sensitivity curve of pure PVA sensor for NO2 and PVA with different concentrations from Ag at (120, 160, 200)°C

Conclusions

In this study, PVA and PVA/Ag nanofibers were successfully prepared by electrospinning. According to XRD, the electrospinning process produced high-quality PVA/Ag fibers, and according to FESEM measurements, the electrospinning process produced a uniform structure and smooth surface, indicating that the diameter of the fibers decreased with the addition of Ag. The orthorhombic phase of PVA/Ag nanofibers exhibited high sensitivity to a wide concentration range of NO2 at different temperatures (120, 160, and 200 °C), suggesting the potential application of nanofibers as sensor materials in homeland security, factory interiors, environmental protection, etc. . Advice. Leave healthy. For these PVA/Ag nanofiber networks, the best sensor performance can be achieved by optimizing the fabrication process and selecting an appropriate operating temperature.

Reference

1. F. A Chayad, A. R Jabur, and N. M Jalal, “Effect of NaCl solution addition on improving some of the physical properties of nylon 6 solutions used for electro spinning purpose,” *Eng. Technol. J.*, vol. 34, no. 7, pp. 1265–1274, 2016.
2. A. R. Jabur, M. H. Abdulmajeed, and S. Y. Abd, “Effect of Cu nanoparticles addition on improving the electrical conductivity and mechanical properties of PVA electrospun polymeric film,” in *AIP Conference Proceedings*, 2018, vol. 1968, no. 1, p. 30016.
3. A. R. Jabur, “Multiwall carbon nanotube/polyvinyl alcohol nanofibers film, electrical conductivity improvement,” *Eng. Technol. J.*, vol. 38, no. 3, pp. 431–439, 2020.
4. A. R. Jabur, E. S. Al-Hassani, A. M. Al-Shammari, M. A. Najim, A. A. Hassan, and A. A. Ahmed, “Evaluation of stem cells’ growth on electrospun polycaprolactone (PCL) scaffolds used for soft tissue applications,” *Energy Procedia*, vol. 119, pp. 61–71, 2017.
5. A. T. Hang, B. Tae, and J. S. Park, “Non-woven mats of poly (vinyl alcohol)/chitosan blends containing silver nanoparticles: fabrication and characterization,” *Carbohydr. Polym.*, vol. 82, no. 2, pp. 472–479, 2010.
6. S. Xiao, W. Xu, H. Ma, and X. Fang, “Size-tunable Ag nanoparticles immobilized in electrospun nanofibers: synthesis, characterization, and application for catalytic reduction of 4-nitrophenol,” *RSC Adv.*, vol. 2, no. 1, pp. 319–327, 2012.
7. . Huang, S. Virji, B. H. Weiller, and R. B. Kaner, “Polyaniline nanofibers: facile synthesis and chemical sensors,” *J. Am. Chem. Soc.*, vol. 125, no. 2, pp. 314–315, 2003.
8. R. R. Arvizo, S. Bhattacharyya, R. A. Kudgus, K. Giri, R. Bhattacharya, and P. Mukherjee, “Intrinsic therapeutic applications of noble metal nanoparticles: past, present and future,” *Chem. Soc. Rev.*, vol. 41, no. 7, pp. 2943–2970, 2012.
9. M. M. G. Fouda, M. R. El-Aassar, and S. S. Al-Deyab, “Antimicrobial activity of carboxymethyl chitosan/polyethylene oxide nanofibers embedded silver nanoparticles,” *Carbohydr. Polym.*, vol. 92, no. 2, pp. 1012–1017, 2013.
10. N. Mahanta and S. Valiyaveettil, “In situ preparation of silver nanoparticles on biocompatible methacrylated poly (vinyl alcohol) and cellulose based polymeric nanofibers,” *RSC Adv.*, vol. 2, no. 30, pp. 11389–11396, 2012.
11. J. Zeng *et al.*, “Controlling the nucleation and growth of silver on palladium nanocubes by manipulating the reaction kinetics,” *Angew. Chemie*, vol. 124, no. 10, pp. 2404–2408, 2012.
12. D. R. Raj, S. Prasanth, T. V Vineeshkumar, and C. Sudarsanakumar, “Ammonia sensing properties of tapered plastic optical fiber coated with silver nanoparticles/PVP/PVA hybrid,” *Opt. Commun.*, vol. 340, pp. 86–92, 2015.
13. Y. Wei, S. Han, D. A. Walker, P. E. Fuller, and B. A. Grzybowski, “Nanoparticle core/shell architectures within MOF crystals synthesized by reaction diffusion,” *Angew. Chemie Int. Ed.*, vol. 51, no. 30, pp. 7435–7439, 2012.
14. K. Choo, Y. C. Ching, C. H. Chuah, S. Julai, and N.-S. Liou, “Preparation and characterization of polyvinyl alcohol-chitosan composite films reinforced with cellulose

nanofiber," *Materials (Basel).*, vol. 9, no. 8, p. 644, 2016.

15. S. A. Habeeb, "Improvement of the Physical Properties of Electro-spun Polyacrylonitrile Nano-fibers Using the Fe2O3 Nanoparticles for Wastewater Treatment." University of Babylon, 2021.
16. S. M. Sze, Y. Li, and K. K. Ng, *Physics of semiconductor devices*. John wiley & sons, 2021.
17. A. R. Jabur and R. Al-Tuhafi, "Preparation and Characterization of NiTi/PVA Nanofibers by Electrospinning," *Eng. Technol. J.*, vol. 39, no. 11, pp. 1674–1680, 2021.
18. W. Hittini, Y. E. Greish, N. N. Qamhieh, M. A. Alnaqbi, D. Zeze, and S. T. Mahmoud, "Ultrasensitive and low temperature gas sensor based on electrospun organic-inorganic nanofibers," *Org. Electron.*, vol. 81, p. 105659, 2020.
19. K. S. Hemalatha and K. Rukmani, "Poly vinyl alcohol-CeO2 nanocomposite films: a promising material for NO2 sensors at high temperatures," *Mater. Res. Express*, vol. 6, no. 8, p. 85008, 2019.
20. H. H. N. Ali, "Synthesis, Characterization and Gas Sensor Performance of In2O3-AgxO nano Composites Prepared by Chemical Bath Deposition," *MS. C Sci. Phys. Univ. Anbar Dep. Phys*, 2016.
21. K. S. Hemalatha and K. Rukmani, "Concentration dependent dielectric, AC conductivity and sensing study of ZnO-polyvinyl alcohol nanocomposite films," *Int. J. Nanotechnol.*, vol. 14, no. 9–11, pp. 961–974, 2017.

Study of Artin Cokernel of the Group $(D_n \times C_{11})$, Where n is an Even Number

Bassim Kareem Mihsin [1]

© 2023 The Author(s). This open access article is distributed under a Creative CommonsAttribution (CC-BY) 4.0 license.

Abstract: In this work,we find the cyclic decomposition of Artin Cokernel $AC(D_n \times C_{11})$ where n is an even number and we find the Artin characters table $Ar(D_n \times C_{11})$, where n is an even number such that ; $n = q_1^{\tau 1} \cdot q_2^{\tau 2} \dots q_m^{\tau m} \cdot 2^{\gamma}, q_i \neq 2$ and q_i are distinct primes for all $i = 1, 2, 3, \dots, m$,then:

$$AC(D_n \times C_{11}) = \bigoplus_{i=1}^{2(\tau_1+1)(\tau_2+1)\cdots(\tau_m+1)(\gamma+1+)-1} C_2$$

and if $n = 2^{\gamma}$, γ is any positive integer then $AC(D_n \times C_{11}) = \bigoplus_{i=1}^{2\gamma} C_2$.

Key Words: Irreducible characters table, Artin Cokernel , groups D_n and C_n .

Author details

[1] General Directorate of Education in Karbala, Iraq

Citation information

Cite this article as:

Mihsin, B.K., (July 2023), *Study of Artin Cokernel of the Group (D_n×C_11), Where n is an Even Number*, Proceedings of the Minar Congress, Turkey, (9) pp 95-112, DOI: http://dx.doi.org/10.47832/MinarCong9-9

http://dx.doi.org/10.47832/MinarCong9-9

[1] basmk3756@gmail.com

Introduction

The commutative group "of all Z-valued characters of a finite group G "(Kirdar,1982). Pointwise addition operation to group that produced by unit characters which involve all cyclic subgroups of the group G (Artin characters), $\bar{R}(G)/T(G)$ is defined as finite commutative group that is denoted Artin Cokemel to group G, which is called as $AC(G)$. "To determin the cyclic decomposition of $AC(G)$ will be not taken in to account according to this work. $AC(G)$ had been defined and studied by(Lam 1967) where G known as cyclic group. 2-parts of $A(G)$was studied by (Yamacchi, 1970). Arbitrary characters $A(G)$ of cyclic subgroups had been studied by (David ,1976). p-group $A(G)$ was studied by (Knwabuez , 1996). $AC(G)$ cyclic decomposition had been studied by (Yassien 2000), where G known as group of elementary commutative group . Abed (2006), "found $Ar(C_n)$ where C_n the cyclic group of order n". Abbass (2008), found $Ar(D_n)$. In this paper, we found $Ar(D_n \times C_{11})$and we study $AC(D_n \times C_{11})$of the non- commutative group $(D_n \times C_{11})$where n be an even no.see more (Basheer,2006; Isaacs,1976; Moori,2006; Jaber,2019; Jaber, 2020; Mohmood, 2015 ; Mirza,2006& Abaas,2018).

The commutative group "of all Z-valued characters of a finite group G "(Kirdar,1982). Pointwise addition operation to group that produced by unit characters which involve all cyclic subgroups of the group G (Artin characters), $\bar{R}(G)/T(G)$ is defined as finite commutative group that is denoted Artin Cokemel to group G, which is called as $AC(G)$. "To determin the cyclic decomposition of $AC(G)$ will be not taken in to account according to this work. $AC(G)$ had been defined and studied by(Lam 1967) where G known as cyclic group. 2-parts of $A(G)$was studied by (Yamacchi, 1970). Arbitrary characters $A(G)$ of cyclic subgroups had been studied by(David ,1976). p-group $A(G)$ was studied by (Knwabuez , 1996). $AC(G)$ cyclic decomposition had been studied by (Yassien 2000), where G known as group of elementary commutative group . Abed (2006), "found $Ar(C_n)$ where C_n the cyclic group of order n". Abbass (2008), found $Ar(D_n)$. In this paper, we found $Ar(D_n \times C_{11})$and we study $AC(D_n \times C_{11})$of the non- commutative group $(D_n \times C_{11})$where n be an even no.see more (Basheer,2006; Isaacs,1976; Moori,2006; Jaber,2019; Jaber,2020; Mohmood,2015; Mirza,2006 & Abaas,2018).

Preliminaries

We have to present elementary bases,remarks and some theorems related to Artin characters, matrix representation and characters in this section, that will be given according to next sections.

Definition (1.1): Curits and Reiner (1981)

Assume G be a group, the induced character on G ,where H is subgroup of G and ϕ be a character of H, is given by:

$$\phi^{\uparrow G}(\eta) = \frac{1}{|H|}\sum_{x \in G} \phi^{0}(x\eta x)^{-1} \quad , \quad \text{where } \eta \in G \text{ and } \phi^{0} \text{is defined by:}$$

$$\phi^{0}(\mu) = \begin{cases} \phi(\mu) & \text{if} \quad \mu \in H \\ 0 & \text{if} \quad \mu \notin H \end{cases}$$

Theorem (1.2): Yassien (2000)

Suppose that G be group, H be cyclic subgroup and $\mu 1, \mu 2, \ldots, \mu k$ "are chosen representatives are for the k- conjugate classes of H contained" in CL_η , $\eta \in G$, then:

$$\phi^{\uparrow G}(\eta) = \frac{|G_G(\eta)|}{|C_H(\eta)|}\sum_{i=1}^{k} \phi(\mu_i) \qquad \text{if } \mu_i \in H \cap CL_\eta$$

$$\phi^{\uparrow G}(\eta) = 0$$

Definition (1.3): Yassien (2000)

The Artin character of G is all character induced from the principal character of cyclic subgroup of G where G is a finite group.

Definition (1.4): Abid (2006)

The Artin character of a finite group G can be displayed in a table called Artin characters table of G which is called $Ar(G)$.

Example (1.5)

Assume that C_{11} = < z > be cyclic group of order 11, the Γ- classes on C_3 [I] = {1} and [z]={ z , z^2 , … , z^{10}},with z^{11} = [I] .

The Artin characters table of:

Table 1.1

Ar (C_{11})=

Γ-classes	[I]	[r]
$\lvert CL_a \rvert$	1	1
$\lvert C_{C_{11}}(CL_a) \rvert$	11	11
∂_1	11	0
∂_2	1	1

where ∂_1 *and* ∂_2 are the Artin characters of C_{11}.

Definition (1.6): Kirdar(1982)

A knowledge of characters of finite group G is shown by a table which is called Artin characters table, pointed by $Ar(G)$ that to be $l \times l$ matrix with Γ-classes columns and rows represents all irreducible characters values for all Artin characters on G, that ι represents Γ-classes number.

Example (1.7)

To find the irreducible characters of $C_{11}$is given by:

Table 1.2.

≡*(C_{11})=

Γ-classes	[1]	[r]
ϑ_1	1	1
ϑ_2	10	-1

such that the irreducible valued characters of C_{11},say ϑ_i , $i = 1,2$.

Theorem [Artin] (1. 8): Serre (1977)

Assume G be a finite group, each irreducible character on G we write as a linear combination of Artin's characters with factor rational numbers.

2. The Factor Group AC(G):

Theorem (2.1): Kirdar(1982)

Assume R be a principle domain ,T is a matrix of $n \times n$ involved in R, then there exist matrices J and F are taken to be invertables where $J.T.F = D$ be amaatrix with diagonal form .Djj is called by dj with elements of natural number m; $0 \le m \le m \Rightarrow dj = 0$ and $j < m \Rightarrow dj \neq 0$ and $1 < j < m \Rightarrow dj / dj + 1$.

Theorem (2.2): Yassien (2000)

$AC(G) = \bigoplus_{j=1}^{i} C_{d_j}$ where $d_j = \pm D_j(T(G))/D_{j-1}(T(G))$, and i is the number of all distinct $\Gamma-$ classes and C_{d_j} is cyclic sub group of order d_j.

Proposition (2.3): Abbas (2008)

Assume D_n (represent dihedral group), where n is even number then rational valued characters table of D_n be as follows:

Table 2.1.

$(\equiv^* D_n) =$

Γ –classes	Γ -Classes of C_n $[r^k]$	[S]	[Sr]
ϑ_1		0	0
ϑ_1	≡ *(C_n)	0	0
⋮		⋮	⋮
ϑ_{l-1}		-1	1
ϑ_l	1 1 ⋯ 1	1	1
ϑ_{l+1}	1 1 ⋯ 1	-1	-1
ϑ_{l+2}		1	-1

Where $\vartheta_l + 2(r^k) = 1$ and $\vartheta_l + 2(r^k) = -1$ when k are even(odd) number respectively,such that C_n contains l is the no of Γ –classes.

Theorem (2.4): Abid (2006)

The characters table of C_q^δ where q a prime number be as follow:

Table 2.2.

Γ-classes	[1]	$[r^{q^{\delta-1}}]$	$[r^{q^{\delta-2}}]$	$[r^{q^{\delta-3}}]$	⋯	[r]
ϑ_1	q^δ	0	0	0	⋯	0
ϑ_2	$q^{\delta-1}$	$q^{\delta-1}$	0	0	⋯	0
ϑ_3	$q^{\delta-2}$	$q^{\delta-2}$	$q^{\delta-2}$	0	⋯	0
⋮ ⋮ ⋮	⋮ ⋮	⋮ ⋮	⋮ ⋮	⋮ ⋮	⋮ ⋮	⋮ ⋮
ϑ_S	q	q	q	q	⋯	0
ϑ_{S+1}	1	1	1	1	⋯	1

Remark (2.5): Abid (2006)

Suppose $n = q_1^{\tau 1} \cdot q_2^{\tau 2} \dots \dots \dots q_m^{\tau m}$ n , $q_1, q_2, \dots \dots, q_m$ be any positive integer are distinct primes then:

$Ar(C_n) = Ar\left(C_{q_1}^{\tau 1}\right) \otimes Ar\left(C_{q_2}^{\tau 2}\right) \otimes \dots \dots \otimes Ar\left(C_{q_m}^{\tau m}\right)$Where $\otimes$.is the tensor product.

Proposition (2.6): Mirza (2006)

The two matrices $T\left(C_{q^\delta}\right)$ and $J\left(C_{q^\delta}\right)$ where q and δ be prime (positive integer)respectively number are given by:

$$T\left(C_{q^\delta}\right) = \begin{bmatrix} 1 & 1 & 1 & \cdots & 1 & 1 \\ 0 & 1 & 1 & \cdots & 1 & 1 \\ 0 & 0 & 1 & \cdots & 1 & 1 \\ \vdots & \vdots & \vdots & \ddots & \vdots & \vdots \\ 0 & 0 & 0 & \cdots & 1 & 1 \\ 0 & 0 & 0 & \cdots & 0 & 1 \end{bmatrix}$$

$$and\ J\left(C_{q^\delta}\right) = \begin{bmatrix} 1 & -1 & 0 & 0 & \cdots & 0 & 0 \\ 0 & 1 & -1 & 0 & \cdots & 0 & 0 \\ 0 & 0 & 1 & -1 & \cdots & 0 & 0 \\ \vdots & \vdots & \vdots & \vdots & \ddots & \vdots & \vdots \\ 0 & 0 & 0 & 0 & \cdots & 1 & -1 \\ 0 & 0 & 0 & 0 & \cdots & 0 & 1 \end{bmatrix}$$

which is $2(\delta + 1) \times (\delta + 1)$ square matrix .$F\left(C_{q^\delta}\right) = I_{2(\delta+1)}$ where $I_{2(\delta+1)}$ is an identity matrix and $D\left(C_{q^\delta} \times C_{11}\right) = dig\{1,1,1, \dots,1\}$.

Remark (2.7) : Abid (2006)

From now on if $n = q_1^{\tau 1} \cdot q_2^{\tau 2} \dots \dots \dots q_m^{\tau m} \cdot 2^\gamma$ where $q_1, q_2, \dots \dots, q_m$ are distinct primes then:

1) $J(C_n) = J\left(C_{q_1}^{\tau 1}\right) \otimes J\left(C_{q_2}^{\tau 2}\right) \otimes \dots \dots \otimes J\left(C_{q_m}^{\tau m}\right) \otimes J(C_{2^\gamma})$

2) If n = 2^γ , γ is any positive integer,then we can write T(C_n)

$$\mathrm{T}(C_n) = \begin{bmatrix} & & & & 1 & 1 \\ \sigma_1(C_n) & & & & 1 & 1 \\ & & & & \vdots & \vdots \\ 0 & 0 & \cdots & 0 & 1 & 1 \\ 0 & 0 & \cdots & 0 & 0 & 1 \end{bmatrix}$$

where $2(\gamma + 1) \times 2(\gamma + 1)$ is square matrix,$\sigma_1(C_n)$ is the matrix obtain by neglecting last two columns {1 , 1 , … , 1 , 0} and {1 , 1 , … , 1} and the last two rows {0 , 0 , … , 1 , 1} and {0 , 0 , … , 0 , 0 , 1} from the matrix $T(C_{2^\gamma})$ in proposition (2.6).

3) $T(C_n) = \begin{bmatrix} & & & H \\ & & & 0 \quad 1 \\ & \sigma_2(C_n) & & H \\ & & & 0 \quad 1 \\ 0 & 0 & \cdots & H \\ 0 & 0 & \cdots & 0 \quad 1 \end{bmatrix}$, where $H = \gamma.times \begin{Bmatrix} 1 & 1 \\ 1 & 1 \\ \vdots & \vdots \\ 1 & 1 \end{Bmatrix}$

Where $\sigma_2(C_n)$ is the matrix obtained by neglecting the last columns the{1 , … , 1 , 0 , 1 , … , 1 , 0 , … , 1 , 0} and {1 , 1 , … , 1} and the last two rows {0 , 0 , … , 1 , 1} and {0 , 0 , … , 0 , 1} from the tensor product $T(C_{q_1}^{\tau 1}) \otimes T(C_{q_2}^{\tau 2}) \otimes \ldots\ldots \otimes T(C_{q_m}^{\tau m}) \otimes T(C_{2^\gamma})$.

Theorem (2.8): Abbas (2008)

Suppose Dn is a dihedral group, where n is even number then the Artin characters table of Dn as follows by:

$Ar(Dn) =$

Table 2.3.

Γ-classes	[1]	$\left[r^{\frac{n}{2}}\right]$	Γ-Classes of C_n				[S]	[Sr]
$\lvert CL_a \rvert$			2	2	….	2	n/2	n/2
$\lvert C_{D_n}(CL_a) \rvert$			N	N	….	n	2^2	2^2
∂_1	**2Ar(C_n)**						0	0
∂_2							0	0
:							:	:
:							:	:
∂_l							0	0
∂_{l+1}	N	0	…….				2	0
∂_{l+2}	N	0	…….				0	2

The group$(D_n \times C_{11})$ (2.9)

The tensor product group $(D_n \times C_{11})$, where(D_n represent dihedral group) with order 2n and non- commutative group such that:

D_n= {$S^i r^k$: 0 ≤ k ≤ n-1 , 0 ≤ j ≤ 1}, where $r^n = 1$, $S^2 = 1$, $Sr^k S = r^{-k}$ and C_{11} with order 11 and it called cyclic group forming of elements {I , Z , Z^2 , Z^3 , … , Z^{10}} with (Z^{11}) = I . The product group $(D_n \times C_{11})$ have order 22n.

$(D_n \times C_{11})$ = {(q , c): q ∈ D_n, c ∈ C_{11}} and $\lvert D_n \times C_{11} \rvert = \lvert D_n \rvert \cdot \lvert C_{11} \rvert$=2n . 11 = 22n

3. The main results

The general form of Artin's characters table of the group $(D_n \times C_{11})$ will be obtained as n is an even number according to this section.

Proposition (3.1)

Suppose $(D_n \times C_{11})$ be a group have order$22n$ then the general formula of the Artin's characters table of the group $(D_n \times C_{11})$where n is an even number can be represented by the following formula:

$Ar(D_n \times C_{11})$=

Table 3.1.

	Γ **-classes of** $D_n \times \{I\}$								Γ **-classes of** $D_n \times \{Z\}$							
Γ-classes	**[1 , I]**	$[r^{\frac{n}{2}}, I]$	Γ − classes of $D_n \times C_{11}$				**[S , I]**	**[Sr, I]**	**[1, z]**	$[r^{\frac{n}{2}}, I]$	Γ − classes of $D_n \times C_{11}$				**[S , z]**	**[Sr, z]**
$\|CL\alpha\|$	**1**	**1**	**2**	**2**	**…**	n	$\frac{n}{2}$	$\frac{n}{2}$	**2**	**2**	**2**	**2**	**…**	n		$\frac{n}{2}$
$\|D_n \times C_{11}\|$	$22n$	$22n$	$11n$	$11n$	…	$11n$	**44**	**44**	$22n$	$22n$	$11n$	$11n$	…	$11n$	**44**	**44**
$\partial_{(1,1)}$	11Ar(D_n)								0							
$\partial_{(2,1)}$																
⋮																
$\partial_{(l,1)}$																
$\partial_{(l+1,1)}$																
$\partial_{(l+2,1)}$																
$\partial_{(1,2)}$	Ar(D_n)								Ar(D_n)							
$\partial_{(2,2)}$																
⋮																
$\partial_{(l,2)}$																
$\partial_{(l+1,2)}$																
$\partial_{(l+2,2)}$																

The Artin's characters table of the group D_n can be write by Ar(D_n).

Proof:

Let $g \in (D_n \times C_{11})$; g (q , I) or g (q, z), q $\in D_n$, I, z $\in C_{11}$

Case (I):

Assume H is a cyclic subgroup of $D_n \times \{1\}$ and φ the principal character of H, Φj Artin characters of D_n such that $1 \le j \le l+2$, then:

we obtain by theorem (1.2):

1) H = < (r , I) > 2) H = < (S , I) > 3) H = < (Sr , I) >

and $\Phi_j(g) = \begin{cases} \frac{|C_G(g)|}{|C_H(g)|} \sum \varphi(hi) & if\ hi \in H \cap CL(g) \\ 0 & if\ H \cap CL(g) = \varphi \end{cases}$

1) H = < (r , I) >

i) if g = (1 , I) and g ∈ H.

$$\Phi(\mathrm{j}\,,1)\,((1\,,\mathrm{I})) = \frac{|C_{\mathrm{Dn}\times \mathrm{C11}}(g)|}{|C_{11}(g)|}\cdot\varphi(g) = \frac{22n}{|C_{11}(1\,,\mathrm{I})|}\cdot 1$$

$$= \frac{11\cdot 2n}{|C_{<r>}(1)|}\cdot\varphi(1) = 22\Phi_{\mathrm{j}}(1)$$

since $\mathrm{H}\cap \mathrm{CL}(1\,,\mathrm{I}) = \{(1\,,\mathrm{I})\}$.

ii) if $g = \left(\mathrm{r}^{\frac{n}{2}}\,,\mathrm{I}\right)$ and $g \in \mathrm{H}$.

$$\Phi(\mathrm{j}\,,1)\,(g) = \frac{|C_{\mathrm{Dn}\times \mathrm{C11}}(g)|}{|C_H(g)|}\cdot\varphi(g) = \frac{22n}{|C_H(g)|}\cdot 1 = \frac{11\left|C_{D_n}\left(\mathrm{r}^{\frac{n}{2}}\right)\right|}{\left|C_{<r>}\left(\mathrm{r}^{\frac{n}{2}}\right)\right|}\cdot\varphi(g)$$

$$= 11\Phi_{\mathrm{j}}\left(\mathrm{r}^{\frac{n}{2}}\right)$$

since $H\cap CL(g)\,,\varphi(g) = 1$.

iii) if $g = (\mathrm{r}^{i}\,,\mathrm{I})$, $\mathrm{i}\neq\frac{n}{2}$ and $\mathrm{i}\neq \mathrm{n}$ and $g \in \mathrm{H}$.

$$\Phi(\mathrm{j}\,,1)\,(g) = \frac{|C_{\mathrm{Dn}\times \mathrm{C11}}(g)|}{|C_H(g)|}\cdot\left(\varphi(g)+\varphi(g^{-1})\right) = \frac{11n}{|C_H(g)|}\cdot(\mathrm{I}+1)$$

$$= \frac{11\cdot n}{|C_H(g)|}\cdot(\mathrm{I}+1) = 11\cdot 2\mathrm{n}$$

$$= 11\cdot\frac{2|C_{\mathrm{Dn}\times \mathrm{C11}}(q)|}{|C_{<x>}(\mathrm{q})|}\cdot\left(\varphi(g)+\varphi(g^{-1})\right) = 11\cdot\Phi_{\mathrm{j}}\,(g)$$

$Since\ H\cap CL(g) = \{g\,,g^{-1}\}\ and\ \varphi = \varphi\,(g^{-1}) = 1$,

$g(q\,,\mathrm{I}), q\in Dn\ and\ q\neq r^{\frac{n}{2}}, q\neq 1.$

iV) if $g\notin$ H.

$$\Phi(\mathrm{j}\,,1)\,(g) = 11\cdot 0 = 11\cdot\Phi_{\mathrm{j}}\,(q)$$

Since $H\cap CL(g) = \varphi$.

2) $\mathrm{H} = <(\mathrm{S}\,,\mathrm{I})> = \{(1\,,\mathrm{I})\,,(\mathrm{S}\,,\mathrm{I})\}$.

i) if $g = (1\,,\mathrm{I})$, $\mathrm{H}\cap\mathrm{CL}(1\,,\mathrm{I}) = \{(1\,,\mathrm{I})\}$.

$$\Phi(l+1\,,1)\,(g) = \frac{|C_{\mathrm{Dn}\times \mathrm{C11}}(g)|}{|C_H(g)|}\cdot\varphi(g) = \frac{22n}{2}\cdot 1 = 11n = 11\cdot\varphi_{l+1}(1)$$

ii) if $g = (\mathrm{S}\,,\mathrm{I})$ and $g \in \mathrm{H}$.

$$\Phi(l+1\,,1)\,(g) = \frac{|C_{\mathrm{Dn}\times \mathrm{C11}}(g)|}{|C_H(g)|}\cdot\varphi(g) = \frac{44}{2}\cdot 1 = 22$$

$$= 11 \cdot 2 = 11 \cdot \varphi_{l+1}(S)$$

since $H \cap CL(g) = \{g\}, \varphi(g) = 1$

otherwise $\varphi_{l+1}(g) = 0$ since $H \cap CL(g) = \varphi$.

3) $H = <(Sr)> = \{(1, I), (Sr, I)\}$.

i) if $g = (1, I)$, $H \cap CL(1, I) = \{(1, I)\}$.

$$\Phi(l+2, 1)(g) = \frac{|C_{Dn \times C11}(g)|}{|C_H(g)|} \cdot \varphi(g) = \frac{22n}{2} \cdot 1 = 11n$$

$$= 11 \cdot \varphi_{l+2}(1)$$

ii) if $g = (Sr, I)$ and $g \in H$.

$$\Phi(l+2, 1)(g) = \frac{|C_{Dn \times C11}(g)|}{|C_H(g)|} \cdot \varphi(g) = \frac{44}{2} \cdot 1$$

$$= 22 = 11 \cdot 2 = 11 \cdot \varphi_{l+2}(Sr)$$

since $H \cap CL(g) = \{(Sr, I)\}$.

otherwise $\varphi_{l+2}(g) = 0$ since $H \cap CL(g) = \varphi$.

Case (II):

Let $D_n \times \{z\}$ be group, H is a cyclic group, then:

1) $H = <(r, z)>$ 2) $H = <(S, z)>$ 3) $H = <(Sr, I)>$

And φ the principal character of H , Φ_j Artin characters of D_n such that $1 \leq j \leq l+2$ we obtain by theorem (1.2)

$$\Phi_j(g) = \begin{cases} \frac{|C_G(g)|}{|C_H(g)|} \sum \varphi(hi) & if\ hi \in H \cap CL(g) \\ 0 & if\ H \cap CL(g) = \varphi \end{cases}$$

1) $H = <(r, Z)>$

i) if $g = (1, I)$ or $g = (1, Z)$, and $g \in H$.

$$\Phi(j, 2)(g) = \frac{|C_{Dn \times C11}(g)|}{|C_H(1, I)|} \cdot \varphi(g) = \frac{22n}{|C_H(1, I)|} \cdot 1 = \frac{22 \cdot n}{|C_{<r,Z>}{}^{(1,I)}|} \cdot 1$$

$$= \frac{22|C_{Dn}(1)|}{|C_{<r>}{}^{(1)}|} \cdot \varphi(1) = 22\Phi_j(1)$$

Since $H \cap CL(1, I) = \{(1, I)\}$.

ii) if $g = (1, \mathrm{I})$ Or $g = \left(\mathrm{r}^{\frac{n}{2}}, \mathrm{I}\right)$ Or $g = \left(\mathrm{r}^{\frac{n}{2}}, \mathrm{Z}\right)$ Or $g = (1, \mathrm{Z})$ and $g \in \mathrm{H}$.

a) if $g = (1, \mathrm{I})$ or $g = (1, \mathrm{Z})$ and $g \in \mathrm{H}$.

$$\Phi(\mathrm{j}, 2)\,(g) = \frac{|C_{\mathrm{Dn}\times \mathrm{C11}}(g)|}{|C_H(g)|} \cdot \varphi(g) = \frac{22n}{|C_H(g)|} \cdot 1 = \frac{22 \cdot n}{|C_{<r,Z>}(g)|} \cdot 1$$

$$= \frac{22 \cdot |C_{D_n}(1)|}{|C_{<r>}(1)|} \cdot \varphi(1) = 22\Phi_{\mathrm{j}}(1)$$

since $H \cap CL(g) = \{g\}, \varphi(g) = 1$.

b) if $g = (\mathrm{r}^{\frac{n}{2}}, \mathrm{I})$ or $g = (\mathrm{r}^{\frac{n}{2}}, \mathrm{Z})$ and $g \in \mathrm{H}$.

$$\Phi(\mathrm{j}, 2)\,(g) = \frac{|C_{\mathrm{Dn}\times \mathrm{C11}}(g)|}{|C_H(g)|} \cdot \varphi(g) = \frac{22n}{|C_H(g)|} \cdot 1 = \frac{\left|C_{D_n}\left(\mathrm{r}^{\frac{n}{2}}\right)\right|}{|C_{<r,Z>}(g)|} \cdot \varphi\left(\mathrm{r}^{\frac{n}{2}}\right)$$

$$= 22\Phi_{\mathrm{j}}\left(\mathrm{r}^{\frac{n}{2}}\right)$$

since$H \cap CL(g) = \{g\}, \varphi(g) = 1$.

iii) if $g = \{(\mathrm{r}^i, \mathrm{I}), (\mathrm{r}^i, \mathrm{Z})\}$, $\mathrm{i} \neq \frac{n}{2}$ and $\mathrm{i} \neq \mathrm{n}$ and $g \in \mathrm{H}$.

$$\Phi(\mathrm{j}, 2)\,(g) = \frac{|C_{\mathrm{Dn}\times \mathrm{C11}}(g)|}{|C_H(g)|} \cdot \left(\varphi(g) + \varphi(g^{-1})\right) = \frac{11n}{|C_H(g)|} \cdot (1+1)$$

$$= \frac{22 \cdot n}{|C_H(g)|} = \frac{22|C_{\mathrm{Dn}}(q)|}{|C_H(q)|} \cdot \left(\varphi(g) + \varphi(g^{-1})\right) = \Phi(q)$$

since $H \cap CL(g) = \{g, g-1\}$ *and* $\varphi = \varphi(g-1) = 1$,

$g(q, Z), q \in Dn$ *and* $q \neq r^{\frac{n}{2}}, q \neq 1$.

iV) if $g \notin$ H.

$\Phi(\mathrm{j}, 2)\,(g) = 0$

since $H \cap CL(g) = \varphi$.

2) $\mathrm{H} = <(\mathrm{S}, \mathrm{z})> = \{(1, \mathrm{z}), (\mathrm{S}, \mathrm{z})\}$.

i) if $g = (1, \mathrm{z})$ and $g \in \mathrm{H}$.

$$\Phi g(l+1, 2)\,(g) = \frac{|C_{\mathrm{Dn}\times \mathrm{C11}}(g)|}{|C_H(g)|} \cdot \varphi(g) = \frac{22n}{2} \cdot 1 = 11n = 11 \cdot \varphi_{l+1}(1)$$

ii) if $g = (\mathrm{S}, \mathrm{Z})$ and $g \in \mathrm{H}$.

$$\Phi(l+1, 2)\,(g) = \frac{|C_{\mathrm{Dn}\times \mathrm{C11}}(g)|}{|C_H(g)|} \cdot \varphi(g) = \frac{44}{2} \cdot 1 = 22$$

otherwise $\Phi(l+1, 2) = 0$ since $\mathrm{H} \cap \mathrm{CL}(g) = \varphi$.

3) $H = < (Sr , z) > = \{(1 , z) , (Sr , z)\}$.

i) if $g = (1 , Z)$, $g \in H$.

$$\Phi(l + 2 , 1)\,(g) = \frac{|C_{Dn \times C11}(g)|}{|C_H(g)|} \cdot \varphi(g) = \frac{22n}{2} \cdot \varphi(g) = \frac{22n}{2} \cdot 1 = 11n$$

$$= 11 \cdot \varphi_{l+2}(1)$$

since $H \cap CL(1 , Z) = \{(1 , Z)\}$

ii) if $g = (Sr , Z)$ and $g \in H$.

$$\Phi(l + 2 , 2)\,(g) = \frac{|C_{Dn \times C11}(g)|}{|C_H(g)|} \cdot \varphi(g) = \frac{44}{2} \cdot 1$$

$$= 22 = 11 \cdot 2 = 11 \cdot \varphi_{l+2}(Sr)$$

since $H \cap CL(Sr , Z) = \{(Sr , Z)\}$

otherwise $\varphi_{(l+2 , 2)}(g) = 0$ since $H \cap CL(g) = \varphi$.

Proposition (3.2):

If $n = 2^{\gamma}$,where γ is any positive integers number,then the matrix T of the group $Dn \times C11$ is given by :

$$T(D_n \times C_{11}) = \begin{bmatrix} 2.\ \sigma_1(C_n) \otimes T(C_{11}) & \begin{matrix} 1 & 1 & 1 & 1 \\ 1 & 1 & 1 & 1 \\ \vdots & \vdots & \vdots & \vdots \\ 0 & 1 & 1 & 1 & 1 \\ 0 & 0 & 1 & 1 & 0 \\ 1 & 0 & 1 & 0 & 1 \\ 1 & 1 & 1 & 0 & 0 \end{matrix} \\ \begin{matrix} 0 & 0 & \cdots \\ 0 & 0 & \cdots \\ 1 & 1 & \cdots \\ 1 & 1 & \cdots \end{matrix} & \end{bmatrix}$$

Which is $2(\gamma + 3) \times 2(\gamma + 3)$ and $\sigma_1(C_n) \times C_{11}$is similar to the matrix in (2.7).

Proof:

The Artin's character table $Ar(D_n \times C_{11})$ can be obtained by theorem (3.1) and the Irreducible character table ($\equiv^*\ (D_n \times C_{11})$)will be obtained by proposition (2.3).

Therefor the matrix $T(D_n \times C_{11})$it can be found by the definition of $T(G)$.

$$T(D_n \times C_{11}) = Ar(D_n \times C_{11}) \cdot \left(\equiv^*\ (D_n \times C_{11})\right)^{-1}$$

$$= \begin{bmatrix} \Sigma & \Sigma & & \begin{matrix} 1 & 1 & 1 & 1 \\ 1 & 1 & 1 & 1 \\ \vdots & \vdots & \vdots & \vdots \\ 1 & 1 & 1 & 1 \\ 0 & 1 & 1 & 0 \\ 1 & 0 & 1 & 0 \\ 1 & 1 & 1 & 0 \end{matrix} \\ 0 & \Sigma & & \\ \begin{matrix} 0 & 0 & \cdots & 0 \\ 0 & 0 & \cdots & 0 \\ 1 & 1 & \cdots & 1 \\ 1 & 1 & \cdots & 1 \end{matrix} & & & \end{bmatrix} == \begin{bmatrix} 2.\ \sigma_1(C_n) \otimes T(C_{11}) & \begin{matrix} 1 & 1 & 1 & 1 \\ 1 & 1 & 1 & 1 \\ \vdots & \vdots & \vdots & \vdots \\ 0 & 1 & 1 & 1 & 1 \\ 0 & 0 & 1 & 1 & 0 \\ 1 & 0 & 1 & 0 & 1 \\ 1 & 1 & 1 & 0 & 0 \end{matrix} \\ \begin{matrix} 0 & 0 & \cdots \\ 0 & 0 & \cdots \\ 1 & 1 & \cdots \\ 1 & 1 & \cdots \end{matrix} & \end{bmatrix}$$

Such that $2(\gamma+3)\times 2(\gamma+3)$,where $\Sigma = 2\sigma_1(C_n) = \begin{bmatrix} 2 & 2 & 2 & \cdots & 2 \\ 0 & 2 & 2 & \cdots & 2 \\ 0 & 0 & 2 & \cdots & \vdots \\ \vdots & \vdots & \vdots & \ddots & \vdots \\ 0 & 0 & 0 & \cdots & 2 \end{bmatrix}$

, 0 is zero matrix , are with size $(\gamma+1)\times(\gamma+1)$.

Proposition (3.3):

If $n = 2^{\gamma}$,where γ is any positive integers number, then the matrices $J(D_n \times C_{11})$ and $F(D_n \times C_{11})$ are taking the forms:

$$J(D_n \times C_{11}) = \begin{bmatrix} J(C_n) \otimes J(C_{11}) & & & & & & 0 & 0 \\ & & & & & & 0 & 0 \\ & & & & & & \vdots & \vdots \\ & & & & & & 0 & 0 \\ 0 & 0 & 0 & \cdots & 0 & 0 & -1 & -1 \\ 0 & 0 & 0 & \cdots & 0 & 0 & 0 & 0 \end{bmatrix}$$

And

$$F(D_n \times C_{11}) = \begin{bmatrix} & & & & & 0 & 0 & 0 \\ & I_{2\gamma\times 2\gamma} & & & & 0 & 0 & 0 \\ & & & & & \vdots & \vdots & \vdots \\ -1 & -1 & \cdots & -1 & -1 & 0 & 0 & 1 \\ 1 & 1 & \cdots & 1 & 1 & 1 & 0 & -1 \\ 0 & 0 & \cdots & 0 & 1 & 0 & 1 & 0 \end{bmatrix}$$

Where $I_{2\gamma\times 2\gamma}$ is the identity matrix, they are $2(\gamma+3)\times 2(\gamma+3)$ square matrix ,then $J(D_n \times C_{11}) \cdot T(D_n \times C_{11}) \cdot F(D_n \times C_{11}) = D(D_n \times C_{11})$.

Proof:

By using theorem (2.1) , the matrix $T(D_n \times C_{11})$ from proposition (3.2) and the previous forms of $J(D_n \times C_{11})$ and $F(D_n \times C_{11})$ then we have:

$$J(D_n \times C_{11}) \cdot T(D_n \times C_{11}) \cdot F(D_n \times C_{11}) = \begin{bmatrix} 2 & 0 & 0 & 0 & \cdots & 0 & 0 & 0 & 0 \\ 0 & 2 & 0 & 0 & \cdots & 0 & 0 & 0 & 0 \\ 0 & 0 & 2 & 0 & \cdots & 0 & 0 & 0 & 0 \\ \vdots & \vdots & \vdots & \ddots & & 0 & 0 & 0 & 0 \\ 0 & 0 & 0 & 0 & \cdots & 2 & 0 & 0 & 0 \\ 0 & 0 & 0 & 0 & \cdots & 0 & 1 & 0 & 0 \\ 0 & 0 & 0 & 0 & \cdots & 0 & 0 & 1 & 0 \\ 0 & 0 & 0 & 0 & \cdots & 0 & 0 & 0 & 1 \end{bmatrix}$$

$$= D(D_n \times C_{11}) = diag\{2\,,2\,,\ldots,2\,,1\,,1\,,1\}$$

Such that $2(\gamma+3)\times 2(\gamma+3)$ square matrix.

Theorem (3.4):

If $n=2^{\gamma}$,where γ is any positive integers number, then the cyclic decompositionof Ac $(D_n\times C_{11})$ is:

$$\text{Ac}\ (D_n\times C_{11})=\bigoplus_{i=1}^{2\gamma} C_2 = \bigoplus_{i=1}^{2} AC(D_n)\ .$$

Proof:

By proposition (3.2) we find $T(D_n\times C_{11})$ and by proposition (3.3) we have $J(D_n\times C_{11})$ and $F(D_n\times C_{11})$ Hence.

$$J(D_n\times C_{11}).T(D_n\times C_{11}).\ F(D_n\times C_{11})$$

$$=diag\{2\ ,2\ ,\dots,2\ ,1\ ,1\ ,1\}$$

$$=\{d_1,d_2,\ ,\dots,d_{\gamma,}\ ,d_{\gamma+1},d_{\gamma+2}\ ,d_{\gamma+3}\}$$

Then by theorem (2.2) we have:

$$AC(D_n\times C_{11})=\bigoplus_{i=1}^{2\gamma} C_2 = \bigoplus_{i=1}^{2} AC(D_n)\ .$$

Example (3.5):

To find $\text{Ac}(\text{D}_{33554432}\times \text{C}_{11})$ by theorem above:

$\text{Ac}(\text{D}_{33554432}\times \text{C}_{11})=$

$$\text{Ac}(\text{D}_{524288}\times \text{C}_{11})=\text{Ac}(\text{D}_{2^{19}}\times \text{C}_{11})=\bigoplus_{i=1}^{38} C_2 = \bigoplus_{i=1}^{2(19)} C_2$$

$$=\bigoplus_{i=1}^{2} A=C(D_{2^{19}})=\bigoplus_{i=1}^{2} AC(D_{524288}).$$

$$\text{Ac}(\text{D}_{33554432}\times \text{C}_{11})=\text{Ac}(\text{D}_{2^{25}}\times \text{C}_{11})=\bigoplus_{i=1}^{50} C_2 = \bigoplus_{i=1}^{2(25)} C_2$$

$$=\bigoplus_{i=1}^{2} AC(D_{2^{25}})=\bigoplus_{i=1}^{2} AC(\text{D}_{33554432}).$$

Propsition (3.6) : If $n = q_1^{\tau_1} \cdot q_2^{\tau_2} \cdots q_m^{\tau_m} \cdot 2^{\gamma}$ where q_i are different primes , and $q_i \neq 2$for all i = 1,2, … , m, γ and τ_i any positive integersthen::

$$T(D_n \times C_{11}) = \begin{bmatrix} 2 \cdot \sigma_2(C_n) \otimes T(C_{11}) & & & & & M \\ & & & & & M \\ & & & & & M \\ 0\ 0 & \cdots & \cdots & \cdots & 0 & 1111 \\ 0\ 0 & \cdots & \cdots & \cdots & 0 & 0110 \\ 1\ 1 & \cdots & \cdots & \cdots & 1 & 0101 \\ 1\ 1 & \cdots & \cdots & \cdots & 1 & 1101 \end{bmatrix}$$

,Where $M = \gamma \cdot times \begin{Bmatrix} 11\ 11 \\ 11\ 11 \\ \cdot\cdot\ \cdot\cdot \\ \cdot\cdot\ \cdot\cdot \\ 11\ 11 \\ 01\ 10 \end{Bmatrix}$,Which is $2[(\tau_1+1)(\tau_2+1)\dots(\tau_m+1)(\gamma+1)+2] \times 2[(\tau_1+1)(\tau_2+1)\dots(\tau_m+1)(\gamma+1)+2]$Square matrix, $\sigma_2(C_n) \times C_{11}$ is similar to the matrix in remark(2.7).

Proof:

The Artin's character table $Ar(D_n \times C_{11})$ can be obtained by theorem (3.1) and from proposition (2.3), and example (1. 7) and by the tensor product we obtained the Irreducible valued character table ($\equiv^* (D_n \times C_{11})$) . then matrix $T(D_n \times C_{11})$can be found by using the definition of $T(G)$:

$$T(D_n \times C_{11}) = A_r(D_n \times C_5) \cdot (\equiv^* (D_n \times C_{11})^{-1}$$

$$= \begin{bmatrix} 2 \cdot \sigma_2(C_n) \otimes T(C_{11}) & & & & & M \\ & & & & & M \\ & & & & & M \\ 0\ 0 & \cdots & \cdots & \cdots & 0 & 1111 \\ 0\ 0 & \cdots & \cdots & \cdots & 0 & 0110 \\ 1\ 1 & \cdots & \cdots & \cdots & 1 & 0101 \\ 1\ 1 & \cdots & \cdots & \cdots & 1 & 1101 \end{bmatrix}$$

Which is : $2[(\tau_1+1)(\tau_2+1)\dots(\tau_m+1)(\gamma+1)+2] \times 2[(\tau_1+1)(\tau_2+1)\dots(\tau_m+1)(\gamma+1)+2]$ Square matrix.

Proposition (3.7):

If n $= q_1^{\tau_1}, q_2^{\tau_2}, \dots, q_m^{\tau_m}, 2^{\gamma}$, such that q_i are different primes and $q_i \neq 2$ for all $i = 1, 2, \dots, m$, γ and τ_i any positive integers then the matrices $J(D_n \times C_{11})$ and $F(D_n \times C_{11})$ are taking the forem:

$$J(D_n \times C_{11}) = \begin{bmatrix} J(C_n) \times J(C_{11}) & \begin{matrix} 0 & 0 \\ 0 & 0 \\ \vdots & \vdots \\ 0 & 0 \\ -1 & 1 \\ 0 & 0 \end{matrix} \\ \begin{matrix} 0 & 0 & \cdots \\ 0 & 0 & \cdots \end{matrix} & \begin{matrix} 0 & 1 & -1 \\ 0 & 0 & 1 \end{matrix} \end{bmatrix}$$

And

$$F(D_n \times C_{11}) = \begin{bmatrix} & & & & & 0 & 0 & 0 \\ & I_k & & & & 0 & 0 & 0 \\ & & & & & \vdots & \vdots & \vdots \\ -1 & -1 & \cdots & -1 & -1 & 0 & 0 & 1 \\ 1 & 1 & \cdots & 1 & 1 & 1 & 0 & -1 \\ 0 & 0 & \cdots & 0 & 1 & 0 & 1 & 0 \end{bmatrix}$$

where $k = 2[(\tau_1 + 1)(\tau_2 + 1) \dots (\tau_m + 1)(\gamma + 1) - 1] \times 2[(\tau_1 + 1)(\tau_2 + 1) \dots (\tau_m + 1)(\gamma + 1) - 1]$ and I_k is an identity matrix of the order k, they are: $2[(\tau_1 + 1)(\tau_2 + 1) \dots (\tau_m + 1)(\gamma + 1) + 2] \times 2[(\tau_1 + 1)(\tau_2 + 1) \dots (\tau_m + 1)(\gamma + 1) + 2]$ square matrix.

Proof:

By choosing previous forme of $J(D_n \times C_{11})$ and $F(D_n \times C_{11})$ and taking the form $T(D_n \times C_{11})$ from proposition (3.6) and by using theorem (2.1) then:

$$J(D_n \times C_{11}) \cdot T(D_n \times C_{11}) \cdot F(D_n \times C_{11}) = \begin{bmatrix} 2 & 0 & 0 & & \cdots & 0 & 0 & 0 \\ 0 & 2 & 0 & & \cdots & 0 & 0 & 0 \\ 0 & 0 & 2 & 0 & \cdots & 0 & 0 & 0 \\ \vdots & & & \ddots & & 0 & & \\ 0 & 0 & 0 & \cdots & 2 & 0 & 0 & 0 \\ 0 & 0 & 0 & \cdots & 0 & 1 & 0 & 0 \\ 0 & 0 & 0 & \cdots & 0 & 0 & 1 & 0 \\ 0 & 0 & 0 & \cdots & 0 & 0 & 0 & 1 \end{bmatrix}$$

$$= D(D_n \times C_{11}) = diag\{2\,, 2\,, \dots, 2\,, 1\,, 1\,, 1\}$$

Which is $2[(\tau_1 + 1)(\tau_2 + 1) \dots (\tau_m + 1)(\gamma + 1) + 2] \times 2[(\tau_1 + 1)(\tau_2 + 1) \dots (\tau_m + 1)(\gamma + 1) + 2]$ square matrix.

Theorem (3.8): If $n = q_1^{\tau_1} \cdot q_2^{\tau_2} \cdots q_m^{\tau m} \cdot 2^{\gamma}$, such that q_i are different primes and $q_i \neq 2$ for all $i = 1,2, \dots, m$, γ and τ_i any positive integers then the cyclic decomposition of $Ac(D_n \times C_{11})$ be:

$$Ac(D_n \times C_{11}) = \bigoplus_{i=1}^{2(\tau_1+1)(\tau_2+1)\dots(\tau_m+1)(\gamma+1)-1} C_2$$

$$= \bigoplus_{i=1}^{2} Ac(D_n) \oplus C_2$$

Proof:

By proposition (3.2) we found $T(D_n \times C_{11})$ and by proposition (3.7) we have $J(D_n \times C_{11})$ and $F(D_n \times C_{11})$ Hence :

$J(D_n \times C_{11}) \cdot T(D_n \times C_{11}) \cdot F(D_n \times C_{11}) = diag\{2,2,2 \dots,2,1,1,1\}$

$= \{d_1, d_2, \dots, d_{(\tau_1+1)(\tau_2+1)\dots(\tau_m+1)(\gamma+1)-1}, d_{(\tau_1+1)(\tau_2+1)\dots(\tau_m+1)(\gamma+1)},$

$d_{(\tau_1+1)(\tau_2+1)\dots(\tau_m+1)(\gamma+1)+1}, d_{(\tau_1+1)(\tau_2+1)\dots(\tau_m+1)(\gamma+1)+2}\}$

Then by theorem (2.2) we have :

$$Ac(D_n \times C_{11}) = \bigoplus_{i=1}^{2(\tau_1+1)(\tau_2+1)\dots(\tau_m+1)(\gamma+1)-1} C_2$$

$$= \bigoplus_{i=1}^{2} Ac(D_n) \oplus C_2$$

Example (3.9):

Calculating $Ac(D_{1800} \times C_{11})$, $Ac(D_{51510368} \times C_{11})$ by theorem above:

$$Ac(D_{1800} \times C_{11}) = Ac\left(D_{5^2\times3^2\times2^3\times C_{11}}\right)$$

$$= \bigoplus_{i=1}^{2(2+1)(2+1)(3+1)-1} C_2$$

$$= \bigoplus_{i=1}^{71} C_2 = \bigoplus_{i=1}^{2} Ac(D_{5^2\times3^2\times2^3}) \oplus C_2$$

$$Ac(D_{51510368} \times C_{11}) = Ac\left(D_{19^2\times13\times7^3\times2^5\times C_{11}}\right)$$

$$= \bigoplus_{i=1}^{2(2+1)(1+1)(3+1)(5+1)-1} C_2$$

$$= \bigoplus_{i=1}^{287} C_2 = \bigoplus_{i=1}^{2} Ac(D_{19^2\times13\times7^3\times2^5}) \oplus C_2 \ .$$

Conclusions

A new method has been found according to this research addition to that the cyclic decomposition of Artin Cokernel$Ar(D_n \times C_{11})$ of the factor group $AC(D_n \times c_{11})$, so we suggest to develop this research for future work.

References

1. Abaas, S. T.(2018). "Some Results on Artincokernel of the groupD_n×C_13where n is an odd number"Sci. (Lahore),30(6).pp. 869-874.
2. Abbas, H. H., (2008)."On Artin Cokernel of Dihedral Group Dn When n is an Even Number", Jornal of Kerbala University, Vol. 6, No. 3 Scientific.
3. Abid , A. S.,(2006). "Artin Characters Table of Dihedral Group for Odd Number", M. Sc. thesis University of Kufa.
4. Basheer , A. M.,(2006) "Representation Theory of Finite Group", AIMS, south Africa.
5. Curits, C. and Reiner, I.,(1981). "Methods of Representation Theory with Application to Finite Groups and order", John Wiley and Sons, New York.
6. David,G.,(1976). "Artin's Exponent of Arbitrary Characters of Cyclic Subgroup", Journal of Algebra, 61, PP 58 - 76.
7. Isaacs, I. M.,(1976). "Character Theory of Finite Groups", Academic Press, New York.
8. Jaber, N. H.(2019) "Artin's characters table of the group Q_2n×D_3wheren=p_1.p_2...p_3 andp_1.p_2...p_3are primes number" Journal (IJEAIS) ,Vol.3 ,pp 1-8, 2019.
9. Jaber, N. H.(2020). "Artin's characters table of the group Q_2m×D_4where m is an odd number" Journal,(IJEAIS),Vol.4,pp 66-87.
10. Kirdar, M.S.,(1982).("The Factor Group of the Z-valued Class Function Modulo The Group of the Generalized Characters",Ph.D. thesis, University of Birmingham.
11. Knwabusz, K., (1996)."Some Definitions of Artin's Exponent of Finite Groups",USA,National foundation Math, GR.
12. Lam, T.Y.(1968) "Artin Exponent of Finite Group", University of Colombia Journal of Algebra, 9,PP 94-119, New York.
13. Mahmood, N. R. and Z. Makkikadhim,(2015)."on Artincokernel of the group Q_2m×D_3 where m=2p and p is prime number" Journal European Academic Research,Vol.III. PP. 1902-1919.
14. Mirza, R.N. , (2006).On Artin Cokernel of Dihedral Group Dn when n is an odd number " M.Sc. thesis, University of Kufa.
15. Moori, J.,(2006)."Finite Groups and Representation Theory, "University of Kawzulu-Natal.
16. Serre, J. P.,(1977)."Liner Representation of Finite Groups",Springer-Verlage.
17. Yamacchi, K.,(1970)."On 2-Parts Artin Exponent of Finite Group ", Sci- Rep.Tokyo, Daigaku Sect.
18. Yassien, H. R.,(2000)."On Artin Cokernal of Finite Groups",M.Sc. thesis University of Babylon.

Inhibitory Effect and Antioxidant Activity of the Internal Membrane Decomposition of Egg Shells

Sheren Fadhel Abbas [1]

© 2023 The Author(s). This open access article is distributed under a Creative CommonsAttribution (CC-BY) 4.0 license.

Abstract: Different samples were collected from the internal membrane of the white and red eggshells local and imported to prepare protein hydrolyases using the enzyme Flavourzyme and studied the chemical composition of the raw material used moisture, ash, protein and fats where the proportions of chemical content were comparable to the samples prepared for the different species of hen and age, The decomposition lasted for two hours during which the degree of decomposition was estimated every half on hour. The hydrolyses of the internal membranes of the imported red egg shells were 0.5990%, the hydrolysates showed the highest reductive strength of the imported white eggs, 9.899%, while the protein decomposition of the eggshells of the eggshells in relation to the feasibility of ferrous ion binding of local red eggs was 40.547. Acquisition of hydrogen peroxide showed that the hydrolysates prepared from the internal membranes of locally red eggs and imported red eggs was a close result, reaching 333.92, whereas the ability of the hydroxyl root to decompose was the protein decomposition of the internal membranes of the shells of flat white eggs. 21.433% and Degradable internal membranes of eggs imported white super Oxide ability to seize the radichal of the highest negative value of the samples prepared 27.061% while did not appear to Tallit Albrootinh for all kinds of internal membranes effective inhibitory to bacteria.

Key Words: Egg Shell, Member shell Egg, Protein Egg.

Author details

[1] Department of Food Sciences, Collage of Agriculture, University of Bashar Iraq

Citation information

Cite this article as:

Abbas, S.F., (July 2023), *Inhibitory Effect and Antioxidant Activity of the Internal Membrane Decomposition of Egg Shells*, Proceedings of the Minar Congress, Turkey, (9) pp 113-120, DOI: http://dx.doi.org/10.47832/MinarCong9-10

http://dx.doi.org/10.47832/MinarCong9-10

[1] Sherenalfrah@gmail.com

Introduction

Egg shells and membranes are byproducts that are inedible but contain active biological compounds [1]. Eggs contribute to human nutrition since ancient times, it is one of the easiest and most receptive foods available of pigments and antioxidants [14].

Egg shells with their shells form 2-10% of the total egg and the shell is rich in mineral elements, especially calcium up to 92.5% as well as contain all the basic components of nutrition that ensure a reasonable reduction of food integration in humans [8].

The aim of this study was it the use of eggshells residues that cause significant pollution to the environment, which is one of the pollutants that cause undesirable odors, therefore, the study used to take advantage of the internal crusts of eggs and remove, dry and then grinded and used as proteolytic antioxidant protein and has the inhibitory effect of bacteria.

Materials and methods

1. Sample collection:

Separating the membrane : samples were collected from the inner membrane of the local and imported hen eggs with its both types red and white by removing the inner membrane of eggs which containing protein through separating them by soaking eggs in temperature 55c˚for 1-2 hours after that the membranes floated upward then dried and grind them and the samples have been kept in plastic containers until use.

Preparetion of the decomposed protein:

Prepared decomposed protein for all samples by taking the percent of 3gm : 3ml of water and I have determined the working conditions of the ideal enzyme from 7pH and temperature 50C˚ degree , where enzyme flavourzyme added by 0.1ml and the decomposition lasted for two hours during this time I followed up the degree of decomposition from zero to two hours.

Microbiology:

Used in the study was obtained bacteria from the Faculty of Agriculture / Department of Food Science at the University of Basra(pseudomonas aeruginosa, Salmonella typhi, Escherichia coil, Bacilluscereus, Staphylococcus aureus.

2. Estimated the chemical content of the inner egg-shells:

- Moisture: Moisture content of samples were estimated by putting 1 gm of samples in Aluminum plates known weight and dried using air drying oven with temperature of 105C˚ until the weight is proven according to[3].
- Ash: Ash content was estimated by burning the samples in Muffle Furnace with the temperature of 550C˚ as it mentioned in [3].
- Protein: Protein content of the samples were estimated by calculating the total percentage of Nitrogen and according to Semi – microkjeldahl [3].

- Fat: The fat of the samples were evaluated by Soxhlet device and by using Hexane as solvent according to the mentioned method in [3].
- The preparation of Protein Hydrolysate: Followed the mentioned method of [2].
- Measuring Antioxidant Assay: Antioxidant effectiveness was estimated by using the system of Linolic acid according to Osawa and Namiki [11].
- Reductive force: Estimated the capability of the decomposer to reduce Ferric ion into Ferrous by following the method of Zhu [12].

$$\text{Reductive force}=100-\frac{\textbf{Read the absorbance of the sample}}{\textbf{Read the absorbance of the control sampled X100}}$$

- The Chelating ability of Ferrous Ion: Followed the method of [11] to calculate the capability of blinding Ferrous

$$\text{Bonding template\%}=\frac{\textit{Read the absorbance of thecontrol sampley}-\textit{Read the absorbance of the sample}X100}{\textit{Read the absorbance of the control sampled}}$$

- The capability of capturing Hydrogen Peroxide: Estimated the capability of capturing Hydrogen Peroxide as it was mentioned in Ruch [13]

$$\text{The ability to absorb peroxide\%}=\frac{\textit{Read the absorbance of the sampledy}}{\textit{Read the absorbance of the control sampled }]100}$$

- Hydroxyl Radical Scavenging: Tested the ability of the samples to capture Hydroxyl radicals and according to the mentioned method in Girgih [2].

$$\text{Hydroxyl Radical Scavenging\%}=\frac{\textit{Read the absorbance of thecontrol sampley}-\textit{Read the absorbance of the sample}X100}{\textit{Read the absorbance of the control sample}}$$

- The capability of capturing the negative of Oxide: I followed the mentioned method in Zhouyong [14].

$$\text{Capturing the superoxide Radical\%}=\frac{\textit{Read the absorbance of thecontrol sampley}-\textit{Read the absorbance of the sample}}{\textit{d Read the absorbance of the control sample }X100}$$

- Statistical analysis: The obtained results were analyzed statistically using the GenStat program and the LSD test was applied to calculate the value of significant differences at the level of significance P ≤ 0.05 based on the method of (Duncan, 1955). All data presented in the tables are the average of the sum of three iterations of each test.

Results and discussion

1. **Chemical analysis of internal egg shell components:**

Table (1) shows the chemical composition (%) of the internal and imported egg shells (red and white). The moisture content of the internal egg shells(locally and imported) of red and white eggs were 3.12,3.45% while the humidity of the imported and red egg shells were 2.22,0.64%. The variation in moisture ratios is due to egg age, storage conditions and the ability of crusts to absorb moisture and its effect in the surrounding atmosphere [7].

The highest ash content of imported white eggshells were 47.17%, while the lowest ash content of imported white eggshells was 20.45, while the ash content of domestic white and

red eggshells were 21.69|%, and 25.13% were similar. Chemotaxis of crusts depending on chicken breed and type of food [13].

The table shows that the protein ratios in the internal membranes of the local white and red eggs are higher than the ratios in the internal membranes of the imported white and red eggshells (1.410 and 1.41) and the lowest protein for the imported eggs (0.32 and 0.89), this variation in ratios depending on the fact that the membranes are rich in proteins.

While the fat percentage of the egg shells of the internal membranes of domestic and imported eggs in both white and red types was the highest index of the egg shells of the imported white eggs, 6.16% and the lowest fat percentage in the shells of the egg shells of the imported red eggs was 1.43%. To the type of hen, the type of food, the age of the hen, the purity of the materials used, the efficiency and accuracy of the equipment and the methods of extraction [5].

Table 1. Chemical Composition (%) of Eggshells

v	Internal egg shell specimens	Moisture%	Protein%%	Ash%	Fat%	R.L.S.D
1	**Imported Red Eggs**	0.64	0.32	20.45	1.43	0.003
2	**Imported White Eggs**	2.22	0.89	43.17	6.16	0.010
3	**Local Red Eggs**	3.12	1.41	21.69	2.61	0.020
4	**Local White Eggs**	3.45	1.33	25.13	2.89	0.002
	R.L.S.D	0.012	0.011	0.0212	0.012	0.010

2. Degree of Hydrolysis:

Table (2) displays the degree of protein degradation of the protein hydrolases generated from the interior membranes of two types of white, imported, and local red and imported egg shells using flavourzyme enzyme efficacy of048.357 units / gm. The findings revealed that both imported white and brown egg membranes had breakdown percentages of 043.20 and 42.97%, respectively. These outcomes were comparable to Muhamy's Ahkaka [4]. After hydrolysis for 30 minutes, the level of enzymatic hydrolysis was reached. It was decided to arrive at the stable stage after 300 minutes, and this was supported by [6].

Table 2. the degree of decomposition and protein of the samples

V	Samples internal eggshell	Degradation degree%	Protein degree%
1	**Local White Eggs 1**	**59.23**	0.789
2	**Local Red Eggs**	**31.34**	0.442
3	**Imported White Eggs**	**43.20**	0.388
4	**Imported Red Eggs**	**42.97**	0.432
	R.L.S.D	**0.0031**	0.0021

3. Results of antioxidant activity values for prepared protein decomposers:

The antioxidant activity was determined by using the linolenic fatty acid system. The results of the proteins decomposition of domestic and imported internal membranes prepared with flavourzym enzyme showed that the antioxidant activity increased by increasing the incubation period and the highest activity obtained from the internal egg membranes of imported red eggshells 0.5990% and the lowest rate was Internal red locally eggs 0.3221% and that this variation in effectiveness is due to the effect of several factors, including hydrolisate and enzyme type and molecular weight [8,12]

Table 3. The antioxidant activity values using the linoleic fatty acid system(%)

v	Internal eggshell samples	Antioxidant activity have
1	**Local White Eggs**	0.4774
2	**Local Red Eggs**	0.3221
3	**Imported White Eggs**	0.3737
4	**Imported Red Eggs**	0.5990
	R.L.S.D	0.021

4. Reduced power of decomposers:

The results in Table (4) demonstrated the reduction potential of the protein decomposition of the internal egg membranes. The highest reduction of the protein decomposition of the local egg membrane was 9.850%, and the lowest ratio of the egg membrane sample was local red (9.788%). The presence of amino acids with antioxidant activity may be the cause [4].

Table 4. The reductive power values of the decomposers

v	Internal eggshell samples	Reductionist force
1	**Local White Eggs**	9.850
2	**Local Red Eggs**	9.788
3	**Imported White Eggs**	9.899
4	**Imported Red Eggs**	9.845
	R.L.S.D	0.0010

5. Ferrous ion binding capability:

Table (5) show the ability to bind ferrous to the hydrolisaes of the internal protein membranes of the locally white 40.547% and red4.224% and white domestic 8.955% crusts. The local and imported white eggs were slightly spaced and this is due to the amount of concentrations used when the concentrations increase[7].

Table 5. Shows the values of the degradability of the ferrousion

v	Internal eggshell samples	Connect the ferrousion
1	**Local White Eggs**	19.651
2	**Local Red Eggs**	40.547
3	**Imported White Eggs**	4.224
4	**Imported Red Eggs**	8.955
	R.L.S.D	0.0021

6. Ability to capture hydrogen peroxide:

The different values of the hydrogen peroxide capture of the internal and imported white and red eggshell hydrolisaes used in the research varied and decreased. The value of the decomposers of the local egg shells 229.96% These values are consistent with theimported white egg 278.57% while the local and imported red egg for word 333.92,333.92% they obtained [9].

Table 6. Hydrogen Peroxide Capability

v	Internal eggshell samples	Hydrogen peroxide capture values
1	**Local White Eggs**	229.8
2	**Local Red Eggs**	333.92
3	**Imported White Eggs**	278.57
4	**Imported Red Eggs**	333.92
	R.L.S.D	0.0010

7. The ability to capture the hydroxyl root

The results in Table (7) show the susceptibility of proteolytic preparations prepared from the inner shells of egg shells[9].

Table 7. Hydroxyl Root Capability

v	Internal eggshell samples	Hydrogen peroxide capture values
1	**Local White Eggs**	19.800
2	**Local Red Eggs**	20.966
3	**Imported White Eggs**	21.433
4	**Imported Red Eggs**	20.455
	R.L.S.D	0.0031

8. Ability to grab the Radical of the negative superoxide:

The results of the ability to capture the negative superoxide root in Table (8) of the proteolytic decomposition of the internal membranes of locally and imported egg shells, where the value of locally white eggs was 22.93 and imported white eggs 27.06 and that this difference is due to the ability to seizure varies by molecular weight and amino acid sequence in the decomposers. Consistent with what he said [12].

Table 8. Negative Super Oxide Radical Capability Values

v	Internal eggshell samples	Were taken for negative superoxide root capture values
1	**Local White Eggs**	22.938
2	**Local Red Eggs**	4.651
3	**Imported White Eggs**	27.061
4	**Imported Red Eggs**	11.839
	R.L.S.D	0.0210

9. Factors affecting the stability of antioxidant activity:

The results showed in Table (9) the effect of temperature, pH and enzyme type on the stability of the antioxidant activity of the prepared decomposers. With the stability of the type of enzyme used, which is the enzyme Flavozyme and that one to stabilize the temperature of the prepared samples better because oxidation tests are affected by temperatures, the decrease and rise, so the temperature was stabilized 50 C and these effects came in accordance with what came [12].

Table 9. Factors affecting the stability of antioxidant activity

v	Samples	Temperature	pH	Enzyme
1	**Local White Eggs**	50	9.15	Flavouzyme
2	**Local Red Eggs**	50	8.15	Flavouzyme
3	**Imported White Eggs**	50	8.22	
4	**Imported Red Eggs**	50	8.47	

10. Inhibitory effect against bacteria of protein decomposers of internal membranes of local and imported white and red eggs:

Table (10) shows the inhibitory activity of bacteria towards the decomposition of the internal membranes of local and imported white and red eggshells of the local and imported white and red eggs.

Table 10. the microbial transplantation of the photolytic decomposition of the internal membranes

v	Bacillus	Pesecto	Staphelo	E.coil
1	**Local White Eggs**	----------	----------	----------
2	**Local Red Eggs**	----------	----------	----------
3	**Imported White Eggs**	----------	----------	----------
4	**Imported Red Eggs**	----------	----------	----------

References

1. A.H.Keiko.,T.N.Kuroda.,G.W.Froning.Heat-induced Egg White Geles as Aff By PH.Journal Series(1998).NO.11.V.19
2. A.M. King. Review of the Uses of Poultry Eggshells and Shell Membrane.'or International Journal of Poultry Science. (2011) 10 (11): 908-912, 2011ISSN 1682-8356
3. AOAC . Official Methods of Analysis: Official Method for Protein. Method (1995)No. 920.87. Association of Official Analytical Chemists, Washington.
4. D.S. Dandare., I.J.Ezeonwumelu.,C.P.Ezeh.,H.Auta.Determination of in Vitro Antioxidant and Radical Scavenging Activities of Different Extracts of Allium sativum (Garlic). IOSR Journal of Pharmacy and Biological Sciences (2014). Volume 9, Issue 5 Ver PP 69-73.
5. G.K.Girish.,L.G.Lobol.,J.A.Jacobson.,Y.Morag.,B.Miller.,D.A.Jamadar. Ultrasound of the Shoulder: Asymptomatic Findings in Men. American Journal Roentgenology. October(2011). Volume 197, Number4.
6. H.G.Huang .R. Z.Jiang.,W.Chen.[6] Purification of Hepta-peptied With Iron binding activity from shrimp processing by- products hydrolysates.Advance Jouenal of Food Scienes and Technology,(2012).4(4):207-212.
7. I.G.Ihami.,I.Zubeyr.,H.M.Emastas,H.Y.Aboul-Eneind. Radical scavenging and antioxidant activity of tannic acid. Arabian Journal of Chemistry.(2010).NO2.V12.PP345-432.
8. K.Zhu.,K.L.Kraemer.,S.Xu .The Process of Innovation Assimilation by Firms in Different Countries .A Technology Diffusion Perspective on E-Business.Management Science.(2006).NO 5.V23 .PP342-432.
9. M.Acneil.,T.Saladin.[9] The Peaks over Threshold Method for Estimating High Quantiles of Loss Distributions. Proceedings of the 28th International ASTIN Colloquium, Cairns, August .(1997). 23-43
10. P.S.Peter.,S.Surai., B.Ksparks.Nutrition and Embryonic Development. 2. Antioxidant Properties and Discrimination in Embryonic .Tissues.(2001).NO54.V23.
11. T.Osawa.,M.Namiki. A Novel Type of Antioxidant Isolated from Leaf Wax of Eucalyptus leaves Journal Agricultural and Biological Chemistry.(1981). Volume 45, 1981 - Issue.
12. W.R.William.,L.D.Zweben.Combine Study Research Combined pharmacotherapies and behavioral interventions for alcohol dependence: the COMBINE study: a randomized controlled trial Group W. Adams, D. Diakosavvas, R. Roberts, J. Sharpley. (2006).NO4.V31.PP231-432.
13. V.Leehamilto .Chains of Command: Responsibility Attribution in Hierarchies Hamilton, V. L. Chains of Command: Responsibility Attribution in Hierarchies1. Journal of Applied Social Psychology, .(1986).16(2), 118–138. doi:10.1111/j.1559-1816.1986.tb02283.x'
14. Z.Dong.,G.T.Zhaogang.,X.M.Li.,M.Xu.,Y.Zhou., H.Ren.[14]Antioxidant Activities of Peptide Fractions Derived from Freshwater Mussel Protein Using Ultrasound-Assisted Enzymatic Hydrolysis. Czech Journal. Food Scinsce.(2017), 35,(4): 328–338.

Effect of Gibberellin Spraying On Yield of Bean and Its Components

Raam Shaker Mahmoud [1], Ammar Al-Zubade [2]

© 2023 The Author(s). This open access article is distributed under a Creative CommonsAttribution (CC-BY) 4.0 license.

Abstract: A field experiment was conducted at the research field station of the Field Crops Department, College of Agricultural Engineering Sciences, University of Baghdad, Jadriya, during the year 2017-2018— the experiment aimed to study the effect of growth regulator gibberellin on broad bean growth and yield. In a factorial experiment according to RCBD design, the first factor was gibberellin spraying stages (the beginning of vegetative growth and the beginning of flowering), while the second factor was gibberellin concentrations (100, 200, and 300 mg L-1), in addition to the comparison treatment, which was sprayed with water only. It was flowering by giving it the highest average plant height, number of pods, and seeds per pod. The results showed the superiority of the spraying stage at the beginning of flowering by giving it the highest mean of plant height, number of pods, and number of seeds per pod. In the spraying phase at the beginning of flowering (S2) and a concentration of 300 mg L-1, the highest average number of pods per plant reached 20.00 pods per plant. In comparison, a treatment at the beginning of flowering (S2) and a concentration of 200 mg L-1 achieved the highest average number of seeds per pod, reached 4.50 Seed in the pod, and achieved the spraying stage at the beginning of vegetative growth (S1) and the concentration was 200 mg L-1, the highest average was 133.3 g.

We conclude from this study that spraying gibberellin at the beginning of flowering affected growth indicators and increased yield by increasing the averages of its components, especially by increasing the concentration of gibberellin at 200 and 300 mg L-1.

Key Words: Legume, foliar application, growth regulator, sustainablity

Author details

[1] – [2] Field Crops Department, College of Agriculture, University of Baghdad, Baghdad, Iraq

Citation information

Cite this article as:

Mahmoud, R.S., Al-Zubade, A., (July 2023), *Effect of Gibberellin Spraying On Yield of Bean and Its Components*, Proceedings of the Minar Congress, Turkey, (9) pp 121-127, DOI:

http://dx.doi.org/10.47832/MinarCong9-11

http://dx.doi.org/10.47832/MinarCong9-11

Introduction

The broad bean, Vicia faba L., is considered one of the winter leguminous crops, as it occupies second place after Poaceae family in terms of importance. Its seeds are characterized by high protein content, estimated at 20-40%, and contain a high percentage of essential amino acids such as lysine, lecithin, and argentine, in addition to its high content of Carbohydrates (48-54%), minerals, fiber, and vitamins (Jacob and Nimr, 2010). Thus, they constitute an essential part of people's food and their importance in improving soil properties through the nitrogen fixation process (Ibrahim, 2011 and Kandi, 2007) and a significant energy source. Pods and green or dry seeds are used for nutrition (Akhidue, Ofuya, 2005). Beans are grown in different parts of the world; China produces about 50% of global Production, and Egypt 10.8%. Neighboring countries such as Syria, Jordan, Iran, and Turkey produce 9,124, 13,99, 10,00, and 8,404, respectively (FAO 2008). The cultivation of beans is widespread in Iraq the governorates of Baghdad, Babel, Tamim, and Nineveh, with an area of 5000 hectares and a production rate of 2.8 tons h-1 (Ministry of Agriculture, 2012). It is spread as an important food crop in the Middle East region and is involved in human use in the animal feed industry (Chafi and Bensoltan 2009).

Due to its crucial role in enhancing biological activity, plants require growth regulators in order to reach maturity. Numerous studies have shown that treating plants with a particular growth regulator improves plant structure, yield quality, and seed output.(Khalaf and Rajbo 2006 E.A.E etal.,2018,(Shihab and Hamza 2020).

Statistics indicate that the Production of broad beans in Iraq is relatively low compared to global Production and neighboring countries. Recently, advanced methods have been shown in agriculture to increase Production, including spraying growth regulators on field crops, and growth regulators are organic chemical compounds created inside the plant and prepared in the laboratory and affect growth by activation or inhibition as well.

Gibberellin is one of the stimulating plant hormones as it has an effect in stimulating hydrolysis enzymes necessary for the conversion of nutrients and cell division, such as alpha-amylase Beta-amylase, leaf and fruit growth, and stem elongation through its effect on cell elongation and increased division (Salloum et al., 2011, Singhandmuht, 2006). Gibberellin spraying is important for its effect on DNA and ATP and on stem elongation, especially cambium cells, leaf growth, flowering and fruit development (Hodey, 1994, and Salloum et al. 2011, Al-Jubouri et al. ,2012. Moreovere, Mustafa (2017) mentioned that spraying Anise seed with gibberellin (distilled water only with 6 mg. litter-1) achieved the highest values for the traits such as the plant hight cm, number of leaves, number of branches , wet weight g, dry weight g,Content of chlorophyll , Content of carbohydrates, Content of auxin, Content of gibberellin %, Content of volatile oil, Yield of volatile oil. Furthermore, Al_Zubaidi and Muafaq 2016) stated that when spraying gibberellin at concentrations of 150 and 200 mg.L-1 on soybeans, it gave a coefficient of (200 mgL-1) the highest average weight of 100 seeds was 12.82 gm, while the control treatment without spraying gave 11.01 gm, while the 150 mg

treatment gave the highest yield 3.446 µg ha-1, while it was the lowest yield in the comparison coefficient, as it reached 2.762 µg h-1 and the concentration 150 mg.L-1 gave the highest mean in plant height, number of branches, leaf area, and pods number per plant, and the yield was (90.3 cm, 4.83 branches. 2011 cm2, 122.9 pods, 3.446 µg.H-1), respectively. Al-Zubaidi (2015) mentioned that the spraying of gibberellin at concentrations of (100, 200, and 300 mg L-1) on barley plants had the highest height at a high concentration of gibberellin. In the same regards, Ismael and Nasralla (2014) showed that the levels of 100 mg GA3.L-1 and water spraying showed highest agronomic record such as number of total branches per plant, ect. In addition, R.S.H.and Zeboon(2019)claimed that all growth parameters were increased g by foliar spraying with gibberllic at level of 400 mgL. Furtheremore, Raam shakir (2016) found that gibberllin spraying along with two inhabetors were resulted significantly superior in all growth measured. Therefore, This research aim to investigate the magnitude effect of gibberellin application on broad bean and its yield components.

Materials and Methods

A field experiment was conducted at the research field station of the Field Crops Department, College of Agricultural Engineering Sciences, University of Baghdad, Jadriya, during the year 2017-2018—the experiment aimed to study the effect of growth regulator gibberellin on broad bean growth and yield. The experiment included two factors: the stages of gibberellin spraying; the first stage is the beginning of vegetative growth (S1) and the second stage is the beginning of flowering (S2) , second factor is gibberellin spraying concentrations (100, 200 and 300 mg L-1) as well as the comparison treatment according to the factorial experiment of randomized complete block design (RCBD). After preparing the land by plowing, smoothing and leveling it, the experiment field was divided into plots (3m * 2 m), and distance between lines was (40 cm) and between plants (20cm). Spanish variety seeds used, the germination rate was 100%, the seeds were sown 3 seeds per hole at a depth of (5 cm) on November 8, 2017, nitrogen fertilizer was added (50 kg N.h-1) in two batches, the first at planting , the second at the beginning of flowering and pod formation (Al-Zubaidi, 2014). After the completion of germination, the plants were thinned to one plant. All crop service operations were carried out, including weeding, hoeing, irrigation and fertilization, according to the plant's needs. The spray solution was prepared by grinding gibberellin tablets (10%), weighed to the required weights, and dissolved in distilled water in an amount of (1 liter) according to the concentrations in the field. The plants were sprayed until complete wetness in the early morning when the dew was gone. Data were collected, classified and analyzed according to the RCBD design, and the averages were compared using L.S.D. at a significant level of 0.05 (steel and torrie, 1980). The studied traits:

1. Plant height (cm): It represents the average final height of three plants taken randomly one week before harvest and measured using a graduated ruler from soil surface level to the end of the growing apex of the main stem.
2. Number of branches (plant branch-1): The average number of branches per plant was calculated from three plants in each experimental unit one week before harvest.

3. Leaf Chlorophyll Index (SPAD): The leaf chlorophyll index was measured with a Chlorophyll Metter Spad-502 Plus device, by taking the readings of three leaves from three branches of each plant and extracting their average.
4. The number of pods per plant (plant pod-1) was calculated in three randomly taken plants, and the average number of pods in each experimental unit was recorded.
5. The number of seeds per pod (Seed pod-1): 5 pods were taken randomly from the plants that were used in measuring the number of pods and according to the number of seeds in the pod.
6. Weight of 100 seeds (g): A random sample (100 seeds) was taken from the total seeds of the experimental unit and weighed with a sensitive scale.
7. Seed yield per plant (gm): It was calculated on basis of average yield for three plants taken randomly from each experimental unit.

Results and discussion

1. Growth indicators

Table 1 showed a significant effect of stages and concentrations of gibberellin spraying and their interaction on plant height, corophyll percentage and number of branches per plant. The treatment of spraying gibberellin at beginning of flowering (S2) achieved the highest plant height and the percentage of chlorophyll reached 110.35 cm and 52.29%, respectively. At the same time, the spraying stages had no significant effect on the number of branches. We note from the same table that the concentration of 200 mg L-1 gave the highest average plant height and number of branches 108.3 cm and 7.67 branches per plant, respectively. In comparison, the concentration of 300 mg L-1 achieved highest percentage of chlorophyll, amounting to 53.60, the comparison treatment gave the lowest height and number branch per plant and chlorophyll percentage was 97.7 cm, 6.17 branch per plant, and 49.20, respectively. The results showed a significant interaction between the treatment of gibberellin spraying at the beginning of flowering and with two concentrations of 200 and 300 mg L-1, which did not differ significantly, as it gave the highest mean of 115.7 and 116 cm, respectively. They achieved the same stage with the concentration of 300 mg L-1 the highest percentage of chlorophyll reached 53.91.

In contrast, the concentration achieved 200 mg L-1, the highest number of branches reached 8.67 branch per plant, compared to comparison treatment (0), which recorded the lowest plant height and the percentage of chlorophyll reached 88.7 cm and 47.63 cm at the beginning of vegetative growth(S1), respectively. The lowest number of branches reached 6.00 branch per plant at the flowering stage (S2). The reason for the increase in plant height and the number of branches at high concentration may be due to the role of gibberellin in elongating the stems through its effect on the elongation of cells and increasing their division and its ability to influence the activation of the formation of branches in the plant, which positively affects their increase (Mukhtar, (Cheyed 2013, Baqir, Zeboon et al. 2019, Nada and Hamza 2019).

Table 1. Effect of gibberellin spraying stages on growth indicators of bean

Gibberellin concentrations (mg L^{-1})	Plant height (cm)			Chlorophyll percentage			Branches Number per plant		
	S1	S2	Mean	S1	S2	Mean	S1	S2	Mean
0	88.7	106.7	97.7	47.63	50.77	49.2	6.33	6.00	6.17
100	98.0	103.0	100.5	46.97	52.57	49.68	8.33	6.33	7.33
200	101.0	115.7	108.3	52.07	53.53	52.80	6.67	8.67	7.67
300	100.0	116.0	108.0	53.29	53.91	53.60	7.00	8.23	7.61
Mean	96.9	110.6		49.99	52.69		7.08	7.30	
LSD 0.05 Spray stages	2.21			1.93			N.S		
LSD 0.05 Concentrations	2.70			2.36			0.29		
LSD 0.05 Interactions	3.82			3.35			0.41		

* S1= beginning stage of vegetative growth , S2= stage the beginning of flowering

2. Yield indicators

The results of Table 2 showed a significant effect of stages and concentrations of gibberellin spraying and the interaction between them on the number of pods per plant, the number of seeds per pod, the weight of 100 seeds, and the seed yield per plant. The results of the table show that spraying treatment at the beginning of flowering (S2) gave the highest average number of pods per plant, number of seeds per pod, and seed yield per plant was 17.41 pods per plant, 3.91 seeds per pod, and 18.87 gm per plant, respectively. While the highest weight of 100 seeds at beginning of vegetative growth (S1) was 149.92 gm. It is noted that the treatment of 300 mg L-1 gave the highest averages for the number of pods per plant, the number of seeds per pod, the weight of 100 seeds, and the seed yield per plant was 17.50 pods, 3.98 seeds, 182.00 gm, and 20.06 gm, respectively. While the comparison treatment recorded the lowest average yield of 6.17 pods per plant, 3.45 seeds per pod, 124.50 gm and 18.09 gm, respectively. led to an increase in yield. The table shows that a significant overlap was achieved between the spraying phase at the beginning of flowering (S2) and a concentration of 300 mg L-1, the highest average number of pods per plant reached 20.00 pods per plant, while a treatment at the beginning of flowering (S2) and a concentration of 200 mg L-1 achieved the highest average number of seeds per pod reached 4.50 Seed in the pod and achieved the spraying stage at the beginning of vegetative growth (S1) and the concentration was 200 mg L-1, the highest average was 133.3 g. The reason for the increase is that spraying at the appropriate time may not be necessary to spray a high concentration of gibberellin by taking the plant enough from the growth regulator, while the treatment of overlap between the beginning of flowering and the comparison treatment (without spraying) recorded the lowest yield of the plant, which reached 15.05 gm per plant. This result in line with (Cheyed 2008, Joody 2010, AL-Naqeeb and Al-Zubadie 2017, Habeeb and Hanshal 2017).

Table 2. Effect of gibberellin spraying stages on yield indicators of bean

Gibberellin concentrations (mg L^{-1})	pods number per plant			number of seeds per pod			weight of 100 seeds (gm)			Seed yield per plant (gm)		
	S1	S2	Mean	S1	S2	Mean	S1	S2	Mean	S1	S2	Mean
0	7.67	13.00	10.33	3.07	3.83	3.45	119.4	129.5	124.5	17.13	15.05	18.09
100	12.33	17.00	14.67	3.93	3.40	3.67	133.0	106.4	119.7	16.68	21.95	18.32
200	14.33	19.67	17.00	3.33	4.50	3.92	133.3	84.90	109.1	19.50	18.20	19.85
300	15.00	20.00	17.50	3.59	4.37	3.98	214.0	150.0	182.0	19.85	20.28	20.06
Mean	12.33	17.41		3.48	3.91		149.9	117.7		18.29	18.87	
LSD 0.05 Spray stages	0.82			0.22			2.90			1.08		
LSD 0.05 Concentrations	1.00			0.27			3.55			1.32		
LSD 0.05 Interactions	1.42			0.38			5.02			1.87		

* S1= beginning stage of vegetative growth, S2= stage of the beginning of flowering

Conclusions

We draw the conclusion from this study that spraying gibberellin at the beginning of flowering had an effect on growth indicators and increasing yield through increasing the averages of its components, most notably by increasing the concentration of gibberellin at concentrations of 200 and 300 mg L-1. This was determined by looking at the results of the experiment.

References

1. Ari, Rajala. 2003 . plant growth regulators to manipulate cereal growth in northern growing conditions. Univer of Helsinki . Department of applied Biology . Publication NO.13 .
2. Chen ,S.Y.,Y.R.Kuo and C.T.Chien .2008. Roles of gibberllines and abscisic acid in dormancy and germination of red bayberry (Myricarubra)seeds .Tree Physiol .28(9):1431-1439.
3. Groot.S.P.C.andC.M.Karssen .1987.Gibberellins regulate seed germination in tomoto by endosperm weakening:astudy with gibberellins – deficient mutants .Plant 171:525-531.
4. Iqbal,N.,R.Nazar .,M.Iqbal R.Khan.,A.Masood and N.A.Khan .2011.Role of gibberellins in regulation of soure - sink relations under optimal and limiting environmental condition .Current Science .100.7-10.
5. R.S.H.Mahmood .,N.H.Zeboon 2019.Effect of folar spraying with Gibberellic and humid acid on wheat growth. Int.j.Agricult.stat Sci.Vol 15 No.2pp.621-625.
6. Al-Zubadidi.Raam,SH.,Muafaq A.S.AL-Naqeeb .2016. Effect of nutrition and gibberellin on growth of barley and oat hydroponic system . Fourth Scientific international conference for Iraq Association of Genetic Environmental Resources.
7. Reaam Shakir.2016.Effect of spraying Gibberellin and Ethephon on the Yield and it Component of rapseed. Alfuratagriculture vol 8(3).
8. E.A.E .Genaidy and H.A.Zahran ,.A.K.G.Atteya,S.K.Al-Taweel.2018.Effect of gibberellic acid and zinc sulphate on vegetative flowering ,seed yield and chemical consistent of jojoba plant (Simmondsia chinsis).Indian J.Agric .Res.

9. Esmail A.E.Genaidy and Hamdy A.Zahran.Sudad K.Al-Taweel .Amiea K.G.2018.Oil Content Vegetative and Reproductive Teaits of jojoba plant AsAffected by Foilar Application of Gibberellic Acid.IOSR Jorn. Of Ager. And VeterinarySci.(IOSR-JAVS) Vol.11 iss.2pp.53-58.
10. Thomas, J. M. 2004. Control of proteinsynthesis in barley aleurone layersby the plant hormones, Gibberellicacid.
11. Khalaf, A. S., & Al-Rajbo, A. S. A. 2006. Seed technology. Dar Ibn Al Atheer Printing and Publishing. University of Mosul. Iraq.
12. AL-Naqeeb, M. and R. Al-Zubadie (2017). "EFFECT OF FOLIAR AND GIBBERELLIN ON GRAIN YIELD AND ITS COMPONENTS OF BARLEY." IRAQ JOURNAL OF AGRICULTURAL RESEARCH 22(10).
13. Baqir, H., et al. (2019). "The role and importance of amino acids within plants: A review." Plant Archives 19(2): 1402-1410.
14. Chafi, M. and A. Bensoltane (2009). "Vicia faba (L), a source of organic and biological manure for the Algerian arid regions." World J Agric Sci 5(6): 698-706.
15. Cheyed, S. (2008). "Effect of gibberelic acid on viability and seed vigour of sorghum sorghum bicolor (L.) meonch resulted from different plant population." M. Ph (Doctoral dissertation, Thesis. University of Baghdad, College of Agriculture, Department of Field Crops).
16. Cheyed, S. H. (2013). "EFFECT OF GIBBERELIC ACID ON VIGOUR OF SORGHUM SEEDS PRODUCED FROM DIFFERENT PLANT POPULATIONS." Iraqi Journal of Desert Studies 5(1).
17. Habeeb, S. T. A. and M. A. Hanshal (2017). "THE ROLE OF HUMIC ACID, GIBBERELLINS AND SMOKED WATER IN IMPROVING THE FLORAL AND FRUIT TRAITS FOR THE TOMATO YIELD." Euphrates Journal of Agriculture Science 9(4): 1-12.
18. Ismael, S. and A. Nasralla (2014). "BIOLOGICAL ACTIVETY OF GA3 AND THE FOENICULUM VULGARE MILL EXTRACT ON VEGETATIVE CHARACTERS OF CHAMOMILE (MATRICARIA CHAMOMILLA L.)." Iraqi Journal of Agricultural Sciences 45(8-special issue).
19. Joody, A. T. (2010). "Effect of GA3 and Method Application of Humic Acid on Some Vegetative Characteristics of Plum PRUNUS SALICINA L." Humic acid 1(1).
20. Mustafa, S. (2017). "The biological effectiveness of gibberellic acid seeds soaking and foliar to abscisic acid in the growth, anise oil yield and its chemical content." Iraqi Journal of Agricultural Sciences 48(5).
21. Nada, H. S. and J. H. Hamza (2019). "PRIMING OF MAIZE SEED WITH GIBBERELLIN (GA3) TO TOLERATE DROUGHT STRESS 2. FIELD EMERGENCE AND ITS PROPERTIES." Iraqi Journal of Desert Studies 9(1): 1-12.

22. إبراهيم،رائدحمدي.2011 . استجابة صنفين من الباقلاء fabaVicia L . للرش بالزنك .مجلة الكوفة للعلوم الزراعية 3(2) : 85-92
23. الزبيدي، رئام شاكر محمود.2015 .تأثير التغذية الورقية ومنظمات النمو في نمو الشعير والشوفان المزروعة في جهاز الأستنبات والحقل . أطروحة دكتوراه مقدمة من قبل قسم المحاصيل الحقلية– كلية الزراعة- جامعة بغداد.
24. حامد، ملاذ عبد المطلب، عبد الجبوري، علاء الدين عبد المجيد. 2012. تأثير حامض الجبرليك في أنبات البذور وحاصل فول الصويا .مجله الانبار للعلوم الزراعية ،المجلد:10 العدد(1)
25. عطية، حاتم جبار ونادر فليح المبارك. 1999. دور منظمات النمو النباتية وموعد الزراعه في نمو وحاصل الذرة الصفراء. مجلة العلوم الزراعية العراقية. 30 (2):353 -364
26. سلوم، محمد غسان ومنى جمال وعبيره معلا . 2011 . الفيزيولوجيا البيئية النباتية . الجزء العلمي. كلية العلوم. جامعة دمشق. دار الطبع سوريا .
27. ياسين، بسام طه.2001 . أساسيات فسيولوجيا النبات. جامعه قطر
28. عطيه ،حاتم جبار، خضير عباس جدوع .(1999). منظمات النمو النباتية النظرية والتطبيقية.دار الكتب للطباعة والنشر.

Synthesis and Characterization of Ultraviolet Photodetector Based On Zns/PEDOT: PSS Organic/Inorganic P–N Heterojunction

Ikhlas H. Shallal [1], Morooje A. Aboode [2], Nisreen S. Turki [3]

© 2023 The Author(s). This open access article is distributed under a Creative CommonsAttribution (CC-BY) 4.0 license.

Abstract: Three samples of inorganic/organic (ITO/ ZnS/ PEDOT: PSS) photodetector has been fabricated from p-type (PEDOT: PSS) and n-type Zinc sulfide (ZnS) film, on a patterned indium tin oxide (ITO) coated glass substrate. The ZnS film was deposited by the thermal evaporation method at different thickness (100,200and300) nm. The current-voltage (I–V) characteristics of the fabricated samples exhibit a typical rectifying behavior. The (ITO/ ZnS/ PEDOT: PSS) has a high photo current which is increased from 0.267 A to 0.416A with increasing of ZnS layer thickness from (100-300) nm while the dark current was 0.057 A, at thickness (100nm) and increased to 0.171A at thickness (300 nm).It was observed that the ITO/ZnS (100nm)/PEDOT: PSS photodetector show higher photo responsivity is 64.4 A/W at 320nm.

Key Words: Organic, Inorganic, heterojunction, detector, thin films.

Author details

[1] College of Education for Pure Science/Ibn Al Haithem, Department of Physics, University of Baghdad, Baghdad, Iraq

[2] Solar Energy Research Center, Renewable Energy Directorate, Ministry of Higher Education and Scientific Research, Baghdad, Iraq

[3] College of Science for Women, Department of Physics, University of Baghdad, Baghdad, Iraq

Citation information

Cite this article as:

Shallal, I.H., Aboode, M.A., Turki, N.S., (July 2023), *Synthesis and Characterization of Ultraviolet Photodetector Based On Zns/PEDOT: PSS Organic/Inorganic P–N Heterojunction*, Proceedings of the Minar Congress, Turkey, (9) pp 128-139,DOI: http://dx.doi.org/10.47832/MinarCong9-12

http://dx.doi.org/10.47832/MinarCong9-12

[1] akhlas.h.s@ihcoedu.uobaghdad.edu.iq

[2] morooj_a@yahoo.com

Introduction

In recent years, organic optoelectronic devices like organic photodetectors (OPDs),organic thin film transistors (OTFTs),,organic light-emitting devices (OLEDs),and organic solar cells (OSCs).[1,2]

Organic photodetectors devices have a great deal of interest possibility; they provide particular features, in cost, weight and flexibility compared to classical and traditional inorganic semiconductors. [3,4] Nowadays, they have various applications, such as optical communication, in which shown potential in optical interconnections in data transmission systems, also they have used in environmental pollution monitoring, biomedical imaging sensing, and sensing, photometric metrology. In these applications, a high response and sensitivity of the utilized OPDs are critical to be acceptable for need in practical applications. [5]

Organic semiconductors, which include polymers and small molecules, have a number of attractive characteristics for optical sensing such as high absorption coefficients through visible wavelengths (VIS) and compatibility with large-area deposition processes like screen printing and ink-jet. [6]

Wide band gap (WBG) semiconductors are itself considering significant materials especially for UV photodetectors, since it permits room temperature employment, and supplies intrinsic visible-blindness.[7,8] The thermal conductivity of these materials are apparent significantly higher values compared with silicon, that makes them appropriate for high temperature and power applications.[9]

Zinc Sulphide (ZnS) thin films are an important (II- IV) semiconductors material, exists mainly in two forms an hexagonal wurtzite structure and cubic sphalerite structure [10,11].ZnS have a great important in various optoelectronic application such as , optical switching devices, light Emitting Diode (LED) in blue to ultraviolet (UV) region, photo catalysts and lasers[12,13,14] due to their distinguishing optical properties such as, wide optical band gap (3.5-3.9) eV, high value refractive index (2.35) and high transmittance.[15,16]

Photodetectors devices are photodiode with rectifying current density-voltage (J-V) characteristics. There are many parameters that affect and describe the performance of detectors. Among these parameters, responsivity which is the most significant parameter in photodetectors and is expressed by the following equation:[17].

$$\mathcal{R} = \frac{I_{ph}}{P_s} \quad \text{or} \quad \frac{V_{ph}}{P_s} \ldots\ldots\ldots\ldots\ldots\ldots (1)$$

Where the Iph and Vph: represent the current and output voltage due to the lighting effect respectively

Ps: is the power of the incident radiation. Responsiveness R is measured in units of (Amp/Watt) or (Volt/Watt).

The other parameter is the Quantum efficiency (η), which is defined as the ratio between the numbers of photo-generated charge carriers (N carriers) to the total number of fallen and absorb photons (N photons), and it is given by the following equation: [15]

$$\eta = \frac{N_{carriers}}{N_{photons}} = \frac{(I_{ph}/q)}{(P_s/hv)} \dots\dots\dots (2)$$

The quantum efficiency (η) is also a function of the wavelength (λ) of the incident photons, and the relationship that relates the spectral response R can be written as:[16]

$$\eta(\lambda) = \mathcal{R}(\lambda)\frac{h\,c}{q\,\lambda} \dots\dots\dots\dots\dots (3)$$

Since (hc/q) is equal to (1.24) ,the equation (3) can be written as follows:[17]

$$\eta(\lambda) = 1.24\ \frac{\mathcal{R}(\lambda)}{\lambda} \dots\dots\dots\dots (4)$$

η(λ) is an abstract number with no units.

The third parameter is the Noise Equivalent Power (NEP.) which is defined as the input radiation power required producing an optical signal so that the signal-to-noise ratio is one unit. That is, (SNR = 1) at the detector's output. It is given by the following equation:[18]

$$(NEP) = \frac{I_N}{\mathcal{R}} \dots\dots\dots\dots\dots\dots (5)$$

$$I_N = \sqrt{2\,q\,I_d\,\Delta f} \dots\dots\dots\dots\dots (6)$$

Where IN: represent the noise current. NEP is measured in Watts. Id: dark current (saturation current at reverse bias).

The detectivity is the most important parameters of the detector. It depends on the temperature, the cut-off frequency, the incident wavelength, the detector area, the frequency bandwidth, as well as the voltage applied to the detector, the noise associated with the detection) and it represents the reciprocal of the equivalent power to the noise as in the following equation:[19]

$$D = \frac{1}{NEP} \dots\dots\dots\dots (7)$$

(D*), is the specific detectivity and it is a criterion for the comparison between the types of detectors and is given by the equation:[19]

$$D^* = \mathcal{R}_\lambda \frac{(A\,.\,\Delta f)^{1/2}}{I_N} = \mathcal{R}_\lambda \left[\frac{A}{2\,q\;I_d}\right]^{1/2} \dots\dots\dots (8)$$

And it measured in (cm.Hz1/2/ Watt).

Device fabrication

A single layer device was manufactured by deposition layer of ZnS thin film with a thickness of (100,200,300∓20nm), on an (ITO) substrate, by the thermal evaporation technique, by using (Edwards E 306A) system, under vacuum pressure (10-5 Torr). Prior to depositing the ZnS film, The substrates were cleaned successively, by using acetone, deionized water, and propanol ultrasonic bath, resulting in a ZnS film of thickness (100,200and300) nm, Then PEDOT: PSS was coated by spin-coating technique at the speed of (1000 r.p.m) for 30sec, all samples were annealed at 70 °C for 30 minutes to evaporate the solvent in a thin film. The (p–n) heterojunctions of (ITO/ZnS/PEDOT: PSS) were fabricated with different ZnS thickness as; [ITO/ZnS(100nm)/PEDOT:PSS], [ITO/ZnS(200nm)/PEDOT:PSS], and [ITO/ZnS(300nm)/PEDOT:PSS],all samples annealed at (523,623)K. Figure (1) shows the stages of manufacturing the photodetector.

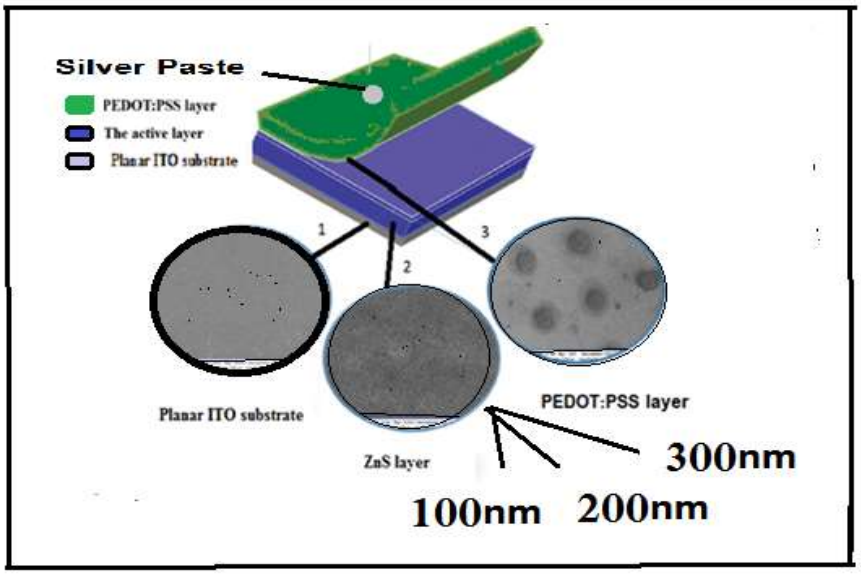


Figure 1. Detailed structure of the detector

Characterization and testing

ZnS film of thickness (100,200and300) nm, and PEDOT: PSS were examined by using scanning electron microscopy (SEM) and the Atomic Force Microscope (AFM)measurement Photocurrents of the samples were measured by Keithley 619).. The spectral responsivity (Rλ) was calculated for each wavelength (λ) by measuring the photocurrent generated (Iph) for each incident wavelength and using the system consisting of:

- Light source, which gives a spectral distribution within wavelengths (300-900nm)
- 2. Monochrometer that covers the wavelength (300-900nm) type (Edmund industrial optical model-0453954) from the company (Optometics-USA. Inc).

By using a 300 W Xe lamp supplied with a manual monochromatic, to examine the quantum efficiency of the samples, The electrical characteristics were collected by a Keithley 619.

Results and Discussions

SEM and AFM Measurements: Figure (2) illustrates the SEM micrographs of ZnS with (100,200, and 300 nm), and PEDOT: PSS thin films, respectively. The morphology of all the samples shows a dense uniform grains. It was observed that the grain size decreases with the increase of thickness.

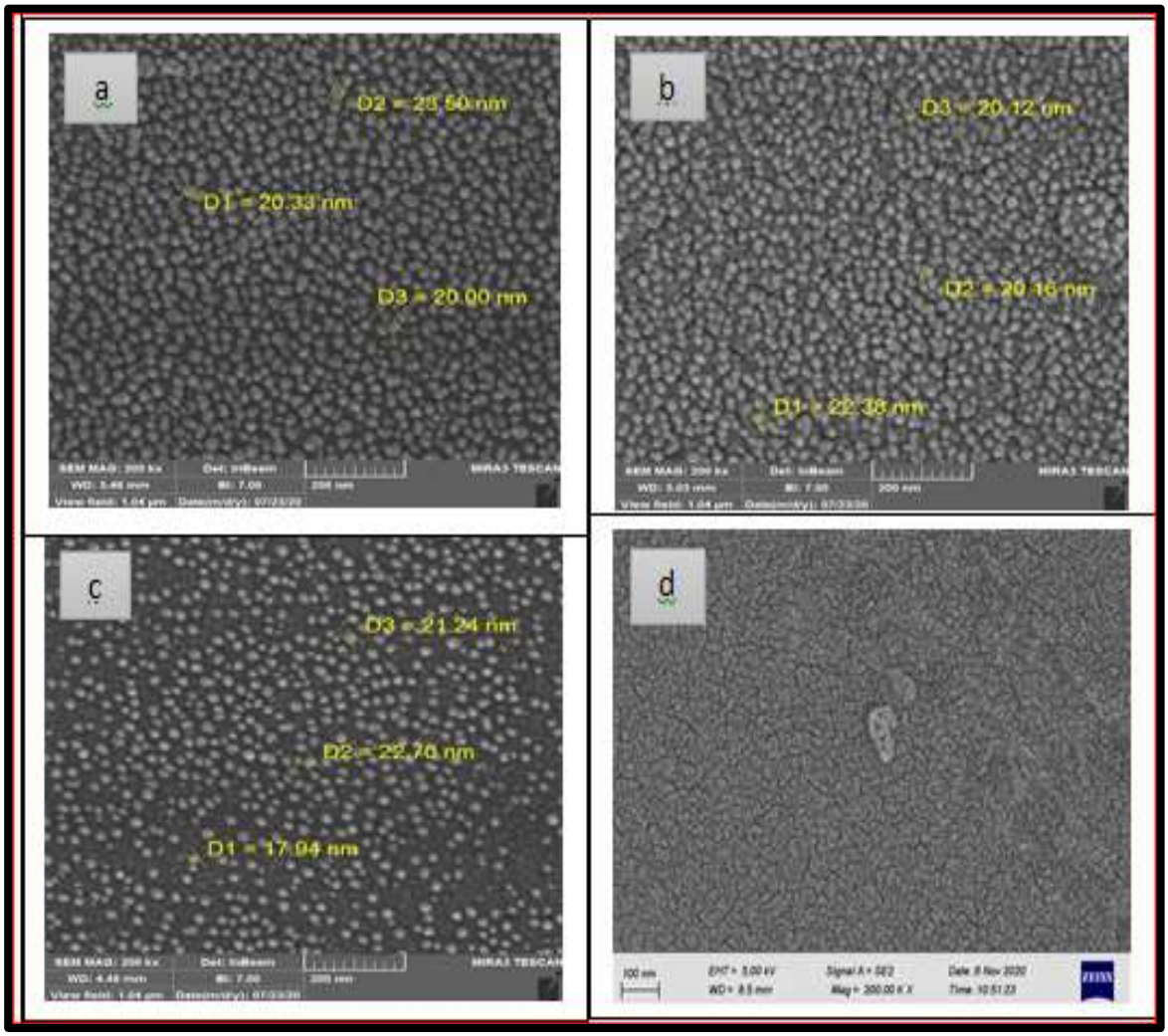


Figure 2. SEM image and of ZnS thin films with different thickness (a):100nm, (b) 200nm (c): 300 nm and (d): PEDOT: PSS films

Figure (3) shows the AFM surface morphology of ZnS and PEDOT: PSS thin films. as seen, the films are homogeneous without voids. It was observed from table (1), the average diameter of grain size decrease with increases in film thickness, also observed that surface roughness and Root Mean Square increase with increases in film thickness for ZnS films.

Table 1. Results of AFM measurements of ZnS and PEDOT: PSS thin films

sample	Thickness (nm)	Root Mean Square RMS (nm)	Roughness (nm)	Ten point Height (nm)	Average Diameter (nm)
ZnS	100	1.75	1.46	7.61	57.43
	200	2.14	1.84	8.05	48.57
	300	2.14	1.73	9.58	75.16
PEDOT:PSS		9.81	8.3	37.9	68.62

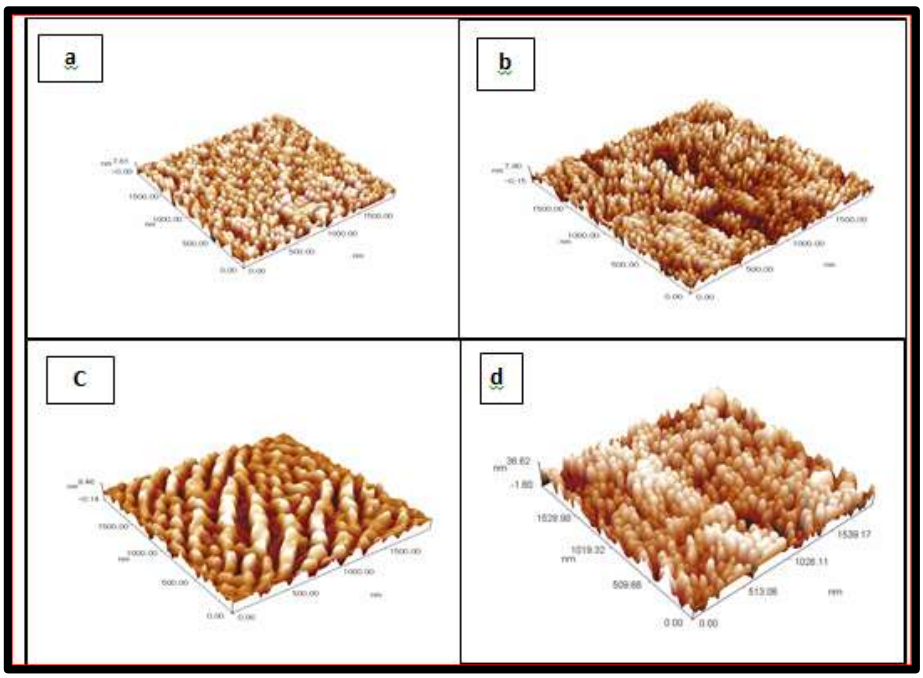


Figure 3. AFM images of ZnS thin films with different thickness (a):100nm, (b) 200nm (c): 300 nm and (d): PEDOT: PSS film

(Current – Voltage) characteristics of (ITO/ZnS/PEDOT:PSS):Figure (4) shows the (I-V) characteristics of the (ITO/ZnS/PEDOT: PSS) photodetector, it is clear that all samples behave like a diode at the bias voltage from (0 – 4V)). Both the dark and photocurrent current increase with increasing of the ZnS film thickness. The dark current was 0.057 A, and increased to 0.171A, while the photocurrent increased from 0.267 A to 0.416A with increasing of ZnS layer thickness from (100-300) nm, as presented in table (2).

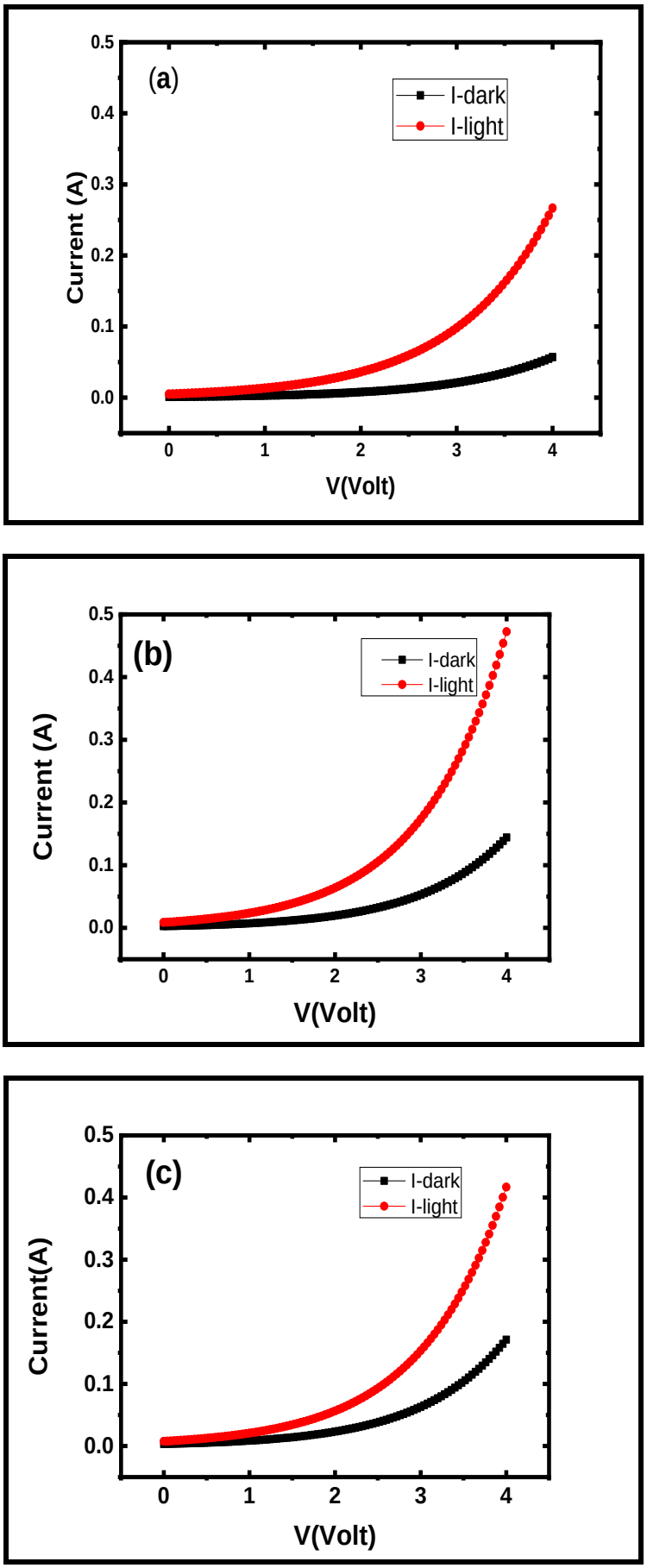


Figure 4. (Current - Voltage) of (ITO/ZnS/PEDOT:PSS) with different thickness of ZnS layer (a):100nm, (b) 200nm (c): 300 nm

Table 2. Results of (Current – Voltage) of (ITO/ZnS/PEDOT:PSS)

Sample	Thickness (ZnS) (nm)	Photocurrent (Iph) A	Dark Current (Id) A	Sensevity S=(Iph)/(Id)
ITO/ZnS/PEDOT:PSS	**(100nm)**	**0.267**	**0.057**	4.68
	(200nm)	**0.472**	**0.144**	3.28
	(300nm)	**0.416**	**0.171**	2.43

Parameters of (ITO/ZnS/PEDOT: PSS) Photodetector: Figure (5) shows the responsivity of the ITO/ZnS/PEDOT: PSS) photodetector, as shown the responsivity increased from 64.46A/W to 218.99 A/W for ZnS layer with 300 nm thickness.

The photodetector shows a clear wide response to the UV spectrum shorter than 400 nm, and the cutoff response wavelength is located at around 320 nm**.**

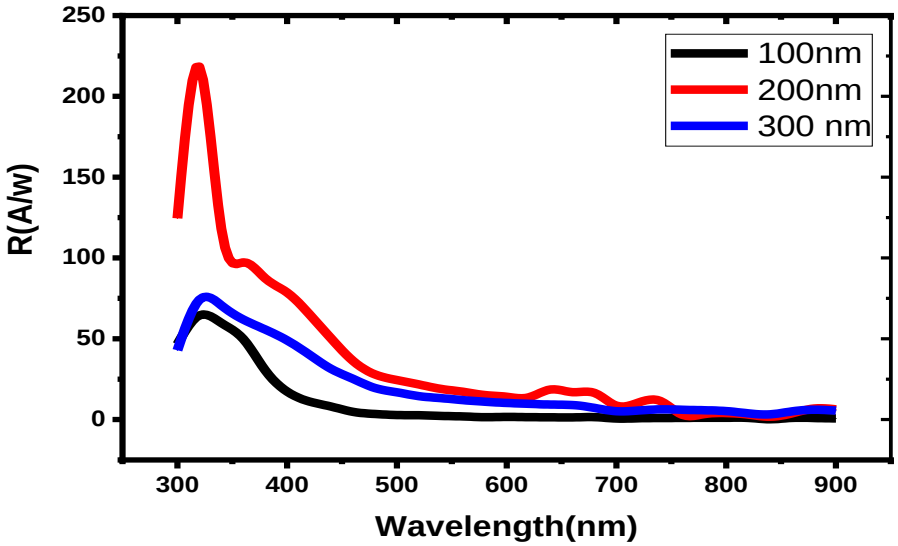


Figure 5. Responsivity of (ITO/ZnS/PEDOT:PSS) with different thickness of ZnS layer

Noise equivalent power (NEP) is defined as the minimum incident power that is required to produce a photocurrent equal to the photodetector noise current at a specified frequency and within a given bandwidth. NEP is calculated by using equation (5). Figure (6) show the NEP values, which decrease with the increase in ZnS thickness. The high value of the NEP was (9.60x10 -15) (W-1) at a thickness of (100nm), due to low noise current.

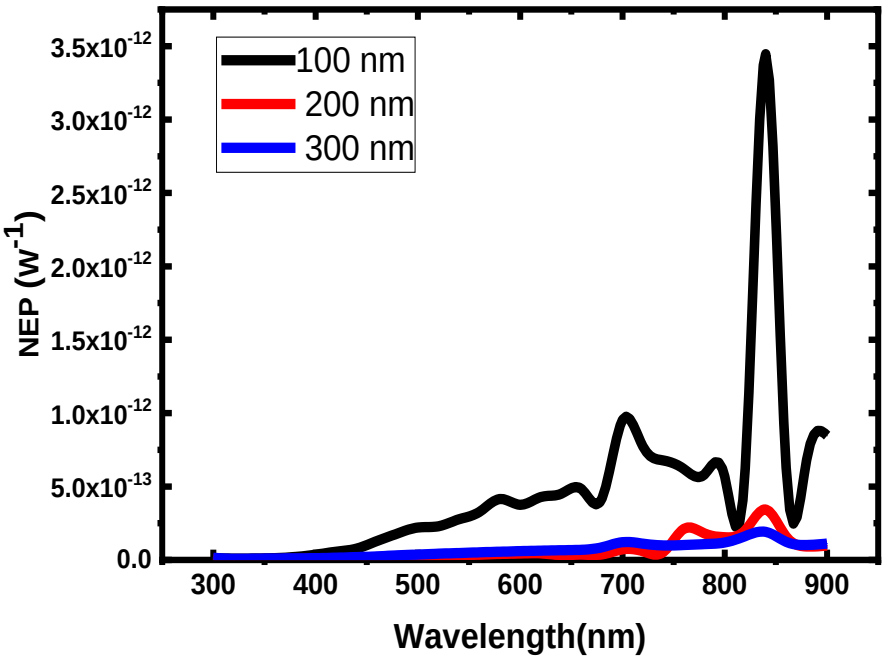


Figure 6. Noise equivalent power of (ITO/ZnS/PEDOT:PSS) with different thickness of ZnS layer

Figure (7) show the detectivity of the (ITO/ZnS/PEDOT: PSS) photodetector. As we noted, the values of the (D*) increasing with increasing of the thickness, and the highest value of the detectivity was at the thickness (300nm), which is (35.2 x1013) (cm .sec-1/2W-1), due to the increase in the light current and the lack of (NEP).

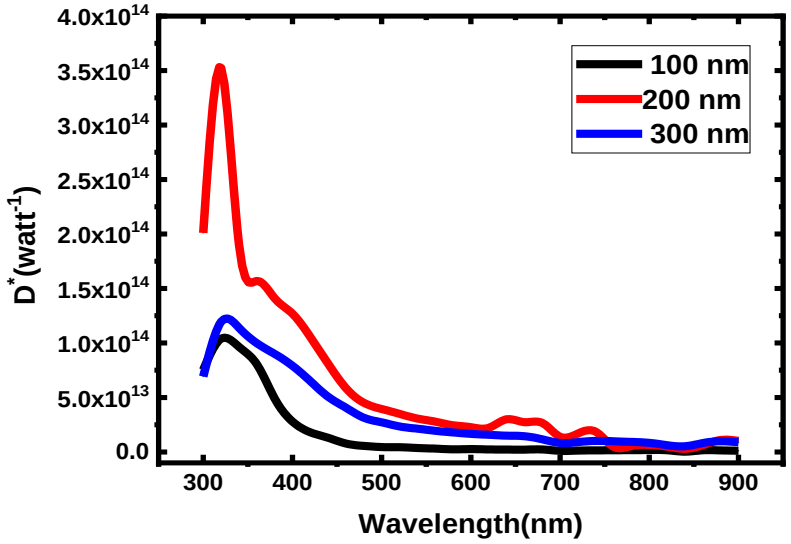


Figure 7. Specific detectivity of (ITO/ZnS/PEDOT:PSS) with different thickness of ZnS layer

The external quantum efficiency (QE) is one of the important parameters as it reflects the relationship between the numbers of charges extracted for each number of incident and absorbed photons.

The quantitative efficiency (QE) was calculated from the responsiveness (R) using the equation (2). Figure (8) show the highest value of the efficiency was equal to 84.63%) at the thickness of the ZnS layer (300nm).

All the data of the Photodetector Parameters (ITO/ZnS/PEDOT: PSS) are listed in table (3).

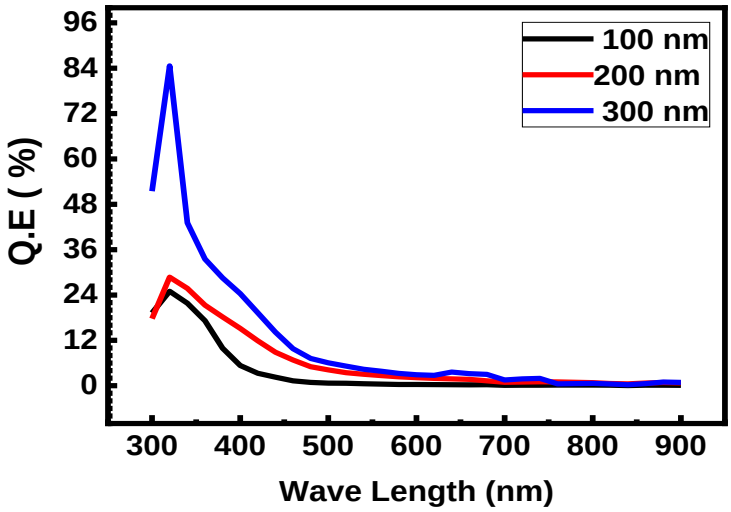


Figure 8. Quantum efficiency of (ITO/ZnS/PEDOT:PSS) with different thickness of ZnS layer

Table 3. Parameters of (ITO/ZnS/PEDOT: PSS) photodetector

Sample	Thickness (ZnS) (nm)	R_λ (A/W)	NEP*10^{-15} (W^{-1})	D^*x10^{13} (cm .$sec^{-1/2}W^{-1}$)	Q.E. (100%)
ITO/ZnS /PEDOT: PSS	100nm	64.46	9.60	10.4	24.97
	200nm	74.08	8.36	11.95	28.70
	300nm	218.99	2.83	35.2	84.63

Conclusions

In summary, Three samples of (ITO/ ZnS/ PEDOT: PSS) heterojunctions are fabricated,. The current-voltage (I–V) characteristics of the fabricated samples exhibit a typical rectifying behavior. The (ITO/ ZnS/ PEDOT: PSS) has

a high photo current which is increased from 0.267 A to 0.416A with increasing of ZnS layer thickness from (100-300) nm while the dark current was 0.057 A, at thickness (100nm) and increased to 0.171A at thickness (300 nm).

A high response of 218.99 (A/W) at 320 nm is observed at a bias of 4 V.

The measurement of the photodetector parameters (ITO/ ZnS/ PEDOT: PSS), includes that responsivity, noise equivalent power (NEP) and the specific directivity, it was found that the highest spectral response at the thickness (300nm). While the noise equivalent power (NEP) of the detectors decreases with the increase in the ZnS thickness.

We think that this organic\inorganic photodetector can be a promising candidate and can be used to fabricate low-cost and high-performance for UV detection.

References

1. Jeramy D. Zimmerman , Vyacheslav V. Diev , Kenneth Hanson , Richard R. Lunt ,Eric K. Yu , Mark E. Thompson , and Stephen R. Forrest ;"Porphyrin-Tape/C 60 Organic Photodetectors with 6.5% External Quantum Effi ciency in the Near Infrared"; J.Adv. Mater. 22, (2010): 2780–2783
2. Yu Han, Xiaohua Zhang, Fan Zhang, Dan Zhao, Junsheng Yu," Improved charge transfer, mobility and morphology for high performance panchromatic organic photodetectors by adding PC71BM in P3HT:IEICO-4F", Organic Electronics 75 (2019): 105410.
3. Dezhi Yang, Xiaokang Zhou, Dongge Ma;"Fast response organic photodetectors with high detectivity based on rubrene and C60" Organic Electronics 14 (2013): 3019–3023.
4. B. Arredondo, C. de Dios, R. Vergaz, A.R. Criado b, B. Romero, B. Zimmermann, U. Würfel," Performance of ITO-free inverted organic bulk heterojunction photodetectors: Comparison with standard device architecture", Organic Electronics 14 (2013): 2484–2490.
5. Wenhai Li, Dong Li, Guifang Dong, Lian Duan, Jialin Sun, Deqiang Zhang1,and Liduo Wang," High-stability organic red-light photodetector for narrowband Applications", Laser Photonics Rev. 10, No. 3, (2016): 473–480.
6. Tim P. Osedach, _ Scott M. Geyer, John C. Ho, Alexi C. Arango, Moungi G. Bawendi, and Vladimir Bulović," Lateral heterojunction photodetector consisting of molecular organic and colloidal quantum dot thin "; APPLIED PHYSICS LETTERS 94, (2009): 043307.
7. Feng Huang, Jing Zhou Li, Zhu Hua Xu, Yuan Liu, ," A Bilayer 2D-WS2/Organic-Based Heterojunction for High-Performance Photodetectors ",Nanomaterials , 9, (2019): 1312.
8. Joshua M. Pearce,"Photovoltaic Materials and Electronic Devices", , Michigan Technological University,USA, (2016).
9. T. Qasuria, "Investigation of the Organic Semiconductor Sensors for the Telemetry System Applications", Ghulam Ishaq Khan Institute of Engineering Sciences and Technology, Pakistan. (2012).
10. Mukherjee, P. Mitra, A. Mukherjee, and P. Mitra, “Characterization of Sn Doped ZnS Thin Films Synthesized by CBD,” Mater. Res., 20(2), (2017): 430–435. doi: 10.1590/1980-5373-mr-2016-0628.
11. B. A.Hasan and M. O. Salman, “Electrical Properties of ZnS Thin Films,” Iraqi J. Phys., 7(8), (2009).
12. R. Zein and I. Alghoraibi, “Influence of bath temperature and deposition time on topographical and optical properties of nanoparticles ZnS thin films synthesized by a chemical bath deposition method,” J. Nanomater., vol. 2019, (2019): 1-13. doi: 10.1155/2019/7541863.

13. S. G. Pandya, “Structural, Optical and Electrical Properties of Chemically Deposited Zinc Sulphide Thin Films,” Int. J. Recent Sci. Res., 7(12) , (2016): 14700–14703.
14. V. K. Ashith and K. Gowrish Rao, “Structural and Optical Properties of ZnS Thin Films by SILAR Technique obtained by acetate Precursor,” IOP Conf. Ser. Mater. Sci. Eng., 360(1), (2018): 012058. doi: 10.1088/1757-899X/360/1/012058
15. R. Vishwakarma, “Effect of substrate temperature on ZnS films prepared by thermal evaporation technique,” J. Theor. Appl. Phys., 9(3), (2015): 185–192. doi: 10.1007/s40094-015-0177-5.
16. M. Benavides and C. Alexandra, “Optimization of Organic Photodetectors from the Visible to the Near Infrared Spectra for Industrial Applications,” Msc. thesis , Friedrich-Alexander-Universität Erlangen-Nürnberg (FAU), (2019).
17. H. Ren, J.-D. Chen, Y.-Q. Li, and J.-X. Tang, “Recent Progress in Organic Photodetectors and their Applications,” Adv. Sci., 8(1), (2021): 2002418.
18. Sravanthi Kache,"Optimization of Charge Collection Efficiency in MSM Photodetector ",Msc. Thesis, University of Missouri- Columbia,(2005).
19. Salah M. Saleh Al-Khazali ,Husam S. Al-Salman , A. Hmood," Low cost flexible ultraviolet photodetector based on ZnO nanorods prepared using chemical bath deposition", Materials Letters, 277, (2020): 128177.

Evaluation of Some Heavy Metals and Microbial Contamination in Some Imported Food Sauce

Miyada Kh Hassan [1]

© 2023 The Author(s). This open access article is distributed under a Creative CommonsAttribution (CC-BY) 4.0 license.

Abstract: Canning, as a preservation technique, is extensively used to extend the shelf life and to maintain the quality of perishable foods. This study was conducted to assess the microbial contamination and give information about the concentration of the heavy metals (Zn, Cu, Pb and Cd) in canned sauce (Pasta sauce, basil sauce, Garlic sauce, Pizza sauce, Wing sauce, macaroni souse, mixed pickle, Mayonez, Tahin sauce, Pure Pomegranate syrup, Classical Sauce, Ketchup sauce, and Hot sauce) that collected from locally markets in Baghdad city during the period 1/9/2022 to 1/2/2023. The results indicated there was no bacterial contamination in all samples but there was a fungal contamination (mold and yeast) in (Pasta sauce, Garlic sauce, Mixed Pickle and Sesame sauce). Detection of investigated heavy metals including zinc, copper lead and cadmium, revealed the presence of Zinc and Copper in acceptable levels depending on the Iraqi standard specification, while Lead and Cadmium surpassed the permissible safe limits with concentration 0.25 ppm in Tahin sauce for Lead, and with concentrations 0.08, 0.07 and 0.11 ppm in canned Pesto basil sauce, Psti macaroni souse and Tahin sauce, respectively, for Cadmium.

Key Words: Food contamination, Food sauce, Heavy metals.

Author details

[1] Department of Biology, Collage of Science, University of Baghdad, Iraq

Citation information

Cite this article as:

Hassan, M.K., (July 2023), *Evaluation of Some Heavy Metals and Microbial Contamination in Some Imported Food Sauce*, Proceedings of the Minar Congress, Turkey, (9) pp 140-149, DOI: http://dx.doi.org/10.47832/MinarCong9-13

http://dx.doi.org/10.47832/MinarCong9-13

[1] miyada.k.765@sc.uobaghdad.edu.iq

Introduction

The subject of human health has garnered significant focus from experts in the realms of food, nutrition, and public health. Canned food, which has become one of the most widely consumed food categories globally, emerged prominently in the commercial sphere during the early 20th century. The production of these food items has grown substantially on a global scale. Canned food is preserved within hermetically sealed, sterile containers (Pascall et al., 2022).

Canned food products can deteriorate and become unsafe to consume due to various factors. These include the existence of microorganisms such as bacteria, yeast, and mold. To mitigate this, thermal treatments and sterilization processes are applied to these foods, effectively eliminating these microorganisms. However, if these treatments are not executed correctly, it can result in the proliferation of these microorganisms, ultimately leading to foodborne illnesses (Karlovsky et al., 2016).

Heavy metals play a crucial role in maintaining the balance within living cells. When present in elevated concentrations, these elements bring about various harmful impacts and toxicities in both human health and the environment, posing a serious threat to living organisms. Presently, specific heavy metal pollutants have been identified as causing detrimental effects on crop quality, thus exerting an influence on both food security and human well-being. Naturally occurring foods have been found to contain heavy metals like chromium, cadmium, copper, lead, and mercury. There is evidence indicating that these heavy metals act as environmental contaminants in raw foods (Munir, 2022). In numerous cases, vegetables absorb heavy metals from polluted water used for irrigation; in some nations, agricultural land is irrigated using sewage and industrial wastewater (Stasinos and Zabetakis, 2013).

Zinc stands out as a crucial inorganic element concerning human health. Its deficiency can lead to stunted growth in children, reduced fertility, dry mouth, headaches, and nausea. Excessive intake of zinc, on the other hand, can result in toxicity, causing electrolyte imbalances, nausea, anemia, and lethargy. Consuming elevated doses of zinc (ranging from 50 to 150 milligrams) can induce vomiting, diarrhea, headaches, and fatigue (Noaman and Al-Mayaly, 2015).

While copper (Cu) is vital for agricultural crops, excessive levels of this element can have severe repercussions on terrestrial ecosystems, as well as on the health of animals and humans. The accumulation of heavy metals in organisms can increase soil rhizosphere pollution, negatively impacting the immune systems of humans and ruminants, potentially leading to neurological issues, kidney failure, digestive problems, and heart ailments (Akhtar et al., 2022).

Numerous prior studies have focused on evaluating the health risks associated with the consumption of heavy metals, including copper (Cu) and cadmium (Cd), through the ingestion of contaminated food crops. (Liu et al., 2005; Ilechukwu et al., 2021).

Heavy metals like lead and cadmium cause neurological and kidney damage. Food contamination by heavy metal mainly occurs through pollution of water and soil (Balali-Mood, 2021).

The lead is classified as toxic metal and cause accumulation effect that lead to dangerous diseases like anemia, kidney toxicity and may result in injury to the central nervous system and brain. Lead impacts human of all ages, but the affected of lead are most dangerous in young children (Aloosh and Al-Azzawi, 2015).

Cadmium is a toxic metal that enters the soil–plant system via low-quality urban wastewater irrigation that is most often polluted industrial discharges with a heavy load of toxic metals (Ebrahimi et al., 2020). Cd is highly toxic heavy metals at higher concentrations to human health and is a main source of carcinogenic disorders (Haider et al., 2021). In addition, it may adversely affect the kidneys and stimulate chronic toxicity signs like decreased organ function, infertility, hypertension, and hepatic malfunction (Manouchehri et al., 2022).

Early detection of heavy metals in canned food is important to minimize the frequency of exposure of the human body (Palisoc et al., 2019).

The aim of the study was to determine the microbial contamination and concentration of some heavy metals (Zn, Cu Pb and Cd) which can be found in some canned sauce collected from some Iraqi markets.

Methods

Thirteen distinct food samples stored in cans were collected from various markets in Baghdad city. The assortment of samples included Pasta sauce, basil sauce, Garlic sauce, Pizza sauce, Wing sauce, macaroni souse, mixed pickle, Mayonez, Tahin sauce, Pure Pomegranate syrup, Classical Sauce, Ketchup sauce, and Hot sauce. These samples were subsequently transported to the laboratory.

To ensure proper experimentation, all glassware was cleaned using an acid wash, followed by rinsing with distilled water, and then drying. The procedure involved digesting the samples using concentrated nitric acid (5 ml), heating them until the solution became transparent. The solution was transferred to a 50 mL volumetric vial, with the volume being completed by adding distilled water. Subsequently, the elements (zinc, copper, lead, and cadmium) were analyzed using a flameless Atomic absorption spectrophotometer (Novaa, German).

In parallel, for the detection of bacteria and fungi, the samples were cultured in nutrient agar and malt extract agar respectively, which were utilized for the purpose of isolation. All culture media were prepared according to the instructions of the manufacture companies,

and sterilized by autoclave at 121°C for15 min. Then 1 ml of samples were collected by sterile tip of micropipette and cultured on cultured media. All the media plates were incubated at 37°C ± 1°C for 24–48 h for bacterial contamination and at 25°C ± 1°C for 7 days for fungal contamination then the plate examined for microbial growth.

Result and discussion

1. Detection of microbial contamination

Generally the canned foods are considered safe because they are processed under controlled conditions. When canned food shows any spoilage bulging can ends, leakage spurting fluids, mold or off-odor do not use it. Canned sauce may contain toxins if not properly processed (Abdulhay, and Salloom, 2013). Microbial contamination in canned sauce illustrated in table (1).

Table (1) Microbial contamination in sauce samples

no	Sample	Bacterial contamination	Fungal contamination
1	Pesto (Alla genivese)Pasta sauce produce by Barilla G.E.R. Fratelli (Italy)	-	+
2	Pesto (Alla genivese)basil sauce produce by Barilla G.E.R. Fratelli (Italy)	-	-
3	Sarimsak (Garlic sauce) Produced by (ARIHAN) Mersin / Turkey	-	+
4	Pizza sauce produced by Gulf food products Co, Amman	-	-
5	Hot Buffalo (Wing sauce) produced by American Garden U.S.A.	-	-
6	Psti (Pesto Rosso) macaroni sauce Produced by Barilla Italy	-	-
7	Camel (mixed pickle) produced by ADF foods LTD (India)	-	+
8	Mayonez Produced by TAMEK GiDA (Turky)	-	-
9	Tahin sesame Paste produced by Gulf food products Co, Amman	-	+
10	Pure Pomegranate syrup produce by (Alraky) Syrian products	-	-
11	Classical Sauce produced in Al-Wadi Al AKDAR SAL (Italy)	-	-
12	Ketchup sauce produced by Pure food Processing Industries (UAE)	-	-
13	Hot sauce (ALRYAD) produced of Delta food industries (UAE)	-	-

Table (1) revealed absence of bacterial contamination in all samples. While there is a fungal contamination in sample 1 (pesto), sample 3 (Garlic sauce), Sample 7 (mixed pickle) and sample 9 (Tahin sesame pest). This contamination due to combination of many reasons like: do not follow the basic health rules in processes of manufacturing and control of critical points in production and use of appropriate sterilizing temperatures, which eliminate all microorganisms and ensures no contamination of canned sauce (Alegbeleye et al., 2022).

The lack of microbial contamination in various other sauce products serves as evidence of the precision and effectiveness of manufacturing processes in eradicating these

microorganisms. Such contamination could otherwise harm the product. This achievement is attributed to the incorporation of modern technologies within the industry, which minimize any contact between the product and workers (Bahramia, 2020).

The canning process plays a significant role in eliminating a majority of microorganisms, thereby minimizing their impact on the quality and safety of food. Nevertheless, it's important to note that undesirable chemical contaminants have been discovered in canned foods, and this can be linked to the canning procedure (Zheng et al., 2021).

2. Detection of heavy metals in canned sauce

Table (2) includes concentrations of Zn, Cu, Pb and Cd in various canned sauce collected from different local markets in Baghdad city during study period from September 2022 to February 2023.

Table (2) concentration of (Zn, Cu, and Cd) in sauce sample

no	Sample	Mean ± SD (ppm)			
		Zn	Cu	Pb	Cd
1	Pesto (Alla genivese)Pasta sauce produce by Barilla G.E.R. Fratelli (Italy)	2.0 ± 0.107	0.5± 0.014	0.11± 0.502	0.04± 0.216
2	Pesto (Alla genivese)basil sauce produce by Barilla G.E.R. Fratelli (Italy)	9.0 ± 0.132	1.5 ± 0.064	0.15 ± 0.773	0.08 ± 4.059
3	Sarimsak (Garlic sauce) Produced by (ARIHAN) Mersin / Turkey	7.5 ± 0.016	1.0 ± 0.051	0.17 ± 0.495	0.05 ± 0.570
4	Pizza sauce produced by Gulf food products Co, Amman	3.0 ± 0.044	8 ± 0.037	0.12 ± 1.096	0.04 ± 0.506
5	Hot Buffalo (Wing sauce) produced by American Garden U.S.A.	2.5 ± 0.013	9± 0.739	0.11± 0.069	0.04± 0.010
6	Psti (Pesto Rosso) macaroni sauce Produced by Barilla Italy	6.5± 0.056	0.9± 0.010	0.13± 0.049	0.07± 0.009
7	Camel (mixed pickle) produced by ADF foods LTD (India)	4.0± 0.062	0.75± 0.054	0.12± 0.012	0.05± 0.494
8	Mayonez Produced by TAMEK GiDA (Turky)	2.0± 0.043	0.2± 0.471	0.07± 0.997	0.02± 0.550
9	Tahin sesame Paste produced by Gulf food products Co, Amman	45.0± 0.002	2.5± 0.412	0.25± 0.406	0.11± 0.013
10	Pure Pomegranate syrup produce by (Alraky) Syrian products	2.0± 0.094	0.3± 0.306	0.09± 0.554	0.03± 0.602
11	Classical Sauce produced in Al-Wadi Al AKDAR SAL (Italy)	5.0± 0.009	0.25± 0.720	0.08± 0.533	0.04± 0.160
12	Ketchup sauce produced by Pure food Processing Industries (UAE)	2.0± 0.302	0.21± 0.018	0.07± 0.665	0.02± 0.017
13	Hot sauce (ALRYAD) produced of Delta food industries (UAE)	3.5± 0.490	0.32± 0.062	0.08± 0.022	0.03± 0.228

2.1. Zn

The table (2) shows the concentration of Zn in sauce samples ranged from 45.0 to 2.0 ml/l. Highest mean value of zinc was 45 ppm in sample 9 (Tahine sesame paste), while the lowest mean value was 2 ppm in sample 1 (Pesto), sample 8 (Mayonez), sample 10 (Pure pomegranate), and sample 12 (Ketchap).

In accordance with Iraqi standards, the permissible threshold for zinc concentration is set at 50 mg/kg. However, the United States Environmental Protection Agency (US-EPA) and the European Commission (EC) have not established specific thresholds for zinc concentration, as outlined by the Alimentarius, a collaboration between FAO and WHO in 1994. Conversely, FAO (2020) has stipulated a maximum limit of 40 mg/kg for zinc in canned fish. Notably, none of the examined samples surpassed the contamination limits established by Iraq for canned foods.

Zinc, a major coating material used to prevent corrosion of iron and steel, it may transfer to the food in can (El Moussawi et al., 2019).

2.2. Cu

The concentration levels of Copper in the various samples of canned sauce studied are detailed in Table (2). Notably, the highest Copper concentration was observed in Hot Buffalo (Wing sauce) at 9 mg/l, whereas Mayonez and Ketchup sauce exhibited the lowest concentration at 0.2 mg/l. In accordance with the FAO/WHO guidelines from 2011, these concentrations were found to be within permissible limits.

As highlighted by Ahmad et al., (2016), copper (Cu) levels tend to be elevated in soil that has been exposed to wastewater irrigation. Factors like a low soil pH and the excessive use of pesticides or insecticides can contribute to the accumulation of copper in the soil. This accumulation has the potential to subsequently transfer to consumable items, including canned food products.

2.3. Pb

The results in table (2) revealed highest concentration of lead 0.25 mg/l in Tahin sauce while the lowest concentration of lead 0.07 mg/l in Mayonez was observed, The permissible upper limit for lead concentration in prepared foods specifically designed for infants or young children is set at 200 µg/kg. FAO/WHO (CIFA, 1992).

Commission Regulation (EC) No 1881/2006 sets maximum levels 0.2 mg kg−1 for lead in legume vegetables, cereals and pulses. In current study, none of the samples exceeded the limits for contaminants in canned foods except Tahine sauce. The variation in lead concentration may related to some reasons like the chemical properties of the food contact material and the food stuff, temperature during the storage, exposure to light (Abdulhay and Salloom, 2015).

2.4. Cd

As outlined in Table (2), it is evident that the concentration of Cd in the analyzed canned sauce samples exhibited a range from 0.02 mg/l in Mayonez and Ketchup sauce to 0.11 mg/l in Tahin sesame Paste. The outcomes of this study aligned with the findings of Khalafalla et al., (2016), who documented Cd concentrations spanning from 0.039 to 0.057 mg/kg in canned meat collected from Egypt. In contrast, Kowalska et al., (2020) recorded lower values for Cadmium, ranging from 0.005 to 0.019 mg/kg, in canned food products from Poland.

The maximum level for cadmium established by Commission Regulation (EC) No 1881/2006 is 0.05 mg kg−1 for canned fruits and vegetables. However, the current findings for Cadmium surpassed this threshold in canned Pesto basil sauce, Psti macaroni sauce, and Tahin sauce, with concentrations of 0.08, 0.07, and 0.11, respectively.

The introduction of Cadmium into food items can occur through spices, as these substances might contain Cadmium concentrations as high as 200 ng/g. Contamination of Cadmium in food products may arise from various factors, including the manufacturing process, equipment used, and the materials and storage methods involved (Müller et al., 1996).

Conclusion

In this research, an examination was conducted on thirteen distinct samples of canned sauce that are accessible in the markets of Baghdad city, focusing on the presence of microbial contamination and four different elements. The study indicated there was no bacterial contamination in all samples but there was a fungal contamination in four samples (Pasta sauce, Garlic sauce, Mixed Pickle and Sesame sauce). While for heavy metals, the findings indicated that the concentrations of Copper and Zinc, which were the subject of investigation, fall within the globally accepted permissible limits. However, the concentrations of cadmium and lead exceeded the allowable thresholds. Among the studied sauces, the highest concentration of lead was identified in Tahine sauce, while Pesto basil sauce, Psti macaroni sauce, and Tahin exhibited elevated levels of cadmium.

References

1. Abdulhay, H. S. and Salloom D. F. 2013. Detection of Microbial and Chemical Contamination in Canned Meat Available in Baghdad Local Markets. Journal of the College of Basic Education.
2. Ahmad, K.; Ashfaq, A.; Khan, Z.I.; Ashraf, M.; Akram, N.A.; Yasmin, S.; Noorka, I.R. 2016. Health risk assessment of heavy metals and metalloids via dietary intake of a potential vegetable (Coriandrum sativum L.) grown in contaminated water irrigated agricultural sites of Sargodha, Pakistan. Hum. Ecol. Risk Assess. 22, 597–610.
3. Akhtar, S.; Khan, Z.I.; Ahmad, K.; Nadeem, M.; Ejaz, A.; Hussain, M.I.; Ashraf, M.A. 2022. Assessment of lead toxicity in diverse irrigationregimes and potential health implications of agriculturally grown crops in Pakistan. Agric. Water Manag. 271, 107743.
4. Alegbeleye O. Odeyemi O. a Strateva M. and Stratev D. 2022. Microbial spoilage of vegetables, fruits and cereals. Applied Food Research 2:100122.
5. Alimentarius, C. (1994). "Joint FAO/WHO food standards programme." Codex Committee on methods of Analysis and Sampling: 19th session, Budapest, Hungary, Criteria for evaluating acceptable methods for evaluating acceptable methods for codex purposes
6. Aloosh M. K. and Al-Azaawi M. N. 2015 Removal of lead and chromium from industrial wastewater by locally Citrobacter spp. Isolates. Iraqi Journal of Science, 56(2A): 983-997.
7. Bahramia A, Moaddabdoost Z., Keith B., Seid S., and Jafari M. 2020. Efficiency of novel processing technologies for the control of Listeria monocytogenes in food products. Trends in Food Science & Technology. V 96: 61-78.
8. Balali-Mood M, Naseri K, Tahergorabi Z, Khazdair MR and Sadeghi M (2021) Toxic Mechanisms of Five Heavy Metals: Mercury, Lead, Chromium, Cadmium, and Arsenic. Front. Pharmacol. 12:643972.
9. CIFA (Committee for Inland Fisheries of Africa) 1992. Report of the third session of the working party on pollution and fisheries. (FAO Fisheries report No.471). Rome: United Nations.
10. Commission Regulation (EC) 1881/2006 setting maximum levels for certain contaminants in foodstuffs, issued by the European CommissionOfficial Journal of the European Union, L364/5 (2006).
11. Ebrahimi, M.; Khalili, N.; Razi, S.; Keshavarz-Fathi, M.; Khalili, N.; Rezaei, N. 2020. Effects of lead and cadmium on the immune system and cancer progression. J. Environ. Health Sci. Eng., 18: 335–343.
12. El Moussawi S. Noureddine, Ouaini R., Matta J., Chébib H. and Cladière M. 2019. Camel Simultaneous migration of bisphenol compounds and trace metals in canned vegetable food Food Chem. pp. 228-238

13. FAO/WHO. 2011. Report of the fifth cession of the codex committee on contaminants in food. Hague, Netherland.
14. Food and Agriculture Organization of the United Nations (FAO). 2020. The State of World Fisheries and Aquaculture 2020. In Brief: Sustainability in Action; FAO: Rome, Italy, ISBN 978-92-5-132692-3.
15. Haider, F.U.; Liqun, C.; Coulter, J.A.; Cheema, S.A.; Wu, J.; Zhang, R.; Wenjun, M.; Farooq, M. 2021. Cadmium toxicity in plants:Impacts and remediation strategies. Ecotoxicol. Environ. 211, 111887.
16. Ilechukwu, I.; Osuji, L.C.; Okoli, C.P.; Onyema, M.O.; Ndukwe, G.I. 2021. Assessment of heavy metal pollution in soils and health riskconsequences of human exposure within the vicinity of hot mix asphalt plants in Rivers State, Nigeria. Environ. Monit. Assess. 193: 1–14.
17. Iraqi Central Organization for Standardization and Quality Control(ICSQC) 2001."Drinking Water Standards", No.417
18. Karlovsky, P., Suman, M., Berthiller, 2016. Impact of food processing and detoxification treatments on mycotoxin contamination. Mycotoxin Res 32, 179–205.
19. Khalafalla, F.A., Ali, F.H., Hassan, A.R.H. and Basta, S.E. (2016). Residues of lead, cadmium, mercury and tin in canned meat products from Egypt: an emphasis on permissible limits and sources of contamination. Journal für Verbraucherschutz und Lebensmittelsicherheit, 11(2), 137-143.
20. Kowalska, G., Pankiewicz, U. and Kowalski, R. 2020. Determination of the Level of Selected Elements in Canned Meat and Fish and Risk Assessment for Consumer Health. Journal of Analytical Methods in Chemistry, 2148794.
21. Liu, W.-H.; Zhao, J.-Z.; Ouyang, Z.-Y.; Soderlund, L.; Liu, G.-H. 2005. Impacts of sewage irrigation on heavy metals distribution and contamination in Beijing, China. Environ. Int. 31, 805–812.
22. Manouchehri A, Shokri S, Pirhadi M, Karimi M, Abbaszadeh S, Mirzaei G, Bahmani M. 2022. The Effects of Toxic Heavy Metals Lead, Cadmium and Copper on the Epidemiology of Male and Female Infertility. JBRA Assist Reprod. 26(4):627-630.
23. Müller, M., Anke, M., Hartmann, E. and Illing-Günther, H. (1996). Oral cadmium exposure of adults in Germany. 1: Cadmium content of foodstuffs and beverages. Food Additives and Contaminants, 13(3), 359–378.
24. Munir, N.; Jahangeer, M.; Bouyahya, A.; El Omari, N.; Ghchime, R.; Balahbib, A.; Aboulaghras, S.; Mahmood, Z.; Akram, M.; Ali Shah, S.M.; Mikolaychik, I.N.; Derkho, M.; Rebezov, M.; Venkidasamy, B.; Thiruvengadam, M.; Shariati, M.A. 2022. Heavy Metal Contamination of Natural Foods Is a Serious Health Issue: A Review. Sustainability 14, 161.
25. Noaman, H. K. and Al-Mayaly. 2015. Detection of some heavy metals and bacterial contamination in canned vegetables. Iraqi Journal of Science, 56(2A): 952-958.

26. Palisoc, S.T., Bentulan, J.M.O. & Natividad, M.T. 2019. Determination of trace heavy metals in canned food using Graphene/AuNPs/[Ru(NH3)6]3+/Nafion modified glassy carbon electrodes. Food Measure 13, 169–176.
27. Pascall M.A, DeAngelo K, Richards J, Arensberg MB. 2202. Role and Importance of Functional Food Packaging in Specialized Products for Vulnerable Populations: Implications for Innovation and Policy Development for Sustainability. Foods. 11(19):3043.
28. Stasinos, S. and Zabetakis, I. 2013. The uptake of nickel and chromium from irrigation water by potatoes, carrots and onions. Ecotoxicology and Environmental Safety. European commission. 91, pp:122-128.
29. Zheng, J., Tian, L. and Bayen, S. (2021). Chemical contaminants in canned food and can-packaged food: a review. Critical Reviews in Food Science and Nutrition. 63(4):1-32.

The Effect of Moringa Oleifera Powder On the Ability of Fusarium Spp Isolates to Produce Toxic Metabolites On Wild Eggplant, Atropa Belladonna

Ali F. Merjan [1], Hala Jumaah Asree [2], Hanan Ali Kareem [3]

© 2023 The Author(s). This open access article is distributed under a Creative CommonsAttribution (CC-BY) 4.0 license.

Abstract: This study was conducted to estimate Fusarium spp ability to produce toxin metabolite, and evaluatethem by using Atropa belladonna leaf as detcror plant, F. graminearum was the most significantly isolate who effect in phytotoxicitly to Atropa belladonna leaf plants 67 %, also to evaluate efficiency of Moringa oleifera powder plant in inhibition radial growth Fusarium spp in agar plates, F. verticillioides, F. moniliforme were the biggest isolates affected by of Moringa oleifera powder plant 67 %. Results revealed that Moringa oleifera had significant effect in inhibiting phytotoxicity metabolites of Fusarium spp., F. verticillioides, F. moniliforme were the biggest isolates affected by of Moringa oleifera powder plant in inhibition of the ability to producing phytotoxicity reformulate.

Key Words: Fusarium moniliforms, Atropa belladonna, bioassay, Moringa oleifera, phytotoxic metabolites.

Author details

[1- 2] Biotechnology faculty, AL- Qasim Green University, Babil, Iraq

[3] College of Science, AL- Qasim Green University, Babil, Iraq

Citation information

Cite this article as:

Merjan, A.F., Asree, H.J., Kareem, H.A., (July 2023), *The Effect of Moringa Oleifera Powder On the Ability of Fusarium Spp Isolates to Produce Toxic Metabolites On Wild Eggplant, Atropa Belladonna*, Proceedings of the Minar Congress, Turkey, (9) pp 150-156, DOI: http://dx.doi.org/10.47832/MinarCong9-14

http://dx.doi.org/10.47832/MinarCong9-14

[1] alimerjan@biotch.uoqasim.edu.iq

Introduction

Mycotoxins can be considered one of the most important challenges that threaten food security in Iraq and over all the word. Mycotoxins cause many cancerous diseases in humans and very high rates of death among poultry flocks in broilers (Adamm et al. 2017), turkeys and other poultry, as well as damage to ovarian tissues of laying chicken flocks, abortions and damage to uterine tissues of livestock (Ayelign,et al. 2017).

Recent studies and research have found that medicinal plant powders have significant effects in inhibiting the fungal growth of Fusarium isolates, as well as in disrupting the vital pathways of Fusarium isolates that lead to the production of mycotoxins (Ahmadu, et al. 2021).

Medicinal plants can be considered as one of the promising and important methods in drawing up a successful strategy to reduce the spread of mycotoxins in foodstuffs and poultry industry products, as they are safe materials that do not cause toxic effects on the living body and do not have cumulative effects in living tissues and do not affect in the health of humans and domestic animals if it is mixed in known proportions with the animal feed of poultry.

The Morinca plant was commonly used as one of the most important medicinal plants that widely used to treat many diseases such as diabetes and weight loss. It also has a high effectiveness in inhibiting many pathogenic fungi of plants and humans that produce mycotoxins (Patil,et al. 2022)

Detector plants are one of the most important vital methods for detecting mycotoxins because they are easy, affordable, and cheap, as well as effective ways to detect the presence of toxins in fungal cultures (Mohamed, et al. 2020). However, some of these plants are characterized by their production of mycotoxin metabolite, and their use has been banned, such as the Datura setrmonium plant (Huang, i. 2017)

The wild eggplant Atropa belladonna is one of the wild plants that are widely used as medicinal plants such as the production of Atropine. There are a number of studies indicating the possibility of using it as a plant that detects mycotoxins, so that this paper aimed to figure out possibility for using Atropa belladonna as bio assay organism to detect mycotoxin(Kasseri, et al. 2016).

This study was conducted to study the effect of Moringa oleifera medicinal plants on the effect on Fusarium spp isolates known for their ability to produce different types of mycotoxins, because the research aims to draw a possible strategy to control the ability of fungi to produce food from grains, feed and poultry feeds, this paper aimed to figure out possibility for using Atropa belladonna as bio assay organism to detect mycotoxins.

Material and methods

Sampling and fungal isolates:

Fields inspection to grain stores intended for poultry feed production in AL- Qasim city, 250 gm Poultry feed, cattle feed and corn samples were taken and kept in papers bags and translocate into microbiology of Biotechnology Labrotary.

surface sterilize of 100 grains of each a kind of grain cereal done by 1% chloralax sterilizing solution, randomly were distributed on PDA plates, and incubated in 28 C for Five days. The fungal isolates were purified on PDA plats and identified by (Leslie. 2006).

Plant material collocation:

Moringa oleifera and Atropa belladonna leaf plants were collected from field, the plant samples were Stored to microbiology of Biotechnology Laboratory by paper bags, then the were air dried and grained by coffee grinder

Detection of Toxic metabolite of Fusarium spp by Atropa belladonna leaf:

All Fusarium isolates were grown on Czapek's dox broth medium, for 21days, the filtrates broth were collects by Buchner funnel, the filtered product kept in refrigerator till use.

Number of complete grown leafs of Atropa belladonna leaf were collects, washed and their surface sterilized and placed in 12cm petri dishes and exposed to filtrates broth of each Fusarium isolate with three replicates, a comparison treatment was carried out in which a Czapek's dox broth medium broth was used, as acontrol wihout any inoculation, phytotoxicity ratio of leaf area were calculated after 24 hour.

Effect of Moringa oleifera plant powder in redial growth of Fusarium isolates:

PDA amendment with 1 % of Moringa oleifera plant powder had been used by pourd in 9 cm redial petri dishes to estimating inhibition ability of Moringa oleifera plant powder to fungal isolates, with three replication, a comparison treatment was carried out in which PDA medium was not amendment with any agent. The radial growth of each plates were measured by millimeters after 5 days, when radial growth in control treatment filled the agar plats.

Effect of Moringa oleifera plant powder in inhibition phytotoxicit metabolite of fusarium spp evaluated on A. belladonna leafs:

Czapek's dox broth medium amendment with 1 % of M. oleifera plant powder had been distributed in 250 ml. flasks, autoclaved 121 C o for 20 minutes, then thy were inoculated with inoculum of fusarium isolates separately with three replication, a comparison treatment was carried out in which Czapek's dox broth medium was not amendment with any agent, all flasks were incubated in 28 Co for 21 days. The filtrates of all flasks were collect by Buchner funnel. grown A. belladonna plants leaf were exposed to filtrates broth of each Fusarium isolate with three replicates, a comparison treatment was carried out in which a

Czapek's dox broth medium broth was used, as control treatment, phytotoxicity ratio of leaf area were calculated after 24 hour.

Statistical analysis: Experiments were designed according completes random design CRD, *P* value > 0.5 was estimating by least significant differences L.S.D.

Results:

Fungal isolates identification:

Several fungal isolates were identified according to field inspection had been showed different fungal species as shown below, Aspergillus. nigar, A. flavus, A. ochraceus, Alternaria alternate, Curvelaria sp. , Dreshlair sp Fusarium oxysporium, F. graminearum, F. moniliform, . F. polyfertum F. solani, F. verticillioides and Trichoderma sp.

Because of the high frequency of isolation of fungal species Fusariu graminearum, F. moniliform and F. verticillioides , Therefore, it was focused on in subsequent experiments.

Detection of Toxic Metabolite of Fusarium spp by A. belladonna leaf:

The results shown in Table 1 are clearly indicate the high phytotoxicity of the metabolic secretions of all species belonging to the fungus Fusarium, which was significantly superior to the control treatment at a probability level of 0.05, when phytotoxicity ratio calculating of leaf area of A. belladonna plant

Table 1. Phytotoxicity efficiency of Fusarium spp metabolic active compounds on A. belladonna leaf plants.

Fusarium species	% phytotoxicity of Atropa leaf
*F. graminearum**	67
F. moniliforme	55
F. verticillioides	52
Control treatment	0
L.S.D. $p \leq 0.05$	5. 341

*each value referring to three replication

F. graminearum had the highest effect in phyto toxicity to leaf plant and it differed significantly from the comparison treatment and the other two Fusarium species, other two species were have a significant effect of phytotoxicity to A. belladonna leaf.

Effect of M. oleifera powder plant in redial growth of Fusarium isolates:

The effect of 1% concentration of M. oleifera plant powder significantly on the radial growth of Fusarium species on agar plats technuqe, as shown in table 2 which had previously been shown to produce toxic metabolic compounds.

Table 2. radial growth of Fusarium spp inhibition by effect fo1% concentration of M. oleifera plant powder

Fusarium species	% Radial growth inhibition
*F. graminearum**	44
F. moniliforme	54
F. verticillioides	67
Control treatment	0
L.S.D. $p \leq 0.05$	4. 096

*each value referring to three replication

F. verticillioides had the highest significantly inhibition after exposure to 1 % M. oleifera amendments PDA agar comparison to control treatment and the other two Fusarium species, have a significant inhibition effect of 1 % M. oleifera powder plant (figure 1).

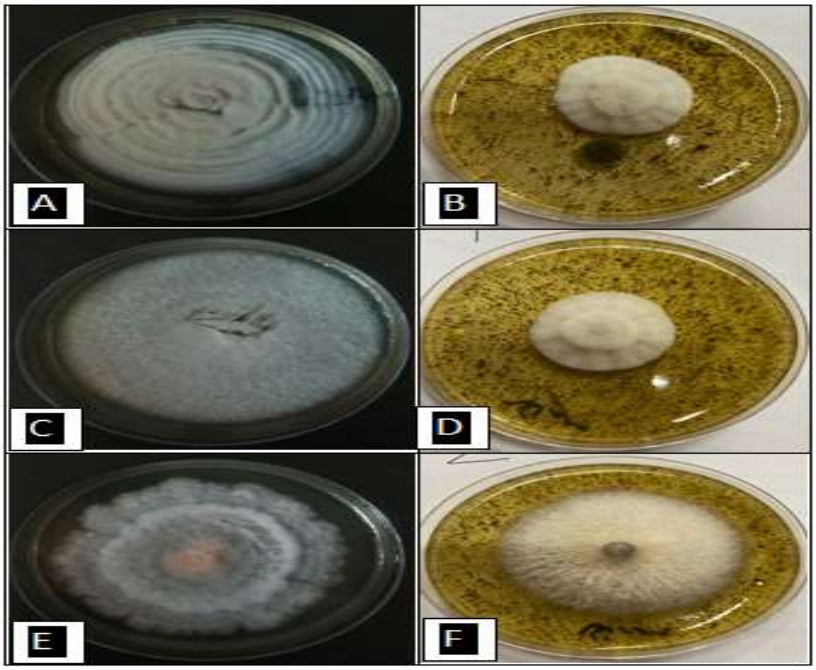


Figure 1. Effect moringa powder plant on the redial growth of Fusarium spp A.Fusarium moniliforme control, B. Fusarium moniliforme+moringa,C. F. verticillioides control, D. F. verticillioides+moringa,E. F. graminearum, F. F. graminearum+moringa.

Effect of M. oleifera plant powder in inhibition phytotoxicit metabolite of Fusarium spp:

Rustles clearly revealing to the efficiency of M. oleifera plant powder that had amendment to a Czapek's dox broth medium in 1 % concentrations shown in table 3, in disrupting the ability of all Fusarium spp in which study included to produce toxic metabolic compounds see table 3.

Table 3: The effect of 1 % of M. oleifera plant powder in the efficiency disruption producing of Fusarium spp active metabolic compounds.

Fusarium species	% phytotoxicity of atropa leaf
*F. graminearum**	21
F. moniliforme	33
F. verticillioides	33
Control treatment	0
L.S.D. $p \leq 0.05$	5. 175

*each value referring to three replication

The suffering of the fungi F. moniliforme, F. verticillioides was the most significant most affected by exposure to 1% morinca powder plant which record 33 % phytotoxicity, note that the rest F. graminearum also significantly affected by exposure to Morinca by 21%, comparisons to the ability of Fusarium spp studied in our research in which they previously had been shown in table 1, that related to phyto toxicity data, (figure 2).

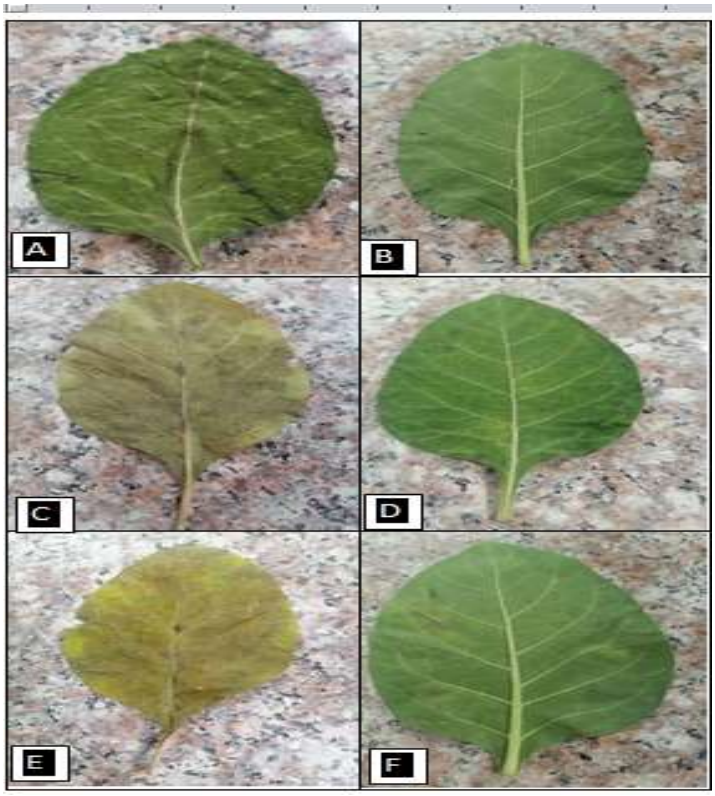


Figure 2. Effect moringa powder plant on the broth cultuer of Fusarium spp Fusarium moniliforme control, B. Fusarium moniliforme+moringa,C. F. verticillioides control, D. F. verticillioides+moringa,E. F. graminearum, F. F. graminearum+moringa

Discussion

Mycotoxins are among the most important bio-pollutants with a high risk to human health and farm animals such as poultry and livestock, so the process of limiting and controlling these products poses a serious challenge for researchers (Patil, et al. 2022). There are vital pathways in fungal cells that are responsible for the production of toxins and vital secretions, and fungal cells need environmental and nutritional requirements to produce these vital substances (Mahlo, et al. 2016).

Morinca has many active compounds like flavonoids, saponins, tannins, catechol tannins, anthraquinones, alkaloids that are abundantly secreted by plant cells, which are used to perform many physiological tasks beneficial to the plant (Mncube, et al. 2019), but these compound can interfere with physiology of fungal cells proses.which lead to inhibition the growing of fungi isolates mycotoxin secreation(Mohamed, et al. 2020).

Conclusions

1. Fusarium isolate which studied in our research have high ability to producing toxic metaboilate
2. **oleifera** pwoderd plant has high effect on radial growth in agar plats of fusarium species.
3. **M. oleifera** pwoderd plant has high effect on toxic metabolite produced by Fusarium isolates in liquid culture.

References

1. Adam, M. A. A., Tabana, Y. M., Musa, K. B., & Sandai, D. A. (2017). Effects of different mycotoxins on humans, cell genome and their involvement in cancer. Oncology Reports, 37(3), 1321–1336. https:// doi.org/10.3892/or.2017.5424.
2. Ayelign, A., Woldegiorgis, A. Z., Adish, A., De Boevre, M., Heyndrickx, E., & De Saeger, S. (2017). Assessment of aflatoxin exposure among young children in Ethiopia using urinary biomarkers. Food Additives & Contaminants. Part A Chemistry, Analysis, Control, Exposure & Risk Assessment, 34, 1606–1616. https://doi.org/10.1080/19440049. 2017.1350290
3. Ahmadu, T., Ahmad, K., Ismail, S.I., Rashed, O., Asib, N., Omar, D., 2020. Antifungal efficacy of Moringa oleifera leaf and seed extracts against Botrytis cinerea causing gray mold disease of tomato (Solanum lycopersicum L.). Braz. J. Biol. 81, 1007–1022
4. Mahlo, S.M., Chauke, H.R., McGaw, L., Eloff, J., 2016. Antioxidant and antifungal activity of selected medicinal plant extracts against phytopathogenic fungi. Afr. J. Tradit. Complement Alter. Med 13 (4), 216–222. https://doi.org/10.21010/ajtcam.v13i4.28
5. Mncube, C.N., Bertling, I., Yobo, K.S., 2019. Investigating the antifungal activity of moringa leaf extract against Fusarium dry rot in vitro. II International Symposium on Moringa. Acta Hortic,, pp. 1306. https://doi.org/10.17660/ActaHortic.2021.1306.29
6. Mohamed, E.A.A., Muddathir, A.M., Osman, M.A., 2020. Antimicrobial activity, phytochemical screening of crude extracts, and essential oils constituents of two Pulicaria spp. growing in Sudan. Sci. Rep. 10 (1), 1–8. https://doi.org/10.1038/s41598-020- 74262-y
7. Patil, S.V., Mohite, B.V., Marathe, K.R., Salunkhe, N.S., Marathe, V., Patil, V.S., 2022. Moringa tree, gift of nature: a review on nutritional and industrial potential. Curr. Pharmacol. Rep. 1–19. https://doi.org/10.1007/s40495-022-00288-7.
8. Huang, M. N., Yu, W., Teoh, W. W., Ardin, M., Jusakul, A., Ng, A. W. T., … Rozen, S. G. (2017). Genome-scale mutational signatures of aflatoxin in cells, mice, and human tumors. Genome Research, 27(9), 1475–1486. https://doi.org/10.1101/gr.220038.116
9. Kasseri, T., & Poór, M. (2016). Ochratoxin A: Molecular interactions, mechanisms of toxicity and prevention at the molecular level. Toxins, 8(4). https://doi.org/10.3390/TOXINS8040111.

The Possible Protective Effect of Rutin to Reduce the Effect of Formaldehyde on Lung Tissue and Oxidative Stress in Rats

Arjwan A Alsudani [1], Hadeel Jabar Neama Almuoswi [2]

© 2023 The Author(s). This open access article is distributed under a Creative CommonsAttribution (CC-BY) 4.0 license.

Abstract: This study aims to know the therapeutic role of one of the types of plant flavonoids (rutin) in reducing the negative effects resulting from inhalation of formaldehyde 40% and its effect on lung function and tissues of rats. As well as clarifying the effective role of rutin in enhancing the effectiveness of antioxidants and reducing the oxidation process, as rutin acts as a natural antioxidant and can be found in many plant species. In this investigation, a total of twenty-four white male rats were used, and these rats were randomly assigned to four groups, with six rats in each group. The experiment was conducted over a period of three weeks and the first group served as a control, while the other groups (G1, G2, and G3) served as experimental groups. The results of evaluating some antioxidants (SOD, CAT, GSTs, and TAOC) and some oxidants (MDA, NO). revealed a clear imbalance between oxidants and antioxidants, increased oxidative stress, pathological changes in lung tissue such as enlargement and widening of the alveoli, and an increase in endothelial thickness. On the other hand, the rutin dosage increased antioxidants, decreased oxidative stress, and improved lung tissue to levels equivalent to the control group.

Key Words: Formaldehyde, Rutin, Lung, Antioxidant, Histological study.

Author details

[1] College of Science, University of Al- Qadisiyyah, Qadisiyyah, Iraq

[2] College of Biotechnology, University of Al-Qadisiyyah, Qadisiyyah, Iraq

Citation information

Cite this article as:

Alsudani, A.A., Almuoswi, H.J., (July 2023), *The Possible Protective Effect of Rutin to Reduce the Effect of Formaldehyde on Lung Tissue and Oxidative Stress in Rats*, Proceedings of the Minar Congress, Turkey, (9) pp 157-172, DOI: http://dx.doi.org/10.47832/MinarCong9-15

http://dx.doi.org/10.47832/MinarCong9-15

[1] orjuwan.mahood@qu.edu.iq orcid.org/0000-0002-4661-7124.

[2] hadeel.jabbar@qu.edu.iq orcid.org/0000-0003-4538-1866.

Introduction

Despite recent advances in modern medicine, medicinal plants continue to make significant contributions to health care. Since ancient times, medicinal plants have been employed in herbal therapy for their antioxidant effects, particularly in underdeveloped nations (Hosseinzadeh et al., 2015). The active ingredients in the composition of medicinal plants are non-toxic or of low toxicity compared to manufactured drugs, and they are produced from metabolic processes in plants and have a role in the treatment of numerous diseases, the most important of which are flavonoids, polyphenols, glucosinolates, terpenoids, phenols, plant sterols, etc., for this reason, Many plants have been used in the pharmaceutical industry in many countries (Gurnani et al., 2014; Padmavathy& Devarajan, 2017). Flavonoids are the secondary metabolites of multiple phenolic compounds and are widely found in plants and the human diet and are involved in the synthesis of many drugs. Since flavonoids have numerous biological, pharmacological, and medicinal properties, including antioxidant, antiviral, anti-inflammatory, antimutagenic, antitumor, and anticancer effects in addition to protecting the heart and blood vessels, they have attracted the attention of scientists working in the field of medicine (Wang et al., 2018; Rengasamy et al., 2019; Donadio et al., 2021; Roy et al., 2022). Due to their numerous health advantages, flavonoids are one of the compounds that are most researched. They have diverse chemical structures, and these structural variations control how they interact and behave biologically (Panche et al ., 2016).

One of the most important flavonoids is Rutin (Rt), a non-toxic bioflavonoid composed of flavonol quercetin and rutinose disaccharide, which is one of the most essential phytochemical components (Stanisicet al ., 2018). Rutin is also known as rutoside, quercetin-3-rutinosid, and sophorin, and its name is derived from its chemical structure. Ruta graveolens is a plant that contains a lot of rutin. (Ganeshpurkar & Saluja, 2017) .

It may also be found in citrus fruits, tea, Passion flowers, buckwheat, apples, and other plants. It is an essential nutrient in meals. Rutin is thought to be safe and non-carcinogenic.

Rutin is a yellow crystalline powder that is odorless and insoluble in cold water and alcohol. It is a flavonol-containing polyphenolic flavonoid. It has the chemical formula C27H30O16, a molecular weight of 610.5 g/mol, and a melting point of 242 °C. Its chemical name is (3, 3', 4', 5, 7- Pentahydroxy flavon - 3- rhamnoglucoside.(Sharma et al., 2013). Rutin is a potent antioxidant with cytoprotective, vasoprotective, neuroprotective, cardioprotective, anti-hypercholesterolemia, anti-spasmodic, anti-inflammatory, anti-stomach, and anti-cancer properties, according to research (Javed et al., 2012; Riaz et al, 2018). Rutin is an excellent antioxidant due to its capacity to bind free radicals and metal ions, and it can eliminate iron ions with double and triple valence, which may lead to the creation of effective free oxygen radicals ROS (Koval'skii et al., 2014). Rutin has a neuroprotective effect, as it binds to free radicals and scavenges them during brain tissue damage (Khan et al., 2012), as quercetin rutin attaches to free radicals and scavenges them during brain tissue injury

(Sharma et al., 2020). It improves sexual function and protects testicular tissues from the effects of diabetes (Al-Rejaie et al., 2016). Rutin has also a protective effect on acute lung damage, as shown by its effects on histological alterations in injured lung tissue and a reduction in lipid peroxide generation (Yeh et al., 2014).

People are now exposed to an atmosphere tainted with formaldehyde, an irritant chemical linked to respiratory ailments. It is an aldehyde produced by the oxidation of methyl alcohol at room temperature. Formaldehyde is utilized in a variety of chemical sectors, including leather products, particle boards, plywood, paper, medicines, resin manufacture, instrument sterilization, embalming of corpses, preservation of biological specimens, and others. According to studies, we can say that Formaldehyde has a strong effect on the respiratory system and an increased risk of asthma because the main exposure to formaldehyde is through inhalation. After all, it is a gas at room temperature and is soluble in water, making it easily absorbed through the respiratory and digestive systems (Costa et al., 2015; Patra & Pariti, 2022). As a consequence, the purpose of this research is to investigate the therapeutic benefits of rutin with its antioxidant characteristics and its role in improving the histological alterations as a result of lung damage produced by inhaling formaldehyde at a 40% concentration.

MATERIALS AND METHODS

Animals

A healthy adult (3 months old) male Albino rat of 24 in number weighing between180 −200 g was obtained from the animal house of the College of Science, University of Al-Qadisiyah. They were kept in cages in a conventional lab setting with a temperature of 23 ± 2°c with 12 h Light/dark cycle and fed with a standard diet and water.

Experimental Design

Animals were divided into four groups (C, G1, G2, G3) containing 6 rats in each group. Group C was considered the control group and group G1 was treated with Rutin both groups were not exposed to formaldehyde (40%) as they were kept in a separate environment. While the other groups (G2 and G3) were exposed to a 40% formaldehyde vapor environment for (1 hour) daily for 3 weeks. They were exposed to 40% formaldehyde by soaking the cotton in it and the cotton was suspended by a metal wire inside the animal cages. As for the G3 group treated with Rutin by oral gavage, they were treated one hour after exposure to formaldehyde.

Preparation of Rutin dose

The dosage of rutin was synthesized using the (Taşl et al., 2018) technique at a concentration of 50 mg/kg body weight.

Samples collection

Directly from the heart, blood samples were taken at the end of the experimental period, and kept in tubes containing anticoagulant (EDTA) to obtain serum. The blood samples were

used for the preparation of serum after centrifugation at 3000 rpm for 15 min and then kept in clean tubes at -20C for measurement of some biochemical parameters. Then the animals were dissected and the lungs were taken, which were placed in Petri dishes containing a physiological solution for cleaning, and then kept in 10% formalin for histological study.

Determination of some biochemical parameters

1. Glutathione-s-transferase (GSTs) determination in blood using the Habig method.
2. Catalase (CAT) determination in blood using the Aebi method.
3. Superoxide dismutase (SOD) levels in blood were determined using the Misra and Fridovich method.
4. Malondialdehyde (MDA) determination using the Guidet and Shah method, and Nitric Oxide (NO) determination in blood using the Hortelance method.
5. Total Antioxidant Capacity (TAOC) determination using the Elabscience Biotechnology Kit.

Histological study

Histological sections of the lungs were prepared depending on Bancroft and Gamble method, using hematoxylin-eosin stain

STATISTICAL ANALYSIS

The data were analyzed by following the one-way analysis of variance (ANOVA) to find out the significant differences between the control group and other groups using the SPSS program (version 21) at a probability level of 0.05.

RESULTS AND DISCUSSION

Biochemical Parameters

Table (1), and Figure (1) show that the level of (MDA) in (G2) treated with formaldehyde increased significantly ($p>0.05$) as compared to the control group (C) and the other groups (G2, G3). In the group (G1) treated just with protein, there was no significant change in the level of (MDA) compared to the control group and a substantial reduction with time (G2, G3). While (G3) treated with formaldehyde and then rutin improved significantly in terms of (MDA). The findings also indicated a substantial rise ($p>0.05$) in Figure(2) in the level of (NO) in (G2) compared to the control and the rest of the groups, and a significant drop ($p>0.05$) in the group (G1) compared to other groups, while the group (G3) showed a clear improvement as it was near to the control group.

Table 1. Effect of Rutin on some biochemical parameters in male rats treated with Formaldehyde

-Numbers denote Mean±SE
-Non-significant differences ($p>0.05$) are indicated by similar letters.
-Significant differences ($p>0.05$) are indicated by different letters.

Groups	Parameters					
	MDA(µ mol/L)	NO(µmol/L)	SOD(U/L)	CAT(U/L)	GSTs(U/L)	T-AOC (U/ml)
Control	4.82±0.02 c	4.46±0.18 b	2.6±0.04 ab	1.37±0.01 a	12,35±0.17a	1.5±0.02 a
G_1	5.01±0.16 c	4.18±0.04 c	2.7±0.02 a	1.33±1.2 ab	12.10±0.2a	1.6±0.15 a
G_2	16.3±0.5 a	21.25±0.33 a	1.22±0.06 c	0.35±0.25 c	6.43±0.36c	0.51±0.04 b
G_3	5.44±1.2 b	4.50±0.16 b	2.52±0.013b	1.29±0.04 b	11.21±0.13b	1.43±1.1 a
LSD	0.029	0.075	0.230	0.047	0-346	0.216

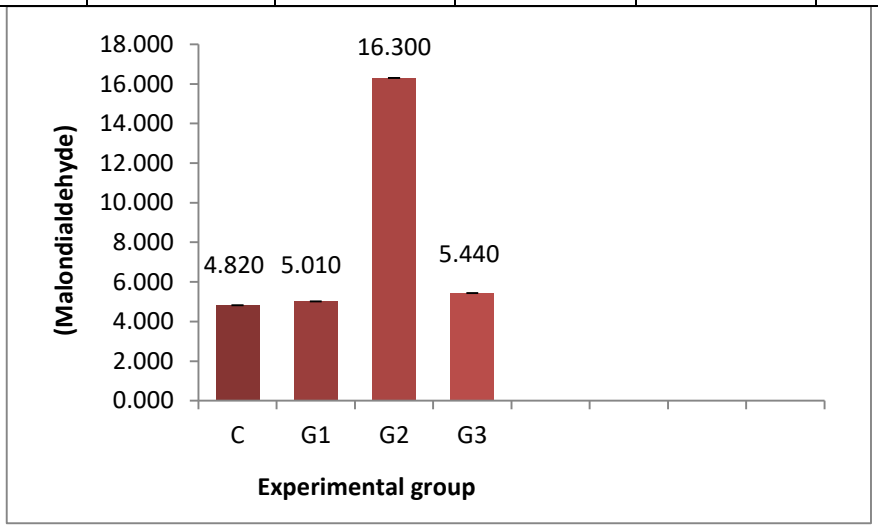


Figure 1. Effect of Formaldehyde with and without Rutin on the levels of MDA in Rats

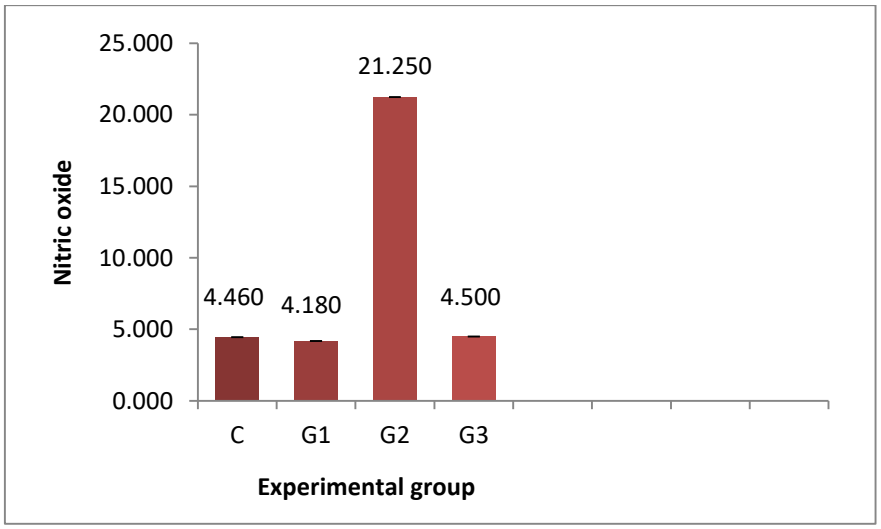


Figure 2. Effect of Formaldehyde with and without Rutin on the levels of NO in Rats

Table (1), Figure(3) shows that the activity of (SOD) in the first group (G1) treated with rutin did not exhibit any significant change compared to the control group (C), however, the group of rats treated with formaldehyde (G2) showed a substantial drop. ($p>0.05$) as compared to the control group and the other experimental groups, and the third group (G3) exhibited a substantial improvement in (SOD) levels and was comparable to the control group.

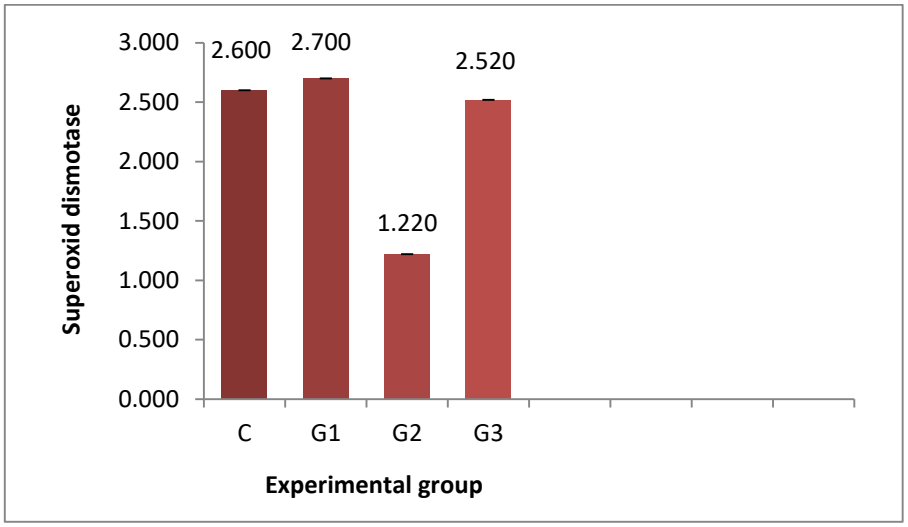


Figure 3. Effect of Formaldehyde with and without Rutin on the activity of SOD in Rats

The results showed that inhaling 40% formaldehyde in the second group (G2) significantly reduced the activity level of (CAT) compared to the control group and the other group's table (1), figure(4), while the first group (G1) treated with rutin was similar to the control group, and the third group (G3) treated with formaldehyde And rutin showed a clear improvement and a significant increase in the level of (CAT) compared to the control group.

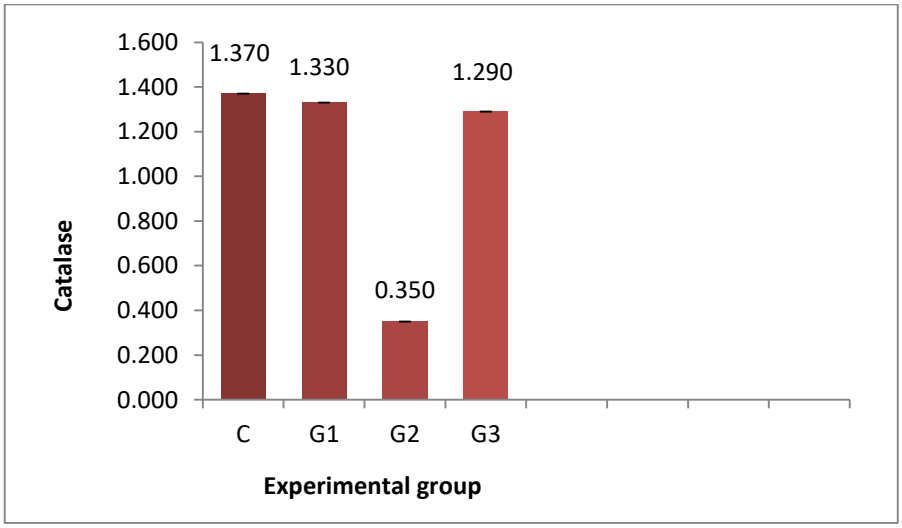


Figure 4. Effect of Formaldehyde with and without Rutin on the activity of CAT in Rats

The findings of the rutin-treated rats (G1), on the other hand, revealed a considerable improvement in the efficacy of (GSTs) and were comparable to the control group table (1), figure(5). When compared to the control and experimental groups, the group (G2) exhibited a substantial drop. Furthermore, when comparing group (G3) to group (G1), a notable improvement and a substantial rise were noticed (G2).

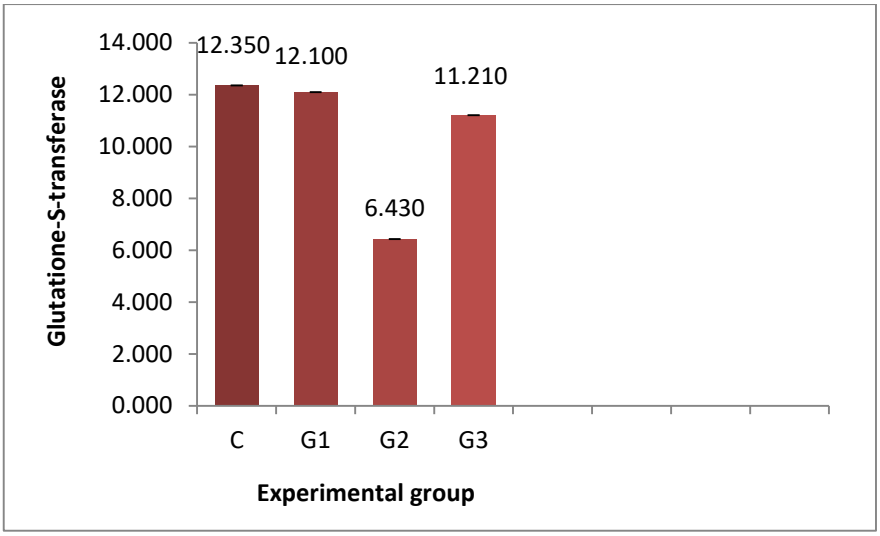


Figure 5. Effect of Formaldehyde with and without Rutin on the activity of GSTs in Rats

The findings revealed a large drop table(1), figure(6) in the level of (TAOC) in the formaldehyde (G2) group compared to (C, G1, G3), while the results of the formaldehyde and rutin (G3) group were comparable to the two groups (C, G1) and showed a major rise A remarkable improvement compared to (G2).

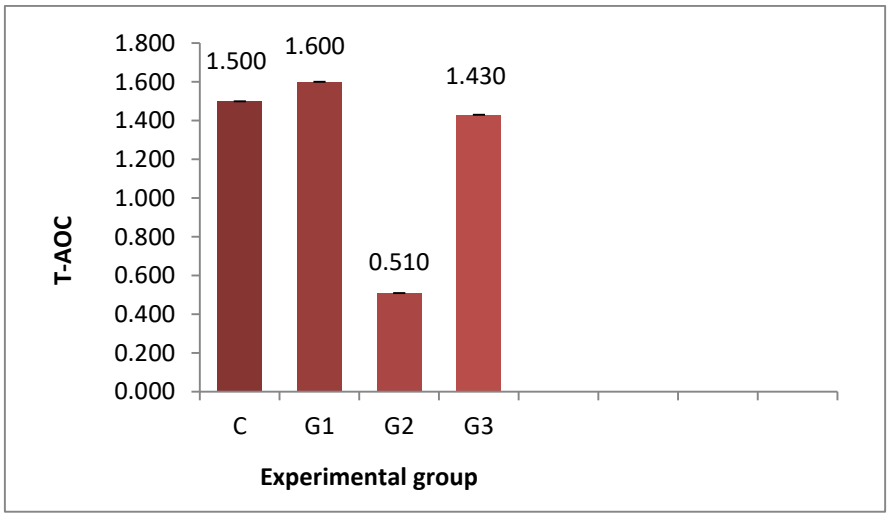


Figure 6. Effect of Formaldehyde with and without Rutin on the Total Antioxidant Capacity (TAOC) level in rats

A balance between antioxidants and oxidants is required for the proper biological activity of cells and tissues, and under normal circumstances, the level of antioxidants and the number of free radicals would be balanced (Singh et al., 2019). This was seen in the rutin-treated group owing to its action in eliminating free radicals and antioxidant capability (Patel & Patel, 2019). Lipid peroxidation is a prominent indication of free radical-caused oxidative damage that affects cell membrane function (Poljsak et al., 2013). The rise in MDA after exposure to 40% formaldehyde may be related to an increase in lipid peroxidation, which

happens when electrons are removed from plasma membrane lipids. This results in a succession of oxidation-reduction processes that yield electrophilic aldehydes such as MDA, a byproduct of lipid peroxidation (Bachi et al., 2013). The rise in No in the formaldehyde-treated group may be connected to oxidative stress since the equilibrium is upset in favor of oxidants owing to increased free radical generation or a reduction in antioxidants (Guglan et al., 2016).

Much research has been conducted to explain the harmful effects of formaldehyde on the reproductive system in male rats, as (Hegazy et al., 2017) indicated. On the other hand, (Leal et al., 2018) reported that formaldehyde exposure induces the development of pulmonary fibrosis. Inhaling formaldehyde and xylene fumes have been shown to have degenerative effects on the lungs and testes of male rats, as well as alter sperm cells and increase sperm abnormalities (Ismail et al., 2021).

SOD protects against oxidative stress by engaging in the cellular defense system against oxidative processes by reducing and neutralizing free radical levels through enzymatic and non-enzymatic antioxidants (Ozougwu, 2016). The reduction in SOD and CAT after inhaling formaldehyde may be ascribed to an increase in the free radical generation since exposure to free radicals from multiple sources increases oxidative stress (Payani et al., 2019).

It might also be due to a low level of GSTs, which shields cells from harmful chemicals by lowering the thiol group of glutathione with poisonous compounds, increasing oxidative stress, and decreasing the enzyme's level (Hasanuzzaman et al., 2017). Low levels of (TAOC) may be related to oxidative stress caused by formaldehyde exposure, leading to increased formation of free radicals, particularly ROS, and therefore an overall reduction in antioxidant capacity (Payani et al., 2019). The G3 group, on the other hand, demonstrated Treatment with formaldehyde and rutin increases antioxidant levels while decreasing oxidants. There is no information available on research that indicates the influence of rutin on formaldehyde-induced lung damage, however, there are studies that illustrate the involvement of rutin in the lung in general (Yehe et al., 2014; Aktas et al., 2017; Bai et al., 2020)

The research found that rutin therapy lowered the amount of MDA, which is consistent with (Sun et al., 2017), who found that rutin reduced the level of MDA in complete Freund's adjuvant-induced arthritic rats because rutin is an anti-peroxide agent and a powerful inhibitor and scavenger of free radicals. Rutin may also lower nitrogen oxide NO generation by decreasing NOS activity. Furthermore, rutin can be oxidized by free radicals, resulting in more stable and less reactive radicals (Wang et al., 2012), which is consistent with (Bai et al., 2020), who stated that rutin reduces the oxidant content of the lung and the production of reactive oxygen species (ROS) by increasing the activity of the antioxidants SOD, CAT, GPX, and preventing mitochondrial damage. Rutin also boosted antioxidant activity, since flavonoids have an important biological function in limiting the generation of free radicals (Ganeshpurkar & Saluja, 2017). Rutin may considerably decrease cyclophosphamide-induced

thymus gland damage, reduce MDA concentration, and boost SOD activity by neutralizing free radicals, particularly ROS (Lan et al., 2022).

Histological study

The results of the current study showed Figure (7) of the histological sections of lung male rats. (A): Cross section through the lung of the control group showing normal alveolus, alveolar sac, bronchioles, and blood vessels. (B): The group of rats treated with rutin (G1) showed the normal histological structure of the lung and was similar to the control group. (C,D): Cross section of the lungs of formaldehyde-treated rats (G2) showing histological changes represented by infiltration of inflammatory cells, dilation of blood vessels, thickening of the wall of the alveoli, and dilation and swelling of the bronchioles. also note swelling and thickening of the walls of the alveoli, expansion of the alveolar sacs, and hemorrhage. this change may affect the functional capacity of the studied tissues. While (E, F): treated with rutin and formaldehyde(G3), show how the tissue structure of the lung began to return to its normal shape except for some traces of bleeding in section (E).

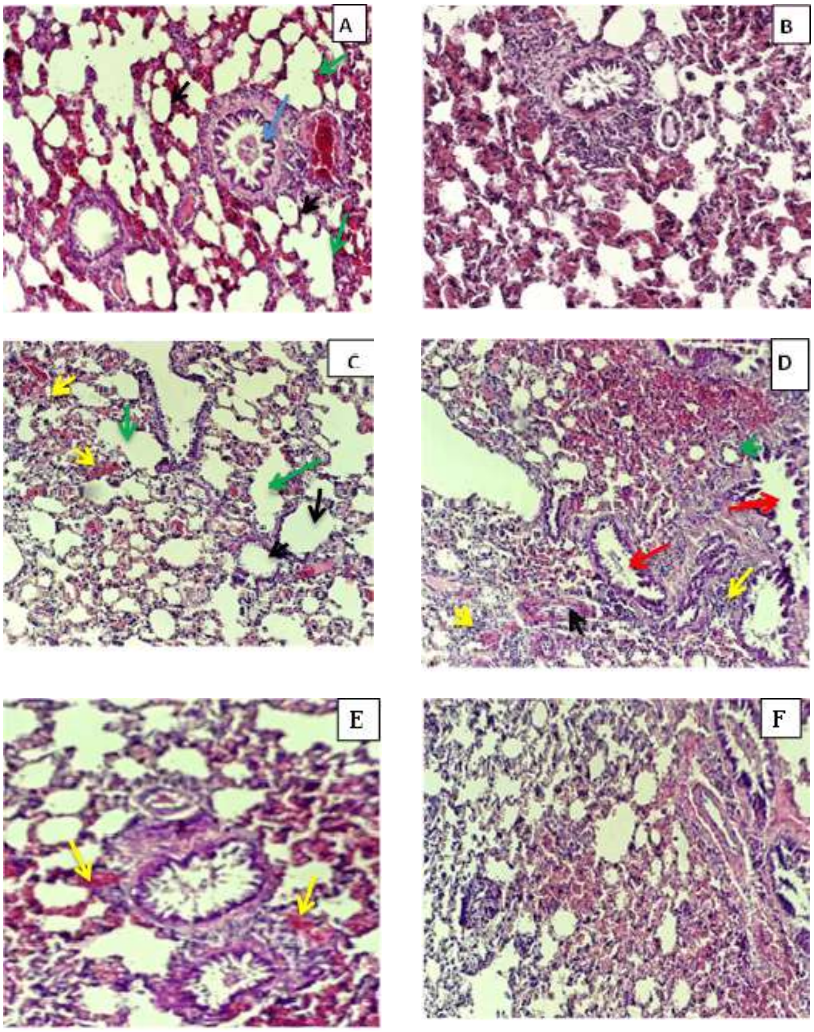


Figure 7. (A) Cross-section of lung in control group showing the normal lung structure with alveoli (black arrow), alveolar sacs (green arrow), bronchioles (blue arrow), and blood vessels (yellow arrow). (H&E X 100). **(B):** Cross section of lung tissue(G1) showing the normal lung structure. (H&E X 100).
(C): cross section of the lung (treated with formaldehyde) (G2) showing swelling of the alveoli with thickening of the walls(black arrow)expansion of the alveolar sacs (green arrow), hemorrhage (yellow arrow). (H&E X 100)
(D) Cross section of lung tissue (G2) (treated with formaldehyde 40% (1 hour) daily for 3 weeks) showing infiltration of inflammatory cells (yellow arrow), dilation of blood vessels (black arrow), thickening of the wall of the alveoli (green arrow), and dilation and swelling of the bronchioles (red arrow). (H&E X 100)
(E&F) show that the lungs treated with formaldehyde and rutin (G3) are similar to the control group, except for some traces of bleeding (yellow arrow). (H&E X 100).

Since formaldehyde directly interacts with tissue components, cytotoxicity is most likely a result of this reactivity, Formaldehyde inflicts various harms on many systems. Its negative effects on the respiratory system have been well documented in epidemiological studies (Tesfaye et al., 2021; Zhao et al., 2021). Alveolar ulceration caused by 40% formaldehyde was caused by the alveolar wall's supporting tissues and surface epithelium being excavated (Costa et al., 2015). Inhaling formaldehyde causes lung harm by producing free radicals in high concentrations, which is the cause of this lung damage. as it decreases (SOD) in inhaled mice, and this leads to a decrease in the detoxification mechanism (Payani et al., 2019). Also, there is a decrease in the activity of (CAT) which leads to the appearance of these harmful effects due to the accumulation of hydrogen peroxide (Li et al., 2017; Reingruber & pontel, 2018). On the other hand, the treatment with rutin leads to an increase in the activity of (SOD) and (CAT) as a result of a decrease in lipid peroxide and an improvement in the mechanism of detoxification. Also, stress is eliminated due to the neutralization of radicals free (Aktas et al., 2017). Additionally, formaldehyde will likely reduce the activity of the enzymes (AAT) and (ALAT), which may be linked to the release of enzymes as a result of epithelial cell damage and lung cell dysfunction. (Leala et al., 2018). Also, the reason for the infiltration of inflammatory cells may be because formaldehyde has caused a decrease in enzyme activity (SDH) significantly decreased, and this affects the functions of the respiratory chain and damage the electron transport chain in the mitochondria in the lung cells, which explains the increase in the infiltration of inflammatory cells in the airway (Chinedum et al., 2014; Leal et al., 2018). There was also a significant increase in the activity of (MDA) in the lung due to oxidative stress and the occurrence of several reactions inside the lung (Miranda da Silva et al., 2015). The results of the research are in agreement with many previous studies. Lung sections from the rats exposed to formaldehyde revealed pulmonary changes in the architecture of the lung and an increase in collagen contents, these alterations were in agreement with what was observed in the rabbit's lungs after 40% exposure (Chinedum et al., 2014), also detected in rats (Mehdi et al., 2014; Ismail et al., 2021) and mice (Afrin et al., 2016). Also study (Ouies & Abd El-Naeem, 2020), showed the effect of formaldehyde on the natural structure of the lung and its immune expression. While all of these parameters have improved when using rutin, because it may contain properties rich in antioxidants, which leads to a reduction in lung injury when exposed to formaldehyde (Bilgin et al., 2020; Tosun et al., 2021). A rutin may be effective in combat increases in capillary permeability Edema due to fluid infiltration From plasma to tissue (Sharma et al., 2013). Also Similarly, Yeh et al. (2014) have determined that rutin has an inhibiting effect on the lipid peroxidation of rats, and Mammadov et al. (2019) found that rutin suppression of increased MDA, rutin also reduced the pathological results of tissue, such as Infiltration of inflammatory cells in the peribronchial and vascular regions, bronchiectasis, pulmonary Arterial vessel wall thickening, pulmonary artery aneurysm. As inhalation of formaldehyde leads to programmed cell death in lung tissue (Liu et al., 2019). The addition of rutin in this study led to the restoration of the natural lung structure with the normal appearance of the alveoli and sinuses (Riaz et al., 2018; Mammadov et al., 2019). Also in the study of Bai et al. (2020) rutin significantly

decreased lung malondialdehyde content, increased lung glutathione content, superoxide dismutase activity, serum total antioxidant capacity, and decreased lung nitric oxide content. In addition, rutin significantly ameliorated histological changes and prevented collagen deposition with the paralleled decrease in lung hydroxyproline content. These results were confirmed by previous studies that showed that treatment with rutin in tissues can prevent and inhibit lung infections. a study of Elma et al. (2022) explained the effect of rutin on blunt trauma pulmonary contusion in mice and how it reduced and improved the effects on lung tissue and contributed to its treatment.

Conclusions

The results in this study showed that formaldehyde inhalation led to a clear imbalance between oxidants and antioxidants, increased oxidative stress, pathological changes in the lung tissue represented by enlargement and widening of the alveoli, and an increase in the thickness of the endothelium. On the other hand, the use of rutin improved antioxidants and reduced oxidative stress and pathological changes in lung tissue, bringing them to levels equivalent to the control group. This indicates that the use of plant flavonoids (rutin) has a role in reducing oxidative stress and the negative effects of formaldehyde.

References

1. Abarikwu, S. O., Iserhienrhien, B. O., & Badejo, T. A. (2013). Rutin-and selenium-attenuated cadmium-induced testicular pathophysiology in rats. Human & experimental toxicology, 32(4), 395-406. https://doi.org/10.1177/0960327112472995
2. Afrin, M., Amin, T., Karim, M. R., & Islam, M. R. (2016). Gross and histomorphological effects of formaldehyde on brain and lungs of Swiss albino mice. Asian Journal of Medical and Biological Research, 2(2), 229-235. https://doi: 10.3329/ajmbr.v2i2.29065
3. Aktas, M., Kandemer, F., Ozkaraca, M., Anedan B., & Kirbas, A. (2017). Protective effects of rutin on acute lung injury induced by oleic acid in rats. Kafkas Universitesi Veteriner Fakultesi Dergisi, 23(3). DOI: 10.9775/kvfd.2016.16977.
4. Al-Roujeaie, A. S., Abuohashish, H. M., Ahmed, M. M., & Alkhamees, O. A. (2016). Effect of rutin on diabetic-induced erectile dysfunction: Possible involvement of testicular biomarkers in male rats. Andrologia, 49(8), 1-9. https://doi.org/10.1111/and.12737
5. Bachi, A., Dalle-Donne, I., & Scaloni, A. (2013). Redox proteomics: chemical principles, methodological approaches and biological/biomedical promises. Chemical reviews, 113(1), 596-698. https://doi.org/10.1021/cr300073p
6. Bai, L., Li, A., Gong, C., Ning, X., & Wang, Z. (2020). Protective effect of rutin against bleomycin induced lung fibrosis: Involvement of TGF-β1/α-SMA/Col I and III pathway. Biofactors, 46(4), 637-644. https://doi.org/10.1002/biof.1629
7. Bilgin, A. O., Mammadov, R., Suleyman, B., Unver, E., Ozcicek, F., Soyturk, M., ... & Suleyman, H. (2020). Effect of rutin on cytarabine-associated pulmonary oedema and oxidative stress in rats. Anais da Academia Brasileira de Ciências, 92. https://doi.org/10.1590/0001-3765202020190261
8. Chinedum, O. K., Ndukaku, O. Y., Ifeanyi, O. E., & Ndubuisi, O. T. (2014). The effect of formaldehyde vapour on the lungs of rabbits. IOSR J Dent Med Sci, 13, 83-93. https://doi.org/10.9790/0853-13928393
9. Costa, S., Carvalho, S., Costa, C., Coelho, P., Silva, S., Santos, L. S., ... & Teixeira, J. P. (2015). Increased levels of chromosomal aberrations and DNA damage in a group of workers exposed to formaldehyde. Mutagenesis, 30(4), 463-473. https://doi:10.1093/mutage/gev00
10. Çuğlan, S., Ekinci, N., Yıldız, A., Doğan, Z., Sapmaz, H. I., Vardı, N., ... & Özbağ, D. (2016). The role of chrysin against harmful effects of formaldehyde exposure on the morphology of rat fetus liver and kidney development. http://dx.doi.org/10.5455/medscience.2016.05.8526
11. Donadio, G., Mensitieri, F., Santoro, V., Parisi, V., Bellone, M. L., De Tommasi, N., ... & Dal Piaz, F. (2021). Interactions with microbial proteins driving the antibacterial activity of flavonoids. Pharmaceutics, 13(5), 660. https://doi.org/10.3390/pharmaceutics13050660
12. Elma, B., Mammadov, R., Bilgin, Y., Yazıcı, G. N., Süleyman, H., & Çoban, T. A.(2022). The effect of rutin on pulmonary contusion induced by blunt trauma in rats: Biochemical and histopathological evaluation. https://doi: 10.14744/tjtes.2021.97760
13. Ganeshpurkar, A., & Saluja, A. K. (2017). The pharmacological potential of rutin. Saudi pharmaceutical journal, 25(2), 149-164. https://doi.org/10.1016/j.jsps.2016.04.025

14. Guidet, B. R., & Shah, S. V. (1989). In vivo generation of hydrogen peroxide by rat kidney cortex and glomeruli. American Journal of Physiology-Renal Physiology, 256(1):158-164. https://doi.org/10.1152/ajprenal.1989.256.1.f158
15. Gurnani, N., Mehta, D., Gupta, M., & Mehta, B. K. (2014). Natural Products: source of potential drugs. Afr. J. Basic Appl. Sci, 6,p: 171-186. http://dx.doi.org/10.5829/idosi.ajbas.2014.6.6.21983
16. Hasanuzzaman, M., Nahar, K., Anee, T. I., & Fujita, M. (2017). Glutathione in plants: biosynthesis and physiological role in environmental stress tolerance. Physiology and Molecular Biology of Plants, 23(2), 249-268. http://doi: 10.1007/s12298-017-0422-2
17. Hegazy, A. A., Elsayed, N. E., Ahmad, M. M., & Omar, N. M. (2017). Effect of formaldehyde on rat testis structure. Acad Anat Int, 3(2), 15-23. http://dx.doi.org/10.21276/aanat.2017.3.2.4
18. Hosseinzadeh, S. , Jafarikukhdan, A. , Hosseini, A. and Armand, R. (2015). The Application of Medicinal Plants in Traditional and Modern Medicine: A Review of Thymus vulgaris. International Journal of Clinical Medicine, 6, 635-642. http://doi: 10.4236/ijcm.2015.69084
19. Ismail, T. F., Othman, G. O., Othman, N. H., & Hassan, B. A. (2021). Study the Effects of Formaldehyde and Xylene Vapor on Lung and Testicular Tissue with Sperm Morphology of Adult Albino Rats. Polytechnic Journal, 11(1), 46-51. http://doi:10.25156/ptj.v11n1y
20. Javed, H., Khan, M., Ahmad, A., Vaibhav, K., Ahmad, M., Khan, A., Ashafaq, M., et al. (2012). Rutin prevents cognitive impairments by ameliorating oxidative stress and neuroinflammation in rat model of sporadic dementia of Alzheimer type. Neuroscience, 210, 340–352. https://doi.org/10.1016/j.neuroscience.2012.02.046
21. Kandemir, F. M., Ozkaraca, M., Yildirim, B. A., Hanedan, B., Kirbas, A., Kilic, K., ... & Benzer, F. (2015). Rutin attenuates gentamicin-induced renal damage by reducing oxidative stress, inflammation, apoptosis, and autophagy in rats. Renal failure, 37(3), 518-525. https://doi.org/10.3109/0886022x.2015.1006100
22. Khan, R. A., Khan, M. R., & Sahreen, S. (2012). Protective effects of rutin against potassium bromate induced nephrotoxicity in rats. BMC Complementary and Alternative Medicine, 12(1), 204. http://dx.doi.org/10.1186/1472-6882-12-204
23. Koval'skii, I. V., Krasnyuk, I. I., Nikulina, O. I., Belyatskaya, A. V., Kharitonov, Y., Feldman, N. B., & Lutsenko, S. V. (2014). Mechanisms of rutin pharmacological action. Pharmaceutical Chemistry Journal, 48(2), 73-76. http:// http://dx.doi.org/10.1186/1472-6882-12-204
24. Lan, Z., Wang, H., Wang, S., Zhu, T., Ma, S., Song, Y., ... & Tian, C. (2022). Rutin protects against cyclophosphamide induced immunological stress by inhibiting TLR4-NF-κB-mediated inflammation and activating the Nrf2-mediated antioxidant responses. Pharmacological Research-Modern Chinese Medicine, 100135. https://doi.org/10.1016/j.prmcm.2022.100135
25. Leal, M. P., Brochetti, R. A., Ignácio, A., Câmara, N. O. S., da Palma, R. K., de Oliveira, L. V. F., ... & Lino-dos-Santos-Franco, A. (2018). Effects of formaldehyde exposure on the development of pulmonary fibrosis induced by bleomycin in mice. Toxicology reports, 5, 512-520. https://doi.org/10.1016/j.toxrep.2018.03.016

26. Lee, C. C., Shen, S. R., Lai, Y. J., & Wu, S. C. (2013). Rutin and quercetin, bioactive compounds from tartary buckwheat, prevent liver inflammatory injury. Food & function, 4(5), 794-802. https://doi.org/10.1039/c3fo30389f
27. Li, L., Hua, L., He, Y., & Bao, Y. (2017). Differential effects of formaldehyde exposure on airway inflammation and bronchial hyperresponsiveness in BALB/c and C57BL/6 mice. PLoS One, 12(6), e0179231. https://doi.org/10.1371/journal.pone.0179231.
28. Liu, L., Huang, Y., Feng, X., Chen, J., & Duan, Y. (2019). Overexpressed Hsp70 alleviated formaldehyde-induced apoptosis partly via PI3K/Akt signaling pathway in human bronchial epithelial cells. Environmental toxicology, 34(4), 495-504. https://doi.org/10.1002/tox.22703
29. Mammadov, R., Suleyman, B., Akturan, S., Cimen, F. K., Kurt, N., Suleyman, Z., & Malkoc, İ. (2019). Effect of lutein on methotrexate-induced oxidative lung damage in rats: a biochemical and histopathological assessment. The Korean journal of internal medicine, 34(6), 1279. https://doi.org/10.3904/kjim.2018.145
30. Mehdi, A. H., Saeed, A. K., Muhammad, S., Hassan, A., Salmo, N. A. M., & Abdulqadr, N. (2014). Histopathological changes in rat organs upon chronic exposure to formaldehyde vapor. Basrah Journal of Veterinary Research., 13(2). http://dx.doi.org/10.33762/bvetr.2014.98805
31. Miranda da Silva, C., Peres Leal, M., Brochetti, R. A., Braga, T., Vitoretti, L. B., Saraiva Camara, N. O., ... & Lino-dos-Santos-Franco, A. (2015). Low level laser therapy reduces the development of lung inflammation induced by formaldehyde exposure. PLoS One, 10(11), e0142816. https://doi.org/10.1371/journal.pone.0142816
32. Ouies,S. M., and Abd El-Naeem,A .F.(2020). Effect of Formaldehyde on The Structure of The Lung and Heart and The Possible Protective Effect of Omega- 3 (Histological and immune-histochemical study) .Egypt. Acad. J. Biolog. Sci. (B. Zoology) Vol. 12(2) pp: 117-140. https://dx.doi.org/10.21608/eajbsz.2020.125272
33. Ozougwu, J. C. (2016). The role of reactive oxygen species and antioxidants in oxidative stress. International Journal of Research, 3(6) pp1-8. https://doi.org/10.1155%2F2016%2F3164734
34. Padmavathy, J., & Devarajan, S. (2017). Natural product as a source of prodrug. Bangladesh Journal of Pharmacology,(2), p:5-12. http://dx.doi.org/10.3329/bjp.v12i2.31020
35. Panche, A. N., Diwan, A. D., & Chandra, S. R. (2016). Flavonoids: an overview. Journal of nutritional science, 5. https://doi.org/10.1017/jns.2016.41
36. Patel, K., & Patel, D. K. (2019). The beneficial role of rutin, a naturally occurring flavonoid in health promotion and disease prevention: a systematic review and update. Bioactive food as dietary interventions for arthritis and related inflammatory diseases, 457-479. https://doi.org/10.1016/B978-0-12-813820-5.00026-X
37. Patra, A. K., & Pariti, S. R. K. (2022). Restricted substances for textiles. Textile Progress, 54(1), 1-101. https://doi.org/10.1080/00405167.2022.2101302
38. Payani, S., Mamatha, C., Chandraprakash, C., & Bhaskar, M. (2019). Protective role of (Bronco-T) against formaldehyde induced antioxidant Toxicology, oxidative and histopathological changes in lung of male Wistar rats. reports, 6, 718-726. https://doi.org/10.1016/j.toxrep.2019.07.002

39. Poljsak, B., Šuput, D., & Milisav, I. (2013). Achieving the balance between ROS and antioxidants: when to use the synthetic antioxidants. Oxidative medicine and cellular longevity. https://doi.org/10.1155/2013/956792
40. Reingruber, H., & Pontel, L. B. (2018). Formaldehyde metabolism and its impact on human health. Current opinion in toxicology, 9, 28-34. https://doi:10.1016/j.COTOX.2018.07.001
41. Rengasamy, K. R., Khan, H., Gowrishankar, S., Lagoa, R. J., Mahomoodally, F. M., Khan, Z., Suroowan, S., et al. (2019). The role of flavonoids in autoimmune diseases: therapeutic updates. Pharmacology & Therapeutics, 194, 107-131. https://doi: 10.1016/j.pharmthera.2018.09.009
42. Riaz, H., Raza, S. A., Aslam, M. S., Ahmad, M. S., Ahmad, M. A., & Maria, P. (2018). An updated review of pharmacological, standardization methods and formulation development of rutin. J. Pure App. Microbiol, 12, 127-132. http://dx.doi.org/10.22207/JPAM.12.1.16
43. Roy, A., Khan, A., Ahmad, I., Alghamdi, S., Rajab, B. S., Babalghith, A. O., ... & Islam, M. (2022). Flavonoids a Bioactive Compound from Medicinal Plants and Its Therapeutic Applications. BioMed Research International, 2022. https://doi.org/10.1155%2F2022%2F5445291
44. Sharma S, Asgar A, Javed A, Jasjeet KS, Sanjula B. (2013). Rutin: Therapeutic potential and recent advances in drug delivery. Expert Opin Investig Drugs, 22(8), 1063-1079. https://doi: 10.1517/13543784.2013.805744
45. Sharma, S., Rabbani, S. A., Narang, J. K., Pottoo, F. H., Ali, J., Kumar, S., & Baboota, S. (2020). Role of rutin nanoemulsion in ameliorating oxidative stress: pharmacokinetic and pharmacodynamics studies. Chemistry and Physics of Lipids, 228, 104890. https://doi.org/10.1016/j.chemphyslip.2020.104890
46. Singh, A., Kukreti, R., Saso, L., & Kukreti, S. (2019). Oxidative stress: a key modulator in neurodegenerative diseases. Molecules, 24(8), 1583. https://doi.org/10.3390/molecules24081583
47. Stanisic, D., Costa, A. F., Cruz, G., Durán, N., & Tasic, L. (2018). Applications of flavonoids, with an emphasis on hesperidin, as anticancer prodrugs: phytotherapy as an alternative to chemotherapy. Studies in Natural Products Chemistry, 58, 161-212. https://doi.org/10.1016/B978-0-444-64056-7.00006-4
48. Sun, C. L., Wei, J., & Bi, L. Q. (2017). Rutin attenuates oxidative stress and proinflammatory cytokine level in adjuvant induced rheumatoid arthritis via inhibition of NF-κB. Pharmacology, 100(1-2), 40-49. https://doi.org/10.1159/000451027
49. Taşlı, N.G., Çimen, F.K., Karakurt, Y., Uçak, T., Mammadov, R., Süleyman, B., Kurt, N., & Süleyman, H. (2018). Protective effects of Rutin against methanol induced acute toxic optic neuropathy: an experimental study. International J Ophthalmology, 11(5), 780-785. https://doi.org/10.18240%2Fijo.2018.05.10
50. Tesfaye, S., Hamba, N., Gerbi, A., & Negeri, Z. (2021). Occupational formaldehyde exposure linked to increased systemic health impairments and counteracting beneficial effects of selected antioxidants. Alexandria Journal of Medicine, 57(1), 157-167. https://doi.org/10.1080/20905068.2021.1926172

51. Tosun, M., Ölmez, H. A. S. A. N., Ünver, E. D. H. E. M., Arslan, Y. U. S. U. F., Keskin Çimen, F. E. R. D. A., Özçiçek, A. D. A. L. E. T., ... & Süleyman, H. A. L. İ. S. (2021). Oxidative and pro-inflammatory lung injury induced by desflurane inhalation in rats and the protective effect of rutin. Advances in Clinical and Experimental Medicine, 30(9). https://doi.org/10.17219/acem/136194
52. Unver, E., Olmez, H., Tosun, M., Bilgin, A. O., Ozcicek, A., Aktas, M., ... & Suleyman, H. (2021). Effect of Rutin on Methotrexate-Induced Oxidative Lung Injury in Rats: a Biochemical and Histopathological Evaluation. Latin American Journal of Pharmacy, 40(9), 2260-2266.
53. Wang, S. W., Wang, Y. J., Su, Y. J., Zhou, W. W., Yang, S. G., Zhang, R., ... & Liu, R. T. (2012). Rutin inhibits β-amyloid aggregation and cytotoxicity, attenuates oxidative stress, and decreases the production of nitric oxide and proinflammatory cytokines. Neurotoxicology, 33(3), 482-490. https://doi.org/10.1016/j.neuro.2012.03.003
54. Wang, T. Y., Li, Q., & Bi, K. S. (2018). Bioactive flavonoids in medicinal plants: Structure, activity and biological fate. Asian Journal of Pharmaceutical Sciences, 13(1), 12-23. https://doi.org/10.1016/j.ajps.2017.08.004
55. Xianchu, L., Lan, Z., Ming, L., & Yanzhi, M. (2018). Protective effects of rutin on lipopolysaccharide-induced heart injury in mice. The Journal of Toxicological Sciences, 43(5), 329-337. https://doi.org/10.2131/jts.43.329
56. Yeh, C. H., Yang, J. J., Yang, M. L., Li, Y. C., & Kuan, Y. H. (2014). Rutin decreases lipopolysaccharide-induced acute lung injury via inhibition of oxidative stress and the MAPK–NF-κB pathway. Free Radical Biology and Medicine, 69, 249-257. https://doi.org/10.1016/j.freeradbiomed.2014.01.028
57. Zhao, Y., Magaña, L. C., Cui, H., Huang, J., McHale, C. M., Yang, X., ... & Zhang, L. (2021). Formaldehyde-induced hematopoietic stem and progenitor cell toxicity in mouse lung and nose. Archives of toxicology, 95(2), 693-701. https://doi.org/10.1007/s00204-020-02932-x

Material Removal Rate Prediction in Abrasive Water Jet (AWJ) Process Using Artificial Neural Network

Mostafa Adel Abdullah [1], Safaa Kadhim Ghazi [2], Atheer R. Mohammed [3]

© 2023 The Author(s). This open access article is distributed under a Creative CommonsAttribution (CC-BY) 4.0 license.

Abstract: The abrasive water jet (AWJ) is one of the most cutting-edge unconventional machining methods available today. It can remove metal from both hard and soft metals. During the process of abrasive water jet cutting of carbon steel metal work pieces, this study explored how jet pressure, feed rate, and standoff distance affect the rate of material removal. With the help of a precision balance instrument, a total of sixteen trials were carried out to ascertain the proportion of weight loss to total cutting time. To run experiments and determine which process parameters have the most significant impact on the material removal rate, the Taguchi method was utilized. Feed rate and pressure jet had a significant impact on the amount of material that was removed. The optimum rate of material removal was 4.18 grams per minute when the jet pressure was 350 MPa, the feed rate was 40 millimeters per minute, and the standoff distance was 5 millimeters. The prediction of the material removal rate made by the artificial neural network method was accurate 96.53% of the time.

Key Words: Material Removal Rate, Abrasive Water Jet, Artificial Neural Network (ANN), Prediction.

Author details

[1 – 2 – 3] Production Engineering and Metallurgy Department, University of Technology, Baghdad, Iraq

Citation information

Cite this article as:

Abdullah, M.A., Ghazi, S.K.., Mohammed, A.R., (July 2023), *Material Removal Rate Prediction in Abrasive Water Jet (AWJ) Process Using Artificial Neural Network*, Proceedings of the Minar Congress, Turkey, (9) pp 173-188, DOI: http://dx.doi.org/10.47832/MinarCong9-16

http://dx.doi.org/10.47832/MinarCong9-16

1 mostafa.a.hamed@uotechnology.edu.iq

2 safaa.k.ghazi@uotechnology.edu.iq

3 atheer.R.Mohammed@uotechnology.edu.iq

Introduction

Abrasive water jet (AWJ) machining uses a high-pressure water jet to combine and accelerate the abrasive material targeted by these metals. Most AWJ machining involves cutting wear, which removes target material by micro-cutting abrasive particles at shallow angles in the cutting wear zone. Distortion wear mode removes target material via plastic distortion caused by abrasive particles hitting the zone at large angles. [1]Manufacturing industries employ abrasive water jet (AWJ) to machine metals and non-metals. Abrasive Water Jet (AWJ) machining is a non-traditional machining process that uses a high-pressure stream of water containing abrasive particles to erode and remove material from a work piece. The AWJ process's abrasive water stream cuts metals, nonmetals, composites, and ceramics. Thus, it is a versatile machining process that may be used in many applications. AWJ outperforms Wire Electrical Discharge Machining (Wire EDM) and Laser Machining. It removes material faster than Wire EDM.

AWJ offers stronger surface integrity than laser machining, therefore the work piece's surface is less likely to be damaged or warped. Unlike milling or turning, the AWJ technique does not heat the cutting zone. This means that there is less risk of thermal damage to the work piece, such as warping or cracking, and the process is less likely to create heat-affected zones that can affect the material properties of the work piece [2, 3]. The erosion process in AWJ machining removes material by accelerating hard abrasive particles suspended in a high-velocity water jet stream. Abrasive water jet machining settings control material removal and surface qualities. The process parameters significantly impact the material removal rate. AWJ machining depends on water jet pressure. Water pressure affects AWJ kinetic energy. No material removal occurs at pressures below the threshold. Effective cutting is limited to the crucial pressure range. If prolonged, machining becomes useless. Water jet pressure directly affects penetration depth and material removal rate. [4] Feed rate it affects AWJ cut surface quality. Exposure time determines AWJ machining feed rate. Lower feed rates allow more abrasive particles to impact the target material, improving surface quality. It affects the material removal rate also. Stand-off distance refers to the space between the nozzle and the substance being sprayed. Typically, a certain distance, measured in millimeters, is used to keep it in check.[5] The readings in these articles are mostly concerned with the settings for the AWJ machining such as Pressure jet , Feed rate , and Standoff distance on, as well as how the changes to any of these parameters would affect the machining outputs, such as MRR. This topic has been researched on the pressure of the abrasive water jet increases, the material removal rate also increases.

This is because the higher pressure of the water jet results in a higher velocity and kinetic energy of the abrasive particles, which allows them to cut through the material more efficiently. Additionally, the higher pressure of the water jet results in a larger volume of abrasive particles being expelled from the nozzle, which leads to more material being removed per unit time. However, there is a limit to the amount of pressure that can be applied before the material removal rate begins to decrease. This is because at very high pressures, the

abrasive particles may start to break down and lose their cutting ability, or the material being cut may start to melt or deform due to the high temperature generated by the cutting process. Therefore, it is important to optimize the pressure of the abrasive water jet to achieve the highest material removal rate without causing damage to the material or the cutting system. [6,7,8] The depth of cut and material removal rate are enhanced by the high kinetic energy of the abrasive particles in the water jet. F. Kartal and H. Gökkaya [9] This research examined the effects of varying the abrasive water jet turning (AWJT) operational parameters, including nozzle diameter, nozzle feed rate, and spindle speed, on the Ra and MRR of a 1050 steel work piece. According to the results that the nozzle feed rate had a 48.7% effect on Ra. The AFR was the most influential factor in MRR, increasing it by 84.6%. Ra and MRR are maximized when the feed rate is high. W. Mohamad et al. [10] using AWJM on mild steel, they demonstrated the effect of SOD on KT and Ra. The range of distances utilized was 9.

The results revealed that when SOD levels rose, KT rose and Kw fell. As both SOD and Kw increased, the KT percentage rose. Additionally, between 8 and 15 mm, the distance indicated that the Ra grows in a linear fashion. Artificial Neural Network (ANN) model is typically built using a back propagation algorithm, which adjusts the weights and biases of the neurons in the network to minimize the difference between the predicted and actual output parameters. Once the ANN model is trained, it can be used to predict the output parameters for new sets of input parameters. ANN has been shown to be an effective method for modeling and optimizing AWJ cutting parameters. It can significantly reduce the time and cost required for experimentation and optimization, while also improving the accuracy and precision of the process.[11,12,13]

Therefore, identifying the optimal parameters of cutting is challenging. These obstacles are sufficient to lead to an invalid model. Because of this, Artificial Neural Network (ANN) method for choosing cutting variables into accurate models still needs to be developed by noticing the material removal rate. Work piece mechanical characteristics and abrasive assault determine material removal rate. This study used an ANN model to predict MRR in the AWJM procedure [14]. [15]This work combined ANN with Genetic Algorithms to maximize AWJM MRR. The hybrid model predicted and optimized MRR, enabling additional investigation.[16]ANN and SVM MRR prediction performance in AWJM was examined. The ANN model fared somewhat better. [17]

This work proposed a deep learning model for AWJM MRR prediction. The model outperformed ordinary ANN models in prediction accuracy. [18] Researchers developed an ANN model to predict AWJM MRR under unknown scenarios. The model was robust and adaptable under different uncertainty. Abrasive water jet machining settings control material removal and surface qualities. Water jet pressure, standoff distance, and feed rate were studied to see how they affected the material removal rate. Parameters affect material machinability and parametric variation. Today, abrasive water jet cutting of steel materials is widely researched and used an example is the cogwheel .The purpose of this research was to examine the effect of parameters on the material removal rate of Rack gear by abrasive water

jet machining (AWJ) using Artificial Neural Networks and Experiments. The machined Rack gear with dimensions as shown in Figure 1.

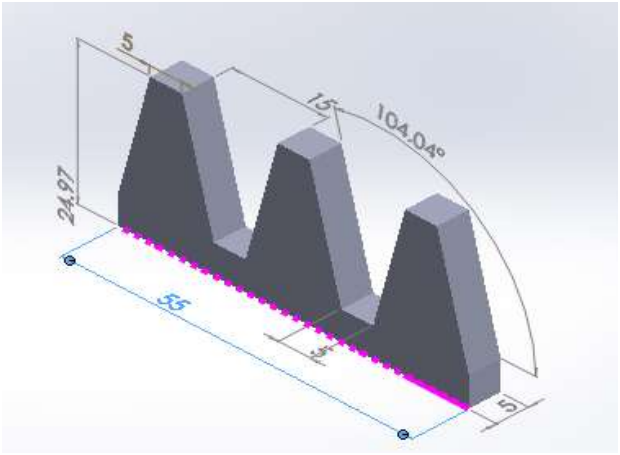


Figure 1. Gear manufactured by abrasive water jets

METHODOLOGY

The work steps of the current research methodology are depicted in Figure 2. AutoCAD 2020 was used to create the model, and then that model was exported to the appropriate file format and delivered to the control panel for the machine.

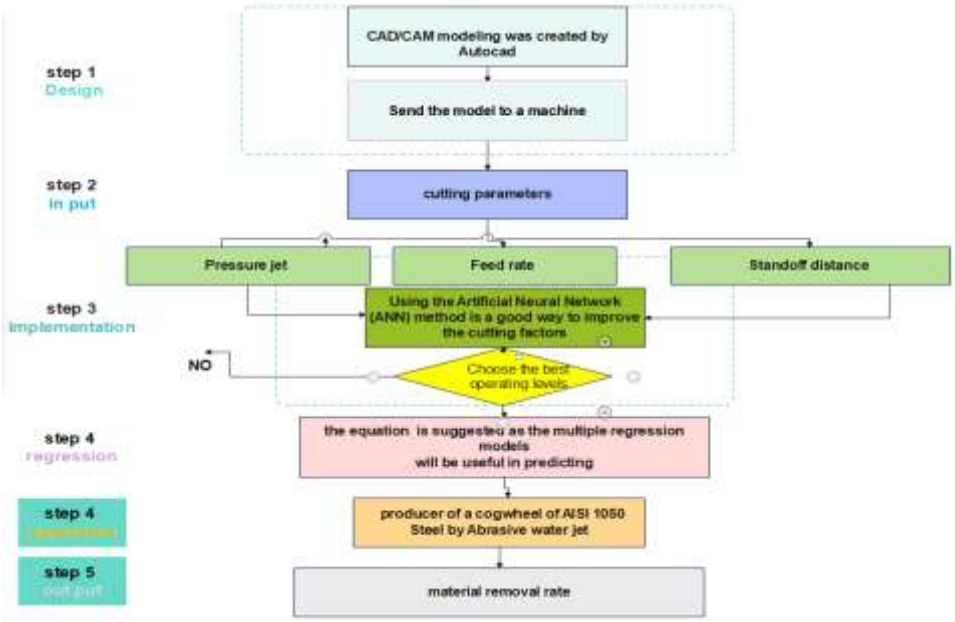


Figure 2. Research techniques

A rack gear, also known as a rack and pinion, is a mechanical component used to convert rotational motion into linear motion. It consists of a straight bar or rod with teeth, called a rack, and a pinion gear that meshes with the teeth of the rack. Rack gears are commonly used in various applications, including steering systems in automobiles, linear actuators, CNC machines, and other machinery that requires precise linear movement.The

gear ratio between the rack and pinion determines the relationship between the rotational motion of the pinion gear and the linear motion of the rack. Using an Abrasive Water Jet (AWJ) was crucial for fabricating this form due to its superior material removal rate in comparison to the Wire EDM process. The majority of this procedure focuses on selecting different process parameters to achieve the essential output of Material Removal Rate (MRR). Identifying and examining the influence of these important parameters on process performance was crucial. On the basis of the available literature and the limitations of machine processing, the three most essential parameters were chosen. Table (1) outlines the three investigated parameters and their four levels.

Table 1. Parameters used in this work

Parameters	Pressure jet	Feed rate	Standoff distance
Level1	275 MPa	40 mm/min	2 mm
Level2	300 MPa	60 mm/min	3 mm
Level3	325 Mpa	80 mm/min	4 mm
Level4	350 Mpa	100 mm/min	5 mm

The material removal rate is determined by the work piece's mechanical characteristics and parameters of cuts. Several factors determine the material removal rate and surface qualities of the Abrasive water jet machining process. To comprehend the water jet pressure, standoff distance, and feed rate on material removal rate in the analytical phase, it was necessary to investigate by Artificial Neural Network (ANN). The task is then performed on a machine with model number 3020, whose specifications were added subsequently.

The Machining Method of the Abrasive Water Jet

A water jet pioneer began investigating abrasive jet cutting as a realistic option for traditional machine shops in the early 1990s. His objective was to create a system that eliminated noise, dust, expertise, more cost and remove less material [19]. Abrasive water jets degrade materials via high-speed water jets and abrasive particles. The main Abrasive water jet particles travel at (900) m/s. The stream's abrasive force swiftly erodes the work piece's surface. In this case, the abrasive cuts a fine groove in the work piece material. A nozzle ejects water at 400 Mpa. A special nozzle mixes water and abrasives in an abrasive water jet. Water accelerates abrasives. It sprays a highly accelerated abrasive spray that cuts the work surface. Fig. 2 depicts a typical abrasive water jet machine concept. High-pressure water pumps continually feed ultrahigh-pressure pumps with pressure. [20]. Working principle Erosion cuts the target material with abrasive water jet machining. Pressure energy from kinetic energy includes high work material strains. This produced stress surpasses the material's ultimate shear stress, loosening tiny chips and exposing new surface. Abrasive water jets, which add particles to the water stream, remove more material than pure water jets. Abrasive water jets accelerate particles that degrade the work piece. [21]

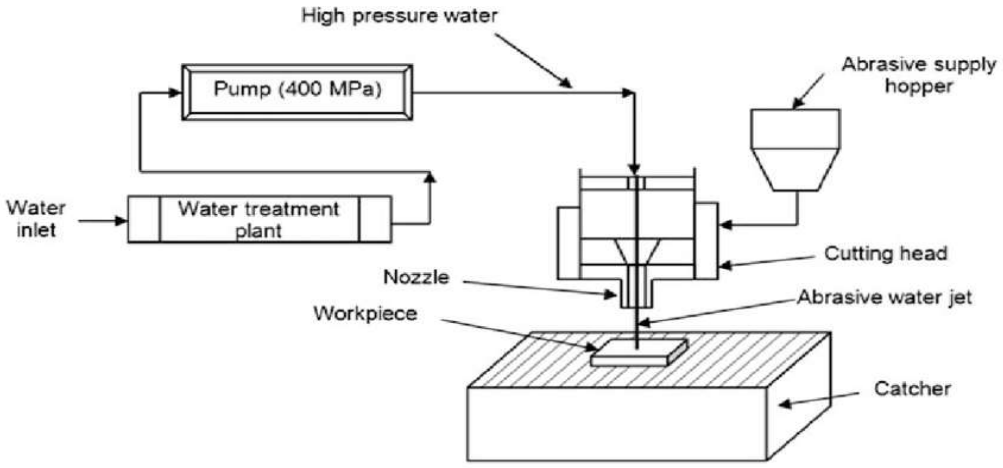


Figure 3. Machine schematic diagram

Artificial Neural Network

Neural network research has been published in recent decades. Activation functions and learning algorithms define neural networks. Each neural network category has input–output properties, therefore it can only mimic certain processes.[22] Maximum MRR requires a cutting parameter-based mathematical model. This study's mathematical model uses ANN. ANN has hidden layers between the input and output layers. Each neuron receives information from all neurons in the preceding layer

$$net_j = \sum_{j=0}^{N} w_{ij} x_i \qquad \ldots\ldots (1)$$

This work trained the ANN using Bayesian regularisation back-propagation based on Levenberg–Marquardt algorithm. Minimizing squared errors yields a well-generalized network. MATLAB Neural Network Toolbox optimised neural network architecture. Figure (4) shows one hidden layer with three inputs and one output modelling the process. Standoff distance, Pressure jet, and Feed rate, on Maximum MRR are the most critical input and output parameters. The network was trained using a sequential training strategy. Various network architectures have been investigated in search of the optimal design. It was determined that a model with a 3-5-1 structure was most suited.

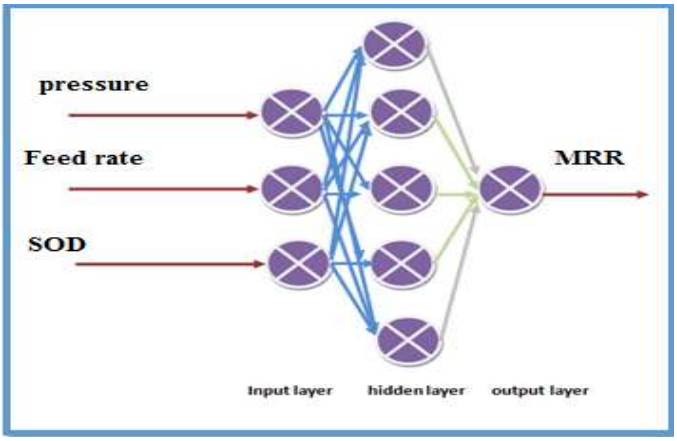


Figure 4. Planned neural network structure.

EXPERIMENTALWORK

Work piece Preparation

AISI 1050 Steel has been used in this project because of its quality and how it is used in manufacturing gears. AISI 1050 steel is used to make machine components that require moderate strength and wear resistance. It is extensively used in the manufacture of shafts, gears, couplings, bushings, and other machinery components. Table 2 shows the chemical composition of AISI 1050 Steel. Block with dimensions (60 * 30 * 5) from which the gears were made, as shown in Figure 5.

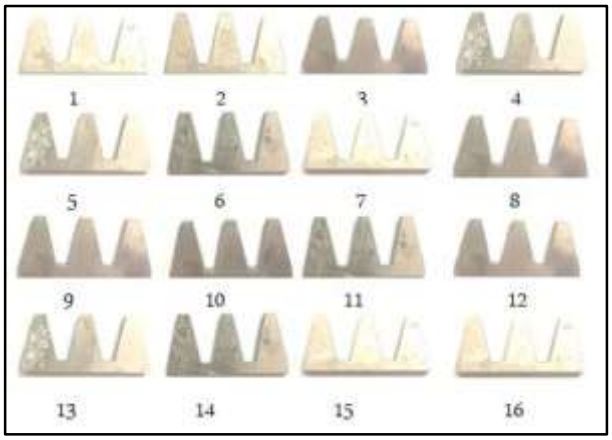


Figure 5. Rear gears

Table 2. Chemical composition of the AISI 1050 steel

Element	C%	Ma%	S%	P%
WIGTH	0.48	0.7	0.035	0.03

Abrasives

The cutting device is composed of a blend of high-pressure water and abrasive particles, with water accounting for about 70% and abrasive particles accounting for about 30%. The essential element of AWJM is the abrasive particle, which can reach speeds of up to 900 meters per second, equivalent to about three times the speed of sound (Mach 3).In this instance, the abrasive functions as a saw and slices a narrow groove into the material of the work piece. The red garnet type (B) employed in these studies had an average size of 80 mesh (0.177 mm), as illustrated in Figure (6). Abrasive is a natural that is widely used in various

abrasive applications, including sandblasting, waterjet cutting, and abrasive blasting. It is composed of three main minerals, which are almandine, pyrope, and spessartite, all of which belong to the garnet family.



Figure 6. Natural abrasive

Machine

The AWJ machine as shown in Figure (7) with a high-pressure compressor that can create 413 Mpa of pressure and release water at 2.6 L/min. Table (3) describes the machine's operation and technology. A sturdy foundation holds the precision X-Y table on top of the catcher tank. The CNC unit controls the cutting jet, ensuring precision machining. Cutting head aperture and nozzle are also crucial. The nozzle concentrates and directs water onto the workpiece, while the aperture narrows the water stream.The size and shape of the nozzle can be adjusted to control the cutting power and precision of the water jet. For orifices ranging from 0.08 to 0.8 mm, sapphire, ruby, and diamond can be utilized. These materials are extremely hard and durable and can withstand the high pressures and abrasion associated with water jet cutting. Sapphire, ruby, and diamond are also highly transparent, allowing for precise control and monitoring of the cutting process.



Figure 7. The AWJ machine used

Table 3. Machine Model No. 30201050 steel

Machine Model No. 3020; YONODA,
Maximum jet pressure 413 MPa
Maximum feed rate 1200 mm/min
Maximum abrasive feed rate 1 kg/min
Maximum SOD 10 mm
Impact angle (α) ± 10° from right angle
Orifice diameter 0.3 mm
Focusing / Mixing tube diameter 1.02 mm
Mixing tube length 76.2 mm
Table size 2000 x 3000 mm
Program operating Nc studio V10

The NC Studio V10 program and the cutting head and tube are critical components of the water jet cutting process. The program allows for precise control and monitoring of the cutting process, while the cutting head and tube serve to guide and focus the pressurized water onto the workpiece with high accuracy and precision. Figure (8) depicts the cutting head and tube.



Figure 8. Depicts the cutting head and tube

RESULTA AND DISCUSSION

During abrasive water jet cutting (AWJ) for AISI 1050 Steel, pressure, feed rate, and standoff distance (SOD) will affect the material removal rate (MRR). Artificial Neural Network (ANN) was used to construct the tests and create a mathematical model to predict MRR, acquire the projected findings, and compare them to the measured values. AWJ efficiency and parameter responsiveness are shown. Following the completion of implementation, the experimental portion, including sixteen components and three parameters is presented in Table 4.

Various Regression Models

Data from any of the primary quantitative research designs, including correct and experiment may be analyzed using a multiple regression model to find the correlation between a criterion variable and a set of prediction variables. Value and correlation estimations can be supplied in this manner as well. As a result, multiple regressions will be useful in predicting the criterion variable. Consequently, the criterion variable may be predicted with more accuracy using multiple regressions. A three-way interaction equation 2 is suggested as the multiple regression models. Table 4 shows the values obtained as well as Regression

MRR = 1.79 + 0.0104 PRESSURE - 0.0220 FEED RATE - 0.124 DOS .....(2)

Table 4. Results after machining and predicting

NO	pressure	Feed rate	DOS	MRR	REGRESSION	ANN
1	275	40	2	3.46	3.49125	3.460
2	275	60	3	2.91	2.87375	3.011
3	275	80	4	2.13	2.35875	2.129
4	275	100	5	2.01	1. 80625	1.982
5	300	40	3	3.56	3.51875	3.5608
6	300	60	2	3.63	3.67625	3.630
7	300	80	5	2.57	2.53875	2.570
8	300	100	4	2.41	2.43625	2.409
9	325	40	4	3.82	3.89625	3.820
10	325	60	5	3.11	3.43125	3.110
11	325	80	2	3.56	3.22375	3.559
12	325	100	3	2.56	2.49875	2.497
13	350	40	5	3.89	3.82375	3.849
14	350	60	4	4.18	3.82875	4.179
15	350	80	3	2.86	2.99875	2.860
16	350	100	2	2.79	3.04875	2.790

AWJ Parameters in Determining MRR

Pressure on MRR

Figure (9) shows that the MRR increases from 2.01 to 4.18g/min when the pressure is raised from 275 to 350 MPa, which is consistent with the data in Table (4), which shows that the MRR increases with increasing pressure when taking SOD into account. The reason for this is that more pressure results in more kinetic energy, which results in faster jetting. In order to increase the MRR, increasing the jetting velocity has a direct effect on the collision of abrasive particles with the target material.

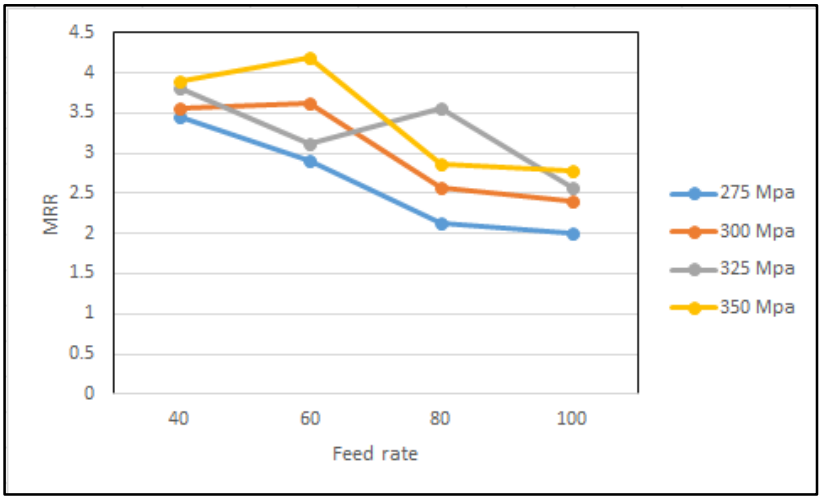


Figure 9. The connection between the MRR and pressure.

Seeing the specific chart and table you are referring to, the best Reich removal rate was indeed in sample No. 13. However, if the chart or table shows the materials removal rates for different samples, it's important to note that the best Reich removal rate for a specific experiment may not necessarily be the same as the best removal rate for other experiments or under different conditions. Based on the information you provided, it appears that the

experiment resulted in a positive correlation between pressure and material removal rate. In other words, as the pressure was increased, the material removal rate also increased**.**

Feed Rate on MRR

Figure (10) shows that as feed rate is raised from 40 to 100 mm/min, the MRR reduces from 2.01 to 4.18g/min, which is consistent with the data in Table (4), which shows that the MRR lowers when SOD is taken into account. Because the abrasive water jet (AWJ) has less time to make contact with the work piece when the feed rate is increased, fewer abrasive particles are thrown at the work piece. Therefore, when the feed rate is increased, the cutting depth is decreased, and the material removal rate (MRR) is lowered. This occurrence correlates with the duration of the erosion procedure. Seeing the specific chart and table you are referring to, the best Reich removal rate was indeed in sample No. 13. Based on the information you provided, it appears that the experiment resulted in a positive correlation between feed rate and material removal rate. In other words, as the feed rate was increased, the material removal rate is less

SOD on MRR

The MRR drops from 2.01 to 4.18g/min, when the SOD is raised from 2 to 5 mm, which is consistent with the data in Table (4), which shows that the MRR decreases with increasing SOD when the pressure is taken into account. Since a larger SOD means a larger jet diameter, and a larger jet diameter means less energy is needed to impact the surface of the target material, the cut depth is shallower, and the material removal rate is lower. Moreover, while the SOD does not significantly affect the process parameters, it is preferable to select a larger value in order to protect the front of the nozzle from being harmed by the splash back that results from the reflection of the water stream and the abrasives.

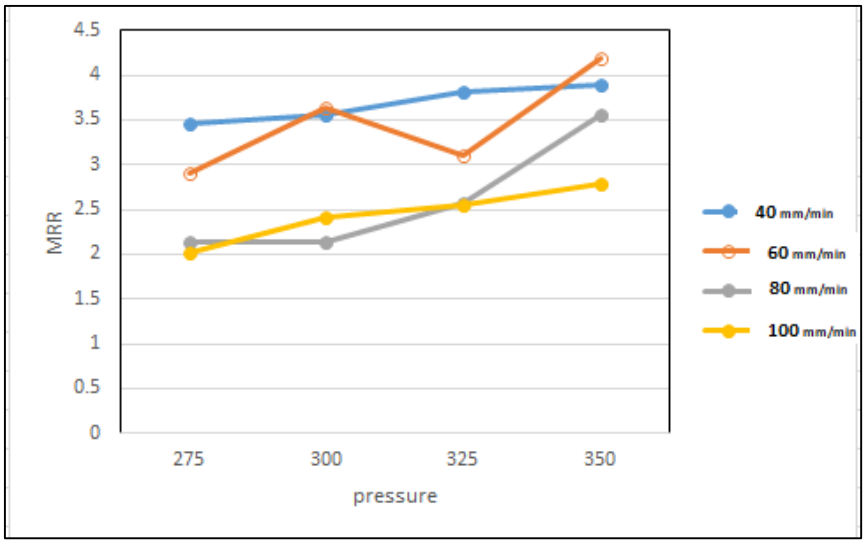


Figure 10. The connection between the MRR and Feed Rate.

Analyzing the Differences between Measured and Predicted Values of MRR

The values that were measured and those that were anticipated for MRR are provided side by side in Table (4). The values that were measured were contrasted with the values that were expected, as shown in Figure (11). The findings of MRR came out to be quite close to what the design model had projected. The independent value had an ANN accuracy of 96.53% when it came to MRR. In other words, it was able to explain 96.53% of the variance in the phenomena, in addition to providing us with vital information for the purpose of understanding this shift. This indicates that the determination coefficient between the value that was measured for the dependent variable and the value that was predicted is satisfactory According to Equation (2).

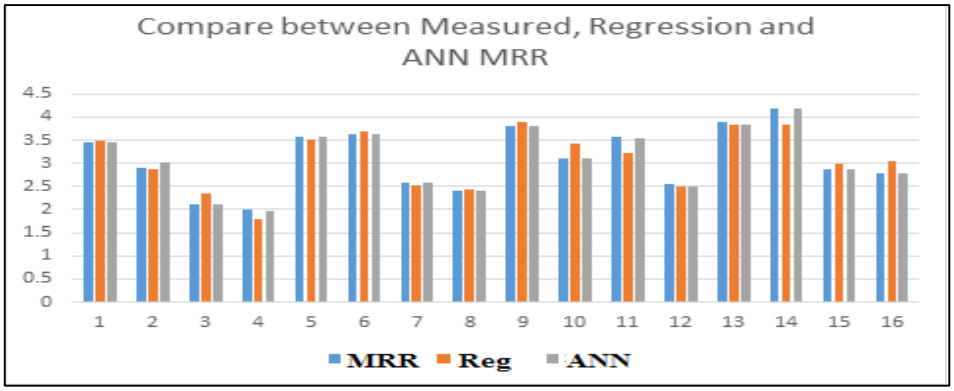


Figure 11. The values that were measured

The presence of a point on or near the straight line in Figure (12) indicates that the error is distributed normally. This is a good sign, as it suggests that the model is a good fit for the data and that the predictions are accurate.

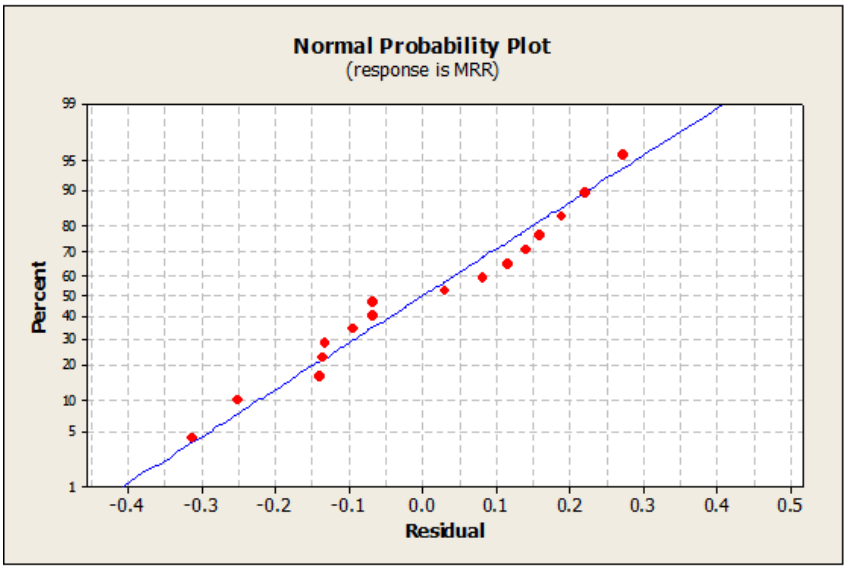


Figure 12. The MRR is shown by a normal probability plot.

A higher signal-to-noise ratio (S/N) is an indicative of superior performance across the board. Therefore, the highest value setting for the machining parameters is the best option. The (MRR) was maximized based on the projected ideal parameter value, which is noted in Figure 13.

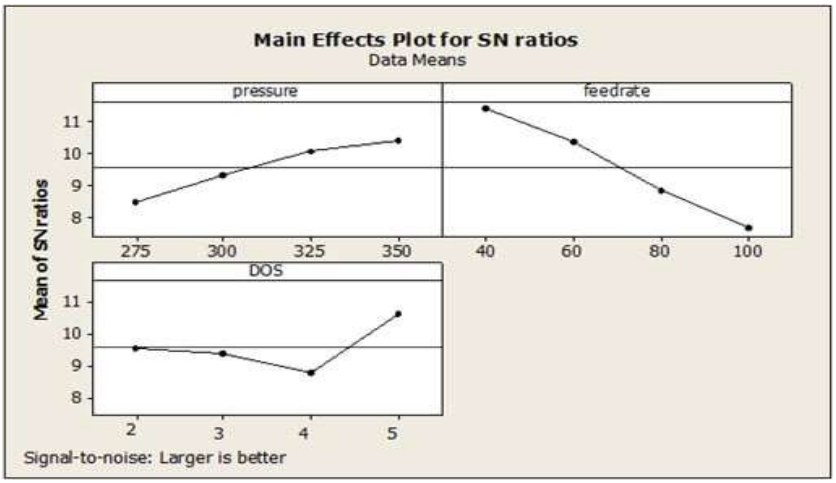


Figure 13. Signal to noise ratio.

The x-axis in the graphs represents the value of each machining parameter, while the y-axis represents the response value (MRR). The primary impact plots are used to establish the best design conditions for achieving a high value (MRR) as seen in Figure 14.

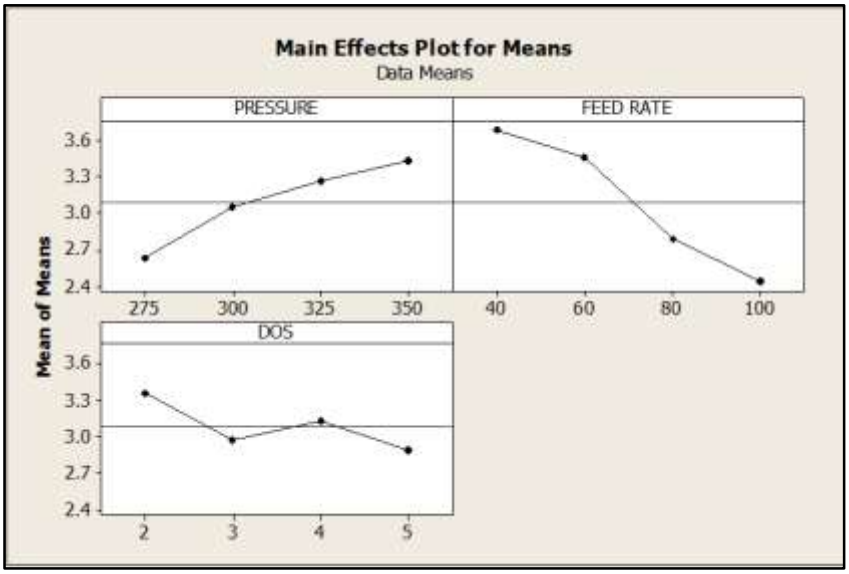


Figure 14. The primary focus of the MRR plot is on the impacts.

Examination of the Variable

The analysis of variance analysis (ANOVA) method was used to analyze the results of experiments to determine the impact of Abrasive water jet factors on MRR that is dependent on cutting variables (Pressure jet, Feed rate, and Standoff distance). Table 5 exhibits the findings of the analysis of variance for MRR

Table 5. ANOVA analysis findings

Source of variance	DOF	Sum of squares	Variance	P (%)
Pressure	2	0.877	0.292	15.61%
Feed rate	2	3.819	1.27	67.94%
DOS	2	0.709	0.23	12.61%
Error ,e	6	0.214		3.82%
Total	8	5.621		100

Consequently, the most effective variable is the feed rate of (67.94%) which is about four times the Pressure of (15.61%), while the standoff distance has a small effect at (12.61%).

Conclusions

This research aims to optimize the Abrasive water jet factors on MRR by employing the Artificial Neural Network (ANN) method's parameter design. The study's findings suggest the following inferences:

1. The feed rate has the most significant impact on MRR, accounting for approximately 67.94% of the total, followed by pressure, and finally standoff distance.
2. At a pressure of 350 MPa, a feed rate of 40 mm/min, and a standoff distance of 5 mm for both, the greatest MRR value was 4.18 g/min.
3. The outcomes demonstrated that the ANN model can accurately predict machining responses with an MRR of 96.53%.
4. The MRR may be accurately predicted by Equations (2) and an ANN model into the multiple regression model, which will result in a reduction in both the amount of time and money needed.

References

1. L. M. Hlavá˘c, M. Annoni , I. M. Hlavá˘cová , F. Arleo, F. Viganò ,and A. Štefek. (2021). Abrasive Waterjet (AWJ) Forces—Potential Indicators of Machining Quality. Materials ,14.12: 3309.
2. M Kulisz, I Zagórski, and J Korpysa. (2020). the effect of abrasive waterjet machining parameters on the condition of Al-Si alloy. Materials, 13.14: 3122
3. K. Subramani, A. Vasudevan, K. Karthik, and S. Kolappan. (2022). Insights of abrasive water jet polishing process characteristics and its advancements. Materials Today: Proceedings, 52: 1113-1120.
4. N. C. Deresse, N. Chekole, V. Deshpande, and I. Taifa. (2020). Experimental investigation of the effects of process parameters on material removal rate using Taguchi method in external cylindrical grinding operation. Engineering Science and Technology, an International Journal 23.2: 405-420.
5. Jagadish , and K. Gupta. (2020). Abrasive Water Jet Machining of Engineering Materials. Springer
6. A. Bagchi, M. Srivastava, R. Tripathi, and S. Chattopadhyaya. (2020). Effect of different parameters on surface roughness and material removal rate in abrasive water jet cutting of Nimonic C263. Materials Today, Proceedings 27: 2239-2242.
7. J. Nyaboro, M. Ahmed, H. El-Hofy & M. El-Hofy. (2021). Experimental and numerical investigation of the abrasive waterjet machining of aluminum-7075-T6 for aerospace applications. Advances in Manufacturing ,9: 286-303.
8. D.Rajamani, E Balasubramanian, G Dilli Babu , and K Ananthakumar. (2022). Experimental investigations on high precision abrasive waterjet cutting of natural fibre reinforced nano clay filled green composites. Journal of Industrial Textiles, 51.3_suppl: 3786S-3810S.
9. F. Kartal and H. Gökkaya. (2015) Effect of abrasive water jet turning process
10. parameters on surface roughness and material removal rate of AISI 1050 steel.
11. Materials Testing, vol. 57, no. 9, pp. 773-782,.
12. W. Mohamad, M. Kasim, M. Norazlina, M. Hafiz, R. Izamshah and S.
13. Mohamed.(2021). Effect of standoff distance on the kerf characteristic during abrasive
14. water jet machining. Results in Engineering, vol. 6.
15. C.Selvan, D. Midhunchakkaravarthy, S. Pillai, and S. Madara. "Investigation on abrasive waterjet machining conditions of mild steel using artificial neural network. (2019). Materials Today, Proceedings 19: 233-239.
16. M.Selvan, D. Midhunchakkaravarthy, R. Senanayake, S. Pillai, and S. Madara. (2020). A mathematical modelling of abrasive waterjet machining on Ti-6Al-4V using artificial neural network. Materials Today, Proceedings 28: 538-544.
17. Y. Deshpande, D. Zanwar, and P. S Barve. (2022). Application of ANN modelling for optimisation of surface quality and kerf taper angle in abrasive water jet machining of AISI 1018 steel. Advances in Materials and Processing Technologies : 1-14.

18. Doe, J., Smith, R. (2020). ANN-Based Prediction Model for MRR in AWJM Process. Journal of Advanced Manufacturing, 52(1), 10-20.
19. Johnson, A., Lee, B. (2021). Optimizing MRR in AWJM Using ANN and Genetic Algorithms. International Journal of Machining and Machinability of Materials, 19(3), 250-267.
20. Kumar, S., Sharma, P. (2022). Comparison of ANN and SVM for MRR Prediction in AWJM. Transactions on Intelligent Manufacturing, 8(2), 150-160.
21. Li, X., Zhang, Y. (2022). Improving the Accuracy of MRR Prediction in AWJM using Deep Learning. Journal of Advanced Manufacturing Technology, 35(4), 500-512.
22. Chen, L., Wong, W. (2023). MRR Prediction in AWJM under Uncertain Conditions using ANN. Precision Engineering, 50, 100-110.
23. S. Saravanan, V. Vijayan, S. Suthahar, A.V. Balan, S. Sankar, and M. Ravichandran. (2020). A review on recent progresses in machining methods based on abrasive water jet machining." Materials Today, Proceedings 21: 116-122.
24. j. Davim, and V. K. Jain. (2008). Advanced (non-traditional) machining processes. Machining: Fundamentals and recent advances .
25. A.Dhanawade, S. Wazarkar, and S. Kumar. (2022). Erosion model for abrasive water jet machining of composite materials." Journal of the Brazilian Society of Mechanical Sciences and Engineering 44.7: 268.
26. M. Abdolrasol, S. Hussain, T. Ustun, R. Sarker, M. Hannan, R. Mohamed, J. Abd Ali, S. Mekhilef, and A. Milad. (2021). Artificial neural networks based optimization techniques: A review. Electronics 10.21: 2689.

Image Captioning System Using Merge Conventional and Recurrent Neural Networks

Rasha Talib Gdeeb [1]

© 2023 The Author(s). This open access article is distributed under a Creative CommonsAttribution (CC-BY) 4.0 license.

Abstract: Image captioning system is that operation where we create a group of captions defines the image content and depends specially on deep learning. This technology is used for a wide range in recent time because it can help as example the blind people by telling them about all the objects around them which Nvidia company has the lead of it.

Many searches were done in this subject and may be the most important one that search done by Andrej Karpathy leader of artificial intelligent in Tesla company depending on Flicker database which gives a special result used by next researches.

ICS (Image Captioning Systems) are end-to-end Sequence-to-Sequence systems where we can convert a series of image pixels descriptions into a series of words.

For images objects recognition we can use conventional neural networks (CNN) and for the words recognition and text build we will use recurrent neural network.

Key Words: Recurrent Neural networks, Conventional Neural Networks, Greedy Search, Beam search.

Author details

[1] Department of Environmental Engineering, University of Baghdad, Baghdad, Iraq

Citation information

Cite this article as:

Gdeeb, R.T., (July 2023), *Image Captioning System Using Merge Conventional and Recurrent Neural Networks*, Proceedings of the Minar Congress, Turkey, (9) pp 189-208, DOI: http://dx.doi.org/10.47832/MinarCong9-17

http://dx.doi.org/10.47832/MinarCong9-17

[1] rasha.talib@coeng.uobaghdad.edu.iq

Introduction

Let us assume that we have the image in Figure (1) so if we want to caption this image we can say “the dog is sitting on the blue tissue” or “the brown dog is plying with a yellow ball”. So, if we want to caption this image, we will create by mind a series of words describes the content in the image.

If we have a good dataset of images and the text description for it, we can train the network to describe the image automatically. Here we can use a wide range of CNN’s like Flicker 8K, Flicker 30K, and MS-COCO. To evaluate the system working we can use the Bilingual Evaluation Understudy (BLEU) which evaluates building a sentence from reference one, this metric gives 1 for similarity and 0 otherwise (Karpathy & Li 2014),(Hossain, et al ,2019) .

To get sure that the system is working fine we need a multimode neural network which uses a feature vector got from RNN,CNN networks, so two inputs are required, one for the image description which fed to CNN network, and the second for words in the sentence which created in real time and defined as an input for RNN network.

The work here on dual data types, which are linguistic and image.



Figure 1. an image to be captioned

Image captioning systems are a problem of artificial intelligence where we must have a similarity between the word resulted with the content of the image. This system needs an image processing task starting with computer vision, which is the task of analyze and recognize the content of the image and a linguistic model that behaves like language processing in human brain, in this field the conversation of the understood image into a sequence of understood words is done(Marc et al ,2018).

Any image captioning system passes through multiple stages which are:

- Images features encoder
- Sequence decoding
- Words Creator
- Encoder-decoder structure
- Multi-modal structure
- Backbone of the object's detector
- Encoder-decoder structure with notice

Objective and expected research contribution

Image captioning system is that operation where we create a group of captions defines the image content and depends specially on deep learning. This technology is used for a wide range in recent time because it can help as example the blind people by telling them about all the objects around them which Nvidia company has the lead of it (Ren et al, 2019).

Many searches were done in this subject and may be the most important one that search done by Andrej Karpathy leader of artificial intelligent in Tesla company depending on Flicker database which gives a special result used by next researches.

The research objectives are summarized in the following points:

- This system is able to help the visually impaired people by connecting this system with Phrase pronunciation system that helps guide the way and avoid obstacles.
- Designing the system that gives the best accuracy by using a merge between conventional and recurrent networks.
- Suggesting the best model that requires less memory and processing power without losing the accuracy or having a long time to give the correct results.

Research methods and materials

We have two main types of neural networks used in ICS as shown in Figure (1-2). The first one called the injection structure, where the second named merge structure. We add a collection of images and words data together and train the RNN on the generated mixture. So, in each train epoch, RNN uses the mixture of two parts data to predicate the next word the network will validate the image information in training task(shin etal,208).

In merge structure we don't give the image data to the RNN, instead of that, the image data are encoded alone and so does for the words and then it is fed to forward feed neural network to build a multi model multi-layer structure.

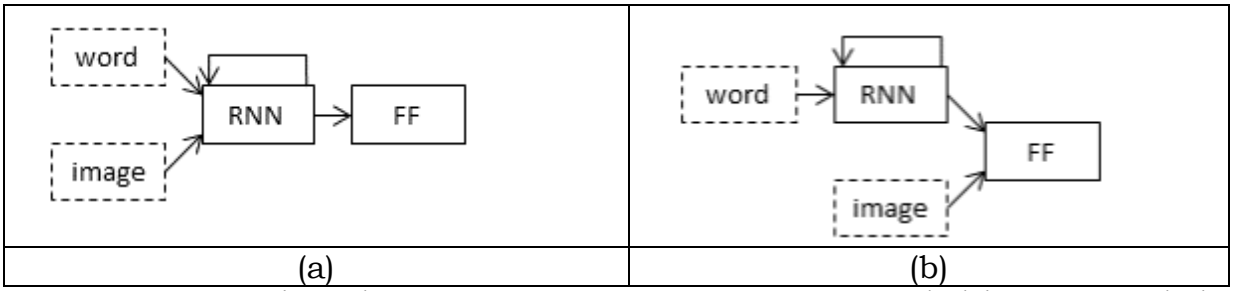


Figure 2. networks used in image captioning systems, (a) injection method (b) merging method

The injection structure gas four main models

Init-inject: here we will use the initial state vector which has a zero main value for the given dimensions. For this state, we can have an image features vector using CNN's which must be from the same size for the hidden state for the RNN and this vector is fed as an initial vector for the RNN(He et al, 2019).

Pre-inject: in this state, we feed the image as a vector so it will become as an initial word. And for the RNN, in each epoch, we can send the words stored in an encoded vector in each time step a series, so, in the first-time step we can send the image vector.

Par-Inject: in this method, and for all time steps, we can merge the two vectors, word vector and the image vector in an equalized dimension impeded space and passed then to be trained using RNN. In all these cases, the images features vectors are created in a structure similar to injection structures and ResNet complex structures, these structures share in affected image vector by RNN hidden state which is the main different between the merge and injection structures.

Depending on networks that were studied, pre-injected networks are much more effective than Par-injection ones, other studies proofed that merge structures are better than injection structures in some cases. Many other studies use Bidirectional RNN, LSTM for much better results. And we can use Pre-trained systems like Glove, word2vec see Figure 3.

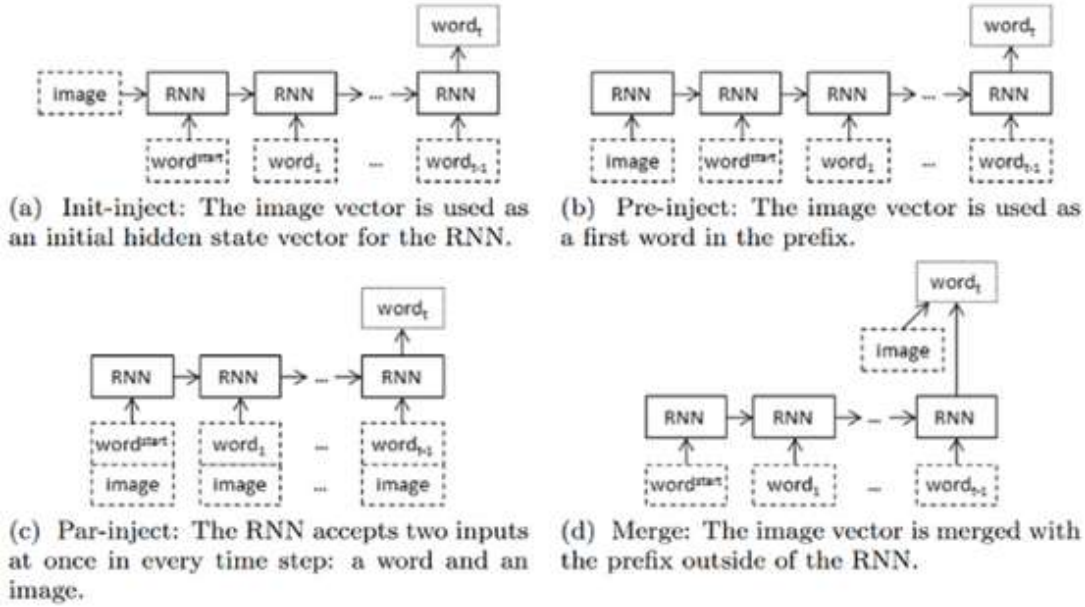


Figure 3. injection methods

Plans designed by Andrej Karpathy

Researcher gives many structure planes to build an image captioning system which can be (Karpathy et al, 2014):

- Plane1:

Let us assume that we want to caption the scene in Figure (4), so first we need to define all the objects inside the image, like the cat and the table then we will create the sentence that describing these objects. The researcher proof that each serial part of words in caption belongs to special part in the image, for the machine these places are unknown. For that reason, we need to create a mapping task to create the captioning model. This work is like what humans does by creating a series of sentences parts by investigating the main parts in the images to get all the objects inside it the crating the caption.

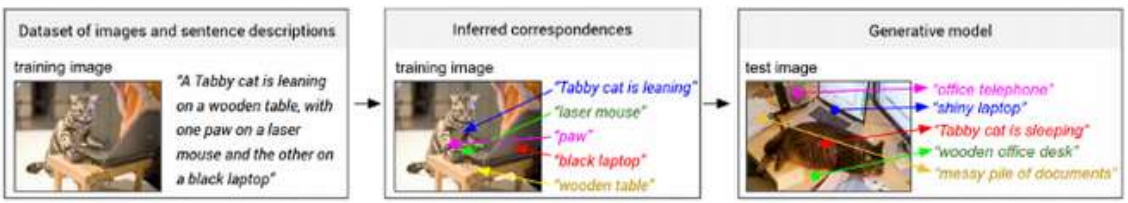


Figure 2. Overview of our approach. A dataset of images and their sentence descriptions is the input to our model (left). Our model first infers the correspondences (middle, Section 3.1) and then learns to generate novel descriptions (right, Section 3.2).

Figure 4. Andrej Karpathy captioning plane

The suggested model creates a multimodal impeded space using booth models to find the adjust states between paragraphs words and positions of it in the image. Here we can use RCNN (Regional conventional neural network) to find the position of the object inside the

image and then train the CNN network on the dataset used which containing 200 classes to recognize all the objects inside them (Wang et al ,2018).

For language modeling, this method suggests using BRNN which gives the best performance for the inter-relations between objects by using n-grams of sentences. Here the impeded word2vec and A300d were used to have the words vector. This way builds a link rate between the image and the sentence which is a result of isolated words and images objects areas rate. If the total rate is strong then the sentence is captioning the image, see Figure 5.

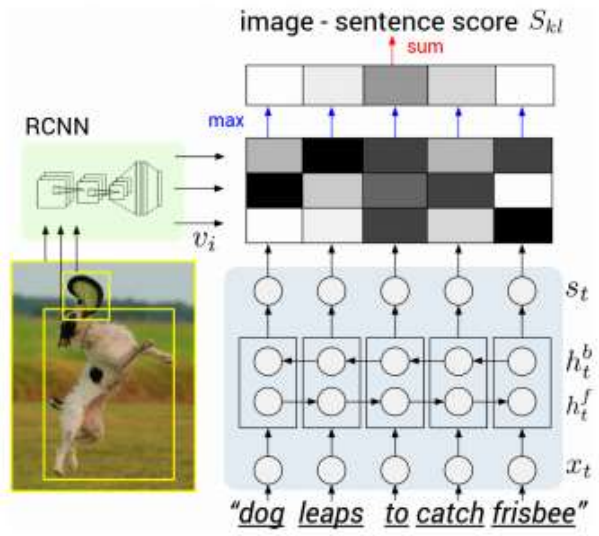


Figure 5. using RCNN in Andrej Karpathy captioning plane

RCNN with create a surround box, so we will look for the part i of the image and create the confidence by comparing with the caption of index t. for that, and for each pair of areas and words, a bullet product is done between the area of index i and the word of index t to compute the similarity rate.

$$S_{kl} = \sum_{t \in gl} \max v_i^T S_t \qquad (1)$$

This equation will define the final result of the sentence.

- Plane2:

This part works with a developed multi dimensions RNN model to create the caption.as shown in Figure 6

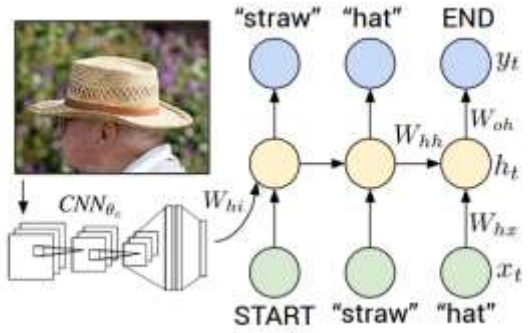


Figure 6. multi dimensions RNN model to create the caption

In this model, we get the $i'th$ pixel of image, and a sequence of input words vector $x1, x2, \ldots, xn$ and then computing the hidden states for this sequence $h1, h2, \ldots, hn$ to get an output sequence $y1, y2, \ldots, yn$. The image feature vector passed one time as an initial hidden state and computes the next hidden state of image vector i and previous states h1-1 and the recent input xt.

We have the recent output yt by using softmax layer which will have the rule of activation function of the hidden state:

$$
\begin{aligned}
b_v &= W_{hi}[CNN_{\theta_c}(I)] \\
h_t &= f(W_{hx}x_t + W_{hh}h_{t-1} + b_h + \mathbb{1}(t=1) \odot b_v) \\
y_t &= softmax(W_{oh}h_t + b_o).
\end{aligned}
\tag{2}
$$

Google structure for image captioning:

This captioning structure was given in a search titled Show and tell: A Neural Image Caption Generate (Oriel et al., 2015) here they used LSTM model instead of RNN. See Figure7

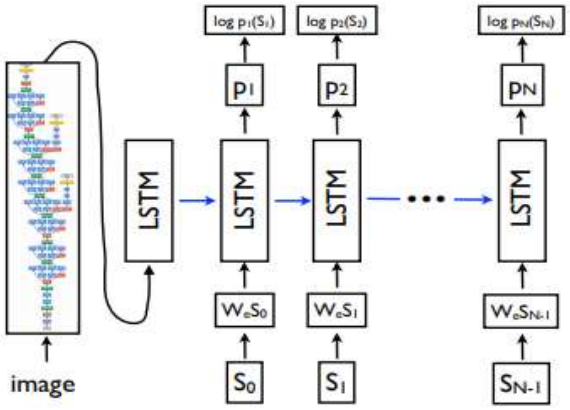


Figure 7. google structure to create the caption

In this state, the image features vector I fed to LSTM sequence at $t = -1$ and just once, then starting from $t = 0$ a sequence of words vector is entered where the last word entered for each step is the word with maximum probability which resulted from hidden state activation function in the studied state, this model is governed by equations:

$$\begin{aligned} x_{-1} &= \mathrm{CNN}(I) \\ x_t &= W_e S_t, \quad t \in \{0 \dots N-1\} \\ p_{t+1} &= \mathrm{LSTM}(x_t), \quad t \in \{0 \dots N-1\} \end{aligned} \tag{3}$$

We use the Beam search to get the best prediction of the caption which selects a number of elected statements K in each time period t. in each period $t + 1$ we take K statement and K word to have $K * K$ available sentence with a higher probability. Then, we elect the words with higher k to be based to the period$K + 1$.

Microsoft structure:

Microsoft publishes her results in a paper titled Rich Image Captioning in the Wild where they depend on encode-decode structure where images are captioned without taking in care the landmarks of the scene and celebrities…etc. where these landmarks and other objects processed in independent stages (Simao et al ,2019).

This model depends on deep Resnet in CNN's and detect if the image contains any celebrities or landmark. Here we depend on a feature input vector as an input for the neural network with a vector of the image too. This model consists mainly of a deep ResNet model to extract features from the image, a linguistic model to describe image contents, a recognition system to recognize landmarks and celebrities, a classifier to predicate the confidence rate as shown in Figure 8.

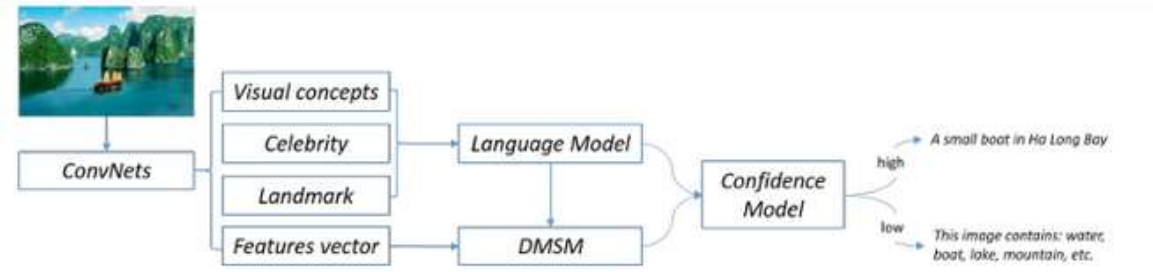


Figure 2: Illustration of our image caption pipeline.

Figure 8. Microsoft structure to create the caption

Structure of image captioning system

Images features encoder:

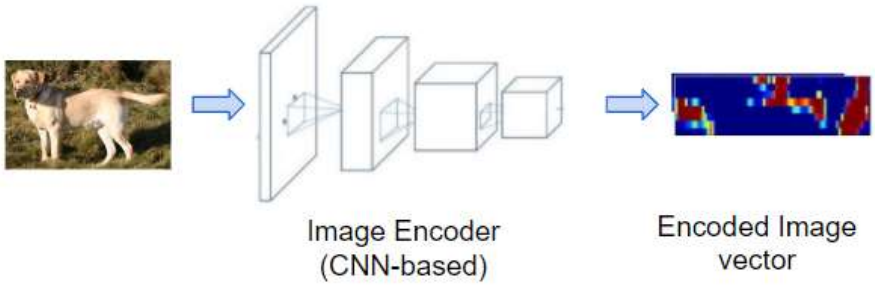


Figure 9. images features encoder in image captioning system

In this stage the source image is taken as input and encoded to have all the main features inside it, this stage depends on CNN networks which use the transfer learning where we can use a pre-trained model and remove the last classification part. Here we can depend on many models like VGG Net, Res Net or any other conventional network (Krizhevsky et al, 2012).

The backbone of this model has several CNN blocks used to extract many features from the image to create a feature map isolates the most important objects in the image. It starts by isolating the simple curves and circles in initial layers until catching objects like eyes and nose in top layers.

Sequence decoding

The encoded input in this stage is processed to create a sequence of tokens which describes the image. Here we can use RNN's that contains a group of LSTMs fed by an embedded layer. See figure10

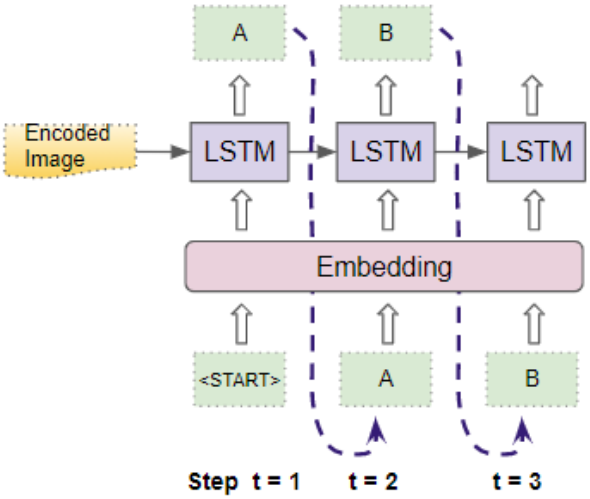


Figure 10. sequence decoding in image captioning system

In this stage we will got the image features vectors as an initial state and define an initial value in smallest input sequence which has the start token and decode the input image vector to create the sequence desired. The prediction here is created using a loop and creating just a single token in each stage then it re-entered as an input to the network in the next loop, after a number of loops an “END” token is created which means that the sequence has ended (Marc et al, 2017).

Words Creator

In this stage we will get a sequence of tokens and create a description which is a sentence in desired language describing the image. This stage consists of a linear layer with a SoftMax layer creates a probability value for each word in linguistic form of the desired language and for each position in the sentence, here we depend on greedy search to build the last sentence by selecting the words with higher probability in each position(Gao et al ,2018) as shown in Figure 11

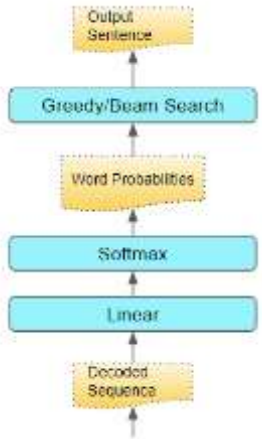


Figure 11. words creator in image captioning system

Where the output image will be the descriptive caption of the studied image.

Encoder-decoder structure:

As we say before, the most used structure in images captioning is the injection structure where it links directly between images encoding results to the decoder sequence and then to the images generator. See Figure 12

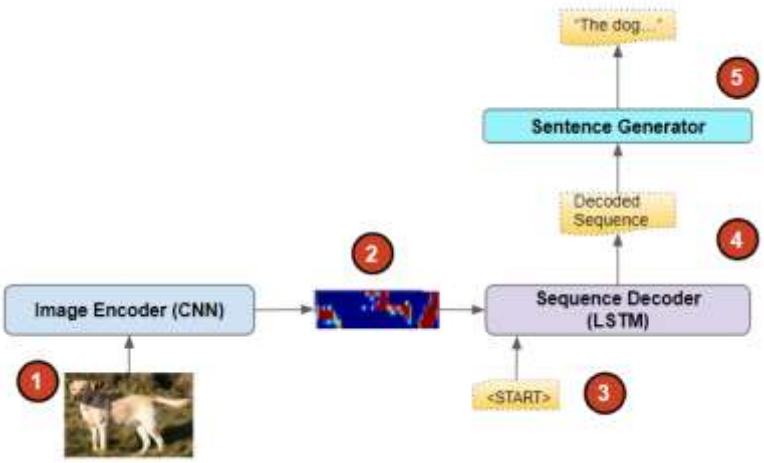


Figure 12. Encoder-Decoder structure

Multi-modal structure:

It is the second important model used in images captioning and named "merge model" which can give more effective results. In addition to connecting the image encoder with the words sequence decoder, the two models works independently of each other. That means, for this model (Zaremba et al 2012): see Figure 13

- CNN network process on images only.
- RNN network works with the captioning part only.

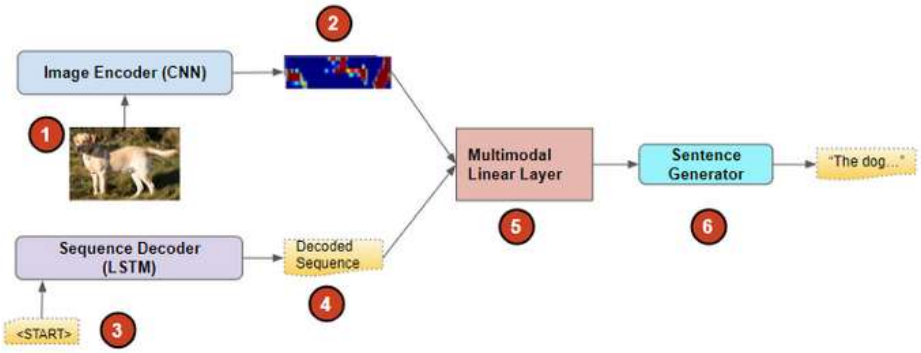


Figure 13. Multi-Modal structure

After that a merging stage between two networks outputs in the multi-modal layer (which might be linear or SoftMax) is done. This model allows us to use transfer learning to encode images and decode sentences. We can use the pre-trained linguistic model for the sentence decoder. There are many ways to create the merge by calculating connectivity, multiply, but the best way with good results is the addition.

Backbone of the object's detector:

This model is used to define a class in an image, it is possible that we have some objects of interest in an image. Instead of using the image classification backbone we can use the pre-trained backbone to detect objects and extract features from the image(Yao et al ,2017). see Figure 14

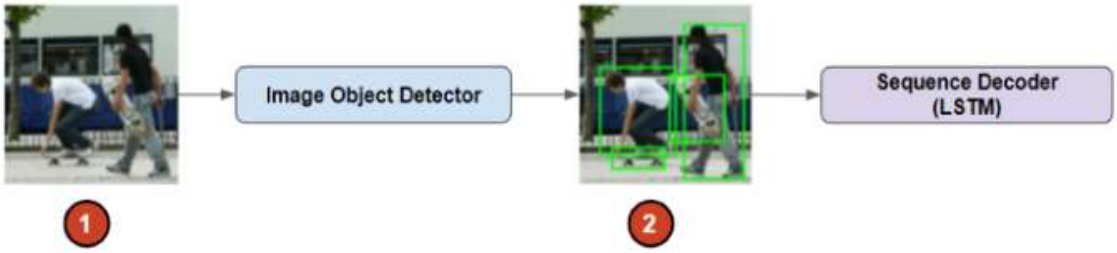


Figure 14. Backbone of the object's detector

The object detection model surrounds the objects with boxes and titling objects inside these boxes so we can enhance the image encoding can be used in next steps for sentence decoder to take all the objects in the image.

Encoder-decoder structure with notice:

The notice system allows us to increase the system performance; it connects and define the relations and the connectivity rate between input and output words which increases the efficiency of image captioning system. when the sequence decoder defines every sentence in every caption, we can detect the part of the image the must relative with the word we have create (Fu et al 2018).

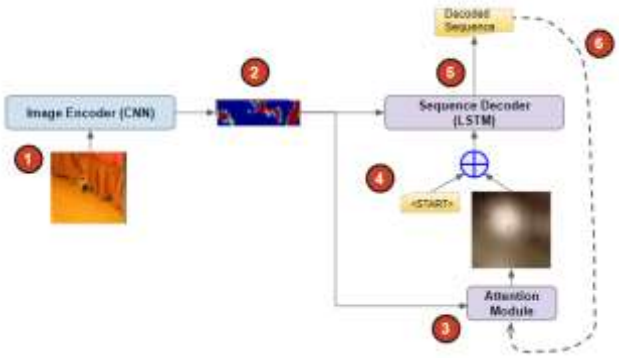


Figure 15. Encoder-decoder structure with notice

Creating of image captioning system

Flicker30K dataset

There are a lot of datasets which can be used effectively in ICS like Flicker30k, Flicker8K. the Flicker30k consists of 31000 images got from flicker website which allows us to build a simple system can be loaded and run on any CPU. This dataset is a group of images linked with five text captions which describes clearly the static objects inside it. These pictures were chosen from six Flicker groups without including any celebrities or landmarks. This group was chosen accurately to include a wide range of scenes and events.

This dataset Flicker8k includes a train set of 6000 images and evaluation set and test set of 1000 images. To evaluate this system, we use the BLEU. Here we have four standard ranges (Abhijit,):

- BLEU-1: 0.401 to 0.578.
- BLEU-2: 0.176 to 0.390.
- BLEU-3: 0.099 to 0.260.
- BLEU-4: 0.059 to 0.170.

Step1: prepare images data:

In this step we will depend on pre-trained model to predicate the images contents, there are many of ready models and the most famous is oxford visual geometry group (VGG). The model used was pre-used using keas and it need to load. To assure of the effectiveness of the model and increasing its speed we can pre-calculate all the features of the images using this pre-trained model and save the results in a file. These features can feed then to the model to predicate an image in the dataset to consume less amount of memory.

When we use the VGG model we had removed the last layer of the CNN model which is the classification layer since we need just the description of the image contents which are the features we have got.

Python Keera's gives us a tool for image resizing to the suitable CNN input of the size 224x224x3 and convert it to a 4096-length vector. Then the features extracted are save in a pickle file.

Prepare text data:

Every dataset has an independent description for each image, the text resulted may need cleaning since each image has a single description that can be used on the image name and its description file. In the next step, we will move over a list of descriptions for all the images and create a dictionary for images descriptions index where each index indicates for a group of one or more of text descriptions. In the next step, we need to clean the description text

where the tokenized task was done to make the processing task simpler to work with. The text cleaning task consists of (Abhijit,):

- Convert all the characters from small to uppercase.
- Remove all punctuation marks.
- Remove all the words less than one character or less than a given number of characters.
- Remove all the words with numbers.

After this clean we can define the size of the dictionary resulted, this decreasing sized dictionary is effective because the smaller ones result smaller models. After this step we can save the images dictionary with descriptions to a new "txt" file where it consists of an image index with description in each row.

After that step we have got an 8092-image description and the cleaned dictionary contain 8763 word, these data were saved in an txt file.

Developing the deep learning model:

This step contains four important steps: data load, definition of the model, fitting the model, end of the task.

Data load:

First it is important to load the pre-prepared images and the text data which can used to fit the model, this data trained on all images and there captions in the training set, in this stage we will manage the model performance on the dataset and use this result to select the saved model.

Train and development sets where defined previously in two files Flickr_8k.trainImages.txt and Flickr_8k.devImages.txt where they contain lists of images files names. And from these names, we can extract the images index and use it to filter the images with their descriptions. Then we will load the images with descriptions of pre-trained set for updated trained data.

Step by step, the model will start developing the image captioning for a single image word by word in each time period and the pre-created sequence of words will fed as an input. So, here we will need the first word to start generating and the last word to verify the end of captioning.

Usually we define the first and the last tokens which can be loaded for captions before text encoding so we can be sure that all the tokens were added to have an accurate result.

After that, we can load image features for a special dataset. Initially we will load all data and returning a subset of interest for a given group of images captions. This text captioning

needs encoding into numbers before it is fed to the model as an input or comparing the prediction states of it.

The first step in encoding task is building a map to attribute every word to an integer which can be done using tokenize class in keas which can learn this attribution task from the captioning proposed data. In addition, we will convert the description dictionary to a list of strings and fit it by the tokenizer so we can encode the text. Every caption will be divided into words and the model must get a word with the image to give the second word. These two words will be fed again to the model as input with the image to give the next word and so on until the model trained.

For example, if we have the input sequence “little girl running in field” which will be divided into six input-output pairs to train the model.

```
X1,     X2 (text sequence),                    y (word)
photo   startseq,                              little
photo   startseq, little,                      girl
photo   startseq, little, girl,                running
photo   startseq, little, girl, running,       in
photo   startseq, little, girl, running, in,   field
photo   startseq, little, girl, running, in, field, endseq
```

Here we must have two arrays, one for the images features and the second for the encoded text, and we will have a single output in the sequence got in second sequence. The input text is encoded as integer fed to the embedded words layer and the images features will fed directly to another part of the model. After that the predictive model will give an output as a probability distribution with all the words in the dictionary. That means, this probability distribution will have 0 value in all positions the word is wrong and 1 if the position is right, and maybe we will need to count the maximum number of words in the longest description.

Prepare the model:

Our model shown in Figure (16):

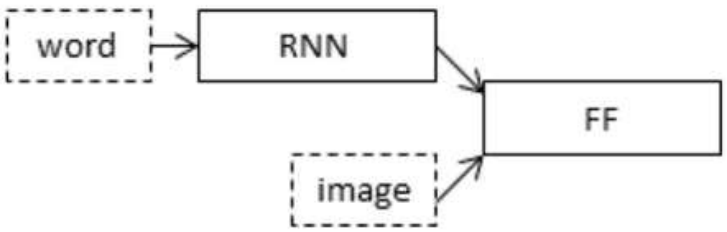


Figure 16. injection model used in the search

This model has three main parts:

- Photo feature extractor: This has 16 layers for pre-trained VGG model on the Image Net with removing of output layer and using the predicated features as input.
- Sequence processor: it is the layer of embedded words to input text process followed with Long-Short term memory Recurrent Net.
- Decoder: the output of each feature extractor and sequence processor is a constant length vector where they are passed into a dense layer to create the last result as predicated word.

The images features extractor model needs a vector of images features with a length of 4096 member processed in dense layer to get 256 captioning objects for the image. Where the sequence processing model needs an input sequence of 34 words fed to embedded layer uses a mask to ignore the added pixels and then into LSTM with 256 memory unit. The two models use a dropout layer with 50% to prevent reaching the overfitting states and increasing the speed of the model.

The decoder will merge the two models by adding operation will the added to a dense layer has a SoftMax function outs all the dictionaries outputs for the next word in the sequence. This Figure shows the neural network structure:

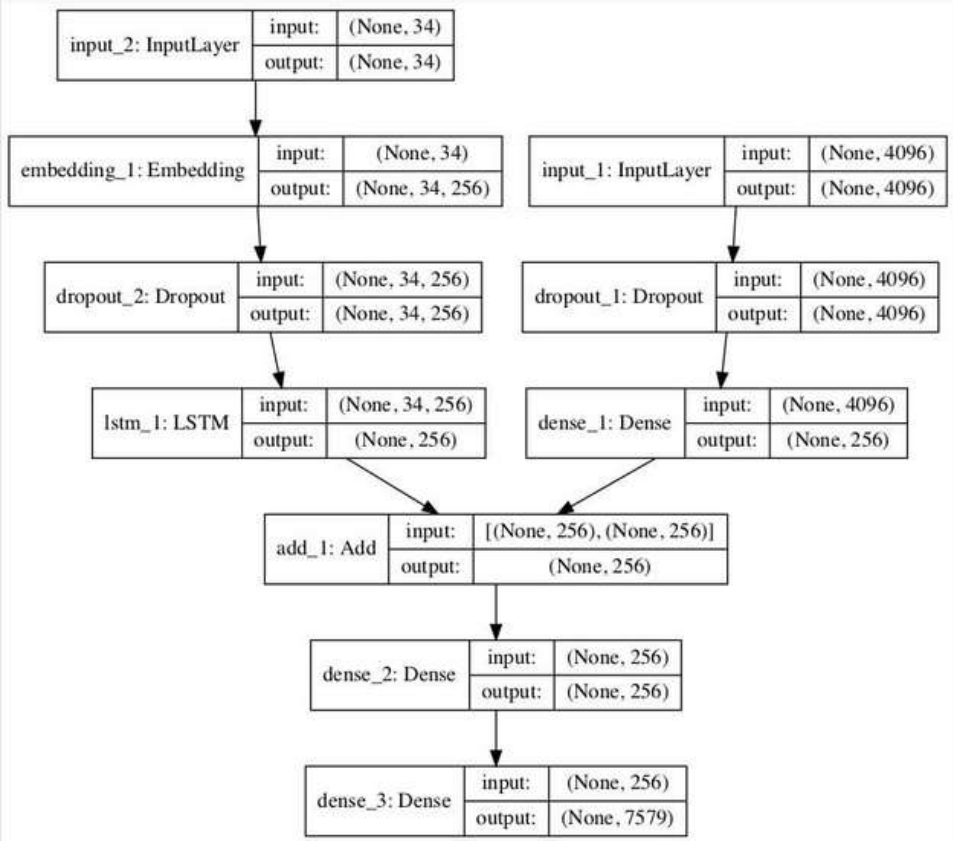


Figure 17. neural network model used in the search

Fitting the model:

We can train The model built very fast but it suffers of overfitting so we will manage the skills of the trained model on the developing set and when the model reaches the maximum training task in the end of the epoch, the model will saved to a file and then we will apply the resulted model on the training set.

Keera's library can do that by using Model Checkpoint which trained to reach the minimum error on the test set and then saving the files contain the result of training and the evaluation error. Every stage will have 20 epochs and each epoch will need at least 30 minutes. The resulted file we be a .h5 file.

Model evaluation:

This model will be evaluated by generating captions for all the images in the test set and evaluate the output using a cost function.

Greedy search and beam search:

To select the right word, we need to perform a search task, these search algorithms are probabilistic which returns the probability of the maximum word predicated.

- Greedy search:

This algorithm will return the word with the maximum probability in the position in the sentence, it is fast and easy to understand and always it gives a right result, Figure (18) shows how this algorithm works.

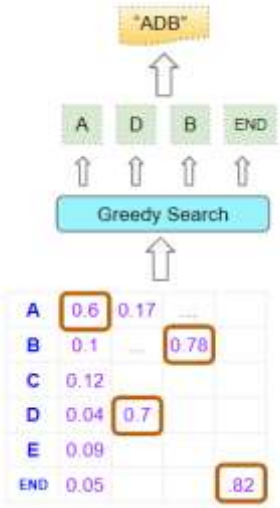


Figure 18. greedy search model

- **Beam search:**

It is a developed greedy search with two mains different:

- In greedy search we take the maximum word probability in the position required where in beam search we take the best N word.
- In greedy search we look to each position of the word alone and when we choose the maximum important word we do not care about the previous and the next word where in beam search we take the N best sequence of the sentence and merge all the previous words with the new word. So, this search more global to give the best sequence see Figure 19.

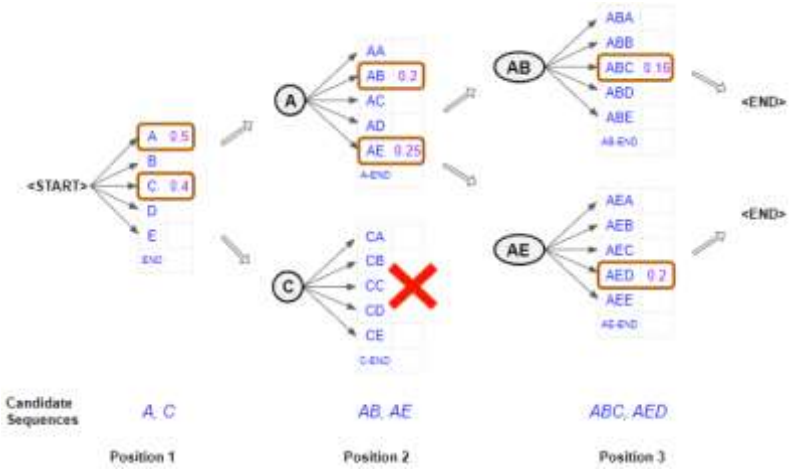


Figure 19. Beam search model

Results and discussion

1. After building this system we find that the injection method is better than merging method to give the best captioning of the image.
2. Beam search was far better than greedy search in resulting more connected words that can describe the images more Appropriately.
3. We can find more active results by using more beams in beam search, in our work we use beam3 and beam5, using more beams means that the system requires more processing power and more time to find the accurate result.

Conclusions and Recommendations

1. As a result of our study, it is recommended to build a captioning system for visually impaired people and blind people, after merging this system with a speaking system.
2. We recommend using a portable system like raspberry Pi as example which can connect with a camera on the glass of the blind person to give him a description of all the situation around him, so we can give him the freedom of movement.
3. We recommend enhancing this system by training more images in a dataset that contain all the objects the visually impaired people can face.

References

1. Karpathy, A., Li,F.,(2014). Deep visual-semantic alignments for generating image descriptions. Arriva: 1412.2306..
2. Marc, T,A (2018). where to put the Image in an Image Caption, arXiv:1703.09137v2 [cs.NE] 14
3. Abhijit, R, .A Guide to Image Captioning , https://towardsdatascience.com/a-guide-to-image-captioning-e9fd5517f350, available[online].
4. Or oil., Alexander, T., Samy, B., Dmitri, E.,(2015). Show and Tell: A Neural Image Caption Generator, arXiv:1411.4555v2 [cs.CV]
5. Kenneth, T,. Xuedong, H., Lei, Z., Jain ,S,.(2016) Rich Image Captioning in the Wild, https://www.microsoft.com/en-us/research/wp content/uploads/2016/06/ImageCaptionInWild-1.pdf, available[online]
6. Marc, T,A,. Albert, G., (2017)What is the Role of Recurrent Neural Networks (RNNs) in an Image Caption Generator?, arXiv:1708.02043v2 [cs.CL]
7. S imago, H., Armin, K., Kofi, B., Joao, S.,(2019). Image Captioning: Transforming Objects into Words, https://papers.nips.cc/paper/2019/file/680390c55bbd9ce416d1d69a9ab4760d-Paper.pdf
8. Krizhevsky, Al., Sutskever, I., Hinton, G.,(2012) Image Net classification with deep convolutional neural networks. In NIPS.
9. Shi, H., Li, P., Wang, B., & Wang, Z. (2018, August). Image captioning based on deep reinforcement learning. In Proceedings of the 10th International Conference on Internet Multimedia Computing and Service (pp. 1-5).
10. Fu, K., Li, J., Jin, J., & Zhang, C. (2018). Image-text surgery: Efficient concept learning in image captioning by generating pseudo pairs. IEEE transactions on neural networks and learning systems, 29(12), 5910-5921.
11. Yao, T., Pan, Y., Li, Y., Qi, Z., & Mei, T. (2017). Boosting image captioning with attributes. In Proceedings of the IEEE International Conference on Computer Vision (pp. 4894-4902).
12. G ao, L., Wang, B., & Wang, W. (2018, February). Image captioning with scene-graph based semantic concepts. In Proceedings of the 2018 10th International Conference on Machine Learning and Computing (pp. 225-229).
13. Fang, F., Wang, H., & Tang, P. (2018, October). Image captioning with word level attention. In 2018 25th IEEE International Conference on Image Processing (ICIP) (pp. 1278-1282). IEEE.
14. He, C., & Hu, H. (2019). Image captioning with visual-semantic double attention. ACM Transactions on Multimedia Computing, Communications, and Applications (TOMM), 15(1), 1- 16.

15. Wang, A., Hu, H., & Yang, L. (2018). Image captioning with Affective guiding and selective attention. ACM Transactions on Multimedia Computing, Communications, and Applications (TOMM), 14(3), 1-15.
16. R en, Z., Wang, X., Zhang, N., Lv, X., & Li, L. J. (2017). Deep reinforcement learning-based image captioning with embedding reward. In Proceedings of the IEEE conference on computer vision and pattern recognition (pp. 290-298).
17. H Ossian, M. Z., Shoal, F., Shiratuddin, M. F., & Lager, H. (2019). A comprehensive survey of deep learning for image captioning. ACM Computing Surveys (Cs UR), 51(6), 1-36.

Cyanobacteria and Microalgae Microcystin-LR of the Reverse Osmosis House Filter Drinking Water in Babel Province, Iraq

Sabaa Hilal Hadi [1], Rana H. Raheema [2],

M.A. Al-Khafaji [3], Abdulazeez A. Hassooni [4]

© 2023 The Author(s). This open access article is distributed under a Creative CommonsAttribution (CC-BY) 4.0 license.

Author details

[1-3] Department of Pathology, College of Veterinary Medicine, AL- Qasim Green University, Iraq

[2] Department of Microbiology, College of Medicine, Wasit University, Iraq

[4] Graduate Studies Division, College of Veterinary Medicine, AL- Qasim Green University, Iraq

Citation information

Cite this article as:

Hadi, S.H., Raheema, R.H., Al-Khafaji, M.A., Hassooni, A.A., (July 2023), *Cyanobacteria and Microalgae Microcystin-LR of the Reverse Osmosis House Filter Drinking Water in Babel Province, Iraq*, Proceedings of the Minar Congress, Turkey, (9) pp 209-218, DOI: http://dx.doi.org/10.47832/MinarCong9-18

Abstract: The purpose of this work is to identify the light-darkness conditions of containers and the location (over or under the sink) of the house water filtration system, water cooler tank transparency that favor to growth of cyanobacteria and microalgae in the internals' parts. The culture results were Cyanobacterium cyclotella atomus, C. meneghiniana, microalgae chlorella vulgaris and scenedesmus arcuastus. These are identifying from group A and B of drinking water samples. A water HPLC system analyzer uses the Microcystin-LR standard was applied and present in moderate quantity in group A samples (0.84 mg/L), While low concentration in group B samples (0.46 mg/L), and absent in group C samples (control group). The aim of this study is creating a plan to serve the community by identifying ways of safe drinking water, this can be accomplished successfully.

Key Words: Cyanobacteria; Microalgae; Microcystin-LR; Drinking water.

http://dx.doi.org/10.47832/MinarCong9-18

1 sabahelal@vet.uoqasim.edu.iq orcid.org/0000-0003-2638-9408

2 rraheema@uowasit.edu.iq orcid.org/0000-0002-1360-1716

3 muna200@vet.uoqasim.edu.iq orcid.org/0000-0003-0022-0989

4 azizakram1985@gmail.com

Introduction

Human health is at risk when cyanobacteria produce scum. Freshwater algae can produce irritants or poisons that grow rather abundantly in eutrophic conditions. In nutrient-rich water, microscopic organisms called microalgae and cyanobacteria, also called blue-green algae (1). In addition, cyanobacteria are microscopically single-celled or filamentous bacteria that share several traits with algae, including a cell wall structure, colors, and the capacity for oxygenic photosynthesis (2). When given the right conditions to thrive, many cyanobacterial species produce poisons. The development of cyanobacteria and the appearance of blooms are aided by a great deal of sunlight, warm temperatures, and nutrient-rich water (3, 4).

A complex of more than 100 species, including some with a tiny (≤ 5 µm) diameter, make up Cyclotella (Kützing) Brébisson. The interspecific resemblance is apparent. The taxonomy of this genus is based on the examination of frustule morphology under scanning electron microscopy (SEM), primarily the smaller specimens (5).

Chlorella vulgaris is a member of the Chlorellaceae family it is a tiny, spherical microalga with a diameter of 5–10 µm. It is often used for human nutrition because of its high protein content and well-balanced amino acid composition. Numerous studies suggest that this species may exhibit mixotrophic activity (6).

Scenedesmus is one of the genera of freshwater algae that are most prevalent in the Chlorophyceae family. They are non-motile and colonial. However, identification is challenging due to the incredibly different morphologies found within species (7).

In addition to affecting the taste and smell of drinking water, the presence of cyanobacteria and microalgae has been connected to human sickness (8). Instances of animal health caused by algae are reported added the number of cyanobacterial incidents is much higher (9) the majority of them caused by cyanobacterial species that accumulate in very dense surface scums. Consequently, the "cyanotoxins" accumulate to levels have negative consequences on health. Dogs were scavenging these material killed by them (10). From tropical marine bathing locations, severe sickness linked to direct skin contact with such mats has been documented (11). There is no nformation available to customers to safeguard themselves if a commercial procedure fails or if they are not inside a commercial treatment plant.

Freshwater is a frequent habitat for the cyanobacterium Microcystis, one of many species that can produce toxins known as microcystins. There are over 60 known congeners of microcystin (12). One of the most prevalent structural changes is microcystin-LR. Studied have been conducted on cyanobacteria in lab animals. Microcystis is frequently discovered along with the toxins it is associated with in studies of algal blooms conducted all over the world.

Microcystis is a cyanobacterium that is most frequently mentioned in the numerous reports of cyanobacteria and their toxins poisoning humans and animals (13). The microcystins have been shown primarily despite the fact that different cyanobacteria's toxin production has been linked with classification as cytotoxins, hepatotoxins and neurotoxins. Studies on animals have shown that acute intravenous or intraperitoneal exposure to microcystin damages the liver severely, while kidneys and lungs were less damaged. (14). additionally, microcystins exhibit tumor-promoting properties by inhibiting protein phosphatases PP1 and PP2A. (15, 16).

This study established a connection between a variety of beneficial elements (light-dark site, transparent water cooler tanks, and sink-mounted water container filtration systems), and their impact on the growth of cyanobacteria and microalgae. One of the most widespread and widely dispersed cyanotoxins, Microcystin-LR, was selected for investigation the negative health effects connected with cyanotoxin ingestion.

MATERIAL AND METHODS

Ethical approval

The scientific committee of the department of veterinary and medicine microbiology approved the research protocol for this study.

Experimental Design

The study included three cases of drinking water samples (DWS) from reverse osmosis filter house type system in Babel, Iraq.

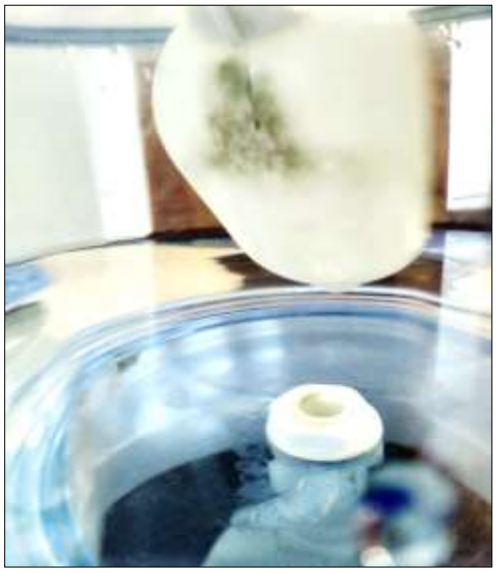


Figure 1. *Cyanobacteria* when growing on the internal parts of the transparence water cooler tank (group A and B)



Figure 2. *Cyanobacteria* when collected from the internal parts of the transparence water cooler tank

(A: DWS from the transparency container and light place (over the sink) water filtration house system, transparency water cooler tank,; (B: DWS from the dark container and dark place (under the sink) water filtration house system, transparency water cooler tank (Picture 1); (C: DWS from the dark container and dark place (under the sink) water filtration house system, dark water cooler tank, The algal bacterial suspension was collected from the internal parts of the water cooler tank in the summer of 2018-2019 (Picture 2) and sent to the Ministry of Science and Technology's lab for the Iraqi Department of Environment and Water. Light conditions may be effective in the growth of cyanobacteria and microalgae in filtered water. For these preliminary tests, the toxin of choice was microcystin-LR. This particular toxin was picked up because of its potential influence on human health has been widely studied in laboratory animals. The World Health Organization recently announced an additional preliminary exposure limit for total microcystin-LR in drinking water of 1 g/L. (17).

Filter cartridges used

The reverse osmosis filter housing used in three cases (Table 1) was marketed.

Table 1. Information on filter cartridges, including types and micron ratings, was taken from the buyer's guide provided by the manufacturer

Filter type	Micron rating
Carbon block Chlorine, Taste and Odor (CTO) 'under sink' cartridge	5 um
Granular Activated Carbon (GAC) 'under sink' cartridge	1 µm
Melt blown pure polypropylene (PP) fiber filter cartridge	1 µm

Biuret assays for quantitation of total protein

The biuret assay is the earliest and cheapest colorimetric (spectrophotometric) method for calculating total protein (18).

Chemicals

Other reagents were HPLC or AR grade and the microcystin-LR standard was purchased from Sigma-Aldrich., Sigma-Aldrich's formic acid (UK) was acquired. Fisher Scientific was also used to get acetonitrile, methanol, and HPLC-grade water (BDH).

Equipment

Photodiode Array Detector Waters 2996 (configured for wavelengths of 230 nm) and Alliance 2695 Separation Module were components of a Waters HPLC system. It was carried out at 358C using a Symmetry C18, octadecyl silyl reverse phase cartridge (2.1mm, 150mm, and 5mm). The Waters Micromass ZQ with an ESI Probe was used for the mass spectroscopic study. The cone voltage was set to 50V, and the operating temperature was 2508C°.

Typical execution

1 mg/mL of the standard microcystin-LR was used as the concentration. Via injecting 25, 50, 75, and 100 ml per run, a standard calibration curve from a 1 mg/mL stock solution of microcystin-LR was produced. The MassLynx V3.5 software was used to control the instrument.

Results and Discussion

The results of the evaluation of three cases group DWS of filters house with light-dark condition as in (Table 2)

Table 2. Shows the evaluation of three cases group DWS of filters house with light-dark condition

Name filters house	Container filters system transparency and its Place	Water cooler Tank Transparency	Bacterial or algae growing
A	Transparence containers and light place (over the sink)	Transparence	++
B	Dark containers and Dark place (under the sink)	Transparence	+
C	Dark containers and Dark place (under the sink)	Dark	-

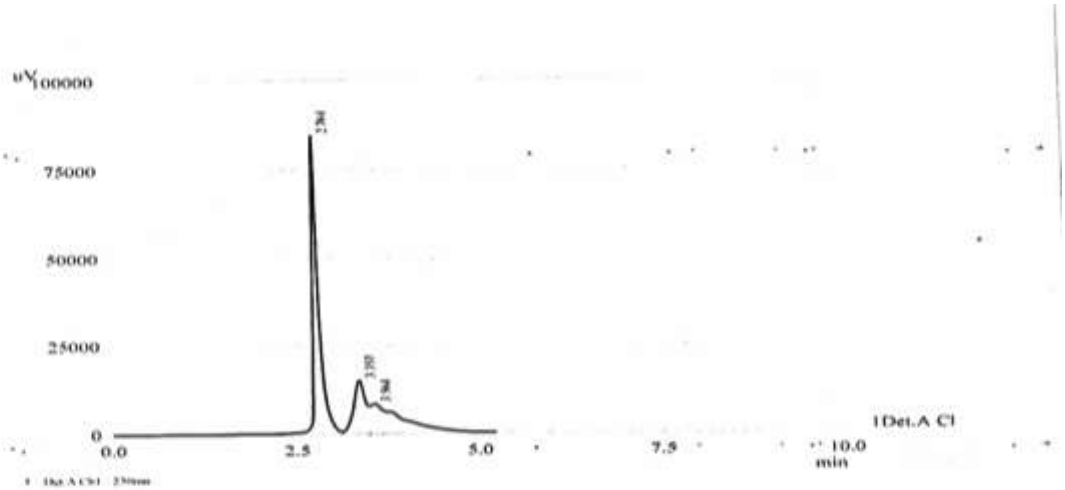
++ High number total protein, + Low number total protein - No growth bacteria

A single chromatographic peak with a concentration of microcystin L.R. of 0.84 mg/L was seen at 2.764 minutes in the case of A group of sample extracts that were examined by HPLC/MS. Additionally, in the B group, the graphic peak was shown at 2.756 minutes, with a Microcystin L.R. concentration of 0.46 Mg/L, whereas group C served as the control group and did not contain Microcystin L.R.

995 m/z mass spectra were being watched. The peak's identity was verified by 2, which throughout the calibration curve's concentration range, adequate sensitivity was attained. Figures 1, 2, and 3 display an overlay of the chromatograms from an official series of injections of calibration with dosages varying from 25 to 100 ng.

In the third case sample, it was discovered that the dark container and its location place under the sink, dark water cooler tank with no transparency played a crucial part in preventing the growth of bacteria or algae, individually or in combination, as in the cases of first and second groups. Water temperature and PH are essential factors for cyanobacteria's growth and bloom formation (19, 20), pH play a vital role in toxin production.

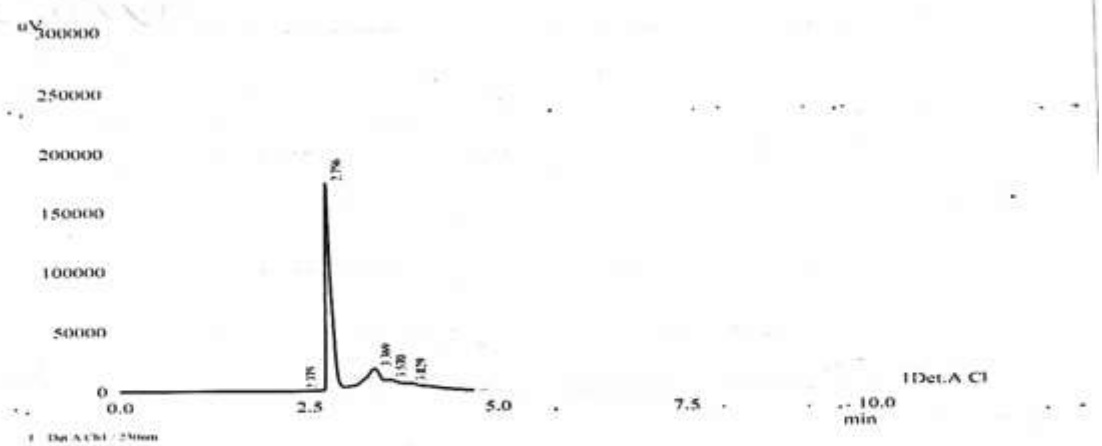
In A and B case samples, mixed colony bacteria were noted as a result of culturing cyanobacterium cyclotella atomus, C. meneghiniana, microalgae chlorella vulgaris and scenedesmus arcuastus as a source of Microcystin L.R. toxin (21) Examine how three factors, such as the inoculum:culture medium volume ratio (5:45, 10:40, 15:35, and 20:30 mL:mL), light:dark photoperiod (8:16, 12:12, and 16:8 h), and type of culture medium, like synthetic media (Guillard's F/2 and Walne's) and wastewaters, affect cell growth.



Detector A Ch1 230nm

Peak#	Ret. Time	Area	Height	Area %	Height %
1	2.764	475981	84308	52.804	78.466
2	3.357	171427	14909	19.018	13.876
3	3.564	253998	8228	28.178	7.658
Total		901406	107444	100.000	100.000

Figure 1. Group A chromatographic peak of Microcystin L.R.



Detector A Ch1 230nm

Peak#	Ret. Time	Area	Height	Area %	Height %
1	2.375	5024	237	0.327	0.113
2	2.756	860553	174254	56.055	82.810
3	3.369	333956	19086	21.753	9.070
4	3.570	137882	9787	8.981	4.651
5	3.829	197783	7063	12.883	3.357
Total		1535198	210428	100.000	100.000

Figure 2. Group B chromatographic peak of Microcystin L.R

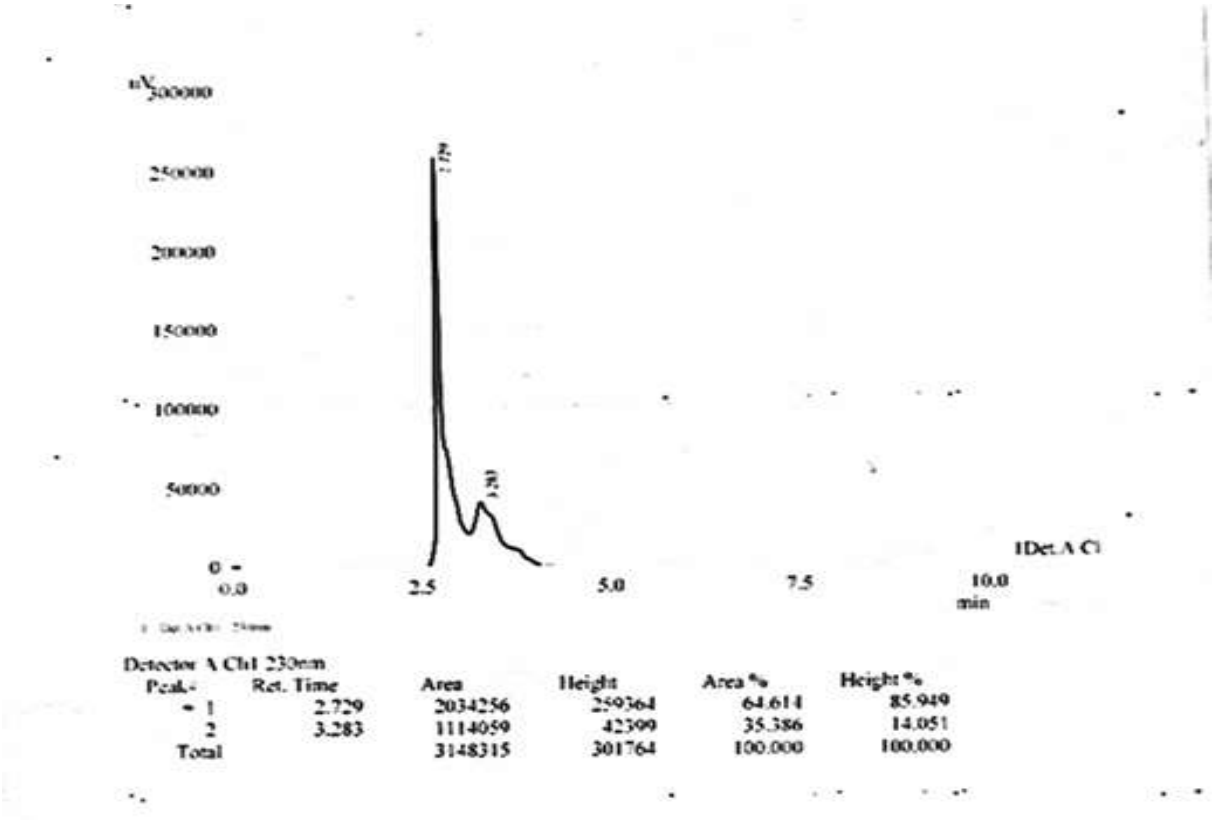


Figure 3. Group C control with no Microcystin L.R

The presence of all above factors caused no growth in the C case group. According to total protein measurements by a spectrophotometer, the organisms grew in groups A and B at moderate and low rates bout 17.87 g/L and 9.3 g/L respectively. Because it is simple to carry out, reagents are simple to prepare, and the assay is significantly less vulnerable to chemical interference with other copper-based assays, the biuret assay is still widely used today. For photosynthetic organisms to thrive and carry out their metabolic processes, light is a crucial factor (22, 23).

An area near a drinking water facility the use of water surface as a source, researchers looked into the chance of long-term low-level exposure to cyanotoxins and its correlation with the occurrence of primary liver cancer (24).

Microcystis is the predominant cyanobacteria, MCs are the cyanotoxins that most frequently measured (25) Determined maximum concentrations (14 g/L) of MCs by Tests for protein phosphatase inhibition were conducted over a three-year period in eight distinct locations within the Lake Erie Western Basin (26) In 2003, 2004, and 2005, a single time point, sampling stations were used to measure intracellular MCs across Lake Erie's Western Basin. Intracellular MCs reached their maximum levels in 2003, 2004, and 2005, at 0.13, 1.64, and 0.14 g/L, respectively.

Taste and odor problems can be solved with activated carbon. Single-cell cyanobacteria and potentially the resulting cyanotoxins will be eliminated or reduced through the use of nanofiltration and ultrafiltration but not removed. While cyanobacteria killed by chlorination.

Conclusions

The existence of microalgae and cyanobacteria in the home filters makes the water used for drinking detestable Cyanobacterium cyclotella atomus, C. meneghiniana, as well as the microalgae chlorella vulgaris and scenedesmus arcuastus, were the results of the cultivation. Compared to how well-lit or dark the containers where the home's water filtration system is situated. Using a water HPLC system analyzer, the Microcystin-LR standard was found in group A samples in a moderate amount 0.84 mg/L and group B samples in a low concentration 0.46 mg/L.

References

1. Chorus, I. (2012) Current Approaches to Cyanotoxin Risk Assessment, Risk Management and Regulations in Different Countries; Federal Environment Agency (Umweltbundesamt): Dessau-Roßlau, Germany, 2012.
2. Ravelonandro, P.H.; Ratianarivo, D.H.; Joannis-Cassan, C.; Isambert, A.; Raherimandimby, M. (2011) Improvement of the growth of Arthrospira (Spirulina) platensis from Toliara (Madagascar): Effect of agitation, salinity and CO2 addition. Food Bioprod. Process. 2011, 89, 209–216.
3. Orefice, I.; Musella, M.; Smerilli, A.; Sansone, C.; Chandrasekaran, R.; Corato, F.; Brunet, C. (2019), Role of nutrient concentrations and water movement on diatom's productivity in culture. Sci. Rep. 9, 1479.
4. Håkansson, H. (2002). A compilation and evaluation of species in the generaStephanodiscus, Cyclostephanos and Cyclotella with a new genus in thefamily Stephanodiscaceae. Diatom Research 17(1): 1-139.
5. Salati, S.; D'Imporzano, G.; Menin, B.; Veronesi, D.; Scaglia, B.; Abbruscato, P.; Mariani, P.; Adani, F.(2017) Mixotrophic cultivation of Chlorella for local protein production using agro-food by-products. Bioresour. Technol. 2017, 230, 82–89.
6. Elzanowski A, Ostell J, Leipe D, Soussov V. "The Genetic Codes". Taxonomy browser. National Center for Biotechnology Information (NCBI), U.S. National Library of Medicine. Retrieved 11 August 2016.
7. Griffiths, D. J. & Saker, M. L. (2003) The Palm Island Mystery Disease 20 Years on: A Review of Research on the Cyanotoxin Cylindrospermopsin. Environ. Toxicol. 18, 78–93.
8. Haider, S., Naithani, V., Viswanathan, P. N. & Kakkar, P. (2003) Cyanobacterial toxins: a growing environmental concern. Chemosphere 52, 1–21.
9. Ballot, A.; Fastner, J.; Wiedner, C. Paralytic shellfish poisoning toxin-producing cyanobacterium Aphanizomenon gracile in northeast Germany. Appl. Environ. Microbiol. 2010, 76, 1173–1180.
10. Edwards, C., Beattie, K.A., Scrimgeour, C.M. and Codd, G.A. 1992 Identification of anatoxin-a in benthic cyanobacteria (blue-green algae) and in associated dog poisonings at Loch Insh, Scotland. Toxicon, 30(10), 1165-1175.
11. Abdelzaher, A., Wright, M., Ortega, C., SoloGabriele, H.M., Miller, G., Elmir, S., Newman, X., Shih, P., Bonilla, J.A., Bonilla, T.D., Palmer, C.J., Scott, T., Lukasik, J., Harwood, V.J., McQuaig, S., Sinigalliano, C., Gidley, M., Plano, L.R.W., Zhu, X., Wang, J.D. and Fleming, L.E. (2010) Presence of pathogens and indicator microbes at a non-point source subtropical recreational marine beach. Applied and Environmental Microbiology 76, 724–732.
12. Cheung, M.Y.; Liang, S.; Lee, J. Toxin-producing cyanobacteria in freshwater: A review of the problems, impact on drinking water safety, and efforts for protecting public health. J. Microbiol. 2013, 51, 1–10.
13. Milutinovi´c, A.; Zorc-Pleskovi˘c, R.; Živin, M.; Vovk, A.; Serša, I.; Šuput, D. Magnetic resonance imaging for rapid screening for the nephrotoxic and hepatotoxic effects of microcystins. Mar. Drugs 2013, 11, 2785–2798.

14. Falconer, I. R., Smith, J. V., Jackson, A. R. B., Jones, A. & Runnegar, M. T. (1988) Oral toxicity of a bloom of the cyanobacterium Microcystis aeruginosa administered to mice over periods of up to one year. J. Toxicol. Environ. Health 24, 291–305.
15. Fujiki, H., Sueoka, E. & Suganuma, M. (1996) Carcinogenesis of Microcystins. In: Toxic Microcystis (eds. Watanabe, M. F., Harada, K. I., Carmichael, W. W. & Fujiki, H.), CRC Press, New York, pp. 202–232.
16. WHO (World Health Organization) (2011), Water sanitation health Guidelines, MANAGEMENT OF CYANOBACTERIA IN DRINKING-WATER SUPPLIES: Information for regulators and water suppliers WHO, Geneva.
17. Layne, E. (1957). Spectrophotometric and turbidimetric methods for measuring proteins. Methods Enzymnl. 3:447-454.
18. Davis, T.W., D.L. Berry, G.L. Boyer and C.J. Gobler, (2009). The effects of temperature and nutrients on the growth and dynamics of toxic and non-toxic strains of Microcystis during cyanobacteria blooms. Harmful Algae, 8: 715-725.
19. Pavlova, V., S. Furnadzhieva, J. Rose, R. Andreeva, Z.L. Bratanova and A. Nayak, (2010). Effect of temperature and light intensity on the growth, chlorophyll a concentration and microcystin production by Microcystis aeruginosa. Gen. Applied Plant Physiol., 36: 148-158.
20. Alejandra Sánchez-Bayo, Victoria Morales, Luis Fernando Bautista, Rosalía Rodríguez, Gemma Vicente and Luis Fernando Bautista, (2020) Cultivation of Microalgae and Cyanobacteria: Effect of Operating Conditions on Growth and Biomass Composition. Molecules, 25, 2834.
21. Gonçalves, A.L.; Pires, J.C.M.; Simões, M.(2016) The effects of light and temperature on microalgal growth and nutrient removal: An experimental and mathematical approach. RSC Adv. 2016, 6, 22896–22907.
22. Vanags,J.; Kunga, L.; Dubencovs, K.; Galvanauskas, V.; Gr¯ıgs, O.(2015) Influence of light intensity and temperature on cultivation of microalgae Desmodesmus communisinflasksandlaboratory-scalestirred ankphotobioreactor. Latv. J. Phys. Tech. Sci. 2015, 52, 59–70.
23. Fleming, L. L., Rivera, C. & Burns, J. (2000) Final Report: Blue Green Algae Exposure, Drinking Water, and Primary Liver Cancer. Final report to the Florida Harmful Algal Blooms Task Force. Florida Department of Environmental Protection, Tallahassee, Florida.
24. Rinta-Kanto, J.M.; Konopko, E.A.; DeBruyn, J.M.; Bourbonniere, R.A.; Boyer, G.L.; Wilhelm, S.W.(2009) Lake Erie Microcystis: Relationship between microcystin production, dynamics of genotypes and environmental parameters in a large lake. Harmful Algae 2009, 8, 665–673.
25. Millie, D.; Fahnenstiel, G.; Dyble Bressie, J.; Pigg, R.; Rediske, R.; Klarer, D.; Tester, P.; Litaker, R.W.(2009) Late-summer phytoplankton in western Lake Erie (Laurentian Great Lakes): Bloom distributions, toxicity, and environmental influences. Aquat. Ecol. 2009, 43, 915–934.

Quintic Spline Exponential Methods for Numerical Solutions of Two-Point Boundary Value Problems in Mid Knots

Ahmed R Khlefh [1]

© 2023 The Author(s). This open access article is distributed under a Creative CommonsAttribution (CC-BY) 4.0 license.

Abstract: In this paper, we develop a class of accurate methods based on the Quintic spline exponential method at mid-nodes for numerical solutions of two-point boundary value problems of the fourth order. Using this exponential spline method, some consistency relations are derived for calculating approximate solutions to problems. Existing finite differentials of the second and fourth orders and spline function-based methods developed in the mid-knots become special cases of this method. The convergence analysis of the proposed method is discussed. Three numerical examples illustrate the practical usefulness of our methodology.

Key Words: Quintic Spline Exponential Method, Two-Point Boundary Value Problem, Exact Solution.

Author details

[1] University of Sumer, Thi-Qar, Iraq

Citation information

Cite this article as:

Khlefh, A.R., (July 2023), *Quintic Spline Exponential Methods for Numerical Solutions of Two-Point Boundary Value Problems in Mid Knots*, Proceedings of the Minar Congress, Turkey, (9) pp 219-229, DOI: http://dx.doi.org/10.47832/MinarCong9-19

http://dx.doi.org/10.47832/MinarCong9-19

[1] arkdsh85@gmail.com orcid.org/0009-0002-2930-5142

Introduction

We consider the fourth-order two-point boundary value problems of the form

$$\psi^{(4)} + p(\eta)\psi = q(\eta) \qquad \eta \in [a,b] \ , \tag{1}$$

With boundary conditions

$$\psi(a) = \mathcal{B}_1,\ \psi(b) = \mathcal{B}_2\ , \psi^{(2)}(a) = \mathcal{B}_3\ ,\ \psi^{(2)}(b) = \mathcal{B}_4 \tag{2}$$

Where $\mathcal{B}_1, \mathcal{B}_2, \mathcal{B}_3, \mathcal{B}_4$ are finite real arbitrary constants and $p(\eta), q(\eta)$ are continuous on $[a,b]$. For arbitrary selections of $p(\eta)$ and $q(\eta)$, the analytical solution of (1) subject to (2) cannot be reached. Other approaches designed to obtain a rough solution to this problem utilizing spline functions and finite difference may be found in the numerical analysis literature.

Al-Said et al. [1,2] solved fourth order obstacle problems using cubic and quartic spline functions, respectively. Using a quintic nonpolynomial spline function, Ramadan et al. [3, 4] found an answer to this issue. In order to create numerical techniques for producing smooth approximations for the solution of equations (1) and (2), this work will build a novel spline approach based on a nonpolynomial spline function that contains a polynomial component and a trigonometric portion.

A quartic non-polynomial spline solution of a system of fourth order boundary value problems at mid knots was presented by Siraj-ul-Islam et al. [5]. We employ a non-polynomial spline with polynomial and exponential components in order to create numerical methods for achieving a smooth, approximative solution to a system of fourth-order boundary value issues. Such an exponential spline was investigated by Zahra [6, 7] for nonlinear fourth-order two-point boundary value problems. There are several approaches to solve boundary-value issues that may be found in the literature. [4,6,8,13].

In order to provide numerical techniques for producing smooth approximations for the solution of the systems (1) and (2), this work develops a novel spline approach based on quintic Spline exponential function that contains a polynomial portion and a trigonometric part. In Part 2, we explain how our technique was derived. In Section 3,, the procedure is laid out in matrix form. Section 4 establishes convergence analysis for the second, fourth, and sixth-order approaches. To demonstrate the applicability and correctness of Section 5, numerical results are provided. Section 6 concludes with the outcomes of the suggested approaches to show their accuracy and practical utility.

Derivation of the Method

This approach is developed by placing mesh points at off-step locations. By using this method, the solution's error is reduced at the locations where it meets additional continuity requirements. $n+1$ subintervals, s.t., are formed from the interval $[a,b]$.
Where,

$\eta_{i-\frac{1}{2}} = a + \left(i - \frac{1}{2}\right)h$ for i $= ,0,1,2 , \ldots . n$. and $h = \frac{b-a}{n}$

The spline exponential function $E_i(\eta)$ has the following form for each of its segments:

$E_i(\eta) = \widetilde{a_i} e^{\tau(\eta-\eta_i)} + \widetilde{b_i} e^{-\tau(\eta-\eta_i)} + \widetilde{c_i}(\eta-\eta_i)^4 + \widetilde{d_i}(\eta-\eta_i)^3 + \widetilde{e_i}(\eta-\eta_i)^2 + \widetilde{f_i}(\eta-\eta_i) + \widetilde{g_i},$ (3)

Where τ is a free parameter that will be applied to increase the method's accuracy and $\widetilde{a_i}$, $\widetilde{b_i}, \widetilde{c_i}, \widetilde{d_i}, \widetilde{e_i}, \widetilde{f_i}$ and $\widetilde{g_i}$ are real finite constants. $\widetilde{E_i}$ becomes a sextic polynomial spline if $\tau \to 0$. Let $\psi(\eta)$ be the exact solution of system (1) and ψ_i be an approximation to $\psi(x_i)$, obtained by the segment $E_i(\eta)$ of the mixed splines function passing through the points $(\eta_i, \psi_i)$and (ψ_{i+1}, ψ_{i+1}).To obtain the necessary conditions for the coefficients introduced in (2), we do not only require that $E_i(\eta)$satisfies (1)at η_i, η_{i+1} and that the boundary conditions are fulfilled, but also the continuity of the first, second, third, fourth and fifth derivatives at the common nodes (η_i, ψ_i). To determine the coefficients of equation (2) in terms of $\psi_i, \psi_{i+1}, \mathcal{T}_i, \mathcal{T}_{i+1}, \mathcal{F}_i$and $\mathcal{F}_{i+1}$.We define the second and fourth order spline derivatives of function values $\psi_{i+\frac{1}{2}}$, $\psi_{i+\frac{1}{2}}$ in order to get the expressions for the coefficients in Equation (3).

- $Ei\left(\tilde{\eta}_{i-\frac{1}{2}}\right) = \psi_{i-\frac{1}{2}}$
- $Ei\left(\tilde{\eta}_{i+\frac{1}{2}}\right) = \psi_{i+\frac{1}{2}}$,
- $Ei^{(2)}\left(\tilde{\eta}_{i-\frac{1}{2}}\right) = \mathcal{T}_{i-\frac{1}{2}}$,
- $Ei^{(2)}\left(\tilde{\eta}_{i+\frac{1}{2}}\right) = \mathcal{T}_{i+\frac{1}{2}}$,
- $Ei^{(4)}\left(\tilde{\eta}_{i+\frac{1}{2}}\right) = \mathcal{F}_{i+\frac{1}{2}}$,
- $Ei^{(4)}\left(\tilde{\eta}_{i-\frac{1}{2}}\right) = \mathcal{F}_{i-\frac{1}{2}}$,
- $Ei^{(4)}\left(\tilde{\eta}_{i+\frac{1}{2}}\right) = \mathcal{F}_{i+\frac{1}{2}}$.

The following expressions can be obtained through algebraic operations:

$$\widetilde{a_i} = \frac{h^4}{32\phi^4 \sinh 2\phi}\left(e^{\phi}\mathcal{F}_{i+\frac{1}{2}} - e^{-\phi}\mathcal{F}_{i-\frac{1}{2}}\right)$$

$$\widetilde{b_i} = \frac{h^4}{32\phi^4 \sinh 2\phi}\left(e^{\phi}\mathcal{F}_{i+\frac{1}{2}} - e^{-\phi}\mathcal{F}_{i-\frac{1}{2}}\right)$$

$$\widetilde{c_i} = \frac{1}{6h}\left(\mathcal{T}_{i+\frac{1}{2}} - \mathcal{T}_{i-\frac{1}{2}}\right) - \frac{h}{24\phi^2}\left(\mathcal{F}_{i+\frac{1}{2}} - \mathcal{F}_{i-\frac{1}{2}}\right)$$

$$\widetilde{d_i} = \frac{1}{4}\left(\mathcal{T}_{i+\frac{1}{2}} + \mathcal{T}_{i-\frac{1}{2}}\right) - \frac{h}{16\phi^2}\left(\mathcal{F}_{i+\frac{1}{2}} + \mathcal{F}_{i-\frac{1}{2}}\right)$$

$$\widetilde{e_i} = \frac{1}{h}\left(\psi_{i+\frac{1}{2}} - \psi_{i-\frac{1}{2}}\right) - \frac{h}{24}\left(\mathcal{T}_{i+\frac{1}{2}} + \mathcal{T}_{i-\frac{1}{2}}\right) + \frac{h^3}{96\phi^4}\left(\mathcal{F}_{i+\frac{1}{2}} + \mathcal{F}_{i-\frac{1}{2}}\right)(\phi^2 - 6)$$

$$\widetilde{f_i} = \frac{1}{2}\left(\psi_{i+\frac{1}{2}} + \psi_{i-\frac{1}{2}}\right) - \frac{h^2}{16}\left(\mathcal{T}_{i+\frac{1}{2}} + \mathcal{T}_{i-\frac{1}{2}}\right) + \frac{h^3}{64\phi^4}\left(\mathcal{F}_{i+\frac{1}{2}} + \mathcal{F}_{i-\frac{1}{2}}\right)(\phi^2 - 2)$$

Where $\phi = h\tau$ for $i = 0,1,2,\dots n$, When the first derivative is continuous, it implies

$$\left(\mathcal{T}_{i+\frac{1}{2}} + 22\mathcal{T}_{i-\frac{1}{2}} + \mathcal{T}_{i-\frac{3}{2}}\right) = \frac{24}{h^2}\left(\psi_{i+\frac{1}{2}} - 2\psi_{i-\frac{1}{2}} + \psi_{i-\frac{3}{2}}\right) - \frac{3h^2}{2\phi^2}\left[\left(\frac{1}{\phi^2} - \frac{1}{6} - \frac{1}{\phi\sinh\phi}\right)\right.$$

$$\left.\left(\mathcal{F}_{i+\frac{1}{2}} + \mathcal{F}_{i-\frac{3}{2}}\right) - 2\left(\frac{\cosh 2\phi}{\phi\sin\phi} - \frac{1}{\phi^2} - \frac{11}{6}\right)\mathcal{F}_{i-\frac{1}{2}}\right], \quad i = 2,3,\dots n-1 \qquad (4)$$

Additionally, the third derivative's continuity suggests:

$$\left(\mathcal{T}_{i+\frac{1}{2}} - 2\mathcal{T}_{i-\frac{1}{2}} + \mathcal{T}_{i-\frac{3}{2}}\right) = \frac{h^2}{4\phi}\left[\left(\frac{1}{\phi^2} - \frac{1}{\sinh\phi}\right)\left(\mathcal{F}_{i+\frac{1}{2}} + \mathcal{F}_{i-\frac{3}{2}}\right) + 2\left(\frac{\cosh 2\phi}{\phi\sin\phi} - \frac{1}{\phi^2}\right)\mathcal{F}_{i-\frac{1}{2}}\right],$$

$i = 2,\dots n-1$

(5)

After subtracting equation (5) from equation (4) and dividing the result by 24, we arrive at:

$$\mathcal{T}_{i-\frac{1}{2}} = \frac{1}{h^2}\left(\psi_{i+\frac{1}{2}} - 2\psi_{i-\frac{1}{2}} + \psi_{i-\frac{3}{2}}\right) - \frac{h^2}{24}\left[\left(\frac{3}{2\phi^4} - \frac{3}{2\phi^3\sinh\phi} - \frac{1}{4\phi\sinh\phi}\right)\left(\mathcal{F}_{i+\frac{1}{2}} + \mathcal{F}_{i-\frac{3}{2}}\right) + \right.$$

$$\left.\left(\frac{\cosh 2\phi}{\phi\sin\phi}\left(\frac{3}{\phi^2} + \frac{1}{2}\right) - \frac{1}{\phi^2}\left(\frac{3}{\phi^2} + 6\right)\right)\mathcal{F}_{i-\frac{1}{2}}\right], \qquad i = 2,3,\dots n-1 \ . \qquad (6)$$

When we remove the ψ's between (5) and (6), we obtain the connection shown below.

$$\left(\psi_{i-\frac{5}{2}} - 4\psi_{i-\frac{3}{2}} + 6\psi_{i-\frac{1}{2}} - 4\psi_{i+\frac{1}{2}} + \psi_{i+\frac{3}{2}}\right) = h^4\left(\delta\left(\mathcal{F}_{i-\frac{5}{2}} + \mathcal{F}_{i+\frac{3}{2}}\right) + \lambda\left(\mathcal{F}_{i-\frac{3}{2}} + \mathcal{F}_{i+\frac{1}{2}}\right) + \omega\mathcal{F}_{i-\frac{1}{2}}\right),$$

$i = 3,4,\dots n-2$.

(7)

Where,

$$\delta = 0.0104\left(\frac{6\sinh\phi - 6\phi - \phi^3}{\phi^4\sinh\phi}\right),$$

$$\lambda = 0.041\left(\frac{6\cosh^2\phi + \phi^3\cosh^2\phi - 6\sinh\phi - 6\phi^3}{\phi^4\sinh\phi}\right)$$

$$\omega = 0.02\left(\frac{18\sinh\phi - 6\phi + 12\phi\cosh 2\phi - \phi^3 + 22\phi^3\cosh 2\phi}{\phi^4\sinh\phi}\right)$$

1- Numerical method

Now, by substituting (x) in the spline relation (7), we obtain $n+1$ linear algebraic equations with n unknowns, $\psi_{i-\frac{1}{2}}, i = 1,2,\dots,n$ as.

$$\left(1 - \delta h^4 p_{i-\frac{5}{2}}\right)\psi_{i-\frac{5}{2}} + \left(-4 - \lambda h^4 p_{i-\frac{3}{2}}\right)\psi_{i-\frac{3}{2}} + \left(6 - \omega h^4 p_{i-\frac{1}{2}}\right)\psi_{i-\frac{1}{2}} + \left(-4 - \lambda h^4 p_{i+\frac{3}{2}}\right)\psi_{i+\frac{1}{2}}$$

$$+\left(1 - \delta h^4 p_{i+\frac{3}{2}}\right)\psi_{i+\frac{3}{2}} = \delta\left(q_{i-\frac{5}{2}} + q_{i+\frac{3}{2}}\right) + \lambda\left(q_{i-\frac{3}{2}} + q_{i+\frac{1}{2}}\right) + \omega\left(q_{i-\frac{1}{2}}\right), \ i = 3,4,\dots n-2 \qquad (8)$$

Four more equations are required in order to calculate $\psi_{i-\frac{1}{2}}, i = 1,2,\dots,n$ .directly for the system (8), two of which are located at each end of the range of integration. The Taylor series

and the technique of indeterminate coefficients are used to generate these boundary equations. These are the boundary equations that correspond to the boundary conditions.

$$-\frac{5}{3}\psi_{\frac{1}{2}}+\frac{5}{6}\psi_{\frac{3}{2}}-\frac{1}{6}\psi_{\frac{5}{2}}-h^2\left(\Delta_0\psi_0^{(4)}+\Delta_1\psi_{\frac{1}{2}}^{(4)}+\Delta_2\psi_{\frac{3}{2}}^{(4)}+\Delta_3\psi_{\frac{5}{2}}^{(4)}+\Delta_4\psi_{\frac{7}{2}}^{(4)}+\Delta_5\psi_{\frac{9}{2}}^{(4)}\right)=$$

$$-\psi_0+h^2\psi_0^{(2)}, \qquad (9)$$

$$-\frac{150}{32}\psi_{\frac{1}{2}}+\frac{139}{2}\psi_{\frac{3}{2}}-\frac{109}{16}\psi_{\frac{5}{2}}+\frac{29}{16}\psi_{\frac{7}{2}}-h^2\left(\bar{\Delta}_1\psi_{\frac{1}{2}}^{(4)}+\bar{\Delta}_2\psi_{\frac{3}{2}}^{(4)}+\bar{\Delta}_3\psi_{\frac{5}{2}}^{(4)}+\bar{\Delta}_4\psi_{\frac{7}{2}}^{(4)}-h^2\right.$$

$$\left.+\bar{\Delta}_5\psi_{\frac{9}{2}}^{(4)}+\bar{\Delta}_6\psi_{\frac{11}{2}}^{(4)}\right)=-\psi_0-h^2\psi_0^{(2)},$$

(10)

$$-\frac{150}{32}\psi_{n-\frac{1}{2}}+\frac{139}{2}\psi_{n-\frac{3}{2}}-\frac{109}{16}\psi_{n-\frac{5}{2}}+\frac{29}{16}\psi_{n-\frac{7}{2}}-h^2\left(\bar{\Delta}_1\psi_{n-\frac{1}{2}}^{(4)}+\bar{\Delta}_2\psi_{n-\frac{3}{2}}^{(4)}+\bar{\Delta}_3\psi_{n-\frac{5}{2}}^{(4)}+\right.$$

$$\left.,\quad \bar{\Delta}_4\psi_{n-\frac{7}{2}}^{(4)}+\bar{\Delta}_5\psi_{n-\frac{9}{2}}^{(4)}+\bar{\Delta}_6\psi_{n-\frac{11}{2}}^{(4)}\right)=-\psi_n-h^2\psi_n^{(2)} \qquad (11)$$

$$-\frac{5}{3}\psi_{n-\frac{1}{2}}+\frac{5}{6}\psi_{n-\frac{3}{2}}-\frac{1}{6}\psi_{n-\frac{5}{2}}-h^2\left(\Delta_0\psi_n^{(4)}+\Delta_1\psi_{n-\frac{1}{2}}^{(4)}+\Delta_2\psi_{n-\frac{3}{2}}^{(4)}+\Delta_3\psi_{n-\frac{5}{2}}^{(4)}\right.$$

$$\left.+\Delta_4\psi_{n-\frac{7}{2}}^{(4)}+\Delta_5\psi_{n-\frac{9}{2}}^{(4)}\right)=-\psi_n+\frac{24}{5}h^2\psi_n^{(2)}, \qquad (12)$$

where the local truncation errors t_1, t_2, t_{n-1} and t_n are connected to the boundary conditions (9-12) . According to the scheme (8) the local truncation error t_i is provided by

$$\left(1-(2\delta+2\lambda+\omega)\right)h^4\psi_i^{(4)}+0.5(1+2\delta+2\lambda+\omega)h^5\psi_i^{(4)}$$

$$+0.04\left(7-3(34\delta+10\lambda+\omega)\right)h^6\psi_i^{(6)}+0.02(5+98\delta+26\lambda+\omega)h^7\psi_i^{(7)}$$

$$+0.0005\left(69-5(70\delta+82\lambda+\omega)\right)h^8\psi_i^{(8)}+0.008(115+8464\delta+726\lambda+3\omega)h^9\psi_i^{(9)}+$$

$$0.0001\left(2497-21(1635\delta+730\lambda+\omega)\right)h^{10}\psi_i^{(10)}+O(h^{11}) \qquad i=3,4,\dots n-2$$

The following type of methods of various orders are generated by the scheme (8 -12):

- **Second Order Method**

  For arbitrary δ *and* λ *and* $\omega=\left(1-2(\delta+\lambda)\right)$

  $$(\Delta_0,\Delta_1,\Delta_2,\Delta_3,\Delta_4,\Delta_5)=\left(-\frac{1}{6},\frac{77}{1151},0,0,0,0\right)$$

  $$(\bar{\Delta}_1,\bar{\Delta}_2,\bar{\Delta}_3,\bar{\Delta}_4,\bar{\Delta}_5,\bar{\Delta}_6)=\left(\frac{41}{256},\frac{1463}{768},0,0,0,0\right)$$

  Local truncation errors for $(\delta,\lambda,\omega)=0.00052(1{,}232{,}1446)$ follow.

  $$\tilde{t}_i=\begin{cases}-\frac{66}{2929}h^6\psi_i^{(6)}+O(h^7) & i=1,n\\ \frac{1}{24}h^6\psi_i^{(6)}+O(h^7) & i=3,4,\dots n-2\\ \frac{560}{1919}h^6\psi_i^{(6)}+O(h^7) & i=2,n-2\end{cases}$$

  (13)

- **Fourth Order Method**

For arbitrary δ *and* $\lambda = \frac{1-24\delta}{6}$, $\omega = (1-2(\delta+\lambda))$

$$(\Delta_0, \Delta_1, \Delta_2, \Delta_3, \Delta_4, \Delta_5) = \left(\frac{1}{132}, -\frac{241}{3456}, -\frac{239}{6912}, \frac{47}{4356}, 0, 0\right)$$

$$(\bar{\Delta}_1, \bar{\Delta}_2, \bar{\Delta}_3, \bar{\Delta}_4, \bar{\Delta}_5, \bar{\Delta}_6) = \left(\frac{653}{146\,3}, \frac{641}{1479}, \frac{19}{7324}, \frac{173}{3072}, 0, 0\right)$$

Local truncation errors for $(\delta, \lambda, \omega) = (0.00144, 0.1724, 0.658)$ follow

$$\tilde{\mathfrak{t}}_i = \begin{cases} -\frac{66}{124301} h^8 \psi_i^{(8)} + O(h^9) & i = 1, n \\ \frac{19}{34200} h^8 \psi_i^{(8)} + O(h^9) & i = 3,4, \dots n-2 \\ \frac{168}{27431} h^8 \psi_i^{(8)} + O(h^9) & i = 2, n-2 \end{cases}$$

(14)

- ***Sixth Order Method***

If $(\delta, \lambda, \omega) = \frac{1}{720}(-1, 124, 474)$

$$(\Delta_0, \Delta_1, \Delta_2, \Delta_3, \Delta_4, \Delta_5) = \left(\frac{9}{51176}, -\frac{8}{127}, -\frac{386}{9149}, \frac{103}{18721}, -\frac{39}{18721}, \frac{19}{65426}\right)$$

$$(\bar{\Delta}_1, \bar{\Delta}_2, \bar{\Delta}_3, \bar{\Delta}_4, \bar{\Delta}_5, \bar{\Delta}_6) = \left(\frac{647}{1487}, \frac{876}{631}, \frac{335}{1791}, \frac{218}{2683}, -\frac{204}{6439}, \frac{220}{43047}\right)$$

Local truncation errors follow

$$\tilde{\mathfrak{t}}_i = \begin{cases} -\frac{28}{18583} h^{10} \psi_i^{(10)} + O(h^{11}) & i = 1, n \\ \frac{1}{3024} h^{10} \psi_i^{(10)} + O(h^{11}) & i = 3,4, \dots n-2 \\ -\frac{79}{20138} h^{10} \psi_i^{(10)} + O(h^{11}) & i = 2, n-2 \end{cases}$$

(15)

2- Exponential Spline solution

A linear system of order $n \times n$ is produced by the system (8) and the boundary conditions (9) through (12) and may be expressed in matrix form as

$$\mathcal{D}\Psi = \mathrm{Z} + \mathrm{T}$$

$$\mathcal{D}\bar{\Psi} = \mathrm{Z}$$

(16)

$$\mathcal{D}(\Psi - \bar{\Psi}) = \mathrm{T}$$

$$\mathcal{D}E \doteq \mathrm{T}$$

where $\Psi = \left(\psi_{i-\frac{1}{2}}\right)$, $\bar{\Psi} = \left(\bar{\psi}_{i-\frac{1}{2}}\right)$, $\mathrm{T} = \left(t_{i-\frac{1}{2}}\right)$ and $E = \left(e_{i-\frac{1}{2}}\right) = \left(\psi_{i-\frac{1}{2}} - \bar{\psi}_{i-\frac{1}{2}}\right)$ for $i = 1,2, \dots, n$,

(17)

Also,

$$\mathcal{D} = \mathcal{D}_0 - h^4 \mathcal{B} \bar{P}$$

$P = diag\left(p_{i-\frac{1}{2}}\right)$ and $\mathrm{Z} = [z_1, z_2, z_3, z_4, \dots, z_{n-2}, z_{n-1}, z_n]^T$, where $p_{i-\frac{1}{2}}$ for $\frac{n}{4} \le i \le \frac{3n}{4}$.

(18)

$$z_i = \begin{cases} 6\mathcal{B}_1 - \frac{5}{2}h^2\mathcal{B}_2 + h^2\left(\delta_0(-\mathcal{B}_1 p_0 + q_0) + \sum_{j=1}^{5}\delta_j q_{j-\frac{1}{2}}\right), i = 1 \\ -2\mathcal{B}_1 - \frac{h^2}{4}\mathcal{B}_1 + h^2\sum_{j=1}^{6}\lambda_j q_{j-\frac{1}{2}} \qquad i = 2 \\ \left(\delta\left(q_{i-\frac{5}{2}} + q_{i+\frac{3}{2}}\right) + \lambda\left(q_{i-\frac{3}{2}} + q_{i+\frac{1}{2}}\right) + \omega q_{i-\frac{1}{2}}\right) \qquad i = 3, \ldots n-2 \\ -2\mathcal{B}_2 - \frac{h^2}{4}\mathcal{B}_2 + h^4\sum_{j=1}^{6}\lambda_j q_{n+j-\frac{13}{2}}, i = n-1 \\ 6\mathcal{B}_2 - \frac{5h^2}{4}\mathcal{B}_2 + h^4\left(\delta_0(-\mathcal{B}_2 p_n + q_n) + \sum_{j=1}^{6}\delta_j q_{n+j-\frac{11}{2}}\right) \quad i = n \end{cases}$$

3- **Convergence Analysis**

Now, our major goal is to produce a bound on $\|E\|_\infty$, where $\|.\|$, denotes the infinite norm, we now return to error equation (16) and convert it as follows:

$E = \mathcal{D}^{-1}T = [\mathcal{D}_0 + h^4 B\psi]^{-1}T = \left[I + {\mathcal{D}_0}^{-1}h^4 B\psi\right]^{-1}{\mathcal{D}_0}^{-1}T,$

we get,

$$\|E\|_\infty \leq \frac{\left\|{\mathcal{D}_0}^{-1}\right\|_\infty \|T\|_\infty}{1 - \left\|{\mathcal{D}_0}^{-1}\right\|_\infty \|B\|_\infty \|\psi\|_\infty}$$

Provided that $\left\|{\mathcal{D}_0}^{-1}\right\|_\infty \|B\|_\infty \|\psi\|_\infty$ .It was shown in that is non-singular and its inverse satisfies the inequality

$\left\|{\mathcal{D}_0}^{-1}\right\|_\infty \leq \frac{5(b-a)^4+10(b-a)^2h^2+9h^2}{384h^2}$

Lemma 1. The matrix given by (18) is nonsingular, provided that $\|B\|_\infty |p|\bar{v} < 1$ where $\bar{v} = \frac{5(b-a)^4+10(b-a)^2h^2+9h^2}{384h^2}$,

finite number; the following statement provides the proof of this lemma [12]. If G is a square matrix of order n and $\|\tilde{G}\| < 1$, then the $(I+\tilde{G})^{-1}$ exists and. $\left\|(I+\tilde{G})^{-1}\right\| \leq (1 - \|\tilde{G}\|)^{-1}$

The discrete boundary value problem has a unique solution as a result of lemma 1 if $\|B\|_\infty |p|\bar{v} < 1$.

We now explore the following three instances using Equations. (13-15):

- **second order convergent method**

  From equation. (13), we have

  $\|T\|_\infty = \frac{1896}{1150}h^6\Upsilon_6, \quad \|w\|_\infty = max_{a\leq x\leq b}|\psi^6(\eta)|$

  And after that comes:

  $$\|E\|_\infty \leq \frac{1897\Upsilon_6 h^2}{1-11520\,(1-\|B\|_\infty\|\psi\|_\infty)} = G_1 h^2 \approx 0(h^2), \qquad (19)$$

  Where,

  $G_1 = \frac{1897\Upsilon_6 h^2}{1-11520\,(1-\|B\|_\infty\|\psi\|_\infty)}$,

- **fourth order convergent method**

  From equation (14), we have

  $\|T\|_\infty = \frac{9587}{3096576} h^8 \Upsilon_{8,} \quad \|\psi\|_\infty = max_{a\le x\le b}|\psi^8(\eta)|$

  And after that comes:

  $$\|E\|_\infty \le \frac{9587\Upsilon_6 h^2}{3096576\,(1-\|B\|_\infty\|\psi\|_\infty)} = G_1 h^4 \approx 0(h^4), \tag{20}$$

  Where

  $G_2 = \frac{1897\Upsilon h^4}{3096576\,(1-\|B\|_\infty\|\psi\|_\infty)}$

- **sixth order convergent method**

  From equation (15), we have

  $\|T\|_\infty = \frac{3307}{1538523} h^{10} \Upsilon_{10,} \quad \|\psi\|_\infty = max_{a\le x\le b}|\psi^{10}(\eta)|$

  And after that comes:

  $$\|E\|_\infty \le \frac{33077\Upsilon_8 h^6}{1538523\,(1-\|B\|_\infty\|\psi\|_\infty)} = G_1 h^6 \approx 0(h^6), \tag{21}$$

  Where

  $G_2 = \frac{33077\Upsilon h^6}{1538523\,(1-\|B\|_\infty\|\psi\|_\infty)}$

Theorem 1

Let $\psi(\eta)$ denote the exact answer to the continuous boundary value problem (1) using the boundary condition (2),and assume that $\psi_{i-\frac{1}{2}}, i = 0,1,\dots,n-1.$

the discrete boundary value problem in (16) is met $E_{i+\frac{1}{2}}\left(\psi_{i+\frac{1}{2}} - \psi_{i-\frac{1}{2}}\right)$.

- $\|E\|_\infty \approx 0(h^4)$, which is provided by (19), is a second order method.
- $\|E\|_\infty \approx 0(h^4)$, which is provided by (20), is a fourth order method
- $\|E\|_\infty \approx 0(h^6)$, which is provided by (21), is a sixth order method

4- Numerical examples and discussion

To compare the performance of proposed method in (16) to other current methods, we now have a look at two numerical samples. Maple22 is used to carry out every computation.

Example 1. Consider the boundary value problem

$$\psi^{(4)} - \psi + 4(2\eta\cos(\eta) + 3\sin(\eta)) = 0 \tag{22}$$

$\psi(0) = 0, \qquad \psi(1) = 0,$

$\psi^{(4)} = 0, \qquad \psi^{(4)} = 2\sin(1) + 4\cos(1),$

The exact solution of (22) is

$$\psi(\eta) = (\eta^2 - 1)\sin(\eta) \tag{23}$$

Example 2. Consider the boundary value problem

$$\psi^{(4)} + \eta\psi + (\eta^3 + 7\eta + 8)e^{\eta} = 0 \tag{24}$$

$$\psi(0) = 0, \qquad \psi(1) = 0,$$

$$\psi^{(4)} = 0, \qquad \psi^{(4)} = -4e,$$

The exact solution of (24) is $\psi(\eta) = \eta(1-\eta)e^{\eta}$. (25)

Table 1. Observed Maximum absolute errors for Example (1).

h	Second order	Fourth order	Sixth order
0.125	6.20×10^{-6}	6.14×10^{-8}	7.2×10^{-11}
0.0625	5.33×10^{-5}	5.03×10^{-11}	9.5×10^{-13}
0.03125	4.01×10^{-5}	8.21×10^{-11}	6.3×10^{-14}

Table 2. Observed Maximum absolute errors for Example (2)

h	Second order	Fourth order	Sixth order
0.125	2.20×10^{-5}	6.14×10^{-8}	5.4×10^{-11}
0.0625	7.5×10^{-6}	3.61×10^{-11}	6.12×10^{-13}
0.03125	4.13×10^{-6}	7.14×10^{-13}	5.11×10^{-14}

Table 3. The observed maximum errors for Example (2)

h	Ramadan et al.[4]	Ramadan et al.[3]	Al-Said et al. [2]	Proposed Method
0.125	1.76×10^{-5}	1.91×10^{-7}	5.69×10^{-4}	3.11×10^{-11}
0.0625	2.98×10^{-10}	3.12×10^{-9}	1.47×10^{-4}	7.15×10^{-13}
0.03125	4.75×10^{-11}	5.02×10^{-11}	3.71×10^{-5}	4.17×10^{-14}

Table 4. The numerical solutions and exact solution of example (2) of n

$\tilde{\eta}$	The proposed method	Exact solution	Absolute error
0	0.0000000000	0.0000000000	0.0000000000
0.1	0.0994653837	0.0994653826	1.1×10^{-9}
0.2	0.1954244376	0.1954244413	3.7×10^{-9}
0.3	0.2834703471	0.2834703497	2.6×10^{-9}
0.4	0.3580379216	0.3580379275	5.9×10^{-9}
0.5	0.4121803120	0.4121803178	5.8×10^{-9}
0.6	0.4373085072	0.4373085120	4.8×10^{-9}
0.7	0.4228880647	0.4228880685	3.8×10^{-9}
0.8	0.3560865459	0.3560865485	2.6×10^{-9}
0.9	0.2213642786	0.2213642800	1.4×10^{-9}
1.0	0.0000000000	0.0000000000	0.0000000

Table 5. The numerical solutions and exact solution of example (1) of n

$\tilde{\eta}$	The proposed method	Exact solution	Absolute error
0	0.000000000000	0.000000000000	0.0000000
0.1	−0.09883508116	−0.0988350824	1.3×10^{-9}
0.2	−0.19072255308	−0.1907225576	4.5×10^{-9}
0.3	−0.26892338327	−0.2689233881	4.8×10^{-9}
0.4	−0.32711140191	−0.3271114075	5.6×10^{-9}
0.5	−0.35956914877	−0.3595691540	5.2×10^{-9}
0.6	−0.36137117847	−0.3613711830	4.5×10^{-9}
0.7	−0.32855101692	−0.3285510205	3.6×10^{-9}
0.8	−0.25824819027	−0.2582481927	2.4×10^{-9}
0.9	−0.14883211158	−0.1488321128	1.2×10^{-9}
1.0	0.0000000000000	0.00000000000	0.00000000

Conclusions

In this study, two instances are taken into consideration for the numerical demonstration of the expositional spline approach, which is designed for the approximate solution of fourth-order two-point boundary value problems. It is demonstrated that this approach is a second-order, fourth-order, and sixth-order convergent method, making it superior to other methods shown in Tables(1-3). The results for the expositional spline method with the exact solution and results of absolute errors are provided in Tables 4 and 5. The numerical results demonstrate the suggested approaches' great accuracy, which is highly encouraging for dealing with the solution of this kind of two-point boundary value problems.

References

1. E.A. Al-Said, M.A. Noor (2002). Quartic spline method for solving fourth order obstacle boundary value problems. Journal of Computational and applied Mathematics, 143 , 107 – 116.
2. E.A. Al-Said, M.A. Noor and T.M. Rassias (2006). Cubic splines method for solving fourth order obstacle boundary value problems. Applied Mathematics and Computations, 174 , 180 – 187.
3. M.A. Ramadan, I.F. Lashien and W.K. Zahra (2009). Quintic nonpolynomial spline solutions for fourth order two point boundary value problems. Communications in Nonlinear Science and Numerical Simulations, 14, 1105 – 1114.
4. M.A. Ramadan, I.F. Lashien and W.K. Zahra (2018)High order accuracy nonpolynomial spline solutions for order two point boundary value problems, Applied Mathematics and Computation 204, 920 – 927.
5. S. Islam, I.A. Tirmizi, F. Haq and S.K. Taseer (2008). Family of numerical methods based on non-polynomial splines for solution of contact problems . Commun. Nonlinear Sci. Numer. Simul. 13 ,1448–1460.
6. W.K. Zahra (2011).A smooth approximation based on exponential spline solutions for nonlinear fourth order two point boundary value problems,.Appl. Math. Comput. 217 ,8447–8457.
7. W.K. Zahra(2011). Finite-difference technique based on exponential splines for the solution of obstacle problems. Internat. J. Comput. Math. 88 , 3046–3060.
8. Ayalew, M., Kiltu, G.G. and Duressa, G.F. (2021). Fitted numerical scheme for second-order singularly perturbed differential-difference equations with mixed shift. Abstr. Appl. Anal. Volume Article ID 4573847, 11 pages.
9. Chekole, A.T., Duressa, G.F. and Kiltu, G.G.(2019) Non-polynomial septic spline method for singularly perturbed two point boundary value problems of order three, J. Taibah Univ. Sci. 13 651–660.
10. El-Zahar, E.R.(2020). Approximate analytical solution of singularly perturbed boundary value problems in MAPLE, AIMS Mathematics, 5 , 2272–2284.
11. Gupta, R., Bhagyamma, D. and SharathBabu, K.(2021). Numerical solution of two-point boundary value problem using transformation technique using quadrature method,Turk. J. Comput. Math. Educ. 12 , 2084–2091.
12. Kiltu, G.G., Duressa, G.F. and Bullo, T.A.(2021). Computational method for singularly perturbed delay differential equations of the reaction-diffusion type with negative shift, 'J. Ocean Eng. Sci. 6 (2021) 285–291.
13. R.A. Usmani(2009). Discrete methods for a boundary value problem with Engineering applications. Math. Comput. 32(1978), 1087 – 1096.

Speed Control for the DC Motor Based on Feedforward PID Controller

Ghaidaa Hadi Salih Elias [1]

© 2023 The Author(s). This open access article is distributed under a Creative CommonsAttribution (CC-BY) 4.0 license.

Abstract: In this paper, Proportional Integral Derivative (PID) controller with the feedforward gain is used to control the speed of the DC motor with and without load disturbance. The comparison between the proposed approach and the conventional PID controller is performed to know the best one. In both cases, with and without disturbance effect, the suggested approach improved system characteristics. Without disturbance effect, the feedforward controller improved the value of settling and rise times with an enhancement percentage of (10.649%) and (22.549%), respectively than a conventional PID controller. On the other hand, in the case of the disturbance effect, it improved the value of settling and rise times with an enhancement percentage of (11.765%) and (20.388%), respectively than a conventional PID controller. As well, it also attained good performance to reduce the load disturbance effect.

Key Words: PID controller; DC motor; Load disturbance; Reference angular speed; Feedforward PID; Conventional PID.

Author details

[1] College of Engineering, University of Kerbala, Kerbala, Iraq

Citation information

Cite this article as:

Elias, G.A., (July 2023), *Speed Control for the DC Motor Based on Feedforward PID Controller*, Proceedings of the Minar Congress, Turkey, (9) pp 230-244, DOI: http://dx.doi.org/10.47832/MinarCong9-20

http://dx.doi.org/10.47832/MinarCong9-20

[1] gadahadi6@gmail.com

Introduction

DC motor is a device that transforms electrical power into mechanical power (Maarif & Setiawan, 2021). It has many kinds such as stepper motor (Shekhawat & Rohilla, 2020), servo motor (Kumar et al., 2017), brushed DC electric motor (Chotai & Narwekar, 2017), and brushless DC electric motor (Yu & Hwang, 2004). Many applications use DC motors such as pendulums (Shao & Li, 2020), mobile robots (Aung, 2007), electric grippers (Nikhil Shewale & Deivanathan, 2018), electric cars (Thakar & Patel, 2019), and cranes (Hairuddin & Yahya, 2022), to benefit from their precise and simple control characteristics (Al-Bargothi et al., 2019).

Controlling the angular speed of the DC motor is very difficult, so, a control system is required (Maarif & Setiawan, 2021). In order to perform speed control for the DC motor efficiently, the control system must withstand any varying environment such as external disturbance (load torque). These external disturbances affect the control system's competence of the DC motor (Pillai et al., 2014)(AL-Samarraie & Abbas, 2012).

In studies, the controllers that are employed for controlling the speed of DC motor are the PI controller (Chaouch et al., 2018), PID controller (Gasparesc, 2016)(Adel et al., 2018) , fractional order PID (Hekimoglu, 2019), combined Adaptive Network with the Fuzzy Inference System (ANFIS) based hybrid PID controller (Guo & Mohamed, 2020), fuzzy logic controller (Tir et al., 2017), model reference adaptive control (Ahmad et al., 2018), and integral state feedback (Munadi et al., 2016).

One of the common controllers among them is the PID controller. It has a simple structure and requires less complexity in the implementation. In addition to be give satisfactorily results for petty external disturbances (Maarif & Setiawan, 2021)(Al-Bargothi et al., 2019)(Pillai et al., 2014).

In this work, a new approach is proposed for improving a conventional PID controller response and reducing the effects of external disturbances. A feedforward PID controller is used for controlling the speed of the DC motor with and without load disturbance.

The proposed approach was compared with the conventional PID controller in standards of settling time (t_s), rise time (t_r), Overshoot (*OS*), and Steady-State Error (*SSE*) to explore which one is the best.

This paper is organized as follows: In the first section, the introduction is described. In the second section, the mathematical model is analyzed. Control strategies for the DC motor are described in section three. In section four, MATLAB Simulink results discussed the step response of the PID and FPID controllers for the DC motor without and with load disturbance, sinewave and pulse responses for PID and FPID controllers with load disturbance. Section five includes the conclusion.

Modelling of the DC Motor

The mathematical model of the DC motor is performed by applying Kirchhoff's voltage law to the electrical part of the DC motor equivalent circuit as shown in Fig. 1. In addition to applying Newton's second law to the mechanical part of the DC motor. The mathematical analysis for both laws is described in Equations (1 and 2), respectively (Hassan et al., 2017)(Hummadi, 2012)(Khan et al., 2015).

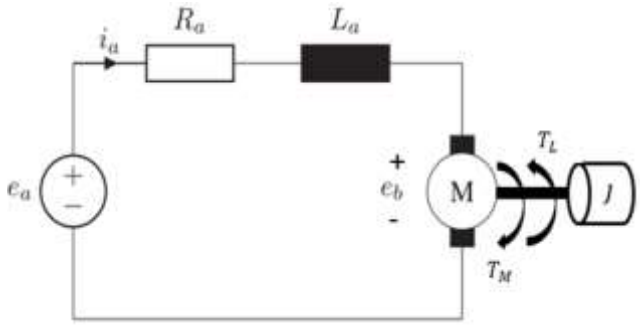


Figure 1. DC motor structure

$$e_a(t) = L_a * \frac{di_a(t)}{dt} + R_a * i_a(t) + e_b(t) \quad (1)$$

$$J * \frac{d\omega(t)}{dt} = -B * \omega(t) + T_M(t) - T_L\,(t) \quad (2)$$

Where, R_a and L_a are the armature resistance and inductance, respectively. i_a denotes the armature current. e_a is the voltage source, e_b specifies the back electromotive force (emf) or induced voltage, J is the inertial load, ω denotes the motor's angular speed, $\frac{d\omega}{dt}$ is the change of motor's angular speed, B is viscous friction, T_M is the motor torque, and T_L is the load torque. The induced voltage and the motor torque are derived by Equations (3 and 4), respectively (Hassan et al., 2017)(Hummadi, 2012)(Khan et al., 2015).

$$e_b(t) = k_b * \omega(t) \quad (3)$$

$$T_M(s) = k_t * i_a(t) \quad (4)$$

Where, k_b and k_t indicate the back emf and the torque constants, in the order. By applying Laplace transform to Equations (1 to 4), the new Equations (5 and 8) are given as follows (Hassan et al., 2017)(Hummadi, 2012)(Khan et al., 2015):

$$E_a(s) = (L_a * I_a(s))\, s + R_a * I_a(s) + E_b(s) \quad (5)$$

$$(J * \mathrm{W(s)})\, \mathrm{s} = -B * W(s) + T_M(s) - T_L(s) \quad (6)$$

$$E_b(s) = k_b * W(s) \quad (7)$$

$$T_M(s) = k_t * I_a(s) \quad (8)$$

The block diagram of the DC motor is formed in Figure 2. As well, the parameters of this motor used in our work experiments are specified in Table 1.

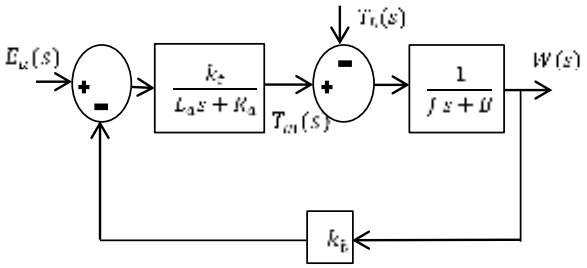


Figure 2. The block diagram of the DC motor

Table 1. Parameters of the DC motor

Parameter	Value	Unit
R_a	2	Ω
L_a	0.5	H
J	0.02	Kg.m²
B	0.2	N.m.sec
k_t	0.1	N.m/A
k_b	0.1	V.sec/rad

Control Strategies

PID Control

One of the famous controllers used in industries is the PID controller. It minimizes the difference between the reference and current signals. The mathematics expression for the PID controller is written as the Equations (9 and 10) (Pendleton et al., 2017) (Farag, 2020):

$$u(t) = k_p * e(t) + k_d * \frac{de(t)}{dt} + k_i * \int e(t)\, dt \qquad (9)$$

$$e(t) = \omega_{ref}(t) - \omega(t) \qquad (10)$$

Where u defines the control input, k_p is the proportional gain, k_d states derivative gain, k_i refers to the integral gain, e represents the error between the reference and current signal, and ω_{ref} is the reference angular speed. The block diagram of that controller is formed in Figure (3) (Pendleton et al., 2017)(Farag, 2020).

The suitable performance of the PID controller depends on the best gains selection. There are many methods for choosing PID gains. One of these methods is called “trial and error”, which is used in this work. It is a simple method, no mathematics is required (Van der Zalm, 2004). The basic idea of this method is that the values of k_d and k_i need to be set first as zero before tuning the k_p. The proportional gain is increased gradually until the output of the control loop oscillates at a constant rate. Increasing the proportional gain will reduce the steady-state error and increase the response speed. As well, the system becomes unstable

when the proportional gain is very high. On the other side, if the proportional gain is too low, the response to system disturbances may be too small. After tuning the proportion gain, the values of k_d and k_i are set gradually until to obtain the best response. The advantage of the integral component is to minimize the steady-state error by multiplying the accumulated error by the integral gain k_i (Farag, 2020)(Jaafar et al., 2014)(Herráez, 2020).

The main function of the derivative item is to dampen the overshoot by multiplying the slope of the error by differential gain k_d. Moreover, the derivative component reduces the speed of the system, and it has a small effect on the steady-state error (Farag, 2020)(Jaafar et al., 2014) (Herráez, 2020)(Syed Hussien et al., 2015a)(Syed Hussien et al., 2015b).

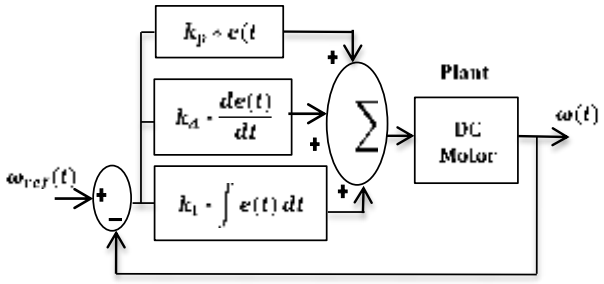


Figure 3. Block chart for DC motor PID control system

Feedforward PID Controller (FPID)

To improve the performance of the PID control system response, the feedforward gain (k_{ff}) is provided to the control system. So, the control input of the PID controller is modified as in Equation (11). The block chat of the DC motor control system is also reformed in Figure 4.

$$u(t) = k_{ff} * (k_p * e(t) + k_d * \frac{de(t)}{dt} + k_i * \int e(t)\, dt) \quad (11)$$

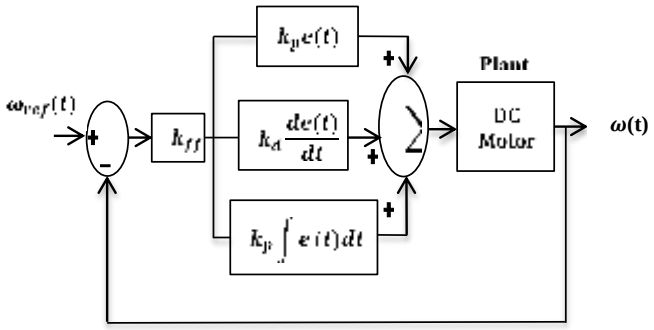


Figure 4. Block chart for DC motor FPID controller

Results and discussion

This section includes four subsections. All tests in subsections were executed by the MATLAB environment to assess the proposed approach. The block diagrams of the conventional PID, and feedforward PID control systems of the DC motor mentioned in section three are structured by MATLAB/Simulink to be simulated.

1. Step response of the DC motor without and with load disturbance

In this subsection, the step response of the DC motor is simulated for two cases. In the first case, the DC motor is assumed without load disturbance. On the other hand, it is assumed with load disturbance of 0.1 Nm between a sample time of 5 and 10 secs.

The step response of the DC motor for both cases: without and with load disturbance are displayed in Figs. (5 and 6), respectively. Figure 5 shows system response without load torque effects. On other hand, Figure 6 demonstrates system response at load torque effects that must be reduced to operate the DC motor control system efficiently.

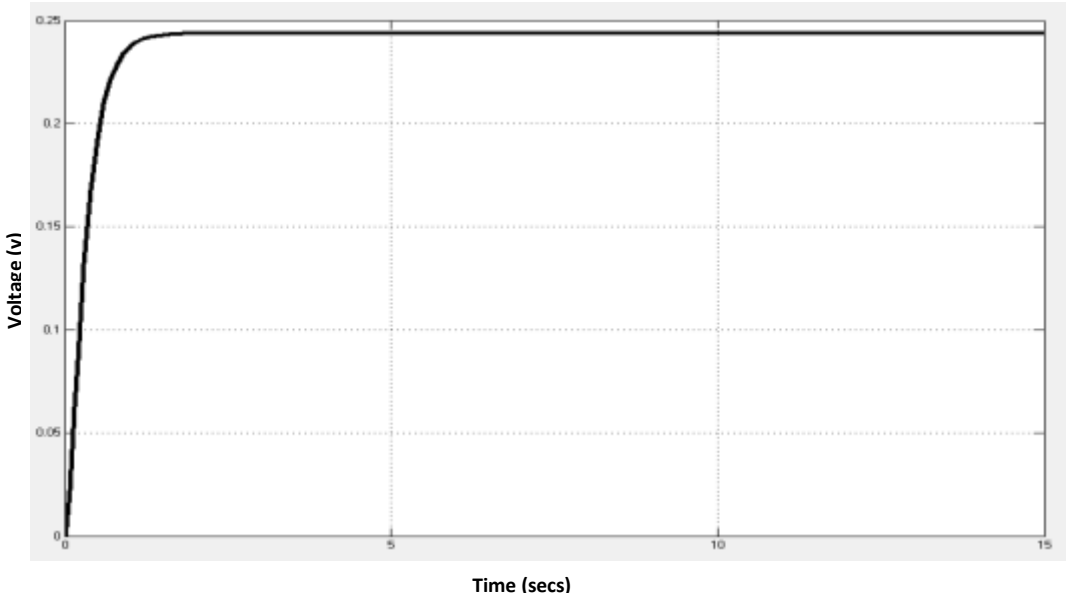


Figure 5. Open loop response of DC motor without load disturbance

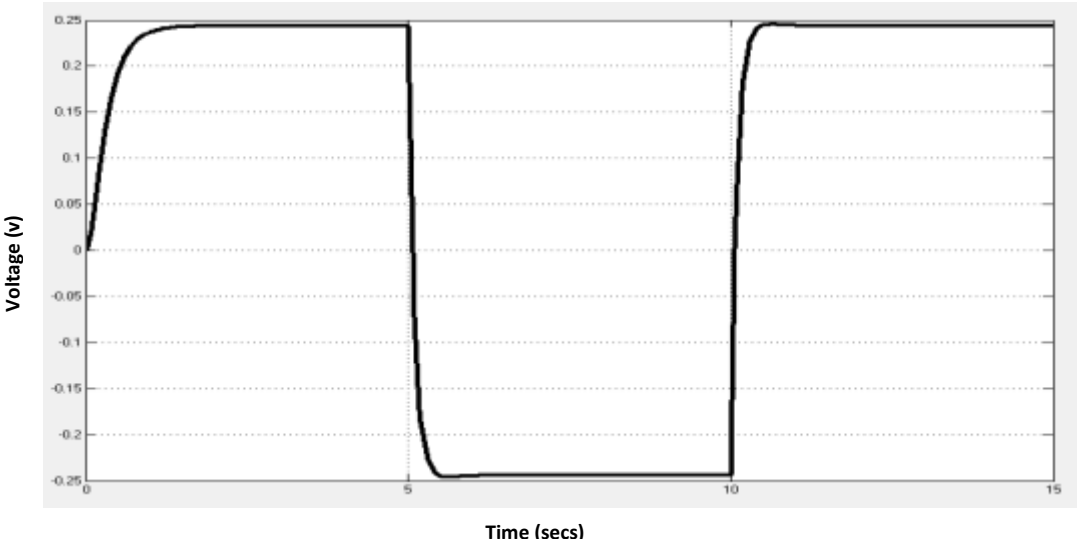


Figure 6. Open loop response of DC motor with load disturbance

2. Step response of the PID and FPID controllers without load disturbance

First of all, the tuning of the PID controller is performed by the trial and error method mentioned in the third section. The same tuned gains (proportional gain, derivative gain, and integral gain) are employed in the PID and the FPID controllers. Besides, five cases of feedforward gain are selected to know its effect on the FPID controller response. The PID and FPID gains are displayed in Table 2. On the other hand, the step response for the FPID for five cases of feedforward gain is shown in Figure 7.

Table 2. PID and FPID controllers' parameters

Controller	Gains			
	k_p	k_i	k_d	k_{ff}
PID	86	36	3.6	-
FPID	86	36	3.6	2
FPID	86	36	3.6	5
FPID	86	36	3.6	10
FPID	86	36	3.6	20
FPID	86	36	3.6	50

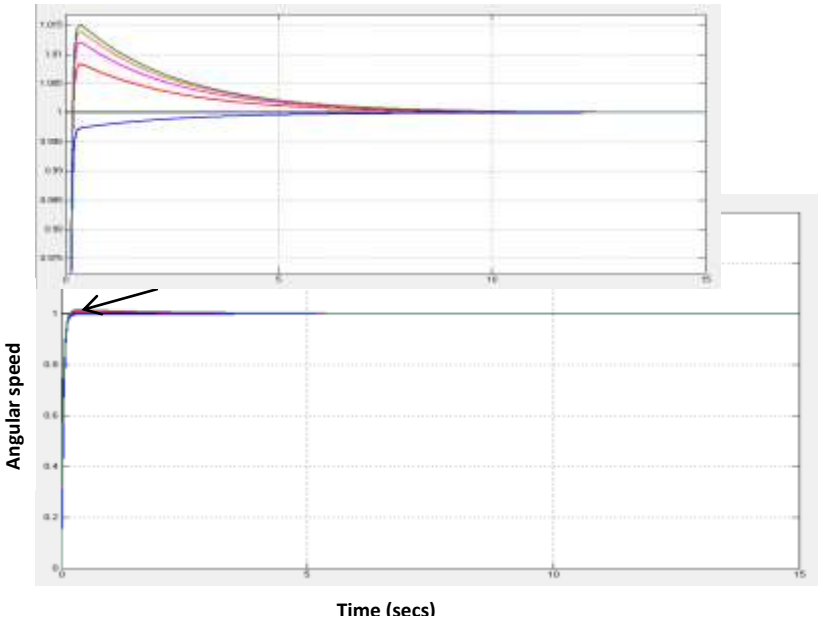


Figure 7. Step response of FPID control system for five cases of feedforward gain

Then, the response system's standards for the FPID controller of the DC motor represented by the settling and rise times, steady state error, and overshoot of the FPID control system for five cases of feedforward gain are stated in Table 3.

Table 3. System response criteria for the DC motor without load disturbance

k_{ff}	t_s *(sec)*	t_r *(sec)*	***OS*** *(%)*	***SSE*** *(rad/sec)*
2	0.156	0.35	0	$1.11*10^{-4}$
5	0.147	0.089	0.325	$2.5*10^{-4}$
10	0.1448	0.009	0.658	$4.17*10^{-4}$
20	0.1438	0.009	1.154	$4.5*10^{-4}$
50	0.1428	0.009	1.45	$5*10^{-4}$

Figure 7 and Table 3 illustrated that in the case of increasing FPID feedforward gain, settling and rise times of system response are decreasing while the overshoot and steady-state error are increasing. Therefore, the derivative and integral gains of the FPID controller are retuned to obtain on smooth FPID response.

The PID and newly tuned FPID gains are arranged in Table 4. According to these tuned gains, the step response for the PID and FPID control systems are simulated and displayed in

Figure 8. Besides, the response system's criteria represented by the overshoot, settling time, rise time, and steady-state error for both control systems are stated in Table 5.

Table 4. Tuned parameters for PID and FPID controllers

Controller	Gains			
	k_p	k_i	k_d	k_{ff}
PID	86	36	3.6	-
FPID	86	8	1.1	17

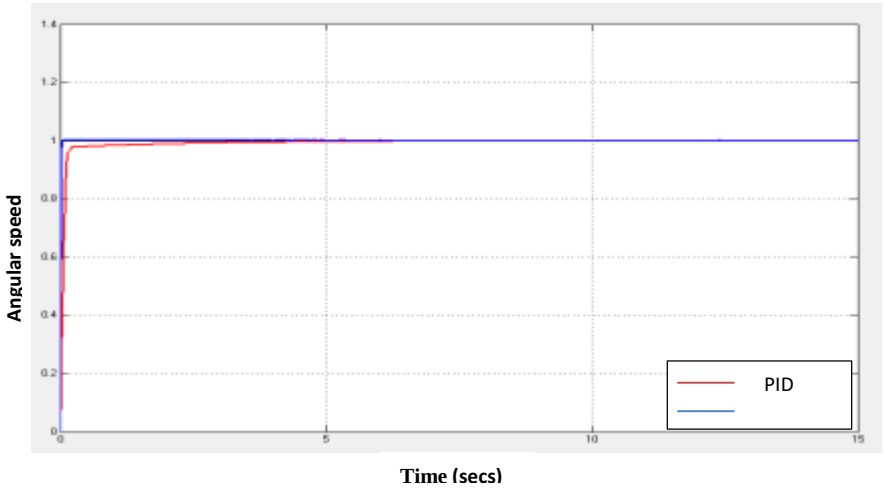


Figure 8. Step response of the PID, FPID control systems for the DC motor without load disturbance

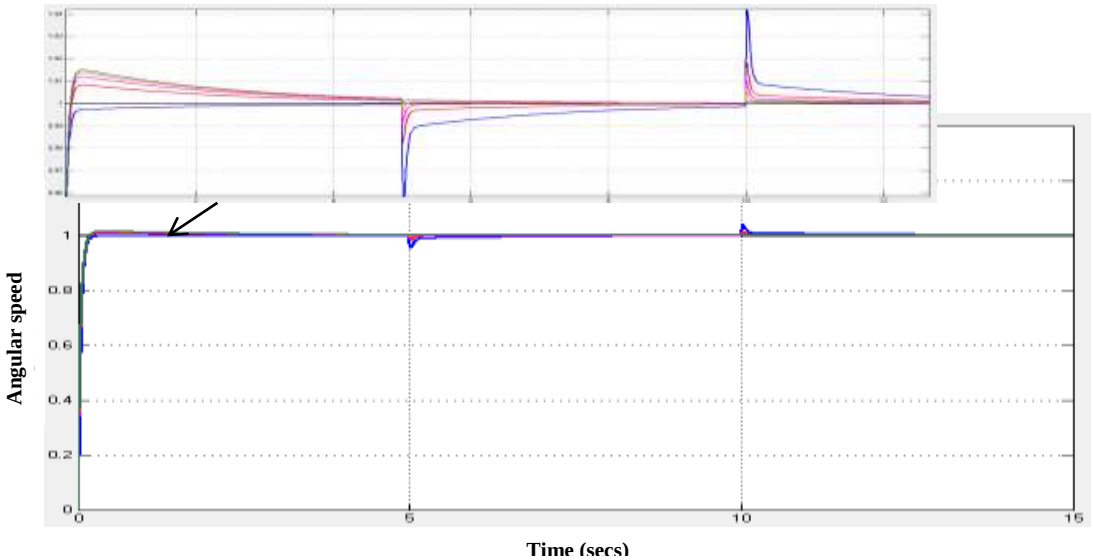


Figure 9. Step response of PID, FPID controllers for the motor with load disturbance.

Table 5. Step response system criteria for the DC motor without load disturbance

Controller	System response standards			
	t_s *(sec)*	t_r *(sec)*	*OS (%)*	*SSE (rad/sec)*
PID	0.385	0.102	0	0.0001
FPID	0.041	0.023	0	0.0003

Figure 8 explained that the FPID controller has more accurate to track reference angular speed than the conventional PID controller. As well, Table 5 refers to that the FPID controller reduced settling and rise times than the PID controller, in addition, to maintaining less value of steady-state error.

3. Step response of the PID and FPID controllers with load disturbance

In this section, the same tests that performed in subsection 4.2 are repeated in this subsection but with load disturbance effect. The simulation result of FPID control system response for five cases of feedforward gain has depicted in Figure 9. On the other hand, the response of the PID and new tuned FPID controller gains are displayed in Figure 10. So, the response system's criteria for the PID and new tuned FPID controllers represented by the settling and rise times, steady state error, and overshoot are specified in Table 6.

Table 6. Control Systems response standards for DC motor with Load disturbance

Controller	System response standards			
	t_s *(sec)*	t_r *(sec)*	*OS (%)*	*SSE (rad/sec)*
PID	0.34	0.103	0	0.0024
FPID	0.04	0.021	0	0.0001

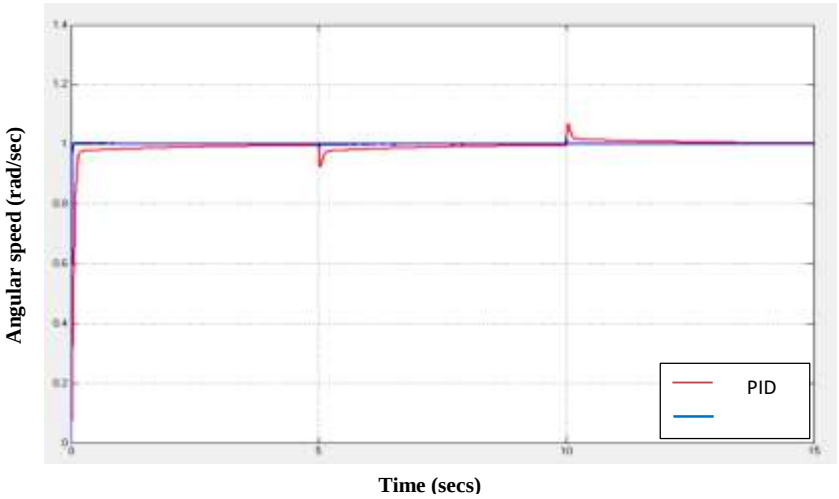


Figure 10. Step response of PID, FPID controllers with load disturbance

Figure 9 clarified that in the case of increasing FPID feedforward gain, the load disturbance effect is decreasing. Figure 10 is explained that the FPID controller has more accurate to track reference angular speed than the conventional PID controller. In addition, it has more power to resistor load disturbance than a conventional PID controller. Tables (1 and 2), refer to that the FPID has reduced settling and rise times than the PID controller, in addition, to maintaining less value of steady-state error

4. Sinewave and pulse responses for PID and FPID controllers with load disturbance

In this test, the sinewave and pulse responses of both control systems for the DC motor with load disturbance have been taken and displayed in Figs. (11 and 12), in the order.

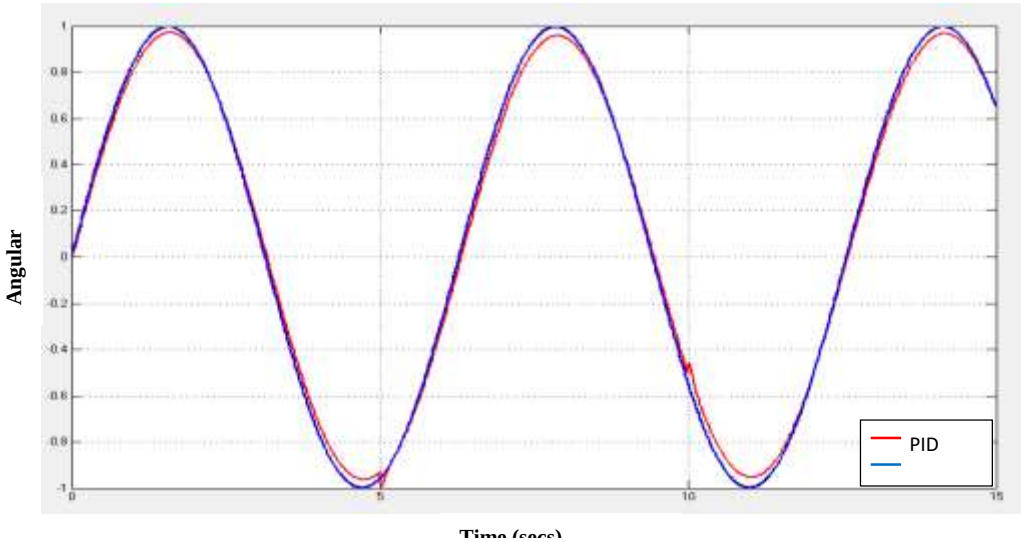


Figure 11. Sinewave response of the PID and FPID controllers for the DC motor with load disturbance

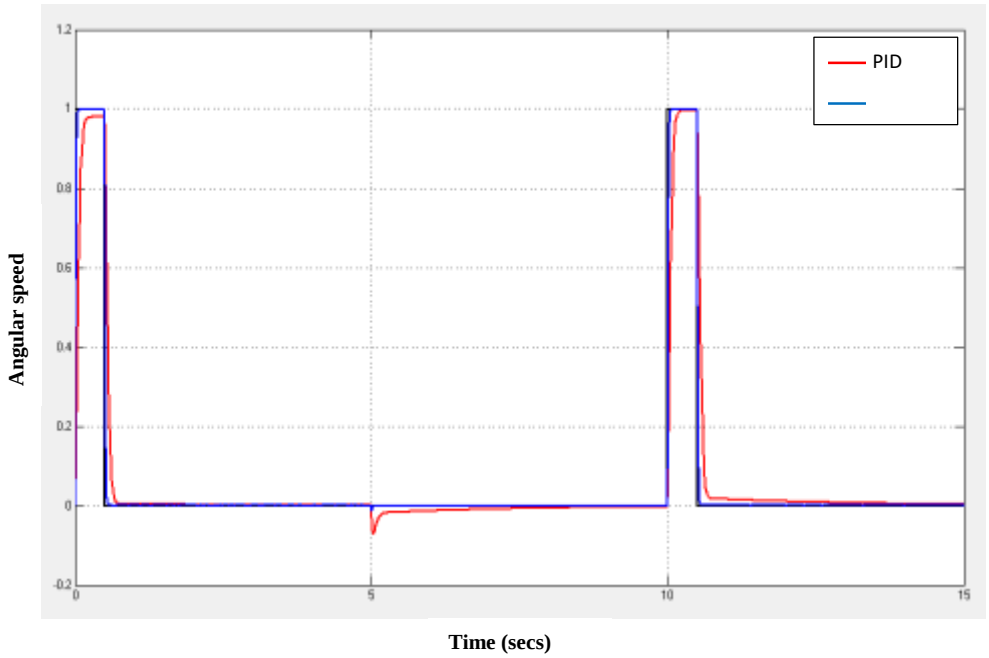


Figure 12. Pulse response of the PID and FPID controllers for the DC motor with load disturbance

The results of Figs. (11 and 12) proved that the FPID controller has more accurate to track reference angular speed than the conventional PID controller. In addition, it has more power to resistor load disturbance than a conventional PID controller. That refers to the power of the suggested approach.

Conclusions

In this paper, the feedforward PID controller was used to control the DC motor with and without load disturbance. The control system was tested with three reference angular speeds, and it was compared with the conventional PID controller to find out which one was better. In all experiments, the outcomes showed that the FPID controller's response reduced the load disturbance effect and improved rise and settling times.

References

1. Adel, Z., Hamou, A. A., & Abdellatif, S. (2018). Design of Real-Time PID tracking controller using Arduino Mega 2560for a permanent magnet DC motor under real disturbances. In 2018 International Conference on Electrical Sciences and Technologies in Maghreb (CISTEM), 1–5. https://doi.org/10.1109/CISTEM.2018.8613560
2. Ahmad, M., Khan, A., Raza, M. A., & Ullah, S. (2018). A study of state feedback controllers for pole placement. In 2018 5th International Multi-Topic ICT Conference (IMTIC), 1. https://doi.org/10.1109/IMTIC.2018.8467276
3. Al-Bargothi, S. N., Qaryouti, G. M., & Jaber, Q. M. (2019). Speed control of DC motor using conventional and adaptive PID controllers. Indonesian Journal of Electrical Engineering and Computer Science, 16(3), 1221–1228. https://doi.org/10.11591/ijeecs.v16.i3.pp1221-1228
4. AL-Samarraie, S., & Abbas, Y. (2012). Design of a Nonlinear Speed Controller for a DC Motor System with Unknown External Torque Based on Backstepping Approach. Uotechnology.Edu.Iq, 12(1), 1–19. http://www.uotechnology.edu.iq/ijcccse_journal/volume 12 2012/no.1.2012/Researches/Dr. Shibly Design of a Nonlinear Speed Controller for a DC .pdf
5. Aung, W. P. (2007). Analysis on Modeling and Simulink of DC Motor and its Driving System Used for Wheeled Mobile Robot. World Academy of Science, Engineering and Technology, 1(8), 299–306. http://urrg.eng.usm.my/eee351/PB4.pdf
6. Chaouch, S., Hasni, M., Boutaghane, A., Babes, B., Mezaache, M., Slimane, S., & Djenaihi, M. (2018). DC-Motor Control Using Arduino-Uno Board for Wire-Feed System. In 2018 International Conference on Electrical Sciences and Technologies in Maghreb (CISTEM), 1–6.
7. Chotai, J., & Narwekar, K. (2017). Modelling and Position Control of a DC Motor. In 2017 International Conference on Advances in Computing, Communication and Control (ICAC3), 1–8.
8. Farag, W. (2020). Track Maneuvering using PID Control for Self-driving Cars. Recent Advances in Electrical & Electronic Engineering (Formerly Recent Patents on Electrical & Electronic Engineering), 13(1), 91–100. https://doi.org/10.2174/2352096512666190118161122
9. Gasparesc, G. (2016). PID control of a DC motor using Labview Interface for Embedded Platforms. 2016 12th International Symposium on Electronics and Telecommunications, ISETC 2016 - Conference Proceedings, 145–148. https://doi.org/10.1109/ISETC.2016.7781078

10. Guo, Y., & Mohamed, M. E. A. (2020). Speed Control of Direct Current Motor Using ANFIS Based Hybrid P-I-D Configuration Controller. IEEE Access, 8, 125638–125647. https://doi.org/10.1109/ACCESS.2020.3007615
11. Hairuddin, W. R. W., & Yahya, N. M. (2022). A Mathematical Model of Geared DC Motor Based of Overhead Crane Control System Prototype. Malaysian Journal of Applied Sciences, 7(1), 44–51. https://doi.org/10.37231/myjas.2022.7.1.299
12. Hassan, A. A., Al-Shamaa, N. K., & Abdalla, K. K. (2017). Comparative Study for DC Motor Speed Control Using PID Controller. International Journal of Engineering and Technology, 9(6), 4181–4192. https://doi.org/10.21817/ijet/2017/v9i6/170906069
13. Hekimoglu, B. (2019). Optimal Tuning of Fractional Order PID Controller for DC Motor Speed Control via Chaotic Atom Search Optimization Algorithm. IEEE Access, 7, 38100–38114. https://doi.org/10.1109/ACCESS.2019.2905961
14. Herráez, D. C. (2020). Self-Driving Car Autonomous System Overview. M.S.c thesis,de Navarra University,Industrial Electronics Engineering.
15. Hummadi, R. M. A.-M. (2012). Simulation of Optimal Speed Control for a Dc Motor Using Linear Quadratic Regulator. Journal of Engineering, 18(3), 340–349.
16. Jaafar, H. I., Yuslinda, S., Shahrieel, M., & Aras, M. (2014). Development of PID Controller for Controlling Desired Level of Coupled Tank System. International Journal of Innovative Technology and Exploring Engineering.
17. Khan, M. R., Khan, A. A., & Ghazali, U. (2015). Speed Control of DC Motor under Varying Load Using PID Controller. International Journal of Engineering, 9(3), 38–48. https://www.cscjournals.org/manuscript/Journals/IJE/Volume9/Issue3/IJE-485.pdf
18. Kumar, P., Chatterjee, S., Shah, D., Saha, U. K., & Chatterjee, S. (2017). On comparison of tuning method of FOPID controller for controlling field controlled DC servo motor. Cogent Engineering, 4(1), 1–20. https://doi.org/10.1080/23311916.2017.1357875
19. Maarif, A., & Setiawan, N. R. (2021). Control of dc motor using integral state feedback and comparison with pid: Simulation and arduino implementation. Journal of Robotics and Control (JRC), 2(5), 456–461. https://doi.org/10.18196/jrc.25122
20. Munadi, Akbar, M. A., Naniwa, T., & Taniai, Y. (2016). Model Reference Adaptive Control for DC motor based on Simulink. In 2016 6th International Annual Engineering Seminar (InAES), 101–106. https://doi.org/10.1109/INAES.2016.7821915
21. Nikhil Shewale, S., & Deivanathan, R. (2018). Modelling and analysis of dc motor actuator for an electric gripper. Journal of Engineering Science and Technology, 13(4), 862–874.

22. Pendleton, S. D., Andersen, H., Du, X., Shen, X., Meghjani, M., Eng, Y. H., Rus, D., & Jr, M. H. A. (2017). Perception, Planning, Control, and Coordination for Autonomous Vehicles. Machines, 1–54. https://doi.org/10.3390/machines5010006
23. Pillai, M. B., Perera, G. V. A. G. A., & Chinthaka, M. K. C. D. (2014). Analysis of a Dc Motor Based Velocity Controller Using Disturbance Observer. Indian Journal of Scientific Research, 5(1), 1–7.
24. Shao, Y., & Li, J. (2020). Modeling and Switching Tracking Control for a Class of Cart-Pendulum Systems Driven by DC Motor. IEEE Access, 8, 44858–44866. https://doi.org/10.1109/ACCESS.2020.2978269
25. Shekhawat, A. S., & Rohilla, Y. (2020). Design and Control of Two-wheeled Self-Balancing Robot using Arduino. Proceedings - International Conference on Smart Electronics and Communication, ICOSEC 2020, October, 1025–1030. https://doi.org/10.1109/ICOSEC49089.2020.9215421
26. Syed Hussien, S. Y., Jaafar, H. I., Ghazali, R., & Abdul Razif, N. R. (2015a). The effects of auto-tuned method in PID and PD control scheme for gantry crane system. International Journal of Soft Computing and Engineering (IJSCE), 4(6), 121–125. http://eprints.utem.edu.my/14047/1/%5B1%5D_F2492014615.pdf
27. Syed Hussien, S. Y., Jaafar, H. I., Ghazali, R., & Abdul Razif, N. R. (2015b). The effects of auto-tuned method in PID and PD control scheme for gantry crane system. International Journal of Soft Computing and Engineering (IJSCE), 4(4), 121–125. http://eprints.utem.edu.my/14047/1/%5B1%5D_F2492014615.pdf
28. Thakar, D. U., & Patel, R. A. (2019). Comparison of Advance and Conventional Motors for Electric Vehicle Application. 2019 3rd International Conference on Recent Developments in Control, Automation and Power Engineering (RDCAPE), 137–142. https://doi.org/10.1109/RDCAPE47089.2019.8979092
29. Tir, Z., Malik, O., Hamida, M. A., Cherif, H., Bekakra, Y., & Kadrine, A. (2017). Implementation of a fuzzy logic speed controller for a permanent magnet dc motor using a low-cost Arduino platform. In 2017 5th International Conference on Electrical Engineering-Boumerdes (ICEE-B), 1–4. https://doi.org/10.1109/ICEE-B.2017.8192218
30. Van der Zalm, G. (2004). Tuning of PID-type controllers. Technische Universiteit Eindhoven: Eindhoven, The Netherlands.
31. Yu, G. R., & Hwang, R. C. (2004). Optimal PID speed control of brush less DC motors using LQR approach. In 2004 IEEE International Conference on Systems, Man and Cybernetics (IEEE Cat. No. 04CH37583), 1, 473–478. https://doi.org/10.1109/ICSMC.2004.1398343

Security Challenges and Threats in Wireless Sensor Networks: A Review

Maytham S. Jabor [1], Aqeel Salman Azez [2], Azhar Hasan Nsaif [3]

Azhar Sabah Abdulaziz [4], Worud Mahdi Saleh [5]

© 2023 The Author(s). This open access article is distributed under a Creative CommonsAttribution (CC-BY) 4.0 license.

Author details

[1-2] Valencia Polytechnic University, Spain

[3] Al Mustansiriyah University, Baghdad, Iraq

[4] Ninevah University, Mosul, Iraq

[5] Diyala University, Diyala, Iraq

Citation information

Cite this article as:

Jabor, M.S., Azez, A.S., Nsaif, A.H., Abdulaziz, A.S., Saleh, W.M., (July 2023), *Security Challenges and Threats in Wireless Sensor Networks: A Review*, Proceedings of the Minar Congress, Turkey, (9) pp 245-264, DOI: http://dx.doi.org/10.47832/MinarCong9-21

Abstract: Wireless Sensor Networks (WSNs) have gained increasing popularity in recent years due to their diverse range of applications. However, owing to their distinctive characteristics—such as limited computational power, energy resources, and a dynamic nature—these networks present unique challenges. Comprising numerous small, low-power sensor nodes, WSNs are deployed in specific areas to gather and transmit data to a base station or sink node. Nevertheless, they remain susceptible to various security threats. A significant concern in WSNs involves attacks compromising data confidentiality, integrity, and availability. Adversaries can intercept and modify transmitted data before forwarding it, thereby undermining its integrity. Additionally, attackers can compromise sensor nodes themselves, thereby gaining unauthorized network access, data manipulation abilities, and the potential to launch subsequent attacks. This paper comprehensively addresses security challenges in WSNs, encompassing attacks on data confidentiality, integrity, availability, and network vulnerabilities. Furthermore, it delves into various attack types against WSNs, such as node compromise, denial-of-service attacks, and network topology breaches. The document provides a thorough review of existing security solutions and protocols proposed to counter these attacks, including encryption, access control, and intrusion detection systems. Lastly, the paper identifies ongoing research challenges and outlines future strategies for enhancing WSN security.

Key Words: Wireless sensor networks, security, attacks, Intrusion detection system

http://dx.doi.org/10.47832/MinarCong9-21

[1] maytham.jebory@gmail.com

[2] aqeelsalman8@gmail.com

[3] bahar299947@gmail.com

[4] azhar.abdulaziz@uoninevah.edu.iq

[5] hawhra11888@gmail.com

Introduction

Wireless sensor networks have gained prominence and progressed toward being one of the most promising and remarkable fields, recently. These networks may unsurprisingly be huge systems consisted of sensor devices which are characterized, in general, of being energy efficient, low-cost, small-sized and low power. Moreover, they serve to gather detailed information about the physical environment. Each device can have a sensor or more, low-power radio(s), embedded processor(s) and is typically battery powered. It would not seem to have a great utility if those devices examined separately. However, the sensor networks' value lies in the fact that of its role in using and co-coordinating a large group of these devices and in allowing very large sensor tasks to be performed[1].

WSNs differ in connection to the data they glean, hence, Wireless sensor networks have several applications, and they can be employed in situations such as observing plants and animals in Ecological Reserves. Furthermore, WSNs can also have another application such as detecting changes in climate, fire discovery, hurricane location, and last but not least to monitor environments and habitats in order to participate in avoidance of natural disasters. We don't lose sight of fact that WSNs make a great contribution in medical applications that depend on sensors to monitor vital signs of a patient, which is known as electronic vital sign monitors. Their applications in the military purposes cannot be overlooked and various other surveillance applications, where they could be harnessed to explore and control an enemy's movements on the battlefield. The sensor nodes are often used in such areas where it is impossible to deploy wired networks[2, 3].

Typically, an authority deploys sensor nodes in a certain area and then, forms a network through wireless communications, automatically. It should be noticed that deployment of homogeneous or heterogeneous sensor nodes can be conducted either in a random way or at locations are determined in advance by using a deterministic scheme., the sensor nodes are most frequently fixed, while, there are moving nodes , which can be deployed depending on the requirements of application[4]. One or more fixed or moving[5] base stations are positioned together with the network

Sensor nodes keep conducting the process of monitoring to the network area after deployment. After an event of interest happens, several functions can be performed by one of the neighboring sensors as follows:

- Generating a report.
- Transmitting the report to a base station through multi-hop wireless links.
  Collaboration can substantially occur when several neighboring nodes perform the detection process to the same event. In such a situation, one of nodes creates a final report after achieving collaboration with the other nodes. The basic processing of the report can be achieved by the base station and then send the report by high quality wired links or wireless links to the outside world for extra processing. Commands or

queries can be transmitted by the Wireless Sensor Network authority to a base station, which, in return, functions to spread the queries or commands into the network. Therefore, a base station functions as a gateway between the Wireless Sensor Network and the outside world[4]. It should be noticed that Wireless Sensor Networks are more susceptible to various forms of security attacks and threats and, which is attributed to an array of reasons among which are the following:

- Multihop decentralized communication.
- Open wireless medium.
- Being deployed in areas which are either hostile and no protected physically[2].

To maintain the security of the wireless network, we should provide protection to it from any types of threats such as unintended uses or unauthorized access. There are three basic security requirements, which are seen very essential to maintain security mechanisms: Confidentiality, Integrity and Availability[6]. **Confidentiality** refers to the prohibition of unauthorized access to information, where only a reliable network node can have an access the resources. **Integrity** refers that the sent information must not altered, or in another way, the process of sending –receiving message must occur without changing or modification. Besides, an access to any sensitive information must not be obtained and must not also changed by an unauthorized persons[7]. Evidently, security achievement in wireless sensor networks will contribute in providing physical protection for the sensors, not only that ,but it also provide protection of communications between network components and protecting data[8]. In this paper, recent research analyses are presented to provide insight into the security mechanism in Wireless Sensor Networks (WSNs). The various types of attacks targeting different network layers are reviewed, highlighting their significant implications and countermeasures. The effectiveness of the reviewed approaches in detecting the attacks to which wireless sensor networks have been subjected is demonstrated.

Security in Wireless Sensor Networks

Security aspect is perceived as one of the main challenges concerning wireless networks especially with regard wireless ad hoc and sensor networks. Basically, susceptibility and vulnerability of these types of networks to attacks are higher than wired networks because they are infrastructure less and dynamic[9] Additionally, those wireless sensor networks may expose to an further vulnerability which are often attributed to placing nodes in a hostile or hazardous environment where physical protection is not guaranteed or provided[10]. Since these networks are broadly used, we are required to find ways to provide protection to them. Sensor networks have, for many years, been subject to too many recurrent attacks and those attacks can fall into two main groups: **Active attacks** and **Passive attacks**.

Active attacks: Basically, include some adjustments to the data stream or it may come in the form of creating false stream, that is to say , those attacker contrive to modify the message content.

Passive attacks : those attacks involve listening to someone's private conversation without her/ his knowing , what's called *eavesdropping on* : or the process of monitoring packets exchanged within a wireless sensor network;[10].

There are the following steps possible for the attack.

- Sender S wishes to send a message to Receiver R.
- S asks R for its encryption key.
- When R returns a key, then that key is intercepted by the attacker and who substitutes his/her key.
- The sender encrypts the message using this bogus key and returns it.
- Since the attacker is the owner of this bogus key, the attacker can read the message [11].

Therefore, we will underline the most widespread types of attacks on wireless sensor network relying on the protocol layers and will review their behavior respectively:

The Physical Layer Attacks

Physical layer serves multiple functions, as follows: selecting frequencies, deflecting signal, generating carrier frequency, modulation, and encrypting data. Furthermore, this layer bears considerable burden and widely suffers the most immeasurable damage arising from the radio jamming attacks[12].

Jamming attacks, can be perceived as a special case of Denial-of Service (DoS) attacks, which pose genuine and serious threats due to the resources constrained property in WSNs. It also disrupts or denies other nodes to use the channel to communicate by occupation the channel that they are communicating on[13]. The main features of these attacks are their effectiveness and simplicity[14]. Jamming can occur in many forms, as reviewed below:

a. **Constant jammer**: In the broad term, this type of jamming, the jammer's technique is to emit a continued jamming signal a radio signal. This process can be executed by two ways: (1) jammer uses a waveform generator that constantly sends a radio signal[15] ,or (2) jammer uses a normal wireless device that continuously sends out random bits to the channel without following any Media Access Control Layer etiquette[16]. Typically, the underlying Media Access Control protocol would permit sending out packets by genuine nodes only in the case of the channel was idle. Consequently, a constant jammer is capable of inhibiting legitimate traffic sources, in an effective way, to get hold of a channel and to send packets [8].
b. **Deceptive jammer**: This process differs significantly from the first case; the technique used by a jammer depends on injecting regular packets constantly to the channel with no gap between successive packet transmissions. Consequently, a regular person who

communicates may be duped into thinking there is a genuine packet and be deceived to continue in the state of reception[17].

c. **Random jammer**: Another form of jamming process is when the random jammer constantly alternates between two phases: *sleep phase* and *jamming phase*. The attacker alternatingly attempts to transmit either random bits or regular packets into networks, here, the aim is to save energy, where the jammer processes sleep for a certain time of period and then develops dynamically for jamming before returning to a sleep phase. The sleeping and jamming phases are either static or random. There is an adjustment between the effectiveness of jamming and energy saving for the reason that it cannot jam in the course of its sleeping period [17].

d. **Reactive jammer**: Reactive jammer begins the process of jamming only when sensing a network activity on a definite channel. However, detecting reactive jamming is much more difficult since it could appear like routine packet collisions[18].

The categories of threats in physical layer and the countermeasures these threats the following:

- **Threat Categories**

Jamming Attacks: Constant, deceptive, random, and reactive jammers disrupt communication channels by emitting signals or interfering with the transmission process.

- **Countermeasures**

1. Spread Spectrum Techniques: Techniques like Frequency Hopping Spread Spectrum (FHSS) and Direct Sequence Spread Spectrum (DSSS) can spread the signal over multiple frequencies, making it harder for jammers to interfere.
2. Channel Hopping: Randomly switching between channels to avoid sustained interference from jammers.
3. Power Control: Adjusting transmission power to mitigate the impact of jamming and manage energy consumption.
4. Receiver Design: Employing advanced receiver designs that can distinguish between weak signals and jamming interference.

Data Link Layer Attacks

Link layer are also subject to attacks, an attacker will attempt to plan, in advance, to disrupt the communication protocol, and over and over again transmits messages in an effort to bring about collisions. This form of collision might require retransmission of any packet influenced by the collision. With this method, it could be potential for an intruder to effortlessly use up a power supply of a sensor by causing oversupply retransmissions[19]. Many types of Threat Categories of attacks against this layer can be reviewed as follows:

a. **Interrogation :** An attack like that, typically , takes advantage of the handshake protocol applied to accomplish communication among nodes, where the attacker is

not capable to consume the target node 's resources by sending a request packet transmission continually , that can induce the victim node on resending a reply to the point that resources become used up[10].

The countermeasures these threats the following:

- Rate Limiting: Implement rate limiting mechanisms to restrict the number of request packets from a single source within a certain time frame.
- Authentication and Authorization: Employ authentication and authorization processes to validate the identity of nodes before processing their requests.
- Intrusion Detection Systems (IDS): Use IDS to detect unusual patterns of continuous requests and take appropriate action.

b. Collisions: The threat of Collisions arise when two nodes try to transmit concurrently on the same frequency and when two nodes collide that leads to a change in the data. As result, this can prompt the node to conduct re-transmission of data through the communication cannel continuously which denies the rest of nodes of sending. If control was not reached concerning the operation of retransmission to stop the operation, that would result in using up the energy of the resources in the sender nodes and the surrounding nodes. An attack like that used to block the services of network, not coming as a direct effect, if there is a situation of at use in the resources of a network[20] .

Countermeasure: Collision Detection and Avoidance

- **Collision Detection:** Network protocols like Ethernet use methods to detect collisions. When a collision is detected, the nodes involved stop transmitting and wait for a random period before attempting to resend.

- **Carrier Sense Multiple Access with Collision Detection (CSMA/CD):** In Ethernet networks, CSMA/CD is used to listen for traffic before transmitting, and if a collision is detected, the transmission is aborted.

- **Switched Networks:** Modern networks often use switches instead of hubs. Switches create individual collision domains, reducing the likelihood of collisions.

c. **Sybil attack: A** malicious sensor disguises or masquerades as multiple sensors, consequently, the routing table will be modified, which will be an error. Therefore, that node can have a significant advantage in electing the head of the cluster. With more votes, the neighboring nodes may be at risk to become a cluster head.

Countermeasures: Node Identity Verification: Utilize cryptographic methods to verify the identity of nodes.

Network and Routing Attacks

a. **Neglect and Greed:** The node that has been taken over by an attacker "*compromised node"* with the neglect and greed attack acknowledges the received packet but neglects to forward it. The controlled messages that the aggressor sends will be acknowledged as valid by all other nodes and that are principally attributed to the fact they are signed correctly, even though those control messages are wrong. Furthermore, its packets are also classified as high priority to be sent first. Seemingly, networks using Dynamic Source Routing are more vulnerable to attack, as the sender node will determine one particular path to get a destination. However, the compromised node can be located along the track and the sending node might not identify it , hence it cannot redirect its movement. The magnitude of effect of such attack within a network is governed by the position of the compromised node and the network region size it will block [21].

b. **Homing**: It is a passive attack because it would require the attacker to monitor the network; the attacker launches this type of attacks for identifying nodes within the wireless sensor network that have special responsibilities. The aim is to identify each node's role correspondingly based upon its position. Additionally, the attack targets the nodes that function a special purpose within the network. These nodes can be relay nodes, global security agents or management nodes. These nodes allure an attacker's interest as their role in the provision of critical services to the network. That is to say, Homing attack is the act of locating the presence of critical resources. As soon as the critical nodes are found, the attack are lunched by adversaries using other active means[21].

c. Sybil: This is the case in which an intruder , in illegitimate manner, claims or steals multiple identities and can also create new multiple identities[22, 23].Eventually, these identities can be employed by an intruder to disturb the functionality of the Wireless sensor network, or exploit the routing protocols and distributed storage[24, 25].

d. **Sink Hole:** Sinkhole attacks are carried out in network layer when an intruder attempts to attract some or most of traffic in a particular region.Essentially , the intruder can utilize many tricks like replaying or duping an advertisement for a high-quality link to the BS, the purpose behind that is to prevent base station from receiving a complete sensing data from nodes . After compromising the node, the intruder can employ it for launching an attack. Technically, the node that is compromised will send fake information to surrounding nodes about its link quality which used in routing metric to select best route during transmitting. Some routing protocols attempt to authenticate the bidirectional reliability of a route with end-to-end acknowledgments that encompass information concerning information reliability or latency. When considering the laptop-class attackers with an influential transmitter that has the ability for providing a high-quality link between a node and the BS, then

the attacker can, in an easy way, deceive the other nodes. The attacker makes influence considerably, which will allure all traffic that head to the BS from nodes, which might be several hops away from the compromised node[26].

e. **Wormhole :**Another form of attack faced by WSNs, this type requires inserting two malicious nodes at least in the network[27]. These infected nodes are connected by a strong link, for instance, a strong wireless signal or a wired liaison. An attack like this one works on misleading the other nodes of the network about the reality of the distance between two bad nodes and suggests a faster path. Practically in regard with wronging their neighboring nodes, those malicious nodes have the ability of replicating data of a distant node in order to convince them that they are within its neighborhood. In general, the routing protocols look for the route that has the shortest number of hops. Furthermore, in this attack, the two malicious nodes provide to achieve a faraway position with an extraordinary hop. This can wrong other nodes that are existed on the real distances separating the two malicious nodes. Eventually, Nodes select this shortest route for sending their data, and those nodes transmit their own data to the malicious nodes[28].

f. **False routing Attack:** An assaulting node operates in the process of routing of data packets for sending it in the incorrect track to deter their access to a legitimate receiver. Simply, the attacker has not only the ability to modify the routing information and creating direct links in the network, but also the ability of changing the path lengths ,or to attract the data packets direction to a particular node or spare them[29].

g. **Acknowledgment Spoofing Attack :** Many routing algorithms that are used in sensor networks at some point need acknowledgments to be used .The nature of the attack is as follows, an attacker could eavesdrop packet that is transmitted from its surrounding nodes and spoof the acknowledgement or send false information[24]. In this way, the attacker has the ability to spread wrong data about the node's status.

h. **Hello Flood Attack : i**n this attack, an attacker takes advantage of "HELLO" packet to be utilized as a weapon with high transmission power to persuade the sensor nodes that are distributed in large area within the WSN, starting with one node then onto the next with more vitality. Generally, several protocols need to broadcast HELLO" packets for the neighbor discovery. In that case, the legitimate nodes that send such packets to the BS could attempt to send over the assailing node assuming that it is the neighbor of theirs. The attacker can exploit that loophole for his own advantage and finally, spoofs the packets [30].

The Transport Layer Attacks

a. **Malicious Flooding Attack:** When the protocol needs to preserve the state at any endpoint of a connection, due to flooding attack, protocol can easily get vulnerable to memory exhaustion[30].Malicious Flooding happens when the

malicious node frequently transmits a considerable array of requests in order to establish connection, which negatively affects and lead to the depletion of resources of legitimate nodes. The huge traffic flooding that produced by these packets will make the network unable to differentiate between legitimate and malicious traffic. In either cases, genuine requests will be overlooked [32].

Countermeasures: Rate Limiting, Connection Queuing, Traffic Filtering, Resource Monitoring, and Captcha and Challenge-Response

b. **Resynchronization Attack:** The attacker makes modification to the packets sequence number for disturbing the communication protocol; it is evident that confirmation of packets might be a conceivable solution[33].

Countermeasures: Sequence Number Verification, Cryptographic Integrity, Connection State Maintenance, Randomized Sequence Numbers, and Time-Based Checks

Application Layer Attacks

a. **Programming Attack:** Nodes could be recreated in exceptional cases, that can be done by sending false information to nodes. This type of attack is likely addressed by the respectability of the program received[33].

Countermeasures: Code Validation and Verification, Digital Signatures, Firmware Integrity Checks

b. **Path-based Denial of Service Attack: The** route that nodes frequently use for data packet can be exploited to access BSs for sending a considerable number of false data packets. As usual, the nodes will be very engaged and sometimes they use up their resources while forwarding those packets, thus preventing genuine packet activity[33].

Countermeasures: Traffic Filtering and Analysis, implement traffic filtering, Rate Limiting, and, Dynamic Routing

c. **Intrusion detection system:** Intrusion detection is a significant subject of research and has multiple applications that affect confidentiality, integrity, and availability. In 2014, based upon the research conducted by Forbes, the most relentless intrusions including a cyber-attack was carried out and compromised customer data, a data security breach of Montana's state health records has compromised the Social Security Numbers and other personal information of some 1.3 million people. Also, an intrusion that struck P.F. Chang's China Bistro which led to the theft of customer data from credit and debit cards, and finally the intrusions that conducted against Evernote and Feedly users.

Countermeasures: Network Monitoring, Intrusion Detection and Prevention Systems (IDPS), Anomaly Detection, Regular Updates and Patching, User Authentication and Access Controls, and Encryption

An intrusion-detection system technology

Intrusion detection is undoubtedly very substantial for a better security policy. There are two key approaches for managing security aspect: prevention-based approach such as authorization, encryption, authentication e.g., and detection-based approach (intrusion detection systems). In any security plan, if intrusion prevention, which is seen as the first line of security, was passed by intruders, detecting approach would be the second line for a security plan and it aims to maintain deterrence for potential cyber-attacks, Intrusion detection offers a deterrence for the attacker and acts an alarm system for a network to manage security plans successfully.

An intrusion-detection system is an indispensable technology, and it has proved its affectivity. It can be defined as software or hardware tools, which is employed to monitor networks for any form of intrusions and serve as detector about internal or external cyber-attacks. Furthermore, an Intrusion Detection System can act as an observer and investigator to systems and user activities. It can also recognize the known attack patterns; detect the activity of abnormal network[34]. The general definition of intrusion-detection system is all about intrusions to network, but concerning Wireless sensor networks, an addition can be made to the definition "physical damages that may incur to sensor devices. On a related level, sensor damage identification is seen considerably important matter to act as fault tolerance and reliability[35].

Recently, researchers have suggested an array of security mechanisms based on intrusion detection system, which present an analysis to work of the nodes, to detect suspicious activity professionally. The researchers commonly concentrate on routing protocol attacks for illustrating their detection methodologies. There is a difference among the researchers' method in two ways, i.e. installing an intrusion detection system agent and detection procedures. Practically, there are three approaches regarding installing an intrusion detection system agent:

(1) Purely centralized system.
(2) Purely distributed system.
(3) Distributed-centralized system.

In the approach 1, the installation of intrusion detection system agent is restricted only at the sink or base station, while in the approach 2, intrusion-detection system agent exist in each sensor node. In the approach 3, for the process of intrusion detection only monitor nodes are used[36].

3.1 Classifications of intrusion-detection system

An intrusion-detection system can be categorized into two forms as follows: ***host-based intrusion-detection system*** **and network-*based intrusion-detection system***. That categorization relies on the logs of data collection, or the auditing of data generated by loadable-kernel modules (LKMs) that acts as interceptor to system calls. Network-based intrusion-detection system performs as detector of attacks by capturing and analyzing network traffic. Moreover, an intrusion-detection system can be categorized according to the detection method as it is described as follows[37]:

Signature-based detection observes events and identifies patterns that correspond to attack signature or sequences that refers to an intrusion. This technique can show low false-positive rates, but does not function, as it should be regarding attacks that were previously unknown, that is to say, used for threats we know[37].

Anomaly-based detection monitors system activity and classifying it as either normal or anomalous one where it performs on defining a profile of normal network behavior and categorizes any abnormality of that profile as an intrusion. The normal profile obtains updates as the system gets knowledge about the behavior of a subject. This method can detect attacks that were previously unknown but might show high rates of false positive; it is capable of detecting novel attacks[37].

Specification-based detection outlines an array of constraints that show the right task of a program or protocol and at the same time, observes the program for performing the determined constraints. However, this technique can likely be able to detect attacks that were previously unknown while showing a low false-positive rate, but is not as effective as anomaly-bases detection regarding the detection process of novel attacks[37].

Wireless Network's IDS Architectures

Moreover, in [37] have divided the architectures of wireless ad-hoc network intrusion-detection system into three types. It is possible to adjust this categorization based upon the requirements of wireless sensor network intrusion-detection system[1]. The three categorizations can be listed as follows:

1. Stand-alone architecture:

In this category, each node performs as an independent Stand-alone intrusion-detection system and holds the responsibility for identifying attacks that are directed only for itself. This type shares no information or makes cooperation with other systems. Obviously, an architecture like that indicates that all the network nodes are able of running an intrusion-detection system IDS[1, 37].

2. Distributed and Cooperative architecture:

In this type of architecture, all nodes run their own intrusion-detection system, in addition to, they participate considerably in a state of cooperation with each other regarding information –sharing for creating a global mechanism of intrusion detection [1, 37].

3. Hierarchical architecture:

In this type of architecture, dividing the network into clusters with cluster-head nodes, practically, the task that those nodes hold is to route within the cluster and also for accepting the accusation messages totally from the other cluster members that indicate something malicious. Furthermore, the cluster-head nodes could also perform as a detector of attacks against the network's other cluster-head nodes, since these nodes represent the primary element of the routing infrastructure [1, 37]

The challenges of designing an IDS for WSN

There are several difficulties that make developing a perfect intrusion detection structure for wireless sensor network non-trivial. There follows, we review the major difficulties to be taken into account when commencing to design an ideal system for detecting intrusion into the wireless sensor network[38].

a. **Resource constraints:** Typically, in traditional networks, the installation of intrusion detection systems is conducted on powerful computers such as mainframes on which IDSs are capable of operating professionally. On the other hand, in wireless sensor network, this is impossible due to the resource constrained sensors in regard with *computation*, *memory* and *power consumption*. Seemingly, it is very challenging task to design a powerful IDS since wireless sensor system consists of several number of small and low-priced sensors and those sensors are characterized of having very limited power, memory, storage capacity, signal bandwidth, and power processing capability.
b. **Dynamic topology change:** the continuing change in topology due to the position of the sensor in some applications of wireless sensor system has made it challenging task for the IDs to keep abreast with this dynamic change[38].
c. **Continuous data streaming:** Immense amounts of data flowing require online intrusion detection system to meet the requirements of type of data, the detection process of internet intrusions , in some applications, the online detection of intrusions is considered tremendously significant and an issue would accept the postponement[38].
d. **Different types of routing protocols**: diverse kinds of routing protocols have been utilized to cater the requirements to be followed concerning the various kinds of wireless sensor network applications. This is why; the intrusion detection scheme design for a type of routing protocols might not be suitable simply for other protocol and result in a very specific detection scheme [38].

e. **Difficulty in building intelligent IDS models**: Due to the lack of the labeled dataset containing both normal profiles and attacks, it becomes an extremely difficult task to utilize the techniques of artificial intelligence that requires training[38].
f. **Lack of standards**: Based upon our knowledge, there is no specific intrusion detection model for wireless sensor network like other kinds of networks. The availability of such a model can participate considerably in facilitating the standardization process and in evaluating of any proposed scheme of intrusion detection system in comparison to other schemes[38].

WSN application Intrusion detection system

Over the course of time, wireless networks have found utility across a diverse spectrum of use cases encompassing outdoor and indoor surveillance applications, telecommunications, and provision of online services. The operational landscape of contemporary networks is marked by a significant diversity in the nature of data being conveyed through these deployed systems. This assortment of network typologies in the present context underscores a pressing exigency for bolstering security mechanisms, owing to the multifarious array of potential cyber intrusions and breaches inherent in the modern milieu. Concurrently, the escalating exchange of data among disparate entities and networks accentuates the necessity for the development and implementation of apropos strategies aimed at fortifying network integrity [39].

An intrusion detection system (IDS) stands as a pivotal security application designed to identify instances of unauthorized access by both external entities and internal users within a system. The conceptual framework of an IDS can be construed as an encompassing entity, which meticulously observes the conduct of a system and offers countermeasures in response to aberrations detected within its operational patterns. In the context of contemporary computing systems, which grapple with a substantial influx of data, it becomes imperative to conceive more sophisticated and adaptable solutions. These security frameworks must demonstrate a degree of versatility across diverse computing platforms while concurrently furnishing an elevated echelon of protective measures. Thus, a pragmatic approach to surmount the challenges that characterize the contemporary landscape involves the integration of machine learning methodologies. This integration serves to streamline the monitoring process and heighten the security posture of wireless networks, thereby ameliorating the associated limitations.

Wireless Sensor Networks (WSNs) are configurations comprising energy-constrained sensors capable of capturing and transmitting data through wireless conduits. Operating under the constraint of finite battery resources, judicious utilization is paramount to avert premature energy depletion, which would lead to node incapacitation and resultant network coverage gaps. WSNs boast a myriad of applications spanning data aggregation,

environmental sensing, digital agriculture, remote monitoring, healthcare, and even military contexts such as border surveillance.

Enhance detection capabilities within vulnerable border regions. The establishment of a conventional communication infrastructure is imperative to ensure the security of such territories. This context necessitates the integration of novel network components, leading to a substantial surge in data generation within the interconnecting networks comprising these communicative entities. The continuous and uninterrupted monitoring endeavors undertaken within these regions precipitate a rapidly evolving paradigm of data interchange [39]. The stratification of network and application layers is realized through the utilization of high-capacity devices, ensuring data integrity and confidentiality. In contrast, the perceptual layer is instantiated through the deployment of a low-power Wireless Sensor Network (WSN). This WSN configuration comprises an array of sensor nodes, engaged in intercommunication through diverse radio frequencies, thereby facilitating an assortment of functions encompassing sensing, surveillance, measurement, and tracking. These wireless nodes, characterized by inherent constraints such as limited processing capability, constricted bandwidth, finite battery longevity, and constrained memory capacity, epitomize resource-constrained entities. The visual representation of the communication interplay amid the layers of the WSN is elucidated in Figure 1. The sensors in this architecture contribute to diverse functions, including sensing, surveillance, measurement, and tracking, albeit operating within the confines of their resource-constrained nature, defined by factors like restricted processing prowess, limited bandwidth, finite battery endurance, and constrained memory capacity. The intricacies of communication between the tiers of the WSN structure are illustrated [40].

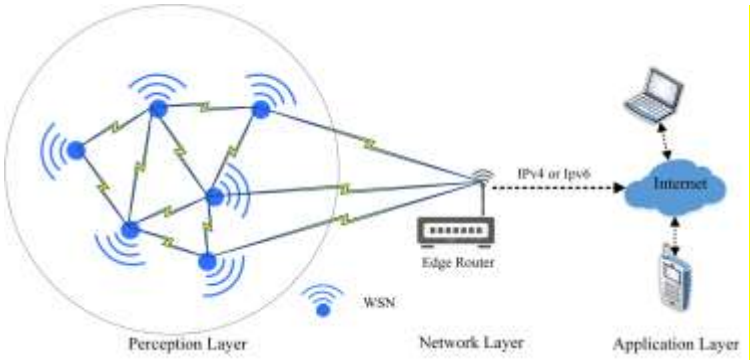


Figure 1. The communication among the WSN layers [40]

The WSN nodes are the basic building block of this layer and share some characteristics that distinguish them from other wireless networks. Among these characteristics are the following Independent nodes without a central control:

- Stationary or mobile WSN nodes
- The transmission range of WSN nodes is also limited
- The WSN network topology is constantly changing
- Multiple hop connections
- Limited bandwidth [40].

Literature Survey

In this section, we will review a number of past studies and theories for designing intrusion detection systems in wireless sensor network. Table 1. show past studies and theories for designing intrusion detection systems in wireless sensor network

Table 1. Past studies and theories for designing intrusion detection systems in wireless sensor network

No. references	Layers	The aim	The result
In [41]	**Physical Layer Security**	a new hybrid-network intrusion detection system based on Dempster-Shafer Theory of Evidence. The proposed method is to combine the features of signature-based and anomaly-based hybrid-network intrusion detection systems	The performance of the proposed method is evaluated in an experimental method with many scenarios in an IEEE 802.11 network and a test using Transmission Control Protocol traffic is also conducted to examine the influence of a jamming attack on forming a Transmission Control Protocol connection.
[42]	**Physical Layer Security**	The defender is to get optimal placements for the hubs and to detect positions for deploying anti-jamming devices on hub locations so that the total fixed cost of hub installation process is reduced and the total transportation is also reduced , (before and after jamming attacks).	to find the positions for placing jamming devices and works on disrupting the operation a wireless network , that results in maximizing the energy consumption and maximum transportation cost
[43]	**Data Link Layer Security**	describes detection algorithms for wireless sensor networks, which identifies a collision attack on the basis of the rate of packet flow to base station node in the network.	Simulation results have demonstrated that the algorithms have low false detection rates, false toleration and a small time to identify attacks.
[44]	**Data Link Layer Security**	detection algorithms for wireless sensor network, which function to detect a collision attack depending	The results of the simulation demonstrate that these algorithms have false detection rates, low false

		on the rate of packet flow to BS node in a wireless network	toleration and a small-time for detecting attacks.
[45]	**Network Layer Security**	a new detection mechanism, called a Cooperative RSS-based Sybil Detection (CRSD) for fixed WSNs, which uses the received signal strength (RSS) to deduce the distance between two identities. Furthermore , it identifies the positions of the identities by means of using the received signal strength information from many surrounding nodes	The analysis and simulation results show the following: 1. Sybil attack causes a significant deterioration in system performance. Cooperative RSS-based Sybil Detection (CRSD) is capable of detecting such attacks in most cases, thereby effectively protecting overall performance
[46]	**Network Layer Security**	The method detects Sybil attacks through anchor nodes position.	The theoretical analysis and experiments demonstrate this method can detect Sybil attacks in an effective way and participates in improving the security of WSNs.
[47]	**Transport layer Security**	a new bandwidth-efficient cooperative authentication (BECAN) scheme in order to filter false data, which is injected by an attacker. Depending on the random graph features of the cooperative bit-compressed authentication technique and sensor node placement, this proposal is able of saving energy by detecting in early stage and removing larger number of injected false data with minor further overheads at the en-route nodes. Additionally, a tiny portion of injected false data is required be verified by the sink, resulting in greatly minimizing the burden of the sink	Theoretical and simulation results show that the scheme is effective regarding energy saving and high probability filtering
[48]	**Transport layer Security**	an energy efficient multipath data transfer scheme to handle the problem that false data injection attack cause. It is possible to conduct that by detecting and filtering the injected false data proactively. Additionally, the multipath data transfer technique serves to inhibit	Simulations demonstrate that this scheme can considerably enhance the false data filtering process performance needles to lose resiliency against data compromisation and node compromisation.

		the direct access of event information via a compromised en-route node	
[49]	**Application layer Security**	a reversible watermarking scheme based on the data sampling interval against node clone attack. The watermark is computed from one data sampling time and integrated into the cluster data. The cluster totally recreates the watermark and statistical judge extract the features of the watermark.	Simulation and performance analysis demonstrate that the proposed scheme is effective in the term of detection results.
[50]	**Application layer Security**	a novel node's location speed time-based detection algorithm to detect node clone attacks in wireless networks	this algorithm greatly contributes in minimizing Communication overheads, Routing Overhead of the entire network and also contributes in improving the network throughput

Conclusions

Wireless Sensor Networks (WSNs) have emerged as a popular and versatile technology with a wide range of applications. However, their unique characteristics pose significant security challenges that must be addressed. Attacks targeting data confidentiality, integrity, and availability, as well as network-level attacks, can compromise the effectiveness and reliability of WSNs. This paper has shed light on the importance of securing WSNs and has reviewed various security solutions and protocols proposed to mitigate these threats. Encryption, access control, and intrusion detection systems have been explored as effective mechanisms to safeguard data and detect malicious activities. Moreover, a variety of attack types, such as node compromise, denial-of-service attacks, and attacks on network topology, have been discussed, emphasizing the need for comprehensive security measures. Looking ahead, future research should focus on addressing emerging threats, developing lightweight and energy-efficient security mechanisms, and designing secure routing protocols for WSNs.

References

1. Jabor MS, Azez AS, Campelo JC, Bonastre Pina A (2023) New approach to improve power consumption associated with blockchain in WSNs. PLoS ONE 18(5): e0285924. https://doi. org/10.1371/journal.pone.0285924.
2. Alrajeh, N.A., Intrusion Detection Systems in Wireless Sensor Networks: A Review. International Journal of Distributed Sensor Networks 2013.
3. Hussain, R.H., A Survey on Security Challenges in Wireless Sensor Networks. Journal of Thi-Qar University, 2017. 12(3).
4. T.Kavitha, Security Vulnerabilities In Wireless Sensor Networks: A Survey. Journal of Information Assurance and Security, 2010.
5. Zhang, Y.Z.Y.F.Y., Securing Wireless Sensor Networks: A Survey. IEEE Communications Surveys & Tutorials, 2008. 10(3): p. 6-28.
6. Poellabauer, W.D.a.C., Fundamentals of Wireless Sensor Networks. Wiley Series on Wireless Communicaions and Mobile Computing.
7. Hossain, M., Security Analysis of Wireless Sensor Network A Literature Review. 2015. 2(1).
8. Atique, S.V.M., Design Issues and Challenges in Hierarchical Routing Protocols for Wireless Sensor Networks, in Computational Science and Computational Intelligence (CSCI), International Conference. 2014.
9. Farooqi, A.H., A survey of Intrusion Detection Systems for Wireless Sensor Networks. Int. J. Ad Hoc and Ubiquitous Computing, 2012. 9(2).
10. T.Kavitha, D.S., Security Vulnerabilities In Wireless Sensor Networks: A Survey. Journal of Information Assurance and Security, 2010. 5.
11. Dinesh Kumar Gupta, Deepika Pathak “Safe Data Transfer Using Logic Gate Based Cryptographic Technique in Wireless Sensor Network”, Available Online at http://www.warse.org/IJATCSE/static/pdf/file/ijatcse351042021.pdf https://doi.org/10.30534/ijatcse/2021/351042021.
12. Aristides, D., Charalampos, and Grammati Aristides, Damianos, Charalampos, and Grammati IEEE COMMUNICATIONS SURVEYS & TUTORIALS, 2009. 11(4).
13. W. Xu, W.T., Y. Zhang, T. Wood, The Feasibility of Launching and Detecting Jamming Attacks in Wireless Networks. ACM international symposium on Mobile ad hoc networking and computing, 2005: p. 46-57.
14. Pelechrinis, I.a.V.K., Denial of Service Attacks in Wireless Networks:The case of Jammers. IEEE Communications Surveys & Tutorials 2011: p. 80-89.
15. W. Xu et al., Channel Surfing and Spatial Retreats: Defenses Against Wireless Denial of Service. ACM Wksp. Wireless Security, 2004: p. 80-89.
16. W. Xu et al., The Feasibility of Launching and Detecting Jamming Attacks in Wireless Networks. ACM Int'l. Symp. Mobile AdHoc Net. and Comp, 2005: p. 46–57.
17. Xu, W., Jamming Sensor Networks: Attack and Defense Strategies. IEEE Network, 2006.

18. Midkiff, D.R.R.a.S.F., Denial-of-Service in Wireless Sensor Networks: Attacks and Defenses. IEEE Communications Surveys & Tutorials, 2008.
19. J. P. Walters, e.a., Wireless sensor network security: A survey. Security in distributed, grid, mobile, and pervasive computing, 2007: p. 367.
20. David Martins., a.H.G., Wireless Sensor Network Attacks and Security Mechanisms : A Short Survey, in Wireless Sensor Network Attacks and Security Mechanisms : A Short Survey.
21. Stankovic, A.W.a.J., Denial of Service in Sensor Networks. Computer, 2002. 35: p. 54–62.
22. J. Newsome, E.S., D. Song, and A. Perrig, The Sybil Attack in Sensor Networks: Analysis & Defenses. in Proceedings of the 3rd International Symposium on Information Processing in Sensor Networks, IPSN '04, (New York, NY, USA), 2004: p. 259–268.
23. S. Raza, L.W., and T. Voigt, Svelte: Real-time intrusion detection in the internet of things. Ad hoc networks, 2013. 11(8).
24. Karlof, C.a.W., D., Secure routing in wireless sensor networks: Attacks and countermeasures. Ad hoc networks, 2003. 1(2): p. 293-315.
25. Douceur, J.R., The Sybil Attack. in Revised Papers from the First International Workshop on Peer-to-Peer Systems, IPTPS '01, (London, UK, UK), 2002: p. 251–260.
26. Saxena, M., Security in Wireless Sensor Networks A Layer-based Classification.
27. Hu YC, P.A., Johnson DB. , Wormhole attacks in wireless networks. IEEE Journal on Selected Areas in Communications, 2006. 24(2): p. 370–380.
28. Guyennet, D.M.a.H., Wireless Sensor Network Attacks and Security Mechanisms : A Short Survey, in International Conference on Network-Based Information Systems. 2010.
29. Chih-Chun Chang, S.M., David J. Nagel, Chih-Chun Chang, Sead Muftic, David J. NagelChih-Chun Chang, Sead Muftic, David J. Nagel, in Chih-Chun Chang, Sead Muftic, David J. Nagel. 2008.
30. Alzaid, H., Foo, E. and Nieto J.G., , January. Secure data aggregation in wireless sensor network: a survey., in In Proceedings of the sixth Australasian conference on Information Security. 2088, 93-105. p. 93-105.
31. Wood, A.D.a.S., J.A, Denial of service in sensor networks. Computer, 2002. 35(10): p. 54-62.
32. Ahmed S. Elqusy , S.E.E.a.A.E.-S., A Survey of Wireless Sensor Network Attacks. Communications on Applied Electronics (CAE) 2017. 6(10).
33. Mukherjee, N., Neogy, S. and Roy, S., , Building Wireless Sensor Networks: Theoretical and Practical Perspectives. 2015, CRC Press.
34. SAHINGOZ, O.C.O.K., A Survey of Intrusion Detection Systems in Wireless Sensor Networks. IEEE, 2015
35. Cao, F.H.a.X., Wireless sensor networks: principles and practice. Auerbach Publications, 2010.
36. Khan, A.H.F.a.F.A., A survey of Intrusion Detection Systems for Wireless Sensor Networks. Int. J. Ad Hoc and Ubiquitous Computing, 2012. 9(2).

37. Ko, P.B.a.C., Challenges in intrusion detection for wireless ad-hoc networks. in Applications and the Internet Workshops, 2003: p. 368373, 2003.
38. Murad A. Rassam, M.A.M.a.A.Z., A Survey of Intrusion Detection Schemes in Wireless Sensor Networks. American Journal of Applied Sciences 2012.
39. Tanya Sood , Satyartha Prakash , Sandeep Sharma , Abhilash Singh Hemant Choubey, Intrusion Detection System in Wireless Sensor Network Using Conditional Generative Adversarial Network", Accepted: 7 May 2022. https://www.researchgate.net/publication/360963737.
40. Rami Ahmad , Raniyah Wazirali , and Tarik Abu-Ain "Machine Learning for Wireless Sensor Networks Security: An Overview of Challenges and Issues", Issues. Sensors 2022, 22, 4730. https://doi.org/10.3390/s22134730.
41. Diego Santoro , G.E.-A., Konstantinos G. Kyriakopoulos, Francisco J. Aparicio-Navarro, David J. Parish, Michele Vadursi, A hybrid intrusion detection system for virtual jamming attacks on wireless networks. Elsevier, 2017
42. 42. Raheleh Khanduzi , A.K.S., Tabu search based on exact approach for protecting hubs against jamming attacks. Computers and Electrical Engineering,Elsevier, 2019
43. Hosamsoleman, A.P., Nasser Mozayyania and SaeedSedighianKashi , , Detection Collision Attacks In Wireless Sensor Network Usingrule-Based Packet Flow Rate. International Journal of Engineering Research and Applications (IJERA), 2013. 3(4): p. 261-268.
44. Punam Dandare, P.V.C., Detection of Collision Attacks and Comparison of Efficiency in Wireless Sensor Network. International Journal Of Engineering And Computer Science, 2016. 5(5): p. 16400-16406.
45. S. Lv, X.W., X. Zhao and X. Zhou, Detecting the Sybil Attack Cooperatively in Wireless Sensor Networks, in International Conference on Computational Intelligence and Security. 2008. p. 442-446.
46. B. Tian, Y.Y., L. Shi, S. Shao, Z. Liu and C. Xu, A novel sybil attack detection scheme for wireless sensor network, in 5th IEEE International Conference on Broadband Network & Multimedia Technology. 2013. p. 294-297
47. R. Lu, X.L., H. Zhu, X. Liang and X. Shen, BECAN: A Bandwidth-Efficient Cooperative Authentication Scheme for Filtering Injected False Data in Wireless Sensor Networks. IEEE Transactions on Parallel and Distributed Systems, 2012. 23(1): p. 32-43.
48. S.V. Annlin Jeba , B.P., Energy efficient multipath data transfer scheme to mitigate false data injection attack in wireless sensor networks. Computers and Electrical Engineering Elsevier, 2013
49. Chen, T.G.a.Y., A node clone attack detection scheme based on digital watermark in WSNs, in First IEEE International Conference on Computer Communication and the Internet (ICCCI), Wuhan. 2016. p. First IEEE International Conference on Computer Communication and the Internet (ICCCI), Wuhan.
50. Patil, D.S.P.a.S.C., A Novel Algorithm for Detecting Node Clone Attack in Wireless Sensor Networks. International Conference on Computing, Communication, Control and Automation (ICCUBEA), Pune, 2017: p. 1-4.

Study The Effects of Different Doses of Tylosin Tartrate On Hematological Parameter and Some Reproductive Hormones On Male White Mice

Awatif I. Muhammed [1], Ban Sahib Abdul-Nabi AL-Nasiry [2]

© 2023 The Author(s). This open access article is distributed under a Creative CommonsAttribution (CC-BY) 4.0 license.

Abstract: The current study aims to evaluate the toxicological and physiological effects of Tylosin tartrate (Tylo. Tart.), in different doses used (250,500,1000) mg/kg, and its effect on various blood parameters and reproductive hormones in male white mice treated daily for 4 weeks compared to the control group. In the present study, attention was paid to recording the changes in the weights of the mice before and after dosing, the study result showed non-significant differences in the weights of mice, indicating that (Tylo. Tart.) was not effect on weights during the dosing periods. Various blood parameters were examined and significant differences were observed in the number of immune cells, that had a prominent role in removing internal or external influences in the tissues of the reproductive organs beside the ratio of male hormones, indicating that (Tylo. Tart.), has a direct effect on male hormones positively reflected on increase the fertility activity of mice was shown visually through the obvious increase in the size of the testicles of treated mice compared to the control group, this was shown through histopathological sections of the testes of mice, a clear activity of (Tylo. Tart.), in different doses to rises the efficiency of spermatogenesis.

Conclusion, the current study proved that the use of (Tylo. Tart.), in various doses has no toxic or side effects, while it has a significant effect on male reproductive efficiency, thus that (Tylo. Tart.), enables to be adopted in the future in veterinary drug formulations interested in fertilization.

Key Words: Tylosin, blood parameter, male hormones.

Author details

[1] Veterinary Drug and Production Research Center, Corporation of Research and Industrial Developmental, Ministry of Industrial and Minerals, Baghdad, Iraq

[2] Zoonosis Diseases Research Unit, College of Veterinary Medicine, University of Baghdad, Baghdad, Iraq

Citation information

Cite this article as:

Muhammed, A.I., AL-Nasiry, B.S., (July 2023), *Study The Effects of Different Doses of Tylosin Tartrate On Hematological Parameter and Some Reproductive Hormones On Male White Mice*, Proceedings of the Minar Congress, Turkey, (9) pp 265-272, DOI: http://dx.doi.org/10.47832/MinarCong9-22

http://dx.doi.org/10.47832/MinarCong9-22

[1] muhammedawatif@gmail.com orcid.org/0000-0001-8297-7066

[2] ban.sn62@covm.uobaghdad.edu.iq orcid.org/0000-0002-3349-4153

Introduction

Tylosin tartarate (Tylo. Tart.), is a broad spectrum time-dependent antibiotic against Gram- negative bacteria such as Haemophilus sp.,Pasteurella sp. and Gram- positive bacteria like Staphylococcus, Streptococcus, and Corynebacterium. (Tylo.Tart.), is belong to the macrolide family, commonly used in companion and farm animals. Its mode of action is based on the inhibition of bacterial protein synthesis that leads to bacteriostatic effect (1,2). As well as, it's used as a food additive in animal feed. This antibiotic is widely used in veterinary medicine to treat a number of bacterial diseases in animals. Recently, it has been widely used as a growth stimulant (3, 4, 5). Typically, Tylosin is used as a mixture of closely related compounds: Tylosin A, B, C and D. Tylosin A is the predominant form (> 80%) and Tylosin D is also the major metabolite being formed in vivo. (Tylo. Tart.), is a naturally created antibiotic from Streptomyces fradia that inhibits bacterial protein synthesis by inhibiting ribosome 50, which is used to manufacture bacterial protein (1). (Tylo. Tart.), is given by injection or orally in the treatment of infections of the respiratory tract and skin infections. Histological changes of (Tylo. Tart.), in the spleen and anti- carcinogenic role were observed in poultry (6). In another study, (Tylo. Tart.), was given orally in different doses in varying periods, ranging from 16- 65 days, they were proven that (Tylo. Tart.), had a significant effect in reducing the level of the hormone LH and FSH (2,7). Furthermore, it has a role in inhibiting testosterone hormone production (2, 8). The current study, aimed to clarify the toxic effects of different doses of (Tylo. Tart.), administered orally for 30 days on blood parameters and male hormones in mice.

Materials Used

Animals and treatment

The study was included 20 male albino mice. were obtained from animal house of Alrazi-Research center. (weighted 20- 25g) at 14- 16 weeks age, They were placed in plastic cages an ambient temperature of 27±2°C with 12h-light and 12h-dark cycle. and provided with water and food ad libitum. They placed in animal house for 30 days for adaptation before starting the experiment. The experiments on animals were performed based on the guidelines of the institutional animal ethics committee.

Experimental Design

20 albino mice divided into 4 groups divided as fallowed:

First group (F1): treated with (Tylo. Tart.), 250 mg/kg only was given orally with 0.2 ml daily for 30 days.

Second group (F2): treated with (Tylo. Tart.), 500 mg/kg only was given orally with 0.2 ml daily for 30 days.

Third group (F3): treated with (Tylo. Tart.), 1000 mg/kg only was given orally with 0.2 ml daily for 30 days.

Fourth group (control): was given orally with 0.2 ml daily Distilled water only for 30 days.

Mice were weighed before and after the dosing period. Animals were euthanized after 30 days of oral administration. The macroscopic pictures were done, in addition Histopathological examination. Blood samples were collected (0.5 ml.) from all mice for necessary tests and kept at -4C0 until use.

Blood parameters measurement:

Blood tests were performed using BECKMAN hematology analyzer included: total count of red and white blood cells, hemoglobin concentration and platelet count.

Hormones level measurement:

Employed ELISA assay to measure hormones such as: LH, FSH, Progesterone and Testosterone.

Histopathology

After incubation period, the histological analysis was performed by examining the morphological changes induced by (Tylo. Tart.), on testis. These organs were collected and fixed with 10% formalin, embedded in paraffin, and cut into 5-µm thick sections (Mescher method 2013). The fixed sections were stained for analysis using hematoxylin and eosin (H and E) staining. The sections were examined under binocular microscope (Olympus CH-2, Tokyo, Japan), and photomicrographs of the fixed organs were obtained. to demonstrate the side effects of (Tylo. Tart.), on the tissue of treated groups compared to the control group.

Statistical Analysis

The SAS software (Version 17) was applied to this investigation to identify how various factors affected the study's variables. In this work, a significant comparison of means was made using the Mean ± SE standard error test performed with one-way analysis of variance (ANOVA).

Results and Discussion

Clinical signs: oral administration of (Tylo. Tart.), using in different doses didn’t show any changes in appearance or behavior of mice also, no mortality were observed, while since the first days of dosing it was observed an

Increase in the sexual ability of mice for all groups dosing with (Tylo. Tart.), compared to control group with an increase in the size of the genitals and their protrusion to the outside with an increase significant in weights of dosing groups of (Tylo. Tart.), compared to control. Through the current study, it was noticed that (Tylo. Tart.), has an effect on body weight indirectly through an increase that was observed visually on genitals, this an increase in

weight is not significant and it's a healthy condition in mice considering (Tylo. Tart.) Is one of the growth stimuli in veterinary medicine that agreed with (9).

Table 1. Body weights of male mice dosing (Tylo. Tart.) in different groups compared to control group.

Body weight (gm.)	(F1)	(F2)	(F3)	control
	27.02±1.01	*28.21±1.21	27.01±1.21	26.22±3.21

(Mean ± SE), * significant difference p≤0.05 **Table 3. Properties of clay soil**

Table 2. shows blood tests of male mice dosing (Tylo. Tart.) in different groups compared to control group

Tests	HGB gm/dl	RBC $\times 10^6/mm^3$	PLT $10^3/mm^3$	HCT %	MCV Fl.	MCH pg.	MCHC g\dl
F1	6.13±0.21	2.28±0.02	251.8±0.21	20.2±0.11	90.9±0.31	26.9±0.23	29.6±0.21
F2	6.00±0.22	2.81±0.01	248.3±0.20	20.3±0.21	72.3±0.21*	21.4±0.21*	29.0±0.20
F3	10.72±0.02*	3.78±0.01	417.5±0.04*	35.8±0.24*	94.8±0.25	28.4±0.26	29.9±0.24
Control	6.01±0.10	2.33±0.01	198.9±0.02	20.0±0.21	85.3±0.21	29.1±0.21	29.1±0.21

(Mean ± SE), * significant difference p≤0.05

Results of Table (2) showed there was a significant difference in the numbers of red blood cells includes: RBC, Hb, PLT, HCT and MCV of mice for all groups dosing with (Tylo. Tart.), compared to control group. And a sharp decrease was observed in MCH of F2 group compared to F1, F3 group and control. A previous study proved that (Tylo. Tart.) helps to absorption of iron from the intestine. Iron is the main component of red blood cells and hemoglobin formation, therefore an unexpected increase is observed in the numbers of red blood cells and their size and contents (10).

Table 3. shows differential white blood cells of male mice dosing (Tylo. Tart.) in different groups compared to control group

Tests	WBC	Neut%	Lymph%	Mono%	Esio%	Baso%
F1	**2.31±0.20**	53.54±0.20*	40.08±0.52*	3.08±0.23	3.21±0.31*	0.09±0.12
F2	2.12±0.20	42.68±0.20*	48.23±0.54*	5.66±0.23*	3.28±0.12*	0.15±0.02
F3	**3.23±0.41**	55.83±0.41*	38.50±0.45*	2.40±0.23	3.12±0.23*	0.15±0.01
control	2.67±0.31	30.67±0.31	64.00±0.51	2.67±0.21	1.67 ±0.10	1±0.01

(Mean ±SE), * significant difference p≤0.05

Results of Table (3) revealed a significant increase in the numbers of basophils and eosinophil's, while a significant decrease in lymphocytes, in addition, a non- significant increase in the numbers of monocytes, and no significant difference in the numbers of white

blood cells of groups treated with (Tylo. Tart.), compared to control. White blood cells are one of the factors of inflammation and immune response in the body. (Tylo. Tart.), directly effects on the digestion process and works to create a balanced microbial environment, the results is increase in the digestive processes in the intestine thus, increasing growth and immune response (11).

Monocytes are among the most important cells of the immune system that repair and remove harmful tissues, moreover, their percentage increased and they had a role in removing internal stimuli or any inflammatory factors that occurred during or after (Tylo.Tart.), dosing. The changes in White blood cells count values are small differences as a result of high doses of (Tylo. Tart.), that corresponding with previous studies (12, 13)

Table 4. shows hormones tests of male mice dosing (Tylo. Tart.) in different groups compared to control group

Tests	FSH mIU/ml	LH mIU/ml	Progesterone ng/ml	Testosterone ng/ml
F1	2.91±0.01*	5.80±0.012*	0.42±0.11	*1.70±0.012
F2	2.51±0.012	5.8±0.012*	0.8±0.012	*1.86±0.012
F3	2.47±0.012	4.3±0.012*	1.0±0.012	1.32±0.012
Control	2.40±0.01	3.65±0.011	1.4±0.02	1.20±0.012

Results of Table (4) revealed significant differences between the groups treated with (Tylo. Tart.), as a significant increase P≥ 0.05 in the level of LH and Testosterone hormones while no significant differences in FSH was observed in all groups that treated with (Tylo. Tart.), compared to control. The results of current study proved that doses used of (Tylo. Tart.), led to an increase in Testosterone hormones level by increasing the stimulating factor of LH hormone, that meaning these doses were absorbed faster and gave a direct effect on the hypothalamic- pituitary-gonadal axis in mice, its role led to an increase in stimulating LHRH hormones levels and increase LH production, thus, led to an increase in testosterone hormones (14). This increase appeared clearly through the increase in the weights of mice treated with (Tylo. Tart.), due to indirect effect of the growth hormone. Results of present study showed that giving (Tylo. Tart.), orally in the doses employed led to an increase in testosterone hormones more quickly than adding it to the feed, as in a previous study (15, 16).

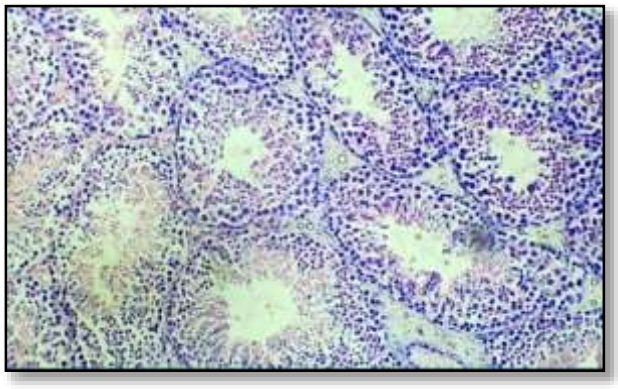


Figure 1.

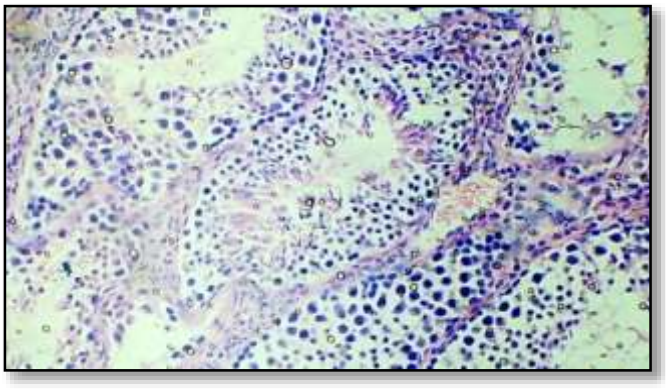


Figure 2.

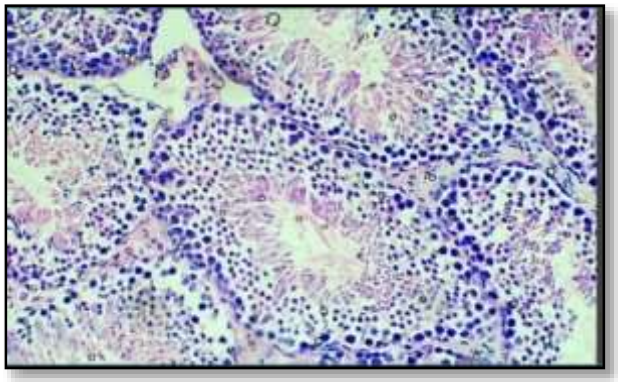


Figure 3.

Figures 1-2-3. Histopathological section of testis of group (F1), (F2) and (F3) treated Tylosin orally at dose 250,500 and 1000 mg/ kg b.w showing remarkable improvements, with closely packed tubular structures and primary spermatocytes, early and late spermatids and large numbers of sperm cells inside the lumen (H & E, ×400).

Conclusions

The administration of (Tylo. Tart.), orally in the doses employed gave non- significant differences in blood indicators, while there were significant differences in the parameters of male hormones and increase in the activity of mice treated with (Tylo. Tart.), with a visually increase in the size of testes, and absence of toxic or side effects during the dosing. Finally, (Tylo. Tart.), can be used in the future in veterinary pharmaceutical formulations or industries.

References

1. Poźniak, B.; Tikhomirov, M.; Motykiewicz-Pers , K.; Bobrek, K. and Świtała, M. (2020). Allometric analysis of tylosin tartrate pharmacokinetics in growing male turkeys. J Vet Sci.; 21(3): 11. doi.: org/10.4142/jvs.2020.21.e35
2. Kang, J.W.; Hossain, M.K.; Park, H.C.; Kim, T.W. and Jeong, S.H. (2020). Physiological influence of tylosin tartrate overdose in vivo in rats. ACTA VET. BRNO; 2020, 89: 283–290. doi.org/10.2754/avb202089030283
3. Baggesen, D.L. ; Wingstr, A.; Carstensen, B.; Nielsen, B.; and Aarestrup, F.M. (1999). " Effects of the antimicrobial growth promoter tylosin on subclinical infection of pigs with Salmonella enterica serotype Typhimuriumm". Am J Vet Res.; 60 : 1201-1206.
4. Vissiennon, T.; Kroger, H.; Kohler, T. and Kliche, R. (2000). "Effect of avilamycin, tylosin and ionophore anticoccidials on Clostridium perfringens enterotoxaemia in chickens." Berl Muench Tieraerztl Wochenschr J.; 113: 9-13.
5. Al-Nasiry, B.S.A.N. (2022). Pathological changes of salmonella typhimurium and treatments with some extracts of Cinnomomum zeylanicum and comparing with chloramphenicol in mice. Biochem. Cell. Arch.; 22(2): 3719- 3925. Doi: 03896.2022.22.3719
6. Baba, T.; Yamashita, N.; Kodama, H.; Mukamoto, M.; Asada, M.; Nakamoto, K.; Nose, Y. and McGruder, E.D. (1998). "Effect of tylosin tartrate on humoral immune responses in chickens." J Vet Med B.; 45: 279-286.
7. Meisel, M.L.; Winterhoff, H. and Jekat, F.W. (1993a)."Effects of tylosin on the pituitary-gonadal axis in male rats". Basic Clin Pharmacol Toxicol.J.; 72: 336-340.
8. Meisel, M.L.; Winterhoff, H. and Jekat, F.W. (1993b)." Tylosin inhibits the steroidogenesis in mouse leydig cells "in vitro". Life Sci; 53: 77-84.
9. Yildiz, S.; Ozturkler, Y.; Uzun, M.; Kaya, M. and Ucar, O. (2004). " Tylosin does not affect GnRH-induced LH secretion in rams". Reprod Toxicol J.; 18: 131-134.
10. Sellers, R.S.; Morton, D.; Michael, B.; Roome, N.; Johnson, J.K.; Yano, B.L.; Perry, R. and Schafer, K. (2007). "Society of toxicologic pathology position paper: organ weight recommendations for toxicology studies". Toxicol Pathol. J.; 35: 751-755.
11. FAOWHO, "Preparation and use of food based dietary guidelines, world health organization". Roma, Italy; v.1,1998.
12. Aly, S.; Ahmed, Y. A. and Mohamed, M.F. (2008). Studies on Bacillus subtilis and Lactobacillus acidophilus, as potential probiotics, on the immune response and resistance of Tilapia nilotica (Oreochromis niloticus) to challenge infections. Biology, Medicine Fish & shellfish immunology; 25: 128-136.
13. Kilpinen, S.; Spillmann, T.; Syrjä, P.; Skrzypczak, T.; Louhelainen, M. and Westermarck, E. (2011). "Effect of tylosin on dogs with suspected tylosin-responsive

diarrhea: a placebo-controlled, randomized, double-blinded, prospective clinical trial". Acta Vet Scand J.; 53:1- 26.

14. Kang, J. W.; Hossain, M. A.; Park, H.; Kim, T. and Jeong, S.H. (2019). Physiological influence of tylosin tartrate overdose in vivo in rats". ACTA VET. BRNO; 89: 283–290.
15. M Kelly, D. and Jones, T. H. (2015)." Testosterone and obesity". Obes Rev. J.; 16 (7): 581-606.
16. Meisel, M.L.; Winterhoff, H. and Jekat, F.W. (1993)."Effects of tylosin on the pituitary-gonadal axis in male rats". Pharmacol Toxicol. J.; 72 (4-5): 336-40.

Using Walnut Peel as a Natural Dye with Natural Wool Fibers

Hiba Swadi [1], Nagham Swadi [2]

Meena M. Abdul-Hussain [3], Ola Subhi [4]

© 2023 The Author(s). This open access article is distributed under a Creative CommonsAttribution (CC-BY) 4.0 license.

Abstract: The research aims to use the dye of walnut shells extracted from the hard shells of the walnut plant, and the dyeing process was applied to the fibers of Iraqi wool, using potassium aluminum sulfate (alum) as a stabilizer for the dye in the acidic and alkaline mediums at different concentrations. Yellow at the acidic medium for all the concentrations used, and dark yellow and brown at the basic medium at concentrations (10%,15%,20%,25%), where the color degree of the dye used at acidic conditions was less compared to the color degree of the dye in the basic medium, and the dye used was characterized by its stability towards Many factors, including high stability towards sunlight, it was observed that the color resulting from the use of the dye was not affected by the rays emitted from the sun, and the results of the examination of washing with soap and water and detergents were (5, 4/5, 4, 3), while the results of acid and base perspiration were recorded (5, 4/5,4) As for the dry rubbing and wet rubbing tests, the results were good and recorded (5,4/5,4,3).

Key Words: Natural Dye, Walnut shells, Wool, Stabilizer.

Author details

[1] Department of chemistry and biochemistry, Collage of Medicine, Al-Nahrain University, Baghdad, Iraq

[2-4] Alteraz for textile and leather Research center, Corporation of Research and Industrial Development, Iraq

[3] Department of chemistry and biochemistry, Collage of Medicine, Al-Mustansiriyah University, Baghdad, Iraq

Citation information

Cite this article as:

Swadi, H., Swadi, N., Abdul-Hussain, M.M., Subhi, O., (July 2023), *Using Walnut Peel as a Natural Dye with Natural Wool Fibers*, Proceedings of the Minar Congress, Turkey, (9) pp 273-283, DOI: http://dx.doi.org/10.47832/MinarCong9-23

http://dx.doi.org/10.47832/MinarCong9-23

[1] haibi.83.83.83@gmail.com

[2] nagham2020999@yahoo.com

[3] meena.Khd@yahoo.com

[4] renasaalaany2014@gmail.com

Introduction

The use of natural plant resources to create dyes for textiles or other materials is known as natural plant dyeing.

These colors are derived from actual plant materials like stems, roots, and fruits, peels, flowers, and leaves. The earliest record to show usage Some natural plant dyes may be found in China as early as 2600 B.C. As According to archeological data, only a few species of plants and animals Back then, ingredients were utilized to extract natural color's (1)

Although the textile industries are considered less polluting the environment compared to other industries, the dyeing process with chemical dyes is one of the main sources of environmental pollution of all kinds. Therefore [2] recently, research and studies tended to use natural dyes instead of chemical dyes due to the toxic and harmful effects of chemical dyes in the field of public health for humans and the field of environmental pollution of all kinds. Pomegranate, banana, beetroot, etc. Various natural dyes were extracted from them, and because natural dyes are non-harmful and non-carcinogenic materials, and they have the ability to dissolve in water, studies and research tended to use and apply this type of dye on natural and industrial textile fibers in addition to leather instead of using dangerous chemical dyes [3, 4,5,6].

Although natural dye has not been designated as a disperse dye, it is believed that some natural dyes can be categorized as such based on their solubility and structural features.(7)

Aim of the Research

Benefiting from plant residues (husks) instead of throwing them away and using them as natural, environmentally friendly dyes for dyeing wool fibers.

The Theoretical Part

Wool is a natural fiber consisting mainly of protein known as keratin and on units of free amino acids [8]. One of the most important types of amino acids: cysteine and contains sulfur. Serine, Analine, which are neutral, and Argnine, which is alkaline. Glutamic acid is a reactive acid. These amino acids contain at least one group of basic amino effect -NH2 group and carboxylic acid group -COOH in addition to the presence of carboxylic groups with the presence of some elements such as carbon by 50%, hydrogen 6%, oxygen 25%, nitrogen 15%, ash 0.5% and sulfur 3% The wool contains lanolin fat and is secreted by cells under the skin, protecting the body from rain and surrounding weather factors.

The structure of the pigment consists of several colored groups, which are chromophores or color carriers such as carbonyl groups, anthraquinones, etc., and exochromes or color assistants such as the amine group, carboxylate, pathochrome, or color enhancer, and hippochrome [9,10]. Natural dyes are divided into three categories: vegetable dyes, animal dyes, and mineral dyes [10].

The dye extracted from the husks of the walnut plant. The nut is known by the scientific name Juglans regia and the colloquial name Wallnut. The length of the tree is about 20 meters. It is found in cold places such as southern Europe, North Africa, eastern Asia, southwestern America, etc. [10] The leaves, stems, fruits, and their green peels and solid structure were used in various fields, including the treatment of various types of diseases, including skin, digestive, and nervous diseases, and the elimination of parasites and worms, in addition to using them as natural dyes [11,12]. The walnut peel is characterized by the fact that it contains several compounds, including the naphthoquinones group and the hexagonal phenolic compounds, which is the main substance responsible for the dye present in the peel (juglone). [13,14,15,16].

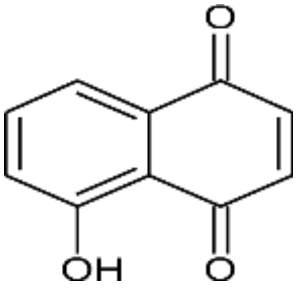


Figure 1. The chemical structure of juglone (17)

The research used many fixatives to fix the dye of walnut shells and compare the colors of the resulting dye without using the fixative, including tannin, potassium aluminum sulfate, and others [17].

The Practical Side

Materials used:

1. Iraqi wool fibers from the General Company for Textile and Leather Industry / Al-Soufi Factory.
2. Dry walnut shells in a powder form (the shells were ground in a mill to turn them into powder).
3. Potassium aluminum sulfate (alum) BDH chemicals Ltd pool England
4. Acid sweating solution (Hysteine monohydrogen chloride, Sodium chloride, Sodium orthophosphate dihydrogen dihydrogen dimer water molecule) The solution was prepared according to the Iraqi standard issued by the Central Organization for Standardization and Quality Control.
5. Base sweating solution (Hysteine monohydrogen chloride, Sodium chloride, Sodium orthophosphate dihydrogen dihydrogen dihydrogen water molecule and Sodium hydroxide). The solution was prepared according to the Iraqi standard issued by the Central Organization for Standardization and Quality Control.
6. Laboratory ethanol alcohol concentration 99% J.T Baker The Netherlands.
7. Hydrochloric acid
8. Sodium hydroxide

Devices used: Several devices were used to conduct laboratory tests in the modeling and packaging centers, as shown in Table

Table 1.

NO.	The device name	Origin	Model	The manufacture company	Capacity
1	Crockmeter	England		James heal	1 sample
2	Washing and Dry Cleaning Color Fastness Tester	England	825	James Heal	8 samples
3	sensitive balance	German	D-72336	KERN	d: 0.01g MAX:1610 g
4	Oven	German	—	Memart	Heat MAX. :250 ℃
5	Water bath Digital	England	LWB-111D	DAIHAN	11
6	Brightness and colourmeter	American	JY9800		1sample
7	Accelerated Weathering Tester	American	14-1621-84-SE	Q-LAB-QUV/SE	48 sample
8	GC mass	American	-------	------	------
9	FTIR spectrophotometer	German	DHAIHAN	TENSOR27	Mid-IR source (4000-400cm)

The method of work: The walnut shells were taken and grinded with a mill with sharp knives. The resulting powder was a powder. The type of active compounds present in the husk powder was detected. The powder was also examined using the FTIR device in the Ibn Al-Bitar Center to know the types of chemical compounds present in the resulting powder, according to the attached figure No. (1). The detection of active compounds using GC mass, according to the attached table No.(2)

Table 2.

NO.	Detection type	The result
1	Tannins test	+
2	Carbohydtate test	+
3	Glycosides test	-
4	Phenols test	-
5	Resins test	-
6	Flavonoids test	+
7	Saponin test	-
8	Alkaloid test	+
9	Protein test	-
10	Coumarins test	+
11	Terpenes test	-
12	Steroids test	-

The alcoholic solvent ethanol was used at a concentration of 99% for the purpose of dissolving the peel powder in the water bath, and two methods were followed to obtain the dye. The solution is cooled, filtered, and re- filtered several times until the dye is obtained, then it is applied to the wool samples to be dyed and at the mentioned concentrations [18]. It has different concentrations to be applied to the wool fibers to be dyed [19].

Dyeing process

The dye was added to the bristles of Iraqi wool after soaking it in plain water for a while, as the samples were dyed with different concentrations of dye extracted from walnut shells (5%, 10%, 15%, 20%) and placed in the dyeing samples attached to the dyeing apparatus, and potassium aluminum sulfate (potassium) stabilizer was added to it. alum) with a concentration of 1% [19] and the dyeing process was carried out using a Gyrosh washing machine.

The dye addition experiments were conducted in the acidic medium and the basic medium, and the degree of acidity (pH values) was adjusted for the samples before and after the dyeing process. The basic pH values were (8-10) after adding sodium carbonate to the dye solution, and the time required to perform the wool dyeing process was (60) minutes at a temperature of 40 degrees Celsius for the first (10) minutes of the dyeing process, and then the temperature was gradually increased until it reached to (60) degrees Celsius for a period of (60) minutes, according to the method [20], and after the end of the period required for dyeing, the dyed wool samples were taken out and washed with tap water to remove excess dye residues.

Tests used: To know the stability of the dye on the used wool fibers

1. Check the colorimetry

   The dyed samples were examined with a Brightness and colourmeter at the National Center for Packaging and L, a, b, and values were extracted, where L represents the degree of whiteness in color, L- the degree of color towards black, a towards red, and a- towards green, and b represents color yellow and b- towards blue.

2. Check for color fastness to washing with soap and water and detergents

   The ability of the dyed patterns to be fixed with water was measured by placing the dyed wool patterns between two white cloths attached to the machine and washed using the Gyrosh washing machine according to the specifications of the Central Organization for Standardization and Quality Control No. 170 of 1989.

   As for the color fastness test by washing with soap and detergent, according to the Iraqi standard specification issued by the Central Organization for Standardization and Quality Control No. 116 of 2018, and the following steps were followed, where (2gm) of soap was used standard soap -without optical brightener per liter of water Added to the samples in the washing machine (Gyrosh) and for a period of (15

minutes), the results of color change and staining were recorded on the white cloth wrapping the dyed sample, and the same method was followed for the used detergent.

3. Examination of acid and base perspiration: color fastness to perspiration, according to Iraqi Standard No. 52 of 1989.

   Acid and base sweat solutions were prepared and added to samples stained with walnut shell dye, and the results were recorded

   Method for preparing an acid sweating solution: To prepare a liter of an acid sweating solution, add 0.5 g of histidine monohydrogen chloride, 5 g of sodium chloride, add 2.2 g of sodium orthophosphate dihydrogen dihydrogen dimolecule water, and add a 0.1 N solution of Sodium hydroxide to bring the solution to a pH of 5,5

   Method of preparing the base sweating solution: To prepare a liter of it, add 0.5 g of histidine-hydrogen monochloride, 5 g of sodium chloride, and 5 g of sodium orthophosphate monohydrogen, and a 0.1 N solution of sodium hydroxide is added to make the pH 8.

4. Examination of the fabric's wet and dry rubbing ability. color fastness to rubbing according to Iraqi Standard No. 906 of 2001.

   Samples were taken and tested with a color fastness tester for wet and dry rubbing (Crockmeter) and the results were recorded based on the gray scale.

5. Testing the dye's stability against sunlight

   Samples stained with the dye were displayed in acidic and alkaline media, in addition to the control treatment to the sun's rays for a period of two weeks, where three quarters of the sample were covered with opaque papers to block the sun's rays, and the remaining quarter was exposed to the sun's rays 105 of 1990.

Results and discussion

The type of compounds present in the resulting dye was diagnosed by FTIR absorption spectrum, and the examination showed an absorption band at frequency 3344.28, which belongs to the N-H and C-H groups that are found in phenolic compounds such as juglane, which is responsible for showing the dye and flavonoids, while at 2926.23 it belongs to the C≡N group and less From 2000 belonging to the C = O and C = C groups, which belong to the group of ketones and amides [21], as shown in Graph No. (1).

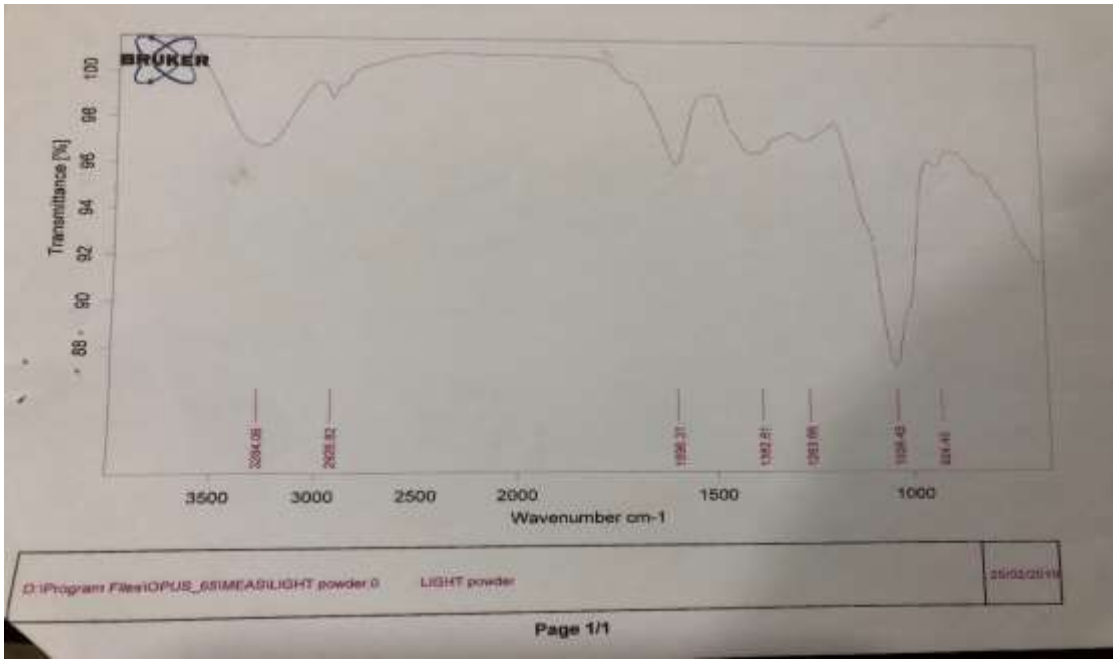


Figure 2. Graph No. (1) FTIR test

Active groups and compounds present in walnut shells were detected in Ibn Al-Bitar Center, which are shown in the results attached to the research Laboratory experiments showed that the colors resulting from dyeing wool with walnut shell dye were yellow in the acidic medium at all concentrations, but in the basic medium, the resulting colors were dark yellow at low concentrations and light brown at high concentrations, as shown in Picture No. (1).



Figure No. (3): shows the colors resulting from dyeing Iraqi wool with walnut shell dye

No. (1): control, in basic medium : No. (2): 10% concentration. No. (3): 15% concentration No. (4): 20% concentration, No. (5): 25% concentration

In acidic medium: No. (6): 10% concentration No. (7): 15% concentration, No. (8): 20% concentration No. (9): 25% concentration

Where the results showed the ability of the Iraqi wool used to be colored with the used dye extracted from walnut shells, due to the ability of the used wool fibers to bind to the dye, and this is due to the formation of bonds between the dye cations and the hydroxyl groups present within the composition of the wool [22] and the high temperatures used that have a role in increasing the susceptibility of the fibers Woolen to dyeing and the susceptibility of the alum used as a stabilizer, as the stabilizer ions spread on the surface of the fibers to be dyed and thus support the success of the dyeing process by forming bonds between the stabilizer ions and the dye used [23] in addition to the effect of the time required for the dyeing process The results of the laboratory tests proved the efficiency of the dye stability on the Iraqi wool bristles, in addition to the efficiency of the alum used as a stabilizer for the used dye, as the results showed more stability of the dye in the basic medium than in the acidic medium towards the examination of washing with soap and water and detergents, as shown in Table No. (2), (3). Where the values of (5-4/5-4)) are considered successful, and 3/4-3)) are acceptable, while 2/3-2-1/2-1 are unacceptable (failed) for the staining test, either for the color change test. So the values (2/3-2-1/2-1) are considered successful and (3/4-3) acceptable. As for (5-4/5-4)), they are considered failed

Table 3. Results of walnut shell dye stability tests on Iraqi wool fibers using soap

NO.	medium type	dye concentration%	Color change	Smudging
1	Basic	10	1	5
2	Basic	15	1	5
3	Basic	20	1	5
4	Basic	25	1	5
5	acidic	10	2/3	5
6	Acidic	15	1/2	5
7	Acidic	20	1/2	5
8	Acidic	25	2	3

Table 4. Results of walnut shell dye stability tests on Iraqi wool fibers using detergent

NO.	medium type	dye concentration%	Color change	Smudging
1	Basic	10	1/2	4/5
2	Basic	15	1	4
3	Basic	20	1	4/5
4	Basic	25	1	4/5
5	Acidic	10	4	2/3
6	Acidic	15	3/4	½
7	Acidic	20	3	5
8	Acidic	25	3/4	3

The results of color change were good depending on the gray scale when exposed to natural sunlight and all concentrations used.

The results of acid and base sweating showed stability of the dye in the two media used, as shown in Table No. (5).

Table 5. The results of the acid and base perspiration tests of the wool fibers dyed with walnut shells dye with the fixative. Values from 4-5/4-5 (successful) and (3-3/4) acceptable, while 3/2- 2-1/2-1)) unacceptable (failed).

NO.	medium type	dye concentration%	Sweating	
			Acidic	Basic
1	Basic	10	4/5	5
2	Basic	15	5	4
3	Basic	20	4	4/5
4	Basic	25	4/5	4
5	Acidic	10	5	4/5
6	Acidic	15	4	4
7	Acidic	20	4/5	5
8	Acidic	25	4/5	4

As for its stability against dry and wet abrasion, it was good, and this is due to the strength of the color resulting from the dye, as shown in Table No. 6.

Table 6. shows the stability of the color of walnut husks dye on Iraqi wool fibers for dry and wet rubbing, where the values of 4-5/4 (5-4) are considered successful, and 3-4/3 are acceptable, but 2-3/2 -1/2-1)) unacceptable (failed).

NO.	medium type	dye concentration%	itching	
			dry	wet
1	Basic	10	5	5
2	Basic	15	3	3
3	Basic	20	4	4
4	Basic	25	4	4
5	Acidic	10	4/5	4/5
6	Acidic	15	4/5	4/5
7	Acidic	20	4	4
8	Acidic	25	4	3

Conclusions

1. The difficulty of dissolving the walnut shell dye used with ethanol
2. The extracted dye is inexpensive and can be applied in the factories of the General Company for Textile and Leather Industries
3. The stability of the dye used after conducting the dye stability tests
4. The color tone of the dye in the basic medium is different from that in the acidic medium.

References

1. Jiangning Che and Xu Yang. A recent (2009–2021) perspective on sustainable color and textile coloration using natural plant resources. Heliyon 8 (2022) e10979.
2. Mousa Sadeghi-Kiakhani and Ali Reza Tehrani-Bagha et al. Use of pomegranate peels and walnut green husks as the green antimicrobial agents to reduce the consumption of inorganic nanoparticles on wool yarns. Journal of Cleaner Production 231 (2019) 1463e1473.
3. M Gobalakrishnan, R Ragavendran et al . A REVIEW ON THE EXTRACTION OF NATURAL DYE FROM THE TREE. International Journal of Creative Research Thoughts (IJCRT). Volume 8, Issue 4 April 2020.
4. K Amutha, S Grace Annapoorani." Eco-friendly dyeing of cotton fabric with natural dye and mordants", A s i a n J o u r n a l o f Multidimensional Research (A J M R) Vol 7, Issue 2, February 2018.
5. A.,Choudhury ."Eco-friendly dyes and dyeing , Advanced matrials and technologies for environmental applications",2(1)145-176,issn :2559-2637,2018.
6. Manal M.EL-Zawahry, Gehan M. Shokry et al. Eco-friendly Dyeing Using Hematoxylin Natural Dye for Pretreated Cotton Fabric to Enhance Its Functional Properties. Egypt. J. Chem. Vol. 64, No. 12 pp. 7135 – 7145,2021.
7. Lizamoni Chungkrang, Smita Bhuyan and Ava Rani Phukan. Natural Dyes: Extraction and Applications. International Journal of Current Microbiology and Applied Sciences. ISSN: 2319-7706 Volume 10 Number 01,2021.
8. Allafi, F., Hossain, M. S., Lalung, J., Shaah, M., Salehabadi, A., Ahmad, M. I., & Shadi, A. Advancements in applications of natural wool fiber. Journal of Natural Fibers, 19(2), 497-512.2022 .
9. Allafi, F. A., Hossain, M. S., Shaah, M., Lalung, J., Ab Kadir, M. O., & Ahmad, M. I. A review on characterization of sheep wool impurities and existing techniques of cleaning: industrial and environmental challenges. Journal of Natural Fibers, 19(14), 8669-8687.2022.
10. Sk, S., Mia, R., Haque, M. A., & Shamim, A. M. Review on extraction and application of natural dyes. Textile & Leather Review, 4(4), 218-233. 2021.
11. Samanta, P. A review on application of natural dyes on textile fabrics and its revival strategy. Chemistry and technology of natural and synthetic dyes and pigments, 1-25.2020.
12. Jonas Frei. A brief History of Juglandaceae. Arnoldian, V.78, Issue 3,2021.
13. Tetiana Yehorenko and Marzhan Kizatove et al. Revealing the Features of the composition of the Walnut Shell from the point of view of the possibility of its use in the food industry. Eastern-European journal of enterprise technologies,1(11,115,) 49-55,2022.

14. Li Zhang, Hong Li et al. Structure and Dyeing Properties of Cotton Fabric Modified by Protein from Waste Feathers. IOP Conf. Series: Materials Science and Engineering 774 (2020) 012043.
15. C. S. Queirós, Ana Lourenço, Sofia Cardoso, Joana P. A. Ferreira." Characterization of walnut, almond, and pine nut shells regarding chemical composition and extract composition".biomass conversion and biorefinary ,2019.
16. Benson Dulo,· Kim Phan et al. Natural Quinone Dyes: A Review on Structure, Extraction Techniques Analysis and Application Potential. Waste and Biomass Valorization 12:6339–6374.2021.
17. Adem Önal, Oguz Özbek et al. Investigation of the dyeing properties of the colorant extracted from Juglans regia L. leaves on cellulosic and protein fabrics. JOTCS; 8(2): 453-460,2021.
18. E Dilara Koçak, Pelin Altay et al. The effect of different mordants on natural dyeing of cotton, viscose and lyocell fabrics with pomegranate bark extracts. Journal of Textile Engineering & Fashion Technology. Volume 8 Issue 6 – 2022.
19. Younes Chemchame and Hajar Benzbir et al. Improvement of Dye Extraction from Common Walnut Stain and Optimization of Wool Dyeing Conditions. International Journal of Chemical Sciences. Research| Vol 18 Iss 3.2020.
20. Barbara Pizzicato and Severina Pacifico et al. Advancements in Sustainable Natural Dyes for Textile Applications: A Review. Molecules , 28, 5954.2023.
21. Nabawia A. El-Zahera and Gehan T. El-Bassyouni et al. Amendments of the Structural and Physical Properties of Cotton Fabrics Dyed with Natural Dye and Treated with Different Mordants. JOURNAL OF NATURAL FIBERS. VOL. 18, NO. 9, 1247–1260.2021.
22. Fatemeh Shahmoradi Ghaheh, Aminoddin Haji and Elaheh Daneshvar. Sustainable Dyeing Process for Nylon 6 Fabrics by Rhubarb Flower Using Different Bio-Mordants. Sustainability, 15, 9232.2023.
23. Aravin Prince Periyasamy. Natural dyeing of cellulose fibers using syzygium cumini fruit extracts and a bio-mordant: A step toward sustainable dyeing. Sustainable Materials and Technologies 33 (2022) e00472.

Evaluation the Pharmacodynamics Interaction of Cyclosporine and Azacitidine On the Treatment of Induced Aplastic Anemia in Rat

Ghanem T. Abdulrazzaq [1], Huda F. Hasan [2]

© 2023 The Author(s). This open access article is distributed under a Creative CommonsAttribution (CC-BY) 4.0 license.

Abstract: The study was done to assess the effective dose and type of relative combination between cyclosporin and azacitidine on the treatment of induced aplastic anemia in rats. Eighty-five rats were divided into five groups: The 1st group: Five female rats were non induced and treated with distilled. The 2nd group: Five female rats were induced and treated with distilled water. The 3rd and 4th groups included twenty-five rats for each one were induced and treated with cyclosporine and azacitidine respectively and each group divided into five equal subgroups with doses of 2, 3, 4, 5, and 6 mg/kg/. The 5th group: Twenty-five rats were induced and treated with a combination of cyclosporine and azacitidine and divided into five equal subgroups with doses of 1, 1.5, 2, 2.5, and 3 mg/kg, for each drug. IL-2 was dependent as a parameter to determine the effective doses and type of drug interaction. IL-2 levels in the group treated with cyclosporine revealed a gradual significant decrease, until reached a plateau in the last two doses. The group that received azacitidine showed gradual, substantial decline in IL-2 levels, the group that treated with a combination of cyclosporine and azacitidine illustrated the best gradual, significant decrease in IL-2 levels until reach to saturation at dose 4 mg/kg as compared with all treated groups. the effective doses of combination cyclosporine with azacitidine and each one alone were (3.68, 5.86 and 5.75) mg/kg respectively and the value of the combination index was 0.51. In conclusion, a combination of cyclosporine and azacitidine revealed a synergistic effect lead to decrease in IL-2 levels during treatment aplastic anemia than did each drug alone.

Key Words: Cyclosporine, Azacitidine, Aplastic anemia, Rats.

Author details

[1 – 2] Department of Physiology and Pharmacology, College of Veterinary Medicine, University of Baghdad, Baghdad, Iraq

Citation information

Cite this article as:

Abdulrazzaq, G.T., Hasan, H.F., (July 2023), *Evaluation the Pharmacodynamics Interaction of Cyclosporine and Azacitidine On the Treatment of Induced Aplastic Anemia in Rat*, Proceedings of the Minar Congress, Turkey, (9) pp 284-292, DOI: http://dx.doi.org/10.47832/MinarCong9-24

http://dx.doi.org/10.47832/MinarCong9-24

[2] dr.hudaalqaraghuli@yahoo.com

Introduction

Aplastic anemia is one type of acquired myeloid hematological system disease, which it is characterized by immune-mediated primary BMF leading to pancytopenia and hypocellular marrow, ultimately leading to an insufficiency of red cells, white cells and platelets in the blood and a fatty substitute of the marrow due to the destruction of early HSCs and HPSC (Brzezniakiewicz-Janus et al., 2020; Sweeney et al., 2021; Peffault et al., 2022). In addition, the immunosuppressive compound cyclosporine A, a well-known inhibitor of calcineurin with a potent immunosuppressive properties (Faheem et al., 2022; Ershad et al., 2023). Cyclosporine blocks T-cell infiltration, activation, and the subsequent release of inflammatory cytokines (Periman et al., 2020). Moreover, it has produced advancements in treating various blood disorders, including autoimmune illnesses and aplastic anemia (Patocka et al., 2021). The principal adverse effects of cyclosporine included nephrotoxicity, hepatotoxicity, tremor, hypertension, gum hypertrophy, gum hyperplasia, hirsutism, as well as GI disturbances including nausea and vomiting (Ershad et al., 2023). Furthermore, azacitidine, a pyrimidine nucleoside analogue of cytidine with antineoplastic activity, has the ability to incorporate into DNA, thereby blocking DNA methyltransferase, focusing on epigenetic gene silencing, which was utilized by cancer cells to silence some genes in order to prevent the development of malignant phenotypes, as well as the FDA authorized it to treat a class of blood and BM diseases (Yang et al., 2021; Sochacka-Cwikła et al., 2022). It's interesting that the medicine combination is most frequently used to treat the worst illnesses, such as cancer, AIDS, arthritis and aplastic anemia (Hasan et al., 2014). The primary goals of combination medications are typically to reduce dosage and toxicity, generate synergistic therapeutic benefits, and prevent or postpone the development of drug resistance (Chou, 2010). The study was done to assess the effective dose and type of relative combination between cyclosporin and azacitidine on the treatment of induced aplastic anemia in rats.

Methodology

Experimental animals

This study was carried out at the animal house/ College of Veterinary Medicine/University of Baghdad. 85 adult female rats were reared in plastic cages in an air-conditioned area under appropriate environmental conditions of (22± 3°C) and relative humidity (60± 5%). The animals were given freshly prepared food and free use of the water supply.

Induction of aplastic anemia

Aplastic anemia was induced according to (Ata, 2016; Hasan et al., 2017).

Experimental design

Eighty five adult rats divided into five groups as follows: The 1st group: Five female rats were treated with distilled water and served as the negative control group without inducing aplastic anemia. The 2nd group: Five female rats were induced with aplastic anemia and

treated with distilled water as the control positive group. The 3rd group: twenty five rats were induced with aplastic anemia and treated with cyclosporine and divided into five equal subgroups with doses of 2, 3, 4, 5, and 6 mg/kg/day. The 4th group: twenty five rats were induced with aplastic anemia and treated with azacitidine and divided into five equal subgroups with doses of 2, 3, 4, 5, and 6 mg/kg. The 5th group: Twenty five rats were induced with aplastic anemia and treated with a combination of cyclosporine and azacitidine and divided into five equal subgroups with doses of 1, 1.5, 2, 2.5, and 3 mg/kg, for each drug.

Determination of interleukin (IL)-2 concentrations

Serum IL-2 concentration was measured quantitatively by using Abcam's IL-2 rat ELISA kit (ab100769) (Kadasa *et al.*, 2015).

Determination the Log dose response curve and effective doses of cyclosporine and azacitidine

After the end of the experiment (30 days), IL-2 was used to determine the log-dose-response curve and maximum effective dose (MED) by using a simple line equation and determining R2 to select the appropriate effective dose that gave the best results (Haley and Knott, 1992).

Determination the type and effective dose of combination cyclosporine and azacitidine by combination index (CI) Equation of Chou-Talalay

The level of IL-2 was utilized as a parameter to calculate the effective dose and type of interaction between cyclosporine and azacitidine according to the Chou-Talalay method (Chou, 2018).

Statistical analysis

The statistical analysis of the data was performed using SAS (Statistical Analysis System, version 9.1). A one-way and two-way ANOVA and least significant differences (LSD) post hoc test were performed to assess significant differences among means. P≤0.05 was considered statistically significant (Taher Abdulrazzaq and Hasan, 2019).

Results

Effects of cyclosporine, azacitidine, and combinations of them on serum IL-2 levels:

The IL-2 levels in the group treated with cyclosporine at doses (2, 3, 4, 5 and 6) mg/kg revealed a gradual significant (P≤0.05) decrease in mean values of (56.54±3.09, 54.67±3.34, 49.55±5.89, 42.98±2.18 and 42.57±3.29) respectively, until they reached a plateau in the last two doses as compared with the positive control group. Also, the group that received azacitidine at the same doses of cyclosporine showed gradual, substantial (P≤0.05) decline in IL-2 levels in mean values (59.41±3.80, 57.02±3.41, 55.68±1.81, 51.58±2.92 and 50.33±0.68), respectively. Whereas, the group that treated with a combination of cyclosporine and azacitidine at doses (1, 1.5, 2, 2.5 and 3) mg/kg for each drug illustrated gradual, significant

(P≤0.05) decrease in IL-2 levels in average values (52.54±1.99, 49.95±0.64, 45.38±2.00, 39.22±0.72 and 36.83±2.63), respectively until reach to saturation at dose 4 mg/kg as compared with all treated groups, with no significant (P≥0.05) differences as compared with negative control group at doses 5 and 6 mg/kg. As shown in the figure (1).

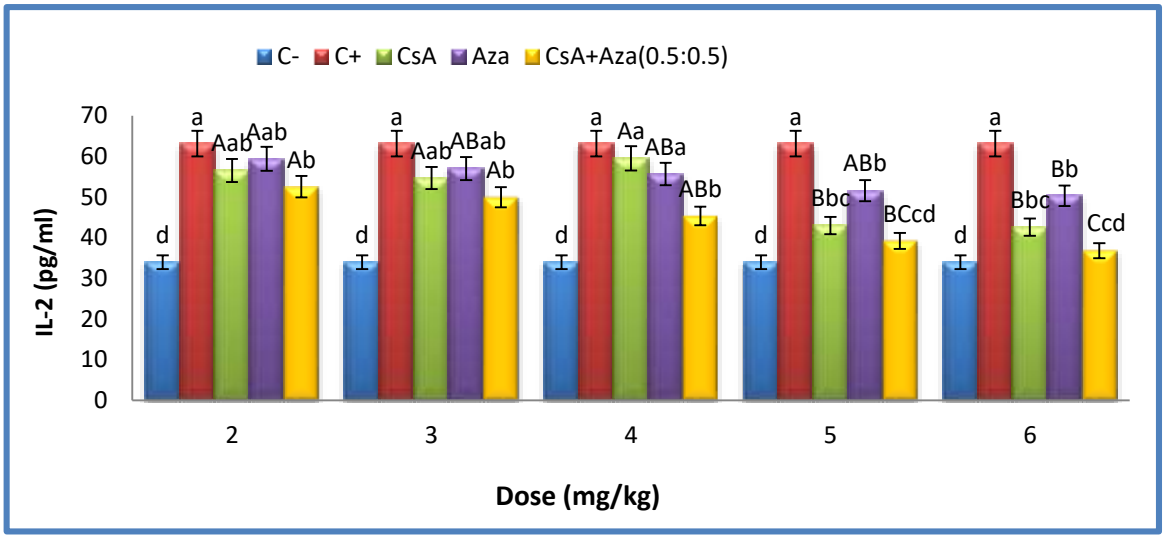


Figure 1. Effect of different doses of cyclosporine, azacitidine and their combinations on serum IL-2 level (pg/ml) for 30 days in rats induced aplastic anemia. LSD: 8.42

*Means with a small letter in the same column significantly different (P≤0.05).

*Means with a capital letter in the same row significantly different (P≤0.05)

*N= 85 female rats.

Determination of the log dose response curve and effective doses of cyclosporine and azacitidine

The log dose-response curve and effective doses of cyclosporine and azacitidine were calculated using a simple linear equation, revealing that the effective dose of cyclosporine was 5.86 mg/kg, as shown in figure (2), and the effective dose of azacitidine was 5.75 mg/kg, as shown in figure (3)

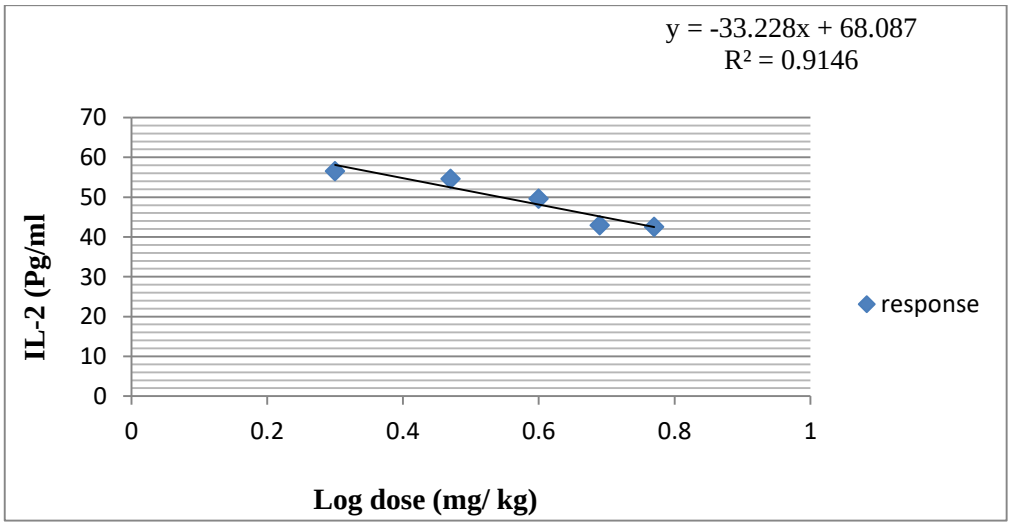


Figure 2. Log dose response curve of cyclosporine on interleukin-2 of female rats.

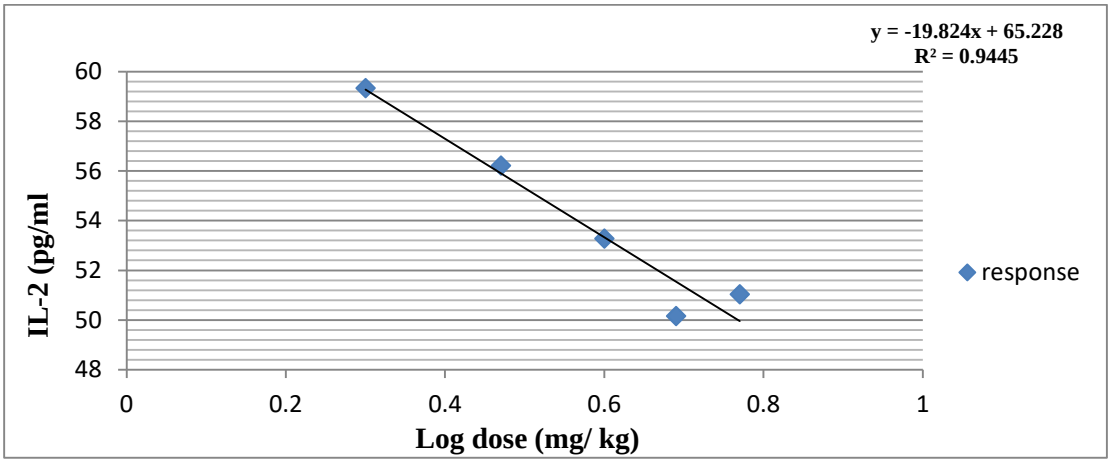


Figure 3. Log dose response curve of azacitidine on interleukin-2 of female rats.

Cyclosporine and Azacitidine Combination Effective Dose and type of Interaction

The effective dose of cyclosporine and azacitidine was 3.68 mg/kg for each drug according to the Chou-Talalay method as shown in figure (4) using the software program CompuSyn, and the type of interaction between cyclosporine and azacitidine was a synergistic interaction according to the value of the combination index (0.51) as explained in figure (5).

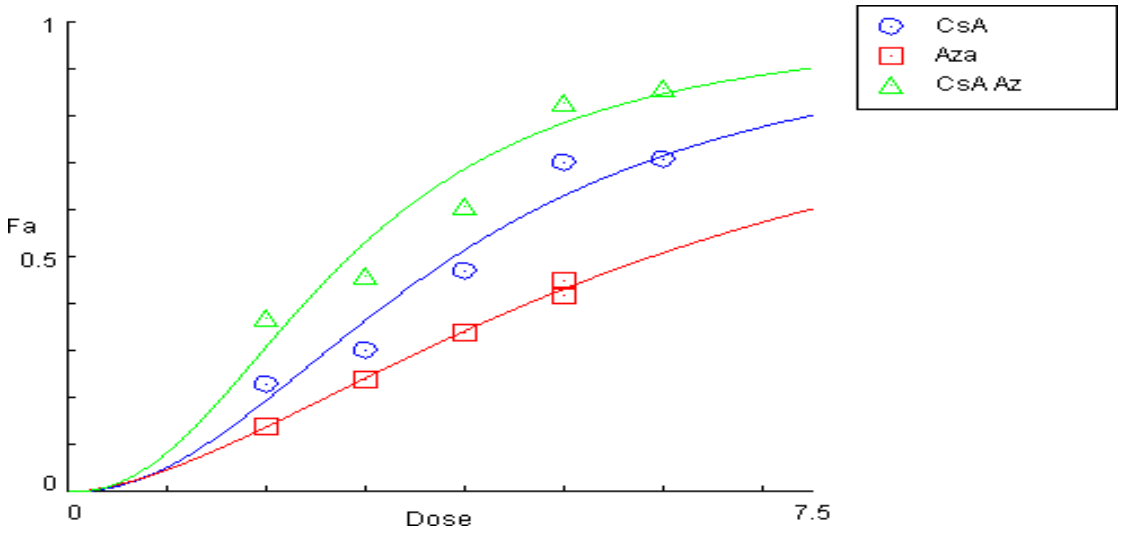


Figure 4. The effective dose of cyclosporine and azacitidine was 3.68 mg/kg, according to the Chou-Talalay method using CompuSyn program software.

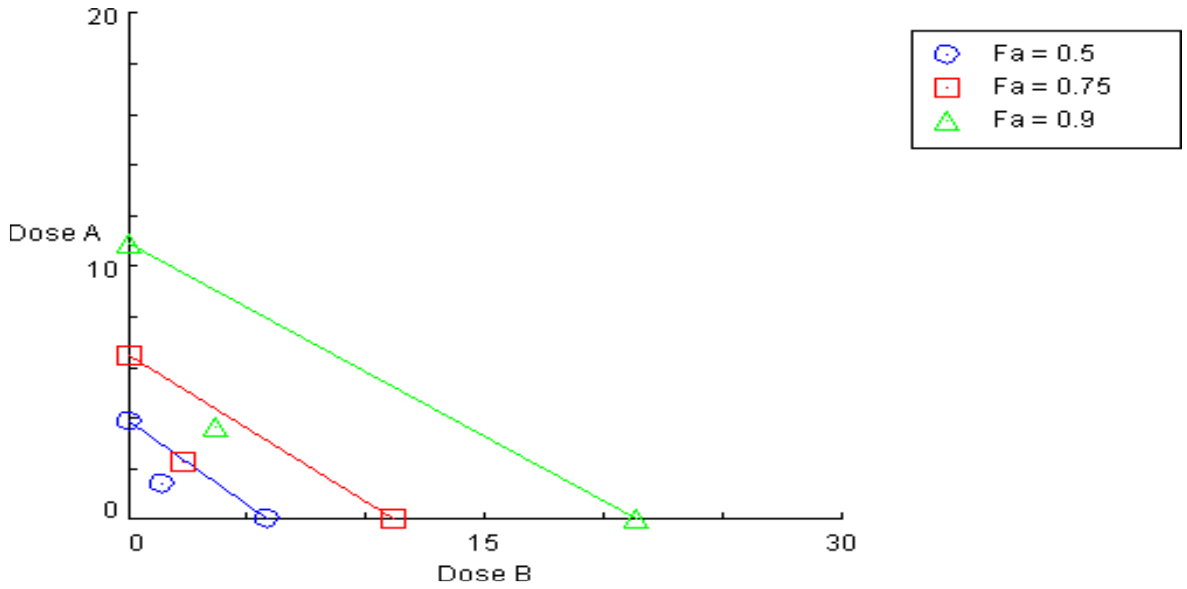


Figure (5): The type of interaction between cyclosporine and azacitidine was a synergistic interaction according to the value of the combination index (0.51), according to the Chou-Talalay method using CompuSyn program software.

Discussion

The elevation in IL-2 serum level in the positive control group was clearly attributed to immune dysfunction, which has been hypothesized to result from abnormal activation of T-helper 1 (Th1) cells and excessive production of hematopoietic negative regulatory cytokines such as IL-2, this explaining agreed with Zhang *et al.*, (2017). In addition, it was reported that IL-2 could stimulate the activation, proliferation, and differentiation of many immune cells, including natural killer (NK), B and T cells (Malek, 2008). So, IL-2 mainly produced by active T-cells and in turn affected the proliferation of T-cells and levels of IL-2 significantly increased in the blood of animals with aplastic anemia when compared to healthy control animals (Dutta *et al.*, 2019; Javan *et al.*, 2021). Furthermore, when stimulated and differentiated, Th1 cells can be produced IL-2 and IFN-γ and activated macrophages and CTLs, and their activity linked to the immune response in the BM compartment of the body, with the higher the level of IL-2, the stronger the immune response in both the BM and peripheral blood (De *et al.*, 2019).

Furthermore, the decline in IL-2 levels in the cyclosporine-treated group was linked to the immunosuppressive activity of this drug by blocking T-cell infiltration, activation, and the subsequent release of inflammatory cytokines, including IL-2 (Periman *et al.*, 2020). Obviously, cyclosporine inhibited antigen-triggered signal transduction in T cells by entering the cytoplasm, binding to an immunophilin, and forming a cyclosporine-cyclophilin complex. This complex inhibited calcineurin, which required inducing IL-2 transcription, resulting in the inhibition of activated T cell proliferation (Ershad *et al.*, 2023). The drug also inhibited the production of lymphokines and the release of interleukin, thereby leading to reduced function of effector T- and B-cells (Brunton et al., 2011; Vashist et al., 2012). Therefore, the subsequent reduction in IL-2 levels further reduced the function of effector T-cells, ultimately leading to immunosuppression (Periman *et al.*, 2020; Yang *et al.*, 2021).

Notably, the azacitidine-treated group had significantly lower IL-2 levels; azacitidine inhibited T cell proliferation and activation, blocking cell cycle progression in the G0 to G1 phase, and decreasing the production of pro-inflammatory cytokines, including IL-2 (Sanchez-Abarca *et al.*, 2010; Goodyear *et al.*, 2010). As well, it was found that azacitidine treatment shifted cytotoxic T cells to regulatory T cells, resulting in a reduction in proinflammatory Th1-cells (Stubig *et al.*, 2014).

Importantly, the group that received a combination of cyclosporine and azacitidine experienced a significantly lower decrease in IL-2 levels than did each drug alone. Of note, these findings suggested a potential synergistic immunosuppressive effect of cyclosporine and azacitidine.

Conclusions

The combination of cyclosporine and azacitidine exhibited pronounced reduction in IL-2 levels of this study. Also, it displayed synergistic potential activity, making it promising as a treatment for aplastic anemia.

References

1. Brzezniakiewicz-Janus, K., Rupa-Matysek, J., and Gil, L. (2020). Acquired aplastic anemia as a clonal disorder of hematopoietic stem cells. Stem Cell Reviews and Reports, 16(3), 472-481.
2. Sweeney, R., Esmail, F., Mirza, K. M., and Nand, S. (2021). Hypercellular bone marrow in aplastic anemia: A case report of two patients. Clinical Case Reports, 9(11), e04845.
3. Peffault de Latour, R., Kulasekararaj, A., Iacobelli, S., Terwel, S. R., Cook, R., Griffin, M., and Risitano, A. M. (2022). Eltrombopag added to immunosuppression in severe aplastic anemia. New England Journal of Medicine, 386(1), 11-23.
4. Faheem, S. A., El-Sayed, N. M., Moustafa, Y. M., Saeed, N. M., & Hazem, R. M. (2022). Pyrvinium pamoate ameliorates cyclosporin A-induced hepatotoxicity via the modulation of Wnt/β-catenin signaling and upregulation of PPAR-γ. International Immunopharmacology, 104, 108538.
5. Ershad, A., Taziki, S., Ebrahimian, M., and Abadi, S. S. D. (2023). Acute cyclosporine overdose: A systematic review. Medicina Clínica Práctica, 6(2), 100358.
6. Periman, L. M., Mah, F. S., and Karpecki, P. M. (2020). A review of the mechanism of action of cyclosporine A: the role of cyclosporine A in dry eye disease and recent formulation developments. Clinical Ophthalmology (Auckland, NZ), 14, 4187.
7. Patocka, J., Nepovimova, E., Kuca, K., and Wu, W. (2021). Cyclosporine A: chemistry and toxicity–a review. Current Medicinal Chemistry, 28(20), 3925-3934.
8. Yang, Y., Hu, N., Gao, X. J., Li, T., Yan, Z. X., Wang, P. P. and Yan, R. (2021). Dextran sulfate sodium-induced colitis and ginseng intervention altered oral pharmacokinetics of cyclosporine A in rats. Journal of Ethnopharmacology, 265(11), 3251
9. Sochacka-Ćwikła, A., Mączyński, M., and Regiec, A. (2022). FDA-Approved Drugs for Hematological Malignancies—The Last Decade Review. Cancers, 14(1), 87.
10. Hasan HF, Khazal KF, Luaibi OK (2014). The effect of crude alcoholic extract of Withania somnifera leaves in experimentally induced arthritis in mice. J.Thi-Qar Sci., 4 (2):45-51.
11. Chou, T. C. (2010). Drug combination studies and their synergy quantification using the Chou-Talalay method. Cancer research, 70(2), 440-446.
12. Ata, S. I. E. (2016).Induction of aplastic anemia in experimental model.Coden IJABFP-CAS-USA. No.7, PP. 1
13. Hasan, H. F., Krair, E. M. and Al-Halbosy, M. F. (2017). Evaluating Anti-Anemic Effect of Mesenchymal Stem Cells and Oxymetholone on Aplastic Anemia Induced in Mice. Indian Journal of Natural Science, 8(44), 12714-12729.
14. Kadasa, N. M., Abdallah, H., Afifi, M., and Gowayed, S. (2015). Hepatoprotective effects of curcumin against diethyl nitrosamine induced hepatotoxicity in albino rats. Asian Pacific Journal of Cancer Prevention, 16(1), 103-108.
15. Haley, C. S., and Knott, S. A. (1992). A simple regression method for mapping quantitative trait loci in line crosses using flanking markers. Heredity, 69(4), 315-324.

16. Chou, T. C. (2018). The combination index (CI< 1) as the definition of synergism and of synergy claims. Synergy, 7, 49-50.
17. Taherabdulrazzaq, G., & Hasan, H. F. (2019). Antagonistic effect of Avena sativa seeds crude extract to chlorambucil effect on fertility of female rats. Biochemical and Cellular Archives, 19(2), 3363-3370.
18. Zheng, K., Wu, L., He, Z., Yang, B., andYang, Y. (2017). Measurement of the total protein in serum by biuret method with uncertainty evaluation. Measurement, 112, 16-21.
19. Malek, T. R. (2008). The biology of interleukin-2. Annu. Rev. Immunol., 26, 453-479.
20. De, R., Dutta, A., Dolai, T. K., Ghosh, K., and Halder, A. (2019). Comparative study of bone marrow and blood plasma levels of IL-2 in aplastic anaemia and their relationship with disease severity. Hematology, 24(1), 84-88.
21. Javan, M. R., Saki, N., and Moghimian-Boroujeni, B. (2021). Aplastic anemia, cellular and molecular aspects. Cell Biology International, 45(12), 2395-2402.
22. Sanchez-Abarca, L. I., Gutierrez-Cosio, S., Santamaría, C., Caballero-Velazquez, T., Blanco, B., Herrero-Sánchez, C. and Perez-Simon, J.A. (2010). Immunomodulatory effect of 5-azacytidine (5-azaC): potential role in the transplantation setting. Blood, the Journal of the American Society of Hematology, 115(1), 107-121.
23. Goodyear, O., Agathanggelou, A., Novitzky-Basso, I., Siddique, S., McSkeane, T., Ryan, G., and Craddock, C. (2010). Induction of a CD8+ T-cell response to the MAGE cancer testis antigen by combined treatment with azacitidine and sodium valproate in patients with acute myeloid leukemia and myelodysplasia. Blood, The Journal of the American Society of Hematology, 116(11), 1908-1918.
24. Stubig, T., Badbaran, A., Luetkens, T., Hildebrandt, Y., Atanackovic, D., Binder, T., and Kröger, N. (2014). 5-azacytidine promotes an inhibitory T-cell phenotype and impairs immune mediated antileukemic activity. Mediators of inflammation, 2014.

Optimization of Wire EDM Parameters for Machining HSS (8X200) by using Grey Relational Analysis (GRA)

Athraa M. S. Ahmed [1], Abd Ulrahman I. Jihad [2]

Heba Saad Qasim [3], Saad K. Shather [4]

© 2023 The Author(s). This open access article is distributed under a Creative CommonsAttribution (CC-BY) 4.0 license.

Abstract: When it comes to machining, manufacturers are always striving for the best possible outcomes. The improvement of the precision and productivity of material processing is the primary goal to enhance Wire Electrical Discharge Machining (EDM) parameters. Whether it's a fragile substance or one that conducts electricity, traditional approaches generally fall short. Maximizing the benefits of machining includes higher product quality, greater production efficiency, and lower production costs. Therefore, industries work hard to fine-tune the EDM settings. Within the scope of this investigation, HSS (8X200) wire EDM parameters are optimized. Finding the ideal machining settings that enhance surface roughness (SR), material removal rate (MRR), and cutting speed (CS) while maintaining economic feasibility is the goal. The Taguchi design parameter and Grey Relational Analysis (GRA) are both utilized in this research. Machining parameters such as pulse on time, pulse off time, servo feed, and servo voltage can be designed, tested, and determined with the use of the Taguchi technique. GRA analyzes experimental data and determines optimal parameter values. In order to evaluate the quality of the machining, wire-cut machines measure SR, MRR, and CS. The settings are validated using the ANOVA. In the fifth experiment, the ideal HSS (8X200) wire EDM parameters were determined. According to the findings of the study, the factors that have the largest influence on SR, MRR, and CS are pulse on time (55.43%), servo feed (17.62%), pulse off time (14.13%), and servo voltage (12.82%).

Key Words: Wire EDM process, Taguchi orthogonal array (TOA), Grey Relational Analysis.

Author details

[1- 3 - 4] Department of Production and Metallurgy Engineering, University of Technology, Baghdad, Iraq

[2] Midland Refineries Company, Baghdad, Iraq

Citation information

Cite this article as:

Ahmed, A.M., Jihad, A.I., Qasim, H.S., Shather, S.K., (July 2023), *Optimization of Wire EDM Parameters for Machining HSS (8X200) by using Grey Relational Analysis (GRA)*, Proceedings of the Minar Congress, Turkey, (9) pp 293-306, DOI: http://dx.doi.org/10.47832/MinarCong9-25

http://dx.doi.org/10.47832/MinarCong9-25

[1] athraa.m.ahmed@uotechnologh.edu.iq

[2] abdouser@gmail.com

[3] heba.s.qasim@uotechnology.edu.iq

[4] saad.k.shather@uotechnology.edu.iq

Introduction

Machining precision components for numerous sectors is essential. High-Speed Steel (HSS) is stiff, brittle, and electrically conductive, making ordinary machining problematic. These materials are employed in durable, wear-resistant, and thermally stable applications. These machining issues demand unique machining procedures(Hai et al., n.d.). Wire EDM is an unconventional HSS machining method. Thin, electrically charged wires erode the workpiece. Standard cutting tools work well for machining hard, brittle materials(Asgar et al., 2021). Optimizing settings produces high-quality components with increased surface polish and dimensional precision, improving product performance. Wire EDM reduces manufacturing time, tool wear, and cost (Dewangan et al., 2019). The worktable, electrode wire spool, and used wire spool make up a Wire EDM machine. The electrode wire is threaded through accurate guides and the workpiece is secured to the worktable. Dielectric fluid between the electrode wire and the workpiece is usually deionized water. It cools, cleans, and insulates the machining area. Energizing the wire and producing an electrical potential difference between it and the workpiece starts machining. The workpiece is positively charged, whereas the wire is negatively charged (electrode). The wire and workpiece spark gap(Asgar et al., 2021). Spark Generation: The wire and workpiece create regulated electric discharges, or sparks, as they approach. High-intensity electrical discharge melts and vaporizes workpiece material quickly. The workpiece is extracted by heat (Mufti et al., 2020). The wire and workpiece melt and vaporize the material fast with controlled electric discharges. Dielectric fluid quickly removes molten and vaporized waste from the cutting area. Continuously feeding electrode wire maintains wire-workpiece gap. The Wire EDM machine cuts electrode wire using CNC instructions to shape, contour, or profile the workpiece. Wire EDM creates fine finishing. Electrical discharges may give machined surfaces a unique texture. Surface quality may need further finishing processes (Complimentary Contributor Copy, n.d.). Fig .1. explained the WEDM mechanism. Controlling electrode wire-workpiece electrical discharges removes material in wire EDM. Systematic optimization of parameter settings is difficult (Dewangan et al., 2019).

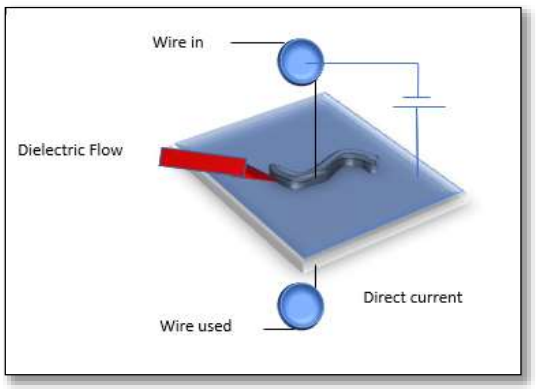


Figure 1. Wire Electrical Discharge Machining Process

There are several benefits to using wire (EDM), a non-traditional technique, when working with hard and brittle materials. In order to improve the effectiveness, precision, and productivity of the procedure, a significant amount of research has been done over the years to investigate wire EDM machining processes and optimization approaches. The relevant research and earlier studies in these fields are covered in this section:

Hammami D and et al (2023). Wire EDM surface finish of 2017T451 and 7075T651 aluminum alloys is evaluated. An L9 Taguchi orthogonal array controls three-factor and three-level WEDM trials to identify process parameter influence. Based on surface roughness (Ra) value, signal-to-noise (S/N) ratio, and ANOVA findings, pulse on time and pulse off time (mare major cutting factors impacting Ra. This paper considers no fissures in the two aluminum alloys' surface topography(Hammami et al., 2023).

Austempered ductile iron ADI-4h's WEDM processing reaction is reported by Sarma P. and et al (2023). Peak current, pulse-on-time, and wire feed have been studied in relation to cutting rate, kerf width, and surface roughness. Mild steel machinability is compared. ADI has strong WEDM machinability, even if mild steel is easier (Hydro et al., 2023).

Benes L. and et al (2023). This study examined the corrosion behavior of (AISI 316Ti) and (AISI 303) stainless steels machined with WEDM in pyrolysis. WEDM machining was tested on both materials using different settings. WEDM, cleaning, and corrosion tests assessed surface topography. At all three stages, electron microscopy examined surface morphology and cross-sections. The surface chemical composition and pyrolysis environment were analyzed. The pyrolysis chamber organic acids did not damage the tested stainless steels. Both steel types had little fissures, or fine precipitated carbides, on their surfaces and subsurfaces, as well as substantial carbon. This presence was linked to the protective or passivation impurities discovered on the surface following the test furnace (Benes et al., 2023).

Asgar1 M. and Singholi A. (2021), showed the advancement of wire EDM with improved material wire electrodes and the best machining conditions. MRR (material Removal Rate), SR (Surface Roughness), Kw (Kurf Width), and machining surface properties were discussed. The study on wire EDM for advanced materials in optimization is focused on more recent elements(Asgar et al., 2021).

Ablyaz T.and et al (2021). This work analyzes polymer composite material (PCM) with WIRE-EDM. Variable voltage (50–100 V), pulse duration (5–15 μs), and pause time (10–50 μs) are input process parameters, whereas cut-width (kerf) is an output parameter. and Titanium plates (1 mm thick) sandwiched on the PCM increase workpiece conductivity. The theoretical model was developed using analysis of variance to determine how process factors affect PCM component cut-width. Voltage and pulse length considerably impact PCM cut-width accuracy (Ablyaz et al., 2021).

Satynarayana K. and et al (2020) were studied cryogenic WEDM process research. Performance factors including pulse on, pulse off, current, voltage, wire tension, and wire feed

affect material removal, tool wear, and surface roughness. The paper's main idea is to combine research philosophy with the finest production practices to aid future industrial and production research (Satynarayana et al., 2020).

Kumar G. and et al (2020). This study optimizes Inconel 750 WEDM parameters using multi-objective optimization. Wire feed rate, pulse-on-time, pulse-off-time, and water pressure were tested using Taguchi L18 orthogonal array (OA). Cutting speed and part surface roughness are predicted output responses (Venkata Rao & Taler, 2020).

Slatineanu L. (2020). These investigations began by enhancing machining machines, wire electrodes, and clamping devices. The second goal was finding the best conditions for improving the machining process in various scenarios. Output metrics included machining productivity, surface accuracy, roughness, wire electrode wear, and surface layer changes (Nagî et al., 2020).

Najm V. (2018). This study uses ANOVA to analyze control parameters like pulse on time (µs), current, and wire tension on heat affected zone, white layer, and Surface Roughness (SR) of high speed steel. Experiments have two primary elements. The results reveal that wire tension impacts surface roughness more than current, pulse on time, or heat affected zone (Najm, 2018).

Boujelbene M. and et al (2017). This study investigates the effects of WEDM process parameters like pulse on time, Servo Voltage, and peak current on Surface Roughness of high alloy steel X155CrMoV12. The goal is to find the optimal machining parameters that minimize SR. The trials were planned using Taguchi's design experiments approach. This study's key findings are: The surface roughness Ra increases with servo voltage, and increasing peak current I degrade WEDM-machined components at given speeds (Boujelbene et al., 2017).

Parthiban M. and et al (2017). Wire electric-discharge grinding (WEDG) for microshaft machining: experimental investigation of diameter accuracy and material removal rate. The impact of process parameters was investigated by repeatedly milling a 2.0-mm High Speed Steel (HSS) pin to a 0.60-mm diameter under different operating circumstances. The experimental data shows that the spark gap affects the rate of material removal by 81% and the precision of the diameter by 50% (Parthiban et al., 2017).

In wire electric discharge machining (WEDM), pulse on time, pulse off time, servo voltage, wire feed, current, and cutting speed were explored by Priyan M and et all (2016). Taguchi's L16 orthogonal array was used for parameter experiments. This study will determine the best WEDM settings for SS 304 machining to improve surface roughness and MRR.Pulse on time increases spark energy as electrical supply increases. Pulse-on time increases MRR, Kerf breadth, and Surface Roughness. Pulse on time most crucial in any reaction (Priyan et al., 2016).

At last, optimizing wire EDM settings for HSS (8X200) materials is crucial for efficient and successful machining. This research study uses Taguchi design parameter approach and

Grey Relational Analysis (GRA) to find the ideal parameter settings (pulse duration, pulse interval, Servo feed, and Servo voltage) to increase surface roughness, material removal rate, and cutting speed at the same experiment. These discoveries will improve HSS (8X200) machining procedures for high-performance component companies.

Methodology

1. **The experimental setup:** This part, displayed the technical details of the wire electrical discharge machining process, including the machines, wires, workpieces, and parameters involved. As can be seen in Fig. 2)a and b), the machining was performed using a wire cut machine 4-axis ELEKTRA DEM 400 A EL PULSE 5. The workshop at Iraq's University of Technology is home to the machine-in location. A High-Speed Steel (HSS) rod cutting 8 by 8 by 200 millimeters was utilized as the workpiece. Using a wire electrical discharge machining (WEDM) machine and a soft brass wire with a diameter of 0.25 millimeters, the rod was cut into nine pieces, each with a thickness of three millimeters (Fig. 3(a): rod of HSS before machining and Fig. 3(b): piece after cutting). The rod's chemical composition was determined using the ASME SEC.II P.A. standards and codes, as indicated in Table 1, by the Midland Refineries Company. Changing certain of the wire EDM process's settings can improve its efficiency. Table 2 shows the work's fixed parameters, whereas Table 3 shows the work's variable parameters. Parameters that can change are the Servo voltage (v), the Servo feed (mm/min), and the Servo pulse on and off times (s).

The following are the parameters that were altered in this study:

[1] Pulse on time (TON): This refers to the cutting time during which voltage is applied through the gap. Higher values of Pulse on time result in higher metal removal rates and lower surface roughness. Pulse on time is typically measured in microseconds.

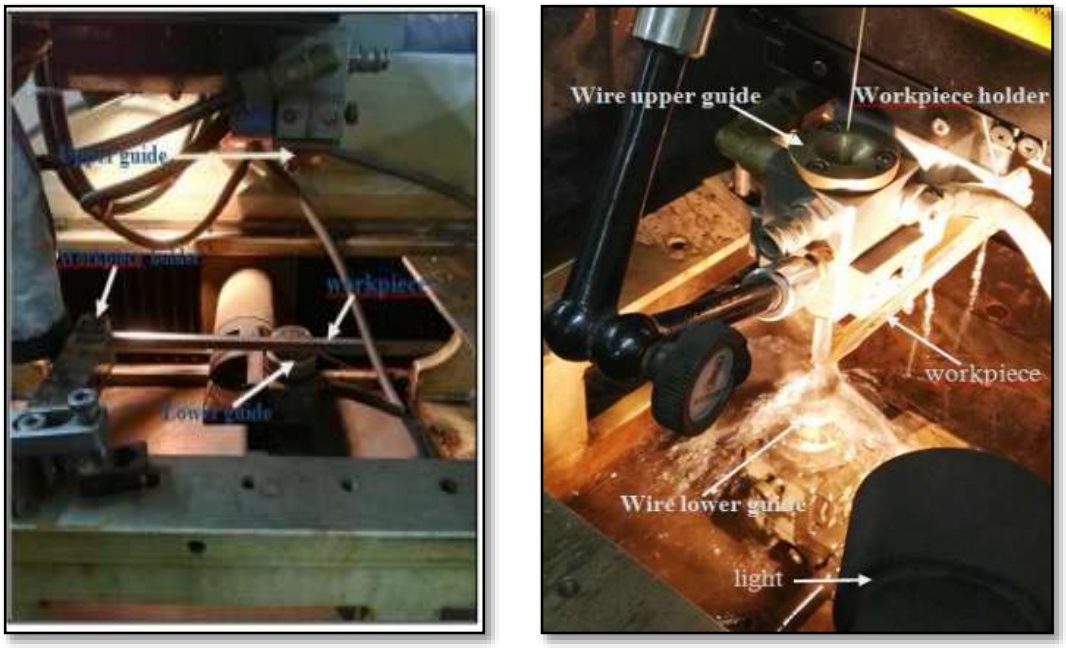
[2] Pulse off time (POFF): This parameter represents the duration of time during which there is no voltage across the gap. During this period, the dielectric fluid flushes away debris before the following discharge. The lowest possible value for pulse off time leads to the highest speed of cutting. This parameter is also measured in microseconds.

[3] Servo feed (SF): Servo feed refers to the feed rate of the table during the machining process. It can be chosen automatically based on servo voltage or set manually. In this study, the value of SF was controlled manually.

[4] Servo voltage (SV): Servo voltage controls the advancement and retraction of the wire. If the mean voltage during machining is upper than the level of set servo voltage, the wire advances. Conversely, if the mean voltage is lower, the wire retracts.



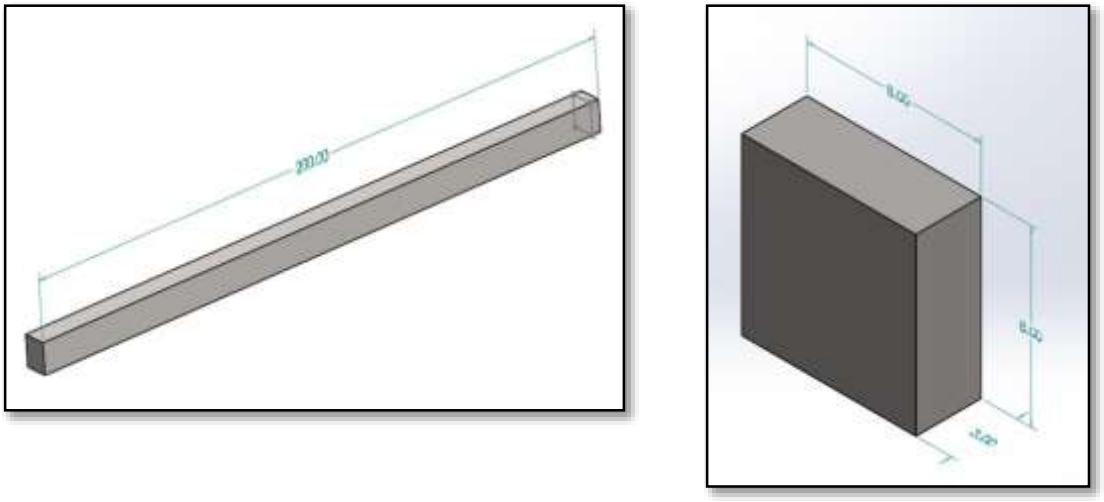
(a)



(b)

Fig.2. (a) Wire EDM Machine (b) Wire EDM Process.





(a) (b)

Figure 3. Workpiece (a) Before machining (b) After machining

Table 1. Chemical Composition of HSS (8X200)

Material	**C**	**Si**	**Mn**	**Cr**	**Mo**	**Ti**	**V**	**Fe**
Weight %	1.1	1.28	0.46	1.08	0.08	0.007	0.01	Balance

Table 2. Wire EDM Machining Conditions

1	Working Material is HSS (8X200)	**4**	Dielectric pure (distilled) water.
2	Brass wire cutting with 0.25 mm Dia.	**5**	Voltage 11 V
3	Wire tension (6) kgf.	**6**	Current 12 A

Table 3. Variable Parameters

Parameter	**Values**
Servo voltage (v)	20, 21, 22
Pulse on (µs)	110, 115, 120
Pulse off (µs)	30, 35, 40
Servo feed (mm/min)	350, 400, 450

2. **The Responses Variables:** Surface Roughness (SR), Material Removal Rate (MRR), and Cutting Speed(CS) have been studied in this work. Smaller value of SR is preferred and larger values of MRR and CS are preferred, so selecting optimal experiments will select relating on Taguchi design and Grey relational analysis.

[1] Surface Roughness (SR): The Pocket surf, a portable version of the Surface Gauge, was utilized to measure the surface roughness of all of the machining surfaces of all of the samples. The value of the average of the three readings that were taken from the Ra instrument for each machining line of sample was recorded. The apparatus that was utilized during the tests explained in Fig.4.

[2] Material Removal Rate (MRR): The rate at which material is removed during the wire EDM process has a significant impact on both the productivity and the expense associated with the machining process. It signifies that they have been erased. The quantity of material removed per unit of time spent machining, which is denoted by the following relationships and expressed as a unit (mm3/min) in Equation (1)(Ahmed, 2018).

$$MRR = Vc * b * H \dots\dots\dots (1)$$

$$b = dw * 2s \dots\dots\dots (2)$$

Where: 1-Material Removal Rate =MRR (mm3/min), 2-Cutting speed = Vc(mm3/min), 3-Cutting width =b (mm), 4-Workpiece thickness =H (mm), 5-Wire diameter =dw (mm), 6-Spark gab = s (mm).

[3] Cutting Speed (CS): It has an impact on the amount of work that can be accomplished throughout the machining process. A wire's cutting speed can be determined by dividing the traveled length by its machining time and then expressing the result in millimeters per minute (mm/min) (Ahmed, 2018). In addition, the WEDM process is not the same for every material because it varies from one material to the next based on the conductivity and melting qualities of a material.



Figure 4. Surface Roughness Apparatus

3. **The Taguchi design parameter:** For optimizing the cutting parameters in wire EDM, it is possible to make use of Taguchi optimization technique. Taguchi technique used for optimization the process's parameters is the essential stage for achieving high quality without an accompanying rise in cost (Durairaj et al., 2013). However, the Taguchi approach was initially developed with the purpose of optimizing individual performance characteristics (Al et al., 2009). The Taguchi design was nine experiments to four parameters with three levels as explained in Table.3. and the design of Taguchi explained in Table.4.

Table 4. Properties of clay soil

Exp.No.	Servo voltage (V)	Pulse on (µs)	Pulse off (µs)	Servo Feed (mm/min)	Surface roughness (Ra)	MRR (mm3/min	Cutting speed (mm/min)
1	20	110	30	350	2.443	7.976	1.227
2	20	115	35	400	3.363	11.050	1.700
3	20	120	40	450	3.427	12.058	1.855
4	21	110	35	450	2.413	8.983	1.382
5	21	115	40	350	3.717	7.618	1.172
6	21	120	30	400	3.457	8.294	1.276
7	22	110	40	400	2.383	9.315	1.433
8	22	115	30	450	2.840	8.847	1.361
9	22	120	35	350	3.633	10.374	1.596

4. **Grey Relational Analysis (GRA):** The application of grey theory in engineering analysis has seen extensive usage, and it indicates the ability to solve the problem of optimally selecting the machining parameters associated with a process that produces many output parameters (Durairaj et al., 2013). The optimal steps to grey relational analysis, more details in reference (Haq et al., 2008) (Rao, 2018)(Panda et al., 2016):

- Step 1: computing S/N (Signal to Noise) ratio for response variables by using equation (3) for MRR and CS (larger is the better) and using equation (4) for SR (smaller is the).

$$\frac{S}{N} = -10 \log \log_{10}(1/n) \sum_{i=1}^{n} \left(\frac{1}{y^2}\right) \dots\dots\dots \quad (3)$$

$$\frac{S}{N} = -10 \log \log_{10}(1/n) \sum_{i=1}^{n} (y^2) \dots\dots\dots . (4)$$

- Step 2: computing normalized value for each response to adopt the different in response units from equation (5), which used for S/N ratio larger is better and equation (6), which used for S/N ratio smaller is better.

$$Zij = \frac{yij - \min(yij, i = 1,2,\dots,n)}{max(yij, i = 1,2,\dots,n) - min(yij, i = 1,2,\dots,n)} \dots\dots\dots (5)$$

$$Zij = \frac{max(yij, i = 1,2,\dots,n) - yij}{max(yij, i = 1,2,\dots,n) - min(yij, i = 1,2,\dots,n)} \dots\dots\dots .. (6)$$

- Step 3: computing (GRC) grey relational coefficient for result of step 2 from equation(7):

$$\mathcal{E}\text{i} = \frac{\Delta \boldsymbol{min} + \boldsymbol{\mathcal{E}\Delta max}}{\Delta \boldsymbol{o} + \boldsymbol{\mathcal{E}\Delta max}} \dots\dots\dots . (7)$$

- Step 4: computing grade of grey relational (GRG) value from relation at equation (8):

$$GRG = \frac{1}{n} \sum_{1}^{n} \mathcal{E}i(Yij) \dots\dots\dots .. (8)$$

From arranged the values of grade relational analysis, the biggest value is the optimal experiment as explained in Table.5. the S/N ration and normalization and in Table.6. explained grey relational coefficient and grade values.

Table.5. S/N ration and Normalization of (GRA)

Exp. No.	S/N			Normalization		
	SR	MRR	CS	SR	MRR	CS
1	-7.7596	18.0351	-1.7768	0.0559	0.0998	0.9001
2	-10.5354	20.8672	-4.6089	0.7751	0.8099	0.1900
3	-10.6974	21.6251	-5.3668	0.8171	1.0000	0.0000
4	-7.6523	19.0684	-2.8101	0.0281	0.3589	0.6410
5	-11.4031	17.6368	-1.3785	1.0000	0.0000	1.0000
6	-10.7732	18.3752	-2.1170	0.8367	0.1851	0.8148
7	-7.5436	19.3831	-3.1249	0.0000	0.4378	0.5621
8	-9.0663	18.9354	-2.6771	0.3945	0.3256	0.6743
9	-11.2061	20.31892	-4.0606	0.9489	0.6724	0.3275

Table.6. Coefficient and grade of (GRA)

EXP. No.	Grey Coefficient			Grade	Rank
	SR	MRR	CS		
1	0.3462	0.3571	0.8335	0.5122	6
2	0.6898	0.7246	0.3816	0.5987	5
3	0.7322	1.0000	0.3333	0.6885	2
4	0.3397	0.4381	0.5821	0.4533	8
5	1.0000	0.3333	1.0000	0.7777	1
6	0.7539	0.3802	0.7297	0.6213	4
7	0.3333	0.4707	0.5331	0.4457	9
8	0.4523	0.4257	0.6056	0.4945	7
9	0.9073	0.6042	0.4264	0.6460	3

Results and Discussion

GRA is especially beneficial when several response factors are evaluated, since it assists in determining the optimum combination of parameters that yields the most desirable outcomes across these variables. Detecting from Table .6. the experiment at rank 1, at experiment five, had the optimal input parameters. This shows that the parameters utilized in experiment 5, namely surface roughness, material removal rate, and cutting speed, are most closely matched with the desired outcomes across all response variables. Thus, grey relational grade may calculate factor influence and identify the optimal amount for each controllable component, at experiment five the input parameters were: (level 2 of servo voltage (SV)= 21 V, level 2 of pule on time (PON) = 115 µs, level 3 of pulse off time (POFF) = 30µs, and level 1 of servo feed (SF) = 350 mm/min. In addition, the total mean of the grey relational grade is estimated for each of the nine tests, and the results of this estimation are given in Table 7. Figure 5 provides a depiction of the relational grade chart for the levels of the processing parameters in grayscale. The bigger the grey relational grade, which ultimately results in an increased number of multiple output characteristics. However, in order to successfully compute the optimal combinations of the method parameter levels, it would be necessary to have knowledge about the relative values of the parameters that correspond to the many output characteristics.

Table 7. Mean (GRG)

Level	Servo voltage	Pulse on	Pulse off	Servo feed
1	0.5998	0.4705	0.5427	0.6454
2	0.6175	0.6237	0.5660	0.5553
3	0.5288	0.6519	0.6373	0.5455
Delta	0.0887	0.1815	0.0946	0.0999
Rank	4	1	3	2

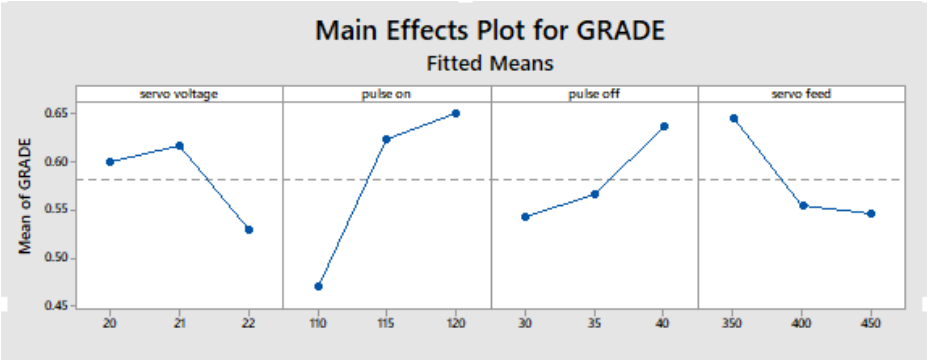


Figure 5. Main Parameters effect on GRG

Analysis of Variance

The primary purpose of the analysis of variance (ANOVA) is to identify the operational parameter that has the greatest influence on the performance characteristics. If a factor has a higher proportion of contribution, it indicates that it has a greater effect on the attributes of the output. The results of the ANOVA are presented in Table.8. for the Grey relational grade, along with the percentage contributions made by each operation variable in descending order of significance.

Table 8. ANOVA Analysis of GRG

Source	DF	Adj SS	Adj MS	F-Value	P-Value	Contribution
Servo voltage	2	0.01323	0.006615	0.44	0.663	12.82%
Pulse on	2	0.05722	0.028609	3.73	0.089	55.43%
Pulse off	2	0.01458	0.007292	0.49	0.633	14.13%
Servo feed	2	0.01819	0.009096	0.64	0.559	17.62%
Error	6	0.08503	0.014172			
Total	8	0.10323				100%

*Where: Df: Degree of freedom.
SS: Sum of square.
MS: Mean square.

Conclusions

Experiments with wire EDM were carried out on machines equipped with brass wire and HSS (8X200). The surface roughness, the rate of material removal, and the cutting speed were measured and for a number of distinct combinations of machining parameters. The following inferences and conclusions can be made:

- The study found the best wire EDM cutting settings using Taguchi optimization and Grey Relational Analysis. Experiment 5 was the best, demonstrating these settings can increase machining quality and efficiency.
- In this work WEDM process gave the results with the most beneficial performance characteristics. (level 2 of servo voltage (SV)= 21 V, level 2 of pule on time (PON) = 115 µs, level 3 of pulse off time (POFF) = 30µs, and level 1 of servo feed (SF) = 350 mm/min.
- This investigation shows that servo voltage, pulse on time, pulse off time, and servo feed the most effecting in this WEDM machining experiments. Pulse on time 55.43%, Servo feed 17.62%, pulse off time 14.13%, and at last servo voltage 12.82%.
- These optimization methods can improve production processes and lower costs. The research also gives a systematic strategy to optimize parameters and increase performance in different processes and sectors.

References

1. Abu-Farsakh M, Coronel J, Tao M (2007) Effect of soil moisture content and dry density on cohesive soil-geosynthetic interactions using large direct shear tests. J Mater Civ Eng 19(7):540–549. https://doi.org/10.1061/(ASCE)0899-1561(2007)19:7(540)
2. Arulrajah A, Rahman MA, Piratheepan J, Bo MW, Imteaz MA (2014) Evaluation of interface shear strength properties of geogrid-reinforced construction and demolition materials using a modified large-scale direct shear testing apparatus. J Mater Civil Eng, ASCE, Vol. 26, No. 5. https://doi.org/10.1061/(ASCE)MT.1943-5533.0000897.
3. Arulrajah A, Horpibulsuk S, Maghoolpilehrood F, Samingthong W, Du Y-J, Shen S-L (2015) Evaluation of interface shear strength properties of geogrid reinforced foamed recycled glass using a large-scale direct shear testing apparatus. Adv Mater SciEng.https://doi.org/10.1155/2015/235424.
4. ASTM (2018) Standard Specifications Manual, American Society for Testing and Materials.
5. Banyhussan, Q. S., Mosa, A. M., Hussein, A. N., & Sigar, E. J. (2023). Evaluating the Shear Strength of Subbase-subgrade Interface Using Large Scale Direct Shear Test. International Journal of Innovation in Engineering, 3(1), 35-47.
6. Bergado DT, Youwai S, Teerawattanasuk C, Visudmedanukul P (2003) The interaction mechanism and behaviour of hexagonal wire mesh reinforced embankment with silty sand backfill on soft clay. Comput Geotech 30(6):517–534. https://doi.org/10.1016/S0266-352X(03)00054-5.
7. Choudhary AK, Krishna AM (2014) Influence of different types of soils on soil- geosynthetics interaction behavior. IJIRSET 3(SPI 4):60–68.
8. Dafalla MA (2013) Effects of clay and moisture content on direct shear tests for clay-sand mixtures. Adv Mater Sci Eng. https://doi.org/10.1155/2013/562726.
9. Giroud, J.P. and Han, J. 2004. Design method for geogridreinforced unpaved roads–I. Journal of Geotechnical and Geoenvironmental Engineering, Volume 130, Issue 8, pp. 775-786.
10. Goud, G. N., & Umashankar, B. (2018). Interface shear strength properties of gravel bases and subgrades with various reinforcements. *International Journal of Geosynthetics and Ground Engineering*, *4*, 1-14.
11. Kamalzare M, Ziaie-Moayed R (2011) Influence of geosynthetic reinforcement on shear strength characteristics of two-layer subgrade. Acta Geotech Slov 8:39–49 Jewell, R. A. (1996). Soil reinforcement with geotextiles. London: Thomas Telford.
12. Kandolkar SS, Mandal JN (2013) Direct shear tests on stone dust. In: Proceedings of Indian Geotechnical Conference, Roorkee, pp 1–6.
13. Liu, C. N., Zornberg, J. G., Chen, T. C., Ho, Y. H., & Lin, B. H. (2009). Behavior of geogrid-sand interface in direct shear mode. Journal of Geotechnical and Geoenvironmental Engineering, 135(12), 1863–1871.

14. Lopes, M. L. (2002). Soil-geosynthetic interaction. In S. K. Shukla (Ed.), Geosynthetics and their applications (pp. 57–61). London: Thomas Telford.
15. Nareeman, BJ, Fattah, MY, (2012), Effect of Soil Reinforcement on Shear Strength and Settlement of Cohesive-Frictional Soil, International Journal of GEOMATE, Vol. 3, No. 1 (Sl. No. 5), pp. 308-313 Geotec., Const. Mat. & Env., ISSN:2186-2982(P), 2186-2990(O), Japan.
16. Nicks JE, Gebrenegus T, Adams M (2015) Strength characterization of open-graded aggregates for structural backfills (No.FHWA-HRT-15-034).
17. Sakleshpur, V. A., Prezzi, M., Salgado, R., Siddiki, N. Z., & Choi, Y. S. (2019). Large-scale direct shear testing of geogrid-reinforced aggregate base over weak subgrade. International Journal of Pavement Engineering, 20(6), 649-658.
18. Sayeed MMA, Ramaiah BJ, Rawal A (2013) Interface shear characteristics of jute/polypropylene hybrid nonwoven geotextiles and sand using large size direct shear test. Geotext Geomembr 42:63–68. https://doi.org/10.1016/j.geotexmem.2013.12.001.
19. SCRB /R6, 2003, Standards and Specifications for Roads and Bridges (2003) (Iraqi Standard Code), Ministry of Housing and Reonstruction.
20. Umashankar B, Hariprasad C, Sasanka Mouli S (2015) Interface Properties of Metal-Grid and Geogrid Reinforcements with Sand. In: International foundations congress and equipment expo 2015, San Antonio, pp 1–9.
21. Voottipruex P, Bergado DT, Ounjaichon P (2000) Pullout and direct shear resistance of hexagonal wire mesh reinforcement in weathered Bangkok clay. Geotech Eng 31(1):43–62
22. Xu, Y., Williams, D. J., & Serati, M. (2020). Investigation of shear strength of interface between roadbase and geosynthetics using large-scale single-stage and multi-stage direct shear test. Road Materials and Pavement Design, 21(6), 1588-1611.

Effect of Toxoplasmosis On Zinc and Thyroid Hormones Levels with Pregnant Women

Aya R. Abduwahab Alheany [1], Ammer Abd. Mohammed [2]

© 2023 The Author(s). This open access article is distributed under a Creative CommonsAttribution (CC-BY) 4.0 license.

Abstract: This study included 115 pregnant women, the case group consisted of 65 women who were infected with toxoplasmosis, while the control group involved 50 pregnant women who were not infected with toxoplasmosis. All the studied women attended Baghdad teaching hospital during the period from 1st February 2021 to 1st March 2022. The results in the current study revealed NS. between the mean ages between the case group (41.84±15.88) years and the control group (40.85±15.48) years. There was HS. (P<0.01) in mean Toxoplasma IgM levels between the case group (2.00±1.17) and the control group (0.09±0.17), and there was also HS. (p<0.01) in mean Toxoplasma IgG levels between the case group (14.20±7.06) and the control group (0.06±0.11). The findings showed HS. (p<0.01) in serum zinc levels between the patients group (56.84±18.87) and the control group (88.09±14.85).

The result also showed HS. (p<0.01) between the mean levels of T3 and TSH (3.16±1.44) and (2.63±1.06) respectively and the control groups (1.37±0.80) and (1.14±0.98) respectively, while NS. (p>0.05) was found between the levels of T4 (3.65±0.97) and the control group (4.02±1.60). There was a correlation between Toxoplasma IgM and serum zinc (22.515), T3 (4.753), T4 (9.261), and TSH (2.795) with HS. (P<0.01), and a correlation between Toxoplasma IgG and serum zinc (17.505), T3 (11.736), T4 (11.377) and TSH (12.878) with HS. (P<0.01).

Key Words: Toxoplasmosis, Thyroid Hormones, Pregnant Women

Author details

[1] College of Medicine, Ibn Sina University for Medical and Pharmaceutical Sciences, Baghdad, Iraq

[2] Department of Medical Laboratory Techniques, College of Health and Medical Technology, Middle Technical University, Baghdad, Iraq

Citation information

Cite this article as:

Alheany, A.R., Mohammed, A.A., (July 2023), *Effect of Toxoplasmosis On Zinc and Thyroid Hormones Levels with Pregnant Women*, Proceedings of the Minar Congress, Turkey, (9) pp 307-312, DOI: http://dx.doi.org/10.47832/MinarCong9-26

http://dx.doi.org/10.47832/MinarCong9-26

[1] aya_alheany@ibnsina.edu.iq

[2] amer.mohammed1968@gmail.com

Introduction

The infection by Toxoplasma gondii is often long-lasting and characterized by the existence of Toxoplasma cyst in muscular & nervous tissues in particular. Moreover, the infection mainly causes a life time protective immunity (cellular and humoral), showing low serum anti-Toxoplasma IgG levels among infected persons (1). Latent toxoplasmosis is can cause different behavioral and hormonal alteration in infected animals & humans and can contribute in causing various psychiatric and neurologic disorders (2). Infected rats and mice developed impaired coordination and performances of the motor neurons, defective learning & decreased avoidance of open predators & spaces (3). They are thought to be evolutionary mechanisms for increasing the chances of host that is ingested by feline (4). In addition, latent toxoplasmosis raises the opportunity for birth giving of male mice and humans (5). Toxoplasmosis Patients with altered levels of testosterone hormone might develop physical symptom e.g. dermal hyper reaction such as erythema, irritation, hirsutism and acne in addition to abnormal muscle growths, renal failure and psychological defects including mood swing, anxiety with depression (6). Many researchers still discuss the impact of latent toxoplasmosis on testosterone.

Published studies demonstrated decreased & increased testosterone concentrations correlated with the seropositive T. gondii among human-beings (6). In present study, the effect of latent toxoplasmosis on serum testosterones was evaluated in males & females. The growth of secondary sexual characteristic of male is regulated by testosterone hormone. Dehydroepiandrosterone (DHEA) is an essential and mainly abundant endogenous circulating steroid hormone in humans produced by the adrenal glands. DHEA acts as progenitor of testosterone & estrogen (7). The hormone prolactin is produced from anterior pituitary gland (due to inhibitory controlling of dopamine) and plays a main part in growth, lactation and reproductive function regulations (8). Localization of sex hormone receptor within immune cell, such as granulocytes, lymphocytes, macrophages & mast cell reveals the direct linkage between the immune & endocrine system and that the endocrine factor is able to modulate the expression of target gene within the immune cell directly (9). Zinc (Zn) is the metal that is found as an essential trace element in all living organisms and tissues. The systematic existence of zinc in tissues is highly affected by the anabolic process balance that regulates the renewal of skeletal and soft tissues (16). Zink is also an important element in the immune system since it functions as an anti-parasitic element (10).

Martial and Methods

From the 1st of February/ 2021 till the 1st of March/ 2022, 115 serum samples were collected from pregnant women who attended Ibn-Albalady Hospital, Al-Ilweia Hospital, Fatimat-Alzahra'a Hospital, Baghdad Teaching Hospital [Medical City Hospital] and Al-Shafaa Hospital in Baghdad province for delivery. The design of this study was based on detecting IgM and IgG antibodies in the sera of pregnant women with toxoplasmosis. The levels of serum T3, T4, TSH, and Testosterone were also measured. Before blood collection, complete

information were recorded in a questionnaire form prepared for this purpose. From each woman, (5) ml of venous blood was obtained, and left for 15 minutes at room temperature, then centrifuged for 5 minutes at 3000 RPM to obtain sera, which were stored at -20 ˚C till use. Toxo. IgM-capture immuno-enzymatic assay is used for the determination of IgM Ab to T. gondii in human sera or even plasma. The serum zinc level was measured by BS 200 technique, while the T3, T4, and TSH levels were tested by ELISA technique

Statistical analysis

The usual statistical methods were used for the analysis and evaluation of the results including:

Descriptive statistics: which included the percentages, frequencies, means, standard deviations & standard errors as well as accumulative percents, which included the Chi-Square test.

Results

Table (1) showed that the mean age of the study group was (41.84±15.88) and the control group (40.85±15.48), with NS. between them (P>0.05).

Table 1. The mean age group of patients and control

	Groups	Mean± Std.	P-Value (CS.)
Age	Cases (n=61)	41.84±15.88	P=0.730
	Control (n=61)	40.85±15.48	P>0.05(NS)

Highly Significant= HS
No significant = NS

Table (2) demonstrated that there was HS. (p<0.01) in the mean *Toxoplasma* IgM levels between the study group (2.00±1.17) and the control group (0.09±0.17), and there was also a HS. (p<0.01) in the mean *Toxoplasma* IgG levels between the study group (14.20±7.06) and the control group (0.06±0.11).

Table 2. the corporation between Study Groups and control group with TOXO IgM & TOXO IgG levels

	Groups	Mean± Std.	P-Value (CS.)
TOXO IgM	Cases (n=61)	2.00±1.17	P=0.000
	Control (n=61)	0.09±0.17	P<0.01 (HS)
TOXO IgG	Cases (n=61)	14.20±7.06	P=0.000
	Control (n=61)	0.06±0.11	P<0.01 (HS)

In table (3), it was shown that there was HS. (p<0.01) in the serum zinc levels between the patients group (56.84±18.87) and the control group (88.09±14.85).

Table 3. The levels of serum zinc in study group and control group

	Groups	Mean± Std.	P-Value (CS.)
Zinc	Cases (n=61)	56.84±18.87	P=0.000
	Control (n=61)	88.09±14.85	P<0.01 (HS)

It was HS. ($p<0.01$) was found between T3 levels in the patient group (3.16±1.44) and the control group (1.37±0.80), and between TSH levels in the patients group (2.63±1.06) and the control group (1.14±0.98), while NS. was detected between T4 levels in the patients group (3.65±0.97) and the control group (4.02±1.60) as shown in table (4).

Table 4. The comparison between T3, T4 and TSH levels

	Groups	Mean± Std.	P-Value (CS.)
T3	Cases (n=61)	3.16±1.44	P=0.000
	Control (n=61)	1.37±0.80	P<0.01 (HS)
T4	Cases (n=61)	3.65±0.97	P=0.124
	Control (n=61)	4.02±1.60	P>0.05 (NS)
TSH	Cases (n=61)	2.63±1.06	P=0.000
	Control (n=61)	1.14±0.98	P<0.01 (HS)

The correlation between *Toxoplasma* IgM and serum zinc (22.515), T3 (4.753), T4 (9.261) , TSH (2.795) showed HS. ($P<0.01$), as shown in table (5).

Table 5. The correlation between TOXO IgM and Zinc, T3, T4 and TSH

Parameters	t-test	P-Value	CS.
TOXO IgM & Zinc	22.515	0.000	P<0.01 (HS)
TOXO IgM & T3	4.753	0.000	P<0.01 (HS)
TOXO IgM & T4	9.261	0.000	P<0.01 (HS)
TOXO IgM & TSH	2.795	0.007	P<0.01 (HS)

The correlation between *Toxoplasma* IgG and serum zinc (17.505), T3 (11.736), T4 (11.377), TSH (12.878) revealed HS. ($P<0.01$) as illustrated in table (6).

Table 6. The correlation between TOXO IgG and Zinc, T3, T4 and TSH

Parameters	t-test	P-Value	CS.
TOXO IgG - Zinc	17.505	0.000	P<0.01 (HS)
TOXO IgG - T3	11.736	0.000	P<0.01 (HS)
TOXO IgG - T4	11.377	0.000	P<0.01 (HS)
TOXO IgG - TSH	12.878	0.000	P<0.01 (HS)

Discussion

Toxoplasmosis is one of the problems of women, especially pregnant women, because the presence of this parasite inside the cells of the host made this microorganism more dangerous. Previous studies have proven that there are changes that occur in the pregnant mother, such as deformation of the fetus and repeated miscarriage. Here, we wanted to take a look at some physiological changes that lead to an imbalance in some levels of thyroid hormones, as well as the zinc levels. It is noted that zinc levels in women infected with toxoplasmosis decreased (56.84±18.87) from its normal levels in the control group (88.09±14.85), $P<0.01$. the results agreed with (Al-Masoudi H. Kh. *et al*, 2020), who reported

that there was a decrease in serum zinc levels in aborted women. The level of serum zinc significantly decreases in women aged (34-43 years) which was (37.73 µg/dl (compared with control group, while level of Vitamin D was significantly decreased in women aged (24-33years), which was (146.3ng/mL) (11). This indicates that *Toxoplasma* consumes zinc and its levels decrease in the bodies of the infected, especially pregnant women. Also the levels of Thyroid hormones decreased in comparison to control group as the T3 was (3.16±1.44), while the control was (1.37±0.80), T4 (3.65±0.97), but the control was (4.02±1.60) and TSH was (2.63±1.06) and the control group was (1.14±0.98) regarding the differences between groups with *Toxoplasma* and normal performance of the thyroid gland compared to two groups affected by Toxoplasma, while in hyporthyroidism and hyperthyroidism groups it was found that the infection with the parasite increased to levels of TSH and T3 with low levels of T4, which showed significant difference compared to the group Hypothyrodisim & Toxoplasma with a decrease in high Compared to the *Toxoplasma* group with normal thyroid performance in T4 levels, there were no differences between the two groups in TSH and T3 levels, while significant differences were found in TSH and T3 levels between *Toxoplasma* group and Hyperthyrodisim and *Toxoplasma* group (12). This study was in a harmony with Procházková, *et al*, 2014). (Procházková) showed that there is a lack of thyroid function due to Toxoplasma, which leads to an imbalance in the levels of thyroid hormones in the bodies of women, including pregnant women (13). Our research proved that the effect of *Toxoplasma* was directly on the decrease in the levels of parasitic living thyroid hormones inside the cells of the patients; this mechanism that *Toxoplasma* uses may be the reason for the low levels of thyroid hormones, the results matches with (Alvarado-Esquivel *et al,* 2019) (14).

References

1. Halonen, S.K. and Weiss, L.M. (2013) Toxoplasmosis. Handbook of Clinical Neurology, 114,125-145. http://dx.doi.org/10.1016/B978-0-444-53490-3.00008-X.
2. Dalimi A, and Abdoli A. Latent Toxoplasmosis and Human HLA. Iraniant. J. Parasitol. (2011). 7 (1): 1–17.
3. Zouei, N. Saeedeh Shojaee, S. and Mohebali, M. et al, The association of latent toxoplasmosis and level of serum testosterone in humans, BMC Research Notes volume 11, Article number: 365 (2018).
4. Tong, W. H. Pavey, Ch. Ryan O'Handley, R. & Vyas, A. Behavioral biology of Toxoplasma gondii infection, Parasites & Vectors volume 14, Article number: 77 (2021).
5. Stelzer, S. BassoJ, W. and Silván, B. et al, Toxoplasma gondii infection and toxoplasmosis in farm animals: Risk factors and economic impact, Food and Waterborne Parasitology V.15, June 2019, e00037.
6. Zouei, N. Shojaee, S. and Hossein Keshavarz et al, The association of latent toxoplasmosis and level of serum testosterone in humans, MBC Research Notes. 2018: 11:265.
7. Abdulmaged M. Traish, Irwin Goldstein, and Noel N. Kim, Testosterone and Erectile Function: From Basic Research to a New Clinical Paradigm for Managing Men with Androgen Insufficiency and Erectile Dysfunction, Eur- Urol. 2007: 52(1) 54-70.
8. Reinhoffer, V. Oláh, M. and Vecsernyés, M. et al, The Regulation of Pituitary Prolactin Secretion: Hypothalamic, Intrapituitary and Intracellular Factors and Signaling Mechanisms, Dimension. 2013: DOI: 10.5772/55571.
9. Gubbels Bupp, M. R. Potluri, T. and Klein, S. L. The Confluence of Sex Hormones and Aging on Immunity, Front Immunol. 2018: 9:1269.
10. SEYREK, K. PAŞA, S. and KIRAL, F. et al, Levels Of Zinc, Copper And Magnesium In Sheep With Toxoplasmosis, Uludag Univ. J. Fac. Vet. Med. 23 (2004), 1-2-3: 39-42.
11. Al-Masoudi, H. Kh. *, Khadhm, A. and AL-Karaawy, F. H. The Impact of Toxoplasma gondii Infection on The Serum Zinc, Vitamin D and Malondialdehyde Levels among Recurrent Miscarriage Women in Babylon Province-Iraq, Sys Rev Pharm 2020;11(7): 443-449.
12. Al-Issawi T. A. M. , and Mohammed, A. S. Effects of Infection with Toxoplasma Gondii to the Levels of Thyroid Hormones European Journal of Molecular & Clinical Medicine, 7(1): 110—114:2020.
13. Procházková, S. K. and Potluková, E. et al, Effects of Latent Toxoplasmosis on Autoimmune Thyroid Diseases in Pregnancy Pols one: 2014: 9(10): e 110878.
14. Alvarado-Esquivel, C. Ramos-Nevarez, A. and Guido, C. A. Association between Toxoplasma gondii infection and thyroid dysfunction: a case-control seroprevalence study BMC Infectious Diseases 19: 826 (2019).

Antimicrobial Effect of Gaultheria Procumbens On Multidrug Resistant Bacteria Causing Wound Infections

Layla Fouad Ali [1], Nagham Shakir AlAttar [2]

© 2023 The Author(s). This open access article is distributed under a Creative CommonsAttribution (CC-BY) 4.0 license.

Abstract: Worldwide, a fast rise of resistant bacteria threatens the effectiveness of antibiotics, so alternatives should be used to overcome this serious problem. In this study a plant extract was used against multidrug resistant bacteria. Eight Klebsiella pneumonia and eight Staphylococcus aureus isolates were obtained from wounds infections. They were isolated and identified by biochemical tests and confirmed by using Vitek-2 test. The plant Gaultheria procumbens was extracted by. Susceptibility test was performed for nine antibiotics against all 16 isolated bacteria, this study brings to light that Klebsiella pneumonia isolates were 100% resistant to most antibiotics but they were sensitive with 12.5%, 75% and 75% to clindamycin, imipenem and meropenem respectively, while Staphylococcus aureus isolates were sensitive with 25% to imipenem and meropenem only. Minimal Inhibitory Concentration was assessed by using microtiter plate for plant extract and meropenem to all isolates. The plant extract subMICs were used against biofilm formation in Klebsiella pneumonia and Staphylococcus aureus isolates. Biofilm inhibition was calculated for each isolate, furthermore, biofilm formation was reduced in most Staphylococcus aureus isolates more than in Klebsiella pneumonia isolates.

Key Words: Antimicrobial, Gaultheria Procumbens, Wound, Infections.

Author details

[1] – [2] College of Science, Biology Department, University of Baghdad, Baghdad, Iraq

Citation information

Cite this article as:

Ali, L.F., AlAttar, N.S., (July 2023), *Antimicrobial Effect of Gaultheria Procumbens On Multidrug Resistant Bacteria Causing Wound Infections*, Proceedings of the Minar Congress, Turkey, (9) pp 313-328, DOI: http://dx.doi.org/10.47832/MinarCong9-27

http://dx.doi.org/10.47832/MinarCong9-27

[1] laylafouadali@gmail.com

[2] dr.naghamattar@mail.com

Introduction

Burns are among the most frequent and pervasive types of trauma that affect skin tissues (1). Patients may require lengthy hospital stays, which can result in nosocomial infections. Furthermore, the germs that live in patients might cause wound infections. (1, 2). When patients experience bacteremia and multiple organ failure syndrome, the risk of invasive wound infection increases. This suggests that 80% of wound infections may be the cause (3, 4). Additionally, other elements including immunological dysfunction, skin barrier degradation, and moist protein-rich eschar promote microbial development because this region is avascular and prevents the delivery of immune cells and immunoglobulins (1, 5).

The emergence of multidrug-resistant (MDR) bacteria caused an increase in burn wound infections, which in turn caused sepsis and death globally (6). The harmful bacteria become more resistant to common antibiotics, and patients may experience significant side effects from taking highly toxic medications like tigecycline and colistin (8). Because of this, empirical antibiotic therapy is insufficient to treat wound infections brought on by MDR bacterial pathogens, and wounds are irreparable (9). The most nosocomial pathogens that has the ability to colonize the skin and cause severe disease locally and systematically infection is Klebsiella pneumoniae and Staphylococcus aureus (10). This bacteria develop antibiotic resistance to many antibiotics like, colistin, carbapenem and fluoroquinolones (11, 12).

Due to the higher surface area involved and the longer length of stay for the patient, burn wounds are typically considered to be richer reservoirs of infection than surgical wounds. The primary factor in the morbidity and mortality of hospitalized burn victims is infection. Infections are to blame for over 75% of burn injury fatalities. The bacteria are spread to the patients who have been hospitalized either by hands, feces, or hydrotherapy (13).

S. aureus and K. pneumonia are two common bacteria identified from burn sites in hospitalized patients. The patterns of antibiotic sensitivity for these organisms frequently shift globally, particularly in emerging nations, which reduces the efficacy of antimicrobial drugs (14). Antimicrobial resistance's effects include a rise in morbidity and a decline in treatment effectiveness. The threat to the public health posed by MDR pathogens and the prevalence of MDR bacteria in hospital environments and patients is a serious issue. Therefore, the information about theses pathogens should be updated as it is very important in management of patients and record the emergence or MDR pathogens in different regions. Most S. aureus produce the enzyme penicillinase which make penicillin ineffective (15). S. aureus is one of normal flora that found in nasal vestibule and different regions in skin. In burn patients the primary barriers of skin are lost and thus exposed to pathogenic bacterial invasion. As a result, during hospitalization, the predominant flora of burn sites will switch from gram positive bacteria to gram negative bacteria such Pseudomonas aeruginosa (16).

A facultatively anaerobic, Gram-ve, encapsulated, non-motile bacteria is Klebsiella pneumoniae. Carl Friedländer initially described the bacteria in 1882 after Edwin Klebs first isolated it in 1875 from the airways of a patient who was dying of pneumonia. One significant

opportunistic and iatrogenic infectious bacterium with significant clinical implications is K. pneumoniae (17). Although it frequently colonizes the digestive and nasal tracts, it is not a disease-causing agent. Even yet, colonization may result in infection when the host immune system weakens, particularly in diabetes patients, people taking glucocorticoid therapy, and people who have had organ transplants. In nature, K. pneumoneae is primarily found in soil, water, and other surfaces (18). K. pneumoniae colonizes several mucosal surfaces in people. Because of the high presence of K. pneumoneae in human gastrointestinal and it is a major reservoir for infection. The studies revealed that K. pneumoniae infections serotypes is the same as colonizing bacteria in gastrointestinal tract. Other studies confirmed that the strains isolated from burn infections is the same as the colonizing strains of K. pneumoniae (19).

Recent years have seen an upsurge in carbapenem resistance in K. pneumoniae due to the widespread usage of these drugs in clinical settings. With a high fatality rate, it first emerged in the 1990s and has since spread widely. The presence of carbapenem-resistant bacteria is a stand-alone risk factor for mortality in patients with nosocomial infections. There are several mechanisms that lead to K. pneumoniae carbapenem resistance (20).

Alternative to antibiotics is needed to overcome the pathogenic resistance. Different portions of plants include essential oils, which are made up of aromatic and volatile substances. Due to the antibacterial actn that EOs have demonstrated, their main function is to protect plants against infections (21). The chemical composition of EOs influences their effects and can be influenced by the quantity of a single component from various plants with various chemotypes. The use of EOs may result in changes to cellular structure, such as the creation of membrane lipids and the deterioration of cell walls and cytoplasmic membranes. According to one theory, EOs control quorum sensing systems by forming biofilms and expressing virulence factors (22).

Because of their potent odors and smells, as well as their capacity to suppress microbiological growth, essential oils are frequently used in the manufacturing of cosmetics, perfumes, and foods. Different EO characteristics have been shown to possess antibacterial qualities, which have been thoroughly examined to determine their potential applicability as alternatives to currently used antimicrobial therapies. Since EOs have been shown to have antibacterial, antiviral, antifungal, and insecticidal characteristics, we can think of them as an alternative to the existing antimicrobials used on humans and animals (21)

The availability of antimicrobials for the treatment of bacterial illnesses in humans and animals is impacted by antimicrobial resistance, which poses a global hazard to animal and public health. Reducing the use of antibiotics in human and veterinary medicine may reduce the issues brought on by the emergence of antibiotic resistance. From the standpoint of uses in aquaculture, earlier studies shown the antibacterial activity of EOs against many microorganisms, including human and animal infections. Different language groups in Yunnan Province, China, have traditionally employed the Ericaceae plant Gaultheria longibracteolata, but little research has been done on it. Our ethnobotanical research in

Yunnan's Lüchun County revealed that this plant is used for a variety of traditional purposes, including food, medicine, and worship. It is appreciated medically for its capacity to ease muscular and nerve pain, and aromatherapy is another complementary medical practice that makes use of it. Both an insecticide and an antibiotic have been employed with it Gaultheria procumbens and Gaultheria fragrantissima, the two species of wintergreen, are the most prevalent sources of wintergreen oil. Wintergreen oil's main component, methyl salicylate, has antibacterial, analgesic, and anti-inflammatory activities and is chemically related to aspirin(22).

The current study is aimed to examine the prevalence and patterns of antibiotic resistance in S. aureus and K. pneumonieae isolated from burn wound infections.

Materials and Method

Isolation and Identification of *Klebsiella pneumonia* and *Staphylococcus aureus* isolates.

Laboratories at a few hospitals in Baghdad gathered burn wound swab samples, which were then grown on MacConkey agar and Mannitol salt agar. Through sub-culturing on these two media and subsequent incubation at 37 oC for 18–24 hours, isolates were obtained from these labs. Suspicious colonies were located using biochemical and morphological methods. Gram staining was used to analyze the microscopic characteristics of colonies and reveal the distinctive morphology of bacteria under a light microscope. Additionally, a motility test was carried out to identify Klebsiella. The Vitek 2 compact system was used to confirm the isolates' identity.

Antibiotic Susceptibility Testing

The modified Kirby-Bauer method (23) was used to test nine antibiotics (clindamycin, tetracycline, trimethoprim-sulphamethaxazole, erythromycin, lincomycin, ceftriaxone, amoxicillin-clavulanic acid, imipenem and meropenem) against all 16 isolates of *K. pneumonia* and *S. aureus*.

Preparation of Essential oil of *Gaultheria procumbens*

Essential oil of *Gaultheria procumbens* was extracted from the dried leaves of the plant. (250g) of dried parts by steam distillation method (Cleavenger). The plant material wiBioled with D.W (1.2L) for 3h; kept at 4º C until used (24).

Determination of Minimal Inhibitory Concentration of Antibiotic and *Gaultheria procumbens* Essential Oil against *Klebsiella pneumonia* and *Staphylococcus aureus* isolates.

96-well micro-titer plates was used. The isolates were cltured in nutrient broth and incubated at 30°C for 24 hours. The broth for Muller-Hinton was made. This approach made

use of 96 U-shaped microtiter plates. Except for the last well (12th well), the plate's wells were all filled with 100 l of Muller-Hinton broth (on the first horizontal line). A range of concentrations were prepared, for antibiotic (3.9-2000 µg/ml) and plant EO dilutions (V:V) (0.39-50%). 100 µL of working stock was put into the first well only, and it was thoroughly mixed. 100 µL was taken from the first well and transferred to the second one, and it was mixed thoroughly. The other wells from 3 to 10 were subjected to the same procedure. From the tenth well, 100 L were collected and then wasted. A total of 100 liters of distilled water were added to the eleventh well, mixed, and then transported to the last well. The bacterial concentrating of 1.5 108 CFU/ml was prepared. After correcting the turbidity to McFarland 0.5, the suspensions were used within 30 minutes after being created. Each of the wells (1–11) received 10 L of bacterial suspension. While the twelfth well is regarded as a negative control, the eleventh well serves as a positive control. To each well, 16 L of resazurin pigment was applied. At 37°C, the plate was incubated for 18 to 24 hours.

Biofilm formation assay

Atshan et al. (2012) evaluated the quantification of biofilm formation by isolates of K. pneumonia and S. aureus as mention (26).

All isolates were grown for 24 hours at 37°C in brain heart broth. After that, it was checked against McFarland standard no. 0.5. A volume (200 l) of an isolated culture was added to three wells of sterile 96-well U-shaped bottom polystyrene microplates. The plate was covered with their covers and incubated for 24 hours at 37°C under aerobic conditions. The six wells that contained bacteria-free tryptic soy broth were regarded as negative controls. All plates were moderately washed three times with distilled water after incubation, dried, and fixed at 65 °C for one hour. Each well received methanol additions for 15 minutes at room temperature. Extra stain was rinsed off the dish by adding more water and running the tap repeatedly. To ensure full drying, the plates were dehydrated at 37°C for around 30 min. 200 l of free ethanol was used to resolubilize the adhering cells for 10 min. The microplate reader at 630 nm measured the optical density of each well.

The data simplification and calculation, classification of bacterial adherence is summarized in Table (1) based on OD630 values obtained for individual isolates of K. pneumonia and S. aureus was employed. Excess stain was rinse by supplement the plate under the consecutively tap water. The plates were dehydrated at 37°C for approximately 30 min to ensured they were completely dried. The adherent cells were resolubilized with 200 µl of free ethanol for 10 min. The optical density of each well was obtained by the microplate reader at 630 nm.

Table 1. Classification of bacterial adherence by microtiter plate method (26)

Mean OD630	Biofilm intensity
OD ≤ ODc*	Non–adherent
2ODc > OD > ODc	Weak
4 ODc > OD > 2ODc	Moderate
OD >4 ODc	Strong

Average OD of the negative control plus three standard deviations is the "Cut off value" (ODc). After calculating the capacity for biofilm formation for all tested isolates and negative controls, the cut-off value (ODc) was determined. Three standard deviations (SD) over the mean of the negative control is what is meant by this term: Each microtiter plate's ODc value was computed separately. Any positive result was a sign that a biofilm was being produced, whereas a negative value indicated that the sample was clear of germs.

Estimation biofilm inhibition

The activity of plant extract as antibiofilm was tested on *K. pneumonia* and *S. aureus* isolates, using 96 well microtitere plate as mention by (27) with modifications. By introducing 100 l of bacterial suspension (108 cells/ml), followed by a 24-hour incubation period at 37 oC, biofilm development was achieved. A growth-free media was employed as a control, and the plate was incubated at 37 oC for 24 hours. after which the antibiofilm material is incubated. The following formula (28) was used to calculate the reduction in biofilm development.

$$\% \text{ Reduction} = \frac{Cotrol\ OD - Test\ sample\ OD}{Control\ OD} \times 100$$

Results and discussion

Isolation and identification of *Klebsiella pneumonia* isolates

After being cultured on MacConkey's agar medium, eight bacterial isolates were isolated from wound specimens; all of the isolates were lactose fermenters and mucoid. MacConkey agar is a differential and selective culture medium for bacteria that is used to isolate and distiguished gram-negative and enteric bacilli depending on the fermentation of lactose (29), while gram-positive organisms cannot grow in the presence of crystal violet and bile salts (30). Eight Bacterial isolates were isolated from wounds specimens by culturing on MacConkey's agar, all isolates were lactose fermenters and mucoid. MacConkey agar, is a differential and selective culture medium used for bacteria, considered to selectively isolate gram-negative and enteric bacilli and distinguish them depending on lactose fermentation (29) a crystal violet and bile salts prevent the growth of gram-positive organisms (30). Also motility was performed and all isolate were non motile. All *Klebsiella* species are gram-negative and often non-motile.

When compared to other members of the Enterobacteriaceae family, they frequently have shorter and thicker shapes (31).

Isolation and identification *Staphylococcus aureus* isolates

After being cultured on mannitol salt agar, eight bacterial isolates were isolated from wound specimens. The chosen isolates that thrived there were yellow colonies. Mannitol salt agar, encourages the growth of one particular species of bacteria while inhibiting the growth of other microorganisms (32). MSA is selective for some Gram-positive bacteria that can withstand high salt concentrations while being selective against the many Gram-negative bacteria. It includes a high concentration of salt (approximately 7.5–10%), which is inhibitory to most bacteria. It is also a differential medium for mannitol-fermenting staphylococci (29). Staphylococcus aureus creates yellow colonies with yellow zones (32).

Identification of *Klebsiella pneumonia* and *Staphylococcus aureus* isolates by Vitek -2 compact system

The Vitek-2 compact device was used to identify the sixteen isolates that grew on MacConkey agar and Mannitol salt agar, respectively. The results showed that all of the isolates were K.pneumonia and S. aureus, respectively.

Antibiotic Susceptibility Testing

Nine antibiotics (clindamycin, tetracycline, trimethoprim-sulphamethaxazole, erythromycin, lincomycin, ceftriaxone, amoxicillin-clavulanic acid, imipenem and meropenem) were used against all 16 isolates of *K. pneumonia* and *S. aureus*, the results showed that *Klebsiella pneumonia* isolates were 100% resistant to most antibiotics but they were sensitive with 12.5%, 75% and 75% to clindamycin, imipenem and meropenem respectively, while *Staphylococcus aureus* isolates were sensitive with 25% to imipenem and meropenem only. Table (2) and Figure (1)

Table 2. Susceptibility percentages of *K. pneumonia* and *S. aureus* toward antibiotics.

Antibiotics	**Resistant isolates of *K.pneumonia***	**Sensitive isolates of *K.pneumonia***	**Resistant isolates of *S. aureus***	**Sensitive isolates of *S. aureus***
Clindamycin	87.5%	12.5%	100%	0%
Tetracycline	100%	0%	100%	0%
Trimethoprim-sulphamethaxazole	100%	0%	100%	0%
Erythromycin	100%	0%	100%	0%
Lincomycin	100%	0%	100%	0%
Ceftriaxone	100%	0%	100%	0%
Amoxicillin-clavulanic acid	100%	0%	100%	0%
imipenem	25%	75%	75%	25%
meropenem	25%	75%	75%	25%

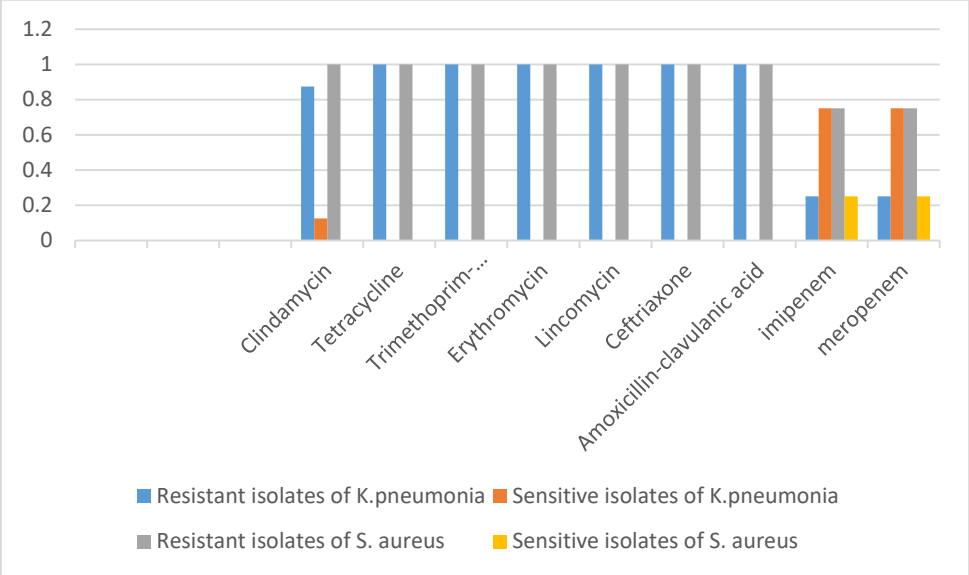


Figure 1. Susceptibility percentages of K. pneumonia and S. aureus toward antibiotics.

Patilaya *et.al.*(2019). eported that *K. Pneumonia* isolates exhibited good sensitivity to meropenem (80%) and indicated low sensitivity to tetracycline (30%) (33). For the carbapenem group of antibiotics tested, Imipenem, Ertapanem, and Meropenem, the susceptibility rates of K. pneumonia isolates were 74.19%, 43.55%, and 27.42%, respectively, according to Adeosun *et al.* (2019) (34). The opportunistic bacterial pathogen *K.pneumoniae* is well known for having a wide range of antibiotic resistance genes. Penicillins, cephalosporins, and carbapenems, which are widely used in critical care settings, are just a few of the lactam medications that the isolates have defenses against. These include the emergence of carbapenemase and porin loss along with the development of extended-spectrum beta-lactamases (ESBL), AmpC -lactamases, Metallo-lactamases (MBL), and carbapenemase (35).

The efflux pumps of MDR K. pneumoniae boost the bacteria's resistance to medications such chloramphenicol, macrolides, quinolones, and -lactams (36). Tetracycline and ampicillin resistance was found in 80.77% and 76.92% of the isolates, respectively, according to Doungjit et al. (2021). Additionally, resistance to the majority of antibiotics, including erythromycin (90.9%), clindamycin (85.4% including inducible resistance), gentamicin, cipro-/levo-/moxi-floxacin, trimethoprim-sulfamethoxazole (58.3%), tetracycline, and rifampin (37), was predicted by methicillin resistance. So, obviously there are multidrug resistant isolates among *K.pneumonia* and *S. aureus*.in this study.

Determination of Minimal Inhibitory Concentration of meropenem against *K. pneumonia* and *S. aureus* isolates.

Minimal Inhibitory Concentration (MIC) of meropenem, which was the most effective antibiotic against *Klebsiella pneumonia* and *Staphylococcus aureus* isolates, was performed against the 16 isolates, the results showed that it was distributed between (250-2000 µg/ml) against K. *pneumonia* isolates, while it was between (31.25-500 µg/ml) against *S. aureus* isolates as shown in table (3).

Table 3. MIC of meropenem against *K. pneumonia* and *S. aureus* isolates.

***K. pneumonia* isolates**	**MIC of meropenem µg/ml**	***S. aureus* isolates**	**MIC of meropenem µg/ml**
K1	500	S1	125
K2	250	S2	500
K3	1000	S3	62.5
K4	500	S4	3.9
K5	2000	S5	500
K6	500	S6	250
K7	250	S7	62.5
K8	1000	S8	125

Brandon Kulengowski *et.al.* mentioned that meropenem MIC's ranged from 4 to 128 mg/ l against *K. pneumonia* isolates (38).

While, Piergiorgio Cojutti *et.al* reported that 26.6% of *K. pneumonia* isolates were susceptible to meropenem (MIC ≤ 2000 µg/ml) and their study was about the resistance increasing among *K. pneumonia* isolates (39). Astudy reported that For *S.aureus* the MIC was 0.06 ± 0.02 mg/l (40).

A member of the carbapenem class of antibiotics, meropenem has a broad spectrum of activity. Numerous Gram-positive and Gram-negative pathogens are successfully inhibited by meropenem, which has remarkable activity against a wide variety of bacteria (41). S. aureus, enterococci, and coagulase-negative staphylococci are the most typical agents that cause infections from surgical incisions. which together account for 46% of all surgical site infections. These infections also have higher rates of MRSA and VRE (42).

Determination of Minimal Inhibitory Concentration of *G. procumbens* E.O against *K. pneumonia* and *S. aureus* isolates.

Minimal Inhibitory Concentration (MIC) of *G. procumbens* E.O was assessed against the 16 isolates, and the results showed that it was ranged from 0.78-25% and 12.5-50% against *K. pneumonia* and *S. aureus* respectively. Table (4)

Table 4. MIC of *G. procumbens* E.O against *K. pneumonia* and *S. aureus* isolates.

***K. pneumonia* isolates**	**MIC of Eo %**	***S. aureus* isolates**	**MIC of Eo %**
K1	6.25	S1	12.5
K2	1.56	S2	25
K3	3.12	S3	50
K4	0.78	S4	12.5
K5	6.25	S5	50
K6	12.5	S6	25
K7	25	S7	25
K8	12.5	S8	25

G. procumbens Eos were substantially more effective against Gram-negative bacteria (MIC, 8.2-10.0 mg/mL) than Gram-positive bacteria (MIC, 13.5-16.7 mg/mL), according to Anna Magiera et al.'s 2019 study (43). Their findings are in agreement with ours, obviously Eo affected *K. pneumonia* more than *S. aureus*, less doses were needed against *K. pneumonia* as in the results of MIC.

Biofilm formation by *K. pneumonia* and *S. aureus* isolates.

A deeper understanding of the physiology, structure, and composition of biofilms—which are believed to be a marker of virulence—has resulted from the development of numerous novel methodologies for biofilm research in recent years (44). In this study, the capability of *K. pneumonia* and *S. aureus* biofilm producing isolates was assessed using 96-well polystyrene microtiter plates that had been pre-sterilized as part of a conventional test for the exposure of biofilm biomass (26).

A microplate reader measured absorbance at 630 nm to assess the biofilm intensity. In light of this, absorbance measurements represented the biofilm's intensity. Thickness created by the examined isolates at the microtiter well's surface. The results showed that all 16 isolates were strong and intermediate biofilm producers. Table (5)

Table 5. Biofilm forming capacity of *K. pneumonia* and *S. aureus* isolates isolates

***K. pneumonia* Strong isolates**	**Mean OD630**	***K. pneumonia* Intermediate isolates**	**Mean OD630**	***S. aureus* Strong isolates**	**Mean OD630**	***S. aureus* Intermediate isolates**	**Mean OD630**
K3	0.23	K1	0.21	S2	0.27	S1	0.18
K5	0.27	K2	0.19	S5	0.27	S3	0.14
K8	0.22	K4	0.20	S6	0.24	S4	0.12
		K6	0.21			S7	0.14
		K7	0.16			S8	0.17

Estimation biofilm inhibition of *K. pneumonia* and *S. aureus* isolates isolates by ***G. procumbens*** Eo.

The 16 isolates of *K. pneumonia* and *S. aureus* were treated with subMICs ***G. procumbens*** Eo, and the biofilm reduction was calculated. The results showed that biofilm formation was reduced in most *S. aureus* isolates more than in *K. pneumonia* isolates, and some isolates in both types of bacteria transformed to week biofilm producers (K2, K7) and (S1, S2, S3, S4, S7 and S8) as shown in table (6) and table (7).

Table 6. Biofilm forming capacity of *K. pneumonia* and *S. aureus* isolates isolates after treating with *G. procumbens* Eo

***K. pneumonia* Strong isolates**	**Mean OD630**	***K. pneumonia* Intermediate isolates**	**Mean OD630**	***S. aureus* Strong isolates**	**Mean OD630**	***S. aureus* Intermediate isolates**	**Mean OD630**
K3	0.17	K1	0.17	S2	0.08	S1	0.10
K5	0.17	K2	0.10	S5	0.13	S3	0.11
K8	0.15	K4	0.17	S6	0.15	S4	0.09
		K6	0.16			S7	0.10
		K7	0.11			S8	0.10

Table 7. Biofilm reduction of *K. pneumonia* and *S. aureus* isolates isolates after treating with *G. procumbens* EO

***K. pneumonia* isolates**	**Biofilm reduction% after treated with *G. procumbens* EO**	***S. aureus* isolates**	**Biofilm reduction% after treated with *G. procumbens* EO**
K1	19%	S1	44.4%
K2	47.3%	S2	70.3%
K3	26%	S3	21.4%
K4	15%	S4	25%
K5	37%	S5	51.8%
K6	23%	S6	37.5%
K7	31.25%	S7	28.5%
K8	31.8%	S8	41.1%

The generation of biofilms on S. aureus ATCC 29213 and E. coli was prevented by Lippia origanoides thymol-carvacrol II chemotype (LTC II) at subinhibitory concentrations (MIC50), according to Martnez et al. (2021) (45). In a different investigation, G. procumbens EO also successfully prevented oral Streptococcus mutans and Candida albicans from forming biofilms (46).

Gram-positive and Gram-negative pathogenic bacteria can both be inhibited by EOs at low dosages. Some EOs have shown to have potent anti-biofilm properties. If EOs are effective at preventing the growth of biofilm, especially in bacteria that are developing AMR (47). The volume, content, and interactions with pathogens of EOs as well as their configuration all contribute to their antimicrobial activity.They have an impact on specific targets inside pathogens (48). The highest activity happens when phenols and aldehydes are present in large amounts. contrasted with weak or no activity from terpene hydrocarbons, esters, or ketones (49). Hydrophobicity affects EO's function by making cells more permeable, which causes cell leakage (50). Hydrophobicity affects EO activity by causing cell leakage by making cells more permeable. EOs also impact how bacteria convert energy, control growth, and maintain nutritional balance (51).

In this study EO had a great effect on the MDR isolates of both bacteria, as antibacterial and antibiofilm, ***G. procumbens*** EO effected *S. aureus* more than *K. pneumonia*, and this may be attributed to presence of the capsule in *Klebsiella*, however, both Gram positive and Gram negative bacteria's capsular polysaccharide has been anticipated to obstruct the transport of antibiotic molecules, giving bacteria an extra intrinsic defense against antibiotics (53). But ***G. procumbens*** EO had a great role in inhibiting bacterial isolates and reducing biofilm formation, so, they might be added to novel antimicrobials.

References

1. Weinstein RA, Mayhall CG. The epidemiology of burn wound infections: then and now. Clin Infect Dis. 2003;37:543–50.
2. Fitzwater J, Purdue GF, Hunt JL, O'Keefe GE. The risk factors and time course of sepsis and organ dysfunction after burn trauma. J Trauma Acute Care Surg. 2003;54:959–66.
3. Escandón-Vargas K, Tangua AR, Medina P, Zorrilla-Vaca A, Briceño E, Clavijo-Martínez T, Tróchez JP. Healthcare-associated infections in burn patients: timeline and risk factors. Burns. 2020;46:1775.
4. Church D, Elsayed S, Reid O, Winston B, Lindsay R. Burn wound infections. Clin Microbiol Rev. 2006;19:403–34.
5. Branski LK, Al-Mousawi A, Rivero H, Jeschke MG, Sanford AP, Herndon DN. Emerging infections in burns. Surg Infect. 2009;10:389–97.
6. Rouse MD, Stanbro J, Roman JA, Lipinski MA, Jacobs A, Biswas B, Regeimbal J, Henry M, Stockelman MG, Simons MP. Impact of frequent administration of bacteriophage on therapeutic efficacy in an A. baumannii mouse wound infection model. Front Microbiol. 2020;11:414.
7. Hujer KM, Hujer AM, Hulten EA, Bajaksouzian S, Adams JM, Donskey CJ, Ecker DJ, Massire C, Eshoo MW, Sampath R. Analysis of antibiotic resistance genes in multidrug-resistant Acinetobacter sp isolates from military and civilian patients treated at the Walter Reed Army Medical Center. Antimicrob Agents Chemother. 2006;50:4114–23.
8. Bahramian A, Shariati A, Azimi T, Sharahi JY, Bostanghadiri N, Gachkar L, Ghalavand Z, Chirani AS, Erfanimanesh S, Hashemi A. First report of New Delhi metallo-β-lactamase-6 (NDM-6) among Klebsiella pneumoniae ST147 strains isolated from dialysis patients in Iran. Infect Genet Evol. 2019;69:142–5.
9. Tabassum R, Shafique M, Khawaja KA, Alvi IA, Rehman Y, Sheik CS, Abbas Z. ur Rehman S: Complete genome analysis of a Siphoviridae phage TSK1 showing biofilm removal potential against Klebsiella pneumoniae. Sci Rep. 2018;8:1–11.
10. Moghadam M, Shariati A, Mirkalantari S, Karmostaji A. The complex genetic region conferring transferable antibiotic resistance in multidrug-resistant and extremely drug-resistant Klebsiella pneumoniae clinical isolates. New Microb New Infect. 2020;36:10063.
11. Ismail MM, Samir R, Saber FR, Ahmed SR, Farag MA. Pimenta Oil as a Potential Treatment for Acinetobacter baumannii Wound Infection: In Vitro and In Vivo Bioassays in Relation to Its Chemical Composition. Antibiotics. 2020. 9:679.
12. Agnihotri N, Gupta V, Joshi M. Aerobic bacterial isolate from burn wound infections and their antibiotics a five-year study. J Burns. 2004;30:241–243.
13. Manus A, Mason A, Manus W, Pruitt B. A decade of reduced Gram negative infections and mortality improved isolation of burned patients. Arch Surg. 1994;129:1306–1309.
14. Donati I, Scammazo F, Gervasoni M, Magliano A, Stankov B, Fraschini F. Infection and antibiotic therapy in 4000 burned patients treated in Milan, Italy, between 1976 and 1988. J Burns. 1993;19:345–348.

15. Burkhard M, Iqbal A, Khatoon N, Iqbal N, Naeem S, Qureshi G. A laboratory study of susceptibility of methicillin-resistant Staphylococcus aureus. Pakistan J Med Sci. 2004;20:229–223.
16. Rokas B, Algimantas T, Rytis R. Staphylococcus aureus infection in the surgery of burns Kaunas University of Medicine Hospital, Lithuania. Medicina. 2003;11:1078.
17. Lari A, Alaghehbandan R. Nosocomial infections in an Iranian burn care center. J Burns. 2000;26(8):737–740.
18. Bagley S. T. (1985). Habitat association of Klebsiella species. Infect. Control. 6, 52–58.
19. Dorman M. J., Short F. L. (2017). Genome watch: Klebsiella pneumoniae: when a colonizer turns bad. Nat. Rev. Microbiol. 15:384.
20. Li B., Webster T. J. (2018). Bacteria antibiotic resistance: new challenges and opportunities for implant-associated orthopedic infections. J. Orthop. Res. 36, 22–32.
21. Logan L. K., Weinstein R. A. (2017). The epidemiology of carbapenem-resistant Enterobacteriaceae: the impact and evolution of a global menace. J. Infect. Dis. 215, S28–S36.
22. Ray C. G., Ryan K. J. (2004). Sherris Medical Microbiology: An Introduction to Infectious Diseases. NY: McGraw-Hill.
23. Vandeppitte, J.; Verhaegen, J.; Engbaek, K.; Rohner, P.; Piot, P., and Heuck, C. (2003). Basic laboratory procedures in clinical bacteriology (2nd Ed.). Geneva: World Health Organization.
24. Abed, I. J.; Hussein, A. R. ; Abdulhasan G. A. and Dubaish, A. N.(2022) Microbiological Effect of Lemongrass Cymbopogon Citratus and Spearmint Mentha Spicata Essential Oils as Preservatives and Flavor Additives in Yogurt, Iraqi Journal of Science, Vol. 63, No. 7, pp: 2839-2849.
25. Wiegand, I.; Hilpert, K., and Hancock, R. E. (2008). Agar and broth dilution methods to determine the minimal inhibitory concentration (MIC) of antimicrobial substances. Nature protocols, 3(2), 163.
26. Atshan, S. S.; Nor Shamsudin, M.; Sekawi, Z.; Lung, LT.; Hamat, R. A., Karunanidhi, A.; Mateg Ali, A.; Ghaznavi-Rad, E.; GhasemzadehMoghaddam, H.; Chong Seng, J.S.; Nathan, J.J., and Pei, C.P. (2012) Prevalence of adhesin and regulation of biofilm-related genes in different clones of Staphylococcus aureus. J Biomed Biotechnol.6: 1-10.
27. Selim, S.; Adam, M.; Hassan, S., and Albalawi, A. (2014). Chemical composition, antimicrobial and antibiofilm activity of the essential oil and methanol extract of the Mediterranean cypress (Cupressus sempervirens L.). BMC Complementary and Alternative Medicine. 14, pp:179.
28. Mathur, S.; Gutte, M.; Paul, D., and Udgire, M. (2013). Study the effect of essential oils on microbial biofilm formation by Klebsiella pneumoniae. Sch. Acad. J. Biosci. 1(3), pp:76-79.
29. Anderson, and Cindy (2013). Great Adventures in the Microbiology Laboratory (7th ed.). Pearson. pp. 175– 176.
30. Anderson, C.; Johnson, T. R.; Case, C. L.; Cappuccino, J. G., and Sherman, N. (2013).7th Edition Great adventures in the microbiology laboratory. 175-176.
31. Ristucci, Patricia; Cunha, Burke (July 1984). "Klebsiella". Infection Control. 5 (7): 343–348.

32. Bachoon, Dave S.; Dustman, Wendy A. (2008). "Exercise 8: Selective and Differential Media for Isolation". In Michael Stranz (ed.). Microbiology Laboratory Manual. Mason, OH: Cengage Learning.
33. Patilaya P, Husori DI and Marhafanny L.(2019) Susceptibility of Klebsiella Pneumoniae Isolated from Pus Specimens of Post-Surgery Patients in Medan, Indonesia to Selected Antibiotics. Open Access Maced J Med Sci. 14;7(22):3861-3864.
34. Adeosun I.J , Oladipo E.K, Ajibade O.A , Olotu T.M , Oladipo A.A , Awoyelu E.H , Alli O.A.T and Oyawoye O.M.(2019). Antibiotic Susceptibility of Klebsiella pneumoniae isolated from Selected Tertiary Hospitals in Osun State, Nigeria. Iraqi Journal of Science. Vol. 60, No.7, pp: 1423-1429.
35. R. Wasfi, W.F. Elkhatib, H.M. Ashour, Molecular typing and virulence analysis of multi-drug resistant Klebsiella pneumoniae clinical isolates recovered from Egyptian hospitals, Sci. Rep. 6 (2016) 38929, https://doi.org/10.1038/srep38929.
36. J.M. Pages, J.P. Lavigne, V. Leflon-Guibout, E. Marcon, F. Bert, L. Noussair, M.H. Nicolas Chanoine, C. Herman, Efflux Pump, the Masked Side of ß-Lactam Resistance in Klebsiella pneumoniae Clinical Isolates, PLoS ONE 4 (3) (2009), e4817. https://doi.org/10.1371/journal.pone.0004817.
37. Doungjit Kanungpean,Shinji Takai and Tsutomu Kakuda (2021) Contamination and Antimicrobial Susceptibility Testing of Staphylococcus aureus Isolated from Pork in Fresh Markets, Nongchok District, Thailand. Veterinary Medicine International. Volume 2021 Article ID 6646846.
38. Mohammad Qodrati, Seyed Ahmad SeyedAlinaghi, Seyed Ali Dehghan Manshadi, Alireza Abdollahi and Omid Dadras (2022). Antimicrobial susceptibility testing of Staphylococcus aureus isolates from patients at a tertiary hospital in Tehran, Iran, 2018–2019. European Journal of Medical Research volume 27.
39. Brandon Kulengowski, Jeffrey J Campion, David J Feola and David S Burgess.(2017) Effect of the meropenem MIC on the killing activity of meropenem and polymyxin B in combination against KPC-producing Klebsiella pneumonia. The Journal of Antibiotics. 70, 974–978.
40. Piergiorgio Cojutti , Assunta Sartor , Matteo Bassetti , Claudio Scarparo and Federico Pea.(2018). Is meropenem MIC increase against KPC-producing Klebsiella pneumoniae correlated with increased resistance rates against other antimicrobials with Gram-negative activity?. Journal of Global Antimicrobial Resistance. Pages 238-241.
41. Sandrine Lemaire, Françoise Van Bambeke, Marie-Paule Mingeot-Leclercq and Paul M. Tulkens.(2005). Activity of three β-lactams (ertapenem, meropenem and ampicillin) against intraphagocytic Listeria monocytogenes and Staphylococcus aureus . Journal of Antimicrobial Chemotherapy, Volume 55, Issue 6, Pages 897–904.
42. Fish DN and Singletary TJ.(1997). Meropenem: a new carbapenem antibiotic. Pharmacother. 17:644–69.
43. DiNubile MJ and Lipsky BA.(2004). Complicated infections of skin and skin structures: when the infection is more than skin deep. J Antimicrob Chemother. ;53(Suppl S2):ii37-ii50.

44. Anna Magiera, Monika Sienkiewicz , MONIKA A. Olszewska , Agnieszka Kicel and Piotr Michel.(2019). CHEMICAL PROFILE AND ANTIBACTERIAL ACTIVITY OF ESSENTIAL OILS FROM LEAVES AND FRUITS OF GAULTHERIA PROCUMBENS L. CULTIVATED IN POLAND. Acta Poloniae Pharmaceutica ñ Drug Research, Vol. 76 No. 1 pp. 93-102.
45. Azeredo, H.M.C.; Rosa, M.F. and Mattoso, L.H.C. (2017). Nanocellulose in bio-based food packaging applications. Ind. Crops Prod. 97, 664–671. doi: 10.1016/j.indcrop.2016.03.013.
46. Martínez A, Manrique-Moreno M, Klaiss-Luna MC, Stashenko E, Zafra G, Ortiz C. Effect of Essential Oils on Growth Inhibition, Biofilm Formation and Membrane Integrity of Escherichia coli and Staphylococcus aureus. Antibiotics (Basel). 2021 Nov 30;10(12):1474. doi: 10.3390/antibiotics10121474. PMID: 34943686; PMCID: PMC8698458.
47. Milos Nikolic, Tatjana Markovic, Milos Mojovic, Boris Pejind, Aleksandar Savic, Tamara Peric, Dejan Markovic, Tatjana Stevic, Marina Sokovic.(2013). Chemical composition and biological activity of Gaultheria procumbens L. essential oil.Industerial Crops and Products.49,561-567.
48. El-Tarabily KA, El-Saadony MT, Alagawany M, Arif M, Batiha GE, Khafaga AF, Elwan HAM, Elnesr SS, E Abd El-Hack M. Using essential oils to overcome bacterial biofilm formation and their antimicrobial resistance. Saudi J Biol Sci. 2021 Sep;28(9):5145-5156. doi: 10.1016/j.sjbs.2021.05.033. Epub 2021 May 20. PMID: 34466092; PMCID: PMC8380992.
49. Dhifi, W., Bellili, S., Jazi, S., Bahloul, N., Mnif, W., 2016. Essential oils' chemical characterization and investigation of some biological activities: A critical review. Medicines. 3, 25. https://doi.org/10.3390/medicines3040025.
50. Bassolé, I.H., Juliani, H.R., 2012. Essential oils in combination and their antimicrobial properties. Molecules 17, 3989–4006. https://doi.org/ 10.3390/molecules17043989.
51. Dhifi, W., Bellili, S., Jazi, S., Bahloul, N., Mnif, W., 2016. Essential oils' chemical characterization and investigation of some biological activities: A critical review. Medicines. 3, 25. https://doi.org/10.3390/medicines3040025.
52. Swamy, M.K., Akhtar, M.S., Sinniah, U.R., 2016. Antimicrobial properties of plant essential oils against human pathogens and their mode of action: An updated review. Evid. Based Complem. Altern Med. 2016, 3012462. https://doi.org/ 10.1155/2016/3012462.
53. Fowler D., Hu J., Hou P., Wong C. Theeffect of sub-inhibitory streptomycin on capsular polysaccharide production and streptomycin resistance in Escherichia coli. J. Exp. Microbiol. Immunol., 2009; 13: 47–52.

أثر التكيّف على الشوارع الحضرية

Adaptation Impact of Urban Alleyways

Inas Hasan Shukur [1], Ahmad N. Al-Shammaa [2]

© 2023 The Author(s). This open access article is distributed under a Creative CommonsAttribution (CC-BY) 4.0 license.

Abstract: Urban alleys are considered one of the main elements of the urban infrastructure, and they were considered an interactive space in the ancient cities, where the need for it stemmed from the need of the people as they were the users of it. From here, the general problem of the research emerged in (the complete lack of knowledge of the impact of adaptation in urban alleys), and a research problem represented by (lack of knowledge about the statement of the impact of adaptation mechanisms on the architecture of urban alleys to reach an interactive urban infrastructure), in order to reach the goal of research in (Building a theoretical framework on the concepts of adaptation and the mechanisms to achieve it in the architecture of urban alleys to reach an interactive urban infrastructure), where the research assumed (it is possible to achieve adaptation in the urban alley to reach an interactive urban alley through the application of its mechanisms within the urban infrastructure), by being a plan The research and its methodology by selecting examples of urban alleys in different countries and using comparative analysis between their types and the possibility of applying adaptation mechanisms to reach indicators to test the hypothesis and access to results, conclusions and recommendations for future research.

Key Words: Adaptation, Coping Mechanisms, Urban Alley, Urban Infrastructure, Interactive Urban Alley.

الكلمات المفتاحية: التكيّف، اليات التكيّف، الشارع الحضري، البنية الفيزيائية الحضرية، الشارع الحضري التفاعلي.

Author details

[1] – [2] Architectural Department, Collage of Engineering, University of Baghdad, Baghdad, Iraq

Citation information

Cite this article as:

Shukur, I.H., Al-Shammaa, A.N., (July 2023), *Adaptation Impact of Urban Alleyways*, Proceedings of the Minar Congress, Turkey, (9) pp 329-344, DOI: http://dx.doi.org/10.47832/MinarCong9-28

http://dx.doi.org/10.47832/MinarCong9-28

[1] enas.hasan@coeng.uobaghdad.edu.com

[2] a.alshammaa@coeng.uobaghdad.edu.iq

الخلاصة

تعد الشوارع الحضرية أحد أهم العناصر الرئيسة للبنية الفيزيائية الحضرية، وكانت تعد فضاءاً تفاعلياً في المدن القديمة، حيث كانت الحاجة له تنبع من حاجة الناس كونهم المستخدمين له. من هنا ظهرت المشكلة العامة للبحث في (بيان النقص المعرفي لتأثير التكيّف في الشوارع الحضرية)، وبمشكلة بحثية متمثلة بـ (بيان النقص المعرفي حول أثر آليات التكيّف على عمارة الشوراع الحضرية للوصول إلى بنية فيزيائية حضرية تفاعلية)، من أجل الوصول إلى هدف البحث في (بناء إطار نظري حول مفاهيم التكيّف وآليات تحقيقه في عمارة الشوارع الحضرية للوصول إلى بنية تحتية حضرية تفاعلية)، حيث افترض البحث بـ (إمكانية تحقيق التكيّف في الشارع الحضري للوصول إلى شارع حضري تفاعلي من خلال تطبيق آلياته ضمن البنية الفيزيائية الحضرية)، وذلك بأن تكون خطة البحث ومنهجيته باختيار أمثلة لشوارع حضرية في دول مختلفة واستخدام التحليل المقارن بين أنواعها وإمكانية تطبيق آليات التكيّف للوصول إلى مؤشرات لاختبار الفرضية والوصول إلى النتائج والاستنتاجات والتوصيات للبحوث المستقبلية.

المقدمة

تعد المدن محاورًا نابضة للحياة الاجتماعية والأحداث، حيث يوفر الفضاء الحضري فرصًا للناس للتواصل والتفاعل مع بعضهم البعض . تعد مراكز المدن التاريخية، على وجه الخصوص، هي بؤر الأنشطة الاجتماعية والاقتصادية والتبادلات التجارية بسبب أهميتها التاريخية والمركزية داخل المدينة، وتسهل شبكة الشوارع والشوارع الحضرية الحركة والتواصل، وهي عنصر حاسم في الفضاءات الحضرية في المدينة، **يقدم القسم الأول من البحث** التعريف بالشارع الحضري وابرز النظريات لاعادة التكيّف في شبكات الشوارع وتأثيرها على كثافة حركة المرور في مراكز المدن التاريخية. ويعرض **القسم الثاني** أساليب واليات وتقنيات تطوير الشارع الحضري، ويركز **القسم الثالث** على الإطار العملي القائم على جمع البيانات وتحليلها من خلال مراقبة الموقع ومن خلال حساب عدد تحركات المركبات والمشاة ويعرض **القسم الرابع** النتائج والمناقشة . يهدف هذا البحث إلى تقديم رؤى حول شبكات الشوارع المستدامة والفعالة التي يمكن تكييفها مع الظروف المحلية للوصول إلى شارع حضري تفاعلي من خلال تحليل البيانات من ملاحظات الموقع، يسلط البحث الضوء على تأثير تصميم شبكة الشوارع الحضرية على كثافة حركة المرور ويدعو البحث إلى أنظمة شبكات شوارع حضرية قابلة للتكيّف .

1- الشارع الحضري Urban Alleyways

قبل البدء بتعريف الشارع الحضري ودوره في المدينة لابد من التعريف بمفهوم التكيّف اصطلاحا بأنه (مناسبة او ملاءمة شيء ما لما يحيطه او التغيير في الاستخدام، كأقصى تقدير مع الاحتفاظ بالهيكل والشكل الاصلي بالإضافة إلى اطالة العمر الانتاجي للمكونات الاصلية) وهو (هو أي عمل لمبنى فوق مستوى الصيانة لتغيير قدرته او وظيفته او اداءه) بمعنى (أي تدخل لضبط او تطوير مبنى ليتناسب مع متطلبات المالك المتغيرة)، وكتعريف اجرائي له بأنه (هو عملية جعل المبنى ملائماً للمتطلبات او الشروط او الظروف البيئية، او هو القابلية على التعديل او التأقلم للشكل او الهيكل لملائمة حالات جديدة، وبمعنى آخر هو أي عمل او أي تدخل يتطلب تعديلا او اعادة استخدام او تطوير ليلائم ظروفا او متطلبات جديدة، فهو الحالة المادية القائمة، ويثير قضايا التوقيت المناسب وتحديد الاولويات والقيمة المضافة المحتملة وهذه القيمة تشتمل على تغيير في الغرض الوظيفي واستراتيجيات الحفاظ على التراث او تجديد المكونات والمباني وتحسينات مهمة في الاداء التشغيلي كانخفاض الطلب على الطاقة وترشيد استخدام المياه والآثار البيئية الاخرى) (البكري ؛ 2021) (البكري والبزاز، 2021)، حيث تلعب الشوارع الحضرية دورًا حيويًا في الأنشطة التجارية وحركة البضائع وأثبتت الشوارع الحضرية أنها أكثر متانة من المباني واستمرت في العمل كشرايين نقل أساسية، وكذلك لدعم نمو المدن وتطورها، لذا يمكن تعريف الشارع الحضري بالنسبة للمدينة على انها (الشوارع الصغيرة)، (وهي خطوط الاشجار والشجيرات داخل المناظر الطبيعية، او انها اماكن عرض الجداريات الثقافية ضمن البنية الفيزيائية الحضرية). (Roukouni et al. ؛2023 ،Mumford ؛2011 ،Hillier 1996) .

إن مصطلح (allee) والذي يشير إلى شوارع مخططة تخطيطا ذا مناظر طبيعية مع الاشجار لحماية المناظر في الحدائق الخاصة، حيث ان هناك حاجة للممرات والاشجار كون ان المشي كان سائدا في هذه المسارات ولم تكن السيارات موجودة بعد، حيث ان الشوارع كانت موجودة منذ (2000 عام)، اضافة لذلك فأن مدن العصور الوسطى كانت تشيد

مبانيها بالقرب من بعضها البعض حيث اماكن العيش والعمل مما يجعل ساكنيها يتحركون ضمن نفس الممر الذي كان يعد فضاءا تفاعليا (interactive space) (zeidler , 1983).

كان تصميم المباني وتنظيمها من قبل المواطنين وليس المخططين، لذا فهم يرتبطون ارتباطا مباشرا باحتياجات الناس في ماهية الحاجة إلى مثل هذه الفضاءات (Gehl , 2011).

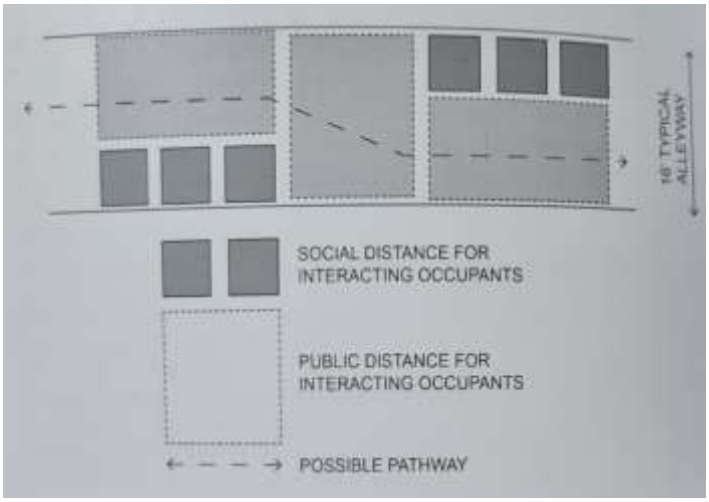
في عهد الثورة الصناعية تغير مفهوم الشوارع الحضرية حيث اصبحت مثل هذه الممرات والشوارع هي الفضاءات المخصصة للافراد من اجل التنقل فيها إلى جميع انحاء المدينة (zeid ler , 1983) ، وقد تكون اماكن لجمع النفايات والخدمات الكهربائية (Gehl , 2011) مما ادى إلى تطور الشوارع مع احتياجاتها واستخداماتها من مناظر وفضاءات طبيعية وممرات حضرية قابلة للمشي إلى ممرات لجمع النفايات والخدمات يُنظر اليه بأنه مظلم وغير آمن .

تواجه العديد من مراكز المدن مشكلة كثافات الحركة العالية، والتي يمكن أن تُعزى إلى عوامل مختلفة، بما في ذلك التغيرات في شكل المدينة، وخاصة تخطيط شبكة الشوارع . تتغير شبكة الشوارع باختلاف الظروف الاجتماعية والاقتصادية، مما قد يؤدي إلى زيادة كثافة الحركة. علاوة على ذلك، ترتبط كثافات الحركة وتوزيع استخدام الأراضي ارتباطًا وثيقًا، حيث إن توزيع استخدام الأراضي داخل منطقة ما يحدد إلى حد كبير أنماط الحركة (Hillier et al.، 1993 ؛ Alsaffar and Alobaydi، 2023)، لذا كيف يعود الشارع الحضري إلى عنصر مفيد وقابل للاستخدام وتفاعلي ضمن العالم العام ؟

2- النظريات الكامنة لاعادة تكيف البنى الحضرية العامة

نظرا لأن الشوارع موجودة بالأصل كبيئات نشطة وفعالة وقابلة للمشي منذ العصور الوسطى وحتى الثورة الصناعية، لذا تعد النظريات الكامنة وراء تنشيط الفضاءات العامة قيمة اساسية لاعادة احياء هذه الفضاءات ، حيث تفسر نظريات (جان هيل Jan Gehl، ونان ايلين Nan Ellin) فعالية هذه الفضاءات العامة من خلال استخدامها كفضاءات متعددة الأغراض، حيث يحدد (هيل Gehl) المسافة المطلوبة للراحة الشخصية داخل الفضاء العام، فالمسافة الاجتماعية هي (1,3 – 3,75) م، أي (4,5 – 12) قدم، والمسافة العامة اكبر من (3,75) م، أي 12 قدم (الشكل 1)، ويمتلك الشارع بعض الاسيجة والاسوار التي تكون العوائق الرئيسية والتي تمنع تفعيل الفضاء (Gehl , 2011)، لذا فأن توضيح نظريات هيل (Gehl) حول كيفية احياء الشوارع واكسابها الخصائص الاساسية بانشاء فضاء قابل للاستخدام بجعل الفضاء مفعم بالحيوية وجعله اجتماعيا وذلك عن طريق صفتين هما المسامية والتواصل واللتين تمكنان من تنشيط الفضاء (Ellin , 2006)، حيث وضعت نان ايلين (Nan Ellin) مقترحا في انشاء فضاءات متكاملة يمكنها معالجة (الجروح) كما تسميها في المناظر الطبيعية وامكانية تطوير بيئة حضرية اكثر استدامة من خلال المسامية والتواصل بين الشوارع الحضرية بوضع جدران مفتوحة توفر الرؤية (stavrides , 2015) وعمل تداخل بين المجتمعات وعرض الثقافات .

فالشوارع الحضرية عبارة عن فضاء شبه عام بين شبكة عامة من الطرق صالحة للاستخدام وبين المساكن الخاصة والمحلات الخاصة وحتى الحدائق، أي انها فضاء انتقالي بين العام والخاص . (stavrides , 2015)



الشكل 1. مخطط توضيحي للترتيبات الممكنة لمستويات الراحة ضمن حدود الشارع الحضري (stavrides , 2015)

3- اليات التكيّف للوصول إلى شارع حضري تفاعلي

ناقش (Ajay et al. , 2020) تحديات الازدحام المروري في المناطق الحضرية واقترح نظامًا ذكيًا لإدارة النقل صديقًا للبيئة يعتمد على تقنية إنترنت الأشياء، وتناول النتائج السلبية لحركة المركبات الخاصة، مثل زيادة استهلاك الوقود، والتلوث، والحوادث، وهدر الوقت. يؤكد البحث على إمكانات إنترنت الأشياء في إدارة الازدحام المروري من خلال ميزات عدة مثل التنظيم والمراقبة وتحليل البيانات. (Mazloumian et al.، 2010) وركز على التباين المكاني لكثافة المركبات كعامل محدد لقدرة الشبكة الحضرية. قدم نهج المحاكاة العيانية لدراسة انتشار الازدحام في شبكات الطرق الحضرية وسلط الضوء على أهمية التقاط التقلبات في متغيرات حركة المرور بدقة. تكشف الدراسة عن العلاقات الأساسية بين متوسط التدفق، ومتوسط الكثافة، وتنوع كثافة المركبات، مما يوفر نظرة ثاقبة لأداء حركة المرور في المناطق الحضرية.

اضافة إلى ذلك، فمن خلال تسليط الضوء على بحث لتقييم سرعة المشاة في مدينة بغداد، فقد تم إجراء تعداد المشاة باستخدام العد اليدوي والفيديو ووجد أن المشاة يمشون أبطأ من غيرهم في البلدان أو المناطق المتقدمة مع سرعة مشي لا تقل عن 29.85 م / دقيقة (Sarsam and Abdulameer ,2014). بشكل عام، تميل المناطق ذات التركيزات العالية من استخدامات الأراضي التي تجذب العديد من الأشخاص، مثل الأنشطة التجارية والثقافية، إلى زيادة كثافة الحركة. من ناحية أخرى، تُستخدم المناطق ذات الكثافة المنخفضة للحركة في المقام الأول للأغراض السكنية (محمد وآخرون، 2020).

تشتهر نوى المناطق الحضرية بوجود مزيج من استخدامات الأراضي التي تتعايش داخل نفس المنطقة، بما في ذلك الأنشطة السكنية والتجارية والثقافية. يمكن أن يؤدي هذا إلى أنماط حركة معقدة حيث يتنقل الأشخاص بين

الأنشطة والوجهات وعادةً ما تتميز كثافة الحركة في النوى التاريخية بارتفاع حركة المشاة، ومحدودية وصول المركبات، ومزيج من استخدامات الأراض، لذا برزت بعض الاليات الممكن اتباعها للوصول إلى شارع حضري تفاعلي ومنها :

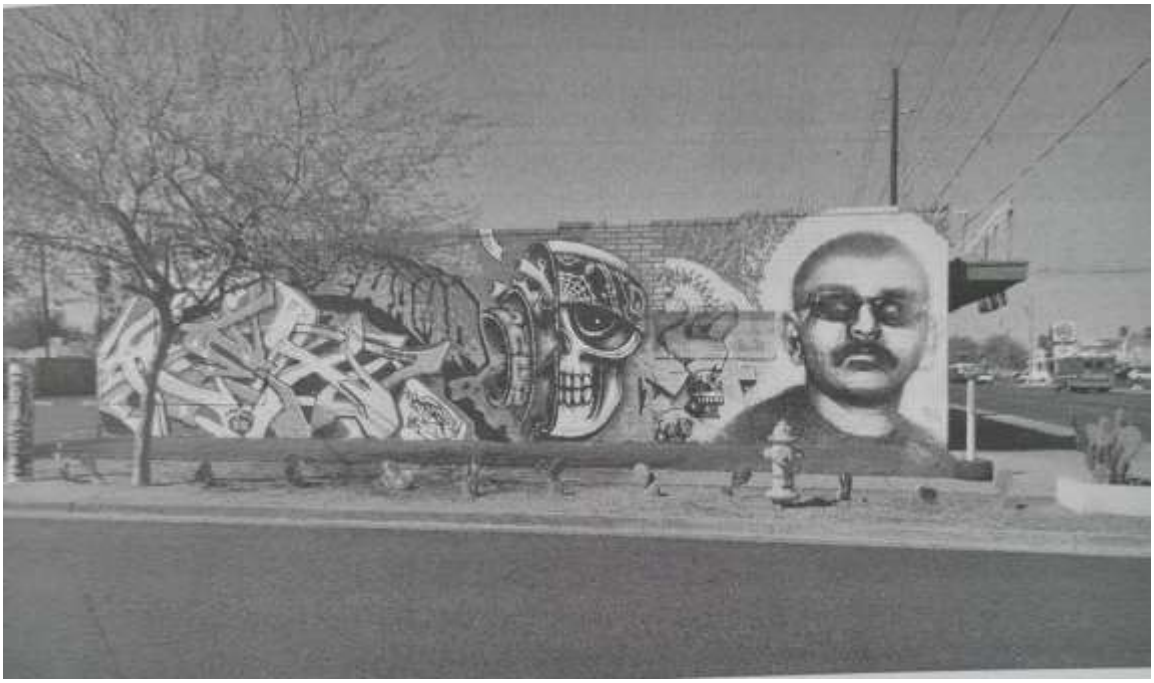
- **مبادئ الاستدامة :**

من أهم مميزات تكيف الشوارع الحضرية هو التوجه نحو مبادئ الاستدامة من خلال معالجة تصريف المياه والتلوث الضوئي واعادة تدوير المواد وتأثير الحرارة وجمع مياه الامطار، لذا جميع هذه المعالجات ممكن استخدامها لتنشيط البنية التحتية للشوارع الحضرية بهدف انشاء مناطق حيوية تجعلها جزءا مركزيا وجعلها وجهات ثقافية بدلا من اهمالها (Work group , 2013)

- **الفن والثقافة في الشوارع الحضرية :**

بدأت العديد من المنظمات الشعبية في مناطق عديدة من العالم بالنمو قبل واثناء وبعد ركود (2007)، حيث ان العديد من المنظمات بدأت بالاهتمام باحتياجات المجتمع والجمهور، فيما يتعلق بالثقافة وبالاستدامة والاقتصاديات المحلية (stavrides , 2015) .

هناك بعض المنظمات التي قامت بمعارض شعبية تعكس اعمال الفنانين في الشوارع الحضرية (الشكل 2) و(الشكل 3) كجزء من النسيج الحضري للمدينة والتي تعكس ثقافات المجتمع في المدينة وبما يتكيف مع العصر الحديث، حيث يتم عرض التراث والتقاليد والمعتقدات في جميع انحاء المدينة على شكل جداريات (Bondnar , 2015) هذا النوع من الفضاءات الحضرية ليس للتعليم الاجتماعي (لتنوع) فقط بل من الممكن ان يكون مكانا للتعبير السياسي، فهي لا تخلق فقط فضاءا حضريا فنيا بل توفر ايضا فضاءات لمختلف المجالات مما يحقق تلاقي التوجهات وتبادل الآراء وخلق أرضية توعية متبادلة (stavrides , 2015)



الشكل 2. الجدار المواجه للجنوب في احد الشوارع الحضرية في كالي، اريزونا (Preiser et.al, 2018)



الشكل 3. جدارية دوغلاس مايلز في احد الشوارع الحضرية، اريزونا **(Preiser et.al, 2018)**

- **التصميم المبدع :**

أحد الحلول التصميمية المستخدمة في الشوارع الحضرية الضيقة في المدن الحضرية هو تصميم المسكن الصغير الذي يدفع المعماريين إلى تصميم مساحات صغيرة ملائمة للعيش ومرنة ومتعددة الاستخدامات، وهذه الحلول تعد تحديا لاستخدامات الاراضي والكثافات المحددة من جميع انحاء المدينة (Preiser et.al, 2018).

4- الجانب العملي (الدراسة العملية)

تم اختيار منطقة الكرخ القديمة في بغداد والتي احتوت على العديد من الشوارع الحضرية الضيقة، حيث حللت الدراسة كثافات الحركة الحالية في منطقة الكرخ وتبحث الدراسة بشكل أساسي في شبكة الطرق واستخدامات الأراضي لفهم تدفق حركة المرور في المنطقة. ولجمع البيانات فقد تم إجراء ملاحظات الموقع لكثافة حركة المرور في شبكة الطرق وتمت مقارنة البيانات التي تم جمعها مع البيانات المتوفرة في مشروع تطوير الكرخ لعام 2014 من قبل أمانة بغداد، حيث تقتصر كثافات الحركة على حركة المركبات والمشاة خلال يوم العمل من الأحد إلى الخميس، وتحديداً خلال أوقات الذروة من الساعة 8 صباحًا حتى 6 مساءً.

غطت النتائج النهائية (الفترة من 2014 إلى 2023)، حيث حددت أوجه التشابه والاختلاف بين المتغيرات التي تؤثر على تشكيل شبكة الشوارع وأثرها على كثافة المرور وتهدف الدراسة إلى تقديم نظرة ثاقبة للوضع الحالي لكثافة الحركة في منطقة الكرخ القديمة والمساعدة في اتخاذ قرارات التخطيط والتطوير العمراني المستقبلية، والهدف الرئيسي هو جمع المعرفة والخبرة المكتسبة من الحسابات النظرية والتصاميم العملية لتقديم شبكة الشوارع كنظام تنقل مستدام وفعال وآمن ويهدف البحث إلى إثبات أن نظام شبكة الشوارع المنفذ بشكل صحيح يمكن أن يكون قابلاً للتكيف مع الظروف المحلية.

- **كيفية تصميم شبكة الشوارع (الشوارع الحضرية):**

تغيرت أنماط شارع الكرخ وتصميماته المجتمعية بشكل ملحوظ في القرن الماضي. تحولت شبكات الشوارع التقليدية الشبيهة بالأشجار إلى تخطيطات الشوارع الشبكية، وأصبحت أكثر تشعبًا. استلزم التطور السريع للمدن دراسة تصميم شبكة الشوارع وأنماطها وخصائصها لفهم ديناميات المدينة. تهدف هذه الدراسة إلى فهم الخصائص الهيكلية لشبكات الشوارع المستخدمة في مراكز المدن التاريخية.

سلط بوكانان الضوء على الطبيعة غير المستدامة للنقل الخاص بالسيارات الخاصة منذ أكثر من نصف قرن في كتابه "المرور في المدن". اقترح حدًا لكثافة حركة المرور يبلغ 200 سيارة / ساعة في كلا الاتجاهين للشوارع المحلية، مما يسمح بكثافة مرورية عالية والاختناقات المرورية فقط على الطرق العامة ذات المعايير المناسبة. من الجدير بالذكر أن بوكانان استخدم عبارة "بيئة الشارع" للتركيز على البيئة الاجتماعية ذات القيم الحضرية والتاريخية بدلاً من علم الأحياء وتلوث الهواء. تهدف دراسة بوكانان إلى فهم تأثير تصميم شبكة الشوارع على البيئات الحضرية وأهميتها التاريخية. من خلال تحديد حدود كثافة حركة المرور والنظر في البيئة الاجتماعية، تأمل الدراسة في تشجيع ممارسات النقل المستدامة وتعزيز التنمية الحضرية الصحية (بوكانان، 1963).

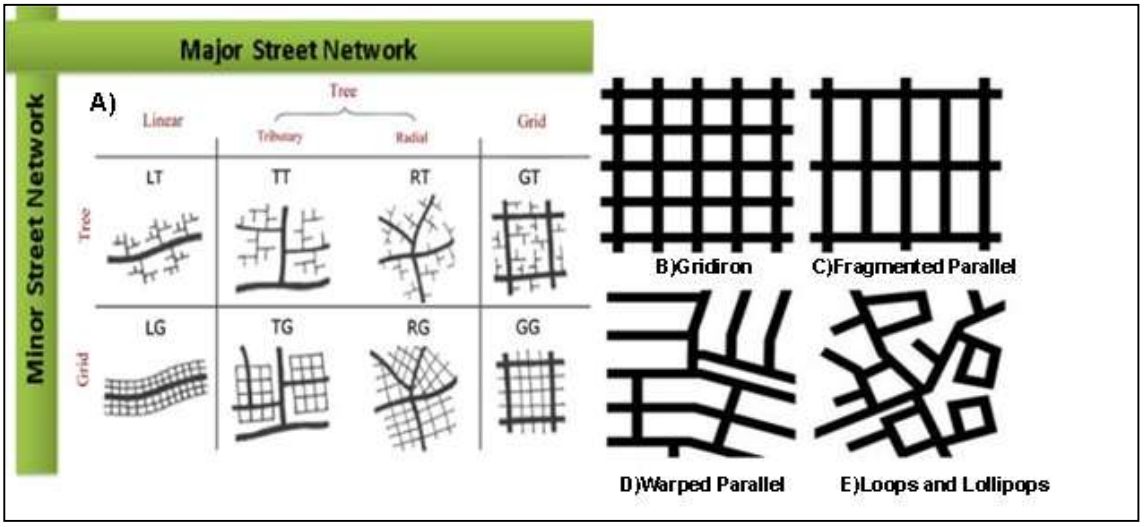
أدرك بوكانان أنه في المدن الصغيرة فقط يمكن أن تتعايش الحياة اليومية مع الاستخدام الكامل للسيارة. في حالات أخرى، كان الإجراء ضروريًا. لن تقوم خطط النقل المتكاملة بتنسيق استخدام الأراضي فحسب، بل ستتحكم أيضًا في الطلب. لا تزال بعض المقترحات صالحة، مثل نظام التصاريح للتحكم في دخول المركبات إلى مناطق محددة، وتسعير الطرق الإلكترونية، ودعم وسائل النقل العام لجعلها أرخص من السفر بالسيارة، ولكن تغيير أنماط العمل بدا معقدًا للغاية. اقترح بوكانان تحسين قدرة النظام الأساسي ومواقف السيارات، ونقل بعض الاستخدامات خارج المناطق المركزية، وإطالة فترة الذروة. لم يكن أي من هذه الحلول مرضيًا تمامًا، ولا تزال المشكلة قائمة حتى اليوم. خلص بوكانان إلى أن حجم الطرق الأساسية اللازمة لاستيعاب الاستخدام الكلي للسيارة كان كبيرًا جدًا لدرجة أن نسيج الأمة لا يمكن استيعابها بسهولة: يجب أن تكون هذه الطرق حول اعتبارات أوسع للبيئة، ومصممة جيدًا، وجذابة بصريًا من جميع الزوايا (بوكانان، 1963).

يمكن أن يؤثر شكل وخصائص الشبكات الحضرية بشكل كبير على العديد من جوانب التنقل، مثل مسافة السفر واختيار الوضع والسلامة، لذا يجب أن تكون الشوارع التي تخدم المناطق السكنية أو التجارية صالحة للعيش وللوصول إلى هذا الهدف، يجب أن تكون وسائط النقل العامة وغير الآلية قادرة على المنافسة مع حركة مرور السيارات (Wachs, 2013 ؛ Currie and Delbosc, 2011 ؛ Gehl,2011).

تشجع الممرات الواسعة السائقين على اكتساب السرعة، لكن السائقين يواجهون مخاطر من حركة المرور منخفضة السرعة (Kang and Fricker , 2013). الانعطاف إلى الشوارع الجانبية أو البحث عن مكان لوقوف السيارات. غالبًا ما يركب راكبو الدراجات على الأرصفة، خوفًا من حركة مرور السيارات الكثيفة والسريعة، مما يعرض المشاة للخطر ؛ يمكن إجراء مقارنة بملاحظات المشاة الذين يحصلون على أرصفة ضيقة بالقرب من ضجيج حركة المرور أو يتم التعدي عليها من خلال وقوف السيارات. يواجه السكان تدهورًا في البيئة وفي المنطقة، بما في ذلك عبور الأطفال

لشوارع خطرة في طريقهم إلى المدرسة. لا يمكن للسائقين المحترفين العثور على مكان لإيقاف سيارات الأجرة أو شاحنة التوصيل الخاصة بهم. يمكن إيجاد حل لتقليل سعة وسرعة السيارات (ماركس، 1957 ؛ برواتش وآخرون، 2012).

تعد دراسة السلامة على الطرق المبكرة من خمسينيات القرن الماضي من قبل ماركس واحدة من أولى الدراسات التي عالجت مشاكل السلامة المتصورة لأنماط شوارع الشبكة مقارنة بالتصاميم الهرمية (ماركس، 1957). استنادًا إلى 5 سنوات من بيانات الاصطدام لـ 86 منطقة سكنية، وجد ماركس ما يقرب من 8 مرات أكثر من حوادث الاصطدام في الشوارع الشبكية و 14 مرة في التقاطعات رباعية الاتجاهات في تصميم الشبكة مقارنة بالتقاطعات على شكل حرف T الموجودة في الترتيبات المتفرعة. كان سبب هذه النتائج هو العلاقة بين زيادة اتصال الشوارع السكنية واحتمال زيادة حركة المرور بسرعات أعلى (Handy et al.، 2003).



الشكل 4. تخطيط ستيفن مارشال يبين بنية شبكة الشوارع الرئيسية وشبكة الشوارع الثانوية (Marshall , 2005)

هي تعتمد مخططًا من كتاب "Streets and Patterns" لستيفن مارشال يؤكد على بنية شبكة الشوارع الرئيسية بشكل منفصل عن شبكة الشوارع الثانوية الموضحة في (الشكل 4) (مارشال، 2005).

استخدم مارشال في كتابه "Streets and Patterns" نظام تصنيف A B C D لوصف أنواع مختلفة من شبكات الشوارع واتجاهاتها المقابلة، مثل الشبكة، والتوازي المجزأ، والتوازي الملتوي، والحلقات والمصاصات. أنواع شبكات الشوارع هذه لها تأثيرات متباينة على وتيرة المشي وركوب الدراجات واستخدام وسائل النقل، كما هو موضح في (الشكل4).

يوفر تصنيف A B C D الذي اقترحه ستيفن مارشال إطارًا مفيدًا لفهم شبكة الشوارع وتطورها. من خلال تصنيف الشوارع إلى أنواع وأنماط مختلفة، مثل شد الحديد، والتوازي المجزأ، والتوازي الملتوي، والحلقات، والمصاصات، يمكننا الحصول على رؤى حول كيفية تأثيرها على تكرار المشي، وركوب الخيل، واستخدام وسائل النقل. على سبيل المثال، مع شبكة الشوارع العادية والمتصلة، يشجع نمط الشبكة على المزيد من المشي وركوب الدراجات مع تقليل استخدام السيارة.

علاوة على ذلك، قد تظهر هذه الأنماط منفردة أو مجتمعة، اعتمادًا على مستوى المركزية في المناطق الحضرية. على سبيل المثال، في المدن المكتظة بالسكان، قد نرى مزيجًا من الأنماط المختلفة التي تعكس الهيكل الحضري الفريد للمدينة. يمكن أن يساعدنا فهم هذه الأنماط وكثافتها على التنبؤ بالتغييرات في استخدام الشوارع والتخطيط وفقًا لذلك لضمان النقل الآمن والفعال لجميع المستخدمين.

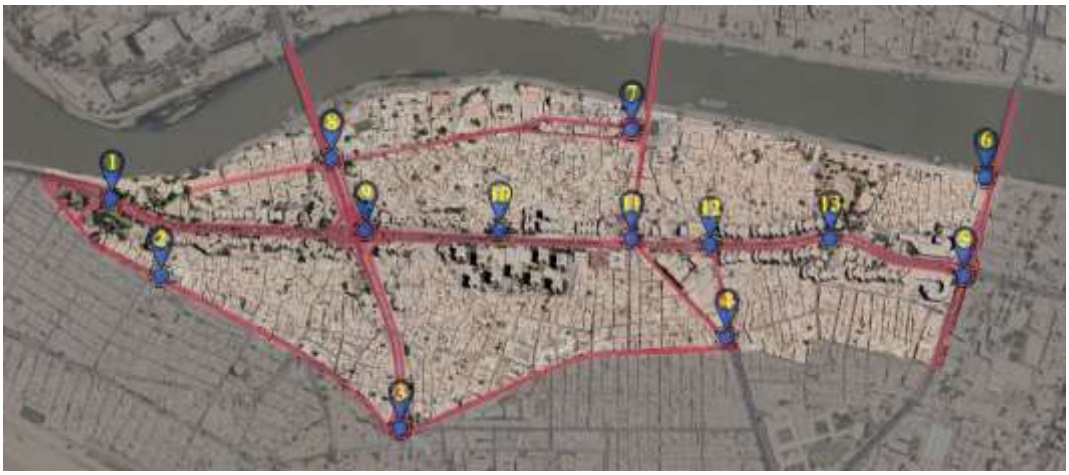
- **حالة دراسية (مركز الكرخ القديم)**
- **نبذة تاريخية :**

الكرخ حي تاريخي يقع على الضفة الغربية لنهر دجلة في بغداد، العراق. إنها واحدة من أقدم مناطق المدينة وأكثرها كثافة سكانية، ولها تاريخ غني يعود إلى القرن الثامن. تتميز الشوارع المتعرجة الضيقة والعمارة التقليدية والثقافة المحلية النابضة بالحياة. الكرخ موطن للعديد من المعالم الثقافية والدينية الهامة. يحتوي الحي على العديد من الأسواق التاريخية، مثل سوق الرحمانية والشواكة، والمعروفين بصناعاتهما اليدوية التقليدية والمنسوجات والمواد الغذائية. على الرغم من أهميته التاريخية، يواجه الكرخ العديد من التحديات، بما في ذلك الاكتظاظ، وتقادم البنية التحتية، والتدهور البيئي. شهد الحي تحضرًا كبيرًا في العقود الأخيرة، حيث تم استبدال العديد من المباني التقليدية بالمجمعات السكنية الشاهقة والمباني التجارية الحديثة (شارع حيفا) . لمواجهة هذه التحديات، أطلقت الحكومة المحلية العديد من المبادرات للحفاظ على التراث الثقافي للحي وتحسين الظروف المعيشية للسكان. وتشمل هذه المبادرات ترميم المباني التاريخية، وإنشاء مساحات خضراء عامة، وتنفيذ بنية تحتية جديدة للنقل لتخفيف الازدحام وتحسين التنقل. لا يزال الكرخ مركزًا ثقافيًا وتاريخيًا مهمًا في بغداد، له طابع وهوية فريدة لا تزال تجتذب الزوار والمقيمين على حد سواء (العبيدي وراشد، 2017) ؛ (الشكل 5)



الشكل 5. مخطط النسيج العمراني لمنطقة الكرخ القديمة (امانة بغداد، 2014) .

ويهدف البحث إلى تحديد كثافة الحركة لكل من المركبات والمشاة في منطقة الكرخ، بغداد، وتم استخدام تقنية مراقبة تعداد البوابة، والتي تضمنت حساب متوسط عدد الحركات في شبكة الطرق بمنطقة الدراسة. تم اختيار ثلاث عشرة نقطة محطة وفقًا لدرجة حضور الناس واستخدامهم للمساحات في الشوارع (الجدول 1)، وتم رسم خط تقاطع وهمي على شبكة الطرق في النقاط المحددة. تم العد خلال أيام العمل وأوقات الذروة على المحاور المرورية، بما في ذلك الشوارع الرئيسية والتقاطعات (الشكل 6).



الشكل 6. خريطة مسح لموقع الكرخ، والنقاط الصفراء هي 13 محطة تم اختيارها

الجدول 1. يبين الإحصائيات الوصفية لكثافات الحركة لمسح الموقع عام 2014. حسب مشروع تطوير الكرخ. (امانة بغداد، 2014)

Traffic Surveys Locations	Total vehicles (per10H)	Total vehicle's peak time (per10H)	Total pedestrians (per10H)	Total pedestrian's peak time (per10H)
Station 1 (Ahmad AlWaeli park)	17828	8456	324	163
Station 2 (Sheikh Maruf street)	3919	1045	334	157
Station 3 (Sheikh Maruf square)	6181	1295	395	246
Station 4 (Allawi street)	8775	3261	543	218
Station 5 (king Faisal 1 square)	4135	1983	255	127
Station 6 (AlAhrar Bridge)	2456	864	854	442
Station 7 (Al Shuhada square)	4527	1896	785	435
Station 8 (Bab AlMoatham Bridge)	17732	5991	465	231
Station 9 (AlTalae'a square)	28809	14530	533	254
Station 10 (Haifa street)	26074	15014	236	184
Station 11(Haifa street square)	12230	4445	316	185
Station 12 (Haifa street)	2645	945	351	142
Station 13 (Haifa street)	1898	826	210	75

تم جمع البيانات لمدة 15 دقيقة كل ساعة من الساعة 8:00 صباحاً حتى الساعة 6:00 مساءً، وتم تسجيل عدد المركبات المتحركة والمشاة في جدول باستخدام برنامج Excel لتحليل البيانات. كان التركيز على ساعات الذروة، عندما يزداد النشاط التجاري وحركة المشاة والمركبات، خاصة خلال أوقات الذهاب إلى العمل ونهاية يوم العمل والمدرسة.

5- النتائج والمناقشة

هدفت هذه الدراسة إلى تحليل الكثافة المرورية في منطقة الكرخ ببغداد باستخدام تقنية مراقبة تعداد البوابة. تضمن النهج اختيار 13 نقطة عد مرورية في منطقة الدراسة وإحصاء عدد المركبات المتحركة والمشاة كل 15 دقيقة

لمدة 10 ساعات. تم إجراء العد خلال أيام العمل وساعات الذروة، مع التركيز على الشوارع الرئيسية والتقاطعات مع ارتفاع نسبة الحضور واستخدام الشوارع.

أظهرت نتائج تحليل الكثافة المرورية زيادة معنوية في الكثافة المرورية في منطقة الدراسة بعد 9 سنوات، خاصة في شارع حيفا شكل 4، وهو المسار الحركي الرئيسي الذي يقسم المنطقة إلى قسمين ويرتبط بثلاثة جسور. لبقية بغداد. ووجدت الدراسة أن حركة مرور السيارات كانت الأعلى في هذا الشارع، بينما انخفضت حركة المشاة بمرور الوقت. ومع ذلك، زادت حركة المشاة في المحطة 7 (ميدان الشهداء)، وهي منطقة سوق تقليدية ذات حركة مرور منخفضة للسيارات (الشكل 7) و (الشكل 8)



الشكل 7. شارع حيفا (محطة 9) تقاطع عالي الكثافة بمنطقة المركبات



الشكل 8. ساحة الشهداء (محطة 7) ذات كثافة عالية لإجمالي مساحة المشاة

يتم عرض نتائج الدراسة الحالية في الشكل 8، والتي توضح كثافة المرور لفترتين مختلفتين من منطقة الدراسة. وكشفت النتائج أن مشروع التطوير من قبل أمانة بغداد عام 2014 لم يحسن الكثافة المرورية في المنطقة، وازدادت الكثافة المرورية بمرور الوقت.

الاستنتاجات :

- من أجل حل العديد من المشكلات الحضرية التي واجهتها المدن الحديثة، لابد من اشراك المجتمع في العمل بالتواصل والمسامية واستخدام الشوارع الحضرية لحل مشكلات تخطيط المدينة المتعددة بما في ذلك زيادة الكثافة وغيرها، ولا يتم ذلك باعادة استخدامها فقط بجعلها اماكن كثر تفاعلية واكثر امانا وانما بنشر الثقافة في جميع انحاء المدينة واثبات ان الشوارع الحضرية الصغيرة يمكن تحويلها إلى فضاءات تفاعلية للعيش .
- تجسد التغييرات في الشارع الحضرية الجوانب المادية للفضاء العام والاندماج الاجتماعي من خلال تعزيز مشاركة الناس في المجالات السياسية والاقتصادية والثقافية والاجتماعية. ومع ذلك، يمكنهم أيضًا إنشاء تحديات فريدة للمخططين والمصممين الحضريين، الذين يجب أن يوازنوا بين احتياجات المستخدمين وأصحاب المصلحة المختلفين مع الحفاظ على الطابع الحضري للمنطقة
- كان الهدف الرئيسي للدراسة هو تحديد شبكة الشوارع الحضرية المحيطة بمنطقة الدراسة ووضع إطار عام للنمو الحضري بناءً على مسوحات حركة المرور. هدفت الدراسة إلى ضمان استمرارية الحركة في منطقة الدراسة، وتعزيز الاستدامة الحضرية، وتسهيل الحركة المتوازنة للمركبات والمشاة دون أي حوادث أو مشاكل بين التدفقات المرورية.
- أظهرت استطلاعات المرور أن شارع حيفا شهد أعلى نسبة تدفق لحركة مرور المركبات خلال ساعات الذروة، حيث بلغ حجم حركة المرور 28809 وكثافة مرورية 11 في عام 2014. ومع ذلك، في عام 2023، زاد تدفق حركة المرور بشكل كبير إلى 50251، مع كثافة حركة المرور 20 تعزى هذه الزيادة إلى ارتفاع عدد السكان ووسائل النقل الشخصية، بما في ذلك سيارات الأجرة والحافلات الصغيرة، حيث لا توجد خدمات البنية التحتية للنقل العام، مثل المترو أو الترام.
- وجدت الدراسة أيضًا أن المناطق ذات الكثافة العالية للمركبات شهدت انخفاضًا ملحوظًا في حركة المشاة. في المقابل، كانت المناطق ذات معدلات المشاة المرتفعة هي تلك التي لم يُسمح للسيارات بالدخول إليها، مثل الأماكن العامة والأسواق التقليدية والمحلات. كانت هذه الشوارع والشوارع الضيقة ذات الزخارف العضوية التقليدية أكثر ملاءمة للمشاة وأكثر أمانًا.
- تسببت الشوارع الحضرية الواسعة والطويلة التي قسمت المنطقة إلى أجزاء في حدوث مشكلات لأنها لم تتطابق مع النسيج التقليدي للمنطقة. أصبحت هذه الشوارع صعبة للوصول إلى المشاة وتسببت في فقدان المنطقة لخصوصيتها. كما أنهم فشلوا في مراعاة العوامل البشرية، كما أن كثافة المركبات العالية في هذه الشوارع جعلتها غير آمنة للمشاة.
- أظهرت الدراسة أن تعزيز بيئة أكثر ملاءمة للمشاة في المناطق الحضرية أمر بالغ الأهمية لضمان الاستدامة والسلامة الحضرية. يمكن تحقيق ذلك من خلال تحسين البنية التحتية للنقل العام وتعزيز التركيبات العضوية التقليدية التي تعطي الأولوية لحركة المشاة.
- تقدم الدراسة رؤى قيمة عن أنماط المرور في منطقة الكرخ ببغداد، والتي يمكن لمخططي المدن وواضعي السياسات استخدامها لتطوير سياسات واستراتيجيات نقل أكثر فاعلية. بشكل عام، تسلط الدراسة الضوء على أهمية المراقبة والتحليل المستمر لكثافات المرور في المناطق الحضرية، وخاصة في المناطق المكتظة

بالسكان والنشطة تجاريًا ويمكن أن تساعد النتائج المخططين الحضريين وواضعي السياسات في تحديد المجالات التي تتطلب تحسينات وتطوير سياسات واستراتيجيات نقل أكثر فاعلية تعطي الأولوية لاحتياجات كل من المشاة والمركبات.

- تهدف الدراسة الحالية إلى زيادة الوعي بأن زيادة حجم حركة المرور لا تؤثر فقط على كثافة حركة المرور بل تؤثر أيضًا على أنماط الحياة الحضرية حيث يبدأ المشاة وسائقو السيارات في تغيير مسارات طرقهم لتجنب الاختناقات المرورية. يؤثر هذا التحول في أوضاع النقل بشكل كبير على طبيعة المناطق المجاورة، لا سيما المناطق السكنية، حيث يؤثر على الخصوصية.

6- التوصيات :

- الاهتمام بتطوير الشوارع الحضرية ضمن المناطق الحضرية في المدينة وخاصة المزدحمة منها كون ان هذه الفضاءات تكون مناطق متنفس للناس وتعمل على احياء تلك المناطق .
- تطوير المساحات العامة والمساحات الخضراء يمكن أن يشجع بشكل فعال نشاط المشاة، ويقلل من الاعتماد على السيارات، ويجعل البيئة أكثر ملاءمة للعيش. من خلال إنشاء ممرات وممرات للدراجات وغيرها من البنية التحتية الملائمة للمشاة، يمكن للأشخاص التنقل بسهولة وأمان أكبر، مما يؤدي إلى تحسين الصحة الجسدية والرفاهية. بالإضافة إلى ذلك، يجب تصميم مناطق وقوف السيارات بطريقة لا تعيق ممرات المشاة.
- يعد تحسين البنية التحتية للنقل العام أمرًا أساسيًا لتقليل حركة المرور وانبعاثات الكربون. يمكن تحقيق ذلك من خلال تطوير طرق جديدة وتحسين الخدمات الحالية ودمج وسائط النقل المختلفة مثل الحافلات والسكك الحديدية الخفيفة والقطارات. من خلال جعل وسائل النقل العام أكثر ملاءمة وسهولة في الوصول إليها، يمكن للناس ترك سياراتهم في المنزل، والحد من الازدحام المروري وتحسين جودة الهواء.
- للتخفيف من الازدحام المروري في الشوارع المزدحمة مثل شارع حيفا، يجب توفير شوارع ثانوية لاستيعاب المركبات. يمكن تحقيق ذلك من خلال إنشاء طرق بديلة تربط الوجهات الرئيسية، مما يسمح للسائقين بتجنب الشوارع الرئيسية المزدحمة. من خلال تقليل عدد السيارات على الطرق الرئيسية، يمكن تحسين تدفق حركة المرور، ويمكن أن تكون تجربة القيادة الشاملة أكثر كفاءة.
- يمكن أن يؤدي تنفيذ خدمات النقل مثل المترو والقطارات إلى تقليل الازدحام المروري بشكل كبير، خاصة خلال ساعات الذروة. يمكن أن توفر هذه الخدمات النقل السريع والفعال إلى الوجهات الرئيسية وتقليل عدد السيارات على الطريق. بالإضافة إلى ذلك، يمكن أن يساعد تنفيذ هذه الخدمات في تقليل انبعاثات الكربون، والتي يمكن أن يكون لها تأثير إيجابي على البيئة.
- يمكن أن يساعد توفير أماكن وقوف السيارات المخصصة للمركبات والحافلات الصغيرة في تقليل الازدحام على الطرق وتحسين تدفق حركة المرور خلال أوقات الذروة. من خلال توفير موقف للسيارات بعيدًا عن الشارع، يمكن للسائقين تجنب إعاقة تدفق حركة المرور على الطرق الرئيسية، وتقليل أوقات السفر الإجمالية وتحسين تجربة القيادة. يمكن أن يساعد هذا أيضًا في تقليل انبعاثات الكربون عن طريق تقليل الوقت الذي تقضيه المركبات في التباطؤ في حركة المرور.

References

1. البكري ، ايناس حسن ، 2021 ، " تكيف المبنى والمواءمة البيئية في العمارة المعاصرة " ، اطروحة دكتوراه ، جامعة بغداد ، كلية الهندسة ، قسم هندسة العمارة
2. البكري ، ايناس حسن ، البزاز ، انعام امين ،2021 " التكيف المستدام لمباني العمارة المعاصرة " بحث منشور ضمن وقائع المؤتمر العلمي الدولي الثالث للعلوم الصرفة والتطبيقية والتكنولوجية لأكاديمية ريمار بالتعاون مع جامعة جيديك التركية
3. Ajay, P., Nagaraj, B., Pillai, B.M., Suthakorn, J., Bradha, M., 2020. Intelligent ecofriendly transport management system based on iot in urban areas. Environ Dev Sustain 1–8.
4. Alobaydi, D., Rashid, M., 2017. A Study of the Morphological Evolution of the Urban Cores of Baghdad in the 19th and 20th Century, in: Eleventh International Space Syntax Symposium at Instituto Superior Técnico, University of Lisbon, Portugal. [online] pp. 31–38. https://www.researchgate.net/publication/318116959
5. Alsaffar, N.H., Alobaydi, D., 2023. Studying street configurations and land-uses in the downtown of Baghdad, in: AIP Conference Proceedings. AIP Publishing. https://doi.org/10.1063/5.0105420
6. Broach, J., Dill, J., Gliebe, J., 2012. Where do cyclists ride? A route choice model developed with revealed preference GPS data. Transportation Research A 46, pp. 1730–1740. https://doi.org/10.1016/j.tra.2012.07.005
7. Buchanan, C., 1963. Traffic in Towns. UK: Penguin
8. City of Austin Downtown Commission Alley Activation Workgroup . 2013 . Activating Austin's Downtown Alleys as Public Space . Austin : City of Austin Downtown Commission Alley Activation Workgroup
9. Currie, G., Delbosc, A., 2011. Understanding bus rapid transit route ridership drivers: An empirical study of Australian BRT systems. Transport Policy18, pp.755–764. https://doi.org/10.1016/j.tranpol.2011.03.003
10. Ellin , N. 2006 . Integral Urbanism . New York .). Routledge
11. Gehl , J. 2011. Life Between Buildings :Using Public Space . Washington: Island Press
12. Hillier, B., 1996. Cities as movement economies. Urban design international 1, 41–60.
13. Kang, L., Fricker, J. D., 2013. Bicyclists commuters' choice of on-street versus off-street route segments. Transportation 40, pp. 887–902.
14. Marks, H., 1957. Subdividing for traffic safety. Traffic Quarterly Institute of Transportation Engineers (July), pp. 308–325
15. Marshall, S., 2005. Streets & Patterns. 1st ed. London and New York: Spon press Taylor and Frank Group. pp.94-96.
16. Mazloumian, A., Geroliminis, N., Helbing, D., 2010. The spatial variability of vehicle densities as determinant of urban network capacity. Philosophical Transactions of the Royal Society A: Mathematical, Physical and Engineering Sciences 368, 4627–4647. https://doi.org/10.1098/rsta.2010.0099.

17. Mohammed, L.R. and Alobaydi, D., 2020a, March. Evolution of the urban form of historic hit citadel: deriving a schematic model for iraqi fortified cities. In IOP Conference Series: Materials Science and Engineering (Vol. 745, No. 1, p. 012180). IOP Publishing
18. Mumford, L., 2011. "What is a City?": Architectural Record (1937). In The City Reader (pp. 123-127). Routledge
19. Preiser ,W., Hardy ,A.& Wilhelm ,J. 2018 . Adaptive Architecture : changing parameters and practice . London & New York , Routledge
20. Roukouni, A., Junyent, I.A., Casanovas, M.M. and Correia, G.H.D.A., 2023. An Analysis of the Emerging "Shared Mobility Hub" Concept in European Cities: Definition and a Proposed Typology. Sustainability, 15(6), p.5222. https://doi.org/10.3390/su15065222.
21. Sarsam, S., and Abdulameer, M., 2014. Evaluation of pedestrians walking speeds in Baghdad city. Journal of Engineering, 20, pp. 1–9. https://www.iasj.net/iasj/article/92298
22. Stavrides , S. 2015 . Common Space as Threshold Space : Urban Commoning in Struggles to Re-appropriate Public Space . Commoning as Differentiated Publicness , spring
23. Wachs, M., 2013. Turning cities inside out: and the resurgence of downtowns in America. Transportation 40, pp. 1159–1172
24. Zeidler , E. H. ,1983. Multi Architecture in the Urban Context . New York :Van Nostrand Reinhold.

دراسة المحتوى الميكروبي لأنواع مختلفة من الخبز والحلويات والمعجنات المباعة في الأسواق المحلية

Study The Microbial Content About Different Types Of Bread, Pastries and Sweets Sold in Local Market

Sahar Sabeeh George [1]

© 2023 The Author(s). This open access article is distributed under a Creative CommonsAttribution (CC-BY) 4.0 license.

Author details

[1] Department of Food Science, College of Agriculture, University of Basra, Basra, Iraq

Citation information

Cite this article as:

George, S.S., (July 2023), *Study The Microbial Content About Different Types Of Bread, Pastries and Sweets Sold in Local Market*, Proceedings of the Minar Congress, Turkey, (9) pp 345-358, DOI: http://dx.doi.org/10.47832/MinarCong9-29

Abstract: This study was conducted in the microbiology laboratories of the College of Agriculture, University of Basra for the year 2021. Modern techniques (Petri film slides) were used to count (total aerobic bacteria, total coliform bacteria, faecal coliform bacteria, Staphylococcus aureus, yeasts, and moulds) as they were collected from five different regions of Basra Governorate, which are (Abi al-Khasib, Old Basra, Algeria, Karma, and al-Ashar) from the shops scattered in these areas, and samples of some sweets, bread, and pastries (cakes with sesame, dumplings, date crumbs, local data, bread, and jerk). Specificity. The highest contamination was observed for the bread sample of the Old Basra region, as the logarithm of the microbial numbers reached (6,1, 1.8, 1, 1.2 and 1) cfu/g for each of (total aerobic bacteria, total coliform bacteria, faecal coliform bacteria, Staphylococcus aurous, yeasts and moulds) on Respectively, while the highest contamination of jerk was observed for the regions of Abi al-Khasib and Karma about the total number of bacteria, and faecal coliform bacteria were found, while there were no growth was found (for faecal coliform bacteria, Staphylococcus aurous, yeasts, and moulds) for the rest of the studied areas below. While the sweets were observed, the highest contamination was in the Abu al-Khasib area and for samples (sesame cakes, dumplings, date stalks, and local data). The average logarithm of the total number of bacteria was (4, 4.6, 5 and 5.3) cfu\g, respectively, while the lowest logarithm averages for the total number of bacteria for the Algeria region were (1, 2.2, 1.2, and 1.2) cfu\g, respectively, according to the above dessert arrangement. Also, no growth of faecal coliform bacteria, yeasts, and moulds was observed for all the sweets selected in the study. However, growth of Staphylococcus aurous bacteria was observed for the dumplings of the Karma region, with an average logarithm of 2.47 cfu/g. And the results obtained fell within the hygiene conditions that make them acceptable and palatable to the consumer.

Key Words: Microbial Contamination, Bread, Pastries, Sweets.

الكلمات المفتاحية: الأحياء المجهرية ، المخبوزات ، الممرضات البكتيرية.

http://dx.doi.org/10.47832/MinarCong9-29

[1] sahersgeorge @uobasrah.edu.iq

الخلاصة

أجريت هذه الدراسة في مختبرات الأحياء المجهرية لكلية الزراعة جامعة البصرة لسنة 2021. إذ استخدمت التقنيات الحديثة (شرائح البتري فلم) لعد (البكتريا الهوائية الكلية وبكتريا القولون الكلية وبكتريا القولون البرازية والمكورات العنقودية الذهبية والخمائر والأعفان) إذ جمعت من خمس مناطق مختلفة من محافظة البصرة وهي (أبي الخصيب والبصرة القديمة والجزائر الكرمة والعشار)، من المحلات التجارية المنتشرة في هذه المناطق وعينات بعض الحلويات والخبز والمعجنات (كعك بالسمسم والزلابية وكليجة التمر و الداطلي المحلي والخبز والجرك). لوحظ وجود فروق معنوية لمتوسطات لوغاريتم الأعداد البكتيرية إلا أنها كانت ضمن الحدود المسموح بها للسيطرة النوعية. إذ لوحظ أعلى تلوث لعينة خبز منطقة البصرة القديمة إذ بلغت لوغاريتم الأعداد الميكروبية (6,1,1.8,1,1.2 & 1) cfu\g لكل من (البكتريا الهوائية الكلية وبكتريا القولون الكلية وبكتريا القولون البرازية والمكورات العنقودية الذهبية والخمائر والاعفان) على التوالي. في حين لوحظ أعلى تلوث للجرك لمنطقتي أبي الخصيب والكرمة بالنسبة للعدد الكلي للبكتريا وتوتجد بكتريا القولون البرازية في حين لم يوجد أي نمو (لبكتريا القولون البرازية والمكورات العنقودية الذهبية والخمائر والأعفان) لبقية المناطق المدروسة أدناه. بينما الحلويات لوحظ أن أعلى تلوث كان لمنطقة أبي الخصيب ولعينات (كعك بالسمسم والزلابية وكليجة التمر و الداطلي المحلي) وبلغ متوسط لوغاريتم أعداد البكتريا الكلية (4, 6.4,5 & 5.3) cfu\g على التوالي بينما أدنى متوسطات لوغاريتم اعداد البكتريا الكلية لمنطقة الجزائر وكانت (1, 2.2, 1.2 & 1.2) cfu\g على التوالي حسب الترتيب الحلويات أعلاه. كما لم يلاحظ أي نمو لبكتريا القولون البرازية والخمائر والأعفان ولجميع الحلويات المنتخبة في الدراسة. لكن لوحظ نمو بكتريا المكورات العنقودية الذهبية لمنتوج الزلابية لمنطقة الكرمة بلغ متوسط لوغارتيم اعدادها 2.47. cfu\g والنتائج التي تم الحصول عليها وقعت ضمن شروط النظافة الصحية التي تجعلها مقبولة للمستهلك ومستساغة ومن المهم توضيح أهمية البحث كونه يبين أهمية الحد من تلوث الأغذية المصنعة محليا وذلك عن طريق نشر الوعي باتباع شروط النظافة الصحة للحد من التلوث والتقليل منه في محلات البيع العامة ولأغلب مناطق المحافظة وذلك لكثرة استهلاك مثل هذه المنتجات.

المقدمة

تعد الحبوب من اكثر الاغذية استهلاكا في العالم لكل نوع منها اصناف مختلفة عديدة اذ تجهز 90% من المدخلات الغذائية للفرد وتشكل حوالي 85% من الانتاج العالمي للغذاء كما يجهز اكبر جزء بالعالم من الطاقة في الدول النامية اذ يوفر ما يتراوح بين 50-90% من اجمالي السعرات الحرارية والبروتين (Tang *et al.*,2010).

تلعب الحبوب دوراً مهماً في النظام الغذائي البشري إذ أستهلك منذ وقت طويل ومن أهم منتجات هي الخبز ومنتجات المخابز بجانب منتجات أخرى كالبسكويت و المعجنات بالإضافة الى استعداد الفرد لاستهلاك وتناول مثل هذه الاطعمة على مدى الأزمان (Oluwajoba *et al*,. 2012).

أدى التحضر في البلدان الى زيادة الطلب على هذه المنتجات ذات السعر المناسب، اذ تعد منتجات المخابز من اهم الأنظمة الغذائية للطبقات الفقيرة في المجتمعات (Ravimannan. 2016).

تعد منتجات المخابز من اهم المواد الغذائية الاساسية في معظم بلدان العالم فهي تحتوي على المكون الرئيسي وهو الحبوب الذي يعد مصدراً رئيسياً ليزودنا بالسعرات الحرارية والبروتين...الخ.

فالحبوب كانت غذاءً اساسياً للإنسان من عصور ما قبل التاريخ واستهلاكها كان منذ فترات زمنية طويلة وبعد ذلك طورت عمليات تصنيع الخبز ومنتجاته و زادت نسب مبيعاته بالعقود الماضية ومن اهم المكونات الأساسية في الخبز ومنتجاته هي الكربوهيدرات، البروتينات، الدهون، الفيتامينات، المعادن (Al-Tulaihan *et al.*,2004).

يؤكل الخبز في جميع انحاء العالم لذا يعد منتوج غذائي مقبول عالميا ولجميع طبقات المجتمع اغنياء، فقراء، ريف، حضر لذا من غير الممكن التقليل من أهميته التغذوية للاستهلاك البشري (Demissie& Natea. (2017، كما من الممكن حدوث تلوث ميكروبي للحبوب الداخلة في تصنيع مثل هذه المنتجات خلال عمليات الخزن بظروف غير صحية وغير ملائمة وهذا يؤدي الى نمو وانتشار الاحياء المجهرية المختلفة المسببة للتلوث (Khanom *et al.*,2016).

كما ممكن ان يحدث تلف وفساد ميكروبي للخبز والصمون وغيرها من المنتجات لكونها تعتبر مستودع ملائم لنمو الفطريات نتيجة لتوفر الظروف الملائمة لنموها كالرطوبة و المكونات الأساسية الداخلة في تصنيع هذه المنتجات مما يسبب تلف فطري نتيجة نمو أنواع مختلفة من الفطريات بعضها يكون منتج للسموم الفطرية وتسبب تعفن وفساد المنتجات النامية عليها خلال الخزن وهذا يحد من العمر الافتراضي للخبز والصمون فالمحتوى المائي دور فعال في زيادة النمو الفطري (Alpers *et al.* ,2021). يحدث تلوث الخبز خلال عملية التصنيع المختلفة ومصدر هذا التلوث هو الهواء المحيط والأليات والعمال اثناء عمليات الإنتاج والبيع للمستهلك وطرق الخزن غير الصحيحة جميع هذه العوامل تؤدي الى حدوث تلوث بكتيري او فطري بالتالي حدوث تغيرات غير مرغوبة مما ينتج عنه تراكم للسموم الناتجة عن نمو الفطريات وبالتالي يؤثر على صحة المستهلك (Garcia *et al* ،. 2019).

التلف الميكروبي يعتمد على خصائص الم نتوج وطريقة الخزن ان من الممكن حدوث انتشار للأحياء المجهرية الدقيقة ويرجع سبب ذلك الى عمليات تجهيز المواد الأولية وطرق الحفظ والتصنيع لذا من الضروري تحديد شروط

الخزن الملائمة لمنع نمو وتكاثر الميكروبات (Olunlade *et al.*(2013 فالخبز ومنتجات المخابز والمعجنات والبسكويت وغيرها من الممكن ان تتعرض الى انواع مختلفة من التلف الفيزيائي، الكيميائي و الميكروبي وان التلف الميكروبي هو الأخطر اذ ممكن ان يحدث نتيجة نمو بعض انواع من البكتريا مثل *Bacillus* Sp وغيرها وكذلك نمو بعض الأعفان المسببة لفساد الخبز وسوف نذكر بعض منها Rhizopus, Mucor, Penicillium, Eurotium, Aspergillus and Monilia (Saranraj and. Geetha.2012) .

تعد المعجنات الحلوة من أكثر المأكولات في تنوعها وتعدد أصنافها: منها الخفيفة التي تقدم مع المشروبات ومنها التي تقدم بعد الوجبة وتعرف بأنها أي نوع من الطعام يعتمد في تكوينه الأساسي على السكر بأنواعه المختلفة. ومن الحلويات الكيك السادة والتورتة بكافة أنواعه والبتيفور والبسكويت والكعك باللوز. تنحصر القيمة الغذائية للمعجنات الحلوة في كونها مصدراً كبيراً للطاقة ولا تمد الجسم بالعناصر الغذائية الأخرى مثل البروتين والفيتامينات والمعادن عدا الشوكولاتة التي تحتوي على بروتينات بالحليب إضافة إلى الحديد الموجود في الكاكاو (Coelho *et al.*,2010).

إن تطور الصناعات الغذائية بشكل كبير أدى الى ارتفاع تواجد أنواع مختلفة من البكتريا الملوثة نتيجة استخدام مكونات جديدة في عمليات تصنيع المنتجات الغذائية والحلويات والمعجنات أو تطبيق عمليات تصنيعية كذلك لأثار تقنيات التعبئة الجديدة وبالإضافة للإنتاج العالي المتزايد للأغذية الجاهزة للأكل وتسويقها (Valero *et al.*,2018) . من الممكن ان تنتقل الى الانسان العديد من الامراض نتيجة تناوله بعض الأغذية الملوثة بالاحياء المجهرية المرضية المتواجدة عن طريق ايدي العاملين والأدوات غير النظيفة المستخدمة في عمليات التصنيع والتعبئة والنقل او عن طريق العاملين الحاملين للبكتريا الممرضة كما يمكن انتقالها للمستهلك عن طريق الحشرات والغبار والهواء وغيرها (WHO,2015).

إن تناول المعجنات والحلويات المكشوفة من الباعة المتجولين يزيد من فرص الإصابة بالأمراض إذ أن ظاهرة انتشار الباعة المتجولين أصبحت تهدد الصحة العامة لأنها تتعلق بصحة الانسان وسلامته. يمكن الوقاية من الامراض المنتقلة عن طريق الأغذية الملوثة وذلك بنشر الوعي الصحي بين الباعة والعاملين باتخاذ الإجراءات الوقائية وتقييد العمال بالنظافة الشخصية والأدوات المستخدمة وغيرها من إجراءات السلامة. ان تواجد بعض الاحياء المجهرية في الغذاء يكون أحد أسباب تلفه وقد تكون ضارة وتسبب بعض حالات التسمم وبالتالي يوثر على الصحة العامة للمستهلك نتيجة لنمو الميكروبات المرضية وتكاثرها فيها مثل بكتريا السل والتيفويد والكوليرا والسالمونيلا بكتريا القولون والباسيلس والخمائر والاعفان وغيرها التي تسبب المرض والتسمم ولا يقتصر التسمم الميكروبي على البكتريا بل قد يحدث عن طريق الفطريات أو الطحالب أو البروتوزوا. (Fung *et al.*,2018)

ومن أهم أنواع البكتريا Bacteria: من أ هم الأجناس البكتيرية التي تسبب فساد الغذاء أو التسمم عن طريقها هي: *Staphylococcus, ,Pseudomonas, Escherichia, Serratia, Salmonella, Shigella, Micrococcus Streptococcus, Bacillus, Clostridium*

الهدف من الدراسة

بسبب الطلب المتزايد في وقتنا الحالي على شراء الخبز والمعجنات والحلويات والبسكويت ومنتجات المخابز المختلفة من قبل المستهلك ولكون المخابز والأفران تختلف بأتباعها لشروط النظافة الصحية وعمليات التخزين وهذا يعتمد على المناطق المتواجدة فيها مثل هذه الأفران في محافظة البصرة لذا استوجب اجراء دراسة ميدانية على مجموعة من المخابز واخذ نماذج لغرض اجراء فحوصات ميكروبية لضمان سلامة الفرد في المجتمع البصري خاصة. واجراء فحص ميكروبي لغرض الكشف عن تواجد بعض الاحياء المجهرية الممرضة والملوثة ومقارنتها مع الأصناف المباعة بالمحلات التجارية مع مثيلاتها لدى الباعة المتجولين وذلك لتزايد الطلب على مثل هذه الأغذية في وقتنا ورخص ثمنها مما يؤثر سلبا على صحة المستهلك لذا وجب إرشاد المستهلكين والسعي لتقديم غذاء صحي وسليم خالي من أي تلوث او احياء مجهرية ممرضة.

طرائق العمل

جمع العينات

جمعت 10 عينات لكل نموذج من خمس مناطق مختلفة من محافظة البصرة وهي (ابي الخصيب والبصرة القديمة والجزائر الكرمة والعشار) اذ جمعت من المحلات التجارية المنتشرة في هذه المناطق واخذت نماذج لعينات بعض الحلويات والخبز والمعجنات (كعك بالسمسم والزلابية وكليجة التمر و الداطلي المحلي والخبز والجرك) وأجريت مجموعة من الفحوصات الميكروبية لمعرفة تواجد بعض أنواع الاحياء المجهرية كالعدد الكلي للبكتريا وعد بكتريا القولون الكلية وبكتريا القولون البرازية والمكورات العنقودية الذهبية والخمائر والاعفان باستخدام تقنية البتري فلم.-

الفحوصات المايكروبية:

1. العد الكلي للبكتريا الهوائية Total count of airplane
2. عد بكتريا Staph aureus
3. عد بكتريا القولون البرازية E.coli.
4. عد بكتريا القولون الكلية coliform
5. عد الخمائر و الأعفان باستخدام تقنية Petrifilm

تم وزن 1غم من كل عينة من عينات الخبز و والمعجنات والحلويات (كعك بالسمسم والزلابية وكليجة التمر و الداطلي المحلي والخبز والجرك) وضعت في انابيب اختبار تحتوي على 9 ml من محلول التخفيف البيتون و بعدها عملت سلسلة من التخافيف زرعت على شرائح البتري فلم واخذ ثلاث مكررات لكل عينة واجريت جميع الفحوصات اعلاه.

طريقة العد باستخدام شرائح Petrifilm^{3M}

استعملت طريقة Petrifilm^{3M} (إنكليزي المنشأ) في عد البكتريا الكلية وعد بكتريا القولون الكلية (coliform) وبكتريا القولون البرازية *E.coli* وعد المكورات العنقودية الذهبية *Staphylococcus aureus* والخمائر والاعفان في المواد الغذائية كالحلويات والجرك والمعجنات المنتخبة من بعض المحلات التجارية لمناطق مختلفة من أسواق

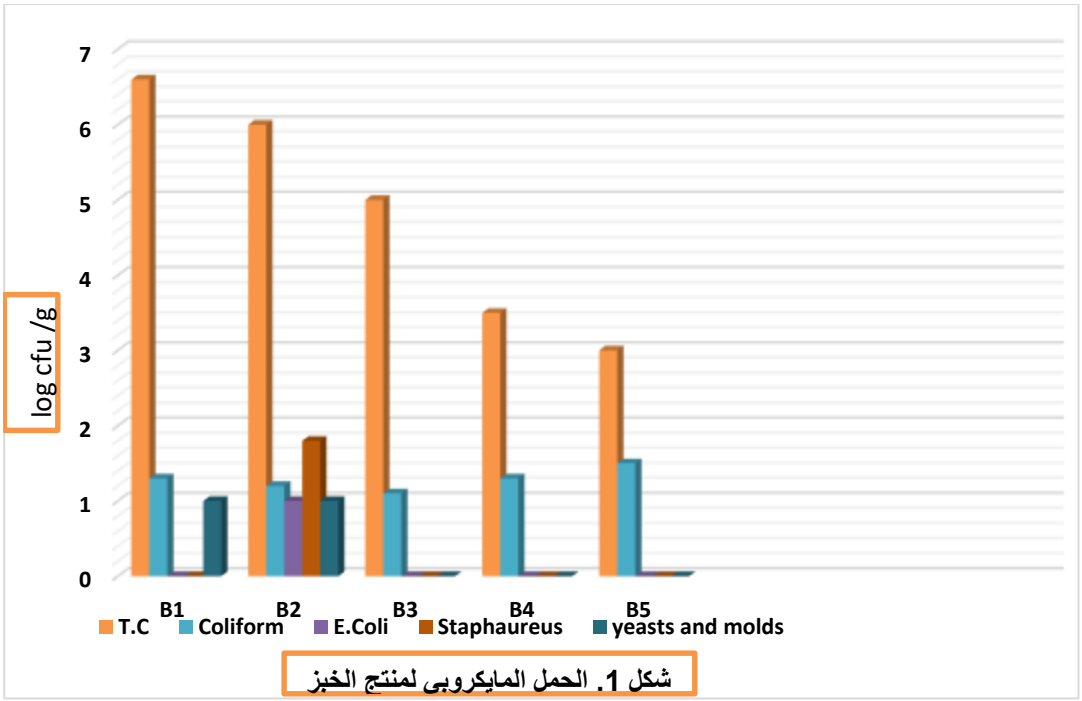
محافظة البصرة وتمتاز طريقة petriflm3M بدقتها واختصارها للوقت والمواد المستخدمة بالطرق الاعتيادية في العد البكتيري اذ تحتوي شريحة مسطحة بها 20 مربع صغير يزرع ml(1) من التخفيف المحضر بهدوء للتأكد من عدم حدوث فقاعات او خدوش لغشاء البتري فلم ونشر بواسطة غلاف بلاستيك مقعر يترك فوق شريحة Petrifilm3M ويضغط من منتصفه لمدة من الزمن بعدها توضع في الحاضنة بدرجة 37 مْ لمدة 24 ساعة بينما حضنت شرائح البتري فلم للخمائر والاعفان بدرجة حرارة 25 مْ لمدة 3-5 أيام بعدها عدت المستعمرات البكتيرية النامية استعملت التخفيف الاول لكل من بكتريا coliform و *E.coli* والخمائر والاعفان و*Staphylococcus aureus* بينما استخدم التخفيف الرابع لحساب للعدد الكلي للبكتريا الهوائية ولجميع العينات في التجربة (Kornacki and Johnson, 2001).

التحليل الاحصائي

حللت البيانات الحالية الخاصة بالتجربة احصائيا باستخدام التصميم العشوائي الكامل Complete Randomized Design CRD والفروق المعنوية باختبار دنكن حسب ما ورد في XLSTAT (2004) .

النتائج والمناقشة

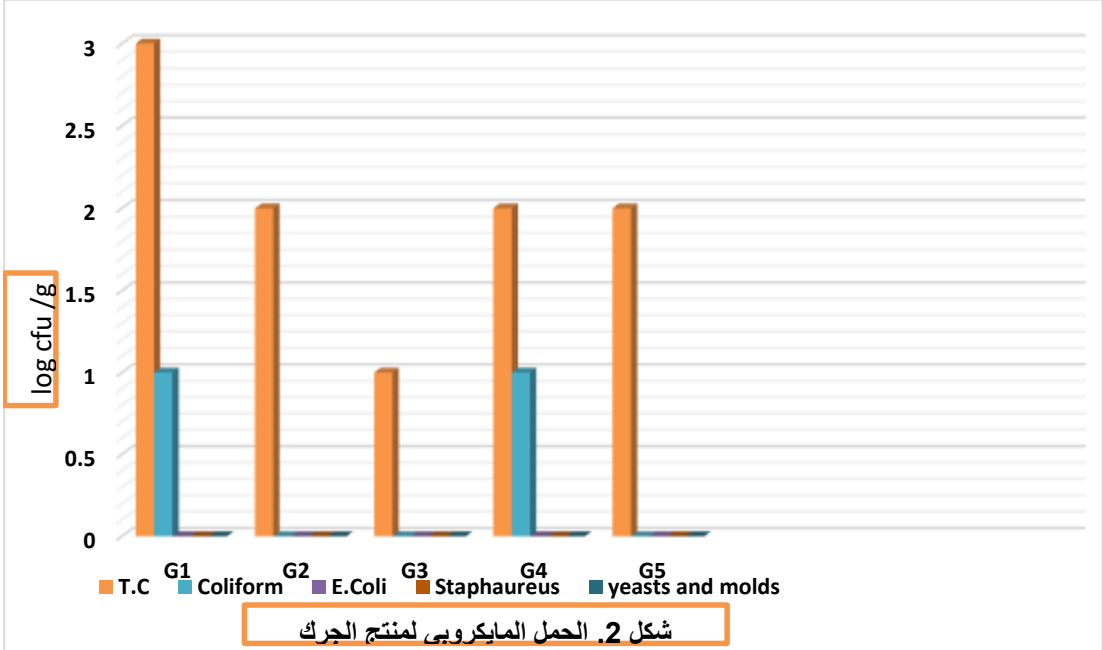
أوضحت النتائج في الدراسة الحالية لفحص نماذج الخبز بان العدد الكلي للبكتريا الهوائية الكلية T.c في عينة خبز منطقة البصرة القديمة أعطت اعلى لوغاريتم لمتوسط العدد البكتيري الكلي وجود فروق معنوية ($P<0.05$) اذ بلغ 6.6 cfu\g وان الحد المسموح به من العدد الكلي للبكتريا من 10-1000 خلية\غرام في حين يلاحظ ان اعداد بكتريا القولون البرازية والمكورات العنقودية لا يتجاوز 10-100 خلية \غرام صالح واخرون. (2014) بينما كان ادنى لوغاريتم لأعداد البكتريا الهوائية الكلية لخبز منطقة الجزائر والتي بلغت 5 cfu\g اما بالنسبة لبكتريا *E. coli* و *aureus Staph* لم يلاحظ وجود اي نمو لهما في عينات خبز مناطق ابي الخصيب والجزائر والكرمة والعشار في حين لوحظ ان اعداد بكتريا القولون الكلية كانت متقاربة في جميع المناطق المنتخبة في الدراسة اما بالنسبة لأكثر منطقة تلوثا ولجميع الاحياء المجهرية المدروسة هي لعينات منطقة البصرة القديمة كما لوحظ نمو بعض الأعفان في عينات منطقتي ابي الخصيب والبصرة القديمة إن تلوث الخبز بالاعفان والخمائر يحصل بعد لحظات من عملية الإنتاج, وخاصةً التلوث الحاصل نتيجة استخدام الآلات والمعدات التداول غير السليم وأن عدد الاعفان المسموح بتواجدها في الخبز اذ تتراوح اعدادها بين(10^{3} – 10) خلية \غم (Ambreen and Samina, 2009) في حين يجب أن لا يتجاوز عدد الخمائر والاعفان 100/غم (Viosencu and Misca, 2005). و يرجع سبب ذلك الى البيئة والمنطقة ومدى نظافتها وتوفر الظروف الصحية اثناء عمليات العجن والخبز والنشر بعد الخبز وقبل بيعها الى المستهلك وتركه معرض للهواء والاتربة والغبار والتي تزيد من الحمل الميكروبي كما موضح في الشكل (1).



شكل 1. الحمل المايكروبي لمنتج الخبز

- **B1**=خبز منطقة ابي الخصيب.
- **B2** =خبز منطقة البصرة القديمة.
- **B3** =خبزمنطقة الجزائر.
- **B4**= منطقة الكرمة.
- **B5**= منطقة العشار.

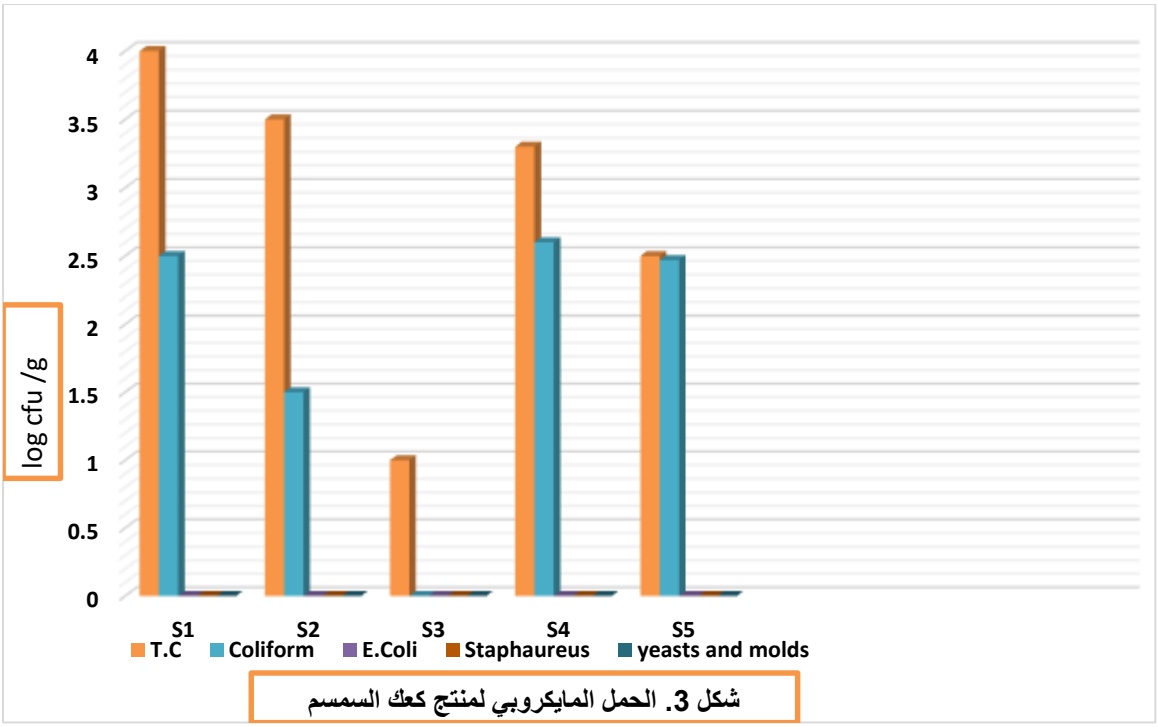
نلاحظ من شكل (2) بان هناك تباين معنوي للوغاريتم اعداد البكتريا الهوائية الكلية بلغت (3 و 1)cfu/g لكل من عينات الجرك وللمناطق ابي الخصيب والجزائر على التوالي بينما كانت الاعداد الكلية للبكتريا الهوائية الكلية متساوية للمناطق البصرة القديمة والكرمة والعشار اذ بلغت 2 cfu/g كما لم يلاحظ أي نمو ميكروبي لبكتريا القولون البرازية *E. coli* و*Staph aureus* و Yest and mold لجميع عينات الجرك وللمناطق اعلاه في حين وجد نمو لبكتريا القولون الكلية لمنطقتي ابي الخصيب والكرمة بمعدل1 cfu/g . وهذا يتفق مع مع ذكره De Vuyst,., & Kerrebroeck. (2021). أن الجرك هو منتوج مخبوز وعملية الشواء بحرارة الفرن تقتل اغلب أنواع الاحياء المجهرية الدقيقة الموجودة في العجينة وهذا يقلل من الحمل الميكروبي او ينعدم. لكن يمكن حصول التلوث للجرك بعد خروجها من الفرن لاحتوائها على مكونات النشا والبروتينات وهي وسط ملائم لنمو الاحياء المجهرية مجددا عند توفر الظروف الملائمة لنموها وخلال عمليات النقل والحفظ والتخزين للمنتوج.



شكل 2. الحمل المايكروبي لمنتج الجرك

- G1=جرك منطقة ابي الخصيب.
- G2=جرك منطقة البصرة القديمة.
- G3 =جرك منطقة الجزائر.
- G4 =جرك منطقة الكرمة.
- G5=جرك منطقة العشار.

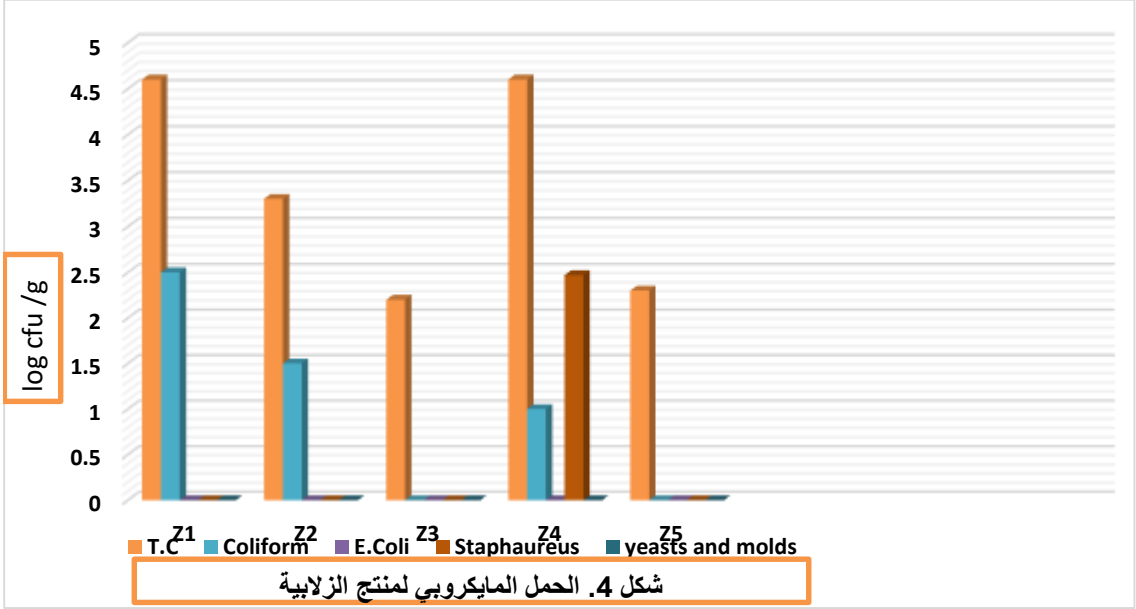
تبين نتائج شكل (3) الفروقات المعنوية بين المعاملات اذ إن منطقة البصرة القديمة هي اكثر المناطق تلوثا مقارنة مع المناطق الأخرى المنتخبة في الدراسة ولجميع الفحوصات الميكروبية التي أجريت في التجربة بينما كانت منطقة الجزائر هي الاقل تلوثا اما مناطق العشار وابي الخصيب والكرمة كانت تتراوح بين هاتين المنطقتين من خلال التلوث الميكروبي لعينات كعك بالسمسم (للبكتريا الهوائية الكلية وبكتريا القولون الكلية وبكتريا القولون البرازية والمكورات العنقودية الذهبية والخمائر والاعفان) على التوالي. اذ لوحظ ان لوغاريتم اعداد للبكتريا الهوائية الكلية لمنتج كعك بالسمسم بلغ (4 و3.5) cfu/g لمنطقتي ابي الخصيب والبصرة القديمة على التوالي في حين كان لوغاريتم اعداد بكتريا القولون الكلية متقاربه الى حد ما مقارنة مع المناطق ابي الخصيب والبصرة القديمة والكرمة والعشار كما لم يلاحظ اي نمو لهذه البكتريا في منطقة الجزائر للبكتريا أعلاه اما بالنسبة لبكتريا المكورات العنقودية الذهبية *staph aurous* لم يلاحظ أي نمو لها ولجميع المناطق لمنتج كعك بالسمسم وكذلك ا بالنسبة لبكتريا *E. coli* لجميع المناطق المنتخبة بالدراسة بينما في دراسة قام بها باحثون في بنغلادش Al-Fuad *et a.*(2018) قارنوا بين المخبوزات والكعك المصنع في المخابز المحلية مع المصنعة في المصانع اذ وجدوا ان نسبة التلوث في المخبوزات ذات العلامة التجارية بلغت 44.6% في حين كانت نسبة التلوث 49.4% في المخبوزات التي تباع في الاكشاك والباعة المتجولين.



شكل 3. الحمل المايكروبي لمنتج كعك السمسم

- S1=كعك بالسمسم لمنطقة ابي الخصيب.
- S2= كعك بالسمسم لمنطقة البصرة القديمة.
- S3 = كعك بالسمسم لمنطقة الجزائر.
- S4 = كعك بالسمسم لمنطقة الكرمة.
- S5= كعك بالسمسم لمنطقة العشار.

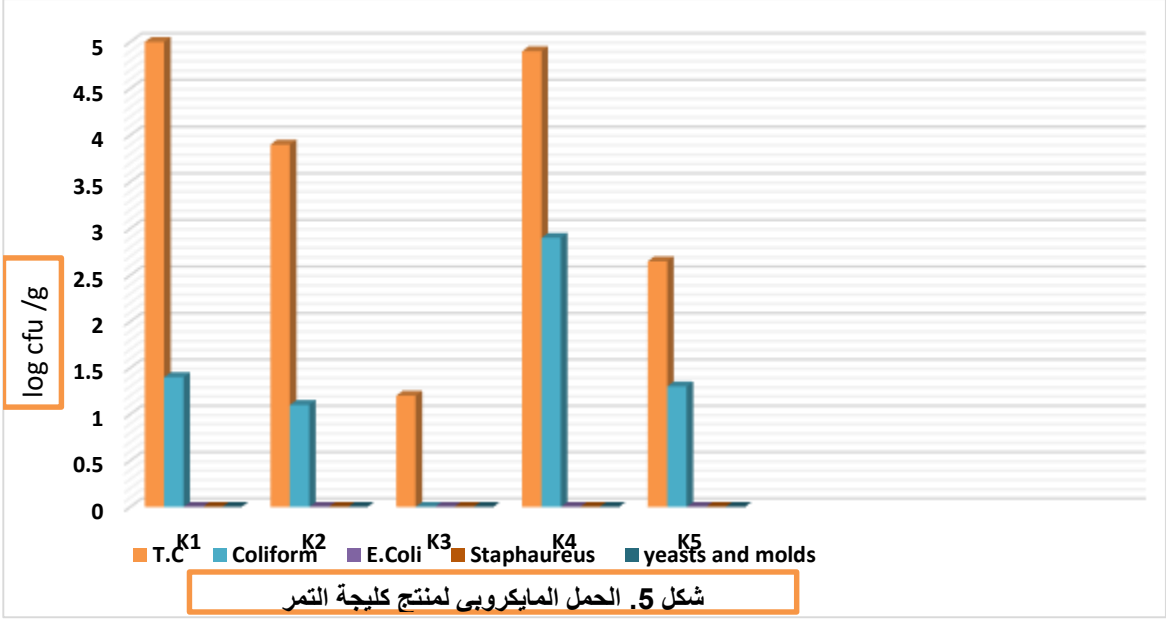
أظهر شكل(4) ان متوسط لوغاريتم اعداد البكتريا الهوائية بلغت (4.6) cfu/g لمنطقتي ابي الخصيب والكرمة على التوالي في حين بلغ متوسط لوغاريتم اعداد هذه البكتريا بلغت 3.3 و2.3 cfu/g للمناطق البصرة القديمة والعشار على التوالي اما منطقة الجزائر بلغت أدني متوسط للوغاريتم اعداد البكتريا الهوائية الكلية لمنتج الزلابية. بينما ظهر تواجد لبكتريا *staph aurous* في منطقة الكرمة اذ بلغ (2.47) cfu/g ولم يلاحظ اي نمولها في المناطق الأخرى المنتخبة بالدراسة اما بالنسبة لبكتريا القولون البرازيه لم يشاهد اي نمو لجميع المناطق المنتخبة في الدراسة كما اشارت النتائج الى ان بكتريا القولون الكلية كانت (2.5و1.5و1) للمناطق ابي الخصيب والبصرة القديمة والكرمة على التوالي في حين لم يظهر أي نمو لها في بقية المناطق أعلاه وأشار الباحثان في دراسة لهما Pundir and Jain.(2011) الى ان البكتريا كالمكورات العنقودية الذهبية وبكتريا القولون الكلية والبرازية والفطريات والاحياء المجهرية اغلبها تنمو على سطح الأغذية المختلفة كالكعك وتسبب في بعض الأحيان تلفها وفسادها عند تواجدها بأعداد كبير اذ تعمل على افراز انزيمات تستطيع ان تحطم بنية الجزيئات المعقدة للأغذية خلال توفر ظروف ملائمة من الحموضة والرطوبة وغيرها من العوامل.



شكل 4. الحمل المايكروبي لمنتج الزلابية

- Z1=زلابية لمنطقة ابي الخصيب.
- Z2=زلابية لمنطقة البصرة القديمة.
- Z3 =زلابية لمنطقة الجزائر.
- Z4 =زلابية لمنطقة الكرمة.
- Z5=زلابية لمنطقة العشار.

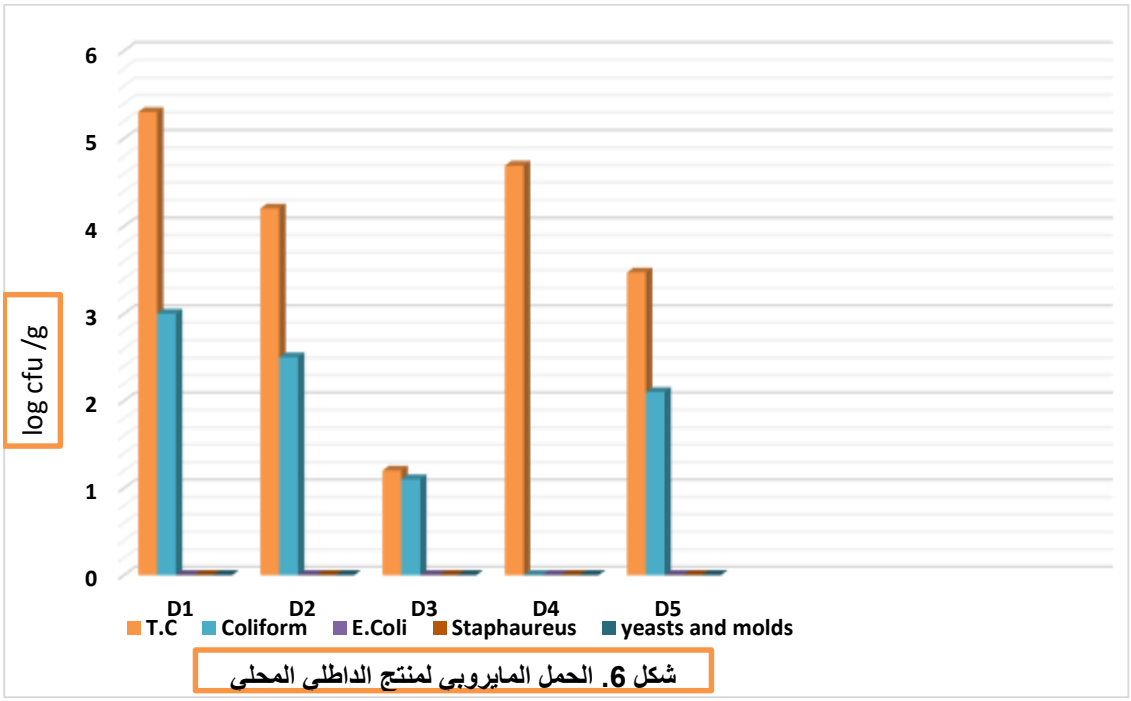
لوحظ في الشكل (5) بان اكثر المناطق تلوثا بالأحياء المجهرية هي ابي الخصيب والكرمة مقارنة مع باقي المناطق المنتخبة بالدراسة بينما أظهرت الدراسة ان منطقة الجزائر هي الأدنى تلوثا ولجميع الفحوصات الميكروبية لمنتج كليجة التمر مقارنة مع بقية المناطق اذ بلغ اعلى متوسط للوغاريتم اعداد البكتريا الهوائية الكلية (5 و 4.9) cfu/g لمنطقة ابي الخصيب والكرمة في حين بلغ ادنى متوسط للوغاريتم اعداد البكتريا الهوائية الكلية 1.2cfu/g لمنطقة الجزائر اما مناطق العشار والبصرة القديمة تراوحت بين (2.65 و3.9) cfu/g على التوالي بينما لوحظ اعلى تواجد بكتريا القولون الكلية Coliform لمنطقه االكرمة والتي بلغت (2.9) cfu/g بينما لم يلاحظ أي نمو للبكتريا في منطقة الجزائر لمنتج كليجة التمر. اما بالنسبة لبكتريا القولون البرازية لم يلاحظ اي نمو لها ولجميع المناطق المنتخبة في الدراسة وكذلك الحال بالنسبة لبكتريا *staph aureus* والخمائر والاعفان وهذا يتفق مع نتائج Al-Fuad *et al.*(2018) الذين وجدوا ان اعداد الاحياء المجهرية في المنتجات المحلية الصنع اعلى من نظيراتها المصنعة في المعامل والمصانع ذات العلامات التجارية معروفة وهذا في منتوجات الكعك والكيك.



شكل 5. الحمل المايكروبي لمنتج كليجة التمر

- K1=كليجة تمر منطقة ابي الخصيب.
- K2=كليجة تمر منطقة البصرة القديمة.
- K3 =كليجة تمر منطقة الجزائر.
- K4 =كليجة تمر منطقة الكرمة.
- K5=كليجة تمر منطقة العشار.

يلاحظ من النتائج المستحصل عليها في شكل (6) ان أعلى متوسطات للوغاريتم اعداد البكتريا الهوائية بلغ (5.3) cfu/g لمنطقه اابي الخصيب لمنتج الداطلي بينما كانت أدنى متوسطات للوغاريتم اعداد البكتيريا الهوائية الكلية لمنطقة الجزائر والتي كانت (1.2) cfu/g اما بالنسبة لمتوسطات إعداد بكتريا Coliform بلغت 3.60 cfu/g لمنطقة الكرمة بينما أظهرت الجزائر ادنى معدلات لنمو هذه البكتريا اذ بلغت 1.1 cfu/g في حين لم يلاحظ نمو لبكتريا *E. coli*و*staph aureus* والخمائر والاعفان لجميع المناطق المنتخبة في الدراسة الحالية وان هذه النتائج الحالية تتفق مع ما توصل اليه الباحثين Kabiru and Madaki.(2017) اللذان لاحظا نمو بعض أنواع بكتريا القولون الكلية والبرازية والمكورات العنقودية وبعض الفطريات ويعزى السبب في ذلك الى تلوث المواد الخام الداخلة في تصنيع الحلويات او احتواء الحلويات على نسب من السكر وهذه الظروف تناسب نمو الفطريات .



شكل 6. الحمل المايروبي لمنتج الداطلي المحلي

- **D1**=الداطلي المحلي لمنطقة ابي الخصيب.
- **D2**= الداطلي المحلي لمنطقة البصرة القديمة.
- **D3** = الداطلي المحلي لمنطقة الجزائر.
- **D4** = الداطلي المحلي لمنطقة الكرمة.
- D5= الداطلي المحلي لمنطقة العشار.

الاستنتاجات

نستنتج من الدراسة الحالية ان الخبز يكون اكثر تلوث من الجرك وذلك بسب بطرق التعامل مع المنتجات اذ ينشر الخبز على اسطح غير نظيفة وغير معقمة مما يؤدي الى تعرضه للتلوث بالبكتريا والأعفان. بينما الجرك يدخل بافران نظيفة ومعقمة وعدم نشره على اسطح غير معقمة بل يتم وضعه في اكياس معقمة نظيفة وكذلك الأدوات المستعلمة في التصنيع نظيفة ومعقمة كما ان المخابز تختلف باتباعها الشروط الصحية حسب البيئة والمحيط الذي ينشا فيه المخبز.

أما بالنسبة للمنتجات المنتخبة وهي (كعك السمسم والزلابية وكليجة التمر والداطلي) اظهرت تلوثا واضحا وعاليا في مناطق ابي الخصيب والكرمة والبصرة القديمة بينما أعطت نتائج اقل تلوثا ولجميع العينات المنتخبة لمنطقة الجزائر أما منطقة العشار أظهرت تلوثا بشكل اقل من بقية المناطق لمنتجات كعك السمسم والزلابية وكليجة التمر والداطلي وممكن ان يعود سبب ذلك الى النظافة في المحلات وهذه تعود الى المنطقة نفسها ونظافة العمال والأدوات والمستخدمة في العرض وغيرها من العوامل الصحية التي يجب اتباعها وتوفيرها في محلات بيع المنتجات الغذائية المستهلكة من قبل الفرد لغرض الحفاظ على صحته وسلامته وتم اختيار هذه المناطق لكونها مناطق تجارية مهمة بالإضافة الى كثرة تسوق السكان منها.

References

1. صالح،احمد عماد والعبد الله،بيان ياسين والنزال، احمد إسماعيل.(2014).دراسة صفات الخبز والنوعية الميكروبية للطحين والخبز المنتج في قضاء تكريت.مجلة جامعة تكريت للعلوم الزراعية المجلد 14،العدد2.

2. Al-Fuad, M. S., Shamimuzzaman, M., Ahmed, R., Ahmmed, H. R., Hasan, M. T., & Roy, R. K. (2018). Packaging and microbial status of local and branded bakery products: a comparative study on Jessore region, Bangladesh. Frontiers in Environmental Microbiology, 4(4), 103-109. doi: 10.11648/j.fem.20180404.12
3. Alpers, T., Kerpes, R., Frioli, M., Nobis, A., Hoi, K. I., Bach, A.,... & Becker, T. (2021). Impact of Storing Condition on Staling and Microbial Spoilage Behavior of Bread and Their Contribution to Prevent Food Waste. Foods, 10(1),.67
4. Al-Tulaihan, A. A., H. Najib and S. M. Al-eid. (2004). The nutritional evaluation of locally produced dried bakery waste (DBW) in the broiler diets. Pakistan Journal of Nutrition, 3, 294-299.
5. Ambreen,A and Samina,K (2009). Microbiological status of bakery products available in Islamabad.Pakistan. j.Agric.Res, 22:93-96.
6. Coelho, A. Í. M., Milagres, R. C. R. M., Martins, J. D. F. L., Azeredo, R. M. C. D., & Santana, Â. M. C. (2010). Contaminação microbiológica de ambientes e de superfícies em restaurantes comerciais. Ciência & Saúde Coletiva, 15, 1597-1606.
7. De Vuyst, L., Comasio, A., & Kerrebroeck, S. V. (2021). Sourdough production: fermentation strategies, microbial ecology, and use of non-flour ingredients. Critical Reviews in Food Science and Nutrition, 1-33.
8. Demissie, S., & Natea, G. (2017). Microbial Quality and Safety of Bread Sold in Cafeteria, Tea and Bread Shop of Jimma Town, Oromia Regional State, Southwest Ethiopia. J Food Ind Microbiol, 3(122), 2.
9. Fung, F., Wang, H. S., & Menon, S. (2018). Food safety in the 21st century. Biomedical journal, 41(2), 88-95..
10. Garcia, M.V.; Bernardi, A.O.; Copetti, M.V.(2019). The fungal problem in bread production: Insights of causes, consequences, and control methods. Curr. Opin. Food Sci. 29:(1–6).
11. Kabiru, M. R., & Madaki, H. M. (2017). Assessment of the microbiological quality of some locally made candies sold at some primary schools at Sharada. Bayero Journal of Pure and Applied Sciences, 10(1), 285-289.
12. Khanom, A., Shammi, T., & Kabir, M. S. (2016). Determination of microbiological quality of packed and unpacked bread. Stamford Journal of Microbiology, 6(1), 24-29.
13. Kornacki, J. L and Johnson, J. L. (2001). Enterobacteriaceae, coliforms and Escherichia coli as quality and safety indicators. Compendium of methods for the microbilogical examination of foods, 69-82.

14. Kornacki, J. L and Johnson, J. L. (2001). Enterobacteriaceae, coliforms and Escherichia coli as quality and safety indicators. Compendium of methods for the microbilogical examination of foods, 69-82.
15. Olulade, B.A., Adeola, A.A and Anuoluwapo, A.O.(2013). Microbial profile of maize-pigeon pea biscuit in storage. Fountain journal of natural and applied sciences 2(2): 1-.9
16. Oluwajoba, S.O., Malomo, O., Ogunmoyela, O.B., Dudu, O.E.O and Odeyemi, A.(2012). Microbiological and nutritional quality of warankashi enriched bread. Journal of microbiology, Biotechnology and food Sciences 2(1): 42-.86.
17. Pundir, R. K., & Jain, P. (2011). Qualitative and quantitative analysis of microflora of Indian bakery products. Journal of Agricultural Technology, 7(3), 751-762.
18. Ravimannan, N. (2016). Study on microbial profile of bread during storage. International Journal of Advanced Research in Biological Sciences, 3, 60-.36
19. Saranraj, P. and M. Geetha.) 2012(. Microbial spoilage of bakery products and its control by preservatives. International Journal of Pharmaceutical and Biological Archives, 3: 38–48.
20. Tang, X., Shen, C., Shi, D., Cheema, S.A., Khan, M.I., Zhang, C. and Chen, Y. (2010). Heavy metal and persistent organic compound contamination in soil from Wenling: An emerging waste recycling city in Taizhou area. China. J Hazard Mater.)173(: 60-653.
21. Valero, A., Rodríguez, M. Y., Posada-Izquierdo, G. D., Pérez-Rodríguez, F., Carrasco, E., & García-Gimeno, R. M. (2016). Risk factors influencing microbial contamination in food service centers. Significance, Prevention and Control of Food Related Diseases, 27-58.
22. Viosencu, D. and Misca, C. (2005). The microbiological parameters in technological process of bread production. Agroalimentary processes and technologies, XI (2):475-480.
23. World Health Organization) WHO(. (2015). estimates of the global burden of foodborne diseases: foodborne disease burden epidemiology reference group 2007-2015. World
24. XLSTAT. (2004). Addinsoft. Pro version 7.5.3 http: //WWW. Xlstat.com/en/ho.

النشاط المضاد للأكسدة لبروتينات الشرش المعزولة من حليب الجمل المتحللة انزيميا واستعمالها في إطالة العمر الخزني للزيوت

Antioxidant Activity of Whey Proteins Isolated from Enzymatically Hydrolyzed Camel's Milk and Their Using in Extending the Shelf Life of Oils

Orass T. AL-Ibresam [1], Rawdah M. AL-Ali [2], Sawsan A. AL-Hilifi [3]

© 2023 The Author(s). This open access article is distributed under a Creative CommonsAttribution (CC-BY) 4.0 license.

Abstract: Camel milk is an important source of nutrients such as proteins and vitamins, including whey proteins, which make inhibition of oil oxidation and microbial growth. The proteolytic have high antioxidant activity due to their amino acid content. The antioxidant properties of camel milk are also attributed to the structural composition of whey proteins upon hydrolysis and their content of bioactive peptides that have antioxidant activities. According to the study, the decomposers showed a high activity in their ability to capture the DPPH radical and bind the ferric ion amounted to 53.19% and 62.88%, respectively, at a concentration of 20 mg/ml, in addition to having a high reducing capacity of 77.199% at the same concentration, and their amino acid content was estimated. The hydrolysates' contribution for enhancing the storage capacity of the oils was studied by decreasing the peroxide number values of sesame seed oil stored at laboratory temperature for 60 days.

Key Words: Camel whey; Proteolytic; Antioxidant; Sesam seeds oil.

الكلمات المفتاحية: شرش حليب الجمل; المتحللات البروتينية; الفعالية المضادة للأكسدة;زيت بذور السمسم.

Author details

[1- 2 - 3] Department of Food Science, College of Agriculture, University of Basra, Basra, Iraq

Citation information

Cite this article as:

Al-Ibresam, O.T., Al-Ali, R.M., Al-Hilifi, S.A., (July 2023), *Antioxidant Activity of Whey Proteins Isolated from Enzymatically Hydrolyzed Camel's Milk and Their Using in Extending the Shelf Life of Oils*, Proceedings of the Minar Congress, Turkey, (9) pp 359-373, DOI: http://dx.doi.org/10.47832/MinarCong9-30

http://dx.doi.org/10.47832/MinarCong9-30

1 orass.yasseen@uobasrah.edu.iq

2 rawdah.ali@uobasrah.edu.iq

3 sawsan.hameed@uobasrah.edu.iq

الخلاصة

حليب الجمل هو مصدر غني للفيتامينات والبروتينات ومنها بروتينات الشرش التي تلعب دوراً مهما في تعزيز العديد من الوظائف الفسيولوجية منها مضادات أكسدة ومضادات ميكروبية وغيرها، يهدف البحث إلى تحضير متحللات شرش حليب الجمل باستعمال أنزيم التربسين لمدة 4 ساعات واختبار فعاليتها المضادة للأكسدة، واظهرت المتحللات البروتينية نشاط مضادا للأكسدة عاليا بفعل محتواها من الأحماض الأمينية ، إذ تُعزى الخصائص المضادة للأكسدة في حليب الجمل أيضًا إلى التكوين الهيكلي لبروتينات الشرش عند التحلل المائي ومحتواها من الببتيدات النشطة بيولوجيًا التي لها أنشطة مضادة للأكسدة. أظهرت المتحللات وفقا للبحث نشاطا عاليا في قابليتها على اقتناص جذر DPPH وربط أيون الحديديوز بلغت 53.19% و69.17% على التوالي عند التركيز 20 ملغم\مل إضافة إلى امتلاكها سعة اختزالية عالية بلغت 77.19% عند التركيز ذاته، كما تم تقدير محتواها من الأحماض الأمينية ومساهمتها في تعزيز القابلية الخزنية للزيوت من خلال خفضها قيم رقم البيروكسيد وقيم حامض الثايوباربيوتريك TBA لزيت بذور السمسم المخزن على درجة حرارة المختبر لمدة 60 يوماً.

المقدمة

تحدث عملية الأكسدة نتيجة التمثيل الغذائي التأكسدي في الجسم وهي تساهم في التقليل من قبول المستهلك للأغذية إذ أنها تعمل على إنتاج مركبات منخفضة الوزن الجزيئي ذات نكهة غير مقبولة فضلا عن كونها سامة و مضرة لصحة الأنسان تتمثل بالجذور الحرة التي تتحرر كنواتج أيضية عرضية إذ تعمل الأكسدة على تحطيم العناصر الغذائية الأساسية كالبروتينات و الحامض النووي (DNA) والدهون، تحدث الأكسدة عن طريق إضافة الأوكسجين أو سحب الهيدروجين أو الكترون بوجود الأنزيمات وعوامل مساعدة أخرى كالحرارة والمعادن والأوكسجين، دعت الحاجة إلى التقليل من الأكسدة وتثبيطها عن طريق إزالة المؤكسدات وكبح الجذور الحرة وتقييد المعادن من خلال إضافة مركبات كيميائية فعالة بتراكيز منخفضة غير سامة ومستقرة و قليلة الكلفة تدعى بمضادات الأكسدة الصناعية (Choe and Min, 2009;Parkin and Damordaran, 2003).

من المعروف إن بيروكسيدات الدهون يمكن أن تسبب تدهورا في الصفات النوعية و التغذوية للغذاء وتقصير عمره الخزني من خلال توليد الجذور الحرة التي تؤدي إلى أكسدة وتحلل الأحماض الدهنية التي تسبب بدورها الضرر الصحي المتمثل بأمراض الكبد والسرطان والشيخوخة. استعملت مضادات الأكسدة الصناعية مثل BHT و BHA على نطاق واسع في الأغذية لفعاليتها العالية للحد من الأكسدة و تلف الأغذية و إطالة العمر الخزني للدهون إلا إن المخاوف بشأن الأثار الصحية التي تترتب على استعمال مضادات الأكسدة الصناعية لذلك كان الاتجاه نحو مضادات الأكسدة الطبيعية التي يتم تحضيرها من مصادر حيوانية أو نباتية لها القدرة على تثبيط تطور الاكسدة (Peng *et al.*, 2010). أثبتت الدراسات إن المتحللات البروتينية تعمل بشكل فعال كمضادات أكسدة طبيعية تعمل على كبح الجذور الحرة و تثبيط بيروكسيد الدهون لاحتوائها على الببتيدات الفعالة حيويا ذات الخصائص المضادة للأكسدة حيث تمتلك فعالية عالية على كبح جذور الأوكسجين التفاعلية ROS وتكبيل أيونات المعادن المؤكسدة وتدعيم النظام الانزيمي المضاد للأكسدة داخل الجسم (Manzanares *et al.*,2019 ;Al-Shamsi *et al.*, 2018).

يمتلك حليب الجمل خصائص مختلفة عن الحليب البقري من حيث تركيبه الكيميائي ومحتواه البروتيني، تمتاز بروتينات شرش حليب الجمل بجودتها من حيث النسب العالية لبروتينات الالفاالبومين واللاكتوفيرين والاكتوفورين والكلوبيولينات المناعية مقارنة بشرش حليب الأبقار. تعد بروتينات شرش حليب الجمل مصدرا مهما للحصول على المتحللات البروتينية التي تعد مدعمات غذائية مهمة في الأغذية الوظيفية (Al-Shamsi *et al.*, 2018).

شهد العقد الماضي اهتماما متزايدا بالأغذية الوظيفية التي تعمل على تعزيز الصحة والوقاية من الأمراض، وتعد الببتيدات الفعالة حيويا المحضرة من متحللات بروتينات شرش حليب الجمل محور اهتمام الباحثين لامتلاكها خصائص مضادة للأكسدة وللميكروبات والسرطان وارتفاع ضغط الدم والسكري وقدرتها على ربط المعادن وتدعيم المناعة (Kamal *et al.*, 2018). هدفت الدراسة إلى تحضير متحللات بروتينية ذات خصائص فعالة حيويا واستعمالها مضادات أكسدة طبيعية بديلة للصناعية لتثبيط بيروكسيد الدهون وإطالة المدى الخزني لها.

طرائق العمل

تم جمع حليب الجمل ذات السنام الواحد من مزرعة جمال محلية في محافظة الانبار غرب العراق تم استعمال إنزيم Trypsin E.C 3.4.21.4 المحضر من شركة Aldrich-Sigma بكفاءة محددة ≥ 250 وحدة / جم.

إنتاج شرش الحليب بالطريقة الحامضية

اتبعت الطريقة المذكورة من قبل Al-Hatim *et al.* (2020) مع بعض التحوير حيث تمت معاملة الحليب حراريا على درجة حرارة 63 م لمدة نصف ساعة بعدها خفضت درجة الحرارة الى 40م، فصل الدهن باستعمال جهاز الفراز، اضيف 10 مل من محلول حامض الستريك 65% لكل 1 لتر من الحليب مع التحريك لمدة 2 دقيقة و بعد مرور 45 دقيقة قطعت الخثرة وجمع الشرش الناضح ليتم تركيزه باستعمال الجهاز المبخر الدوار Rotary Evaporator من نوع Frankin electric, England على درجة 40م ثم تجفيده بجهاز التجفيد Freeze-drying من نوع (Germany, Christ).

تحضير المتحللات البروتينية

استعمل أنزيم Trypsin لتحضير المتحلل البروتيني باتباع الطريقة الموصوفة من قبل Wali *et al.* (2019) حضر المحلول البروتيني بنسبة 10:5 (وزن\ حجم) بالماء المقطر بعدها تم أجريت المعاملة الحرارية للمحلول على درجة حرارة 80م لمدة 2 دقيقة ثم تبريد المحلول إلى درجة حرارة 25م ، أضيف الأنزيم بنسبة 1% من وزن العينة بعد ضبط الظروف المثلى الخاصة بالأنزيم المتمثلة بالرقم الهيدروجيني باستعمال محلول حامض الهيدروكلوريك (1M) ومحلول هيدروكسيد الصوديوم (1M) و ضبط درجة الحرارة على 37م باستعمال حمام مائي هزاز من نوع (Germany GFL) استمر التحلل لمدة 4 ساعات و ثبط عمل الأنزيم بعد انتهاء مدة التحلل برفع درجة حرارة المتحلل إلى 90م لمدة 5 دقائق و بعدها إضافة محلول ثلاثي كلورو حامض الخليك Trichloroacetic acid (TCA) (12%) ثم اجري الطرد المركزي (5000 g) ليتم جمع الراشح وتجفيده.

تقدير درجــة التحــلل

اتبعت الطريقة حسب Hoyle and Merrit (1994) و الموصوفة في Da Silva *et al.* (2018) لتقدير درجة التحلل بواسطة حساب النسبة المئوية للنتروجين الذائب في12% من TCA والنسبة المئوية للنتروجين الكلي في عينة المركز البروتيني المجفد الخام وحسب المعادلة التالية:

$$\text{درجة التحلل\%} = \frac{\text{النتروجين الذائب في 12\% TCA}}{\text{النتروجين الكلي في العينة}} \times 100$$

تقدير الأحماض الأمينية

قدرت الأحماض الأمينية في المتحللات البروتينية لشرش حليب الجمل حسب الطريقة الموصوفة من قبل Al-Hilifi *et al.* (2023) باستعمال جهاز Amino acids analyzer حيث مزج 10-20 ملغم من المتحللات المجفدة مع محلول حامض الهيدروكلوريك(*6N*) في أنبوبة مفرغة من الهواء و على درجة حرارة 110°م لمدة 24 ساعة، وضع

المزيج في جهاز الطرد المركزي 4000 g لمدة 10 دقائق، بعدها حضر مزيج من 250 مايكروليتر من الراشح المفصول مع محلول بيكربونات الصوديوم الهيدروجينية ليوضع في حمام ثلجي لمدة 15 دقيقة ثم حضر مزيج مكون من 375 ميكروليتر من الراشح المفصول و محلول منظم سترات الليثيوم 12.0 N و رقم هيدروجيني 2.90 ، استعمل عمود S4300 و بطولين موجيين 570،440 نانوميتر. اتبعت الطريقة الموصوفة من قبل شركة SW analyzer amino acids Clarity.

الفعالية المضادة للاكسدة

اقتناص جذر Diphenyl-2picrylhdrayzl 1,1 (DPPH) :

اجري اختبار اقتناص جذر Diphenyl-2picrylhdrazyl 1,1 (DPPH) للعينات المحضرة وفق طريقة (2015) Shah and Modi اضيف 0.5 مل من محلول DPPH (0.1 Mm) لكل 1مل من كل تركيز عينات المتحللات البروتينية المحضرة بتراكيز 5-25 ملغم\مل حضن المزيج في الظلام لمدة 30 دقيقة في حرارة المختبر، إضافة الى العينة الضابطة المحضرة بمزج ما ذكر أعلاه عدا العينة المستبدلة بالماء المقطر. قيست الامتصاصية على طول موجي 517 نانومتر. حسبت قابلية الاقتناص لعينة المقارنة Ascorbic acid بالطريقة نفسها، قدرت قابلية اقتناص جذر DPPH حسب المعادلة أدناه:

$$\text{قابلية اقتناص DPPH \%} = \frac{\text{امتصاصية العينة الضابطة} - \text{امتصاصية العينة}}{\text{امتصاصية العينة الضابطة}} \times 100$$

قابلية ربط الحديدوز:

قدرت القابلية على ربط أيون الحديدوز حسب الطريقة الواردة في Hussein *et al.* (2020) حضرت العينات بتراكيز 5-25ملغم /مل وأضيف 0.4 مل من محلول 8-hydroxy quinolone (5 Mm) لكل تركيز من العينات إضافة الى العينة الضابطة المحضرة بخلط كل ما مذكور أعلاه ماعدا العينة التي استبدلت بالماء المقطر، حضنت العينات في الظلام بدرجة حرارة الغرفة لمدة 10 دقائق. قدرت قابلية الربط لعينة المقارنة

Ethylene diamine tetra acetic acid disodium (EDTA-Na_2) بالطريقة نفسها، قيست الامتصاصية على طول موجي 562نانومتر، حسبت قابلية الربط بالمعادلة التالية:

$$\text{قابلية ربط أيون الحديدوز \%} = \frac{\text{امتصاصية العينة الضابطة} - \text{امتصاصية العينة}}{\text{امتصاصية العينة الضابطة}} \times 100$$

القوة الاختزالية:

اجري اختبار تقدير القوة الاختزالية تبعا لطريقة Devi *et al.* (2017) استعملت التراكيز (5-25) ملغم/مل للعينات المدروسة و لعينة المقارنة BHT ، مزج 1مل لكل تركيز من العينات المدروسة مع 2.5 مل من محلول منظم الفوسفات المحضر 0.2M و رقم هيدروجيني 6.6 و2.5 مل من محلول Potassiom ferricyanide 1% حضن المزيج عند درجة حرارة 50°م لمدة 20 دقيقة، ثم اضيف محلول TCA 1% ثم اجري الطرد المركزي بسرعة 3000

g لمدة 10 دقائق لفصل الطبقة العلوية للمحلول ثم اضيف 1مل من محلول FeCl3 0.1% و5 مل من الماء المقطر. حضرت العينة الضابطة بإضافة جميع المواد المذكورة اعلاه عدا العينة المستبدلة بالماء المقطر. قيست الامتصاصية على طول موجـي 700 نانومتر ثم حسبت نسبة القوة الاختزالية من خلال المعادلة التالية حسب ما مذكور من قبل Hemalatha *el al.*(2010):

$$\text{القوة الاختزالية\%} = 100 - [\frac{\text{قراءة امتصاصية العينة}}{\text{قراءة امتصاصية العينة الضابطة}}] \times 100$$

اختبار قابلية المتحلل البروتيني في حفظ زيت السمسم

تم دراسة قابلية المتحلل البروتيني في حفظ زيت السمسم من الأكسدة وإطالة عمره الخزني وذلك بإضافته بثلاث تركيز هي (0.10, 0.15, 0.25%) ومقارنته مع مضاد الأكسدة الصناعي BHT 0.02% وعينة السيطرة . وحفظت المعاملات في عبوات شفافة بدرجة حرارة 40مْ ± 5 مْ ولمدة 60 يوم وتم متابعة تغيرات الأكسدة كل 15 يوم من خلال قياس قيمة البيروكسيد.

قيمة البيروكسيد Peroxide Value PV

تم تقدير قيمة رقم البيروكسيد حسب الطريقة الموصوفة AOAC(1980) للزيت المخزن على درجة حرارة 40 مْ ± 5مْ لمدة (0 ، 15 ،30، 45 ، 60) يوم.

اختبار حامض الثايوباربيوتريك Thiobarbituric Acid (TBA)

قدر حامض الثايوباربيوتريك حسب الطريقة الموصوفة في Mousavi et al.(2015) للزيت المخزن على درجة حرارة 40 مْ ± 5مْ لمدة (0 ، 15 ،30، 45 ، 60) يوم.

التحليل الاحصائي

تم استخدام التصميم العشوائي الكامل (C.R.D) ضمن البرنامج الإحصائي Genstat (2011) لإجراء التحليل الاحصائي واختبرت العوامل المدروسة بأقل استخدام فرق معنوي عند مستوى معنوي ≥ 0.05

النتائج والمناقشة

تقدير درجة التحلل

يظهر الجدول (1) تقدير درجة التحلل لمركز بروتينات شرش حليب الجمل المحضر باستعمال انزيم Trypsin حيث ازدادت درجة التحلل بزيادة زمن التحلل، اذ كانت درجة التحلل بعد مضي 30 دقيقة من زمن التحلل 13.65% ويلاحظ من النتائج ازدياد درجة التحلل تدريجيا لتصل اقصاها عند 240 دقيقة من زمن التحلل حيث سجلت 38.90 %. يمتاز أنزيم Trypsin بكسر الاصرة الببتيدية من النهاية الكاربوكسيلية الطرفية للاحماض الامينية اللايسين والارجنين ولهذا فهو يمتلك الية عمل تمكنه من تحرير سلاسل ببتيدية قصيرة ذات اوزان جزيئية منخفضة (lsen *et al.*, 2004).

جدول 1. درجة التحلل لمتحللات مركز بروتينات شرش حليب الجمل المحضرة بأنزيم Trypsin

درجة التحلل %	زمن التحلل (دقيقة)							
	30	60	90	120	150	180	220	240
	11.65	16.66	19.89	22.77	26.45	30.33	34.67	38.90

تقدير الأحماض الأمينية

يلاحظ من الجدول (1) محتوى متحللات الشرش من الأحماض الأمينية حيث بلغت نسبة الاحماض الامينية الأساسية 37.91% والاحماض الامينية الحلقية 9.11% والاحماض الامينية الكارهة للماء 41.10% وكان حامض البرولين هو السائد 10.21% قد يعود السبب في تباين نسب الاحماض الامينية الى ظروف التحلل ونوع الانزيم المستخدم في التحلل وخصوصية عمله التي تعد من اهم العوامل المؤثرة على التحلل، ان تأثير زمن التحلل قد يكون سبب الاختلاف في تركيزات الأحماض الأمينية يعتمد نوع الأحماض الأمينية وموضعها في سلسلة الببتيد على آلية عمل الانزيم. (Wali *et al.*, 2019; Neto et al., 2019; Al-Hilifi et al., 2023)

جدول (1): الاحماض الامينية لمتحللات شرش حليب الجمل.

Molar percentage%	Amino acids
8.67	Arginine
7.70	Lysine
6.77	Alanine
4.61	Phenylalanine
10.21	Proline
4.48	Threonine
5.04	Leucine
4.30	Methionine
4.12	Glutamic acid
6.32	Serine
8.91	Histidine
7.06	Glycine
4.50	Tyrosine
3.11	Valine

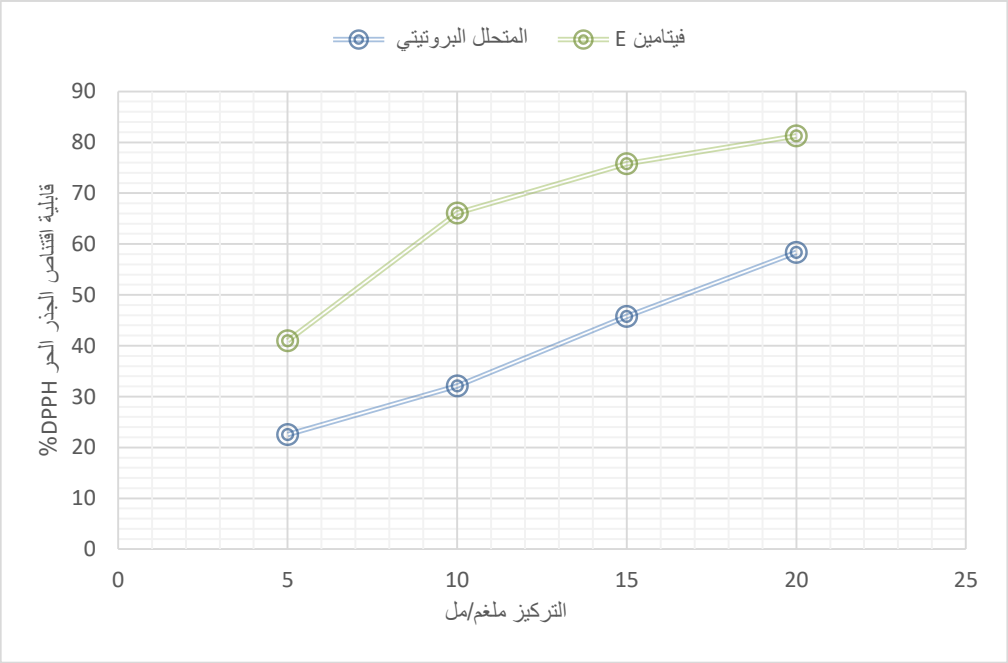
الفعالية المضادة للاكسدة

قابلية اقتناص جذر 1,1 Diphenyl-2picrylhdrayzl (DPPH)

يشير الشكل(1) إلى قابلية المتحللات البروتينية على اقتناص جذر DPPH مقارنة مع عينة المقارنة فيتامين E عند التراكيز 5-20 ملغم / مل، يتضح من النتائج ان زيادة التركيز اثرت معنويا ($P \geq 0.05$) على قابلية الاقتناص، حيث أبدت المتحللات اعلى قابلية اقتناص عند التركيز 20ملغم / مل بلغت 53.19% بينما سجل التركيز 5ملغم /مل اقل قابلية اقتناص بلغت 22.51% مقارنة بعينة المقارنة فيتامين E التي تفوقت في قابليتها على الاقتناص عند جميع

التراكيز. ويعزى ذلك إلى النسبة العالية من الأحماض الأمينية الحلقية مثل الفنيل الالنين والتايروسين المانحة للإلكترون بسبب وجود مجموعة الفينول ذات القدرة على التفاعل مع الاوكسجين وتكوين جذور (Hernández- phenoxyl Ledesma *et al.*, 2005) فضلا عن وجود الاحماض الامينية الكلايسين والكلوتاميك والهستدين الذي يمتاز بامتلاكه مجموعة الاميدازول المانحة للهيدروجين كما يعمل الحامض الأميني الميثيونين على تكوين sulfoxides من خلال تأكسد مجموعة الكبريت بدلا من الجزيئات الحيوية مما يعزز من قابلية المتحللات على اقتناص الجذور الحرة و كبح الأكسدة (Chen and Li, 2012; Qian *et al.*,2008)

أشار (Lin *et al.*, 2012) الى ان نوع الانزيم يؤثر في تحديد النشاط المضاد للاكسدة للمتحللات البروتينية من حيث نوع الاحماض الامينية وموقعها في السلسلة الببتيدية ، ان موقع الاحماض الامينية الكارهة للماء في النهايات الطرفية للسلسلة الببتيدية يعمل على تعزيز الفعالية المضادة للأكسدة. (Nwachukwu and Aluko 2018)

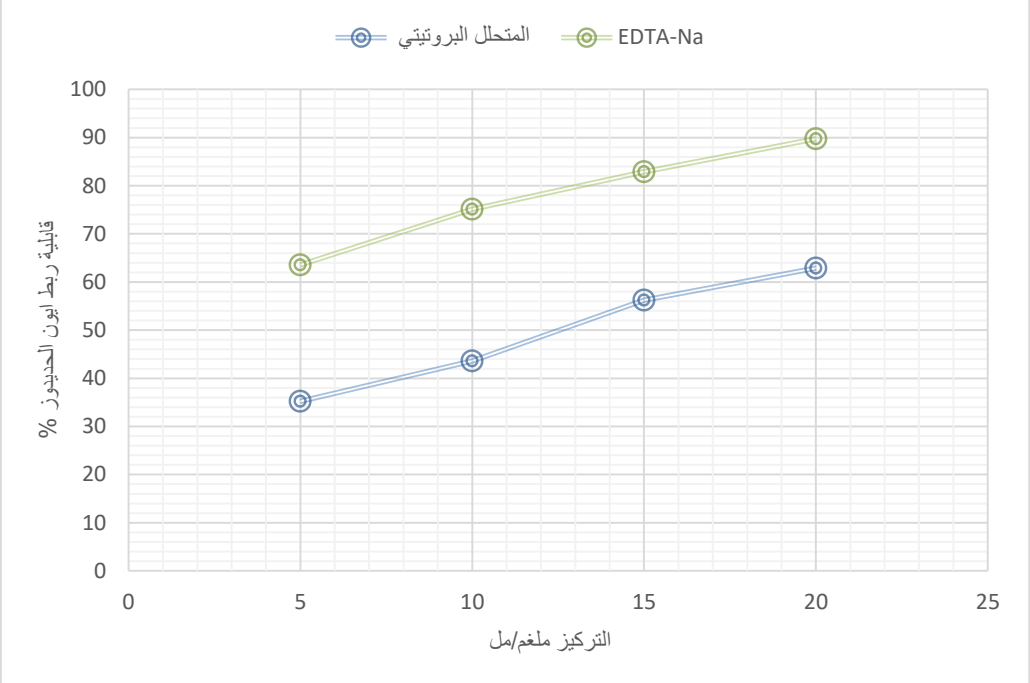


شكل 1. قابلية اقتناص جذر DPPH لمتحللات بروتينات شرش حليب الجمل

قابلية ربط ايون الحديدوز

يوضح الشكل(2) ان قابلية متحللات بروتينات الشرش على ربط ايون الحديدوز قد تأثرت معنويا ($P \geq 0.05$) بزيادة تركيزها بالمقارنة مع $EDTA\text{-}Na_2$ ، تشير النتائج الى ان قابلية الربط عند التركيز 5 ملغم \ مل قد بلغت 37.21% و ازدادت تدريجيا لتصل أقصاها عند التركيز20 ملغم \ مل حيث كانت 69.17% مقارنة بعينة المقارنة $EDTA\text{-}Na_2$ إذ بلغت قابلية الربط 97.31% عند نفس التركيز. ممكن ان يعود السبب في ذلك الى وجود الاحماض الامينية الحلقية كالفنيل النين و التايروسين إضافة الى الارجنين والهستدين و الليوسين التي تعمل على تنظيم العناصر

النزرة في الجسم كذلك وجود الاحماض الامينية الحامضية مثل الكلوتاميك التي تعزز من قابلية الربط بسبب وفرة مجاميع الكاربوكسيل فيها (O'Loughlin *et al.*,2015; Caetano-Silva *et al.*, 2015) .

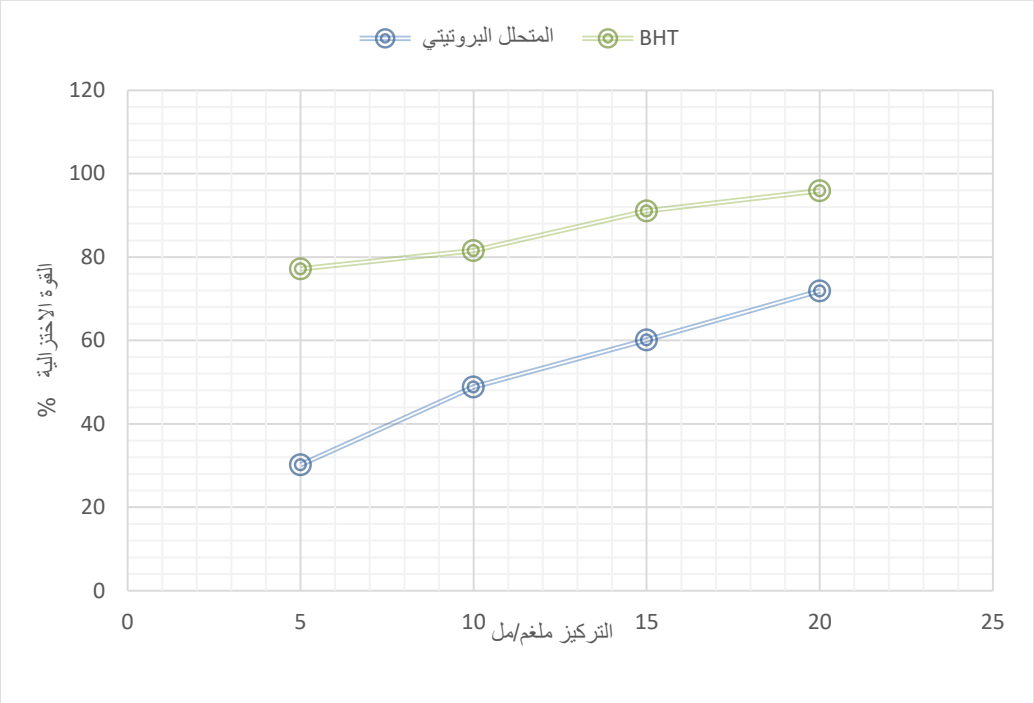


شكل 2. قابلية ربط ايون الحديدوز لمتحللات بروتينات شرش حليب الجمل

القوة الاختزالية

يوضح الشكل (3) القوة الاختزالية لعينات المتحللات المدروسة التي ازدادت بزيادة التركيز مقارنة مع عينة المقارنة BHT ، بينت النتائج ان قيم القوة الاختزالية قد تأثرت معنويا ($P \geq 0.05$) بزيادة التركيز اذ سجلت المتحللات اعلى قوة اختزالية عند اعلى تركيز 20 ملغم\مل اذ بلغت 77.19% بينما انخفضت بانخفاض التراكيز لتسجل اقل قيمة عند اقل تركيز 5 ملغم \ مل اذ بلغت 30.28%. في حين ان القوة الاختزالية لعينة المقارنة المضاف لها BHT عند التركيز 20 ملغم\ مل بلغت 96.72% ويعود سبب في ذلك الى امتلاك المتحللات نسب عالية من الاحماض الامينية ذات المقاومة العالية للاكسدة مثل الميثيونين والهستدين التي تمتلك مجاميع الاميدازول والكبريت المانحة للالكترون Da (silva *et al.*, 2018; Kerasioti *et al.*, 2014).

وقد أكد Bassan *et al.* (2015) على ان وجود نسب من الاحماض الامينية الميثونين البرولين والهستدين يساهم في رفع مستوى السعة الاختزالية للمتحللات البروتينية.

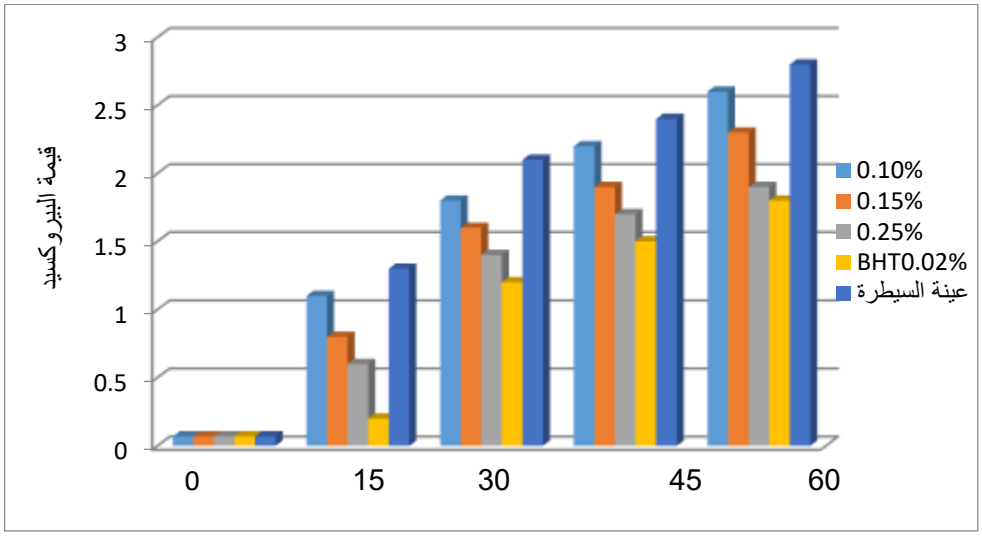


شكل 3. القوة الاختزالية لمتحللات بروتينات شرش حليب الجمل

اختبار قابلية المتحلل البروتيني في حفظ زيت السمسم

تبين الشكل (4) قيم البيروكسيد لعينات الزيت المضاف لها المتحلل البروتيني المحضر من مركز بروتين شرش المخزن على درجة حرارة 40 مْ ± 5مْ لفترة 0 و15 و30 و45 و60 يوم, تظهر نتائج التحليل الإحصائي وجود فروقات معنوية ($P \geq 0.05$) في قيم البيروكسيد لزيت السمسم مع زيادة تركيز المتحلل البروتيني ومدة الخزن اذا اظهر تركيز 0.25% اعلى قابلية لإعاقة أكسدة زيت السمسم بالمقارنة مع باقي المعاملات اذ بلغت قيمة رقم البيروكسيد 1.5 مليمكافىء\ كغم زيت بعد مضي 45 يوما من الخزن بينما عند التراكيز 0.10 و 0.15 بلغت 1.8 و 1.6 مليمكافىء\ كغم زيت على التوالي وهي اقل بالمقارنة مع عينة السيطرة التي سجلت 2.1 مليمكافىء\كغم زيت بعد 45 يوما من الخزن. وتشير النتائج الى حصول زيادة تدريجية في قيم البيروكسيد مع تقدم فترة الخزن واظهرت عينات الزيت المضاف لها المتحلل البروتيني تطور بطيء في معدلات الأكسدة خلال الخزن بالمقارنة مع عينة السيطرة , ارتفعت قيم البيروكسيد من 0.07 مليمكافىء\ كغم زيت عند بداية الخزن لتصل الى 1.8 مليمكافىء\ كغم زيت بعد مرور 60 يوم من الخزن في عينة الزيت المضاف لها المتحلل بتركيز 0.25% وهي مقاربة لعينة الزيت المضاف لها مضاد الاكسدة الصناعي BHT 0.02% والبالغة 1.8 مليمكافىء\ كغم زيت. في حين يلاحظ *ارتفاعا* ملحوظ في قيم البيروكسيد من 0.09 مليمكافىء\ كغم زيت في فترة قبل الخزن لتصل الى اعلى معدل لها 2.8 مليمكافىء\ كغم زيت عند نهاية فترة الخزن. قد يعود السبب في خفض معدلات الاكسدة الى الاحماض الامينية الكارهة للماء التي ممكن ان تعيق عملية الاكسدة وتكون البيروكسيدات, وقابلية الببتيدات على منح الالكترون واقتناص الجذور الحرة (Zhu *et al.*, 2022; Pan *et al.*,2020).

إن وجود الاحماض الامينية اللايسين والميثيونين والهستدين والتايروسين واللايسين يعزز من قدرة المتحللات البروتينية على تثبيط بيروكسيدات الدهون في الأغذية (Vasconcellos *et al.*, 2014; Singh *et al.*, 2014) وقد يعود السبب في ارتفاع قيم االبيروكسيد مع تقدم فترات الخزن الى تأثير درجة الحرارة وتوفر الاوكسجين التي تؤدي الى زيادة معدلات الاكسدة (Wong *et al.*, 2020).



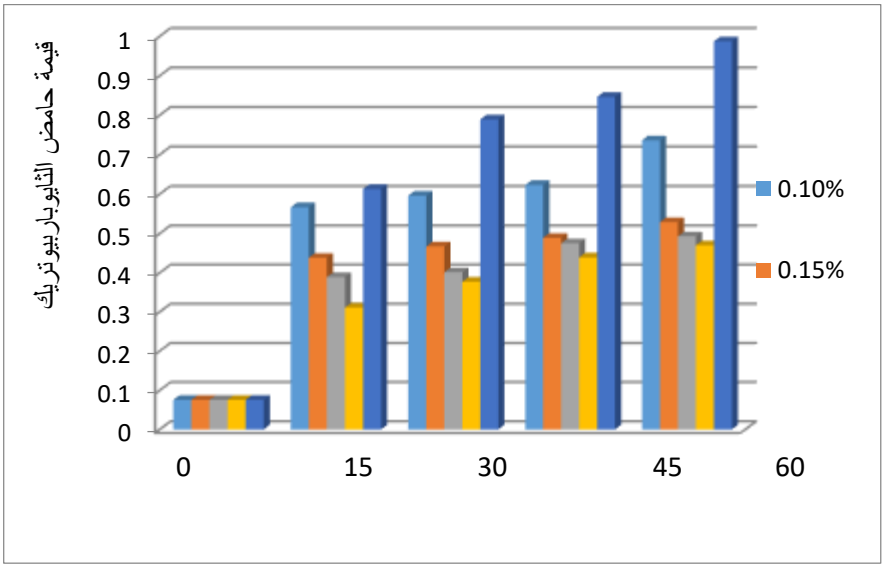
شكل 4. اختبار رقم البيروكسيد لزيت السمسم المعامل بمتحللات بروتينات شرش حليب الجمل

قيمة حامض الثايوباربيوتريك Thiobarbituric Acid (TBA)

تبين الشكل (5) قيم حامض الثايوباربيوتريك TBA ملغم مالنولديهايد\ كغم لعينات زيت السمسم المضاف لها المتحلل البروتيني المحضر من مركز بروتينات شرش حليب الجمل بتراكيز 0.10 % و 0.15 % و0.25% والمخزن في عبوات شفافة على درجة حرارة 40 مْ ± 5مْ لفترة 0 و15 و30 و45 و60 يوم ومقارنتها مع العينة القياسية المضاف لها BHT بتركيز 0.02% وعينة السيطرة بدون أي إضافة , ويلاحظ من نتائج التحليل الاحصائي لا يوجد أي فروقات معنوية ($P \geq 0.05$) في قيم حامض الثايوباربيوتريك TBA لزيت السمسم في الفترة صفر من الخزن التي بلغت 0.08 ملغم مالنولديهايد\ كغم زيت، بينما يلاحظ انخفاض قيم حامض الثايوباربيوتريك TBA لزيت السمسم بزيادة تركيز المتحلل البروتيني ومدة الخزن حيث اظهر تركيز 0.25% اقل قيمة لحامض الثايوباربيوتريك TBA اذ بلغت 0.48 ملغم مالنولديهايد\ كغم زيت بعد مضي 60 يوما من الخزن في حين بلغت قيمة حامض الثايوباربيوتريك TBA 0.73، 0.53 ملغم مالنولديهايد\ كغم زيت عند التراكيز 0.10 و 0.15% على التوالي وهي أقل بالمقارنة مع عينة السيطرة التي سجلت 0.98 ملغم مالنولديهايد\ كغم زيت ومقاربة لقيمة حامض الثايوباربيوتريك TBA لعينة BHT التي بلغت 0.46 ملغم مالنولديهايد\ كغم زيت بعد مضي 60 يوما على الخزن.

بينما كانت قيم حامض الثايوباربيوتريك TBA عند التراكيز 0.10% و 0.15% و0.25% لعينات زيت السمسم بعد مضي 15 يوما من الخزن 0.56، 0.45، 0.37 ملغم مالنولديهايد\ كغم زيت على التوالي مقارنة مع عينة BHT و عينة السيطرة التي بلغت0.30، 0.60 ملغم مالنولديهايد\ كغم زيت على التوالي. وتشير النتائج الى حصول تطور

تدريجي في قيم حامض الثايوباربيوتريك TBA مع تقدم فترات الخزن بالمقارنة مع عينة السيطرة، ارتفعت قيم حامض الثايوباربيوتريك TBA بعد مضي 30 يوما من الخزن لتصل الى 0.58، 0.47، 0.38 ملغم مالنولديهايد\ كغم زيت في عينة زيت السمسم المضاف لها المتحلل بالتراكيز0.10، 0.15، 0.25% على التوالي مقارنة بعينة الزيت المضاف لها مضاد الاكسدة الصناعي BHT 0.02% التي بلغت 0.36 ملغم مالنولديهايد\ كغم زيت، في حين شهد عينة السيطرة ارتفاعا ملحوظ في قيم حامض الثايوباربيوتريك TBA لتصل 0.79 ملغم مالنولديهايد\ كغم زيت بعد مضي 30 يوما من الخزن، وباستمرار فترة الخزن لتصل الى 45 يوما كانت قيم حامض الثايوباربيوتريك TBA 0.61، 0.49، 0.46 ملغم مالنولديهايد\ كغم ز زيت عند التراكيز 0.10، 0.15، 0.25% على التوالي مقارنة بعينة الزيت المضاف لها مضاد الاكسدة الصناعي BHT 0.02% التي بلغت 0.44 ملغم مالنولديهايد\ كغم زيت، في حين بلغت قيمة حامض الثايوباربيوتريك TBA في عينة السيطرة 0.85 ملغم مالنولديهايد\ كغم بعد مضي 45 يوما من الخزن. يعود السبب الى ان طريقة تقدير قيمة حامض الثايوباربيوتريك TBA تكشف عن اكسدة الاحماض الدهنية غير المشبعة التي تعتبر دليل على تزنخ الدهون والزيوت من خلال تفاعل 2 مول من حامض الثايوباربيوتريك TBA مع مول واحد من مالنولديهايد ليكون معقدا اصفر اللون ثم يتحول تدريجيا للون البرتقالي ثم الى اللون الأحمر الوردي نتيجة لتفاعل ثنائي الالديهايد مع ثلاث ذرات من الكاربون الناتجة من اكسدة الاحماض الدهنية غير المشبعة. Guillén-Sans and Guzmán-Chozas 1998).



شكل 5. قيمة حامض الثايوباربيوتريك TBA لزيت السمسم المعامل بمتحللات بروتينات شرش حليب الجمل

الاستنتاجات

هدفت الدراسة إلى تحضير شرش حليب الجمل المحضر بالطريقة الحامضية، وإنتاج متحللات بروتينية باستعمال إنزيم التربسين وتركيزها وتجفيفها، وتقدير نسبة الأحماض الأمينية فيها واختبار فعاليتها المضادة للأكسدة من حيث قابليتها على اقتناص جذر DPPH وربط أيون الحديدوز وقوتها الاختزالية واستعمالها كمضادات أكسدة طبيعية في حفظ زيت السمسم وقياس قيم رقم البيروكسيد خلال فترات التخزين. أظهرت نتائج البحث امتلاك المتحللات البروتينية المحضرة فعالية مضادة للأكسدة عالية لاحتوائها على أحماض أمينية ذات مجاميع فعالة تعزز من النشاط المضاد

للأكسدة فضلا عن قدرتها في اقتناص الجذور الحرة ومنع أكسدة زيت السمسم مما أدى إلى انخفاض قيم البيروكسيد خلال فترات الخزن.

References

1. Al-Hatim, R.R.; Al-Rikabi, A.K.; Ghadban, A.K., (2020) The Physico-Chemical Properties of Bovine and Buffalo Whey Proteins Milk by Using Ultrafiltration Membrane Technology. Basrah J. Agric. Sci (33): 122–134.
2. Al-Hilifi, S. A., Al-Ibresam, O. T., Al-Hatim, R. R., Al-Ali, R. M., Maslekar, N., Yao, Y., & Agarwal, V. (2023). Development of Chitosan/Whey Protein Hydrolysate Composite Films for Food Packaging Application. Journal of Composites Science, 7(3), 94.
3. Al-Shamsi, K. A.; Mudgil, P.; Hassan, H. M. and Maqsood, S. (2018). Camel milk protein hydrolysates with improved technofunctional properties and enhanced antioxidant potential in vitro and in food model systems. Journal of Dairy Science, 101(1): 47-60.
4. AOAC: Association of Official Analytical Chemists (1980). Official Method of Analysis, 13th edn., Washington, DC, pp: 130–143.
5. Bassan, J. C.; Goulart, A. J.; Nasser, A. L.; Bezerra, T. M.; Garrido, S. S.; Rustiguel, C. B.; Gumiarães,L. H. S. and Monti, R. (2015). Buffalo cheese whey proteins, identification of a 24 kDa protein and characterization of their hydrolysates: In vitro gastrointestinal digestion. PloS One, 10(10): e0139550-0139568.
6. Caetano-Silva, M. E.; Bertoldo-Pacheco, M. T.; Paes-Leme, A. F. and Netto, F. M. (2015). Iron-binding peptides from whey protein hydrolysates: Evaluation, isolation and sequencing by LC–MS/MS. Food Research International,(71): 132-139.
7. Chen, Y. C.; Chang, H. S.; Wang, C. T. and Cheng, F. Y. (2009). Antioxidative activities of hydrolysates from duck egg white using enzymatic hydrolysis. Asian-Australasian Journal of Animal Sciences, 22(11): 1587-1593.
8. Choe, E., & Min, D. B. (2009). Mechanisms of antioxidants in the oxidation of foods. Comprehensive reviews in food science and food safety, 8(4): 345-358.
9. Da Silva, J. D. F.; Correa, A. P. F.; Kechinski, C. P. and Brandelli, A. (2018). Buffalo cheese whey hydrolyzed with Alcalase as an antibrowning agent in minimally processed apple. Journal of Food Science and Technology, 55(9): 3731-3738.
10. Devi, K.; Haripriya, S.; Kumar, J.K. N.; Dharini, V. and Kumar, V. (2017). Rational approach to sequential optimization of antioxidative whey protein hydrolysate production. International Journal on Nutraceuticals, Functional Foods and Novel Foods, 16:83-89.
11. El-Ibresam, O. T. Y., & AL-Rikabi, A. K. J. (2022). Effect of pH,temperature and NaCl on antioxidant peptides from Iraqi buffalo whey proteins hydrolysis Arab Journal of Agriculture Sciences (AJAS), 15 (5): 68 – 98.

12. Genstat Discovery Edition.(2011). Genstat Release 10.3DE. VSN International LTD. Rothamsted Experimental station.UK.
13. Hemalatha, S. ; Lalitha, P. and Arupriya, P. (2010). Antioxidant activities of the extracts of aerial roots of Pothos aurea (Linden ex Andrel). Der Pharma Chemica, 2 (6): 84 – 89.
14. Hernández-Ledesma,B.;Davalos,A., Bartolome,B. and Amigo, L. (2005). Preparation of antioxidant enzymatic hydrolysates from α-lactoalbumin and β-lactoglobulin.Identification of active peptides by HPLC-MS/MS. J. Agric. Food Chem ., 53: 588-593.
15. Hussein, F. A.; Chay, S. Y.; Zarei, M.; Auwal, S. M.; Hamid, A. A.; Wan Ibadullah, W. Z. and Saari, N. (2020). Whey protein concentrate as a novel source of bifunctional peptides with angiotensin-I converting enzyme inhibitory and antioxidant properties: RSM study.Foods,9(1):1-15.
16. Guillén-Sans, R. and Guzmán-Chozas, M. (1998). The thiobarbituric acid (TBA) reaction in foods: a review. Critical Reviews in Food Science and Nutrition, 38(4):315–330.
17. Kamal, H., Jafar, S., Mudgil, P., Murali, C., Amin, A., & Maqsood, S. (2018). Inhibitory properties of camel whey protein hydrolysates toward liver cancer cells, dipeptidyl peptidase-IV, and inflammation. Journal of Dairy Science, 101(10), 8711-8720.
18. Kerasioti, E.; Stagos, D.; Priftis, A.; Aivazidis, S.; Tsatsakis, A. M.; Hayes, A. W. and Kouretas, D. (2014). Antioxidant effects of whey protein on muscle C2C12 cells. Food Chemistry, 155: 271-278.
19. Lin, S.; Tian, W.; Li, H.; Cao, J. and Jiang, W. (2012). Improving antioxidant activities of whey protein hydrolysates obtained by thermal preheat treatment of pepsin, trypsin, alcalase and flavourzyme. International Journal of Food Science and Technology, 47(10): 2045-2051.
20. Manzanares, P.; Gandía, M.; Garrigues, S. and Marcos, J. F. (2019). Improving health-promoting effects of food-derived bioactive peptides through rational design and oral delivery strategies. Nutrients, 11(10): 25-45.
21. Mousavi, J.S.R.; Niazmand, R. and Shahidi Noghabi, N.(2015). Antioxidant of purslane(Porulaca oleracea L.) seed hydro-alcoholic extraction on the stability of soybean oil. Journal of Agricultural Science and Trechnology.17(6):1473-1480.
22. Neto, Y. A. H.; Rosa, J. C. and Cabral, H. (2019). Peptides with antioxidant properties identified from casein, whey, and egg albumin hydrolysates generated by two novel fungal proteases. Preparative Biochemistry and Biotechnology, 49(7): 639-648.
23. Nwachukwu, I. D. and Aluko, R. E. (2018). Structural and functional properties of food protein-derived antioxidant peptides. Journal of Food Biochemistry, 43(1): 1-13.
24. O'Loughlin, I. B.; Kelly, P. M., Murray, B. A.; FitzGerald, R. J. and Brodkorb, A. (2015). Molecular characterization of whey protein hydrolysate fractions with ferrous chelating

and enhanced iron solubility capabilities. Journal of Agricultural and Food Chemistry, 63(10): 2708-2714.

25. Olsen, J. V., Ong, S. E., & Mann, M. (2004). Trypsin cleaves exclusively C-terminal to arginine and lysine residues. Molecular & cellular proteomics, 3(6), 608-614.
26. Pan M, Liu K, Yang J, Liu S, Wang S, Wang S. Advances on Food-Derived Peptidic Antioxidants-A Review. Antioxidants (Basel). 2020 Aug 27;9(9):799. doi: 10.3390/antiox9090799
27. Parkin, K. L. and Damodaran, S. (2003). Oxidation of food components. In: Encyclopedia of food sciences and nutrition. Caballero, B.(ed.). 2st edn., (1-10): 4288-4294
28. Peng, X.; Xiong, Y. L. and Kong, B. (2009). Antioxidant activity of peptide fractions from whey protein hydrolysates as measured by electron spin resonance. Food Chemistry, 113(1): 196-201.
29. Qian, Z. L.; Jung, W. K. and Kim, S. K. (2008). Free radical scavenging activity of a novel antioxidative peptide purified from hydrolysate of bullfrog skin, Rana catesbeiana Shaw. Bioreso. Technol.,99:1690-1698.
30. Shah, P. and Modi, H. A. (2015). Comparative study of DPPH, ABTS and FRAP assays for determination of antioxidant activity. International Journal for Research in Applied Science and Engineering Technology 3(6): 636-641.
31. Singh , B.P. ; Vij,S . ; and Hati , S. (2014) . Funactional significance of bioactive peptides derived from soybean .Journal Homepage,54 : 171-179.
32. Vavrusova, M.; Pindstrup, H.; Johansen, L. B.; Andersen, M. L.; Andersen, H. J. and Skibsted, L. H. (2015). Characterisation of a whey protein hydrolysate as antioxidant. International Dairy Journal, 47: 86-93.
33. Wali, A.; Yanhua, G.; Ishimov, U.; Yili, A.; Aisa, H. A. and Salikhov, S. (2019). Isolation and identification of three novel antioxidant peptides from the Bactrian camel milk hydrolysates. International Journal of Peptide Research and Therapeutics, 26(2):1-10.
34. Wong, F.; Xiao, J.; Wang, S.; Ee, K.; Chai, T. Advances on the antioxidant peptides from edible plant sources. Trends Food Sci. Technol. 2020, 99, 44–57.
35. Zhu, Y.; Lao, F.; Pan, X.; Wu, J. Food Protein-Derived Antioxidant Peptides:MolecularMechanism,StabilityandBioavailability. Biomolecules 2022, 12, 1622. https://doi.org/10.3390/biom12111622.

The Effect of Serum Glypican-4 (GLY-4) in Patients with Cardiovascular Disease in Iraq

Bayader Abdul Hussein Mahmeed [1], Hend Ahmed Abass [2]

Wasan T. Al-Rubayee [3], Rayah Sulaiman Baban [4]

© 2023 The Author(s). This open access article is distributed under a Creative CommonsAttribution (CC-BY) 4.0 license.

Abstract: Glypicans, a family of heparan sulfate proteoglycans that are attached to the cell membrane by a glycosyl-phosphatidylinositol anchor, and they include six members, GPC1-GPC6. Glypicans are emerging as an important family of compounds that may play a role in cardiovascular diseases. Therefore, this study aimed to investigate the levels of Glypican-4 (GLY-4) in Iraqi patients with cardiovascular disease. Methods the study included 80 subject divided into 40 patients with cardiovascular disease and 40 controls. Measured Serum GPC4 levels were determined using an enzyme-linked immunosorbent assay. Result Serum GPC4 was significantly associated with cardiovascular disease and negative correlation between gly-4 and Troponin (r= -0.1511), while a positive correlation was found between gly-4 and CRP (r= 0.157). Conclusions the study indicates that elevated serum GLY-4 levels are significantly associated with an increased risk of cardiovascular disease.

Key Words: Cardiovascular disease, Glypican-4, CRP.

Author details

[1-2-3] Department of Chemistry and Biochemistry, College of Medicine, Al- Nahrain University, Baghdad, Iraq

Citation information

Cite this article as:

Mahmeed, B.A., Abass, H.A., Al-Rubayee, W.T., Baban, R.S., (July 2023), *The Effect of Serum Glypican-4 (GLY-4) in Patients with Cardiovascular Disease in Iraq*, Proceedings of the Minar Congress, Turkey, (9) pp 374-379, DOI: http://dx.doi.org/10.47832/MinarCong9-31

http://dx.doi.org/10.47832/MinarCong9-31

1 bayaderb79@gmail.com

2 hendahmedabass80@gmail.com

3 wasanbashaga@gmail.com

4 baban.rs9@gmail.com

Introduction

Glypicans are heparan sulfate proteoglycans (HSPGs) that are linked to the outer cell membrane by a glycosyl-phosphatidylinositol anchor and comprise an approximately 450 amino acid N-terminal protein domain and an approximately 100 amino acid stalk region (1). Most glypicans have an N-terminal domain that is proteolytically broken down by a convertase similar to furin, resulting in two chains that are still linked by disulfide bonds (2). Certain glypicans activity appears to require this processing, but not all of them (3). According to predictions, glypicans' stalk sections will mostly consist of random coils and will typically have 1–5 attachment sites for heparan sulfate (4). There are six glypicans in both mice and people (glypican-1, -2, -3, -4, -5, and -6).

The human GLY-4 gene produces the protein known as glypican-4. Cellular surfaces include heparan sulfate proteoglycans are made of a membrane-associated protein core that has been replaced by a variable number of heparan sulfate chains. Members of the GRIPS family of integral membrane proteoglycans (glypicans-related) have a core protein that is linked to the cytoplasmic membrane by glycosyl phosphatidylinositol. These proteins might be involved in the regulation of growth and the regulation of cell division. At the 3' terminus of GPC3, the GLY-4 gene may also contribute to the Simpson-Golabi-Behmel syndrome (5).

Watanabe and colleagues made the initial discovery of glipican-4 in the kidneys and developing mouse brain in 1995 (6). Gesta and colleagues (7) showed that visceral and subcutaneous fat tissues express glypican-4 genetically in different ways. The scientists discovered that glypican-4 expression in the subcutaneous and visceral adipose tissues appeared to be inversely correlated with body mass index (BMI) and waist-hip ratio (WHR), indicating higher risks for metabolic and cardiovascular problems (7).

In contrast to existing insulin sensitizers, a new adipokine called glipican-4 has been discovered. It is a cell surface proteoglycan that improves insulin receptor signaling and adipocyte development by directly interacting with the insulin receptor (8).

As an insulin sensitizer, glypican-4's binding to the insulin receptor controls insulin activation and downstream signaling. Moreover, the HOMA (Homeostasis Model Assessment) index and WHR, as well as circulating glypican-4 levels, are all strongly linked with poor glucose tolerance and Obesity in patients (9).

Highly charged macromolecules known as heparan sulfate proteoglycans (HSPGs) are present on the surface of almost all cell types. In mammalian cells, syndecans and glypicans are the primary cell surface proteoglycans that transport heparan sulfate. They engage in interactions with a wide range of chemicals, such as growth factors, enzymes, and extracellular matrix components (ECM), and operate as regulators of biological processes, such as hemostasis and embryogenesis [10,11]. They are consequently involved in different

pathogenic illnesses such cancer, atherosclerosis, and thromboembolic disorders, as well as wound healing [8-12].

Glypicans are expressed in the heart [13], although it is unclear how they affect cardiac remodeling and failure. Glypicans control how cells react to different growth factors [14]. The variety of cellular processes that glypicans may have an impact on is highlighted by the knowledge that these growth factors govern cell migration, differentiation, and proliferation [15]. To our knowledge not many studies have been done regarding the serum levels of GLY-4 in cardiovascular disease patients, therefore, this study investigated the levels of Glypican-4 (GLY-4) in a sample of Iraqi patients with cardiovascular disease and the association between GLY-4, troponin and C-reactive protein.

Material and method:

The study was a case - control study. The number of samples that were taken included 80 samples that were divided into 40 patients with cardiovascular diseases and 40 healthy, sex and age matched controls.

The samples were taken from patients attending Al-Imamian Al-Kadhimiyain Medical City, the period of sampling was between September 2022 - December 2022 in which 5 ml of blood was withdrawn, and CRP, Troponine, and GLY-4 were measured using the ELISA methods.

Statistical analysis: Data were analyzed by statistical packages of SPSS 18.5 (Statistical Packages for Social Sciences-version 18.5). All data were presented as a mean±SEM. Statistical differences between data of patients and control groups were determined according to the student's t- test. Correlation between the variables was performed by Spearman correlation coefficient. P values were significant if the P-value is ≤ 0.05

Result: A highly significant differences was found in mean values of both **GLY-4** and CRP between patients and controls P>0.0001, while a significant difference in the mean of troponin was found between patients and controls p=0.02. No significant difference was found in mean of age between patients and controls, (Table-1).

Table 1. comparison of the mean measured parameters in study groups

	Mean ± SD Controls	Mean ± SD Patients	P value
Age	64.4± 7.4	61.65+7.57	0.26 NS
GLY-4	6.79 ±1.29	14.2+ 4.08	<0.0001
CRP	2.21±1.53	11.1+4.45	<0.0001
TROP	0.27± 1.32	11.2+5.5	<0.0001

The table (2) showed a negative correlation between gly-4 and Trop (r= -0.1511), while a positive correlation was found between gly-4 and CRP (r= 0.157).

Table 2. Correlation between gly-4 with Trop and CRP in the study groups

Correlation	GLY-4	
Trop	r = -0.15111851	P = 0.01
crp	r = 0.157308331	P = 0.01

Discussion

Glypican-4 (GLY-4) is a cell surface protein that can enter the bloodstream in a number of different clinical circumstances. Uncertainty exists regarding the relationship between circulating GLY-4 and the future mortality or heart disease risk.

We show in this study that raised serum GLY-4 levels are strongly connected to a higher risk of cardiovascular disease. An insulin-sensitizing adipokine known as circulating GLY-4 has been connected to a number of disorders correlated with insulin resistance, which has linked to the occurrence of cardiovascular events and mortality (16).

Proteoglycans are heparan sulfate proteoglycans made up of a core protein that is covalently attached a heparan sulfate chain or chains. They are present in the secretory vesicles and extracellular matrix, and are ubiquitously expressed on cellular surfaces. The cellular impacts of HSPGs encompass a variety of capabilities, such as: 1) the ability to interact in order to act as a substrate for cellular migration with other membrane surface proteins, 2) the ability to serve as a binding site for circulating molecules, 3) the ability to serve as a receptor for proteases, 4) the ability to serve as a coreceptor that can fine-tune the growth factor receptor activity threshold, and 5) the ability to activate intracellular signaling pathways among the various families of HSPGs, Due to their actions on cardiovascular cells and putative involvement in disease progression, the glypican families of HSPGs have drawn more attention.(17)

In this study, we list the results of the glypican homologs on various kinds of cardiovascular cells and talk about their support to routes that are common to (Inflammatory disease, hypertrophy, and vascular remodeling) Cardiovascular disorders), as well as their potential role in the onset and progression of particular diseases like hypertension, heart failure, and atherosclerosis. Fisher et al. in 2019 have examined the association between plasma GLY 1, 3, and 4 levels of other inflammatory markers and the severity of the illness in a cohort study (18).

Conclusions

Therefore, it may be concluded that a higher risk of cardiovascular disease is significantly related with raised serum GLY-4 levels.

References

1. Venero Galanternik M, Kramer KL, Piotrowski T: Heparan Sulfate Proteoglycans Regulate Fgf Signaling and Cell Polarity during Collective Cell Migration. Cell Rep 2015.
2. Mead, Timothy J., et al. "Proteolysis: a key post-translational modification regulating proteoglycans." American Journal of Physiology-Cell Physiology 323.3 (2022): C651-C665.
3. Briscoe, James, and Pascal P. Thérond. "The mechanisms of Hedgehog signalling and its roles in development and disease." Nature reviews Molecular cell biology 14.7 (2013): 416-429.
4. Cheng, Fang, et al. "Non-conserved, S-nitrosylated cysteines in glypican-1 react with N-unsubstituted glucosamines in heparan sulfate and catalyze deaminative cleavage." Glycobiology 22.11 (2012): 1480-1486.
5. Veugelers, M., Vermeesch, J., Watanabe, K., Yamaguchi, Y., Marynen, P., and David, G. (1998). "GPC4, the Gene for Human K-glypican, Flanks GPC3 on xq26: Deletion of the GPC3-GPC4 Gene Cluster in One Family with Simpson – Golabi - BehmelSyndrome".Genomics.,3 (1),111. doi:10.1006/geno.1998.5465. PMID 9787072
6. Watanabe, K., Yamada, H., Yamaguchi, Y. (1995). K-glypican: A Novel GPI-Anchored Heparan Sulfate Proteoglycan that is Highly Expressed in Developing Brain and Kidney. J Cell Biol., 130(5), 1207-18.
7. Gesta, S., Blüher, M., Yamamoto, Y., Norris, A. W., Berndt, J., Kralisch, S., et al. (2006). Evidence for a Role of Developmental Genes in the Origin of Obesity and Body Fat Distribution. Proc Natl Acad Sci USA., 103(17), 6676-81.
8. Ussar, S., Bezy, O., Blüher, M., Kahn, CR. (2012). Glypican-4 Enhances Insulin Signaling via Interaction with the Insulin Receptor and Serves as a Novel Adipokine. Diabetes., 61(9), 2289-98.
9. Li, K., Xu, X., Hu, W., Li, M., Yang, M., Wang, Y., et al. (2014). Glypican-4 is Increased in Human Subjects with Impaired Glucose Tolerance and Decreased in Patients with Newly Diagnosed Type 2 Diabetes. Acta Diabetol., 51(6), 981-9.
10. Christianson, Helena C., et al. "Cancer cell exosomes depend on cell-surface heparan sulfate proteoglycans for their internalization and functional activity." Proceedings of the National Academy of Sciences 110.43 (2013): 17380-17385.
11. Shriver, Z., Liu, D., and Sasisekharan, R. (2002). Emerging Views of Heparan Sulfateglycosaminoglycan Structure/Activity Relationships Modulating Dynamicbiological Functions. Trends Cardiovasc Med., 12, 71-77.
12. Obunike, J. C., Pillarisetti, S., Paka, L., Kako, Y., Butteri, M. J., Ho, Y. Y., Wagner, W. D., Yamada, N. Mazzone, T., Deckelbaum, R. J., Goldberg, I. J. (2000). The Heparin-Bindingproteins Apolipoprotein E and Lipoprotein Lipase Enhance Cellularproteoglycan Production. Arterioscler Thromb Vasc Biol., 20, 111-118.

13. Traister, A., Shi, W., and Filmus, J. (2008). Mammalian Notum Induces the Release of Glypicans and Other GPI-Anchored Proteins from the Cell Surface. Biochem J., 410(3), 503–11. 10.1042/BJ20070511
14. Fico, A., Maina, F., and Dono, R. (2011). Fine-tuning of Cell Signaling by Glypicans. Cell Mol Life Sci., 68(6), 923–9. 10.1007/s00018-007-7471-6.
15. Filmus, J., and Selleck, S. B. (2001). Glypicans: Proteoglycans with a Surprise. J Clinl Invest.,108(4), 497–501.
16. Huang, K., and Park, S. (2021). Heparan Sulfated Glypican-4 Is Released from Astrocytes by Proteolytic Shedding and GPI-Anchor Cleavage Mechanisms. eNeuro., 8(4). doi: 10.1523/ENEURO.0069-21.2021. PMID: 34301723; PMCID: PMC8387153.
17. Sarrazin, S., Lamanna, W. C., and Esko, J. D. (2011). Heparan Sulfate Proteoglycans. Cold Spring Harb Perspect Biol., 3(7), a004952. doi: 10.1101/cshperspect.a004952. PMID: 21690215; PMCID: PMC3119907.
18. Fisher, J., Linder, A., Bentzer, P. (2019). Elevated Plasma Glypicans are Associated with Organ Failure in Patients with Infection. Intensive Care Med Exp., 7(1). 2. doi: 10.1186/s40635-018-0216-z. PMID: 30618011; PMCID: PMC6323058.

The Effect of Alcoholic Extract of Infected Ceratonia Fruits Infected with Some Fungi on Some Histological Characteristics of White Male Swiss Ratus Rattus Ratus

Zainab Jawad Naki Al-Busaid [1], Zainab Abd Al -Ameer Mohammed [2],
Zainab Shnewer Mahdi Al-Turfi [3], Wijdan Kamal Noor Shalan Al-Qraawy [4]

© 2023 The Author(s). This open access article is distributed under a Creative CommonsAttribution (CC-BY) 4.0 license.

Author details

[1- 2 - 3- 4] Department of Life Sciences, College of Education for Girls, University of Kufa, Baghdad, Iraq

Citation information

Cite this article as:

Al-Busaid, Z.J., Mohammed, Z.A., Al-Turfi, Z.S., Al-Qraawy, W.K., (July 2023), *The Effect of Alcoholic Extract of Infected Ceratonia Fruits Infected with Some Fungi On Some Histological Characteristics of White Male Swiss Ratus Rattus Ratus*, Proceedings of the Minar Congress, Turkey, (9) pp 380-388, DOI: http://dx.doi.org/10.47832/MinarCong9-32

Abstract: The present study was aimed to evaluate the effect of carob alcoholic extract which is infected with Pencillium and three other species belonging to the species Aspergillus, Aspergillus niger, Aspergillus flavus, and Aspergillus terrus due to poor storage, in order to investigate the effect of this extract on the testes tissue of Swiss rats Rattus ratus. The current study was conducted in the animal house belonging to the Department of Life Sciences /College of Education for Girls/ University of Kufa, this study began in March until June 2017 Laboratory animals were divided into three main groups. The first group was treated with low concentration 100 mg / kg. The second group was treated with a high concentration 300 mg / kg of the alcoholic extract. The third group was a control group injected with normal saline 0.9 % NaCl2 tissue samples were taken from the three groups for the purpose of conducting tissue tests after one month of intra peritoneal injection. The results showed that the low concentration 100mg / kg had a somatic effect on the testicular tissue, some changes were observed in the tissue including the dissociation of the epithelial tissue ,expansion of blood vessels and accumulation of red blood cells inside it also there were Edema in the interstitial tissues and expansion in the diameter of the Seminal tubules and it was also observed that there was congestion in the Seminal tubules , decrease in the number of sperm within the cavity. High concentrations of alcoholic extract (300mg / kg showed that the changes on the tissues were higher than what observed for the lowest concentration, the most prominent of these changes is the breakdown of the Seminal tubules and Interstitial tissue There were also a marked decrease in sperm count in addition to an expansion in the diameter of the Seminal tubules, separation in the lining of the Seminal tubules, as the histological sections showed a large expansion in the diameter of blood vessels and aggregation of large numbers of red blood cells inside them.

Key Words: Alcoholic Extract, Ceratonia Fruits_Fungi

http://dx.doi.org/10.47832/MinarCong9-32

[1] zainabj.albusaid@uokufa.edu.iq

Introduction

Medicinal plants have many advantages, benefits, and uses in the treatment of various diseases. One of these medicinal plants is carob or Ceratonia siliqua, which has been used in the treatment of several diseases ,such as low fertility and sexual dysfunction problems, many studies have pointed to its importance in increasing fertility through increasing the production of sex hormones that enhance testicular activity and increase the production of sperm (1) and prevent malignant diseases such as prostate cancer (2) In addition to containing carob fruits quantities of vitamin E (3) which is considered a strong antioxidant, as some studies indicate its role in the regeneration of spermatozoa of mice testis after the damage (4). The storage or preservation of these plants with unsuitable conditions such as high temperature and humidity will affect the characteristics of the plant therapeutic. There are also factors added to the conditions mentioned, which are the biological factors, including insects, bacteria and fungi. The fungal toxins produced by some species of fungi which are the most important problems affecting the therapeutic properties of medicinal plants. There are species of fungus infect seeds and fruits not stored properly. One of the most important species of fungi that cause harm to plants are Aspergillus and Pencillium, which belong to one species and known as the fungus Ascomycetes, various

Species of Aspergillus including Aspergillus niger. These species cause diseases only if inhaled dust is loaded with spores of this species causing damage to the ear and audio channel (5) and the other species are Aspergillus terrus. This species causes animal abortions in cattle and dogs and its responsible for sinusitis and affects the liver, spleen and kidney as well as the pure bone (6). The third species is the most dangerous Aspergillus flavus because it produces serious toxins and causes damage to organs tissue, such as necrosis, tissue fibrosis, liver cancer and immune deficiency (7). As for the penicillium fungus, it is harmful because it produces many toxins, including Ochratoxin these fungal toxins affect the spleen, liver and also affects the brain carcinogenic (8).

The objective of the present study is to assess the effect of alcoholic extract of carob plant infected with Pancillium and Aspergillus due to poor storage in order to investigate its effect on Swiss rats testis tissues.

Material & Methods

Isolation & diagnosis of fungi

The fungus was isolated from C. siliqua fruits by crushing the fruits stored in unsuitable conditions and then weighing 10 g of powder using the balance. Then, the powder was placed in a baker container with 100 ml distilled water and mixed well glass, then a series of were done in sterile plastic test tubes by taking 1 ml of solution and adding 9 ml of distilled water to the dilution 〖10〗 ^ (5) f_0 then transfer 〖10〗 ^ (- 4) f_0 and 〖10〗 ^ (- 3) f_0 from the suspension diluted to sterile petri dishes containing food medium (PDA) about three dishes and incubated in37 ° C for 48 hours and the observation of growth periodically and then

adopted the method of direct examination of fungal colonies based on morphological characteristics such as the shape and color of colony and the shape and color of the diagnosis of fungal species.

Preparation of experimental animals

The present study was carried out in the laboratory animal house follow for biological department of Girls Education Faculty in this study 24 male rats Rattus ratus were used. The animals were divided into three groups, each group included eight adult males aged 9-12 weeks, while the weight was between 200-250 g. The animals were placed under suitable laboratory conditions of suitable temperature, water and dry foodstuffs

Preparation of alcoholic extract

The alcoholic extract of carob fruits was prepared according to reference (9), So take (20) gram from dry fruits , the active ingredients were extracted via soxholate apparatus after that, the extract materials were concentrated by rotatory evaporator at temperature degree (40- 45 C°) after obtained on the dry material, it weighted in order to prepare the stock, from was made up tow concentrations (100,300) Mg/Kg of body weight for the present study was conducted

Animals scarification

Treated animals were killed by anesthetizing the chloroform. A longitudinal incision was carried out, the abdominal cavities of animals were opened, their reproductive organs were removed for each animal after the adipose tissue and other tissues were attached to testis were pushed out, these organs were transformed into formalin (10 %) in order to fixation the tissues for 48 hr. in plastic bottles and was labeled and stored until used to prepare the tissue slices.

Histological study

Histological sections of male reproductive organs were prepared to identify the effect of the extract on the Swiss males rats testis depending on the method (10) as follows:-

Histological preparation included fixation the testis by using formalin 10% for 48 hr. then dehydration process have been done by using graduated concentration of ethyl alcohol 70%, 80%, 90% and 100% for 1.5 hr. to each concentration, then the specimens were clearing by Xylene for 60 min for each time and then embedding with Paraffin wax. The block, where cutting by using Rotary microtome in to histological sections at six micrometer, after that stained by Haematoxylen-Eiosin stain then mounted by Canada balsam and cover slid.

Histological slides examination

Slices were examined by using Compound Microscope, histological study included observation the changes in the structure of seminal tubules and the changes in the diameter of the seminal tubules cavity and the blood vessel.

Results

Diagnosis of fungi

The results of direct examination of petri dishes after complete the incubation period showed infected carob fruits samples with Pencillium and other species of Aspergillus as shown in figures below



Figure 1. Colonies of Aspergillus isolated from the culture medium PDA a- A. niger b-A. flavus



Figure 2. colonies of Pencillium& Aspergillus isolated from the culture medium PDA a-Pencillium b-A. terrus c-A. niger

Histological study

The effect of an alcoholic extract of C. siliqua at the concentration 100 mg/kg showed moderate effect changes such as a decrease in number of sperm inside the cavity and widening in the diameter of the seminal tubules figure (4,6) also there were a congestion and bleeding in the interstitial tissue figure (4,) and we observed a congestion and hemorrhage inside the seminal tubule cavity figure (5,7,8,) .The histological sections treated with the same concentration also showed clear degeneration, necrosis ,and dissociation in the epithelial layer of seminal tubules figure (4,5 ,7 ,8), We observed a blood vessel widening and accumulation of red blood cells within the cavity and manifestation of edema in the interstitial tissue figure (5).), as well as the Histological cross-section of male rats testis treated with 300 mg / kg of C.siliqua alcoholic extracts infected with Aspergillus & Pencillium showed a clear separation and distraction in the epithelial layer of the seminal tubules and the occurrence of necrosis in the interstitial tissue figure (9), we also note a decrease in the number of sperm inside the seminal tubules and a clear widening in there diameter figure (10,11), In addition to a bloody hemorrhage between seminal tubules figure (11) and note the disappearance of sperm inside the cavity and expansion of the diameter and a large distraction in the wall of the seminal tubule figure (9)

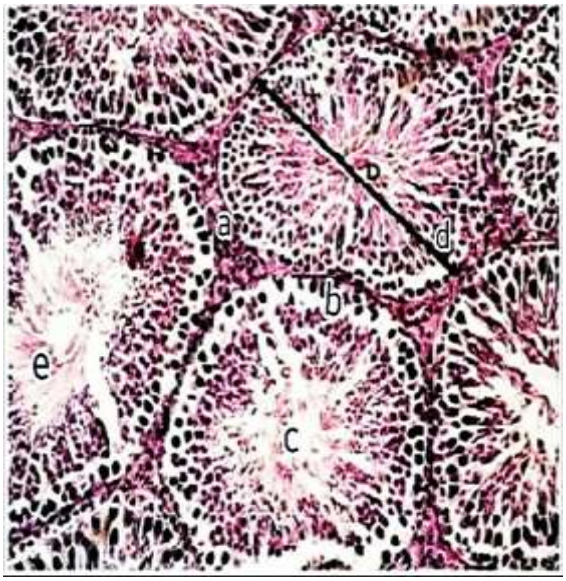


Figure 3. Cross section through testis of control group showing normal histological structure .a - Interstitial tissue b – epithelial layer of seminal tubule c-Cavity of the seminal tubule d – seminal tubule with normal form and diameter e- mature sperm. H & E 100 X

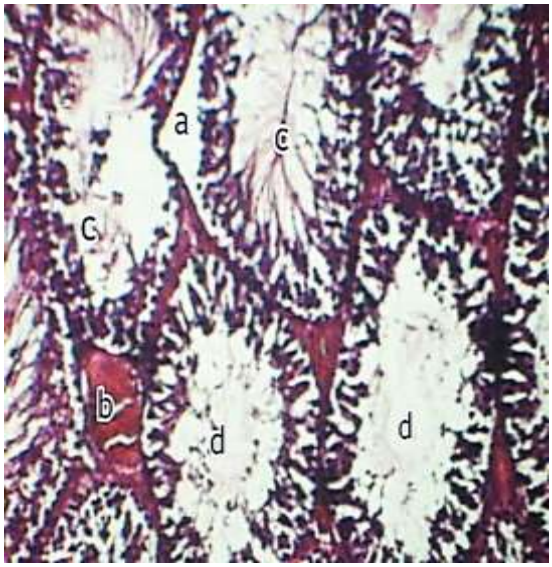


Figure 4. The effect of C. siliqua extract on the testis at the concentration 100 mg/ kg shows a- Dissociation of epithelial layer b- congestion and hemorrhage in the interstitial tissues c- low sperm count d- widening of the seminal tubule diameter. H & E 100 X

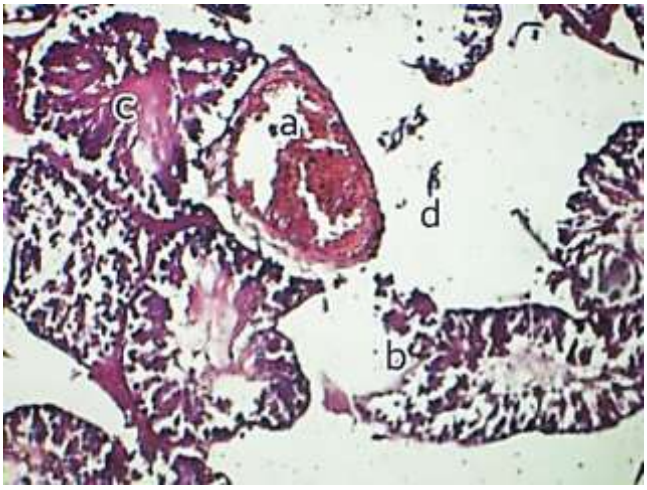


Figure 5. The effect of C. siliqua extract on the testis at the concentration 100 mg/ kg shows a- widening in blood vessel and aggregation red blood cell inside it b-degeneration of seminal tubule layer c-congestion and hemorrhage in seminal tubule d- edema in the interstitial tissue. H & E 100 X

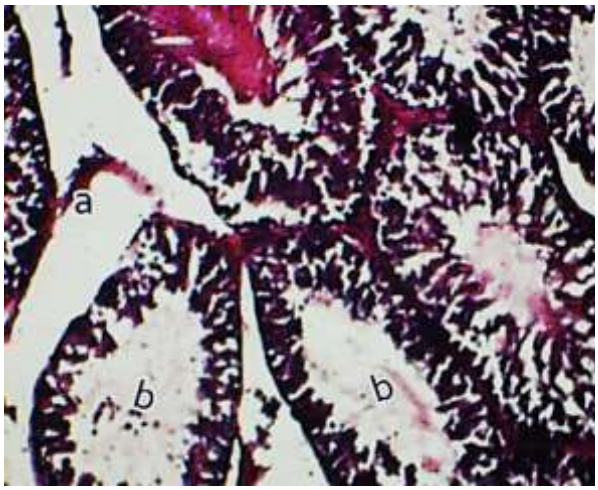


Figure 6. The effect of C.siliqua extract on the testis at the concentration 100 mg/ kg shows a-degeneration in the interstitial tissue b- widening in seminal tubule diameter and decrease the number of sperm within the cavity . H & E 100 X

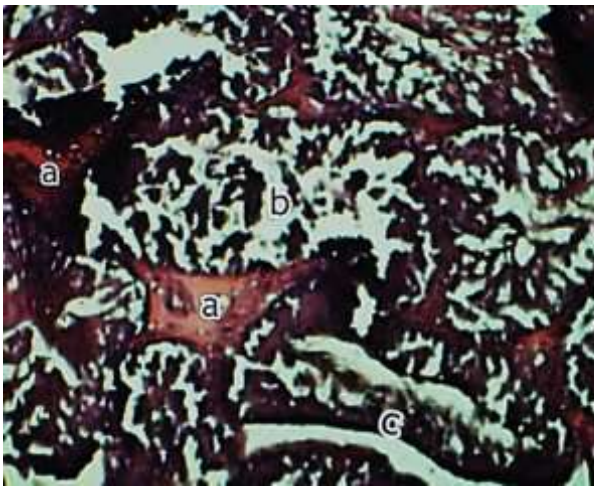


Figure 7. The effect of C.siliqua extract on the testis at the concentration 100 mg/ kg shows a- congestion and hemorrhage in seminal tubule tissue b- necrosis in epithelial layer C - irregularity of the seminal tubule diameter. H & E 100 X

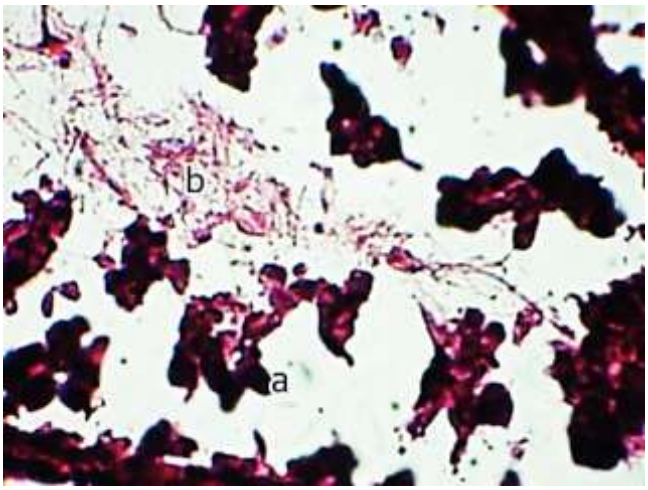


Figure 8. The effect of C. siliqua extract on the testis at the concentration 100 mg/ kg shows a- necrosis and degeneration in seminal tubule epithelial layers b - congestion in the seminal tubule cavity H & E 400 X.

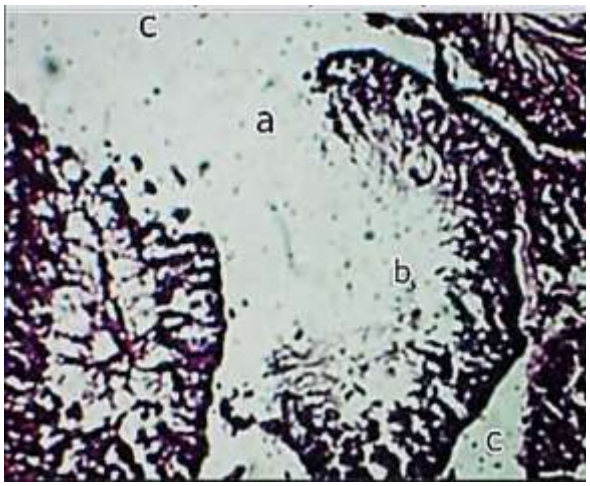


Figure 9. cross section of the rat testis at a concentration (300mg / kg) showing a – distraction in seminal tubule wall b - a widening inside the cavity of seminal tubule and sperm disappearance inside it C – degeneration ad necrosis in the interstitial tissue. H & E 100 X

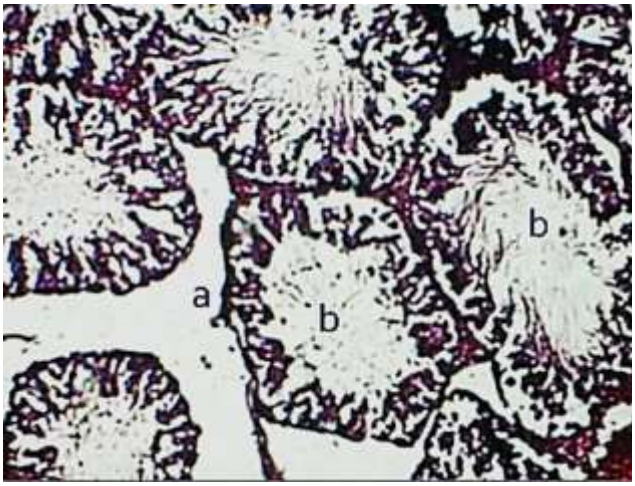


Figure 10. cross section of the rat testis at a concentration (300mg / kg) showing a - significant degeneration and necrosis in the interstitial tissue s b- a significant reduction in the number of sperm and a clear widening in the diameter of seminal tubule . H & E 100 X

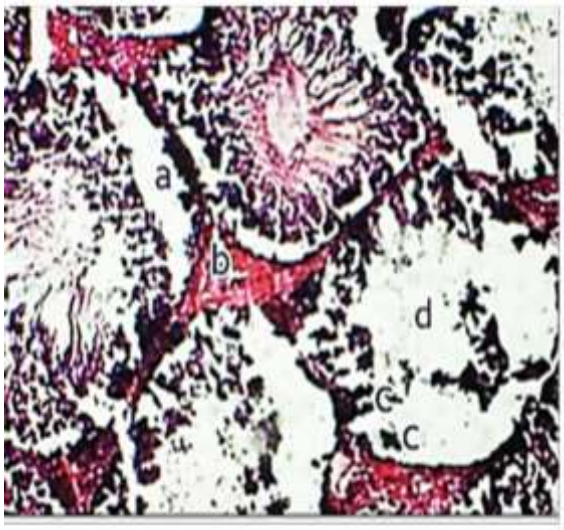


Figure 11. cross section of rat testis at a concentration (300mg / kg) showing a- clear separation in the epithelial layer lining the seminal tubule b- hemorrhage and congestion in interstitial tissue C- degeneration in the epithelial layer d- decrease the number of sperm within the cavity. H & E 100 X

Discussion

The results of the present study showed that low doses 100mg / kg and high doses 300mg / kg of alcoholic carob fruits extract infected with Aspergillus and Pencillium figures (1,2) showed a significant inhibitory in the activity of testicular tissue and manifestation many histological changes, including ,dissociation in the epithelial tissue ,widening blood vessels and aggregation of red blood cells figures (4,5,6,7,9,10) in addition to apparent a congestion and hemorrhage in the interstitial tissues and edema in the tissue structure figures (4,5 ,7) . The results of histological examination also showed that there was a breakdown in walls of seminal tubule and widening it and there were low sperms count inside the cavity of the seminal tubule. Figures (4,6 ,9 ,10).

The results of our study were consistent with a number of studies that indicated the effect of Mycotoxin in animal tissues fed with fodder containing fungal toxins. Researchers 11,12 mentioned that birds have been fed with the fungi A. niger & A. flavus for several weeks, the histological changes have resulted degeneration and necrosis in the liver tissue. As for the tissues of the kidney, there were vasiculation in the cytoplasm of some kidney cells and pyknotic of cytoplasmic nuclei. As for lung tissue, the study of histological sections showed congestion and bleeding in addition of widening blood vessels and edema in different areas of the lung tissue, for the transverse sections of the intestinal tissues, there were an increase in inflammation and cell hypertrophy. These changes are consistent with the results of the present study. The researchers 13 noted that injecting mice with high concentrations (9,12) mg/kg of A.flavus & A. Parasiticus caused the death of mice within 48 hours while other groups of animals were injected with low concentration (3 ,6) mg/kg of aspergillus flavus & Aspergillus Parasiticus, histological examination showed clear changes in the liver tissue such as degeneration, necrosis, and rupture of the cells. There was also abnormal growth and multiplication in the cells, which is the liver injury to cancer and the occurrence of Genetic mutations as well as there were histological changes in renal and lung tissues and these changes were agreed with the results of the current study. In another study by researchers (14) to assess the effect of fungal toxins from Aspergillus in the gastrointestinal tract of dogs, researchers observed bleeding in the epithelial lining the intestine. The researchers (15) found that clotting time in birds treated with fungal toxins was relatively longer than the birds within the control group and pointed to the effect of fungal toxins on the obstruction of the work of proteins responsible for blood clotting, and this leads to bleeding in the tissues and cells and this result also came in line with the results of the current study.

References

1. Mokhtari M Ph. D, Sharifi E MSc, Azadian Sh ,MSc.(2012) The effects of hydro alcoholic extract of Ceratonia siliqua L. seed on pituitary-testis hormones and spermatogenesis in rat. Islmic Azad University , Kazerun Branch, Department of Bilogy , Kazerun, Iran.
2. Awad, A.B., C.s. Fink. (2000). Phytosterols as, anticancer dietary component. J Nutr., 130(9):2127-30
3. Duke, J., (2009) Phytochemical and Ethno botanical Databases Ceratonia siliqua , Green Farmacy Garden 8210 Murpht Road Fulton ,MD 20759 . Agricultural Research Service, Beltsville Area: http //www.ara-grin.gov/duke/Ceratoniasiliquainformationform NPGS/GRIN
4. Jedlinska-Krakowska, M., G. Bomba, K. Jakubowski, T. Rotkiewicz, B. Jana, A. Penkowski .(2006). Impact of Oxidative stress and supplementation with Vitamins E and C on testis morphology in rats. J Reprod Dev.,52(2):203-9
5. Abarca M, Bragulat M, Castella6, Cabanse F. (1994). Ochratoxin A Production by Strains - Aspergillus niger Var .niger)).Appl Environ Microbiol .60(7):2650
6. Lectureg, S., Richard, f. (2012) Jump up to Opportunistic mycoses I:Aspergillosis. Sporotrichosis Archived. (PDF)Rinosopori- diosis& Zygomycosis theoriginal form on 2012 -12 (PDF Newberne, P.M., R. Russo and G.N. Wogan,1966. Acute toxicity of aflatoxin B1 in the dog. Path. Vet. 3: 331-340
7. William JH,Phillips TD,FOLLY PE,stiles JK,Jolly CM Aggarwal D .(2004).Human aflatoxicosis in developing countries :review of toxicology exposure ,Potential health Consequences, and interventions. Am. J.clin Nutr.80n(5):1106-22.PMID 15531656
8. Clark, H.A. and S.M.Shedker .(2006),Ochratoxin A:its Cancer risk and Potential for exposure ,Journal of toxicology and Environmental health B, Vol-9,no.3,pp.265-296, View at Publisher. View at Google scholar View at Scopus
9. Harbone ,J.B.. .(1975).Physiological and Function of Flavonoid .Flavonoids .New York ,Sanfrancisco
10. Bancroft, J. D., Stevens, A. (1996) Theory and Practice of Histological Techniques 4th edn, Churchill liv ingstone London
11. Ortiz, L.T., M.L.Rodriguez ,C. Alzueta, A. Rebole , Centeno, & J. Trevino . 2004. Effect of carob seed (Ceratonia siliqua L.) in broiler chick diet on nutrient digestibility and intestinal Viscosity. EAAP publication NO.110, Toledo, Spain, Wageningen Academic publishers, pp:239-242
12. Jayabarathi P, Mohamudha Parveen R*, .(2010) Biochemical and histo pathological analysis of Aflatoxicosis in growing hens fed with commercial poultry feed. International Journal of Pharmaceutical Sciences Review and Research V.3 P.P 127-13
13. Ochieng, P.J, , Okun, D , Mugenya, I. , Njagi, N. J., John M .(2016) In vivo toxicological and histo pathological Effects of Aflatoxin B1 exposure and related risk
14. Cast. (2003). Mycotoxins: Risks in plant , animals ,and human system . Ames, Iowa, USA, Council for Agricultural Science and Technology :199
15. Raju, M.V.L.N and Devegowda .(2000) Influence of esterified glucomanan on performance and organ morphology inbroilevs exposed to individual aflatoxin ,Ochratoxin and T-2toxin Br.Poult,SC:41:640-650

Identification and Diagnosis of Some Types of Pathogenic Bacteria That Cause Dental Caries in Diabetic Patients

Sumyah H. Torki [1], Salih S. Yagoub [2], Haneen M. Hammed [3],
Tabarak S. Jassim [4], Mastafa H. Al-Musawi [5], Hanan A. Al-Naymi [6]

© 2023 The Author(s). This open access article is distributed under a Creative CommonsAttribution (CC-BY) 4.0 license.

Author details

[1-3-4] Department of Plant Biotechnology College of Biotechnology, Al-Nahrain University, Baghdad, Iraq

[2] College of Education for Pure Science, Diyala University, Diyala, Iraq

[5] Department Clinical Laboratory Science, College of Pharmacy, Mustansiriyah. University, Baghdad, Iraq

[6] Department of Chemistry, College of Education for Pure Science-Ibn AL-Haitham, University of Baghdad, Baghdad, Iraq

Citation information

Cite this article as:

Torki, S.H., Yagoub, S.S., Hammed, H.M., Jassim, T.S., Al-Musawi, M.H., Al-Naymi, H.A. (July 2023), *Identification and Diagnosis of Some Types of Pathogenic Bacteria That Cause Dental Caries in Diabetic Patients*, Proceedings of the Minar Congress, Turkey, (9) pp 389-394, DOI: http://dx.doi.org/10.47832/MinarCong9-33

Abstract: Diabetes Mellitus (DM) there are two type: type-I diabetes, in which the pancreatic beta cells lose their ability to create insulin, and type-II diabetes, in which an issue with the beta cells or a decrease in tissue sensitivity to insulin are required for the development of the illness. Dental caries, periodontal disease, and tooth mobility, all of which are oral problems, are widespread chronic diseases that have become significant health issues. This study was conducted for 3 months in private dental clinics and laboratories of Bilad Alrafidain University Collage, to isolate and diagnose some types of pathogenic bacteria that cause dental caries and the effect of some factors on the incidence of infection, and their impact on patients with diabetes. Isolation results showed 56 bacterial isolates were diagnosed from the samples were collected from patients with dental caries from dental clinics and were divided into 30 samples of dental caries patients with diabetes, 26 samples of Dental caries patients only. 46 isolates of Gram-positive bacteria including the genera Streptococcus ssp., isolates from Staphylococcus ssp. was diagnosed and 10 Gram-negative bacterial isolates, while 30 isolates from dental caries patients with diabetes and 26 isolates from dental caries patients only. The study showed that bacteria Streptococcus ssp. are the main cause of dental caries compared to isolated bacteria, and that the incidence of dental caries had high among people with diabetes.

Key Words: Dental caries, Diabetes, Pathogen Bacteria.

http://dx.doi.org/10.47832/MinarCong9-33

[1] sumyah.hasan@nahrainuniv.edu.iq
[2] drsalih@bauc14.edu.iq
[3] haneen.mushtaq@nahrainuniv.edu.iq
[4] tabarak.sabah@nahrainuniv.edu.iq
[5] mustafa.h.j@uomustansiryah.edu.iq
[6] hanan.a.s@ihcoedu.uobaghdad.edu.iq

Introduction

Diabetes mellitus (DM), a common chronic illness, has become a significant healthcare issue. In India, an estimated 40 million people had diabetes in 2007, and by 2025, it is expected that this figure will nearly double to 70 millionBy 2025, every fifth person with diabetes will be an Indian, according to the International Diabetes Federation's (IDF) Diabetes Atlas. (Goyal *et al.*, 2012). A set of metabolic illnesses caused by abnormalities in insulin secretion, action, or both are brought on by DM and are defined by hyperglycemia.

There are two types of diabetes: Type-I diabetes, in which the pancreatic beta cells cease to be able to make insulin, and type-II diabetes, in which the beta cells must either be defective or have decreased insulin sensitivity for the disease to show. Dental caries, periodontal disease, and saliva-influenced tooth movement are examples of oral problems. (Mathur and Dhillin, 2018).

Patients with diabetes tend to experience severe fluid loss through polyuria, a weakened immune system, decreased connective tissue metabolism, and a variety of microvascular abnormalities. Xerostomia, salivary gland dysfunction, increased susceptibility to bacterial, viral, and fungal infection, periapical abscesses, tooth loss, taste impairment, lichen planus, burning mouth syndrome, and altered orthodontic tooth movements are among the conditions caused by these factors in diabetic patients (González-Moles and Ramos-García, 2021).

Comparing diabetic patients to non-diabetics, dental caries is found to be an extremely common and horrifying occurrence. According to earlier studies, patients with type-II diabetes have a higher chance of developing dental caries than people without the disease. The rise in salivary production and activity that has an effect on dental health is brought on by DM (Shiferaw *et al.,* 2022).

Dental caries is brought on by demineralization, which is brought on by the buildup of microbial plaque flora, a decrease in salivary flow rate, which reduces cleaning, buffer activity, and decreased calcium levels, which are necessary for the restoration of decaying teeth (Dianawati *et al.,* 2020).

Materials and Methodologies

Collection samples

60 samples were collected from patients have dental caries from dental clinics, this samples divided into 30 samples of dental caries patients with diabetes, and 30 samples from patients have Dental caries without diabetes. The patient's age, gender, and place of residence were also recorded. A sterile bonding brush was used to collect the sample, and the swab was then placed in a tube with transport media before being transported to the lab for the implantation of the smears on the proper nutritive medium and the performance of diagnostic tests.

Isolation of Bacteria

Samples were spread by using sterile swabs on the surfaces of various media, including (Nutrient agar, MacConkey agar, Mannitol salt agar, and Mitis Salivarius Bacitracin Agar), Inoculated plates were incubated an aerobic condition for 24-48 hours at 37 °C, and bacteria were identified using morphology, cultural characteristics, and biochemical tests.

Preservation and maintenance of the sample

Isolates were temporarily preserved on Nutrient Agar solid nutrient medium and incubated at 37c for twenty-four hours. They were stored in the refrigerator at 4c and were renewed every two weeks. As for the permanent preservation of isolates, 15 ml of glycerol was added to 85 ml amid a broth of heart and brain broth and distributed in sterile small tubes. Covered tightly, after which inoculation with bacterial colonies and anaerobically incubated at 37C for 24h, and kept in Deep Freezer at -20 °C (Yoo et al, 2005).

Statistical analysis

Chi-square (X2) statistical analyses were used to evaluate the data statistically and identify the key differences.

Results and Discussion

56 bacterial isolates were diagnosed from the samples were collected from patients with dental caries from dental clinics and were divided into 30 samples of dental caries patients with diabetes, 26 samples of Dental caries patients only show in figure (1).

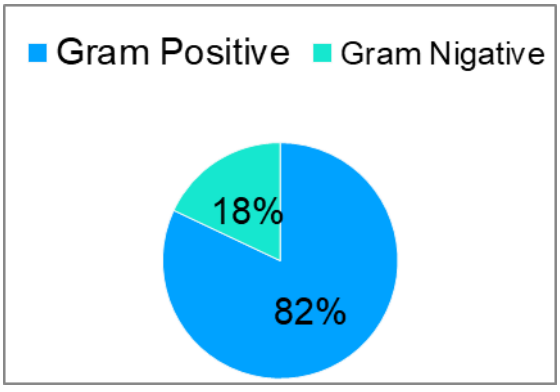


Figure 1. Bacteria that isolate from patients

46 isolates of Gram-positive bacteria including the genera Streptococcus ssp., isolates from Staphylococcus ssp. was diagnosed and 10 Gram-negative bacterial isolates, while 30 isolates from dental caries patients with diabetes and 26 isolates from dental caries patients without diabetes, as Show in table (1).

Table 1. Bacteria that isolate from patients

No.	Isolated Bactria	Number
	Gram positive	
1	Streptococcus ssp.	30
2	Staphylococcus ssp.	16
	Gram Negative	
3	Escherichia Coli	10

That Staphylococcus bacteria is the most common in dental careis , in addition to the fact that Streptococci is one of the genera that predisposes to causing opportunistic diseases through Before other groups of the genus Streptococci that are present on the nose, skin, and alimentary canal (Whary et al, 2015), it is also the cause of acute nosocomial infections (Hetem et al, 2017). In its non-native, it has rapid resistance mechanisms, ease of dissemination represented by plasmids through the process of coupling and transformation, in addition to having surface antigens and lysis enzymes that help it penetrate into different tissues of the body, such as the case in staphylococcus bacteria. As for Gram-negative bacteria, the percentage was the lowest compared to Gram-positive bacteria, and according to what was confirmed by several studies that most of the Gram-negative bacteria originate from inflammation of the respiratory tract or the gastrointestinal tract, and this agrees with both (Huffinagle et al, 2017).

Cultivation Characters

Streptococcus ssp. grown on solid Nutrient agar medium, blood agar medium after being grown in aerobic conditions at a temperature of 37C for 24 hours, showed small, high, irregular, adherent colonies to each other, while Growing it on Blood agar medium, most of it is α hemolytic.

Streptococcus ssp. grown on solid Mannitol salt agar medium, blood agar medium after being grown in aerobic conditions at a temperature of 37C for 24 hours, showed small, yellow color, adherent colonies to each other, while Growing it on Blood agar medium, most of it is β hemolytic.

E. coli isolates were initially diagnosed based on phenotypic traits, after growing them on MacConkey agar medium, blood agar medium, The results showed that the bacteria were fermenting the sugar lactose and cut down pink, smooth, shiny and sharp colonies on the differential agar medium that contains bile salts and crystal violet dye that allows the growth

of Gram-negative bacteria including the enteric family and inhibits the growth of positive bacteria, Growing it on Blood agar medium, most of it is not hemolytic (Wanger et al, 2017).

Microscope Characters

Streptococcus ssp. results of dry trowels prepared from colonies of developing bacteria showed a gram-Positive wave of spherical or oval-shaped pools arranged in pairs or baskets, Staphylococcus ssp. bacteria are Gram-positive cocci about 0.5 – 1.0 µm in diameter. They appear as clusters that resemble grapes, and Gram's stain was used to detect E. coli by creating a smear from the colony that had just begun to grow (18–24 hours earlier) (Levinsion, 2017).

Biochemical test

Biochemical tests were carried out on all isolates, and 26 isolate were positive, while 30 isolate were negative to Catalase test. Positive bacteria analyzed the hydrogen peroxide reagent to water and oxygen. 16 isolate appearance positive to Oxidase test while 40 isolate were negative for the oxidase test through the science of color shifting the colonies when adding the reagent this agrees with (AL-saadi,2014). Only 10 isolate seemed positive to the indole test, and only 16 isolate can Growth on a medium Mannitol salt agar, while 30 isolate exhibited partial lysis of the type alpha hematolytic, 16 isolate showed complete lysis of the type beta hematolytic, and 10 isolate showed gamma hemolytic show in table (2).

Table2. Biochemical test result

Bactria	Catalase test	Oxidase test	Blood Hemolysis	Indole test	Growth on a medium Mannitol salt agar
Streptococcus ssp.	-	-	α-hemolytic	-	-
Staphylococcus ssp.	+	+	B-hemolytic	-	+
E. coli	+	-	Non-hemolytic	+	-

Conclusions

Therefore we conclude that Streptococcus ssp. Bacteria are the main cause of dental caries compared to isolated bacteria, and that the incidence of dental caries was high among people with diabetes.

References

1. Asadi, S.; Kargar, M.; Solhjoo, K.; Najaf, N. and Ghorbani-Dalini, S. (2014) The Association of Virulence Determinants of Uropathogenic Escherichia coli with Antibiotic Resistance. Jundishapur J Microbiol. 7(5): 1-5.
2. Dianawati. N, Setyarini. W, Widjiastuti. I, Ridwan. R.D and Kuntaman. K .(2020). The distribution of Streptococcus mutans and Streptococcus sobrinus in children with dental caries severity level. Dental journal. Vol 53. No 1.
3. González-Moles M.A and Ramos-García P. (2021). State of Evidence on Oral Health Problems in Diabetic Patients: A Critical Review of the Literature. J Clin Med. 10(22):5383. doi:10.3390/jcm10225383.
4. Goyal D, Kaur H, Jawanda MK, Verma S, Parhar S. (2012). Salivary pH and dental caries in diabetes mellitus. Int J Oral Maxillofac Surg.
5. Hetem, D.J.; Rooijakkers, S.H.; Ekkelenkamp, M.B. (2017). "Staphylococci and Micrococcus in Infectious Diseases". 4th ed. pp.1509-1522.
6. Huffnagle, G.B.; Dickson, R.P.; Lukacs, N.W. (2017). The respiratory tract microbiome and lung inflammation: a two-way street. Mucosal Immunology, 10(2), 299.
7. Levinson, W. (2016). Review of Medical Microbiology and Immunology. 14"ed. McGraw-Hill education, Inc. PP 821.
8. Mathur VP, Dhillon JK. (2018). Dental Caries: A Disease Which Needs Attention. Indian J Pediatr.
9. Shiferaw A, Alem G, Tsehay M. and Kibret G.D. (2022). Dental caries and associated factors among diabetic and nondiabetic adult patients attending Bichena Primary Hospital's Outpatient Department. Front. Oral. Health 3:938405. doi: 10.3389/froh.2022.938405.
10. Wanger, A.; Chavez, V.; Huang, R. S. P.; Wahed, A.; Actor, J. K. and Dasgupta, A. (2017). Microbiology and Molecular Diagnosis in Pathology. Elsevier Inc. Rights Reserved. 300pp.
11. Whary, M.T.; Baumgarth, N.; Fox, J.G.; Barthold, S.W. (2015). Biology and diseases of mice. In Laboratory Animal Medicine (Third Edition), 143-149.
12. WHO (World Health Organization). (2003). Basic Laboratory Procedures in Clinical Bacteriology.
13. Yoo, S; Kim. P; Hwang, H; Kim, K; Choe, S; Min, B. and kook, J.(2005). Identification of non- mutans Streptococci origamis in dental.

Determination of Vitamin D Levels in Patients with Autism by High Performance Liquid Chromatography HPLC

Hadeel Sameer Abd Alwahab [1]

© 2023 The Author(s). This open access article is distributed under a Creative CommonsAttribution (CC-BY) 4.0 license.

Abstract: According to our hypothesis, ASD patients have lower levels of serum vitamin D, which have been found to be related to the disease's severity. Additionally, we predicted that a sizable fraction of children who have ASD could benefit from vitamin D3 therapy. Of the 215 children with ASD, 37 of them have received vitamin D3 treatments. Prior to and following the course of treatment, serum 25 D levels, CARS, and ABC have been measured. Serum 25D concentrations had a negative correlation with the ABC overall scores and language subscale scores On the ABC and CARS, symptom scores were considerably lower following vitamin D3 treatment. Additionally, the data imply that treatment outcomes were stronger in younger ASD patients.

Key Words: Autism Spectrum Disorder; Vitamin D; HPLC.

Author details

[1] Departement of Chemistry, College of Medicine, University of Al Nahrain, Baghdad, Iraq

Citation information

Cite this article as:

Abd Alwahab, H.S. (July 2023), *Determination of vitamin D levels in patients with Autism by high performance liquid chromatography HPLC*, Proceedings of the Minar Congress, Turkey, (9) pp 395-402, DOI: http://dx.doi.org/10.47832/MinarCong9-34

http://dx.doi.org/10.47832/MinarCong9-34

[1] hadeelsameer118@gmail.com

Introduction

The occurrence of ASD has risen dramatically over the remaining quite a few decades, from one in 5000 kids in 1975 to one in 88 teens in 2012, a 600% extend inside 30 years. At this point, there is a sturdy consensus that genetic elements play a vital position in ASD. Also, it has grown to be obvious that environmental elements are involved,3,4 which likely interaction with genetic factors. Trends of extended ASD incidence in dark-skinned people as properly as a greater ASD hazard in adolescents of moms with diet D deficiency for the duration of pregnancy, have additionally been reported.

Therefore, nutrition D deficiency at some point of early childhood may additionally be an essential environmental threat thing for ASD. We currently described a baby with ASD, who had suffered from nutrition D3 deficiency. This toddler actually multiplied after diet D3 supplementation, suggesting that nutrition with vitamin D might possibly at once have an effect on core autism signs. Consistent with this finding, sizable enhancement was once pronounced in a very current find out about evaluating nutrition of children with vitamin D3 tiers of122 teens with ASD and normally growing children.

Patients and Methods

Two hundred and fifteen ASD youngsters from the outpatient Department of Pediatric Neurology and Neuron-rehabilitation. ASD analysis used to be made with the aid of pediatricians who have trip with the autism diagnostic remark schedule, in accordance with DSM-IV standards of the American Psychiatric Association. In total, 285 wholesome controls participated in our study.

They were chosen from the hospital's AL-Imamaien-AL-khadumaien's centers of youth recreation and matched with the ASD team with regard to gender and age. For avoiding seasonal effects on 25 D levels, our research had been conducted over a period of six months.

Method

The CARS, which requires a score of less than 30 for regular youth, and the ABC, which requires a score of less than 53 for usual childhood, were used for determining the symptoms of autism. High-performance liquid chromatography (C18) has been utilized in order to evaluate the serum 25(OH) D tiers. The definition of sufficient serum 25(OH)D is higher than or equal to 30ng/mL, insufficient serum 25(OH)D is between 10ng/mL and30ng/mL, and poor serum 25(OH)D is ≤10ng/mL. All adolescents with ASD who had inadequate or insufficient intake of vitamin D have been advised to take supplements of vitamin D3. Only 37 of the 181 ASD teenagers finished the recommended diet D3 administration for three months. Through a nurse, vitamin D3 has been previously supplied intra-muscularly at a 150IU/month dose (in total 3 injections) and orally at a 400IU per day dosage (in total three months). Ranges of serum 25(OH)D have been evaluated before and three months following treatments. In this work, the ABC was evaluated by conducting parent interviews, whereas CARS has been evaluated by the observation of the behavior of adolescents with ASD during

a newborn psychiatric checkup. A rehabilitation health. professional evaluated CARS and ABC both before and after a three-month course of treatment. 37 ASD teenagers who had finished diet D supplementation have been split to 2 groups based on their ages early cure team (n = 20) less than or equal to 3 years, later.

Result

The information on contributors' demographics. 285 healthy controls and 215 ASD youths in total have been enrolled in this research (Table1). The average age of children with ASD used to be 4.760 ± 0.950 years.

Healthy control group members (5.120 ± 1.150 years) had been matched based on sex and age with ASD group. 80.47% (n = 173) of the children with ASD were of the male gender, compared to 19.53% (n = 42) of the females, for the ratio of almost 4:1. There used to be no distinction between the two businesses in terms of the birth records (mom and father's ages at birth, gestational age, and initial weight).

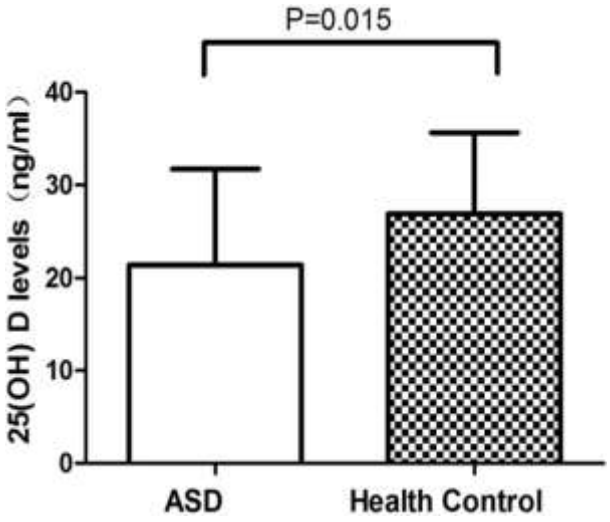


Figure 1. Levels of serum 25(OH) D in ASD children and healthy controls. T-test has been utilized used for comparison.

Table 1. The demographic data of ASD children and healthy controls

Parameters	ASD	Health Control	*P*-value
Number of participants	215	285	
Age (years)	4.76 ± 0.95	5.12 ± 1.15	0.35
Sex			
Male (%)	173 (80.47)	255 (78.95)	0.45
Female (%)	42 (19.53)	60 (21.05)	0.36
Age of the mother at birth (years)	27.55 ± 1.13	26.54 ± 3.24	0.25
Age of the father at birth (years)	28.50 ± 1.87	28.13 ± 2.26	0.36
Gestational age (months)	38.89 ± 2.45	39.23 ± 125	0.32
Birth weight (kg)	3.44 ± 0.41	3.32 ± 0.21	0.42
Boy weight (kg)	15.76 ± 0.23	16.33 ± 0.35	0.26
Height (cm)	107 ± 1.23	110 ± 1.35	0.35

Teenagers with ASD had lower levels of serum 25(OH)D when compared to the healthy controls. High-performance liquid chromatography had been utilized in order to evaluate serum 25 (OH) D tiers. Teenagers with the ASD had significantly lower levels of serum of 25D compared to the healthy controls. In ASD group, there were 13 and 71.2% people who had inadequate diet D, respectively. Among children in good health, none had low vitamin D intake, and 61.80% had an inadequate diet. Between ASD males and ASD girls, there was formerly shown to be little difference in serum 25 (OH) D degrees.

Adolescents with ASD's behavioral issues improving following diet D3 supplementations. All of the ASD adolescents with a shortage in vitamin D and vitamin D sufficiency have been instructed to take vitamin D3 supplements, however, only 37 of the 181 ASD adolescents had gone through with the recommended three months of regular vitamin. A dosage of 150 IU of vitamin D3 was once administered intramuscularly once a month, and a dose of 400 IU was once given orally once a day. Assessments of (levels of CARS, ABC, and serum 25(OH)D) had been done before and three months following the treatments. Following dietary D supplementation, all of the patients have shown almost improved serum 25(OH) D levels (P=0.00, Fig3-A). Additionally, in comparison to the pre-treatment situation, the overall ABC scores, some ABC subscale rankings (language, social skills, body and object usage, social or self-help), and the overall rankings of CARS had all considerably declined (P<0.050, Figs3-B and D-H). Although the ABC subscale's sensory ratings showed a reducing trend after receiving vitamin D treatments, no significant differences have been found between the pre- and post-treatment periods (P=0.185, Fig2-C).

In young ASD adolescents, vitamin D supplementation might wish to be of higher quality. A total of 37 ASD young people who have received vitamin D supplements have been split to 2 groups based upon their ages: the early treatment group (n = 20) less than or equal to 3 years, and the later group of treatment (n =17) were both under the age of three. The discount of whole ABC scores and whole CARS ratings has been once studied for each group.

The discount of whole ABC rankings (P=0.08, Fig4-A) and whole CARS rankings (P=0.016, Fig4-B) in early treatment group has once been extra giant when compared to it in the later therapy group. It can also recommend that nutrition D supplementations should be greater high-quality in the youthful ASD children.

Table 2. Vitamin D levels of all participants

Vitamin D levels	Autistic children (*n* = 215)	Health controls (*n* = 285)	*P*-value
Vitamin D deficiency (<10 ng/mL)	13% (28/215)	0	0.032
Vitamin D inadequacy (10-30 ng/mL)	71.2% (153/215)	61.8% (176/285)	0.028
Vitamin D adequacy (>30 ng/mL)	15.8% (34/215)	38.2% (109/285)	0.025

Table 3. Follow-up table of ASD children with Vitamin D deficiency and inadequacy

	Vitamin D deficiency (<10 ng/mL)	Vitamin D inadequacy (10-30 ng/mL)	Total number
Be advised to receive vitamin D supplementation	28	153	181
Taking vitamin D supplementation	26	68	94
Lost of contact or unable to conduct evaluations	6	51	57
Finished vitamin D supplementation	20	17	37

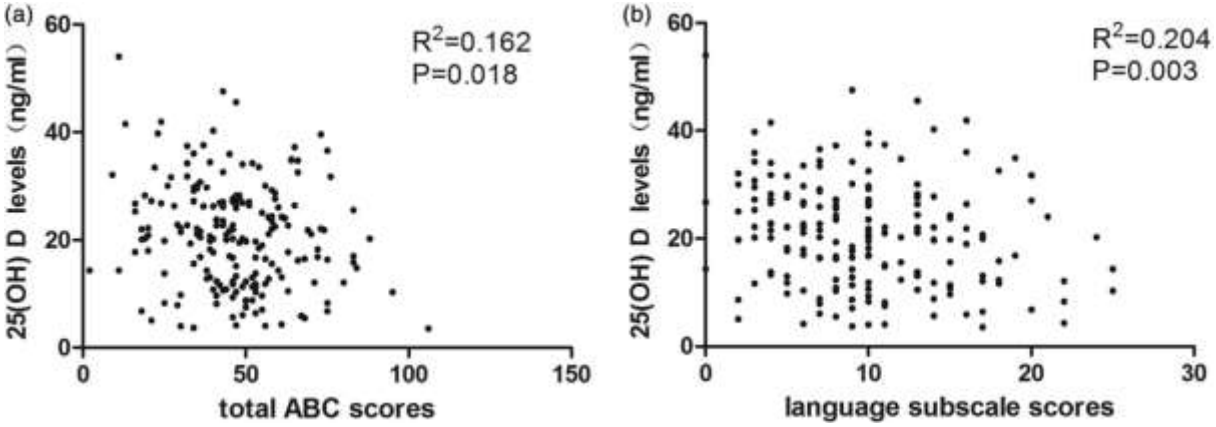


Figure 2. Correlation take a look at used to be utilized in order to consider correlations between ABC scores and 25(OH) D stages. (A) The relation between 25(OH) D ranges and whole ABC score levels. (B) The correlation between 25(OH) D stages and language rankings of the ABC sub-scale.

Discussion

Three key findings emerged from the present research. First, compared to typically developing children, levels of serum 25(OH)D are much lower in children with ASD. Adding vitamin D3 to food improved scientific findings, especially in young persons with ASD. The main findings of the present study are consistent with earlier research that shows reduced vitamin D levels in the ASD, increased incidence of ASD in the adults with dark skin, and increased ASD risks in teenagers whose mothers had vitamin D insufficiency throughout the period of pregnancy. The excellent outcomes of vitamin D3 supplementations are consistent as well with the results that have been reported by one of the recent trials; as far as we know, this represents the first replication of those results. We have also found that younger ASD children were more likely to experience a reduction in overall ABC ratings and overall, CARS ratings after taking vitamin D supplements. This finding might also suggest that, in the event of a deficiency, vitamin D supplementation should start as soon as possible. It's interesting to note that the ABC subscale's language rankings and the 25 (OH) D stages' overall ABC ratings were adversely correlated.

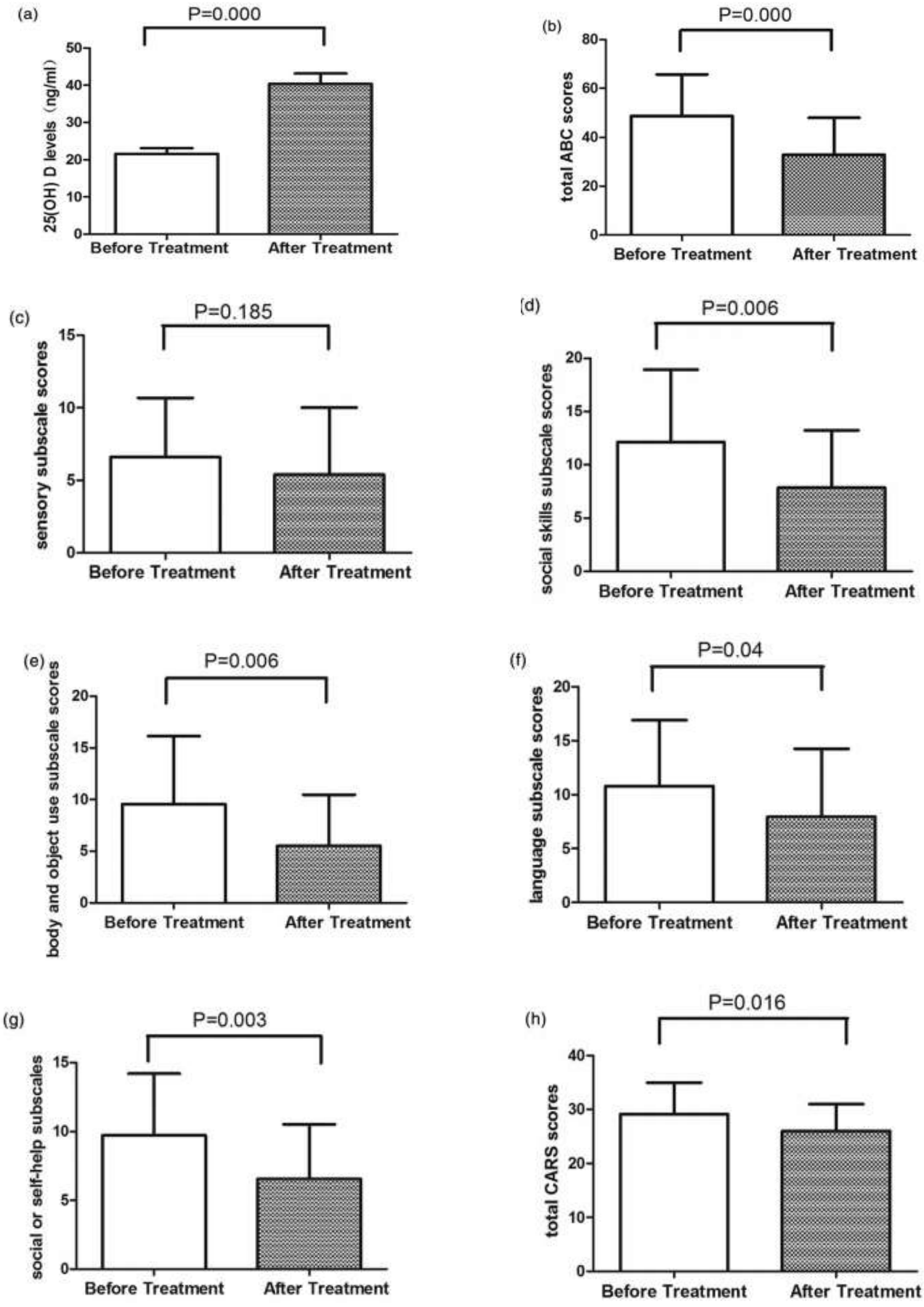


Figure 3. Changes of the levels of 25(OH) D and the behavioral anomalies in the ASD children prior and post treatments.

The comparison has been done using T-test. (A) Modifications in 25(OH)D levels. Changes in the scores of ABC overall (B). (C) Changes in the sensory sub-scale's scores (ABC). (D) Changes in the ABC subscale's social skills scores. (E) Score adjustments for the ABC sub-scale's object and body uses. (F) Language subscale score variations (ABC). (G) Changes in the ABC sub-scale's social or self-help scores. Changes in the overall CARS score values (H).

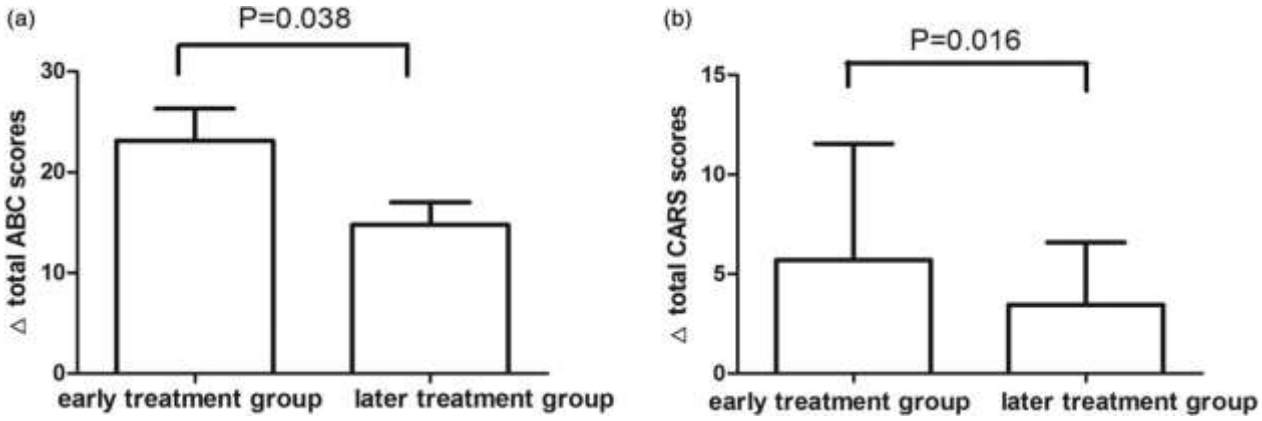


Figure 4. Reductions of the total ABC scores and CARS score values between the early and later treatment groups. The T-test has been utilized for comparisons. (A) Reduction of the total ABC scores. (B) Reduction of the total CAR score values.

Conclusions

This research demonstrates how inadequate levels of vitamin D may be contributing to the ASD. A safe and affordable form of treatment, vitamin D3 supplementation was shown to considerably enhance outcomes in some ASD patients, particularly in younger children. Further research is necessary to determine the precise mechanism by which vitamin D helps treat ASD, though.

References

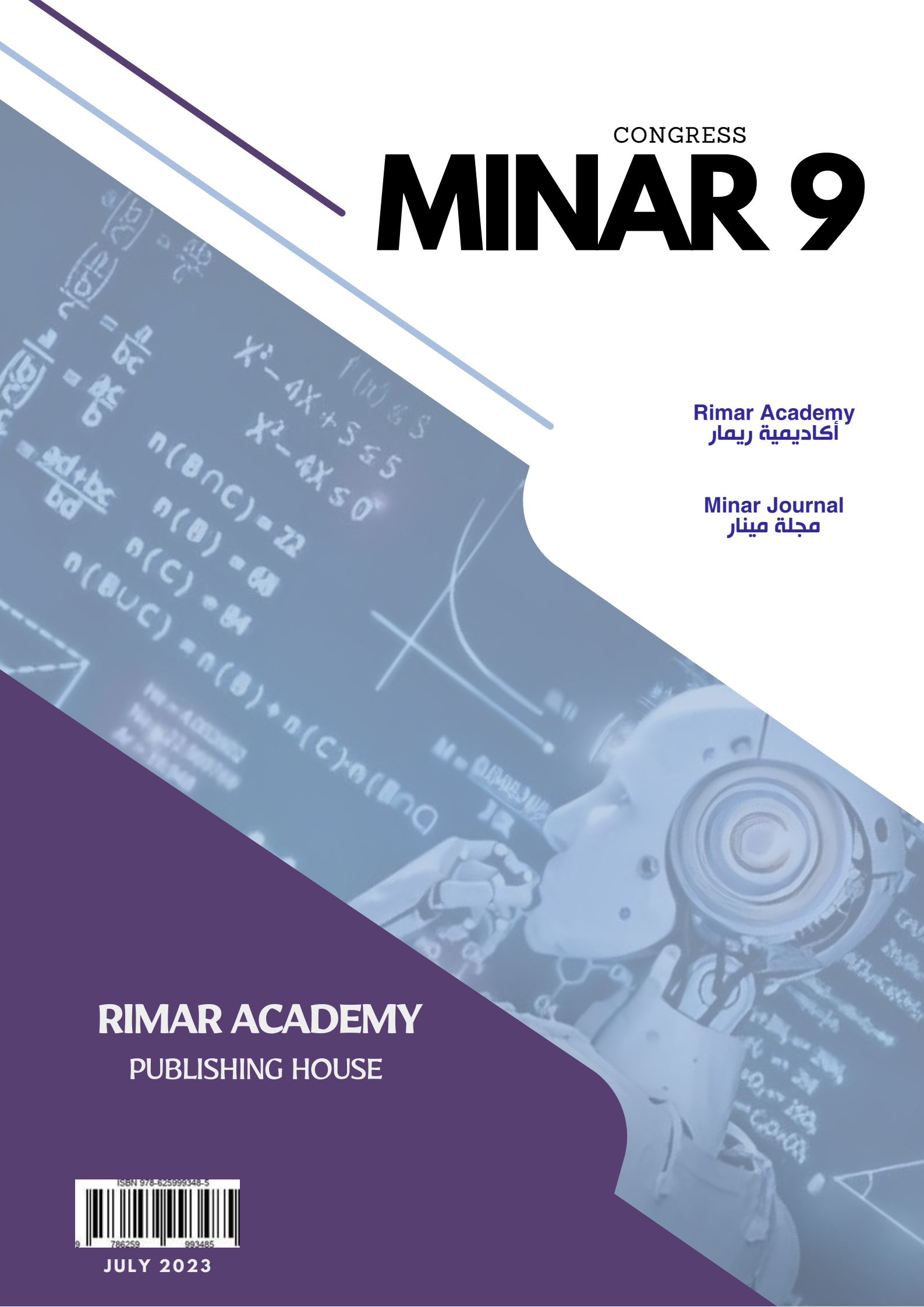
1. Pioggia G, Tonacci A, Tartarisco G, Billeci L, Muratori F, RutaL, et al. Autism and lack of D3 vitamin: a systematic review. Res Autism Spectr Disord 2014;8:1685–98.
2. Cannell JJ. Autism, will vitamin D treat core symptoms? Med Hypotheses 2013;81:195–8.
3. Cannell JJ. On the aetiology of Autism. Acta Paediatr 2010;99: 1128–30.
4. Kinney DK, Barch DH, Chayka B, Napoleon S, Munir KM. Environmental risk factors for autism: do they help cause de novo genetic mutations that contribute to the disorder? Med Hypotheses 2010;74:102–6.
5. Freitag CM, Staal W, Klauck SM, Duketis E, Waltes R. Genetics of autistic disorders: review and clinical implications. Eur Child Adolesc Psychiatry 2010;19:169–78.
6. Meguid NA, Hashish AF, Amwar M, Sidhom G. Reduced serum levels of 25-hydroxy and 1,25-dihydroxy vitamin D in Egyptian children with autism. J Altern Complement Med 2010;16:641–5.
7. Ramagopalan SV, Heger A, Berlanga AJ, Maugeri NJ, Lincoln MR, Burrell A, et al. A ChIP-seq defined genome-wide map of vitamin D receptor binding: associations with disease and evolution. Genome Res 2010;20:1352–60.
8. Cannell JJ. Autism and vitamin D. Med Hypotheses 2008;70: 750–9.
9. Uher R. Gene–environment interactions in severe mental illness. Front Psychiatry 2014;5:48.
10. Neggers YH. Increasing prevalence, changes in diagnostic criteria, and nutritional risk factors for autism spectrum disorders. ISRN Nutr 2014;2014:514026.
11. Bakare MO, Munir KM. Autism spectrum disorders (ASD) in Africa: a perspective. Afr J Psychiatry (Johannesburg) 2011;14: 208–10.
12. DeLuca GC, Kimball SM, Kolasinski J, Ramagopalan SV, Ebers GC. Review: the role of vitamin D in nervous system health and disease. Neuropathol Appl Neurobiol 2013;39:458–84.
13. Molloy CA, Kalkwarf HJ, Manning-Courtney P, Mills JL, Hediger ML. Plasma 25(OH) D concentration in children with autism spectrum disorder. Dev Med Child Neurol 2010;52:969–71.
14. Mostafa GA, Al-Ayadhi LY. Reduced serum concentrations of 25-hydroxy vitamin D in children with autism: relation to autoimmunity. J Neuroinflamm 2012;9:201.
15. Tostes MH, Polonini HC, Gattaz WF, Raposo NR, Baptista EB. Low serum levels of 25-hydroxyvitamin D (25-OHD) in children with autism. Trends Psychiatry Psychother. 2012;34: 161–3.
16. Neumeyer AM, Gates A, Ferrone C, Lee H, Misra M. Bone density in peripubertal boys with autism spectrum disorders. J Autism Dev Disord. 2013;43:1623–29.
17. Gallo S, Jean-Philippe S, Rodd C, Weiler HA. Vitamin D supplementation of Canadian infants: practices of Montreal mothers. Appl Physiol Nutr Metab 2010;35(3):303–9.
18. Koc˘ovská E, Andorsdóttir G, Weihe P, Halling J, Fernell E, Stóra T, et al. Vitamin D in the general population of young adults with autism in the Faroe islands. J Autism Dev Disord 2014;44:2996–3005.
19. Bener A, Al-Hamaq AO, Saleh NM. Association between vitamin D insufficiency and adverse pregnancy outcome: global comparisons. Int J Womens Health 2013;5:523.

CONGRESS

MINAR 9

Rimar Academy
أكاديمية ريمار

Minar Journal
مجلة مينار



RIMAR ACADEMY

PUBLISHING HOUSE

ISBN 978-625999348-5

JULY 2023